Volume 2

APPENDICES

APPENDIX 1

PRELIMINARY FE STUDY

1 Introduction

This is a preliminary FE study on long span perforated beams. General comparison is made to investigate the structural behaviour of beams with standard and non-standard web openings and visualize the behaviour of beams with various web opening shapes.

Sixteen perforated beams with 20m span are globally analysed with the use of FE software ANSYS. Different web openings are examined. However, the spacing and the size of such web openings is controlled for comparison reasons (i.e. same number of web openings at every beam). All web openings should fit to a square of 450mmx450mm. Essentially, it is tried to utilize the maximum possible web opening area within these limits (i.e. lighter beam).

The above perforated beams are categorized to those have filleted web opening edges at the mid-depth (the reason for this shape configuration is discussed in **Appendix 2**), and the normal ones. The latter category consists of web openings such as: C1-2/3/6/7/8/10/13/14/15/16/19/21/22/23, and the ones with filleted web opening shapes such as: C1-4/17. Perforated beams with filleted web openings present narrower web-post widths, as the fillet shape is actually developed out of the 450mmx450mm limits.

The comparison is established in two levels, pinned and fixed end supports of the perforated beam. The Von-Mises stresses along the length of the beam, local horizontal nodal stresses at the edge of the web opening located at mid-span as well as maximum deflections and shape deformations are examined.

All perforated beams are presented as following with random order.

2 FE model

Analysis Type: Geometric and Material Linearity

Section Size: Total Depth: 710mm
Flange Width: 520mm
Flange Thickness: 30mm
Web Thickness: 12mm
Root Radius: 24.1mm

End Post Width:	560mm	*Opening Spacing:*	590mm
Element Type:	Tetrahedral 10node 92	*Element Size:*	50mm
Poison's Ration:	0.3	*Young's Modulus:*	209GPa
Load Type:	35.65kN to all beams (Linear elastic region)		

3 FE results

(C1-2) Cellular Beam – Benchmark Point

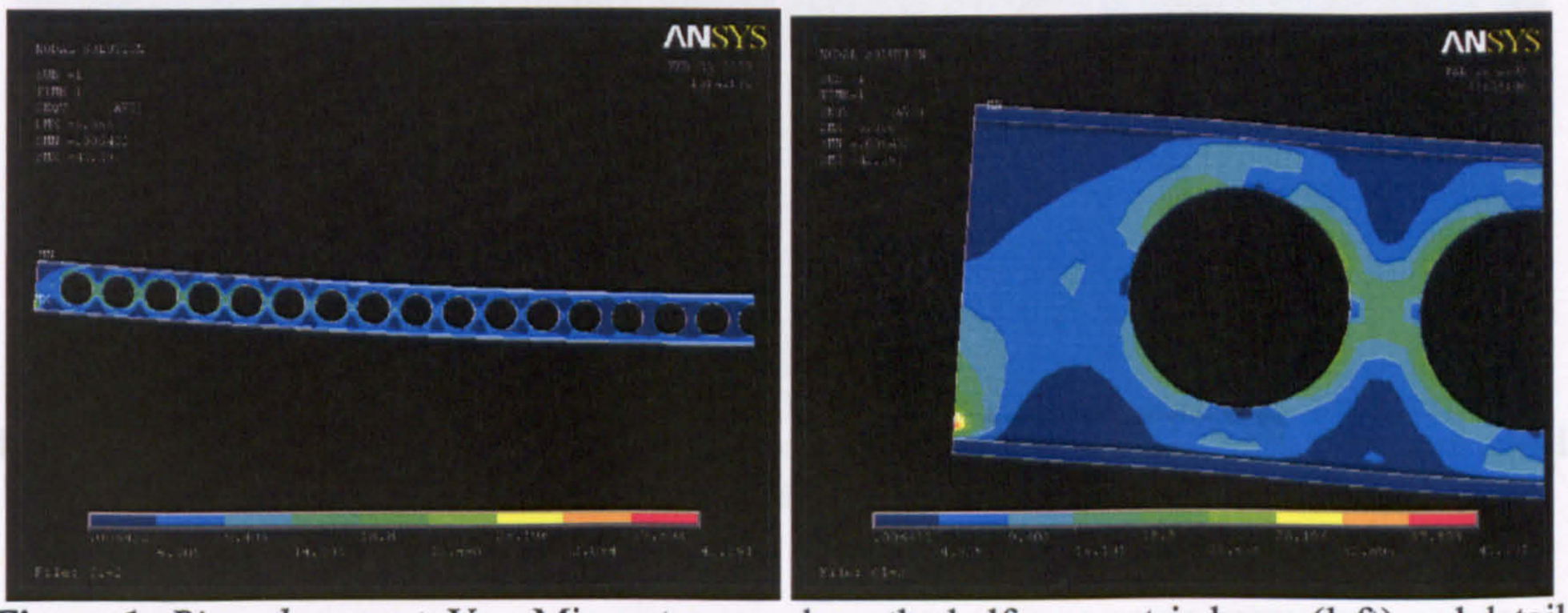

Figure 1: *Pinned support:* Von-Mises stresses along the half symmetric beam (left) and detail of the Von-Mises stresses at the end post (right)

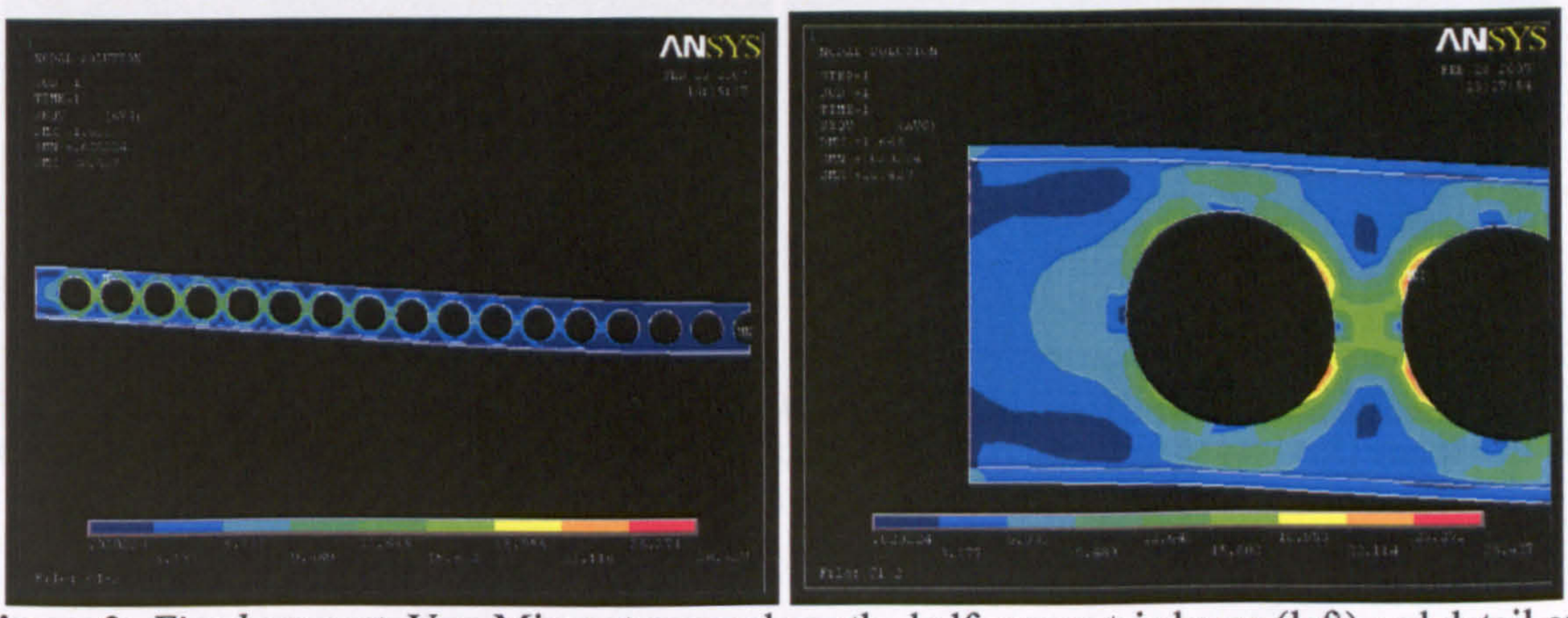

Figure 2: *Fixed support:* Von-Mises stresses along the half symmetric beam (left) and detail of the Von-Mises stresses at the end post (right)

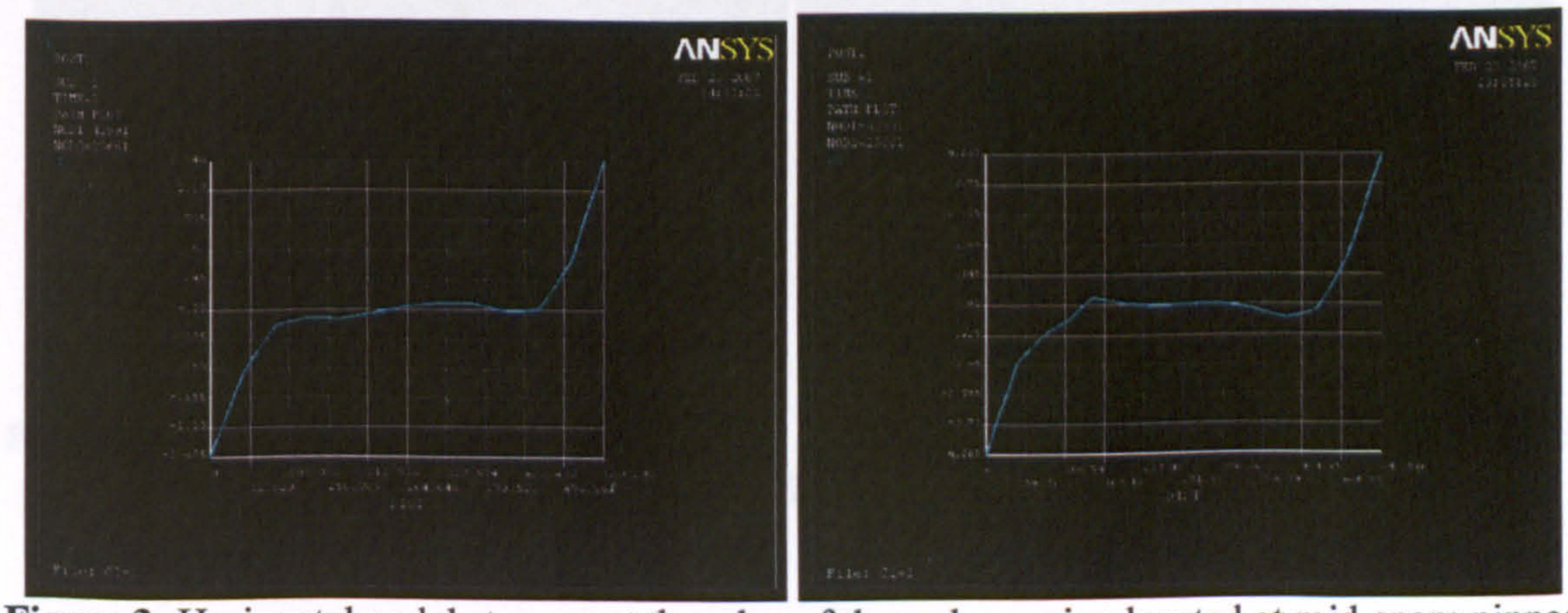

Figure 3: Horizontal nodal stresses at the edge of the web opening located at mid-span: pinned support (left) and fixed support (right)

(C1-3) Castellated Beam

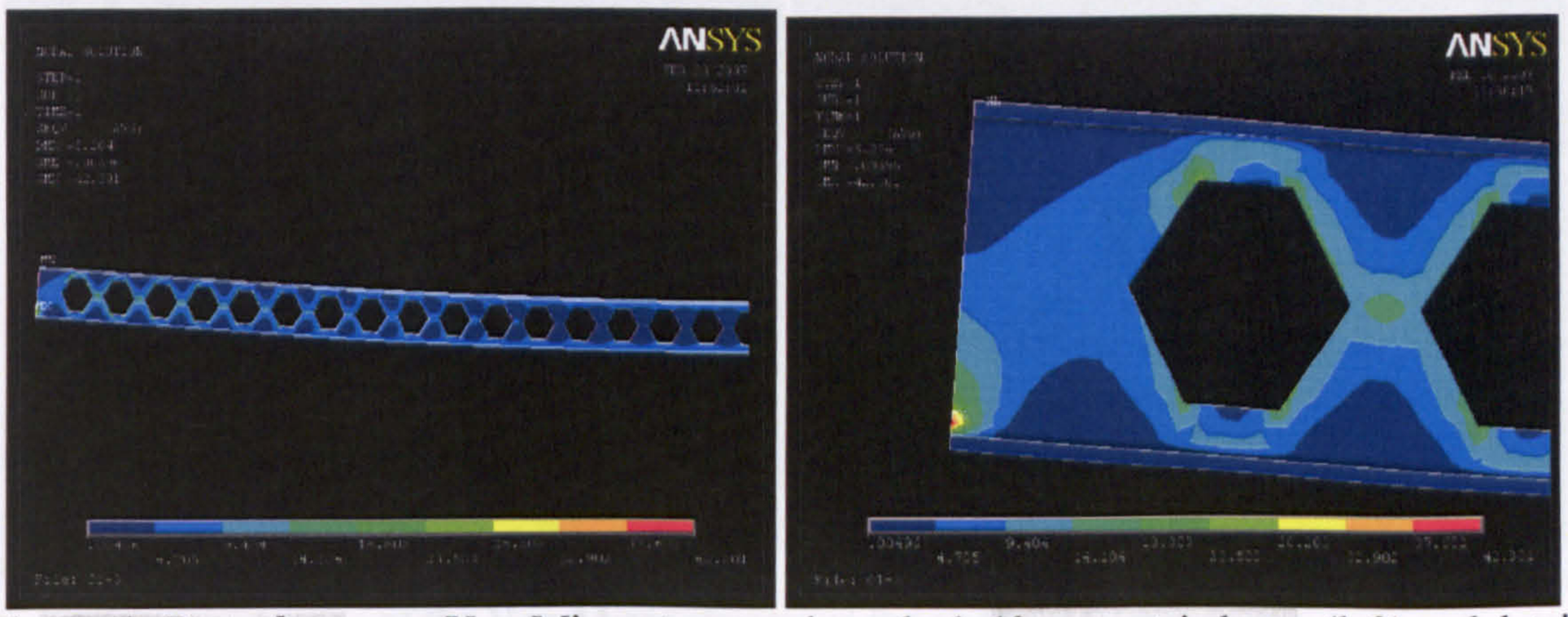

Figure 4: *Pinned support:* Von-Mises stresses along the half symmetric beam (left) and detail of the Von-Mises stresses at the end post (right)

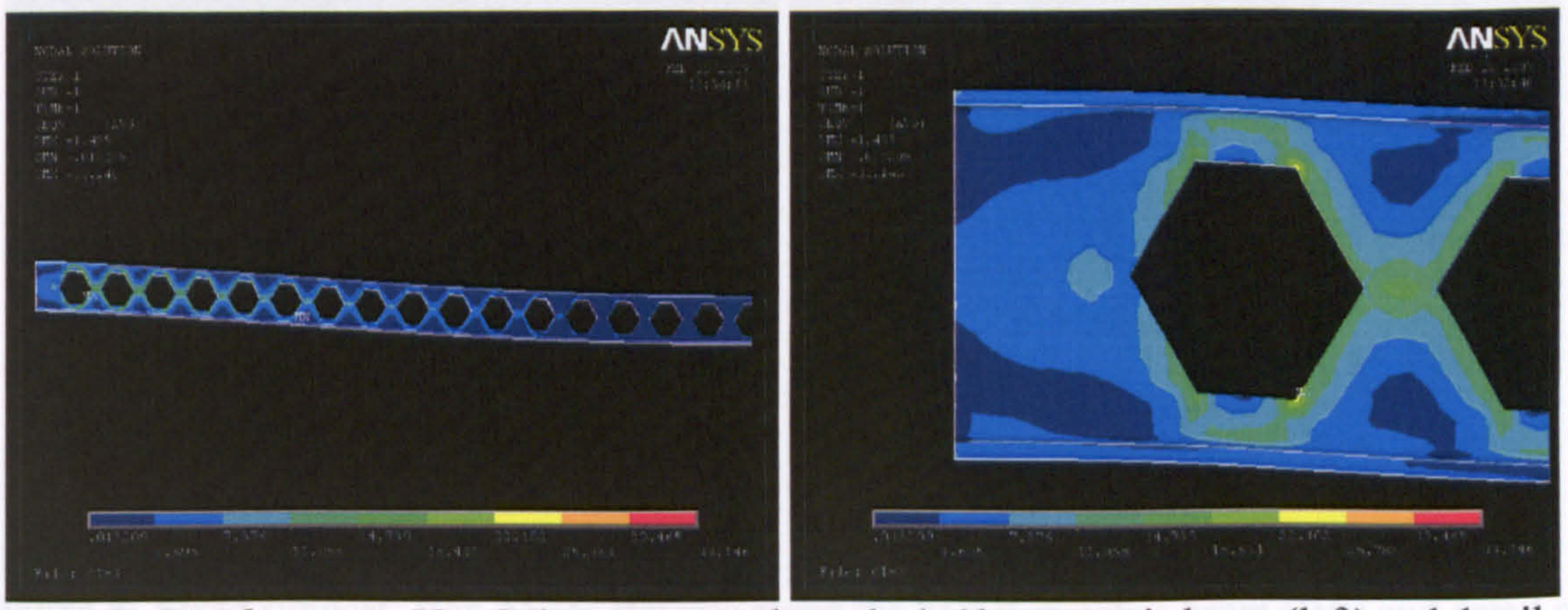

Figure 5: *Fixed support:* Von-Mises stresses along the half symmetric beam (left) and detail of the Von-Mises stresses at the end post (right)

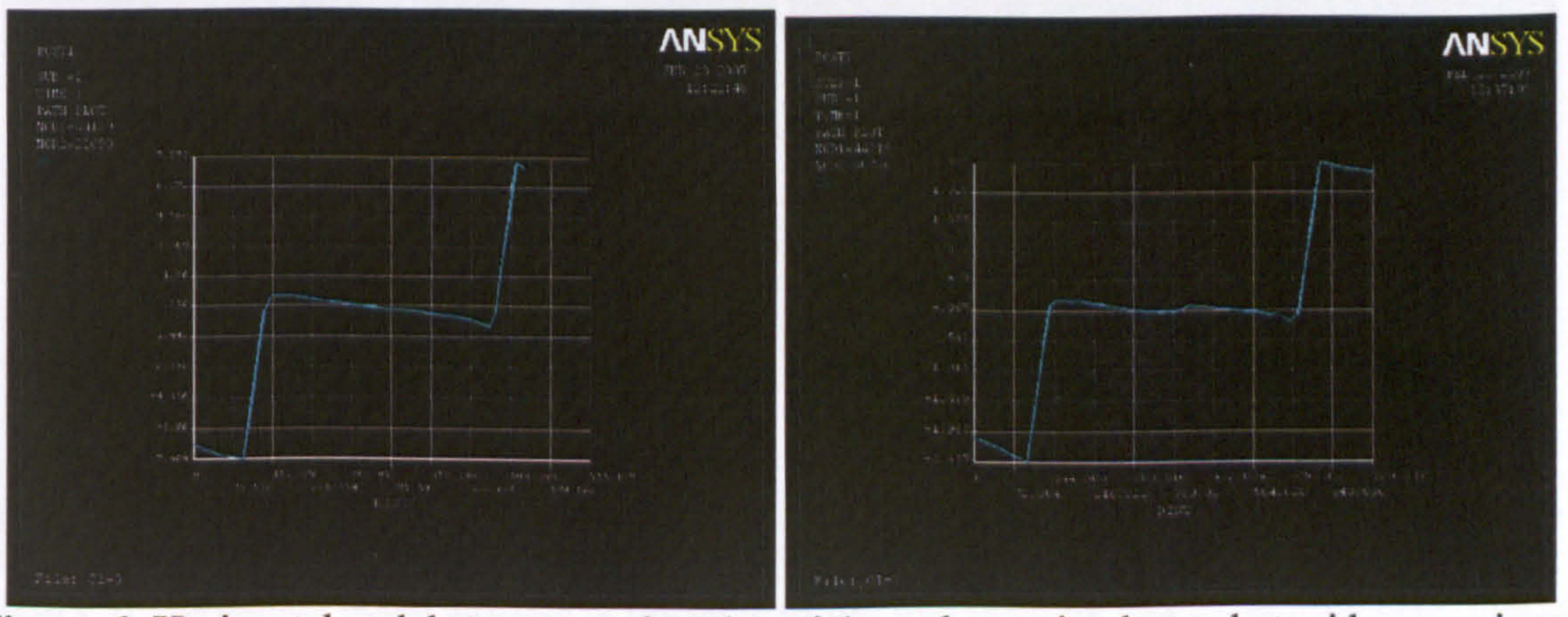

Figure 6: Horizontal nodal stresses at the edge of the web opening located at mid-span: pinned support (left) and fixed support (right)

(C1-15) Polygonal-12 edges

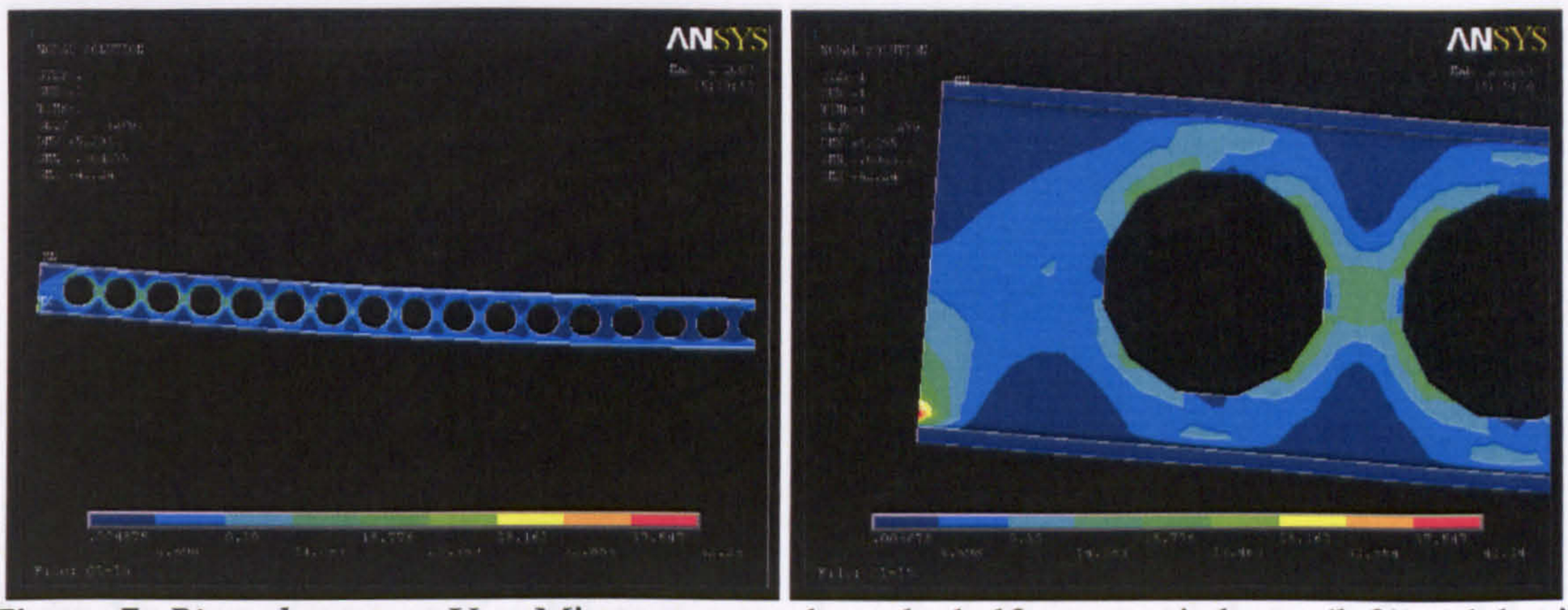

Figure 7: *Pinned support:* Von-Mises stresses along the half symmetric beam (left) and detail of the Von-Mises stresses at the end post (right)

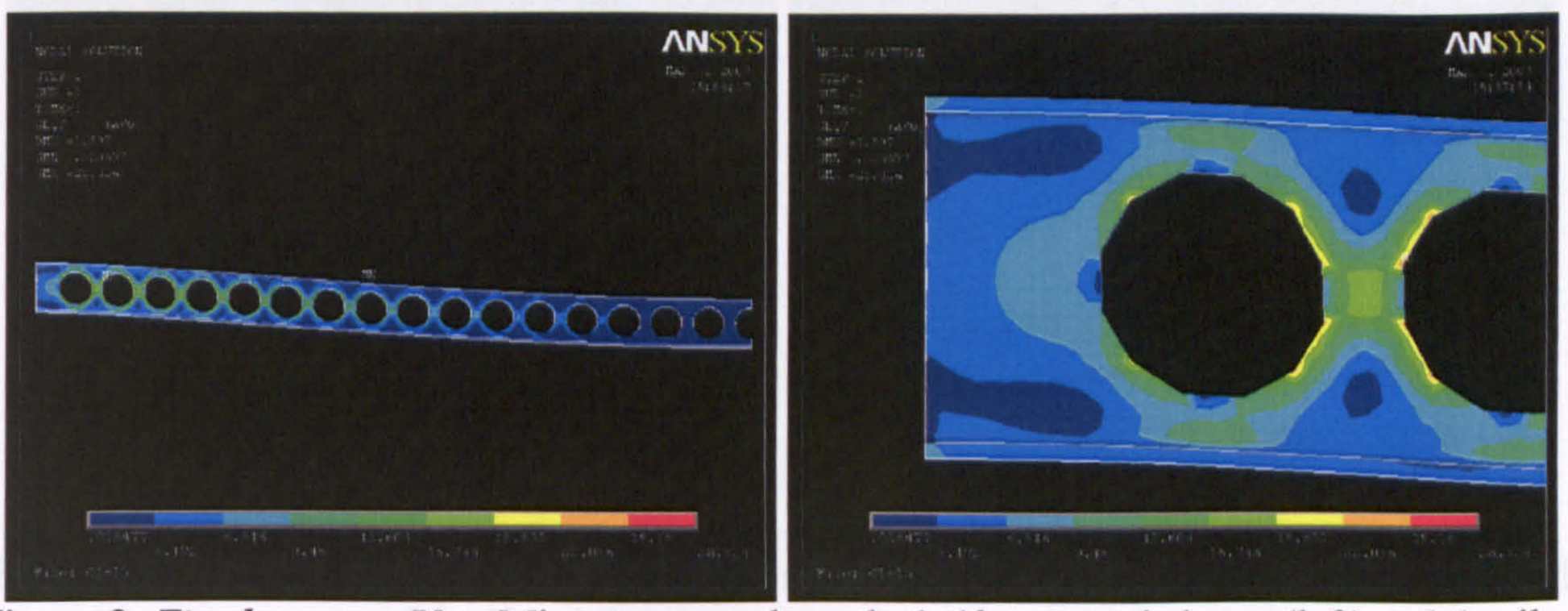

Figure 8: *Fixed support:* Von-Mises stresses along the half symmetric beam (left) and detail of the Von-Mises stresses at the end post (right)

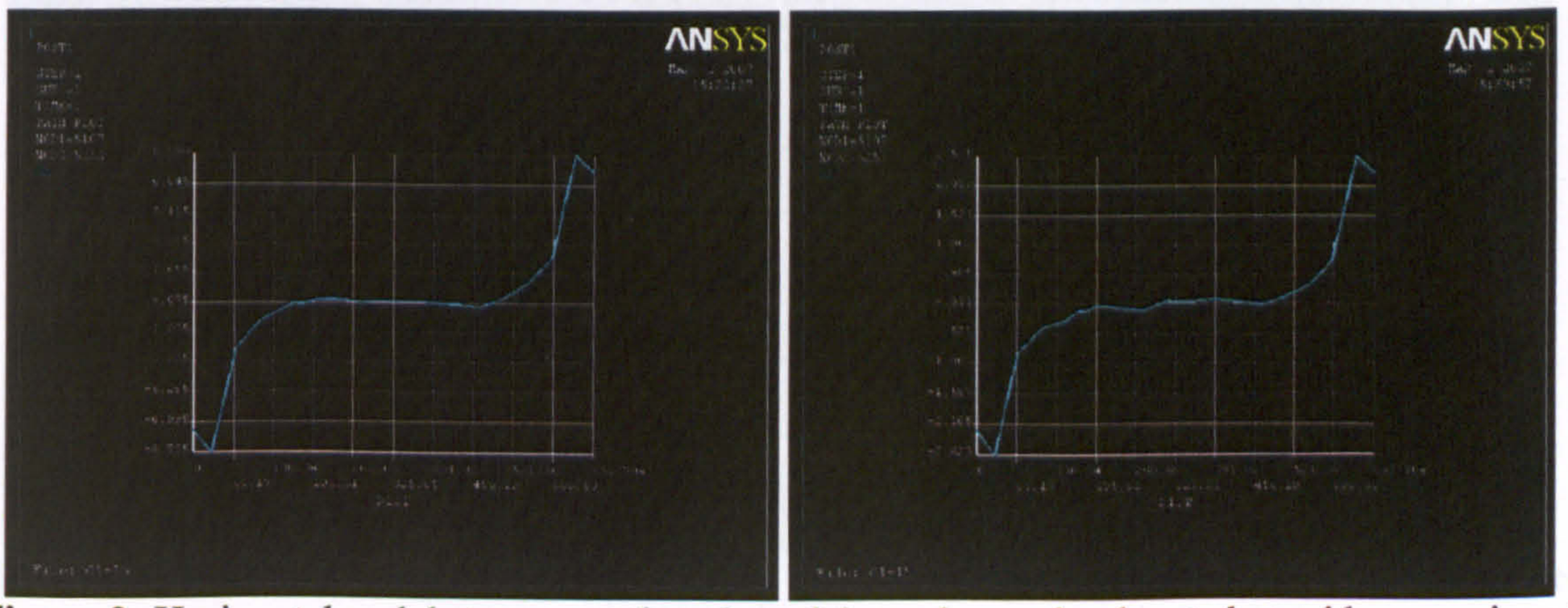

Figure 9: Horizontal nodal stresses at the edge of the web opening located at mid-span: pinned support (left) and fixed support (right)

(C1-16) Polygon-12 edges (15mm rotated, sharp end on the top & bottom)

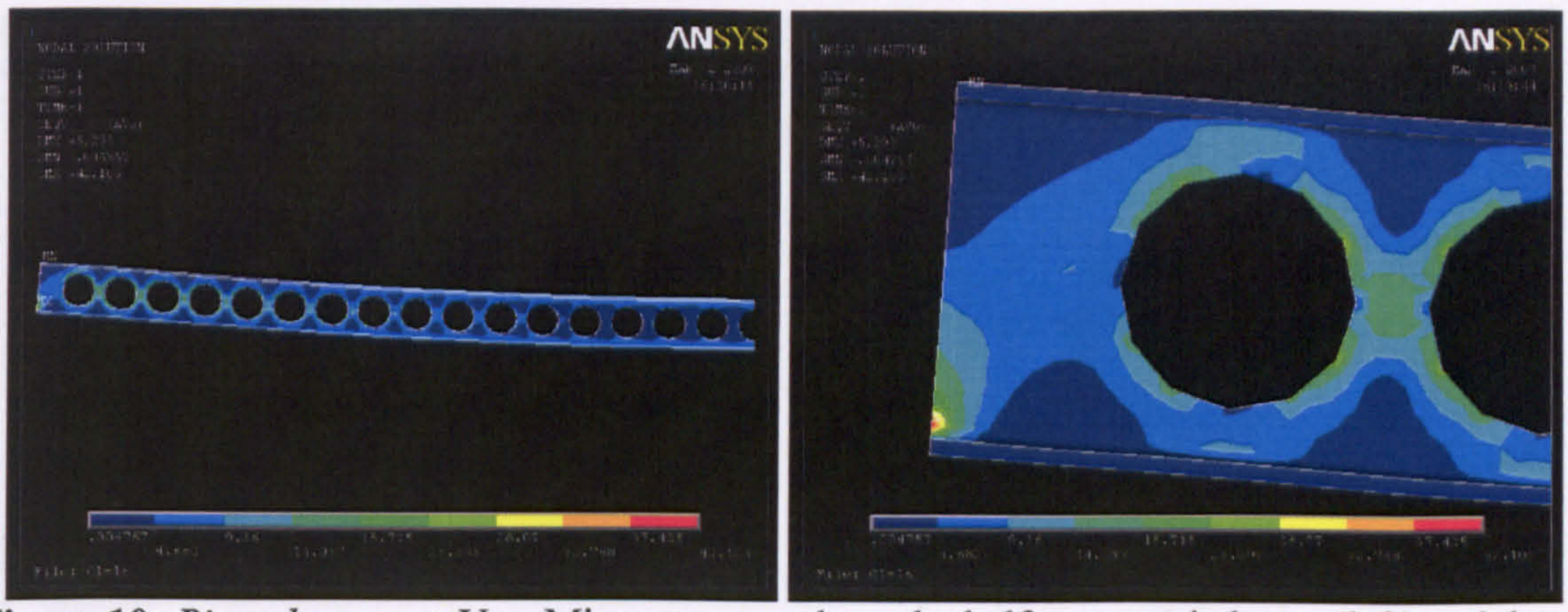

Figure 10: *Pinned support:* Von-Mises stresses along the half symmetric beam (left) and detail of the Von-Mises stresses at the end post (right)

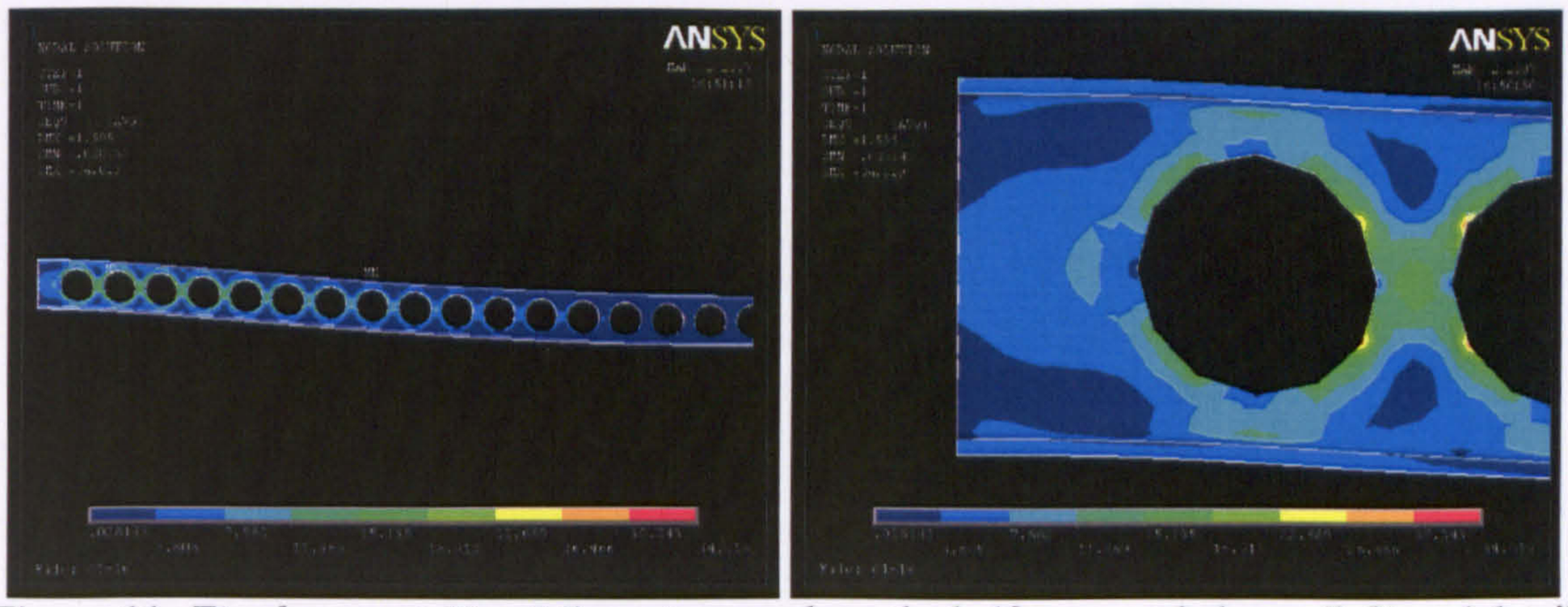

Figure 11: *Fixed support:* Von-Mises stresses along the half symmetric beam (left) and detail of the Von-Mises stresses at the end post (right)

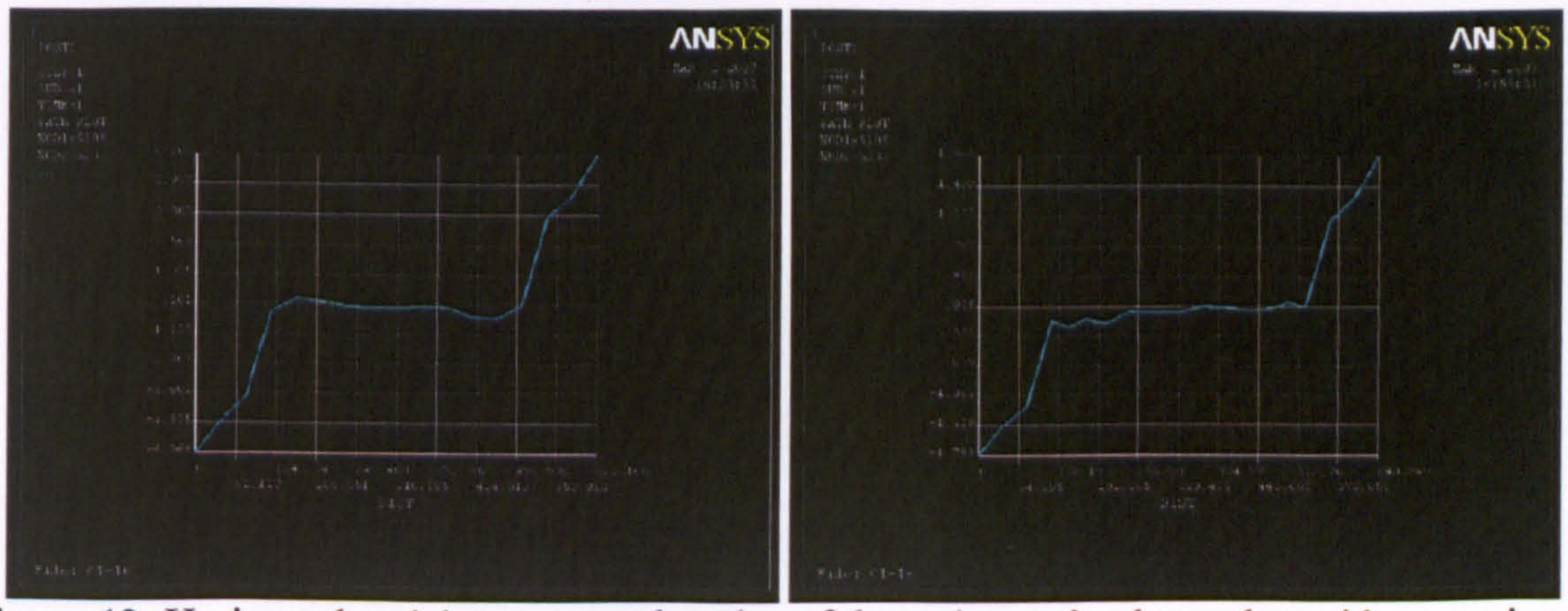

Figure 12: Horizontal nodal stresses at the edge of the web opening located at mid-span: pinned support (left) and fixed support (right)

(C1-4) Cellular with fillets (radius of 25mm)

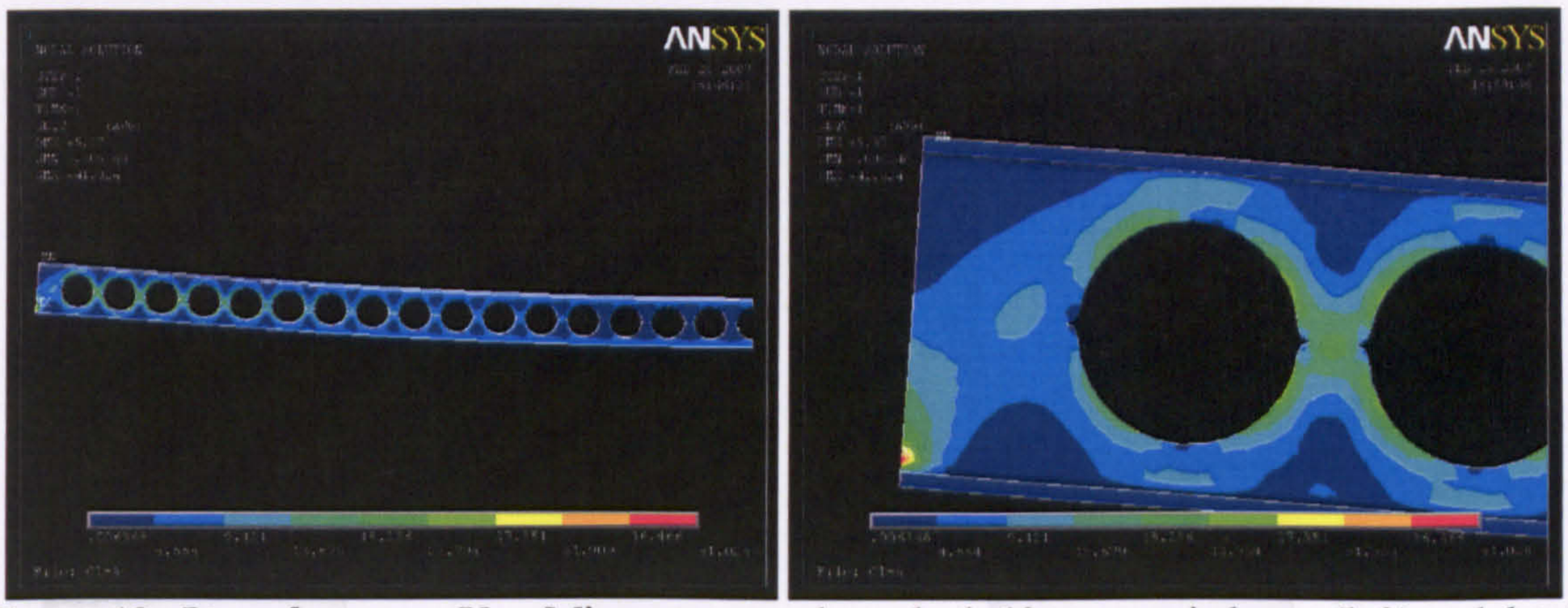

Figure 13: *Pinned support:* Von-Mises stresses along the half symmetric beam (left) and detail of the Von-Mises stresses at the end post (right)

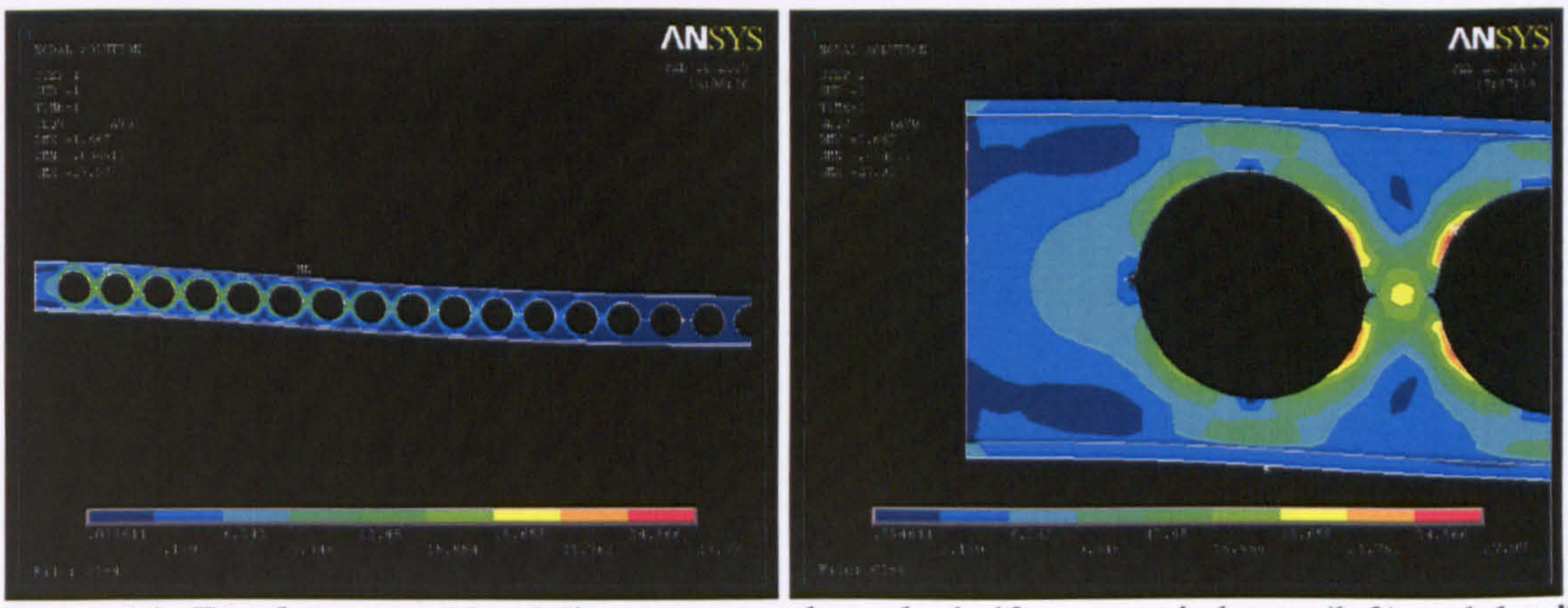

Figure 14: *Fixed support:* Von-Mises stresses along the half symmetric beam (left) and detail of the Von-Mises stresses at the end post (right)

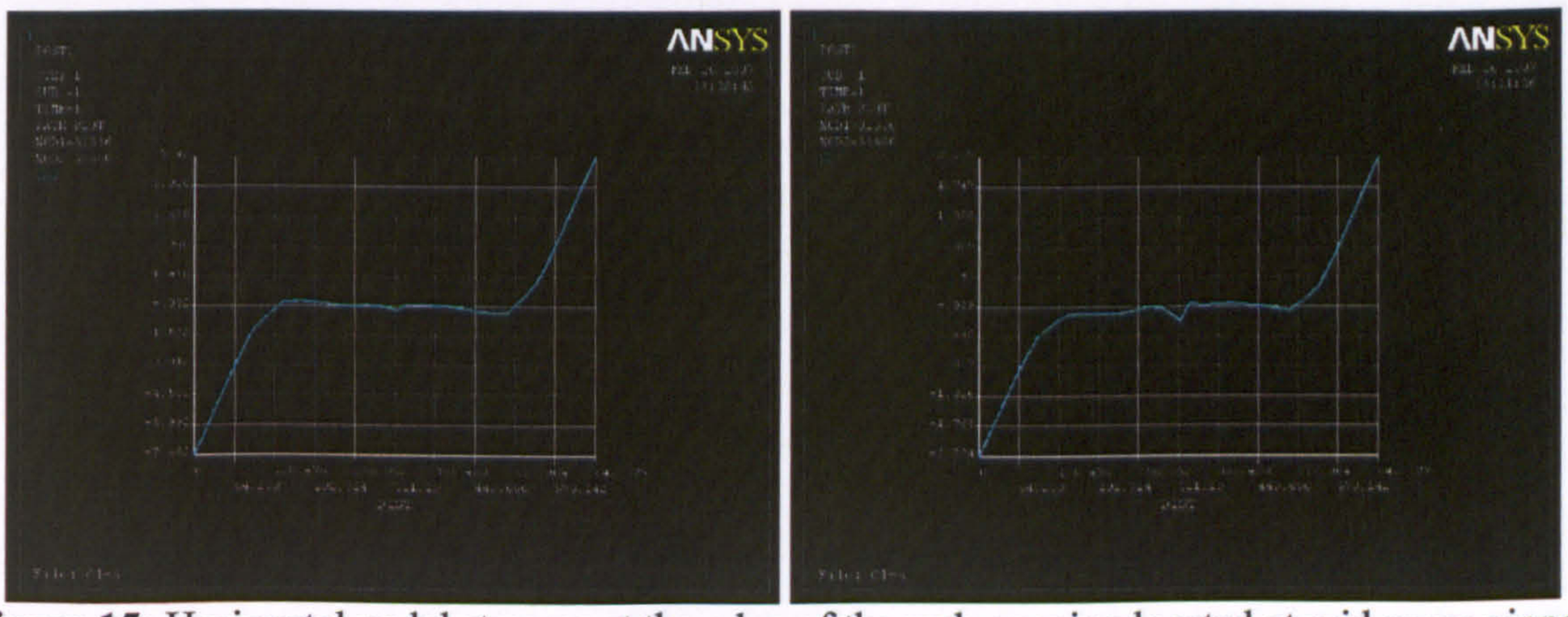

Figure 15: Horizontal nodal stresses at the edge of the web opening located at mid-span: pinned support (left) and fixed support (right)

(C1-17) Cellular with fillets (radius of 50mm)

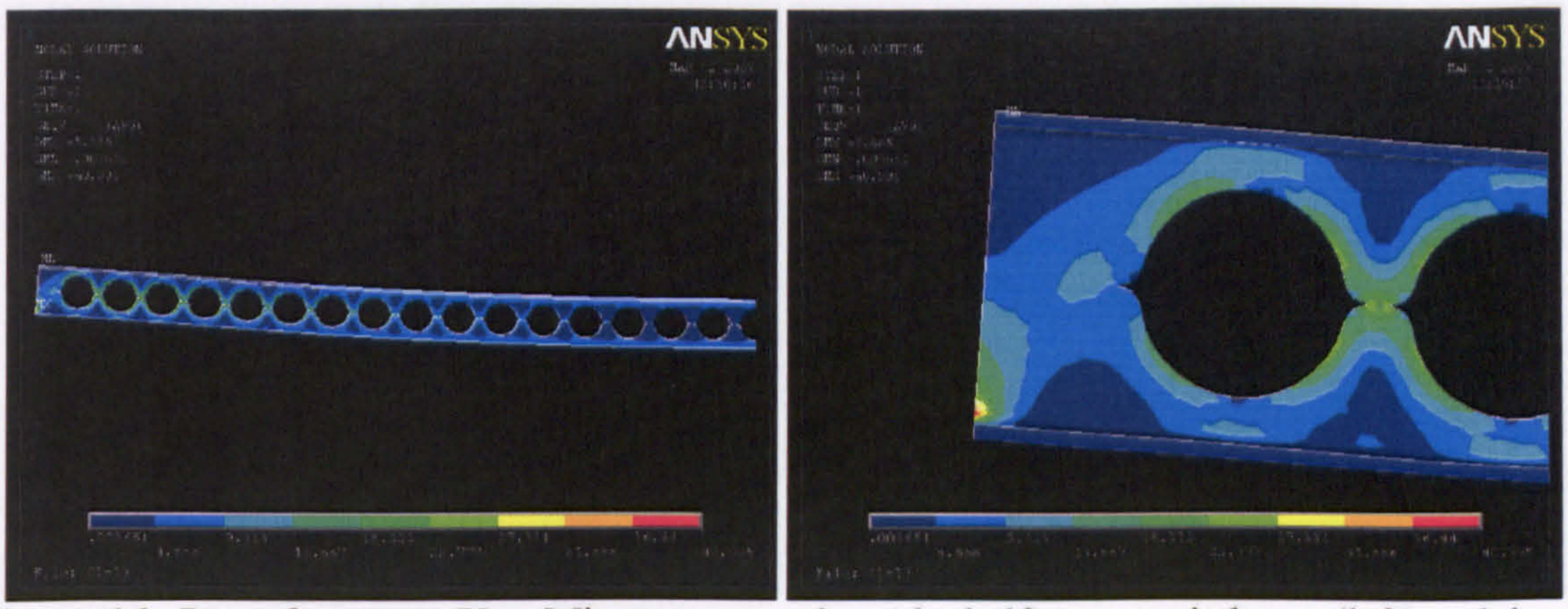

Figure 16: *Pinned support:* Von-Mises stresses along the half symmetric beam (left) and detail of the Von-Mises stresses at the end post (right)

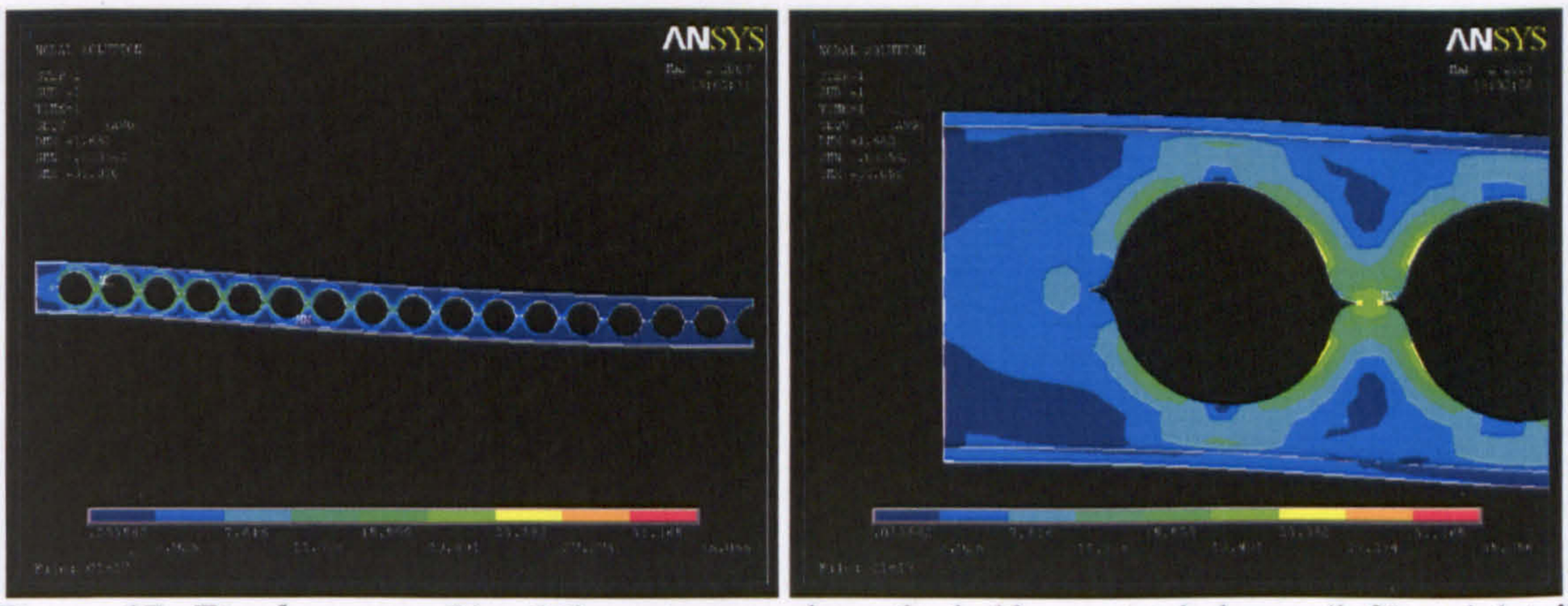

Figure 17: *Fixed support:* Von-Mises stresses along the half symmetric beam (left) and detail of the Von-Mises stresses at the end post (right)

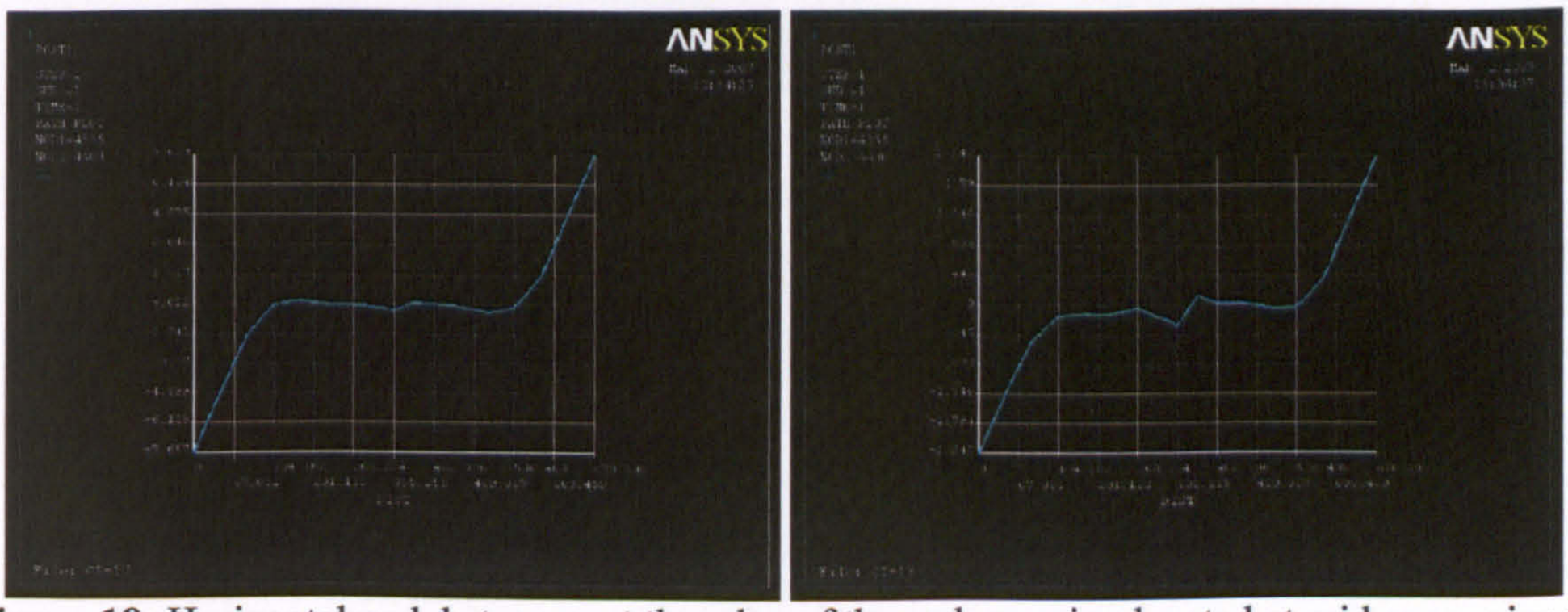

Figure 18: Horizontal nodal stresses at the edge of the web opening located at mid-span: pinned support (left) and fixed support (right)

(C1- 13) Castellated with added depth

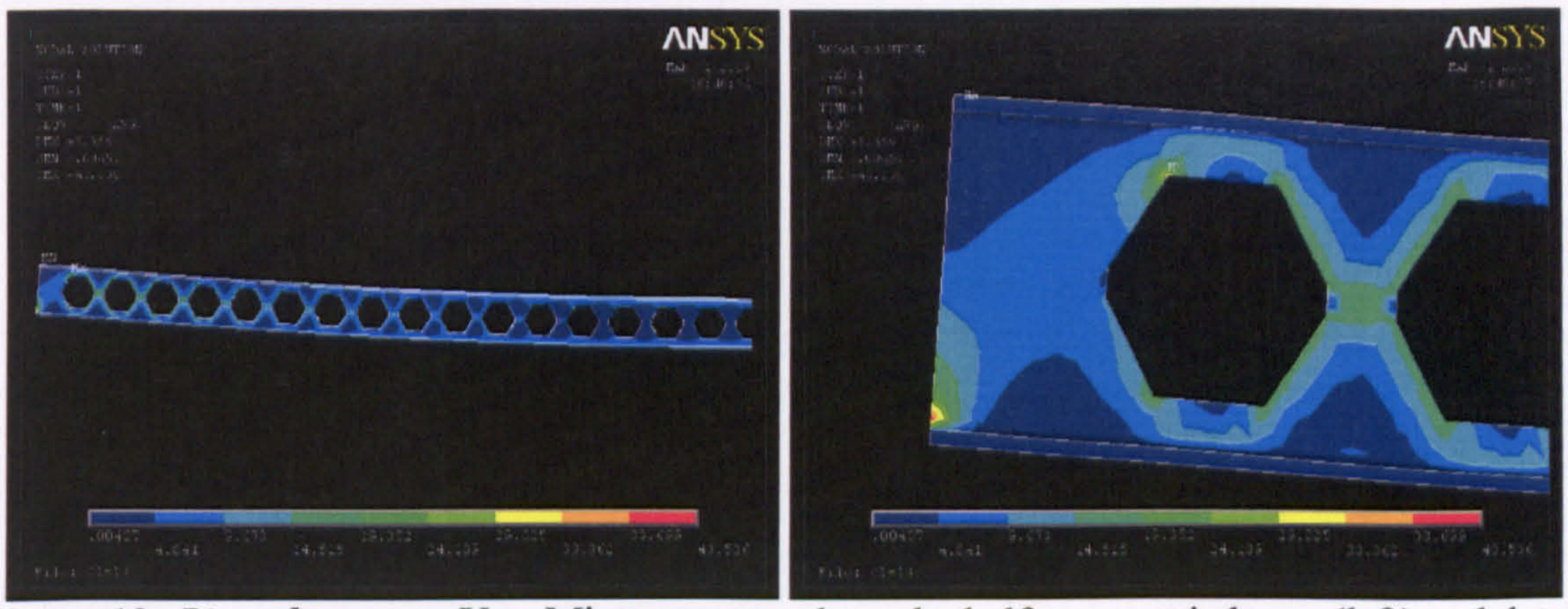

Figure 19: *Pinned support:* Von-Mises stresses along the half symmetric beam (left) and detail of the Von-Mises stresses at the end post (right)

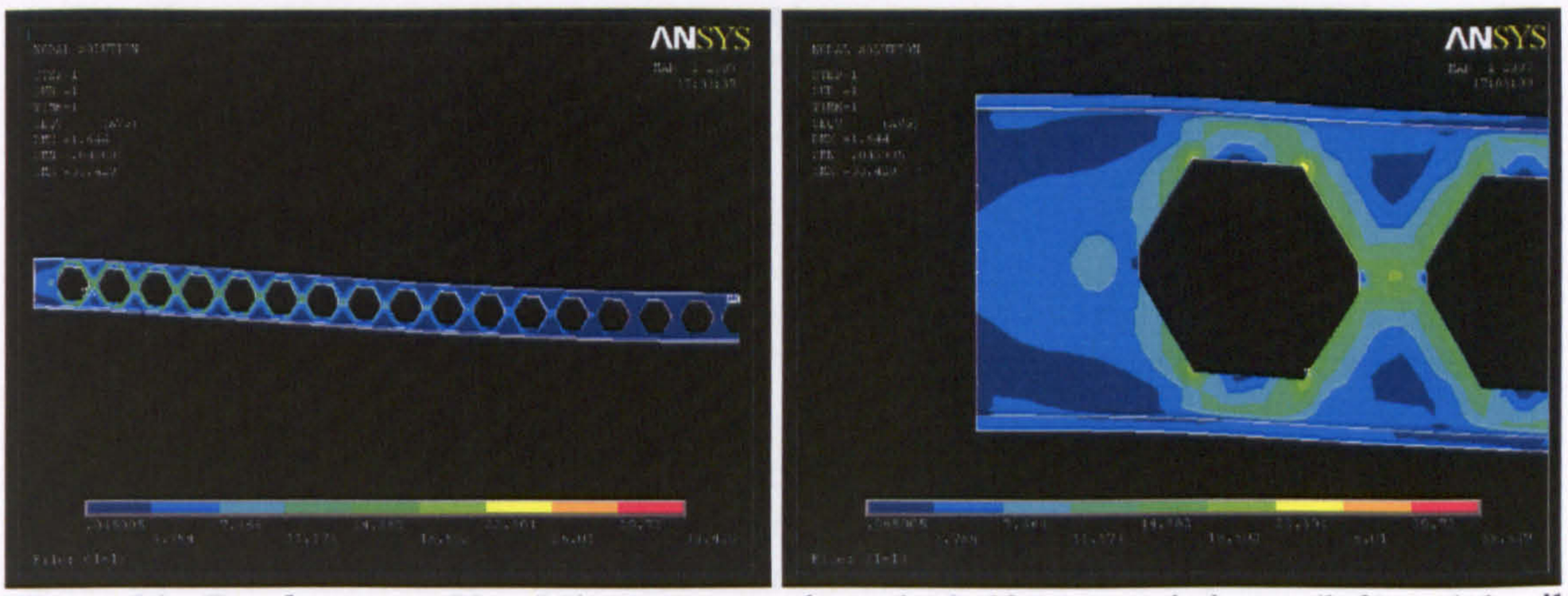

Figure 20: *Fixed support:* Von-Mises stresses along the half symmetric beam (left) and detail of the Von-Mises stresses at the end post (right)

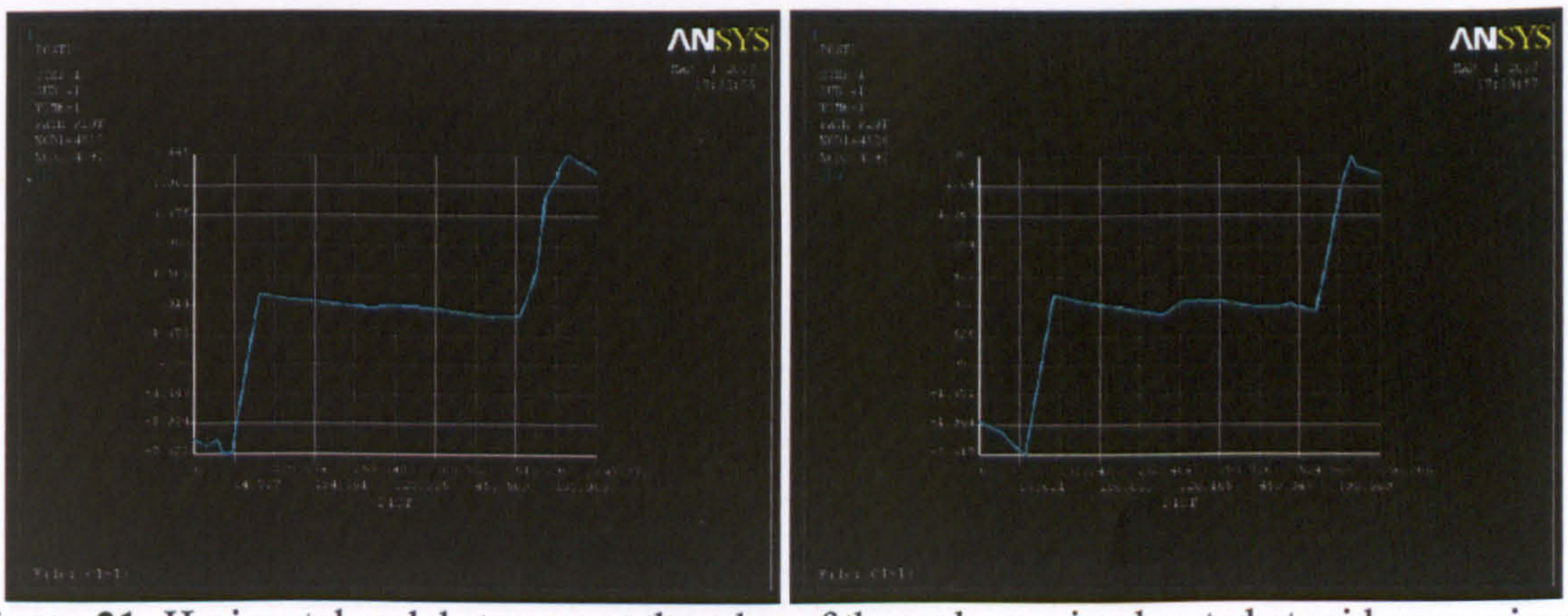

Figure 21: Horizontal nodal stresses at the edge of the web opening located at mid-span: pinned support (left) and fixed support (right)

(C1-14) Castellated with added depth and corner fillets (radius of 25 mm)

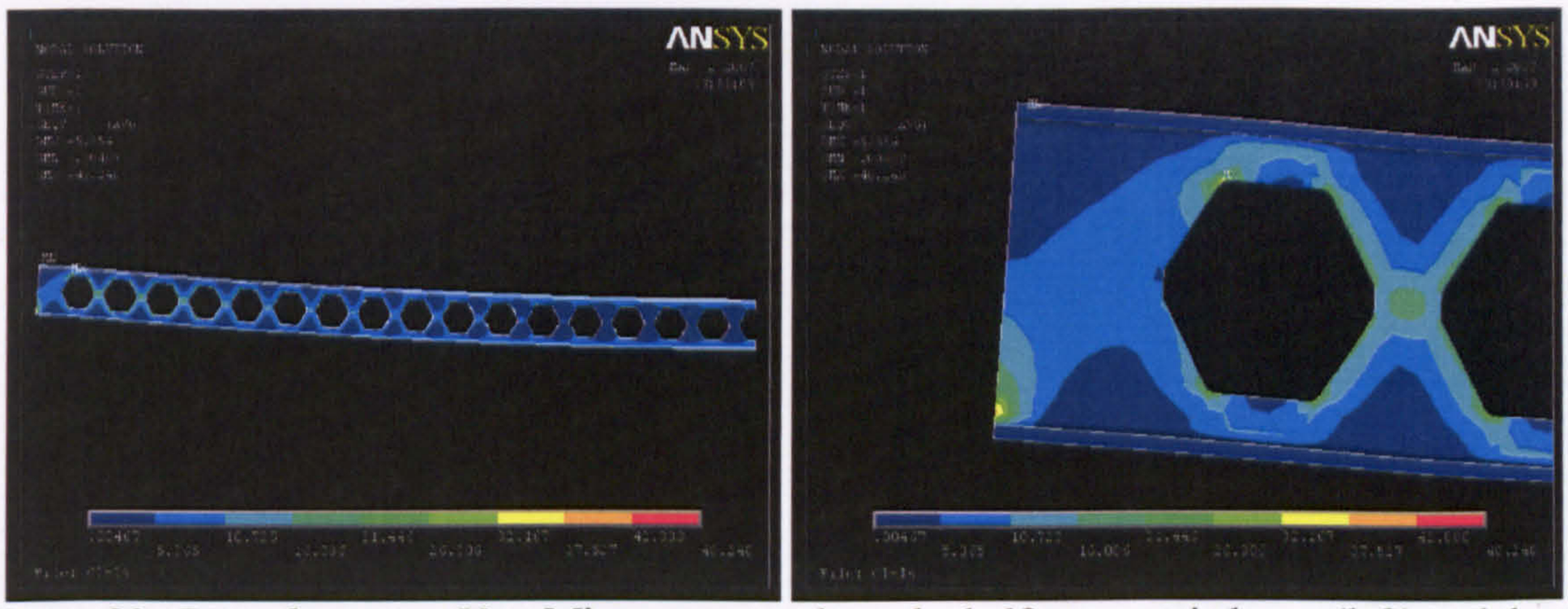

Figure 22: *Pinned support:* Von-Mises stresses along the half symmetric beam (left) and detail of the Von-Mises stresses at the end post (right)

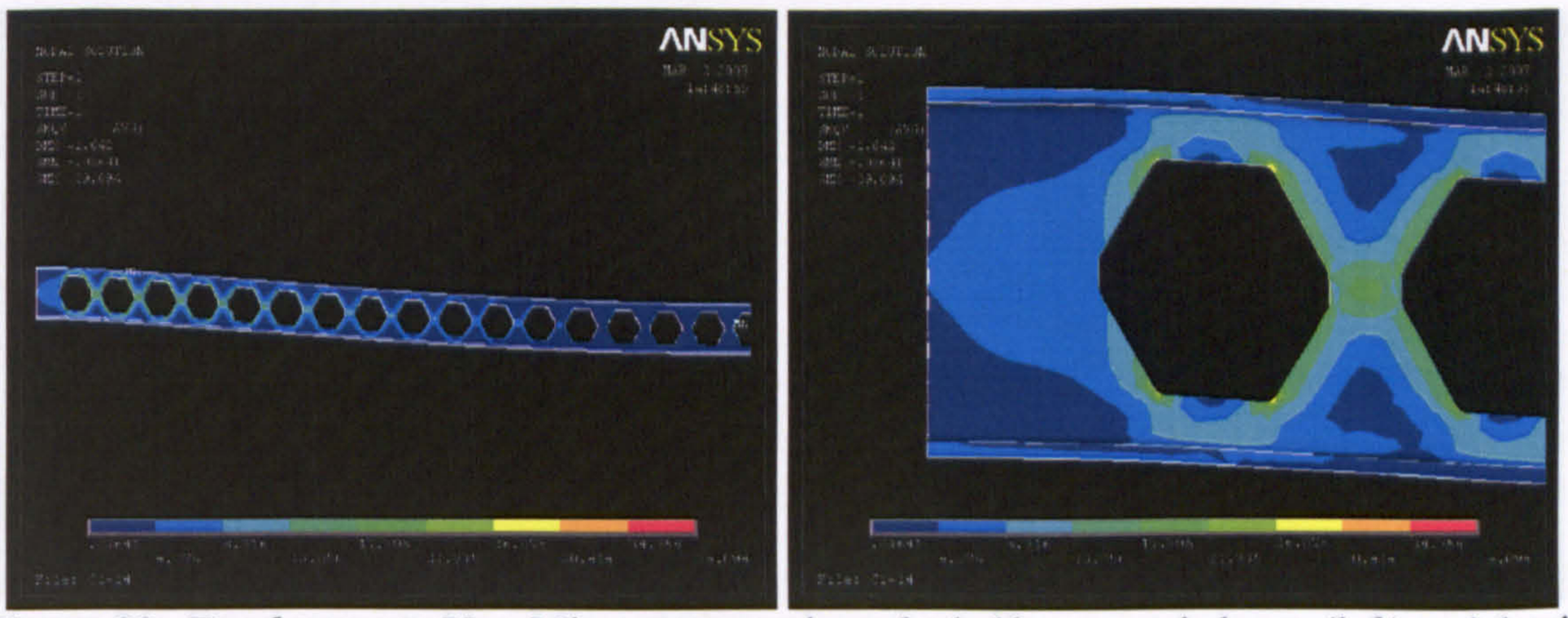

Figure 23: *Fixed support:* Von-Mises stresses along the half symmetric beam (left) and detail of the Von-Mises stresses at the end post (right)

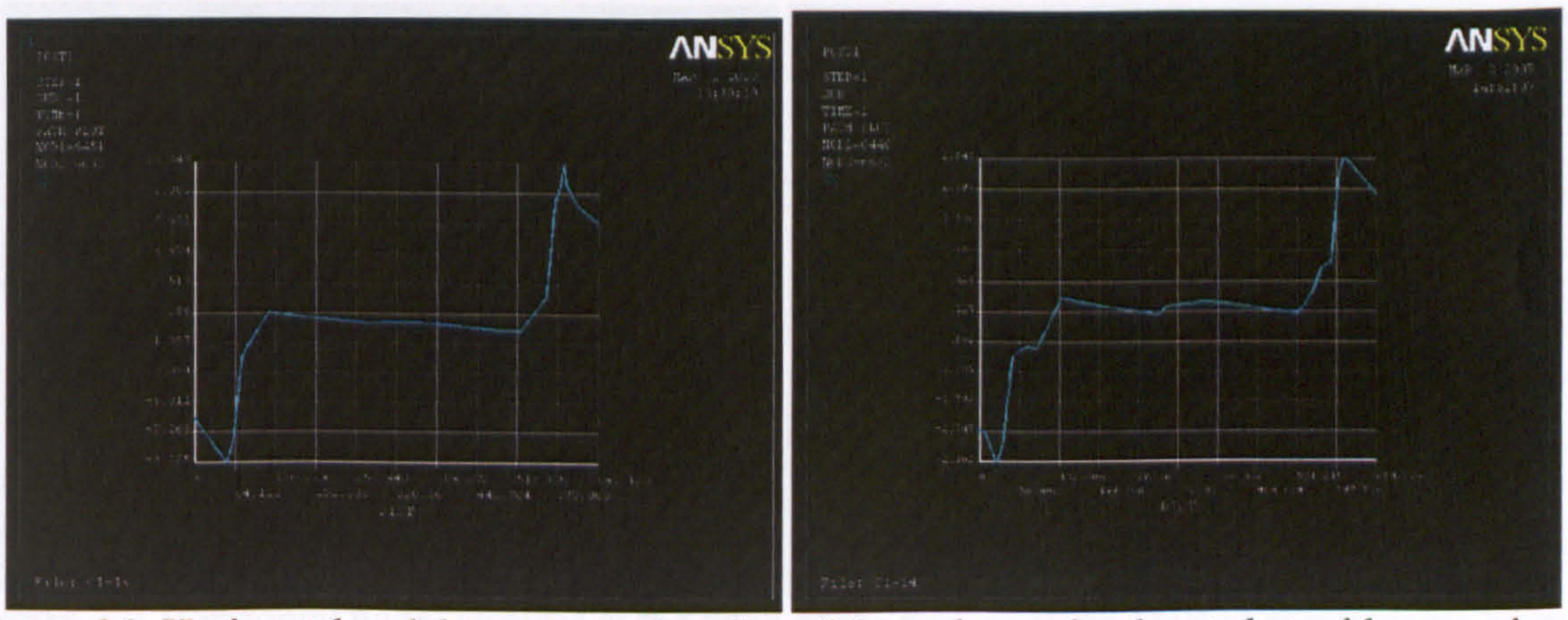

Figure 24: Horizontal nodal stresses at the edge of the web opening located at mid-span: pinned support (left) and fixed support (right)

(C1-7) Square

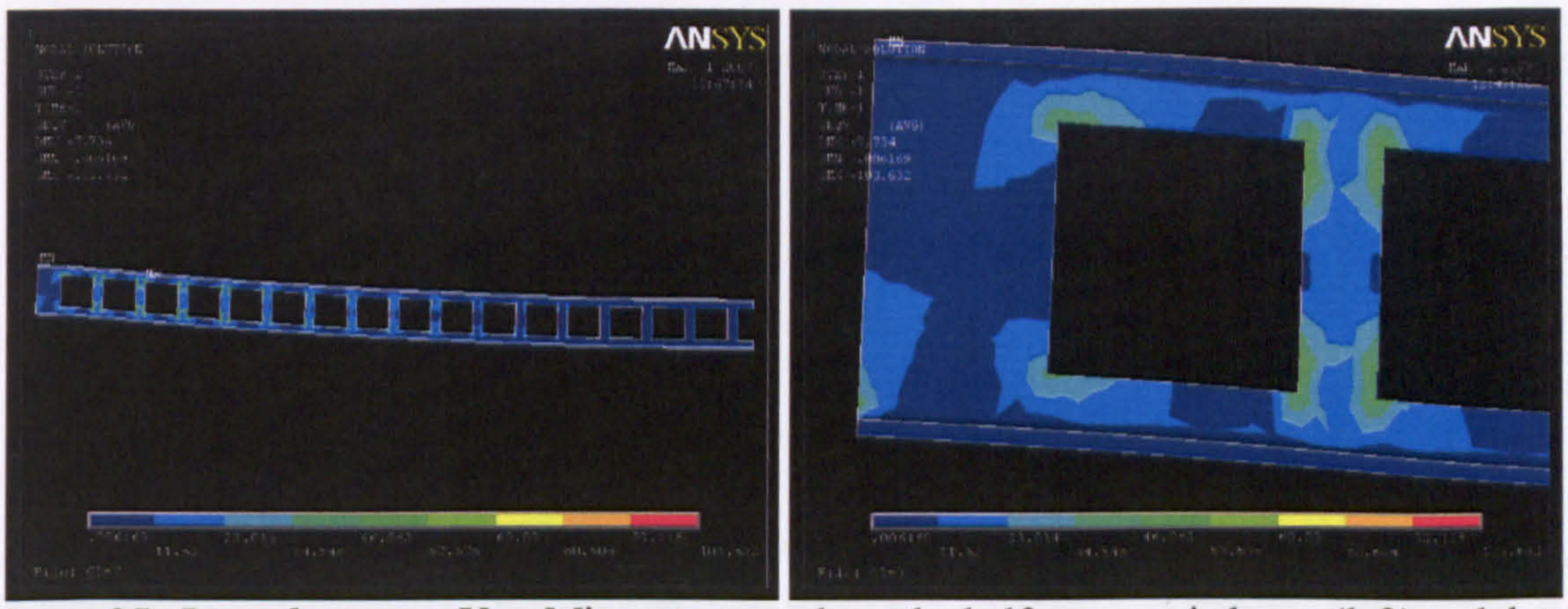

Figure 25: *Pinned support:* Von-Mises stresses along the half symmetric beam (left) and detail of the Von-Mises stresses at the end post (right)

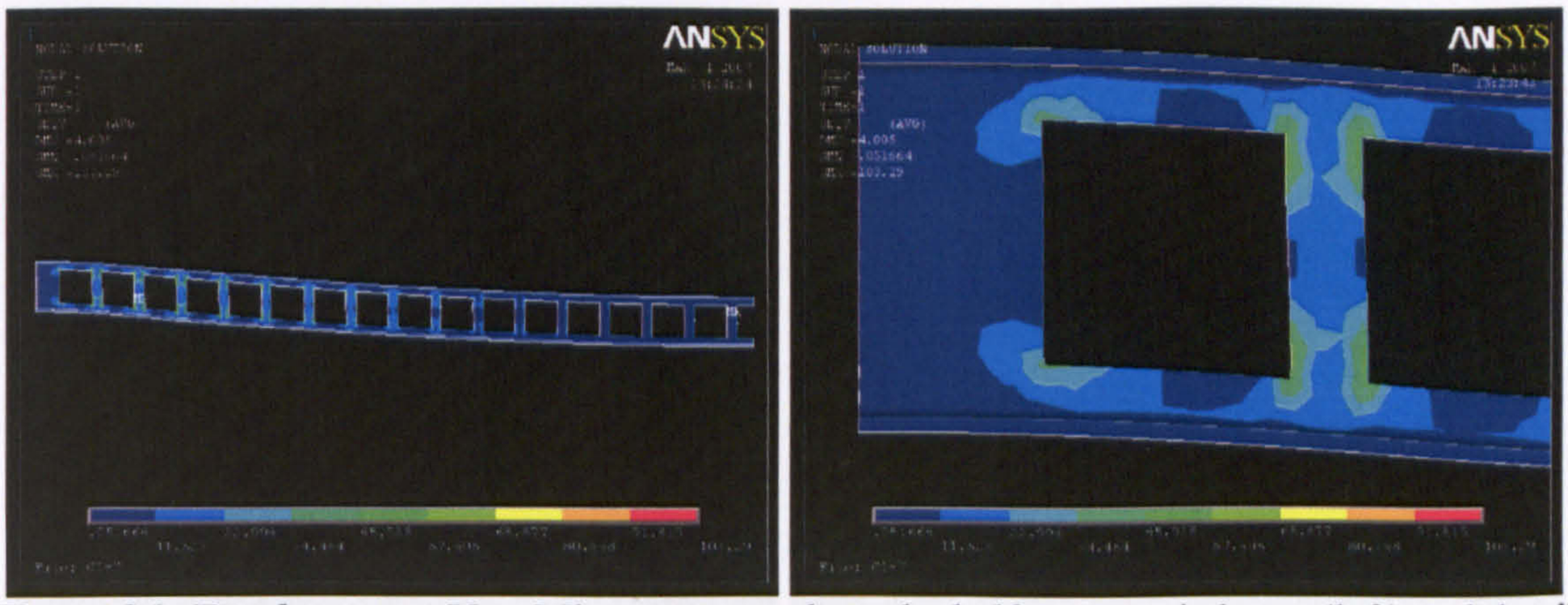

Figure 26: *Fixed support:* Von-Mises stresses along the half symmetric beam (left) and detail of the Von-Mises stresses at the end post (right)

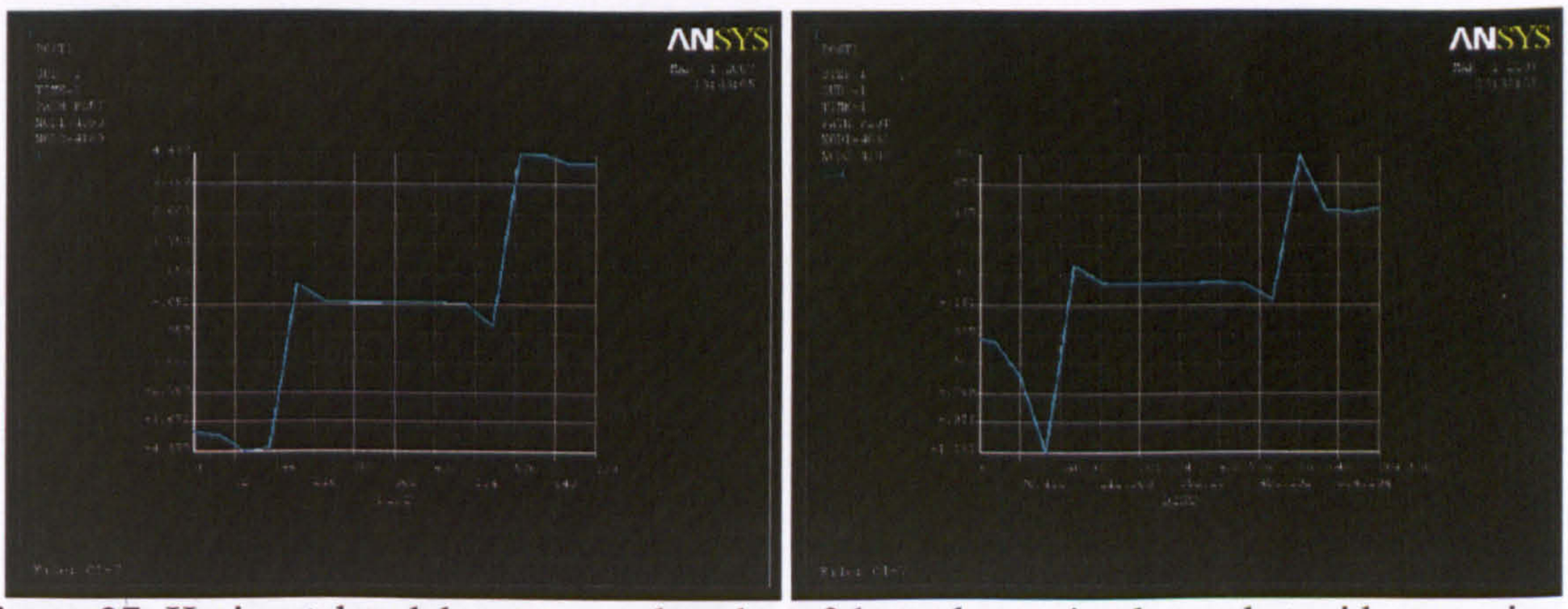

Figure 27: Horizontal nodal stresses at the edge of the web opening located at mid-span: pinned support (left) and fixed support (right)

(C1-8) Square with corner fillets (radius of 25mm)

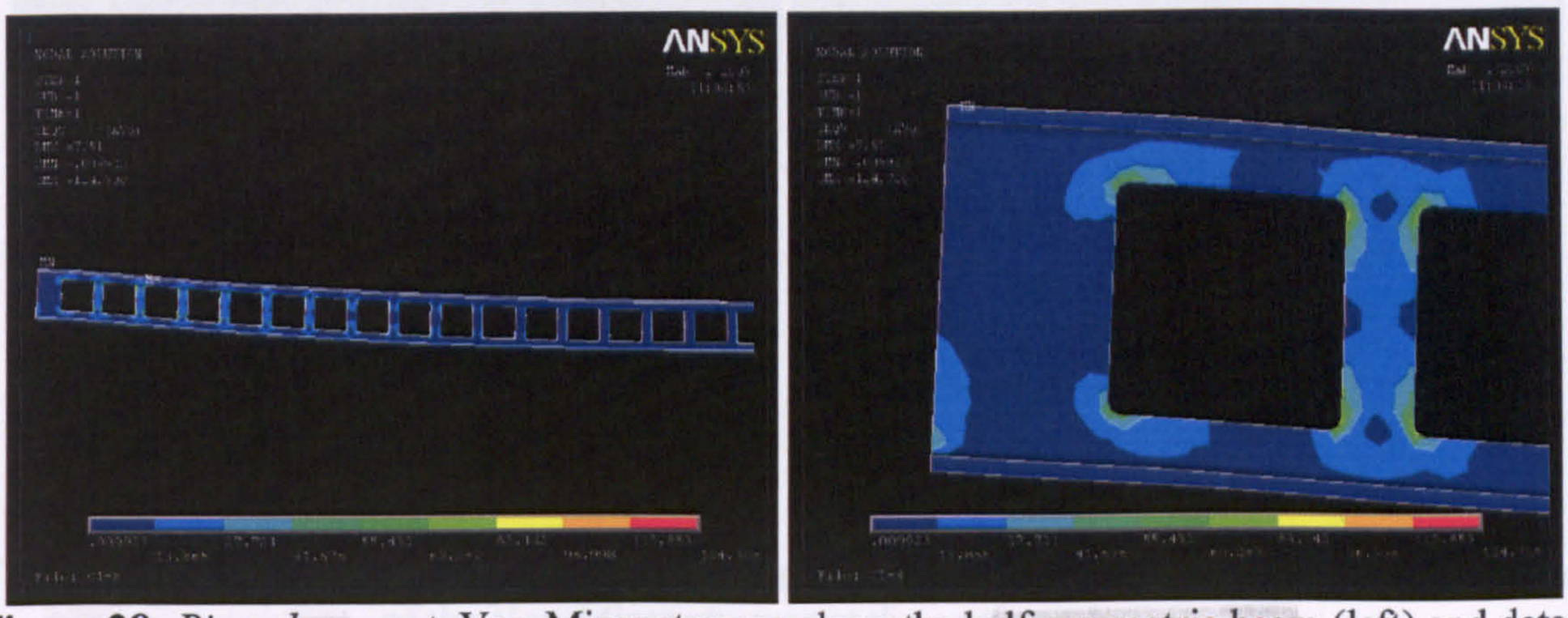

Figure 28: *Pinned support:* Von-Mises stresses along the half symmetric beam (left) and detail of the Von-Mises stresses at the end post (right)

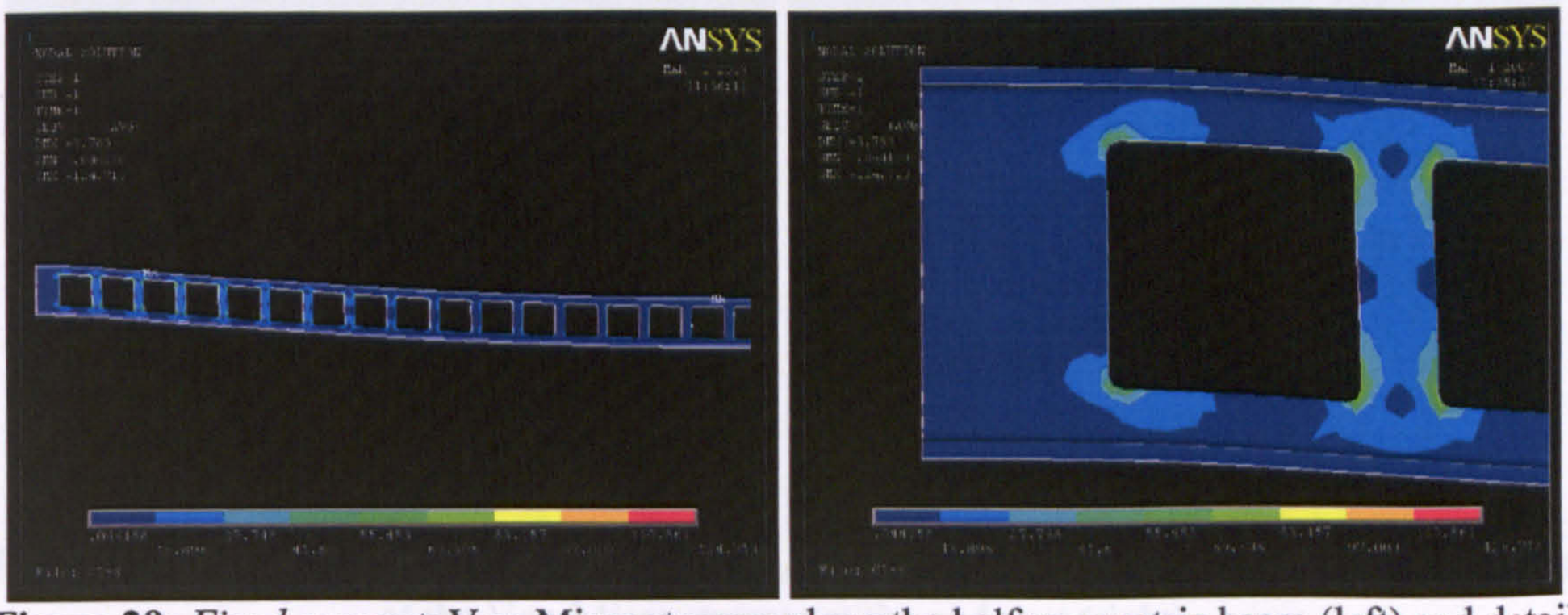

Figure 29: *Fixed support:* Von-Mises stresses along the half symmetric beam (left) and detail of the Von-Mises stresses at the end post (right)

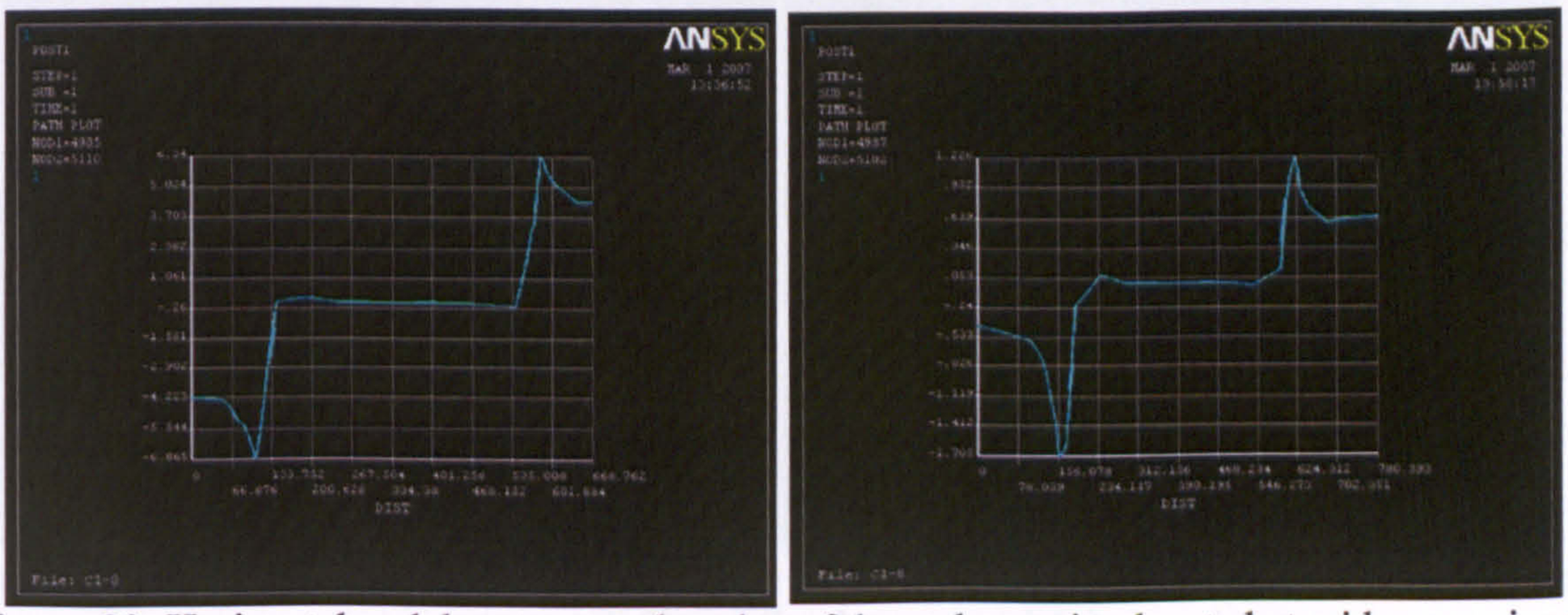

Figure 30: Horizontal nodal stresses at the edge of the web opening located at mid-span: pinned support (left) and fixed support (right)

(C1-21) Transformed Semi-circle

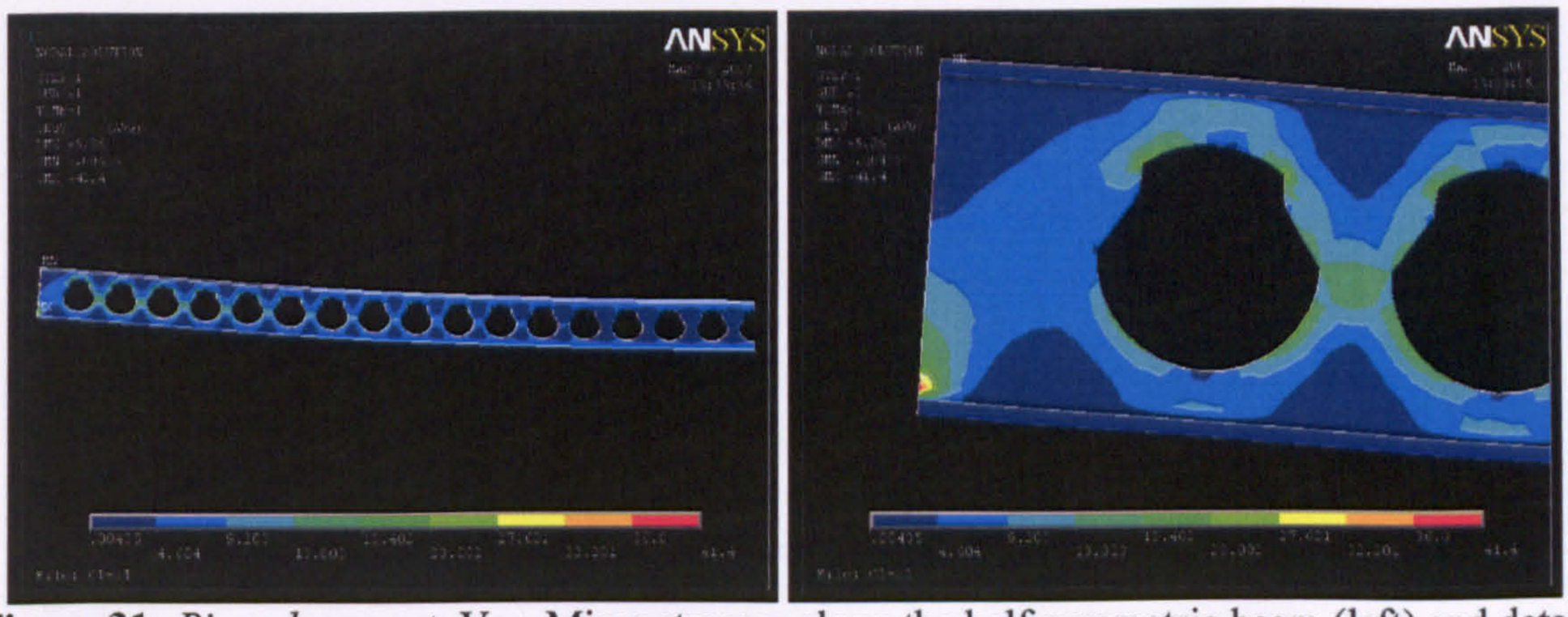

Figure 31: *Pinned support:* Von-Mises stresses along the half symmetric beam (left) and detail of the Von-Mises stresses at the end post (right)

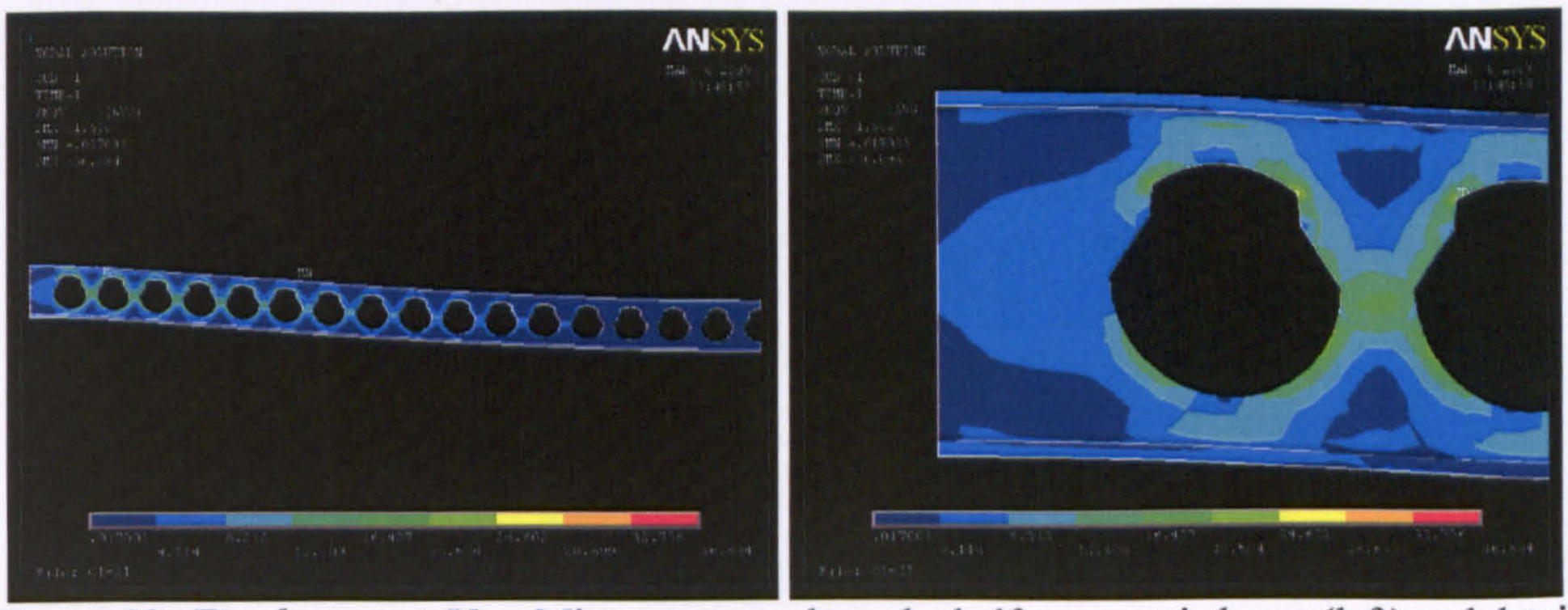

Figure 32: *Fixed support:* Von-Mises stresses along the half symmetric beam (left) and detail of the Von-Mises stresses at the end post (right)

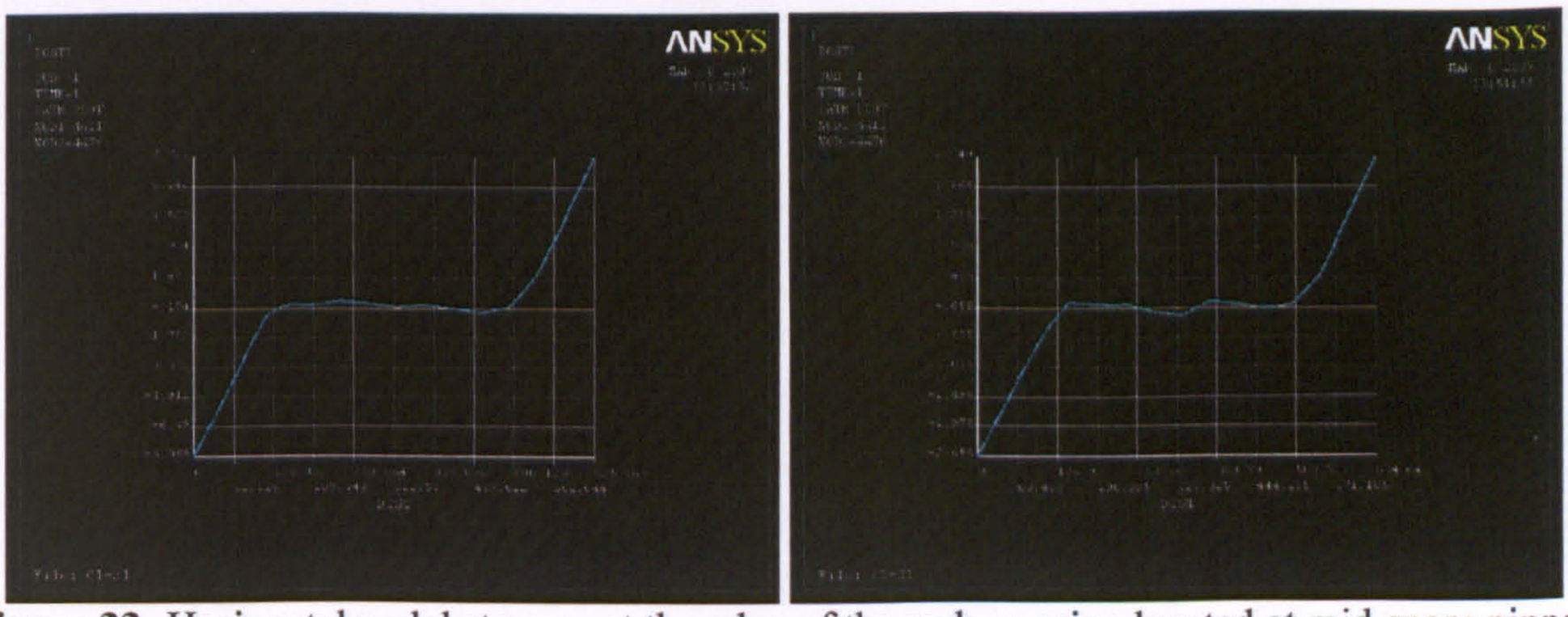

Figure 33: Horizontal nodal stresses at the edge of the web opening located at mid-span: pinned support (left) and fixed support (right)

(C1-22) Transformed Semi-circle (up-side-down)

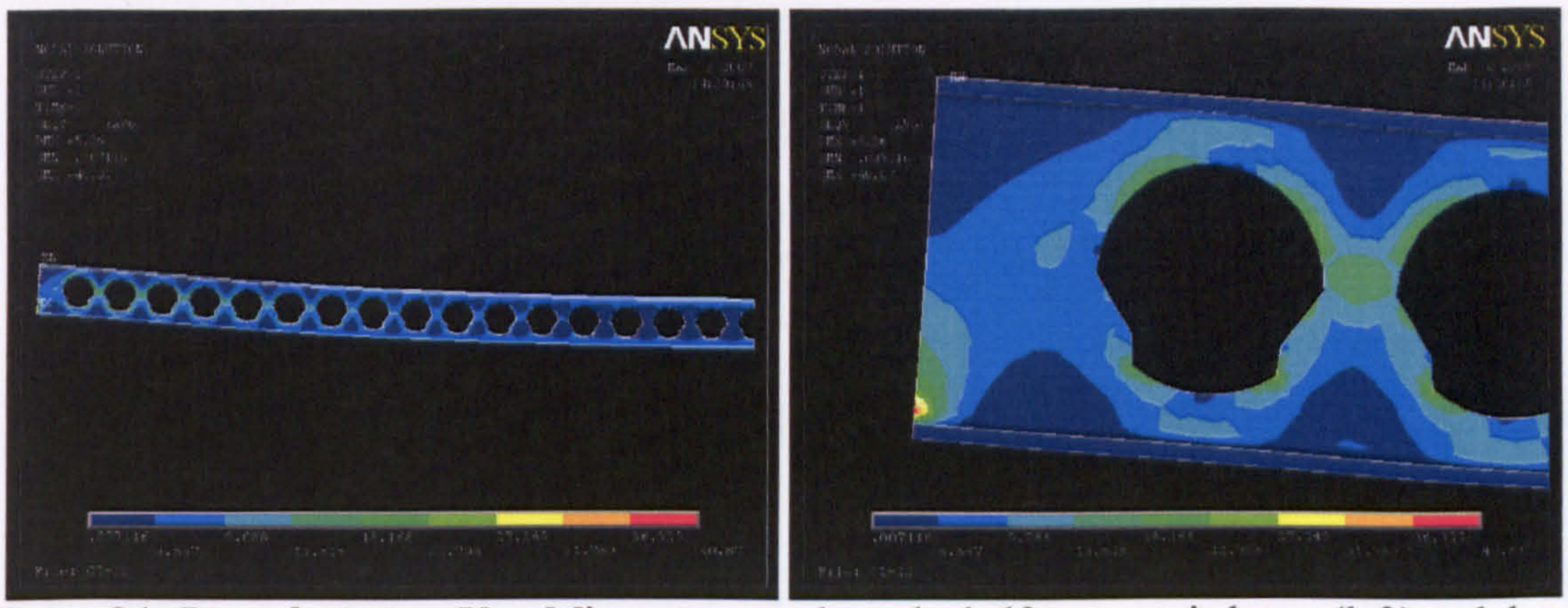

Figure 34: *Pinned support:* Von-Mises stresses along the half symmetric beam (left) and detail of the Von-Mises stresses at the end post (right)

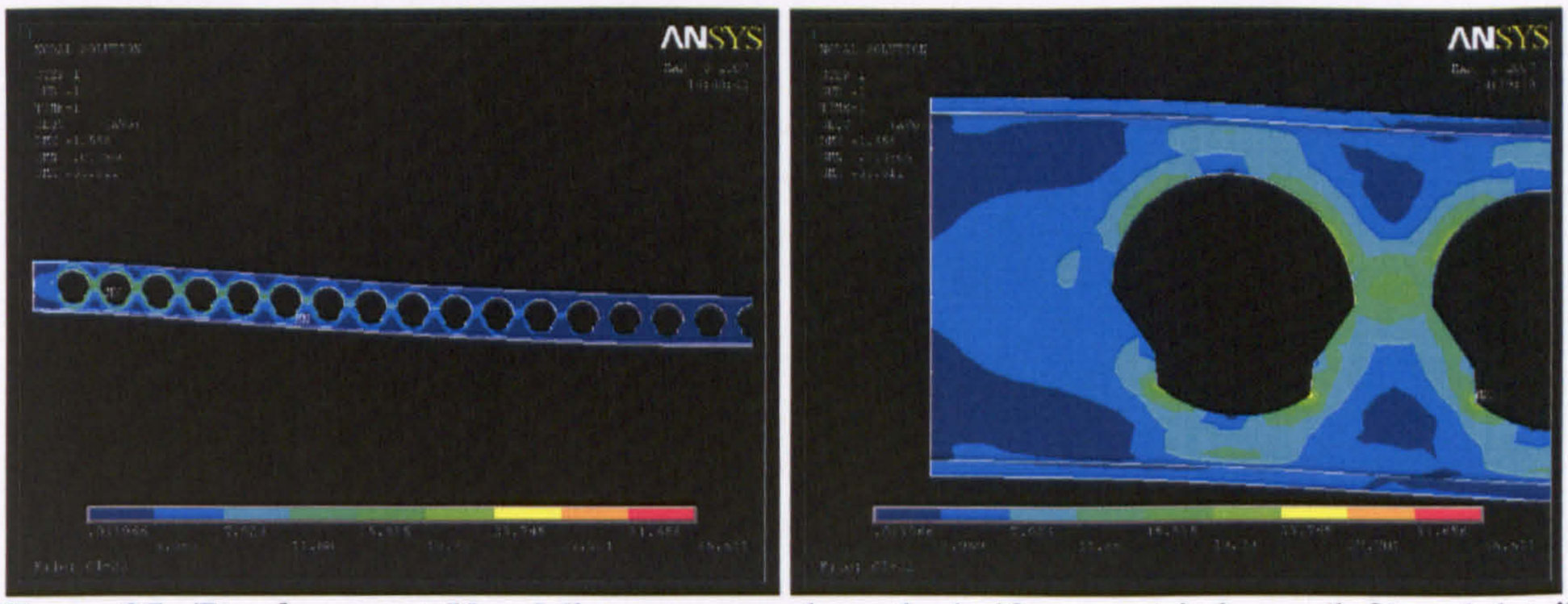

Figure 35: *Fixed support:* Von-Mises stresses along the half symmetric beam (left) and detail of the Von-Mises stresses at the end post (right)

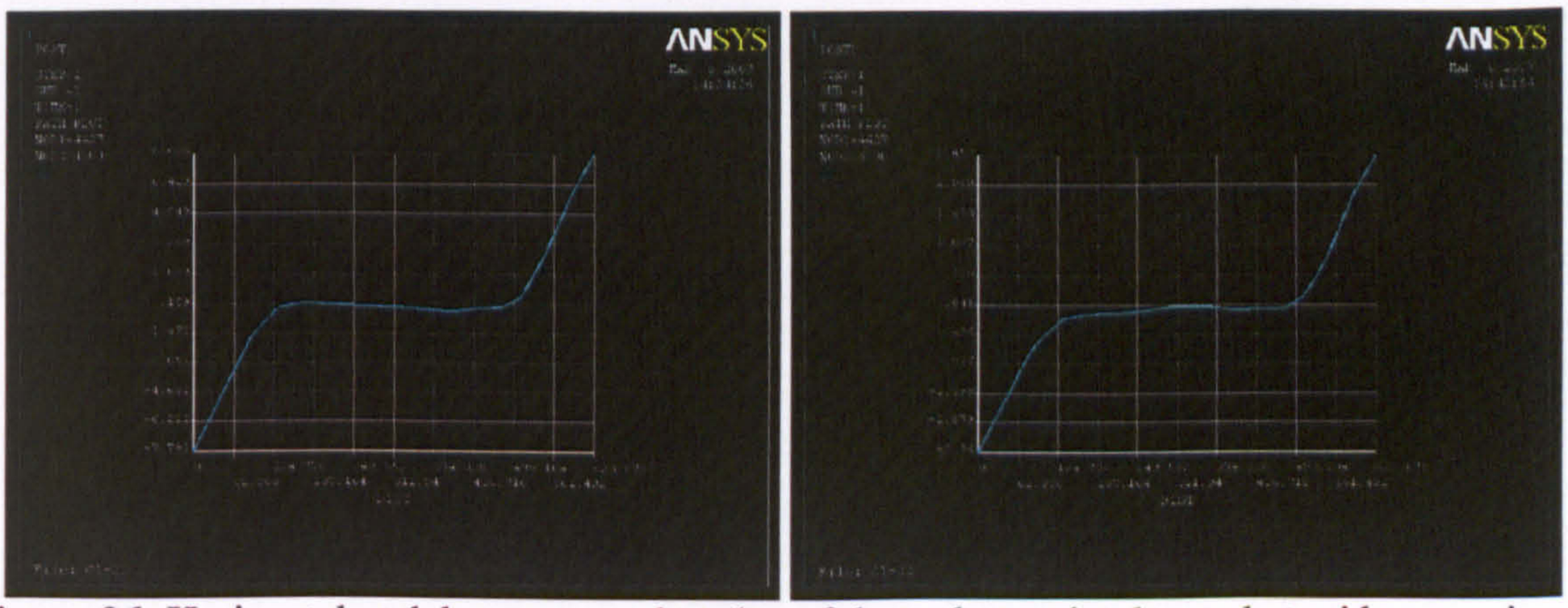

Figure 36: Horizontal nodal stresses at the edge of the web opening located at mid-span: pinned support (left) and fixed support (right)

(C1-23) Top & Bottom Transformed Semi-circle

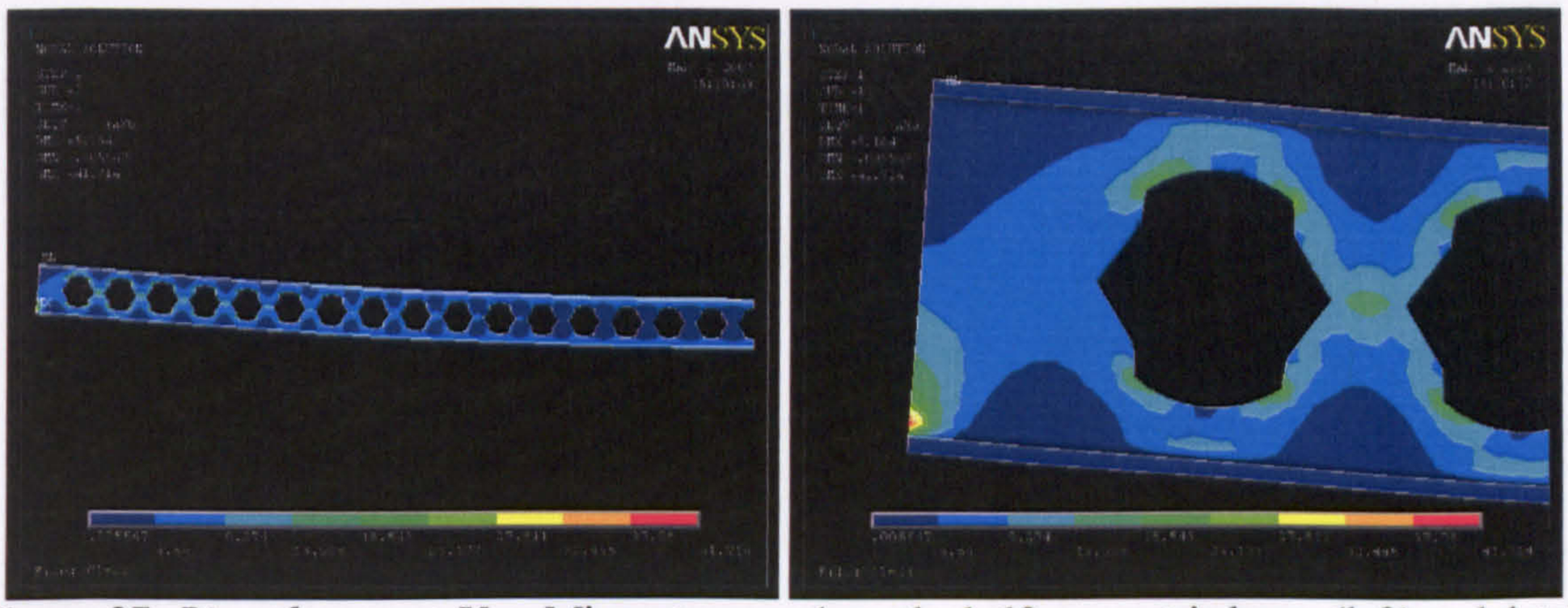

Figure 37: *Pinned support:* Von-Mises stresses along the half symmetric beam (left) and detail of the Von-Mises stresses at the end post (right)

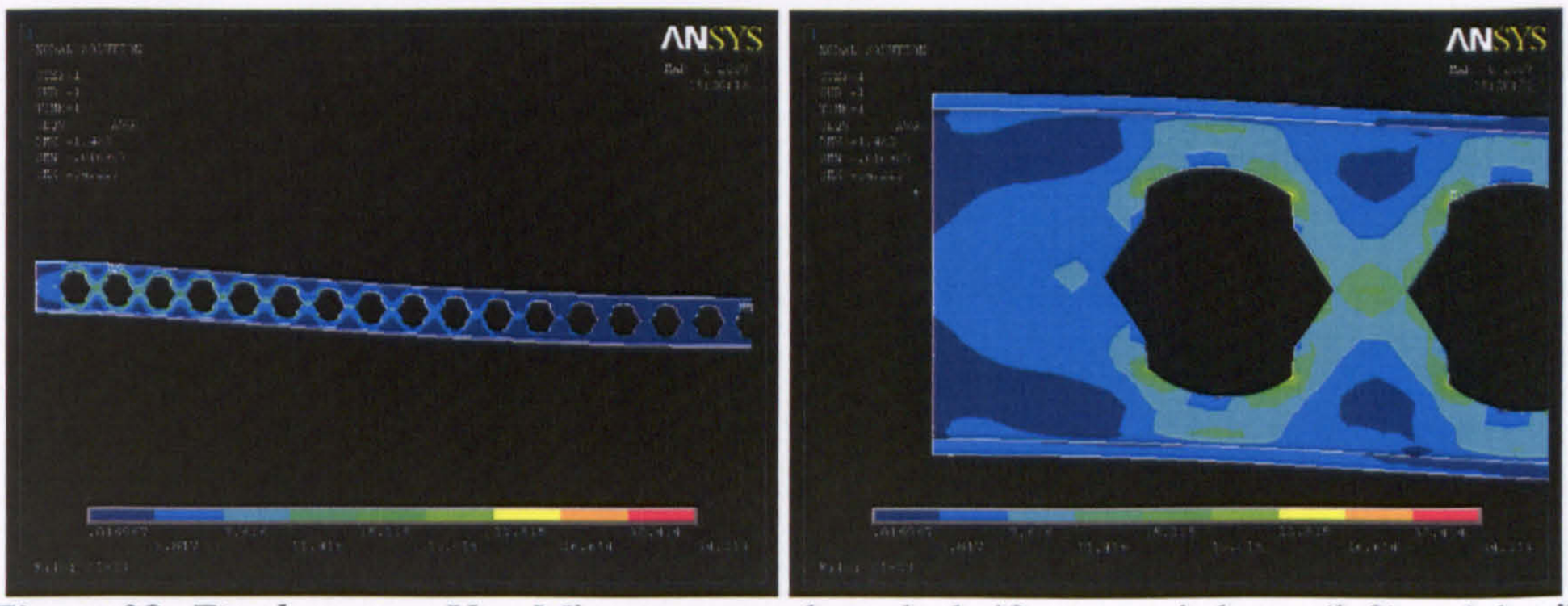

Figure 38: *Fixed support:* Von-Mises stresses along the half symmetric beam (left) and detail of the Von-Mises stresses at the end post (right)

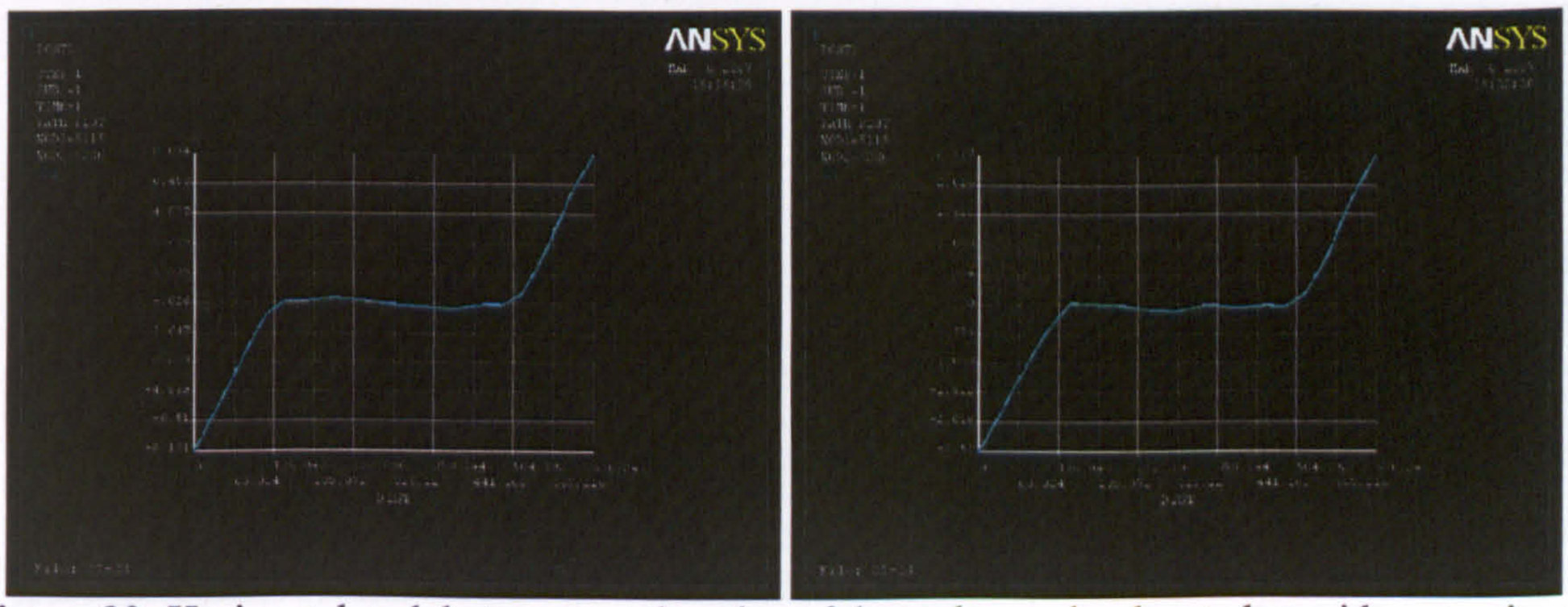

Figure 39: Horizontal nodal stresses at the edge of the web opening located at mid-span: pinned support (left) and fixed support (right)

(C1-19) Inclined ellipse

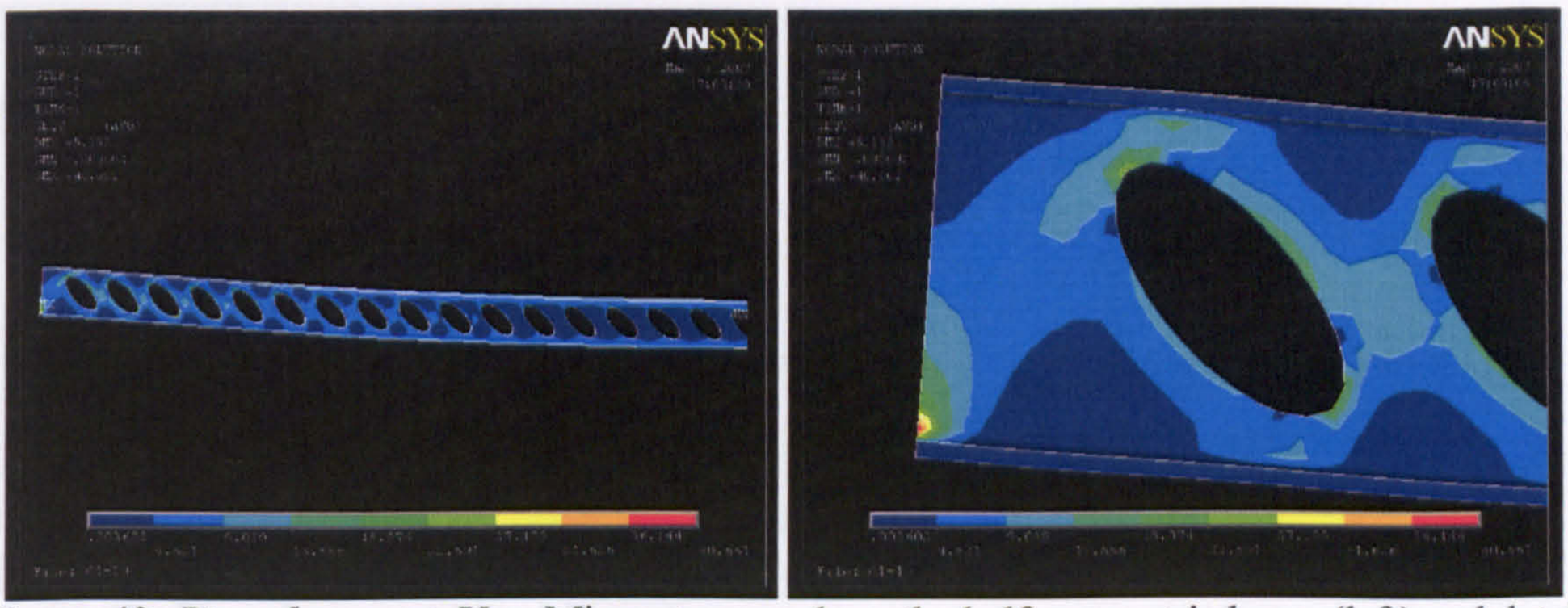

Figure 40: *Pinned support:* Von-Mises stresses along the half symmetric beam (left) and detail of the Von-Mises stresses at the end post (right)

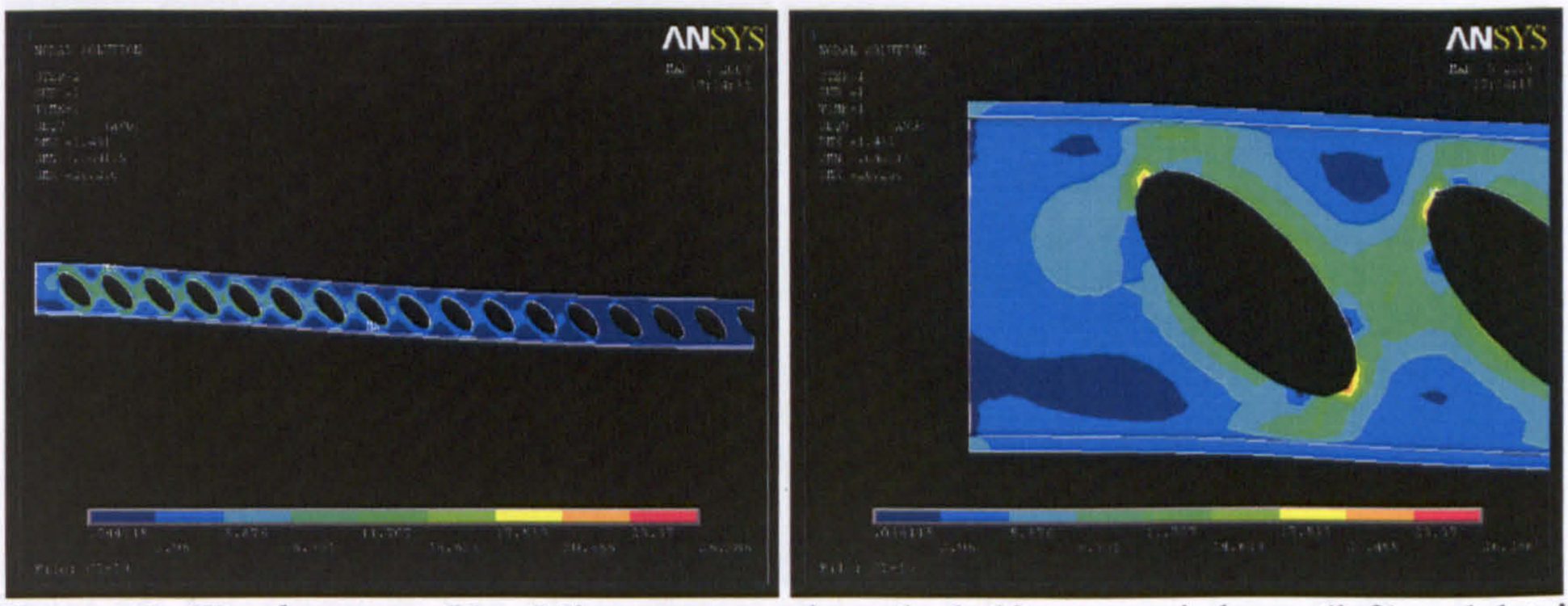

Figure 41: *Fixed support:* Von-Mises stresses along the half symmetric beam (left) and detail of the Von-Mises stresses at the end post (right)

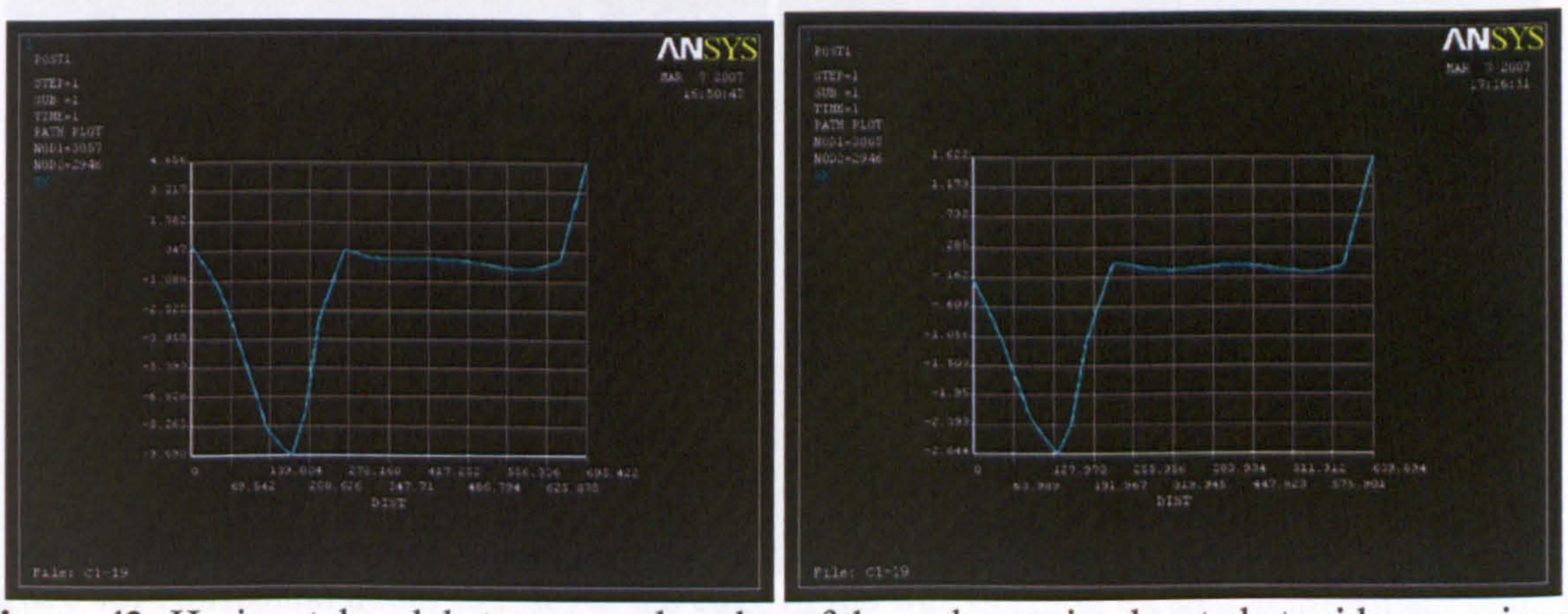

Figure 42: Horizontal nodal stresses at the edge of the web opening located at mid-span: pinned support (left) and fixed support (right)

(C1-6) Vertical ellipse with fillets (25mm) – Included in limits

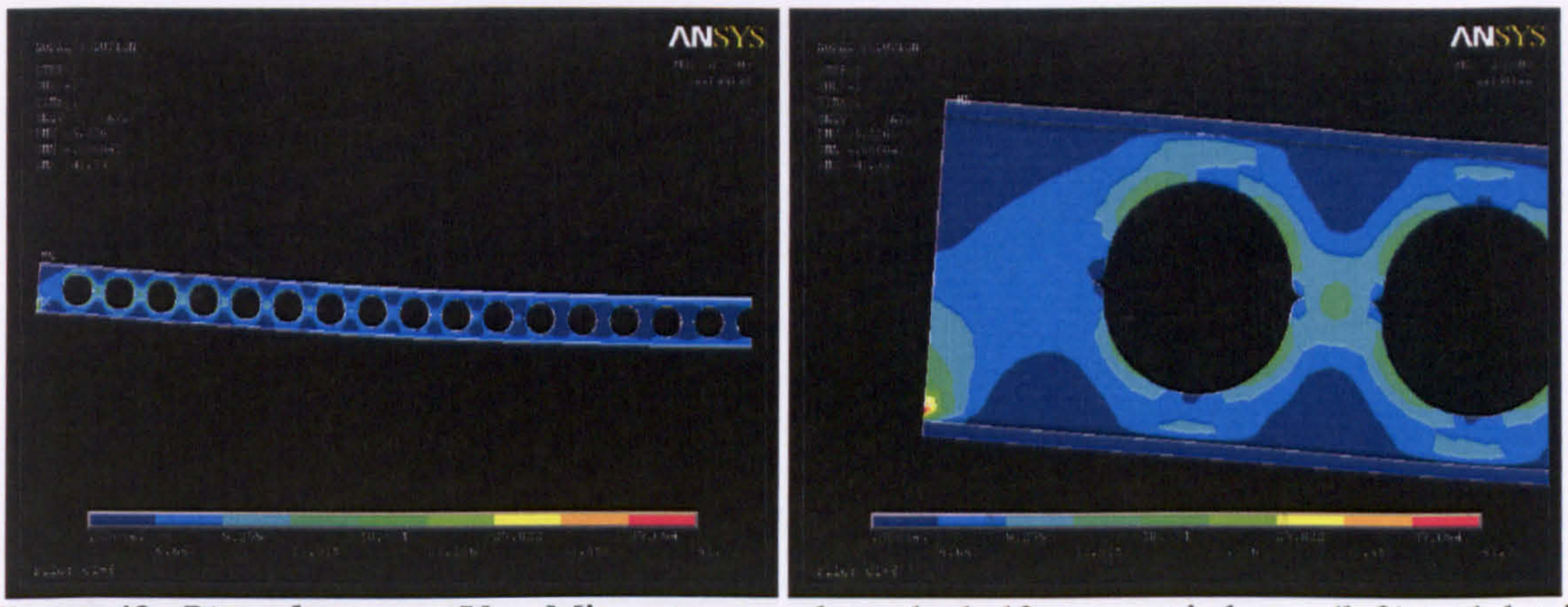

Figure 43: *Pinned support:* Von-Mises stresses along the half symmetric beam (left) and detail of the Von-Mises stresses at the end post (right)

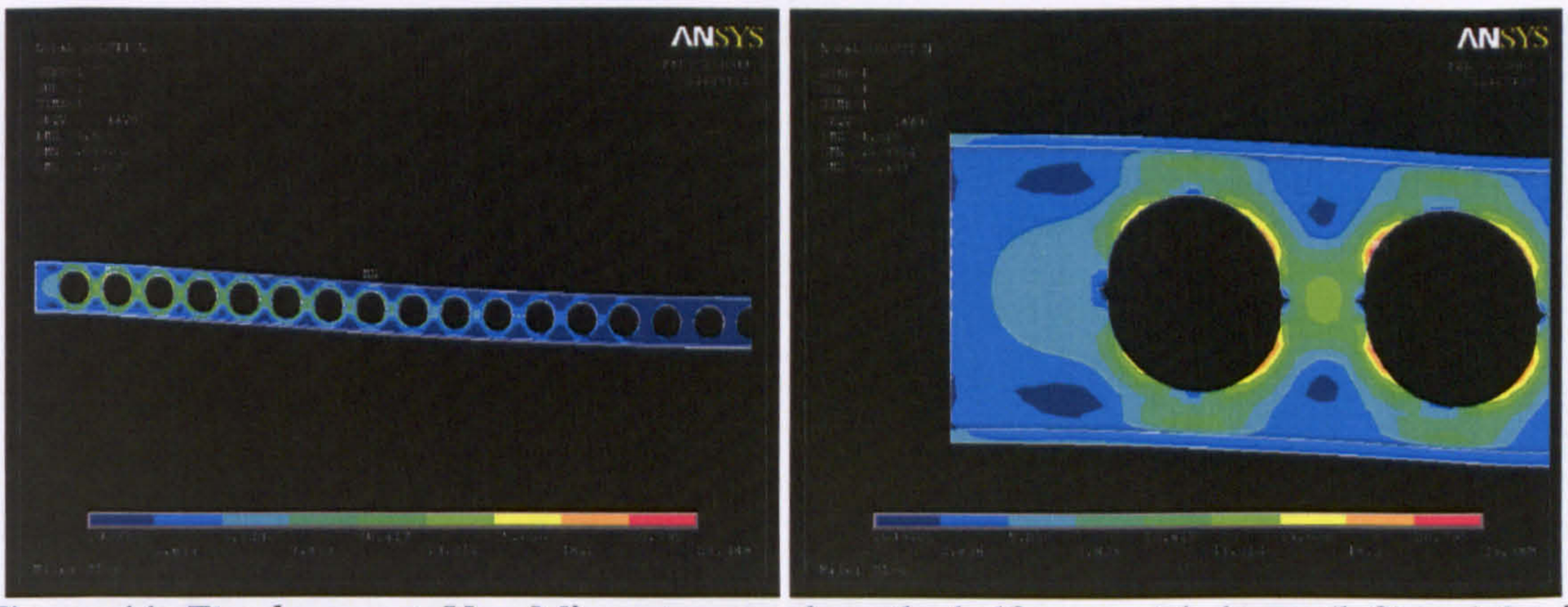

Figure 44: *Fixed support:* Von-Mises stresses along the half symmetric beam (left) and detail of the Von-Mises stresses at the end post (right)

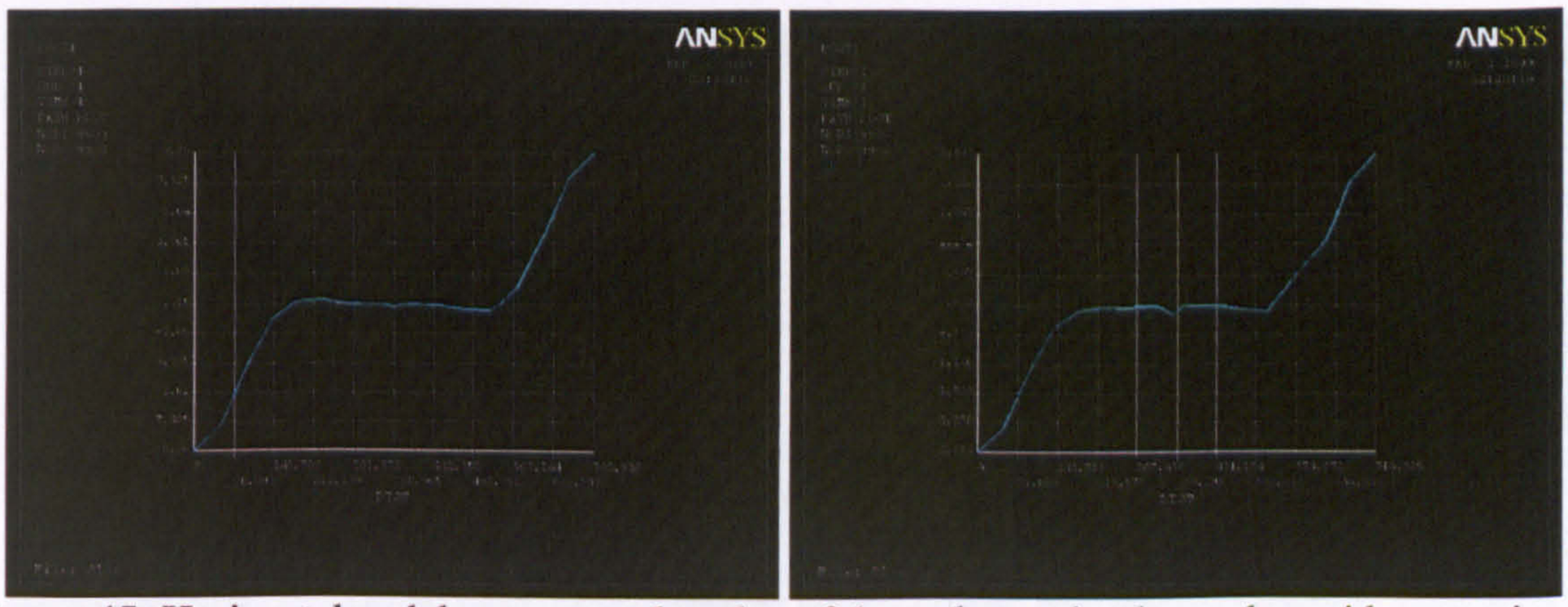

Figure 45: Horizontal nodal stresses at the edge of the web opening located at mid-span: pinned support (left) and fixed support (right)

(C1-10) Rhombus with filleted edges

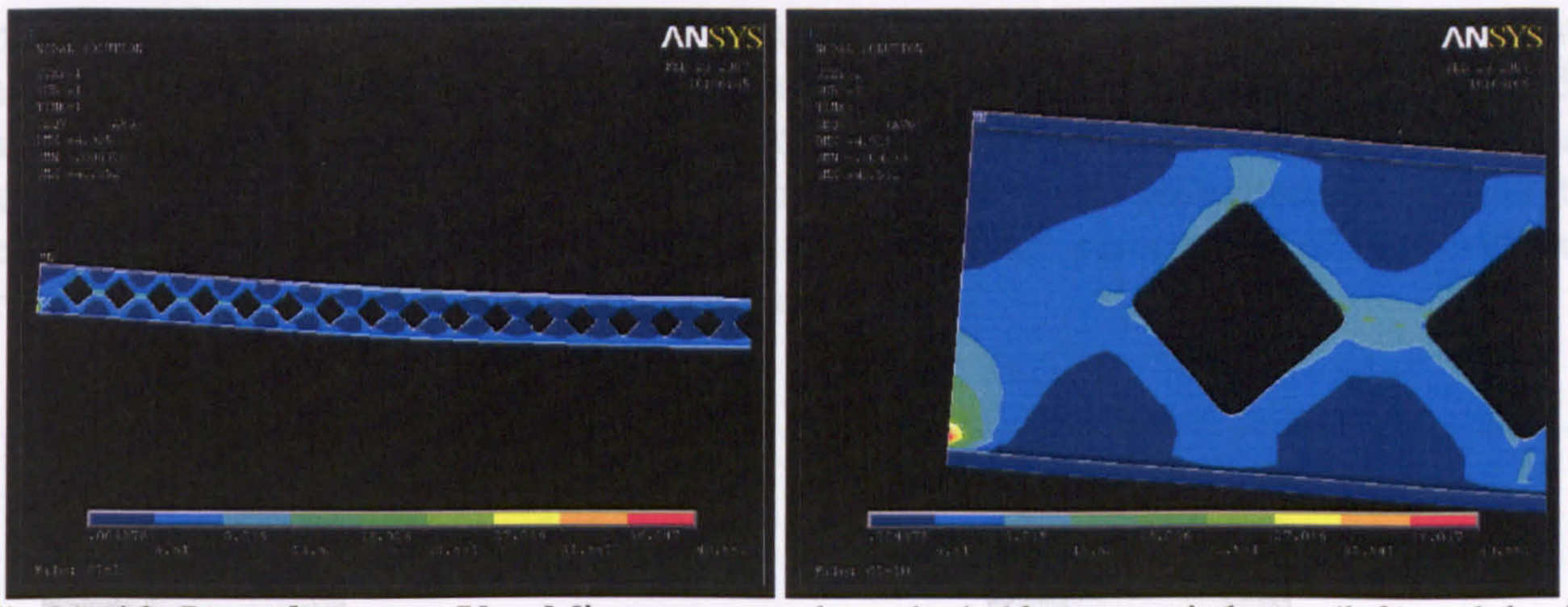

Figure 46: *Pinned support:* Von-Mises stresses along the half symmetric beam (left) and detail of the Von-Mises stresses at the end post (right)

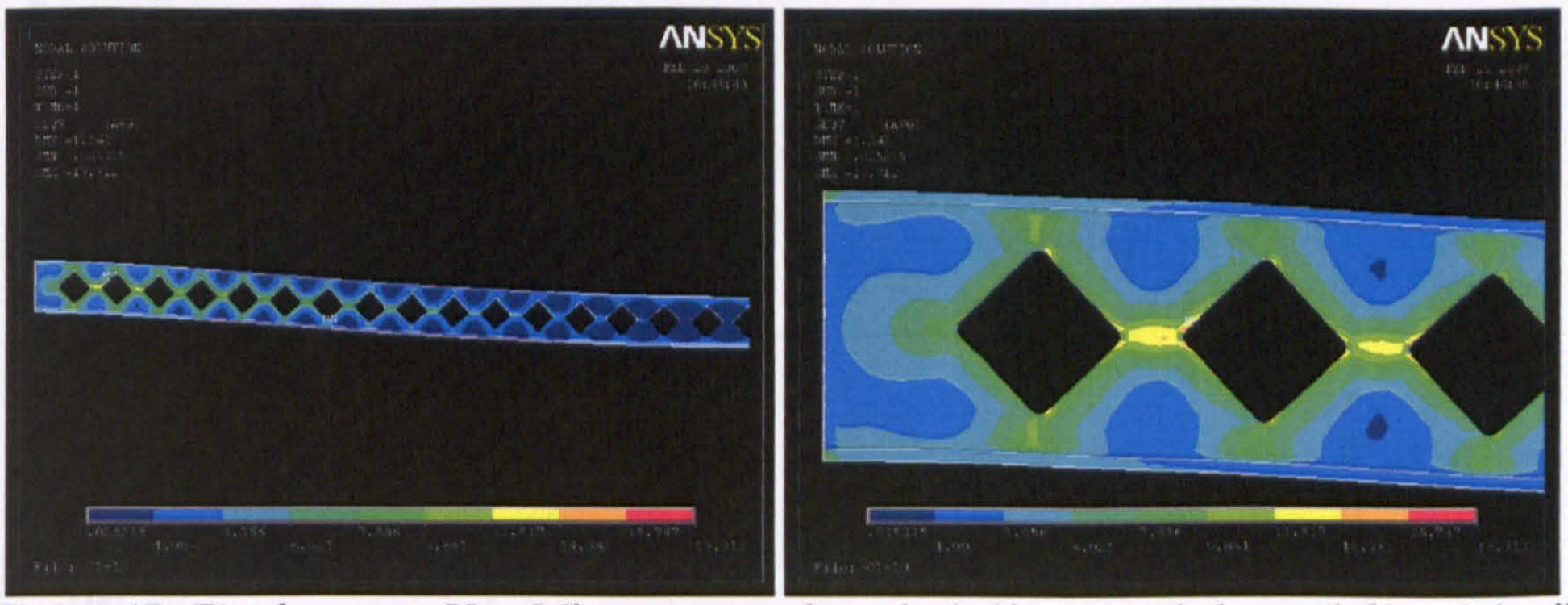

Figure 47: *Fixed support:* Von-Mises stresses along the half symmetric beam (left) and detail of the Von-Mises stresses at the end post (right)

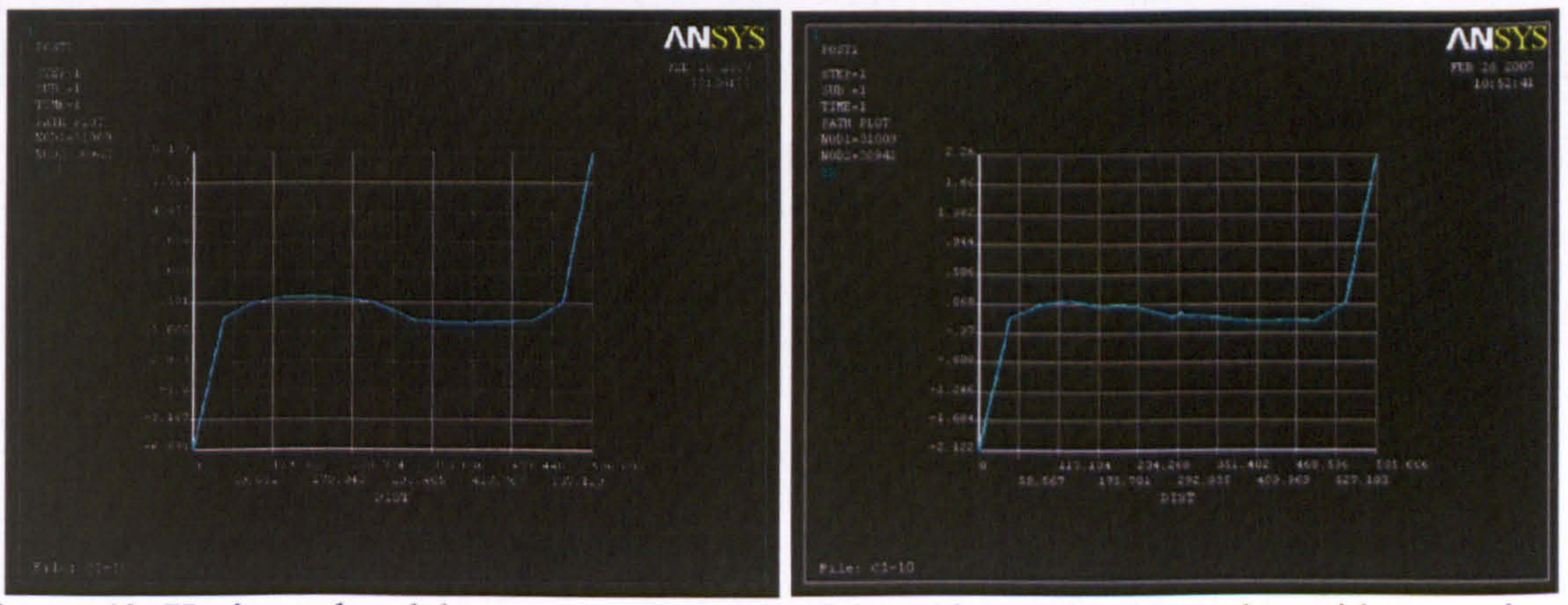

Figure 48: Horizontal nodal stresses at the edge of the web opening located at mid-span: pinned support (left) and fixed support (right)

Table 1 below shows the maximum stresses obtained from FEA for direct comparison. Horizontal, vertical, shear, first principal and Von-Mises stresses are compared in order to draw basic conclusions. This is not a parametric study as many factors are changed

and examined simultaneously, however some overall conclusions are drawn. It is shown that some perforated sections behave similar to the cellular beams (C1-2). In **Figure 49**, the percentages of increase or decrease of certain factors; such as scrap steel and final depth after manufacturing and the web openings area are presented, in respect to cellular beams (C1-2). It is worth to make clear that all are percentages of improvement are made in comparison to the cellular beam.

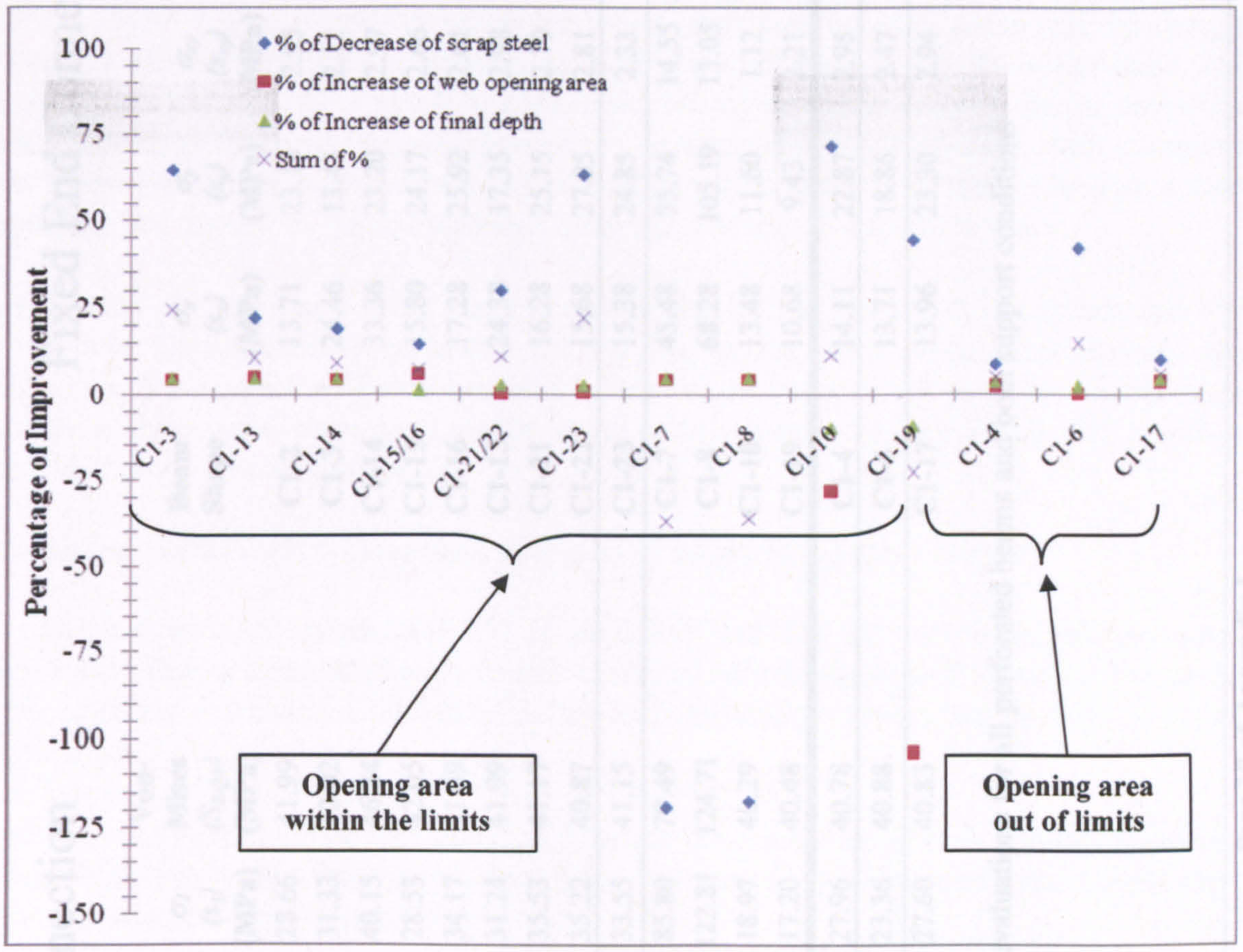

Figure 49: Percentages (%) of improvement for all web beams in terms of scrap steel, web opening area and final beam depth

Pinned End Connection

	Beam Shape	σ_x (s_x) (MPa)	σ_y (s_y) (MPa)	σ_{xy} (s_{xy}) (MPa)	σ_1 (s_1) (MPa)	Von-Mises (S_{EQV}) (MPa)
Within the limits (normal web openings)	C1-2	13.53	24.24	2.98	28.66	41.99
	C1-3	24.78	13.71	2.19	31.33	42.02
	C1-14	32.11	25.32	3.06	40.15	46.34
	C1-15	14.91	26.04	2.67	28.53	42.05
	C1-16	17.12	26.98	2.64	34.17	41.69
	C1-13	23.81	19.06	3.00	31.24	41.99
	C1-21	15.25	26.96	2.82	35.53	41.17
	C1-22	16.43	26.94	2.86	35.22	40.87
	C1-23	15.38	25.31	2.43	33.55	41.15
	C1-7	44.79	75.50	14.57	85.80	79.49
	C1-8	66.85	105.38	13.07	122.81	124.71
	C1-10	18.35	14.49	4.08	18.97	40.29
	C1-19	11.34	10.10	2.42	17.20	40.48
Out of limits (filleted web openings)	C1-4	13.75	23.77	2.99	27.96	40.78
	C1-6	13.24	19.45	2.49	23.36	40.88
	C1-17	13.65	23.73	2.98	27.60	40.83

Fixed End Connection

Beam Shape	σ_x (s_x) (MPa)	σ_y (s_y) (MPa)	σ_{xy} (s_{xy}) (MPa)	σ_1 (s_1) (MPa)	Von-Mises (S_{EQV}) (MPa)
C1-2	13.71	23.18	2.95	27.67	27.89
C1-3	24.46	13.43	2.11	31.22	29.12
C1-14	33.36	23.20	2.97	39.44	37.82
C1-15	15.80	24.17	2.66	27.06	26.51
C1-16	17.28	25.92	2.61	33.16	32.34
C1-13	24.38	17.35	2.98	33.49	30.57
C1-21	16.28	25.15	2.79	33.79	31.98
C1-22	15.68	27.05	2.81	34.67	32.03
C1-23	15.38	24.85	2.33	32.03	29.68
C1-7	45.48	75.74	14.55	86.82	79.29
C1-8	68.28	105.19	13.05	123.00	124.71
C1-10	13.48	11.60	1.12	17.19	17.02
C1-19	10.68	9.43	2.21	16.19	26.29
C1-4	14.11	22.87	2.95	27.29	27.46
C1-6	13.71	18.86	2.47	22.73	22.93
C1-17	13.96	23.30	2.94	26.89	30.29

Table 1: Maximum stress evaluations for all perforated beams and both support conditions

3 Discussion on the Fe results

Compare: cellular (C1-2) against castellated (C1-3) beams

As the circle is the 'perfect' geometrical shape, by using circular web openings in perforated beams (i.e. cellular beam) many advantages are obtained. The stress distribution is uniform; without stress concentrations and the plastic hinges are able to move and to redistribute the load. Also, perforated beams with circular web openings are competitive in the industry as they provide large web opening areas and the design becomes much more flexible complying with the client needs. On the other hand, the hexagonal web opening shape (i.e. castellated beam) is widely used in the industry. Its main benefit is the manufacturing procedure; as there is not wasted steel, with complete use the advantage of profile cutting; hence a deep final beam is formed. The above web openings are named as typical standard ones and are widely used nowadays.

Comparing the cellular (C1-2) and the castellated (C1-3) beams, it is noticed that the stress and displacement evaluations are varying in the same range. The stresses are higher in the castellated beam because of the stress concentrations at the sharp edge points, and the deflections are a higher at the cellular beam, as the circular web opening provides larger opening areas.

Compare: cellular (C1-2) against polygon-12 edges (C1-15/16) beams

A polygon with 12 edges (C1-15) is modeled and the FE results show that such perforated beams behave slightly better than the cellular beams. Following, the same web opening rotated just 15mm (C1-16) and the sharp corners are located at more critical positions.

Between the simply supported perforated beams the results are almost similar. However, when these beams are fixed supported, there is a variation of the results due to the high stress concentrations at these sharp points.

Compare: cellular (C1-2) against cellular with fillets radius of 25mm (C1-4) & 50mm (C1-17) beams

Comparing the cellular beams and the cellular beams with the filleted circular web openings (C1-4), it is seen that the latter ones distribute better the stresses because of the increased edge length of their web openings. Also, it is noticed that insignificant stresses occurred at the sharp-tip point of the fillets (i.e. at the mid-depth of the section), provided that the web openings are widely spaced. Slightly high deflections, due to the irregularity of the web opening shape, are obtained.

However, when bigger radius of the fillet is considered (C1-17), a very narrow web-post is formed with high stress concentrations. An acceptable radius limit should be defined through a comprehensive local FE investigation.

Compare: castellated (C1-3) against castellated with added depth (C1-13) beams

An effective way of increasing the final beam's depth is by using the hexagonal web opening with added extra welded plates between the top and bottom tee-sections. In this way, the final beam is deeper and so the vertical shear capacity is enhanced. It should be mentioned that, this manufacture procedure is not very effective as higher quantity of steel is required as well as the welding line is increased. Therefore, the final product is more expensive.

From FEA it is found that both stresses and deflections are higher compare to the cellular beams. Between C1-3 and C1-13 beams, the horizontal stresses have similar trend, while their magnitudes are slightly higher for standard castellated beams. On the other hand, the deflections are slightly higher for castellated beams with the extra plates.

Compare: cellular (C1-2) against transformed semi-circle (C1-21/22/23) Beams

Debutant web opening shapes are designed based on circular web openings (i.e. C1-21 and C1-22). Similar stresses are found, however the web opening shape with the smaller opening length at the top tee-section (C1-21) behaves slightly better. As it was anticipated, the general assumption that the vertical shear forces are equally resisted from the top and bottom tee-sections is not verified.

In addition to that, the full transformed shape (C1-23) is modelled. Now the perforated beams behave better than C1-21 and C1-22. It is worth to further investigate this web opening (C1-23) configuration, as a relative large web opening area is provided, whereas the stresses and deflections found, are not increased.

Compare: cellular (C1-2) against inclined ellipse (C1-19) beams

When an inclined ellipse is designed in the predetermined limits (C1-19), the opening area is very small. Consequently, the stresses are decreased compare to the cellular beam.

Compare: cellular (C1-2) against vertical ellipse with fillets (25mm) – included in limits (C1-6) Beams

Perforated beams with vertical elliptical web openings with fillets are designed within the limits, and they are heavier than cellular beams. Despite the fact that the web opening area is large enough, from **Table 1** it can be seen that the stresses are decreased. This is a result of the narrow web opening length at the top tee-section and so the increased vertical shear capacity. In addition to that, its overall structural efficiency is presented in **Figure 49**, where the sum of improvement for perforated beams with C1-6 web openings is approximately 15%.

Compare: cellular (C1-2) against rhombus with filleted edges (C1-10) beams

Perforated beams with rhombus web openings are very heavy compare to the cellular beams, as they provide much smaller web opening areas. Consequently, these beams have lower deflections as they have higher stiffness. Low vertical shear stresses are observed due to the narrow opening length at the top and the bottom tee-sections.

4 Conclusions and recommendations

General conclusions are summarized here, as they are important for the selection of the web opening shapes are investigated in this research thesis.

- The use of fillets at the point of the welding line can cause some advantages when the radius is up to a limit and the web openings are widely spaced.
- The general assumption that the vertical shear forces are equally resisted from the top and bottom tee-section is not verified.
- It is interested to investigate what it happening when an inclined ellipse is formed close to the support.
- It is concluded that the shape of the web opening causes different results. There are some important parameters that strongly affect the behaviour of the perforated sections; such as the opening length at the top tee-section.

Studying **Figure 49** and **Table 1**, it is concluded that the web openings C1-6 and C1-23 are improved in terms of web opening area, amount of scrap steel and final beam depth as well as they experience relatively low stresses. Eventually, based on this preliminary FE study it is decided to further investigate these configurations and proceed to non-linear (material and geometric) FE parametric global and local analyses.

APPENDIX 2

MANUFACTURING PROCEDURE

1 Introduction

Designers and engineers usually require perforated sections with certain criteria such as the weight of the beam, the height of the section and the web opening size and spacing. In this research project most of these factors are considered in order to investigate new web openings shapes that follow some or all of these criteria.

Castellated and cellular beams are fabricated from steel I-sections. The castellated beams are produced by one way continuous oxy-cutting/plasma-cut along the length of the beam with a 'zig-zag' pattern (**Figure 1**, left), while the cellular beams are produced by a double way oxy-cutting/plasma-cut along the length of the beam with a more intricate pattern (**Figure 1**, right). The manufacturing way of the cellular beams generates discontinuities to the fabrication.

In both cases, the two halves are then shifted and welded together to produce a beam of a greater depth with hexagonal or circular openings in the web. The final beam has a larger section modulus and greater bending rigidity than the original (parent) section, without an increase in weight. However, the presence of the web openings will change the structural behaviour of the beam from that of the parent (solid) webbed beams. Various experimental tests on castellated and cellular beams have shown that beam slenderness, shape parameters and the loading type are the main parameters, which dictate the strength and the failure modes of such beams.

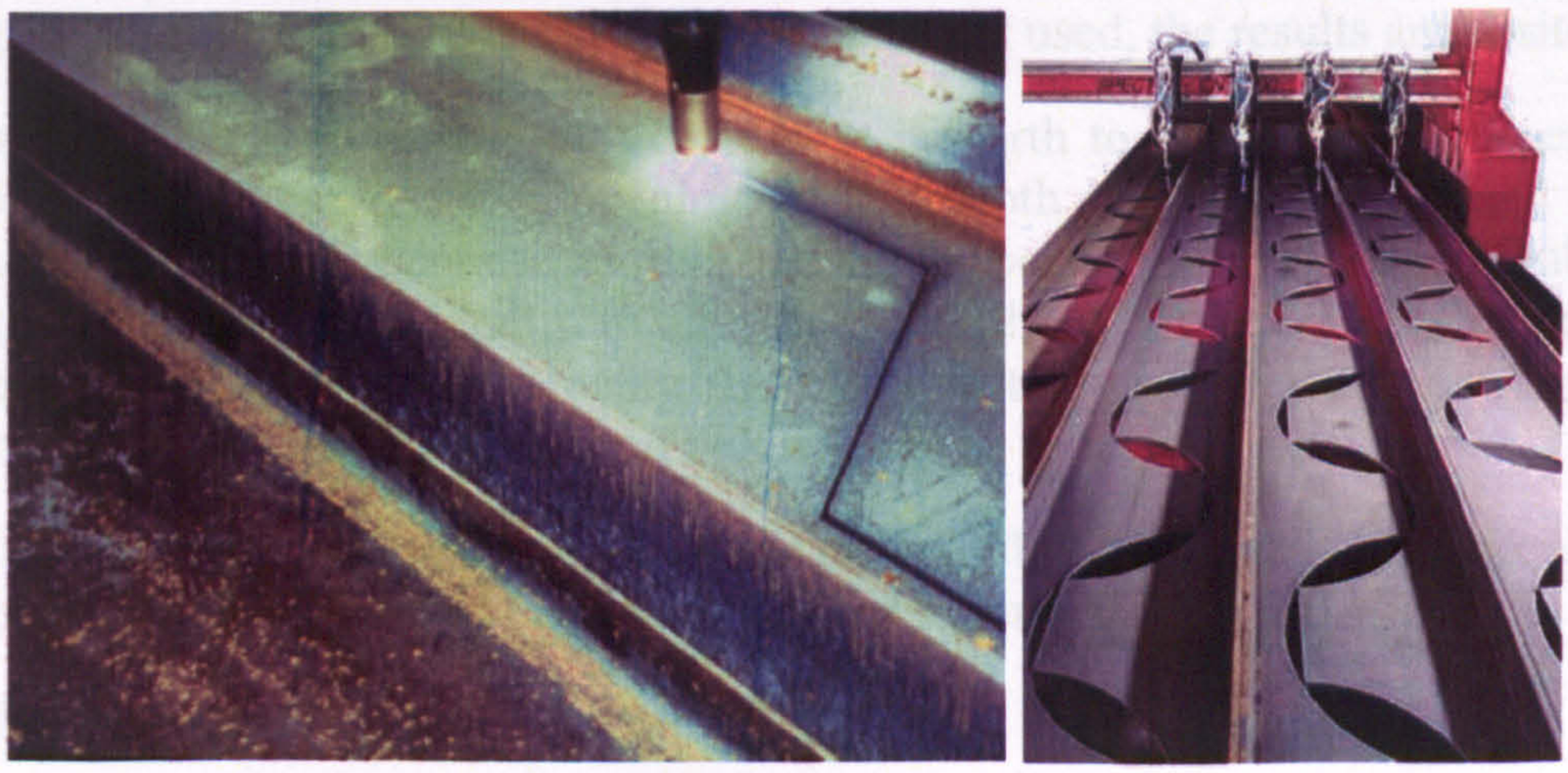

Figure 1: Continuous one-way cut (left) and continuous double-way cut (right) (CMC Steel Products)

The development of automated cutting and welding equipment, leads to an advanced manufacture of such perforated beams in an almost ultimate number of depths and spans, suitable for both light and heavy loading conditions. This research project focuses on the structural improvement of the steel perforated beams with the scope to enhance the functionality and effectiveness of the existing equipment, to develop novel effective steel perforated beams, with the lowest budget of production. This can be accomplished by saving material and manufacturing time.

2 Non-standard web opening shapes

The idea is to design perforated beams with novel non-standard web opening shapes providing the maximum possible web opening area for the integration of services and the minimum self weight. The fabrication precautions should be provided to make the results feasible and to use the advantage of automation in the manufacturing procedure.

3 Choice based on preliminary FE study (Appendix 1)

In **Appendix 1**, preliminary FE analyses on 16 randomly chosen standard and non-standard web opening shapes (combinations of shapes in some cases), are conducted. Global FEA is established for perforated beams with a span of 20m and 33 web openings regularly spaced along the length of every beam. Beams are designed for two different support conditions. It is concluded that C1-23 beam is the most effective among them in all given aspects such as: load carrying capacity, deflections, Von-Mises stresses and stress path at the edges of the examined web openings. This beam seems to be effective in terms of manufacturing as well.

C1-23 beam is a combination of circular and hexagonal web opening shapes. The positive characteristics of these typical web opening shapes are combined. In addition to that, from preliminary FE study it is found that vertical (C1-6) and inclined (C1-19) elliptical web openings behave satisfactorily, mainly due to their narrow opening length at the top and bottom tee-sections. Hence, the web opening shapes with an elliptical profile are also of interest.

Providing a curvy edge at the top and bottom tee-sections, similarly to perforated beams with circular web openings, high stress concentrations at this narrow critical area are prevented. On the other hand, straight web opening edges simplify the manufacturing procedure of perforated beams, such as in the case of beams with hexagonal web openings. Consequently, when both types are correctly used, the results are positive.

Furthermore, from the preliminary FE study is it worth to note that, when perforated beams with filleted circular web openings at mid-depth are utilsed (C1-4 and C1-17), the results are almost identical to the perforated beams with typical circular web openings. It should be noted that web openings with fillets, r, equal to 25mm and 45mm are assessed. The idea of introducing the fillets at the circular web openings has a structural advantage and it is discussed below.

Based on the above concepts, novel non-standard elliptical and filleted circular web openings are mainly examined in this research programme.

4 Novel elliptical web opening shapes

Elliptical web opening shapes are introduced with narrow opening length at the top and bottom tee-sections (**Figure 2**). These web opening shapes consist of a combination of semi-circles with straight lines (**Figure 4.20**).

New profile cut: Following the conventional profile cutting way used to produce perforated beams with hexagonal web openings (i.e. castellated beams), an effective manufacturing method is proposed herein for the novel elliptical web openings (**Figure 2** and **3**). For the optimum use of this profile cutting procedure, it is provided that the diameter of the semi-circles should be equal to the welding length (i.e. $2R=s_o$) and so

the web-post width. This provision can be ignored, however as it is drawn in **Figure 5** below, the advantages of this manufacturing procedure are then eliminated.

In order to manufacture the beams in **Figure 2** and **3**, a simple double-way cut procedure is utilised, and the oxy-cut length is dramatically reduced in comparison with the oxy-cut length utilised to form the circular web openings. Additionally, the starting point of the welding line is now easily identified due to the sharp-tip point (i.e. corner) formed at the mid-depth of the beam. The geometry of the web opening shape is simple, the web opening area can be very large as well as the final depth of the beam is always significantly increased.

In elliptical shapes the width is independent of the depth (i.e. major and minor axis), hence a higher number of deep web openings can be fitted along the length of the beam, in comparison with the perforated beams with circular web openings. Hence, the stiffness of the web-posts is not reduced and the weight of the beam can be effectively controlled and maintained as low as possible, as it is usually required for long span applications, in order to avoid large deflections due to self-weight.

In **Figure 2**, the profile cutting procedure of the parent sections and the final perforated beams with increased final depth are presented for two novel elliptical web opening shapes with different radius, R, of the semi-circles at top and bottom tee-sections and same angle (THETA) of the straight lines. In **Figure 3**, the profile cutting procedure of the parent sections and the final perforated beams are presented for two novel elliptical web openings with same radius (R) of the semi-circles and different angle (THETA) of the straight lines. It is observed that, the final depth of the beam is only dependent on the radius of the semi-circles (i.e. Example 1), and not on the angle of the straight lines (Example 2). Hence, the greater the radius of the semi-circles, R, the smaller is the final depth, *h*, of the perforated beam with such novel elliptical web openings.

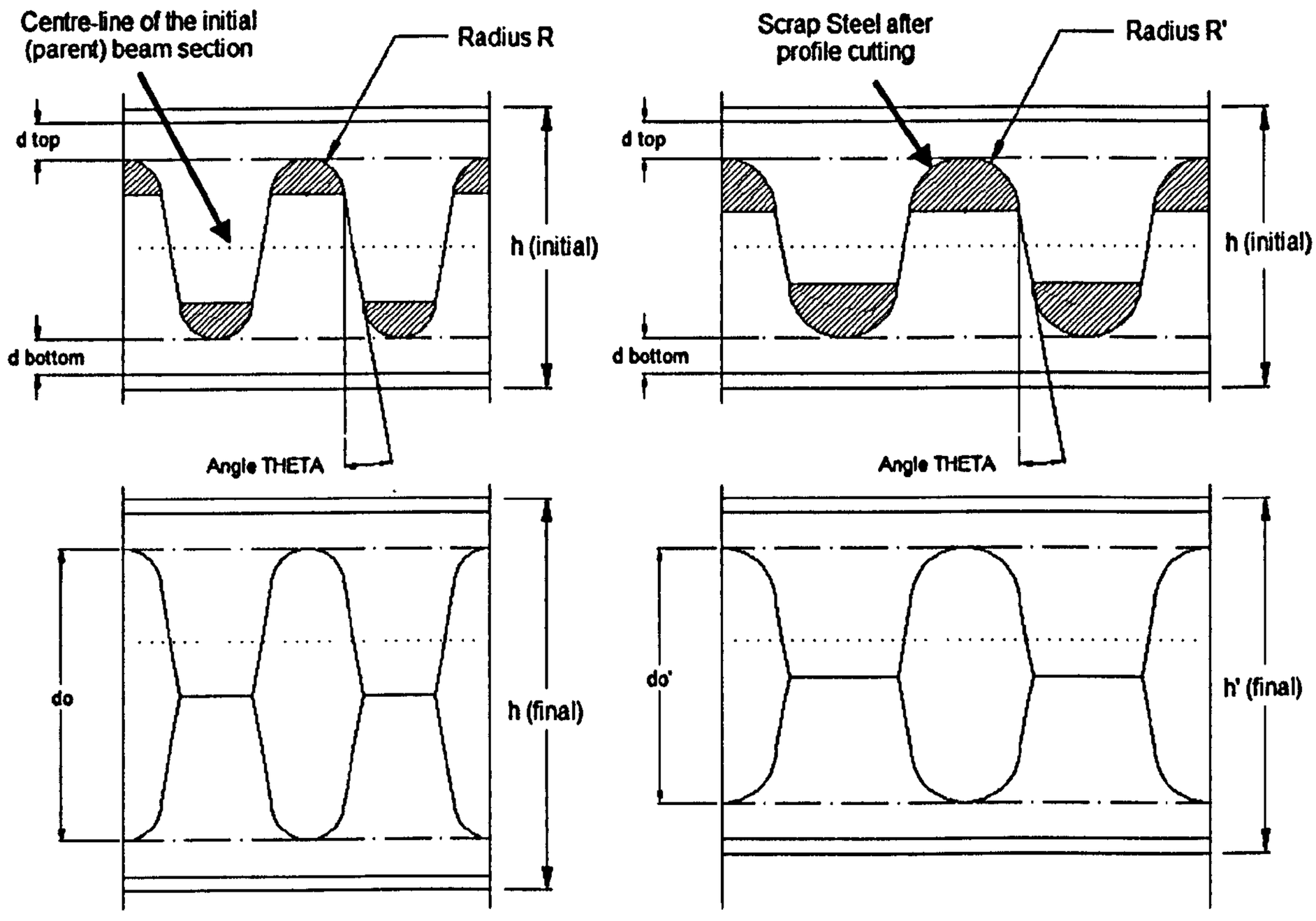

Figure 2: Example 1. Cutting profiles with standard welding length (new profile cut)

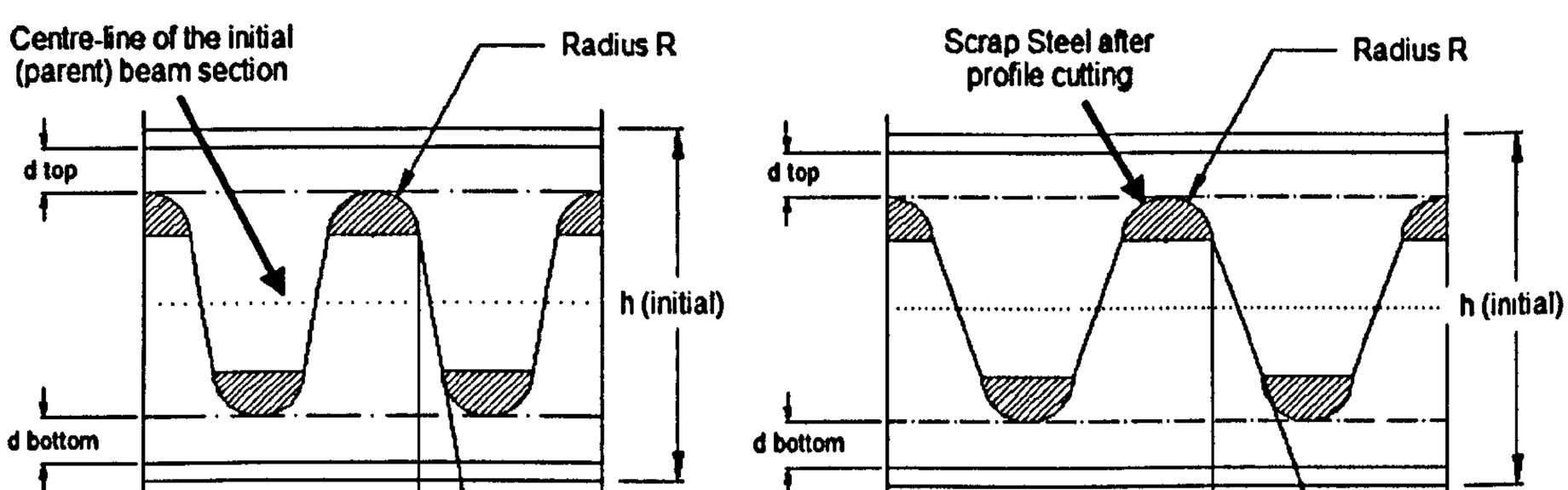

Figure 3: Example 2. Cutting profiles with standard welding length (new profile cut)

5 Novel filleted circular web opening shapes

Perforated beams with circular web openings are widely used in the steel construction industry, as they provide smooth stress distribution in the vicinity of the web openings and a large web opening area.

However, perforated beams with circular web openings are non-economic as a significant amount of scrap steel is wasted. In addition to that, the profile cutting procedure becomes expensive as a double way oxy-cut is utilised. Also, the welding procedure is sometimes difficult, as the automatic welding machines cannot easily indentify the starting welding point on the uniform smooth circular edge. Such a mistake sometimes causes major problems with expensive solutions. It is worth to say that the above disadvantages of perforated beams with circular web openings are appeared only when beams are manufactured with the profile cutting procedure, and they are considered as important from experts.

Modifying the manufacturing procedure and insensitively jeopardize the circular web opening shape, the above problems can be eliminated. Although, the results are not dramatically improved, taking into consideration the amount of annual production for a company, the economic effect is a significant figure. Moreover, as it is aforementioned in the main thesis, such perforated beams can be examined for further crack propagation and fatigue studies.

New profile cut: Following the concept of the conventional profile cutting way of the circular web openings (i.e. cellular beams), the fillets are introduced by rounding the sharp edges of the web-posts as it is shown in **Figure 4**. The same double way profile cutting procedure is utilised again, however there is an advantage on the welding procedure. Also, the amount of the wasted steel at the end of the production is reduced and another portion of the steel actually increases the final beam depth. As it is drawn in **Figure 4**, the greater the fillet radius, r, (i.e. the smaller the 'e' depth), the lower amount of steel is wasted and so deeper beams are produced. However, the smaller the value of 'e', the shorter the welding length is at the web-post. The latter phenomenon needs further investigation for structural integrity, as it is provided in the main thesis.

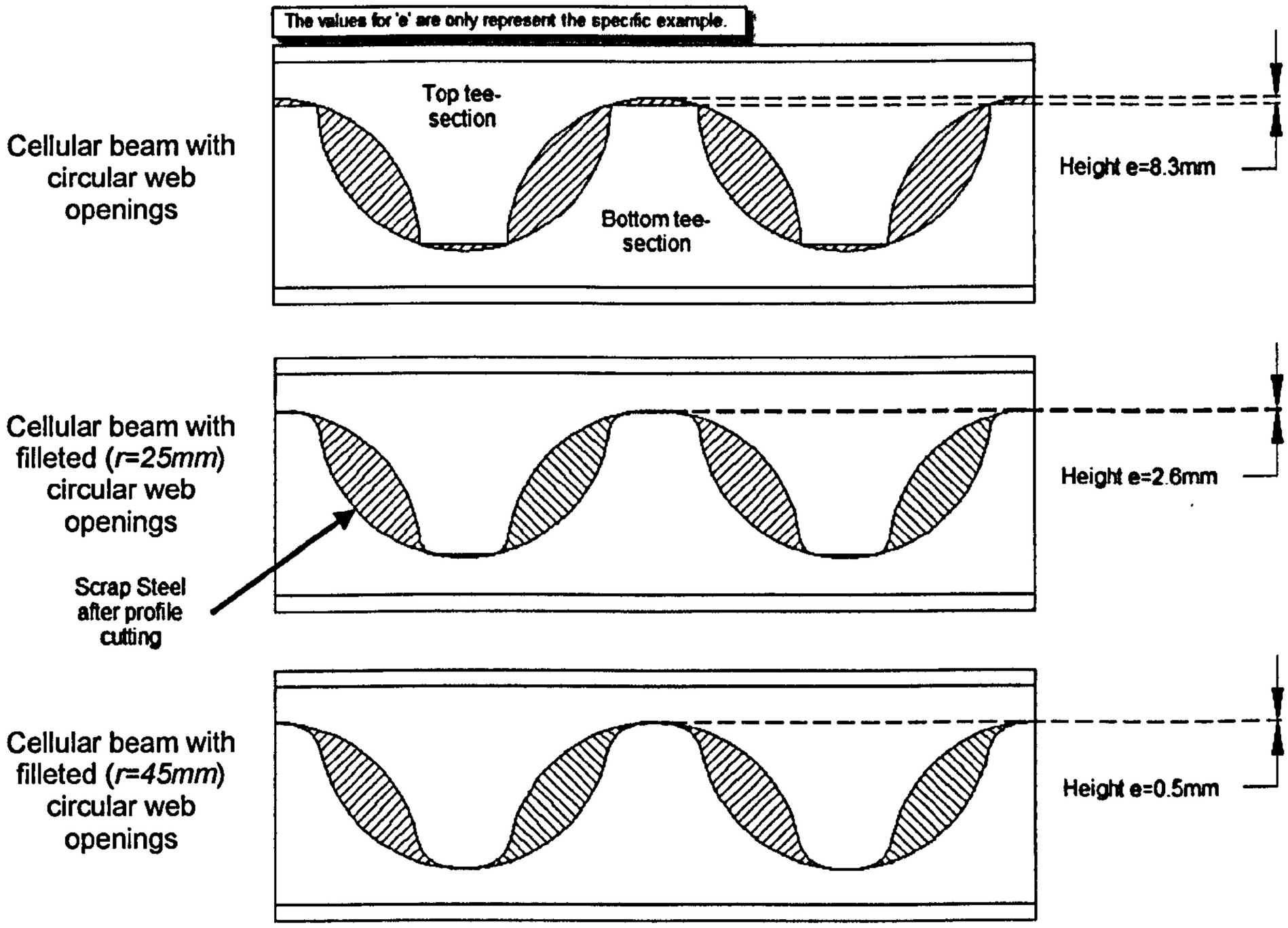

Figure 4: Cutting profiles with variable web-post length (i.e. conventional profile cut) - comparison

6 Overview on the manufacturing procedures (factors)

The manufacturing procedure of the novel perforated beams should result:

- A shorter oxy-cut length.
- A shorter welding line.
- An increased depth of the final beam.
- A large web opening area.

In more detail, **Figure 5** shows the cut-line (Step 1) and the final result after shifting and welding the tee-sections (Step 2) for beams with a standard circular web opening, a novel elliptical (i.e. $2R \neq s_o$) **Figure 2** and **3**) and a novel filleted circular web opening.

Figure 5 shows that when an elliptical web opening is developed, the web-post is enhanced (i.e. more steel area is provided between the two adjacent web openings) and the depth of the final beam is increased. When filleted circular web openings are developed, the web-post area and the welding line are slightly decreased, while the depth of the beam is slightly increased.

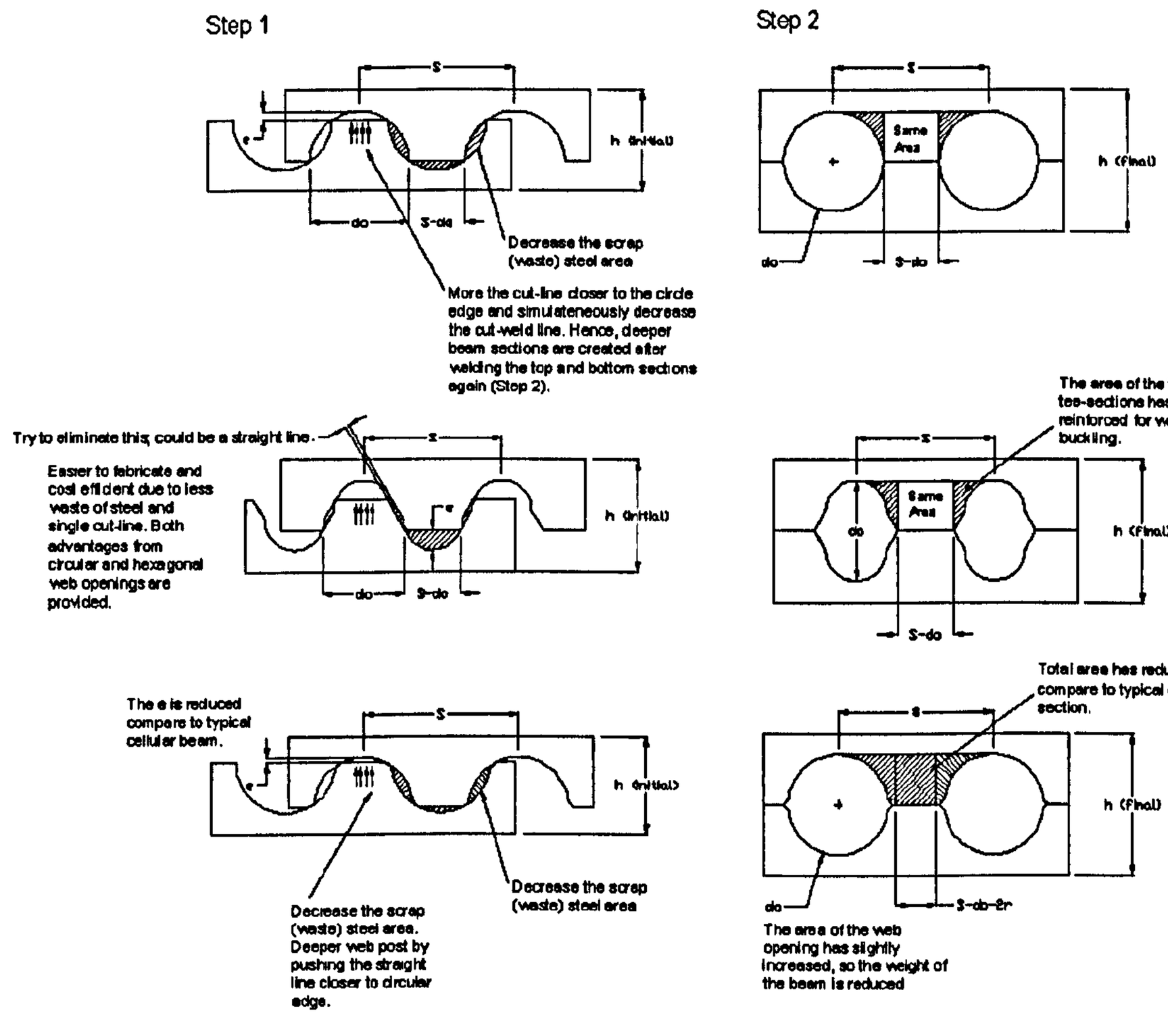

Figure 5: Cutting profiles with variable welding length (i.e. conventional profile cut)

Table 1 presents the factors affected by the manufacturing procedure of the perforated beams with novel elliptical web openings. The factors that can affect the vertical shear and the web-post buckling behaviour of the beams are also designated. Results are synopsised for three manufacturing methods of perforated beams such as: i) the profile cutting with the aforementioned provisions (i.e. $2R=s_o$) (increased depth of the final beam) (e.g. **Figure 2** and **3**), ii) the conventional profile cutting (increased depth of the final beam) (e.g. **Figure 5**), and iii) simple web opening cut-out (i.e. removal) of the steel plate (final depth of the perforated beams is equal to the parent's beam).

In this research programme, perforated beams with simple web opening cut-outs are only considered, in order to be able to assess the results and draw reliable conclusions. In the case of the profile cutting, a more complex study would be considered with numerous factors varying for different steel section sizes. However, the outcome of this research programme could be implemented for both manufacturing procedures.

Manufacturing Procedures	Failure Mode Consideration	Web Openings Shape Parameters	Welding Length	Final Depth of the Beam	Web Opening Area	Critical Open Length	Weight of the Beam	Number of Web Openings
Profile cutting with web-post length equal to the diameter of the semi-circles ($2R=s_o$)	Web-post buckling	R	§	*§	§	§	§	§
		THETA			§		§	§
Profile cutting with variable web-post length	Web-post buckling	R	§	§	§	§	§	§
		THETA	§	§	§		§	§
Web opening cut-out from web	Vierendeel mechanism	R			§	§	§	
		THETA			§		§	
Web opening cut-out from web	Web-post buckling	R			§	§	§	
		THETA			§		§	

Table 1: Factors affect the manufacturing procedure of perforated beams with novel elliptical web openings (*formula is provided)

The formula defines the final depth of a perforated beam with novel elliptical web openings when $2R=s_o$, is given as follows:

$$* \; h_{final} = 2h_{initial} - d_t - d_b - 2\mathrm{R}$$

On the other hand, when the conventional profile cutting method is used for novel elliptical web openings and filleted circular web openings, the bigger the difference between the parent and the final beam depth, the more advanced the manufacturing procedure is considered. This is going to be achieved by eliminating the '*e*' value; as it is shown in **Figure 5**.

7 Web opening area of novel shapes

The formula for the web opening area of the new vertical and inclined elliptical web openings is defined below, in relation to the angle, THETA, and radius, R.

Web opening area of vertical elliptical web opening:

$$A_{ellipse} = [\pi \mathrm{R}^2] + \left[4\mathrm{R} + 2\left({}^{d_o}/_{2} - \mathrm{R}\right) tan\vartheta\right]\left({}^{d_o}/_{2} - \mathrm{R}\right)$$

Web opening area of inclined elliptical web opening:

$$A_{ellipse} = [\pi \mathrm{R}^2] + \left[4\mathrm{R} + \left({}^{d_o}/_{2} - \mathrm{R}\right) tan\vartheta\right]\left({}^{d_o}/_{2} - \mathrm{R}\right)$$

The web opening area of the circular web opening with filleted edges at the mid-depth is defined as shown below:

$$A_{circle\ with\ fillets} \cong \pi \frac{{d_o}^2}{4} + \pi \frac{r^2}{4}$$

APPENDIX 3

VON-MISES CRITERION

Von-Mises criterion is mainly used when the distortion of metals is required, whereas Tresca criterion is dominantly used for representation of maximum shear capacity. Both formulas of Von-Mises and Tresca theorems are presented as following.

The Tresca criterion (**Figure 1**) predicts that yielding will occur when the maximum shear stress at any point reaches a maximum allowable shear stress for that material. For this reason the Tresca criterion is often referred to as the *maximum shear stress criteria*. In one dimension the maximum shear stress is given by:

$$\tau_{max_{1-D}} = \frac{\sigma_y}{2}$$

In three dimensions the maximum shear stress is given by:

$$\tau_{max_{3-D}} = \frac{\sigma_1 - \sigma_3}{2} \leq \tau_{ys}, if\ \tau \geq \tau_{ys}\ then\ yield\ occurs$$

Provided that:

$$\sigma_{tresca} = \sigma_1 - \sigma_3 > \sigma_{max}$$

However, the Von-Mises criterion (**Figure 1**) is based on the assumption that failure occurs when the energy of distortion reaches the same energy for yield/failure in uniaxial tension. It is much less conservative than other yield criteria (e.g. Rankine, Tresca etc.) and thus can help to eliminate over designing when used with ductile materials.

In two dimensional problem types, yield occurs when:

$$\sigma_1{}^2 - \sigma_1\sigma_2 + \sigma_2{}^2 = \sigma_y$$

In three dimensional problem types, yield occurs when:

$$\frac{1}{\sqrt{2}}\sqrt{[(\sigma_1 - \sigma_2)^2 + (\sigma_2 - \sigma_3)^2 + (\sigma_3 - \sigma_1)^2]} = \sigma_y$$

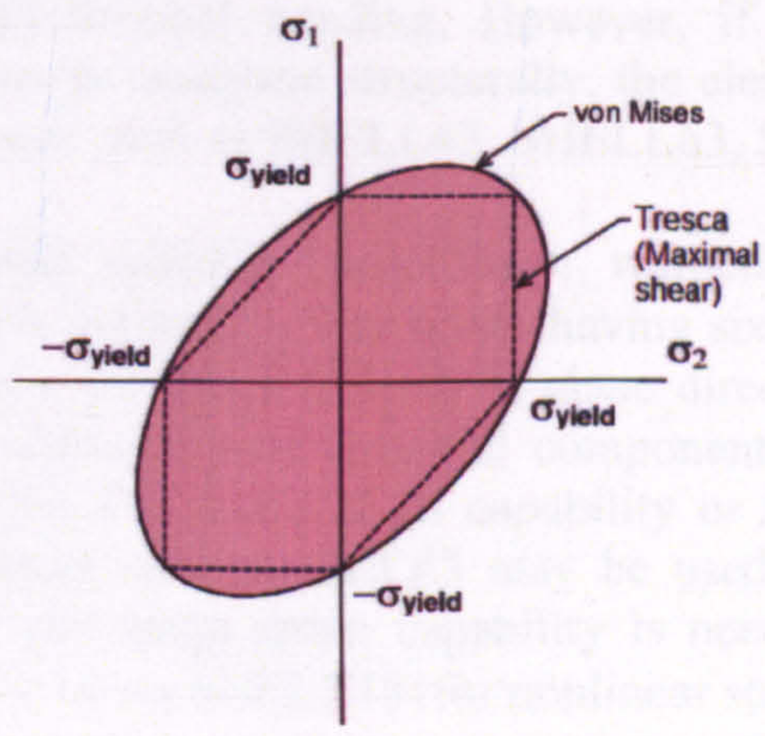

Figure 1: Plane Stresses

APPENDIX 4

GENERAL FE MODEL

1 Rational behind the element selection

For the rational selection of the element type a few approaches modelling a typical perforated beam have been examined.

SOLID45 is defined by eight nodes having three degrees of freedom at each node element needs. SOLID45 uses less CPU time for the element stiffness formation and stress/strain calculations comparable to the full integration option, while the length of the element history saved record is only the $1/7^{th}$ of the full integration option. This element provides a good non-linear convergence with extra deformation but no hourglass effects (similar to SOLID185). It will not suffer from volumetric locking. SOLID45 also supports orthotropic material properties. However, the use of such element does not offer very accurate results while more than one layer of elements is necessary to capture the bending behaviour.

SOLID92 has a quadratic displacement behaviour and is well suited to model irregular meshes (such as produced from various CAD/CAM systems). SOLID92 element is defined by ten nodes having three degrees of freedom at each node. This element supports orthotropic material properties and is well designed for temperature applications. However, this element is conical 3D element which is not suitable for mapped meshes. Similarly to SOLID45 more than one layer of elements is necessary to acquire bending and obtain reliable results.

The following typical shell elements are also examined:

SHELL131 is defined by four nodes, one thickness per layer, a material angle for each layer, and the material properties. If the material is uniform and the analysis has no transient effects, only one layer is needed with a linear temperature variation through the thickness. The conducting shell element is applicable to a 3D, steady-state or transient thermal analysis. SHELL131 generates temperatures that can be passed to structural shell elements in order to model thermal bending. However, if the model containing the conducting shell element is to be analyzed structurally, the element should be replaced by an equivalent structural element such as SHELL43, SHELL63, SHELL181, or SHELL281.

SHELL43 (SHELL143) is well suited to model linear, warped and moderately-thick shell structures while the element is defined by four nodes having six degrees of freedom at each node. The deformation shapes are linear in both in-plane directions. For the out-of-plane motion, it uses a mixed interpolation of tensorial components. SHELL43 also supports orthotropic material properties. For a thin shell capability or if plasticity or creep is not needed, the elastic quadrilateral shell SHELL63 may be used. However, if convergence difficulties are encountered and large strain capability is needed, SHELL181 should be used. Also, it is recommended using SHELL181for nonlinear structures.

SHELL181 is suitable for analyzing thin to moderately-thick shell structures. The element type used for this model is SHELL181, as it is shown in **Figure 1**. It is a 4-node element with six degrees of freedom at each node. SHELL181 is well-suited for linear, large rotation, and/or large strain non-linear applications. SHELL181 accounts for follower (load stiffness) effects of distributed pressures. It may be used for layered applications for modelling laminated composite shells or sandwich construction. The accuracy in modelling composite shells is governed by the first order shear deformation theory (usually referred to as Mindlin-Reissner shell theory). Moreover, SHELL181 provides the option of reduced integration with hourglass control (default) which alleviates the shear locking effects.

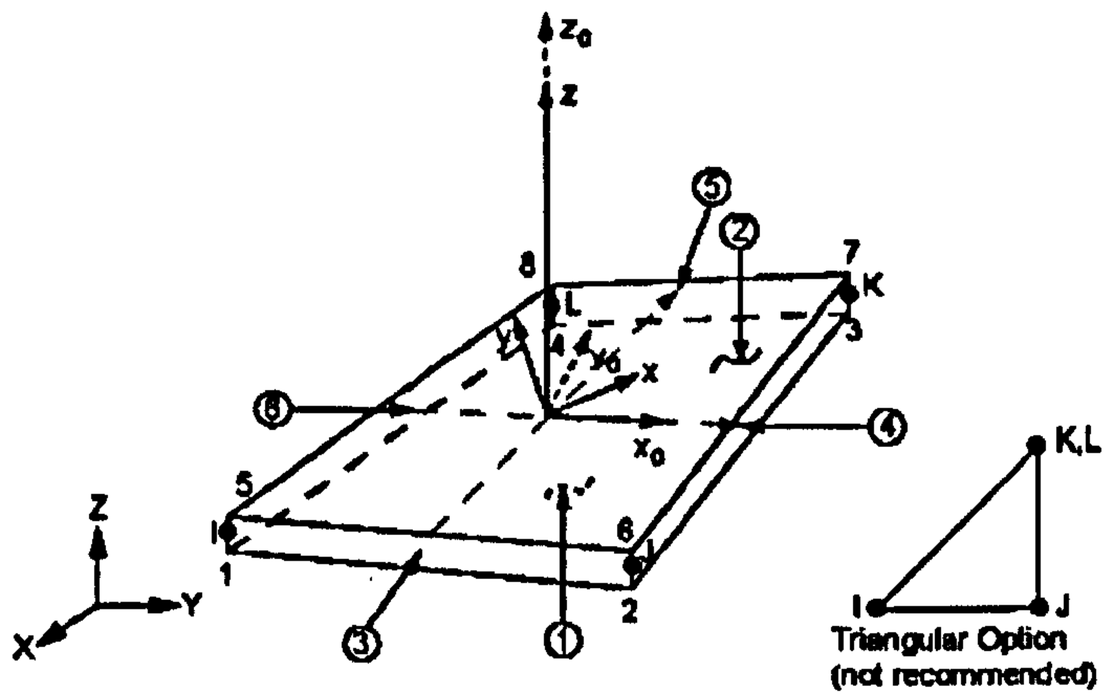

x_0 = Element x-axis if ESYS is not provided.

x = Element x-axis if ESYS is provided.

Figure 1: SHELL181 Element (ANSYS v11.0)

The geometry, node locations, and the coordinate system for this element are also shown in **Figure 1**. The element is defined by four nodes: I, J, K, and L. The element formulation is based on logarithmic strain and true stress measures. The element kinematics allow for finite membrane strains (stretching). However, the curvature changes within a time increment are assumed to be small.

2 Element comparisons

It is decided to use shell elements for perforated steel beams with thin webs and flanges. The membrane bending is interesting while flexible elements are necessary recording the out-of-plane displacements at critical positions. Consequently, the model shown in **Figure 2** was modelled with various shell elements. It is concluded that the results are similar especially between SHELL43 and SHELL143 elements as it was expected. On the other hand, when SHELL181 elements are utilised, a stiffer model is obtained while load capacity at the elastic region is lower. This is used for a conservative design and the increased stiffness helps avoiding the pre-mature local buckling of the perforated beams in the vicinity of the web openings. However, the load carrying capacity recorded is similar.

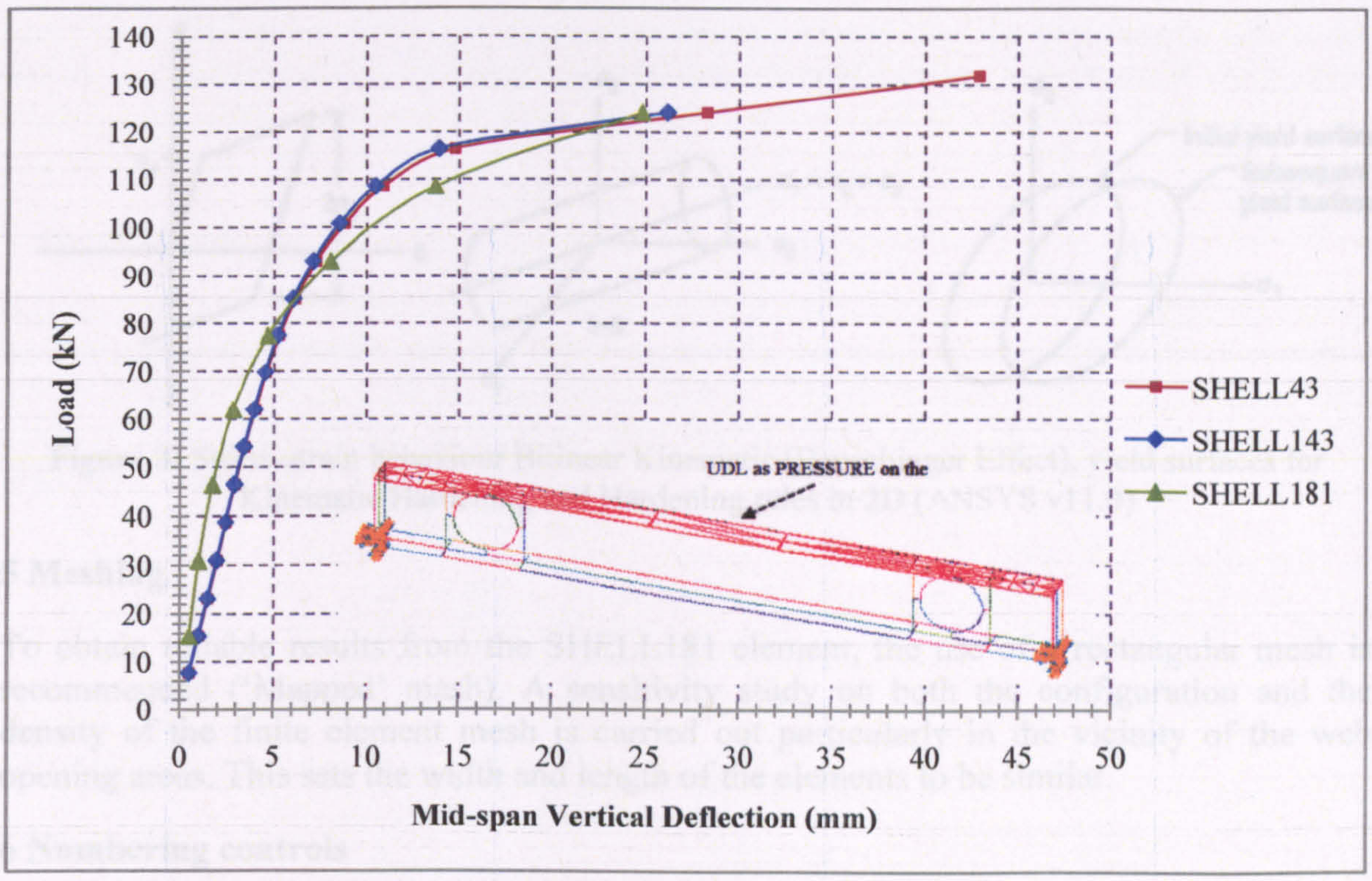

Figure 2: Convergence results of the FE analyses with different element types

3 Real constants

The values of the real constants represent the thicknesses of the steel section components. Thus the thickness of the shell may be defined at each of its nodes. The thickness of the stiffeners is decided to be the same with the thickness of the flanges, to obtain an effective stress distribution along the web of the steel section.

4 Material properties

In most FE analyses of the current thesis, it is assumed that the material properties of the steel are identical across the whole beam. The SHELL181 element required linear isotropic properties as well as bilinear kinematic hardening (BKIN) properties to properly model steel.

The Bilinear Kinematic Hardening option assumes the total stress range is equal to twice the yield stress, so that the Bauschinger effect, shown below in **Figure 3**, is included. This option is recommended for general small-strain use for materials that obey Von-Mises yield criterion, such as most metals. Also, it should be noted that in BKIN option; Rice's hardening rule is applied, which does take stress relaxation with load increase into account. This is taken as the default from ANSYS. Note that the density for the steel is not added in the material model, so the self-weight is not introduced in these models. No modal analysis is conducted.

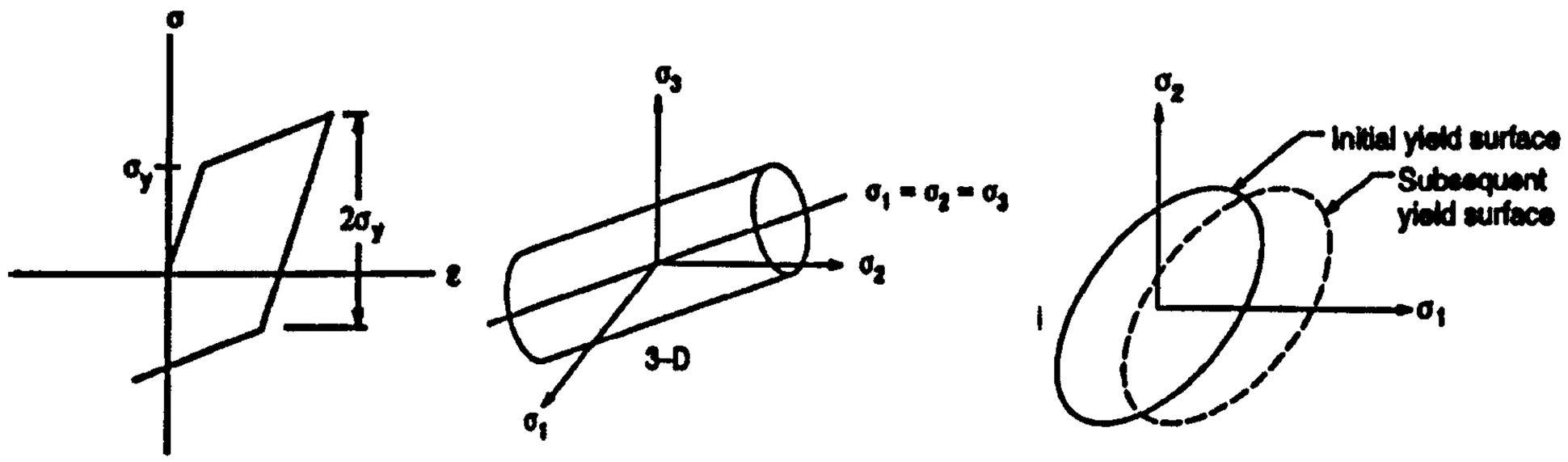

Figure 3: Stress-strain behaviour Bilinear Kinematic (Bauschinger Effect), yield surfaces for Kinematic Hardening and Hardening rules in 2D (ANSYS v11.0)

5 Meshing

To obtain reliable results from the SHELL181 element, the use of a rectangular mesh is recommended ('Mapped' mesh). A sensitivity study on both the configuration and the density of the finite element mesh is carried out particularly in the vicinity of the web opening areas. This sets the width and length of the elements to be similar.

6 Numbering controls

The perforated beam is modelled as different planes represent flanges, stiffeners and web which are glued together. Use of the *AGLUE* command in ANSYS generates new areas by "gluing" input areas. The glue operation redefines the input areas so that they share lines along their common boundaries. The new areas encompass the same geometry as the original areas. This operation is only valid if the intersection of the input areas are lines along the boundaries of those areas. The *AGLUE* command results in the merging of lines and key-points at the common area boundaries. This means one must be aware of area numbering when multiple *AGLUE* commands are applied to avoid any "ungluing" of geometry.

It is worth mentioning that merging key-points before nodes can result in some of the nodes becoming 'orphaned'; that is, the nodes lose their association with the solid model. The orphaned nodes can cause certain operations, such as boundary condition transfers, surface load transfers, and so on, to fail. Care must be taken to always merge in the order that the areas appear. All precautions are taken to ensure that everything is merged in the proper order. Also, the lines and key-points of the lower numbered area are kept.

7 Loads and boundary conditions

Displacement boundary conditions are needed to constrain the model to get a unique solution. The entire model is analysed as unique entity, so no boundary conditions need to be applied at points of symmetry. However, boundary conditions are applied where the supports and loading exist.

The boundary conditions representing the supports are set first. It is decided that both ends of the beam will be simply supported. Because of the fact that shell elements are used in

order to represent the three dimensional model, it is found that the best way to define the simply supported ends is by using a single line of nodes at the very ends of the bottom flange. The uniformly distribute load applied as pressure at the whole surface area of the top steel flange.

8 Analysis type

In this thesis the analyses are large displacement and static. When large displacement is used the true stress-strain relationship is replaced, hence the change in the cross-sectional area during the loading is replacing the initial area. The distinction between the engineering stress, which neglects this change of area, and the true stress is significant. The basic difference can be seen from **Figure 4**.

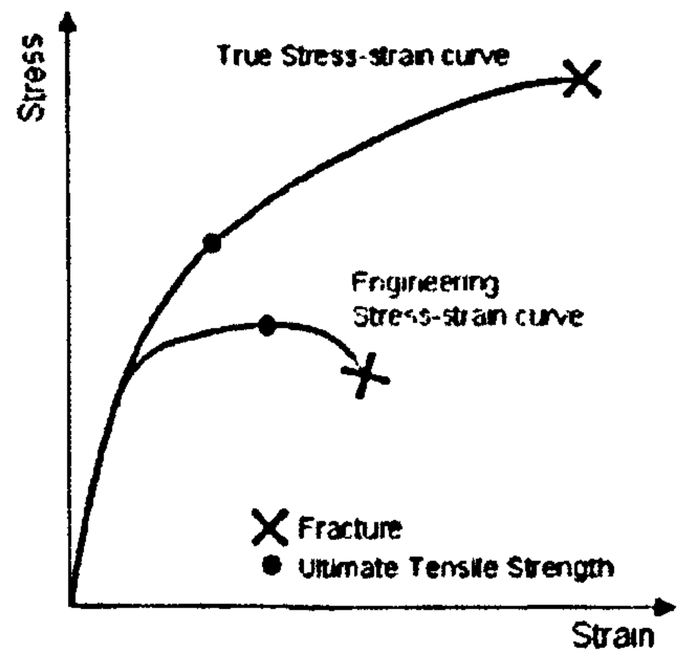

Figure 4: Comparison of Engineering and True Stress-Strain Curves (B.J. Mac Donald, 2007)

The time at the end of the load step 1 refers to the ending load per load step. Automatic time stepping allows ANSYS to determine appropriate sizes to break the load steps into. Decreasing the step size usually ensures better accuracy, but this takes time. The Automatic Time Step feature (ON) determines an appropriate balance. This feature also activates the ANSYS bisection feature, which allows recovery if convergence fails. However, in **Chapter 3** Automatic Time Stepping is not used (OFF) and the reason is the direct control of the load increments. The sub steps are set to indicate load increments used for this analysis. Hence, an instant monotonic loading is applied with scope to simulate the laboratory experimental test.

APPENDIX 5

INTERACTION RESULS FOR UB 457X152X52 (S275)

	Positions, x (mm)	Load carrying capacity, w (kN/m)	$V_{Sd}/V_{o,Rd}$	$M_{Sd}/M_{o,Rd}$
position 1	0	116.8	1.065	0.000
position 2	284	116.8	1.005	0.300
position 3	537	116.8	0.906	0.546
position 4	788	116.8	0.775	0.741
position 5	1039	112.7	0.629	0.873
position 6	1299	104.5	0.482	0.952
position 7	1573	99.1	0.342	0.981
position 8	1866	93.4	0.219	0.995
position 9	2177	89.5	0.107	1.002
position 10	2500	88.5	0.000	1.000

Table 1: Interaction results for $d_o=0.5h$

	Positions, x (mm)	Load carrying capacity, w (kN/m)	$V_{Sd}/V_{o,Rd}$	$M_{Sd}/M_{o,Rd}$
position 1	0	55.6	1.01	0.00
position 2	284	61.0	0.99	0.15
position 3	537	65.6	0.95	0.30
position 4	788	71.0	0.90	0.44
position 5	1039	76.2	0.82	0.59
position 6	1299	78.4	0.71	0.74
position 7	1573	80.2	0.57	0.87
position 8	1866	81.2	0.39	0.96
position 9	2177	76.2	0.20	0.99
position 10	2500	76.2	0.00	1.00

Table 2: Interaction results for $d_o=0.75h$

APPENDIX 6

YIELD PATTERNS

In the following figures the stress concentration in the vicinity of the web openings with depth of 80%, 65% and 50% of the beams' depth are plotted, while the web openings are located at different 'ideal' positions (e.g. position x is equal to 2, 4, 8 and 10) in order to show the movement of the plastic hinges while the shear-moment interaction varies. The web opening positions under investigation are given as follows with the sequence they presented: high shear region, high shear and low moment region, high moment and low shear region and pure moment region. The Von-Mises criteria is used and stresses are plotted to re-present the plastic hinges. Together with the stresses in the vicinity of each web opening, the top steel flange is plotted, as it yields first due to a higher compressive stress than that in the web at HMS (**Figure 2.12**). Also, the formation of the first plastic hinges at the LMS is shown. The universal beam UB 457x157x52 is comprehensively examined, as it is determined as the most critical between the typical mid-range beams considered in this research programme.

Web opening A

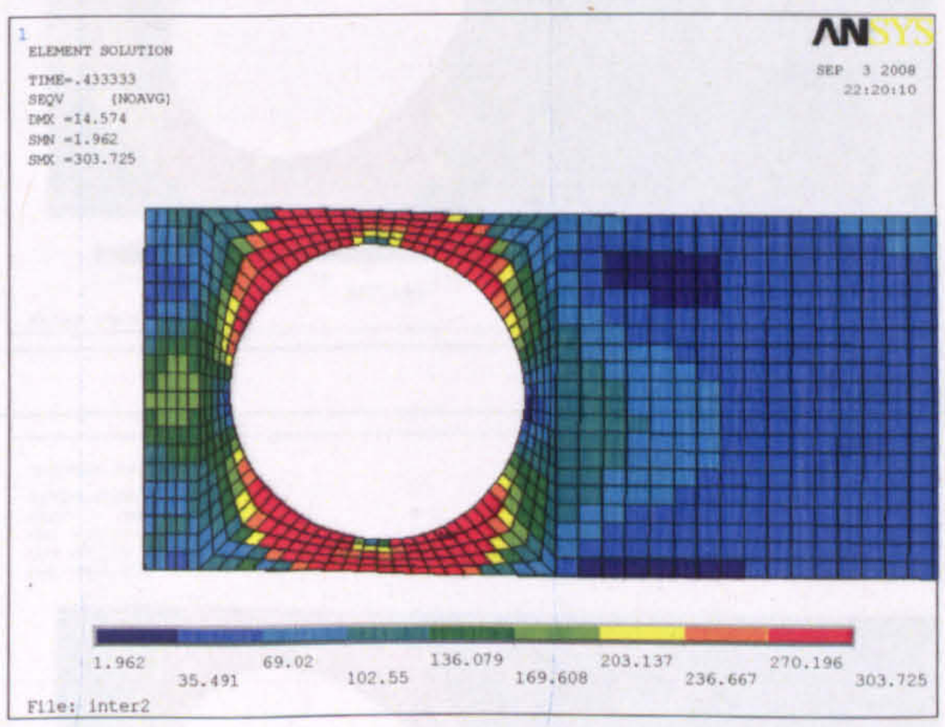

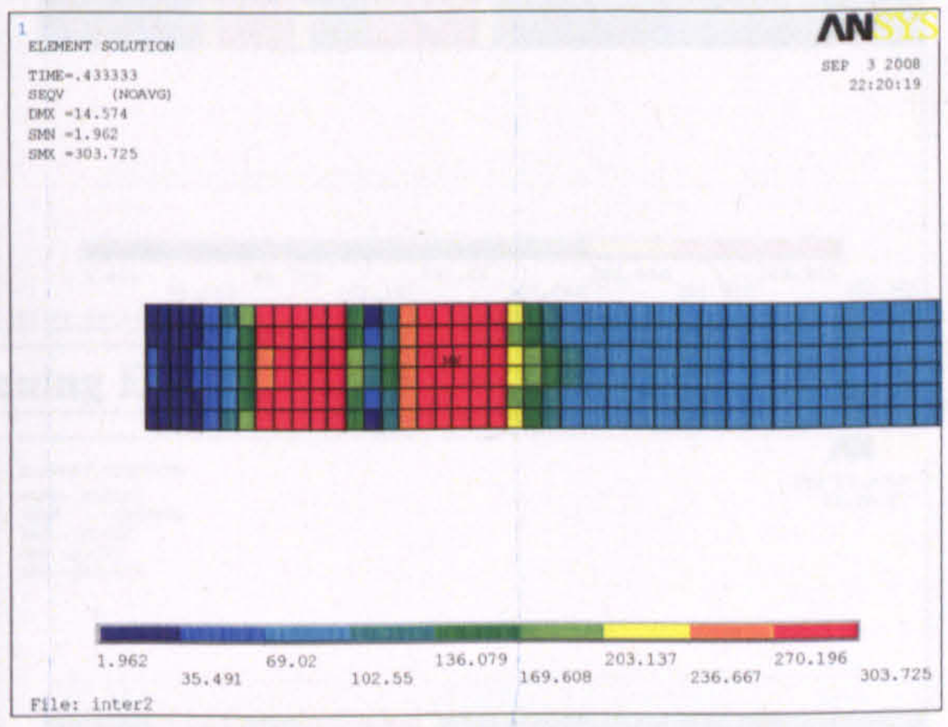

Web opening B

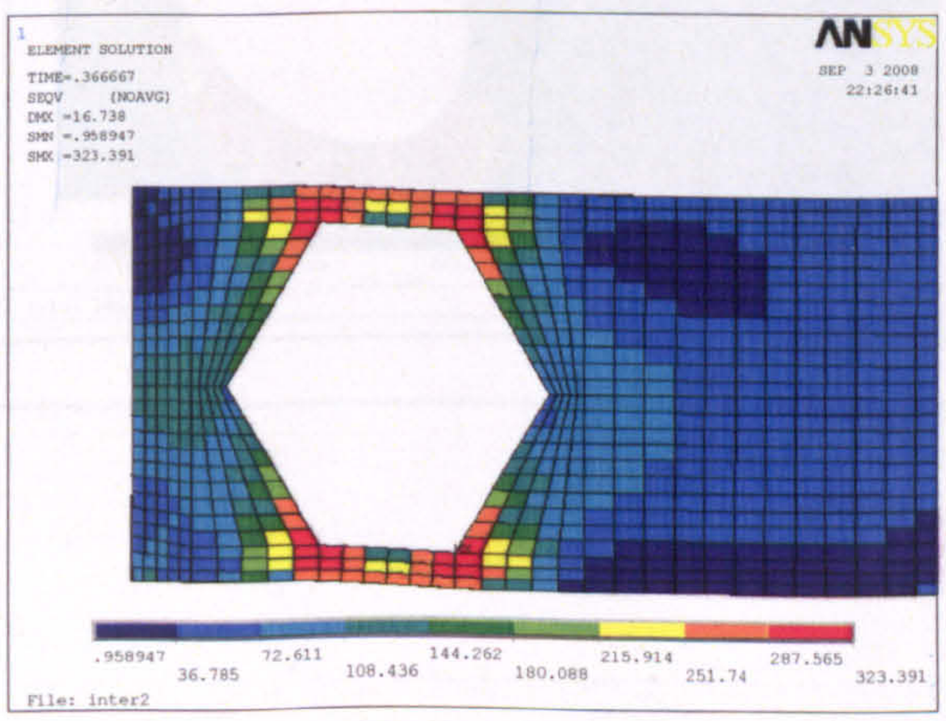

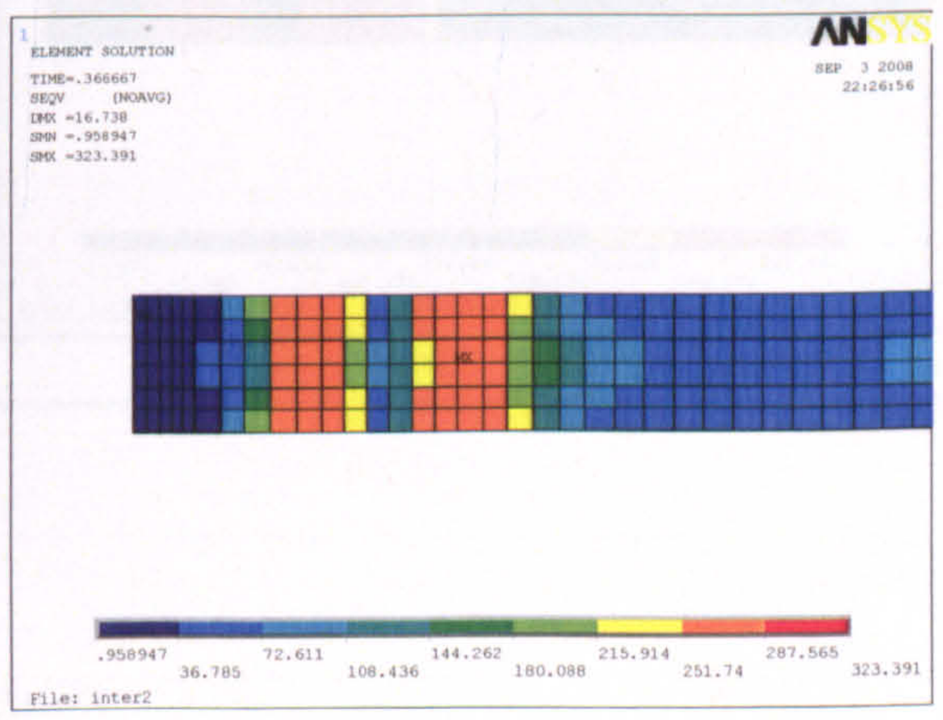

Web opening C

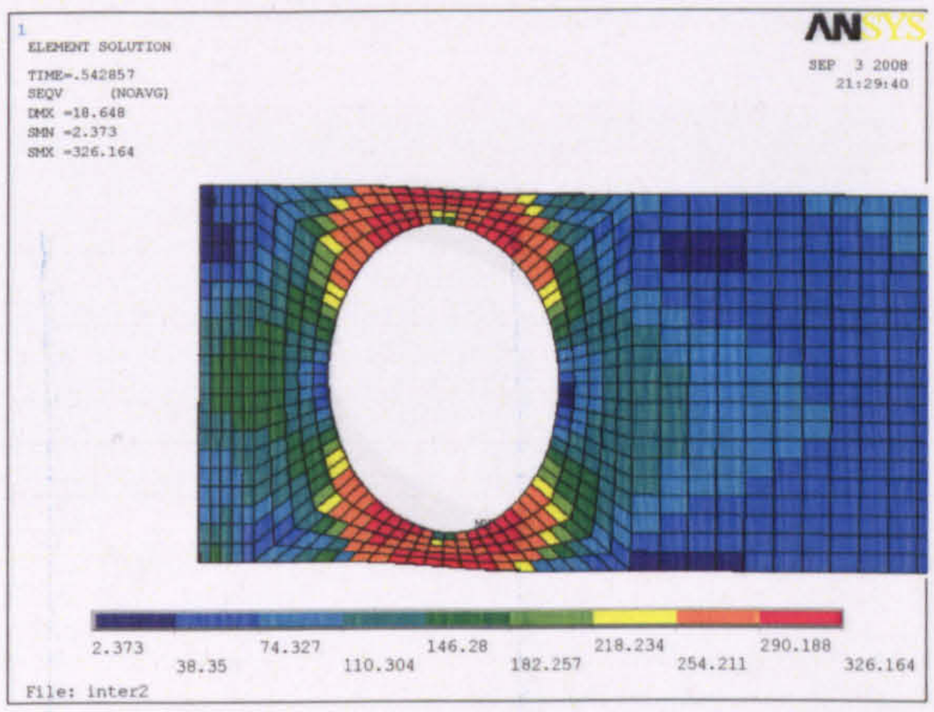

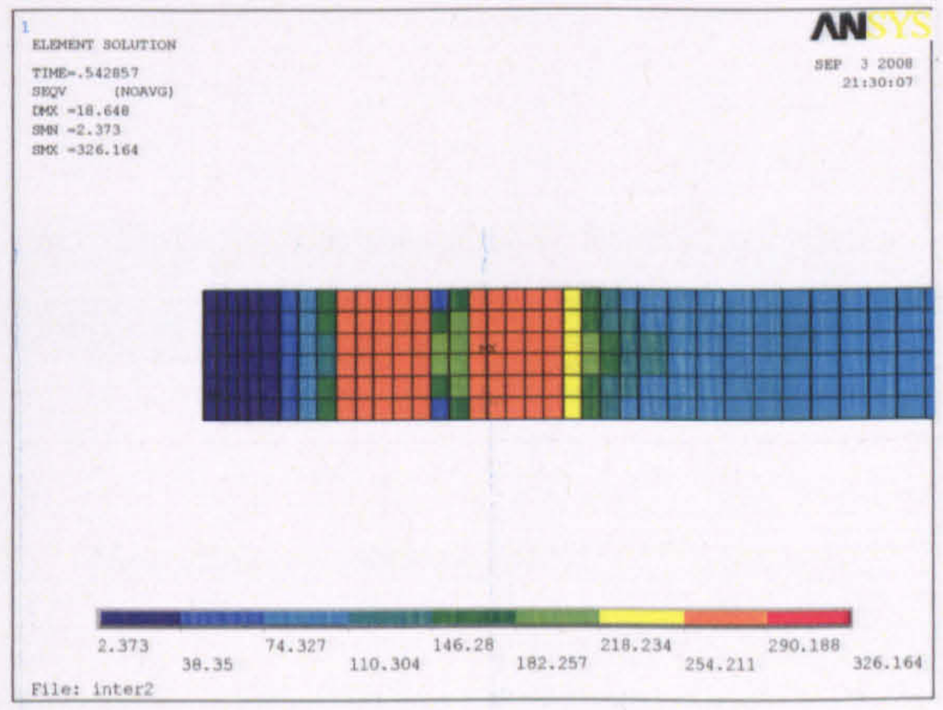

Web opening D

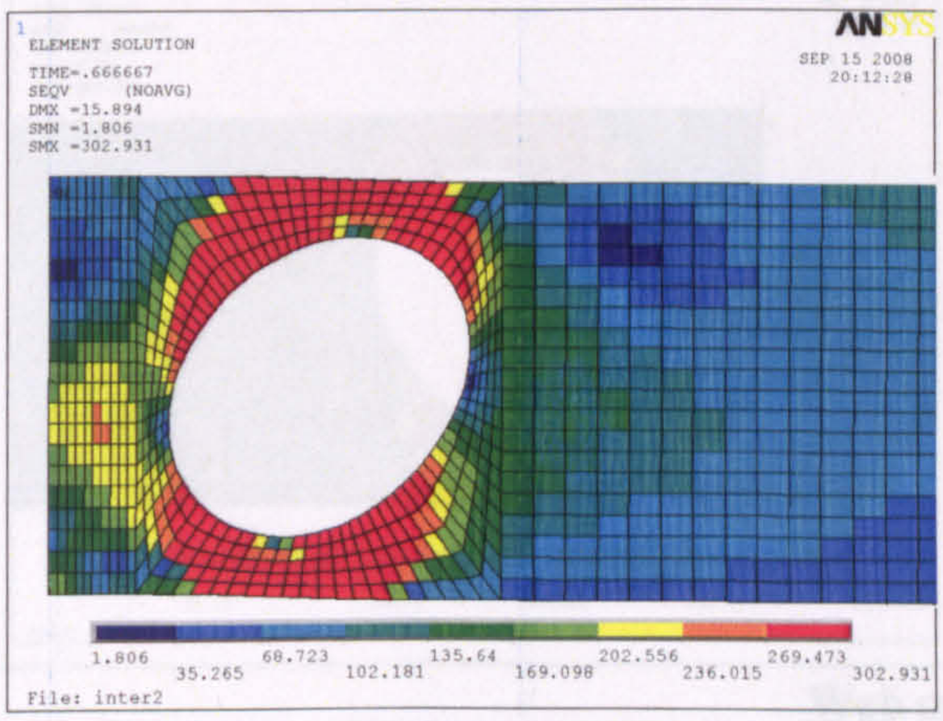

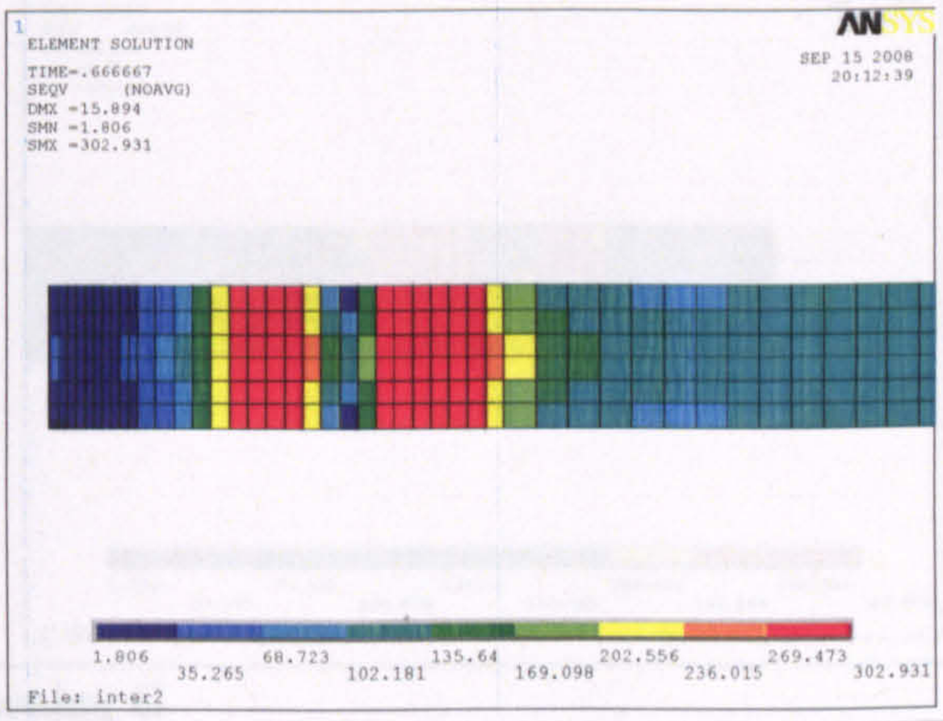

Web opening E

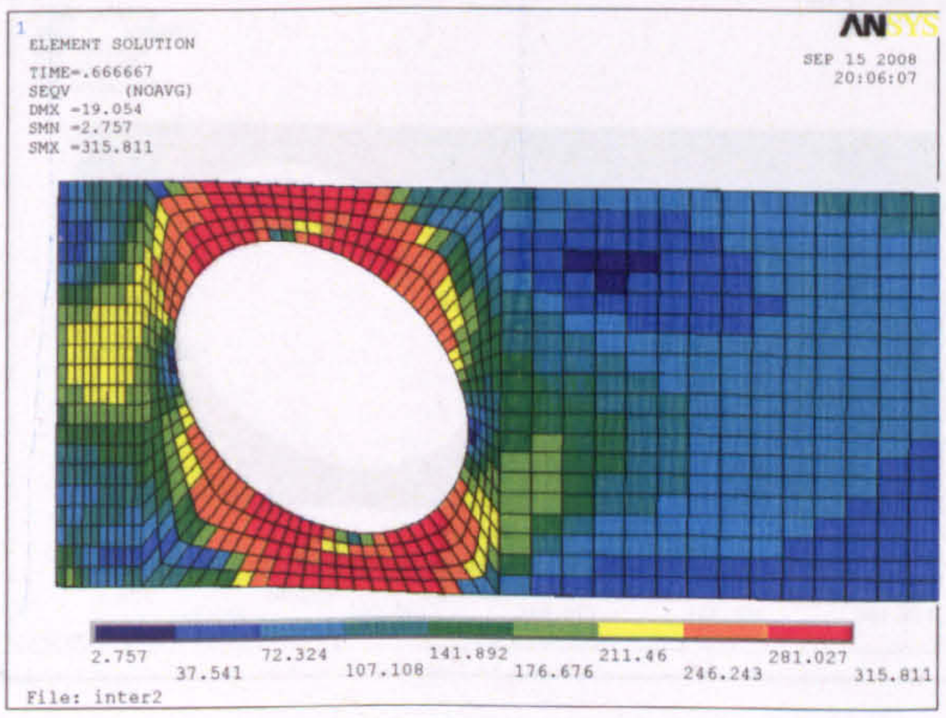

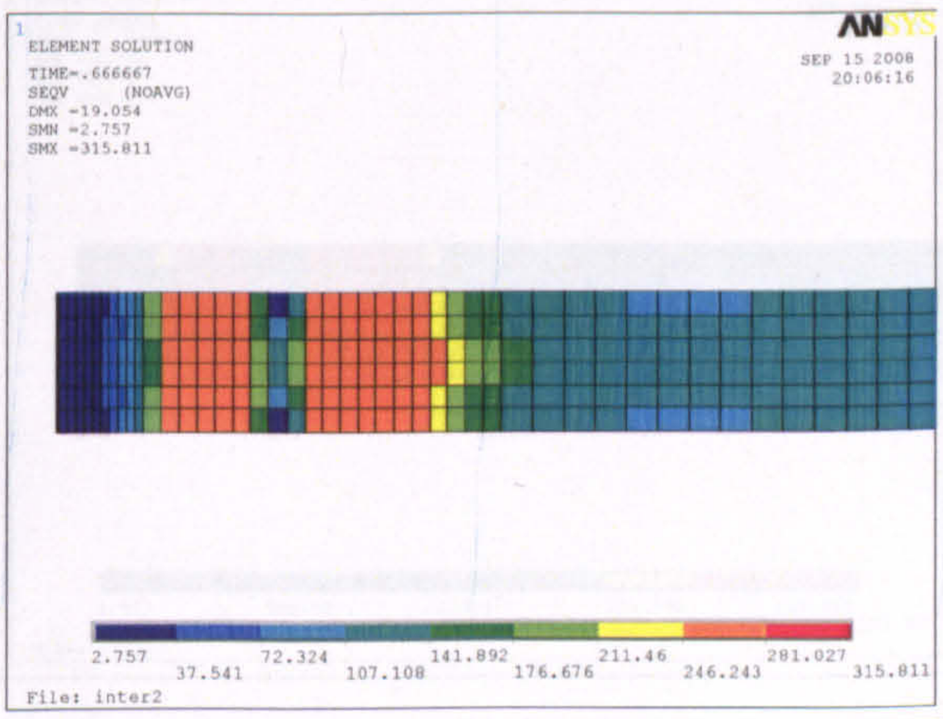

Web opening F

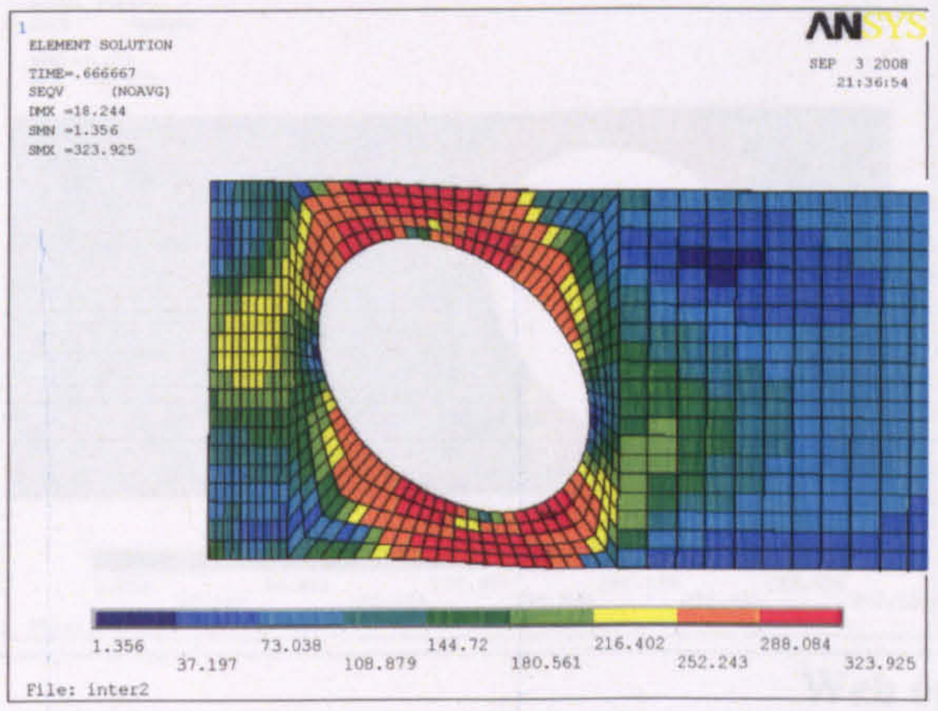

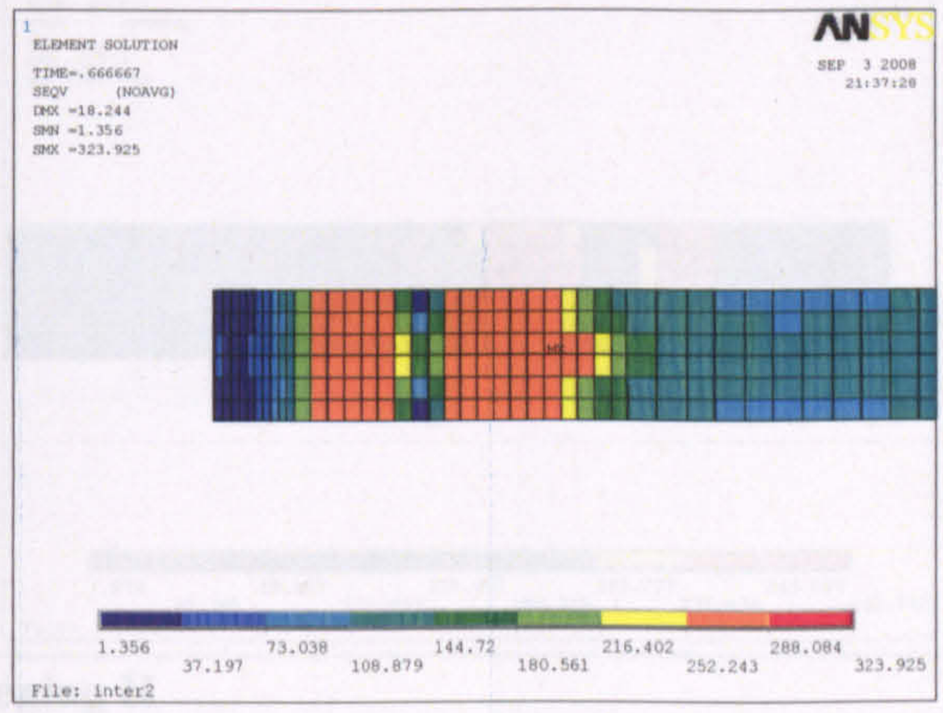

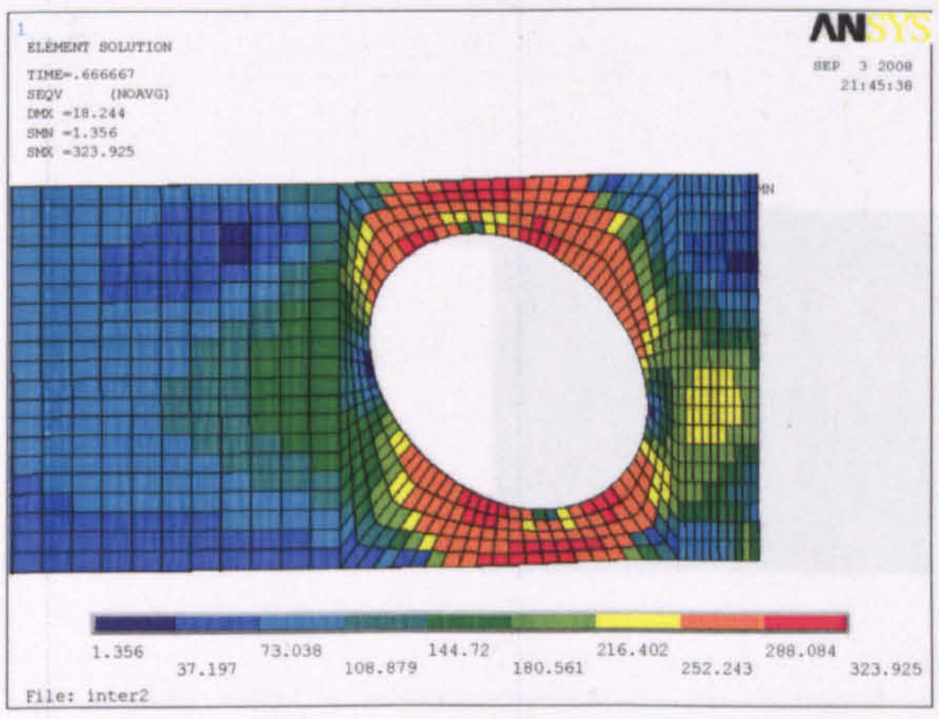

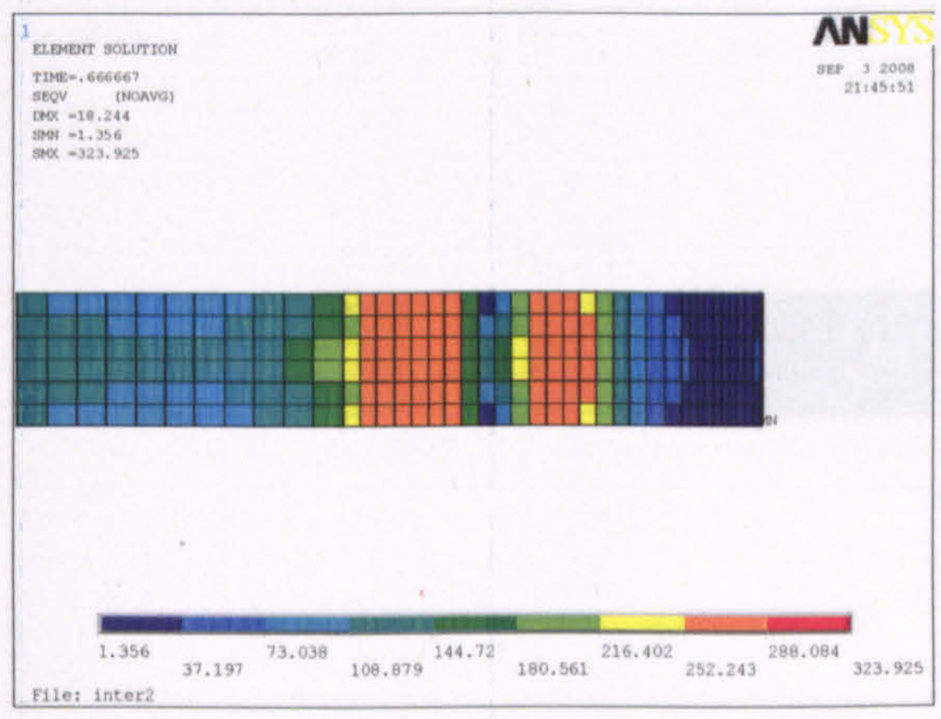

Web opening G

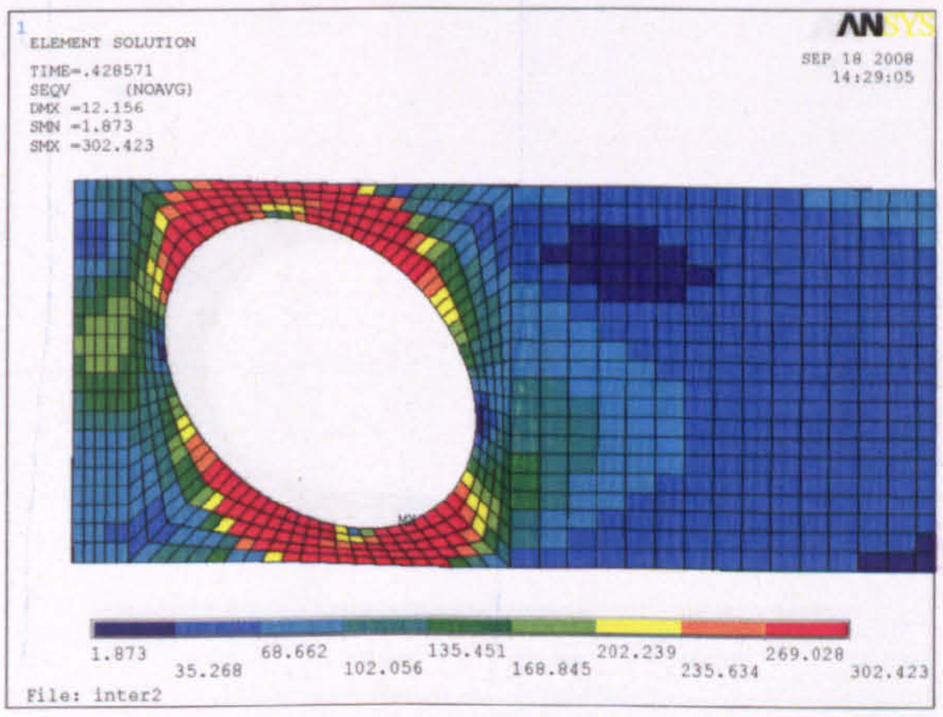

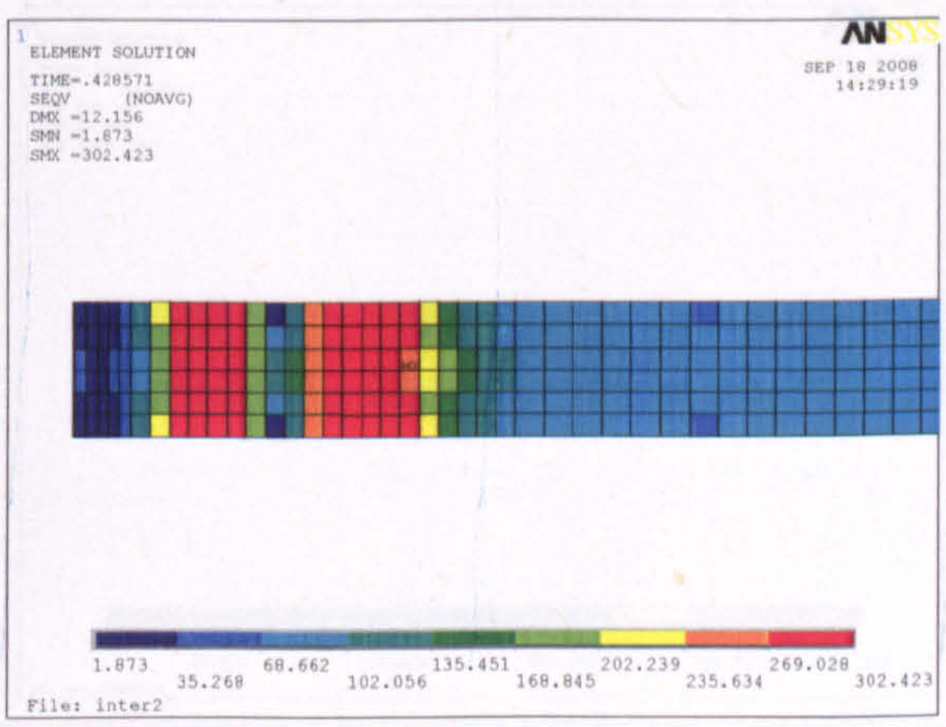

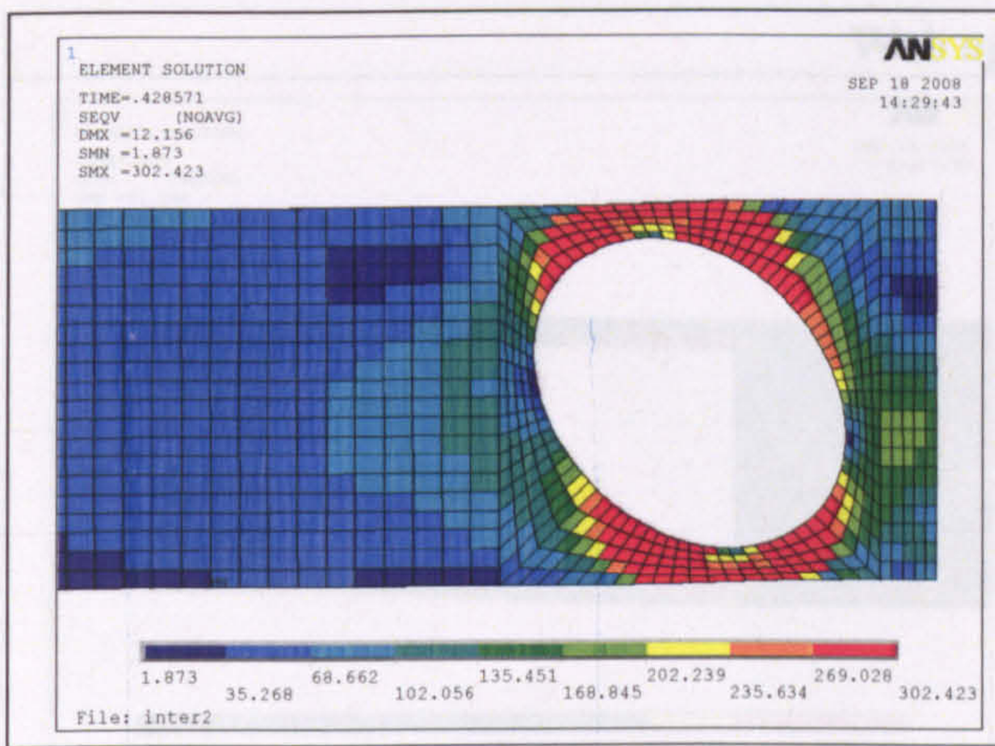

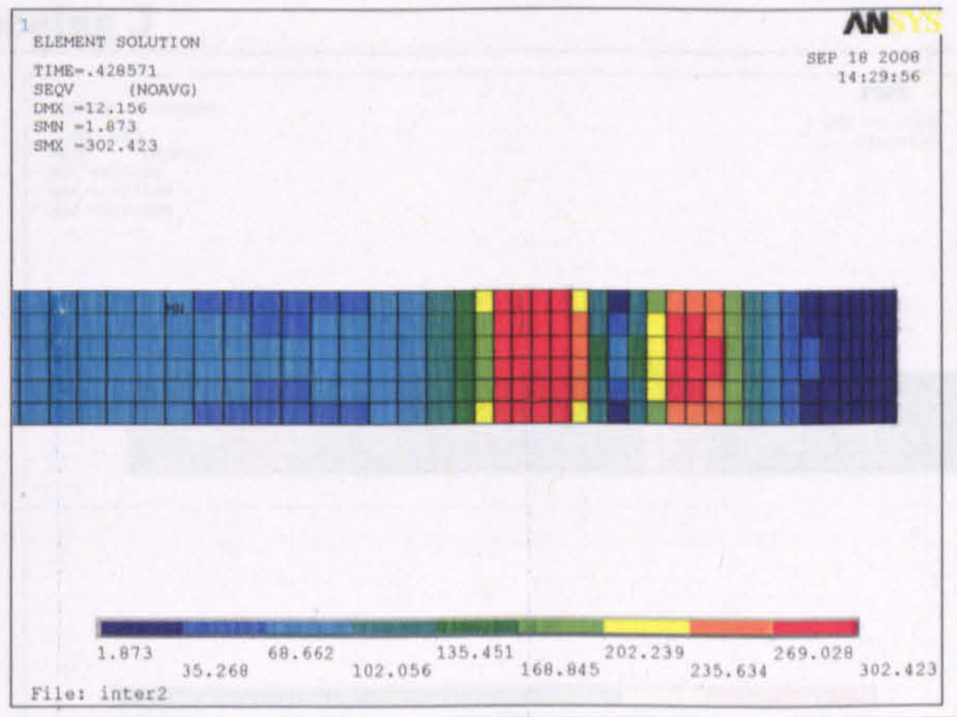

Web opening H

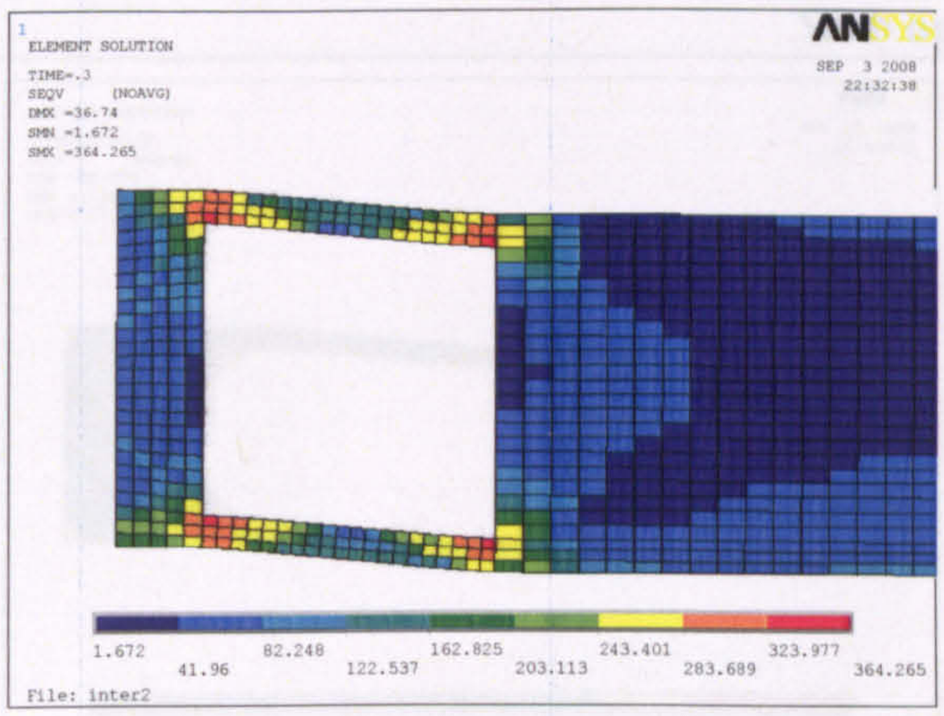

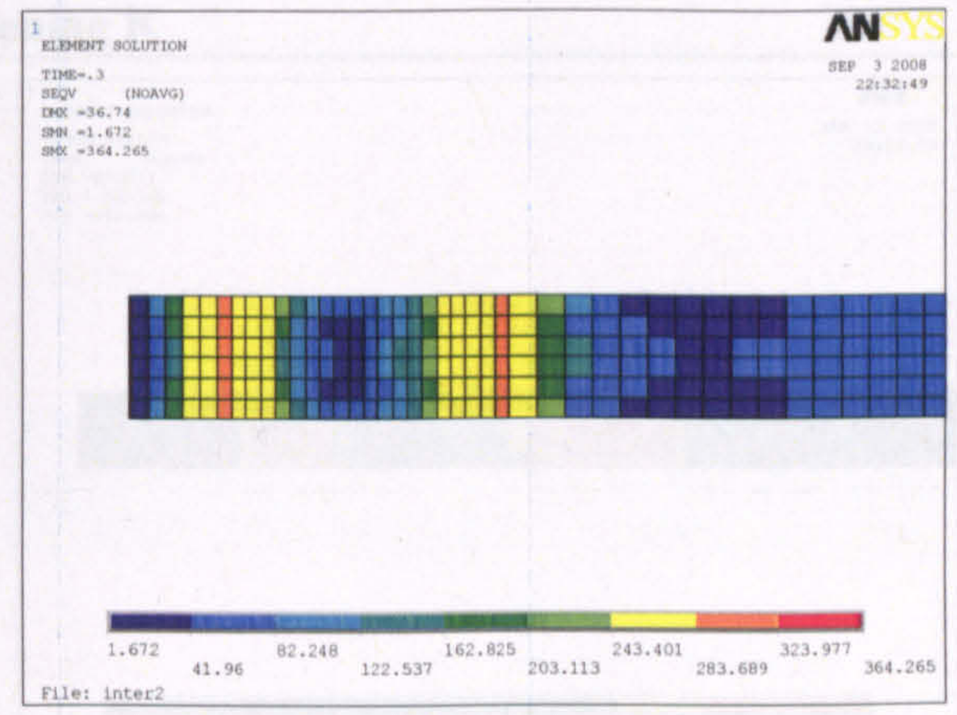

Web opening I

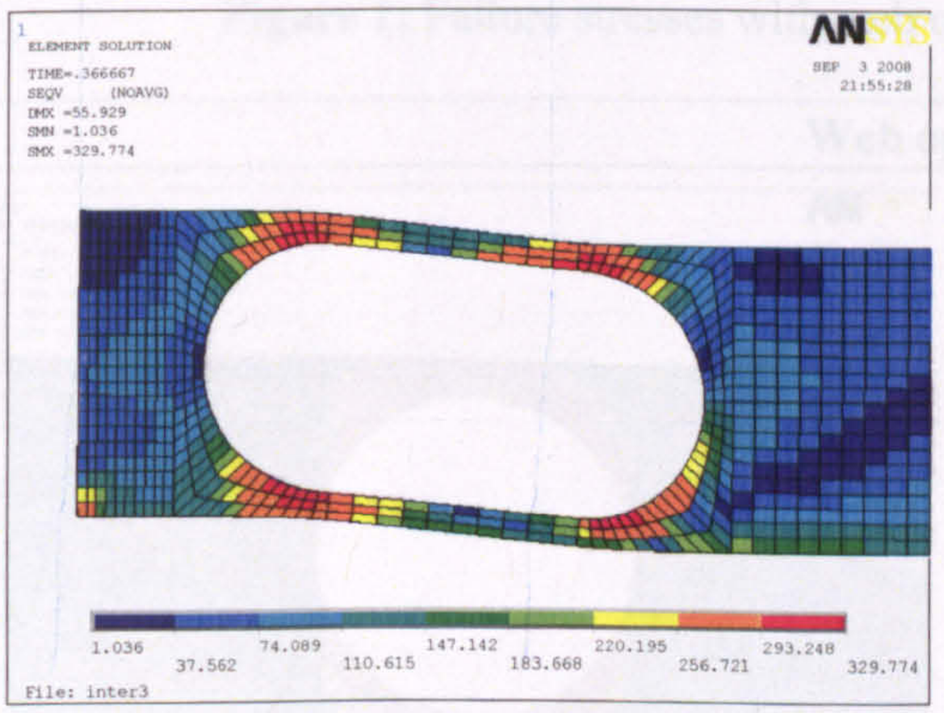

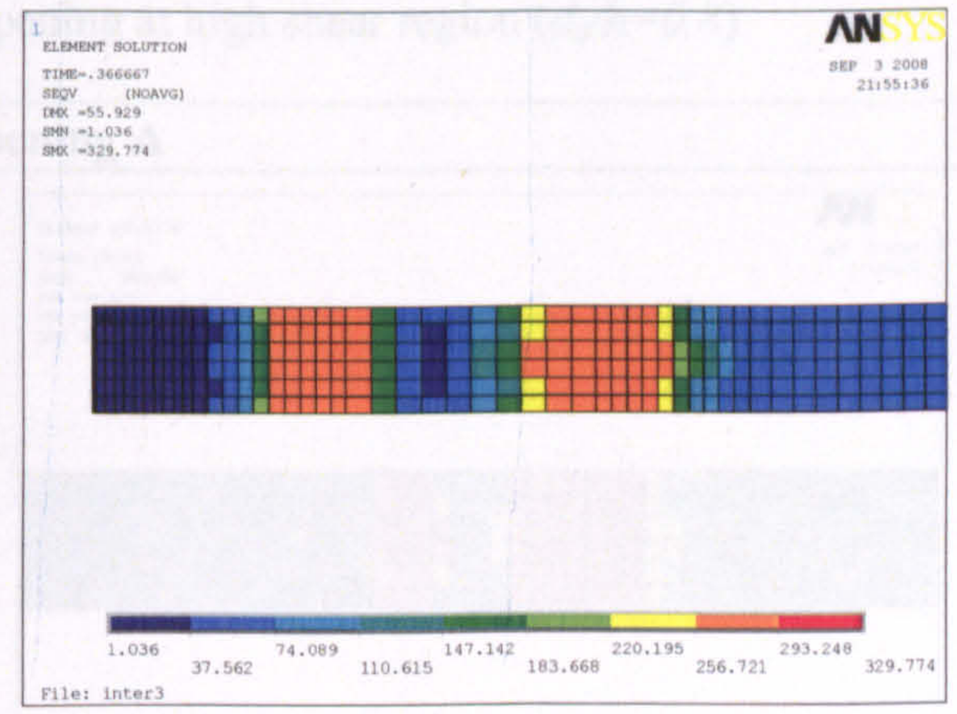

Web opening J

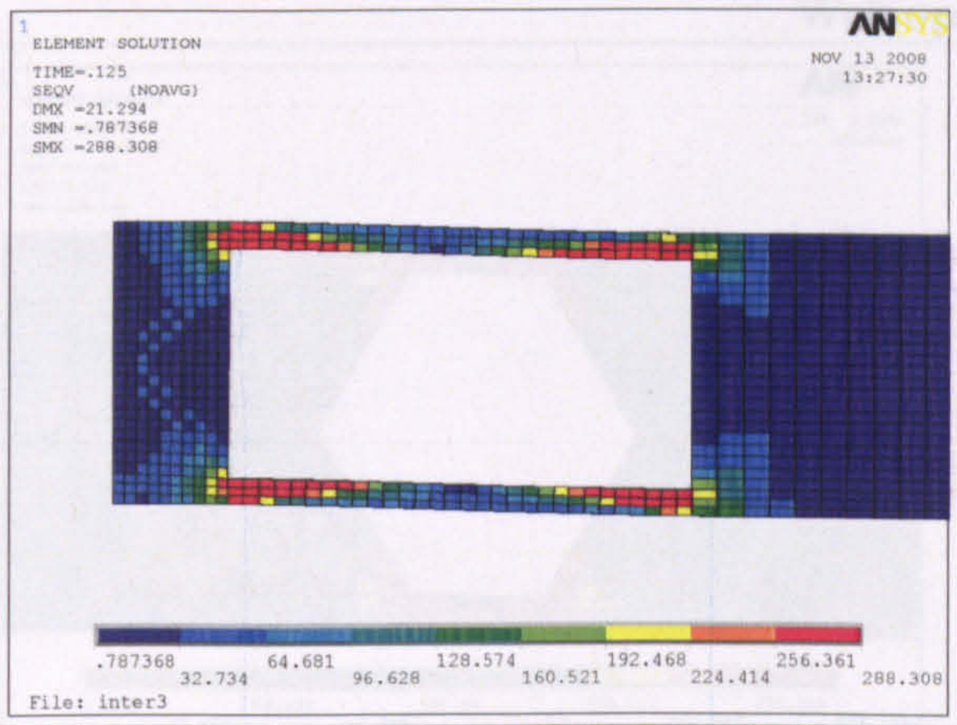

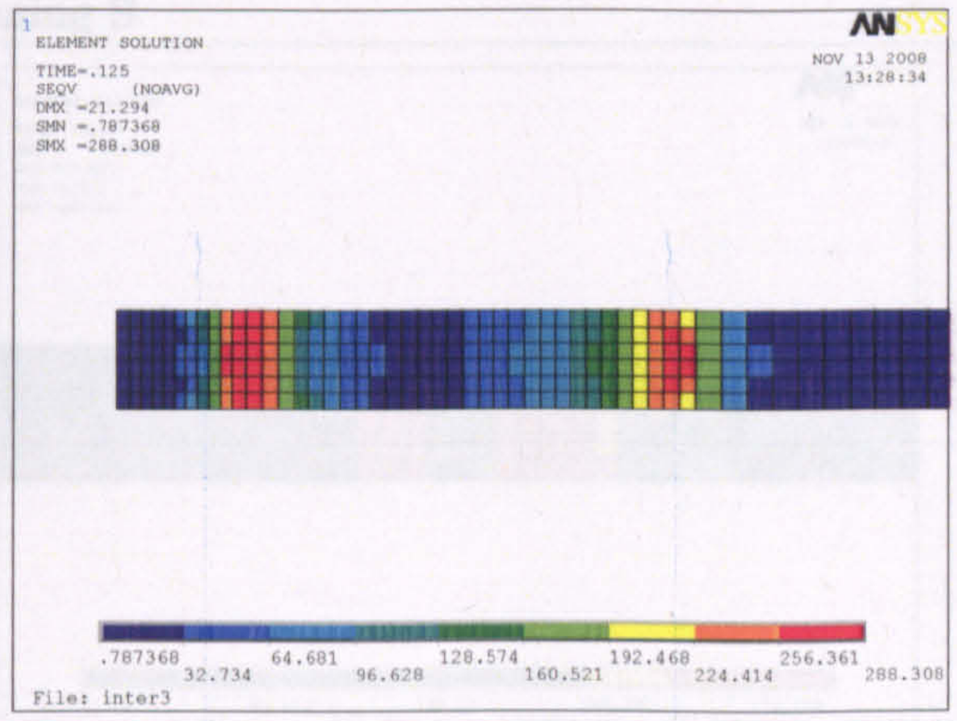

Web opening K

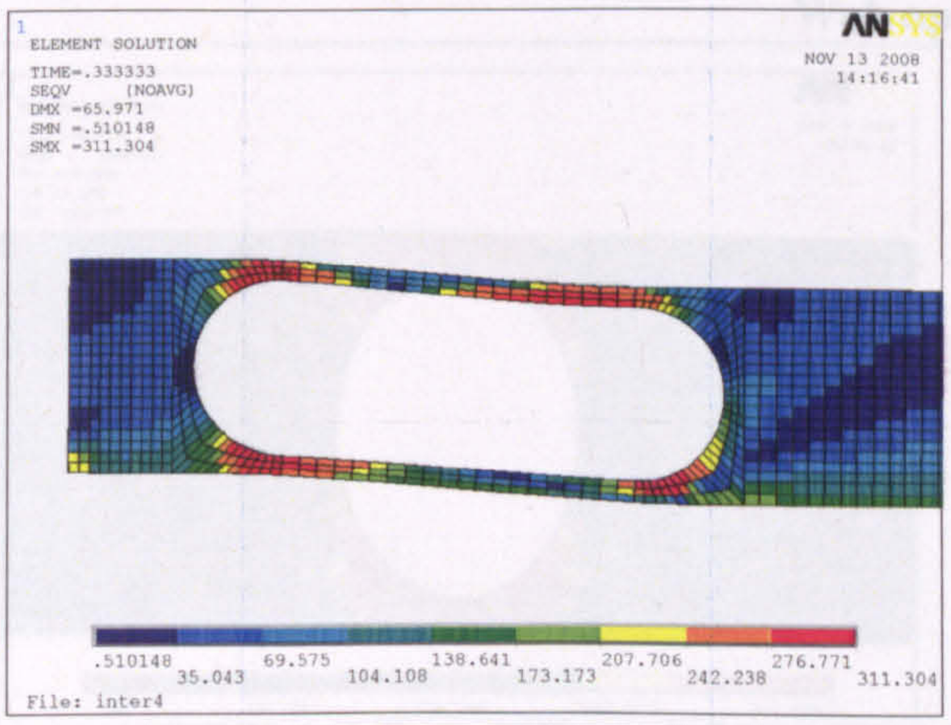

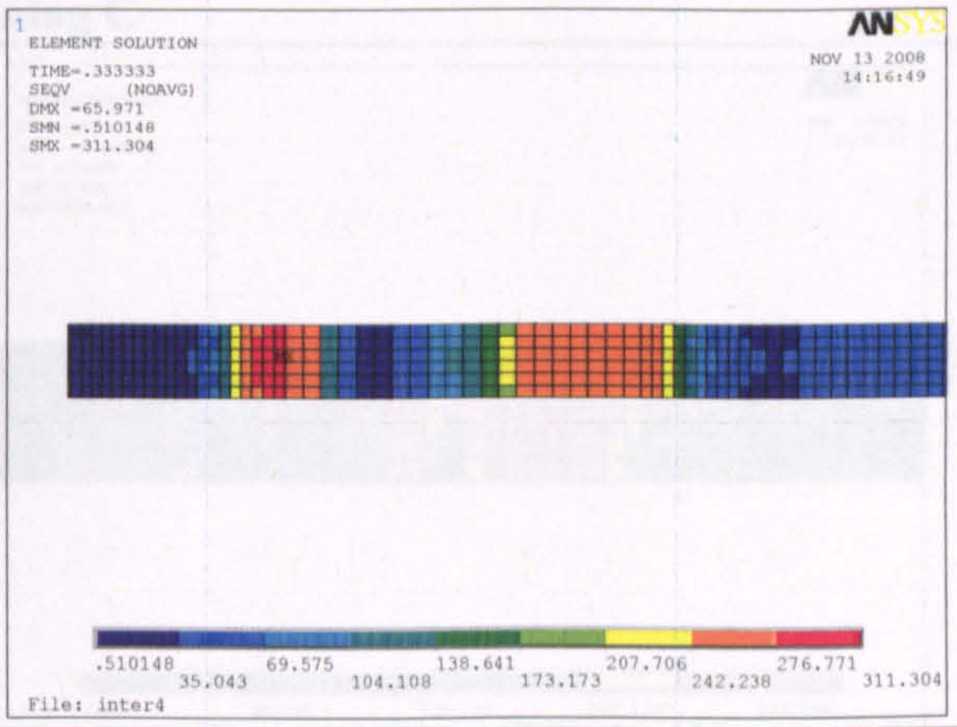

Figure 1: Failure stresses with web opening at high shear region ($d_o/h=0.8$)

Web opening A

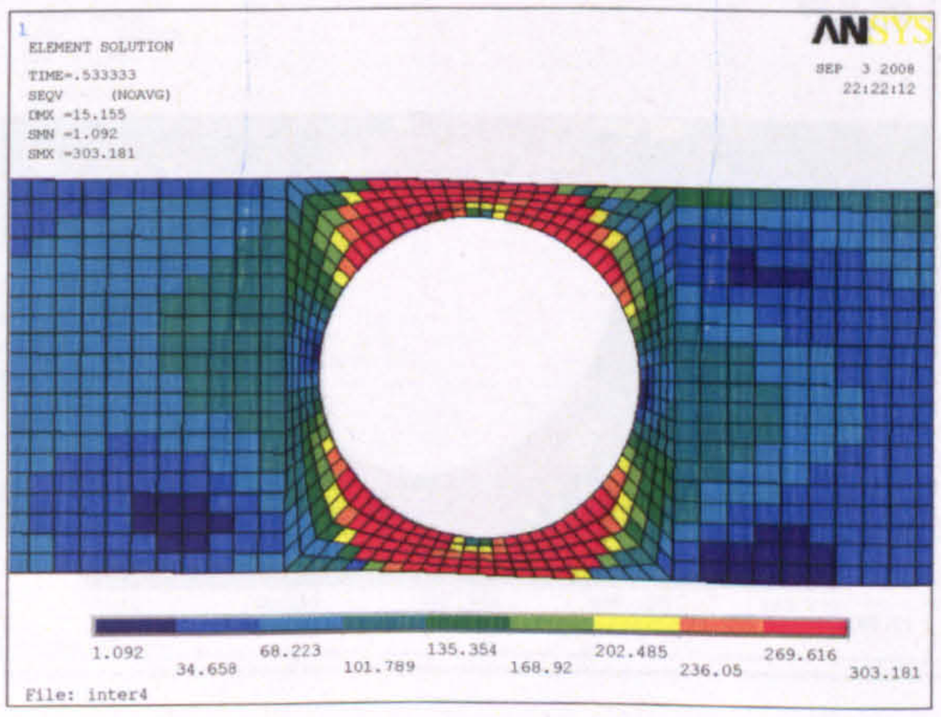

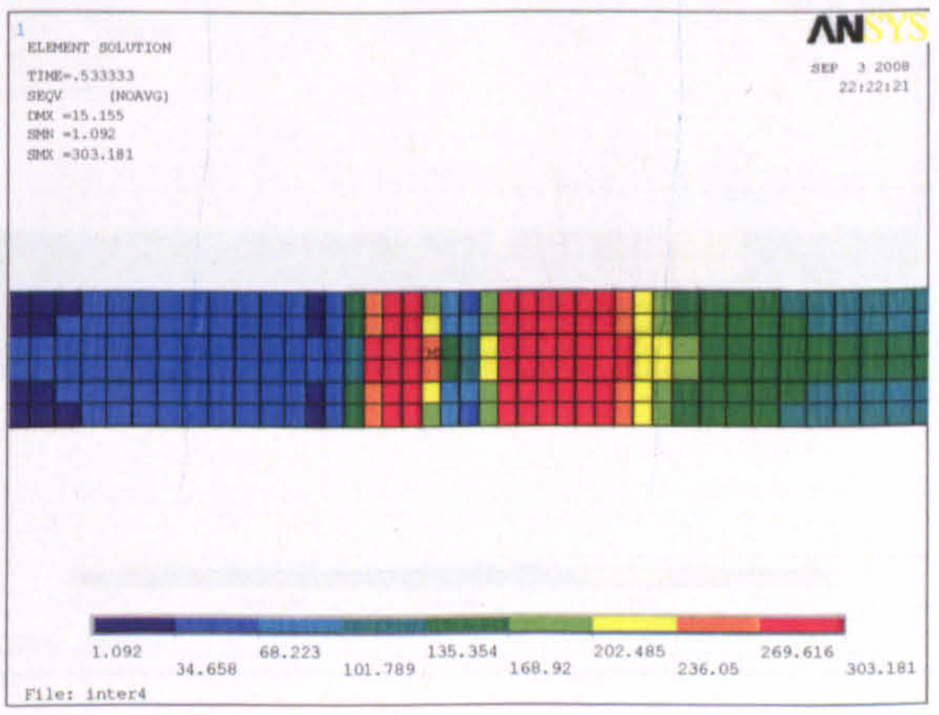

Web opening B

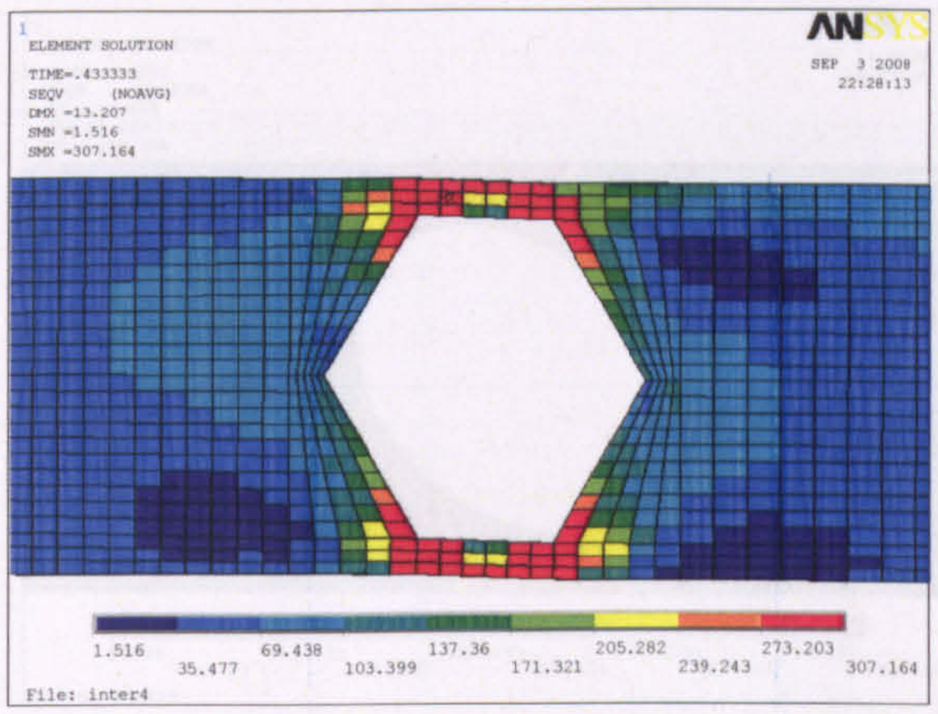

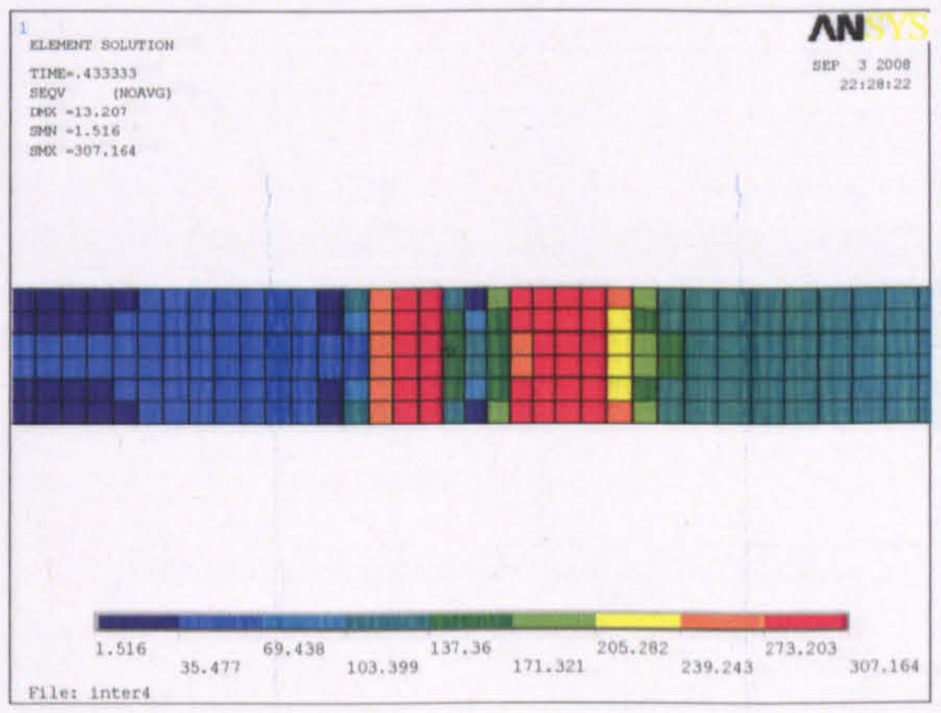

Web opening C

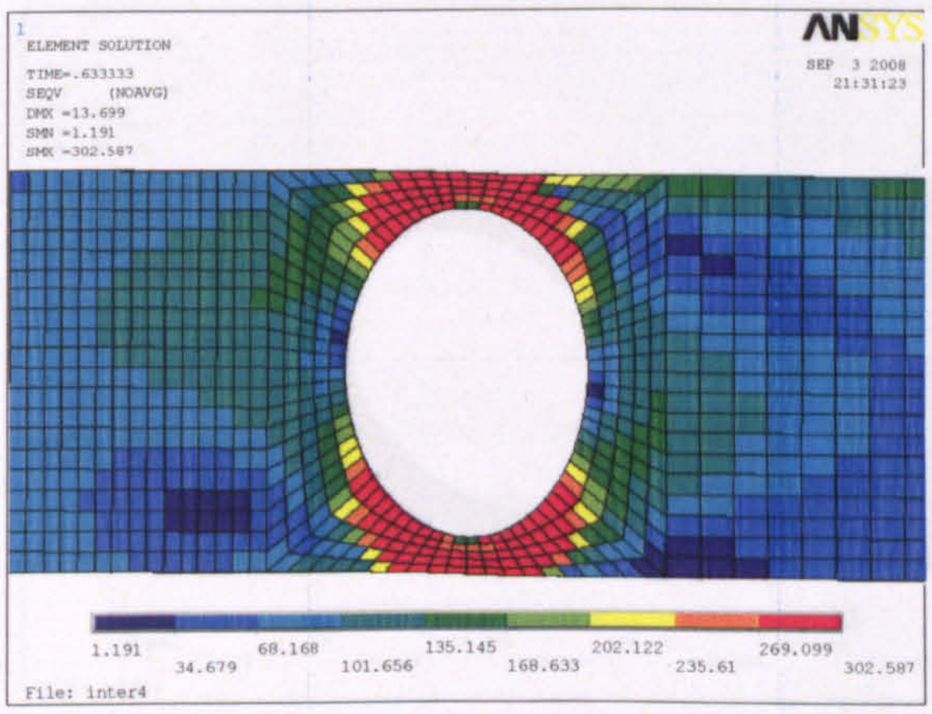

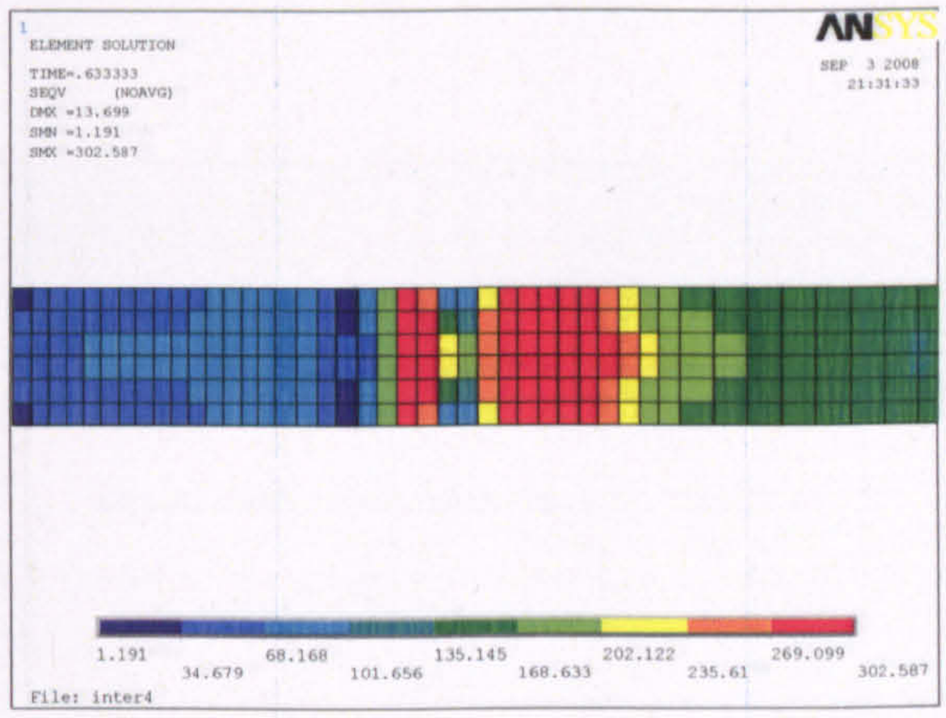

Web opening D

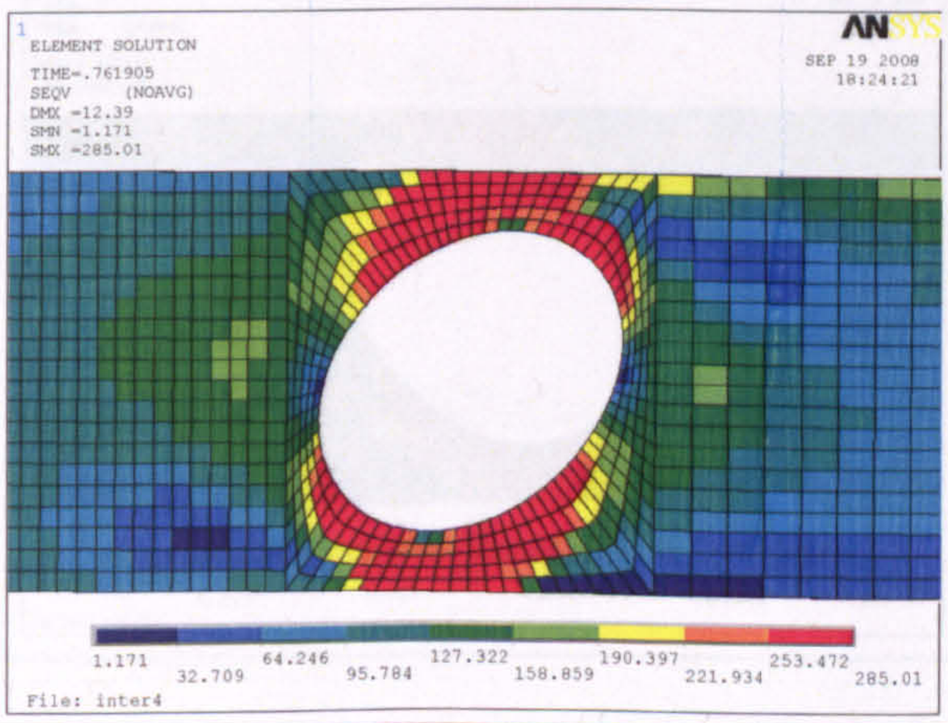

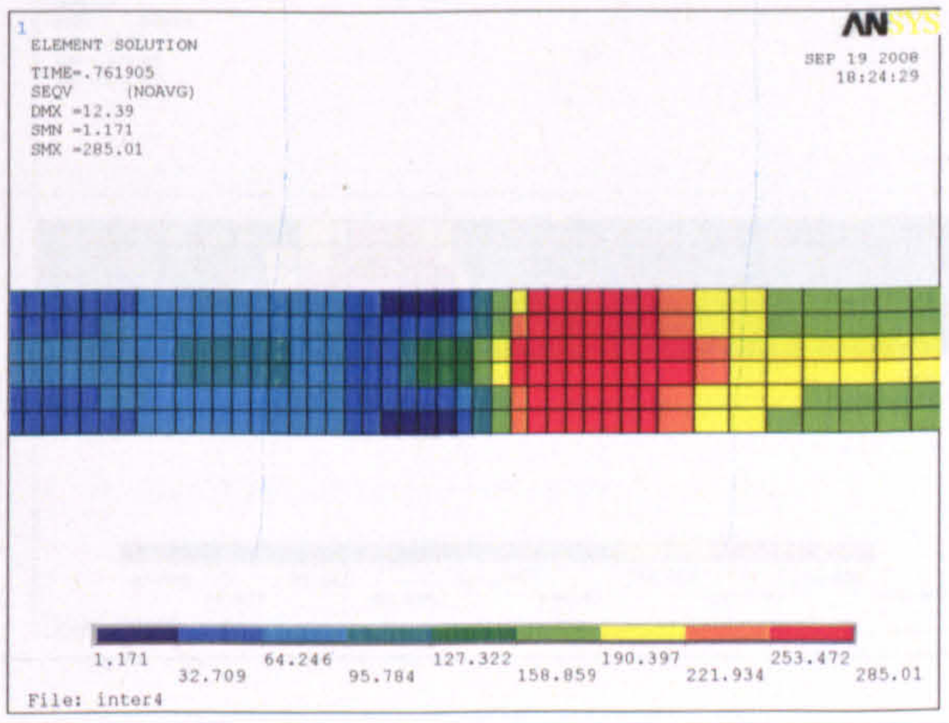

Web opening E

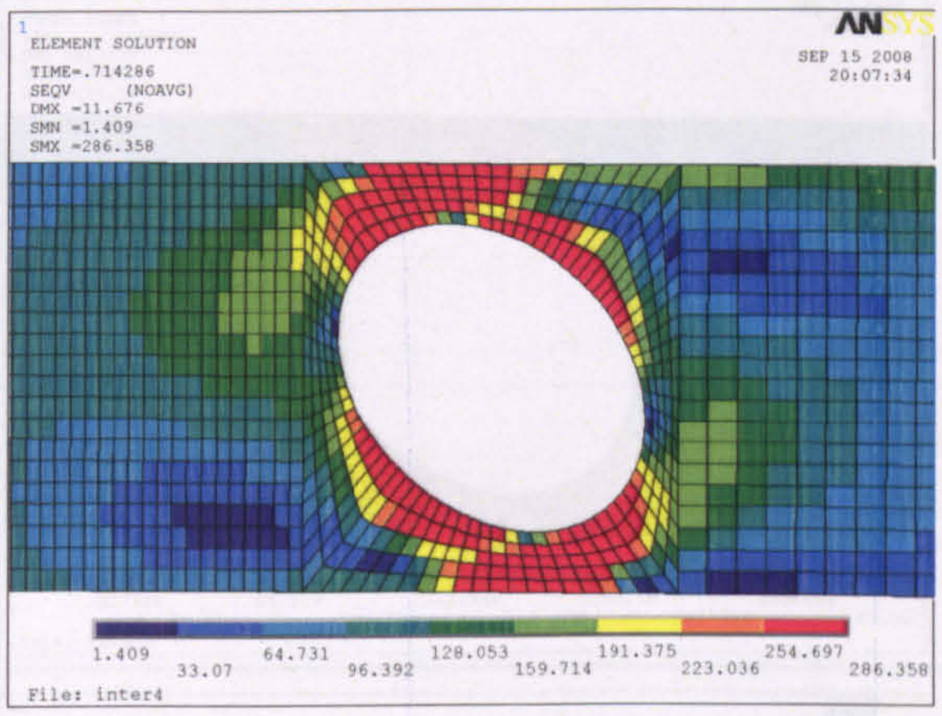

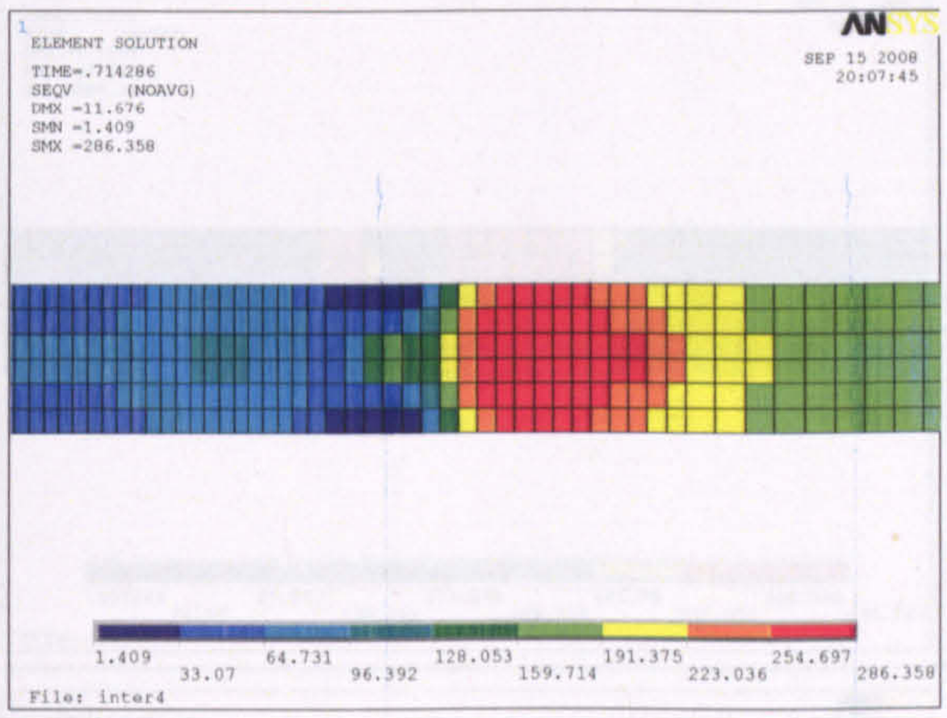

Web opening F

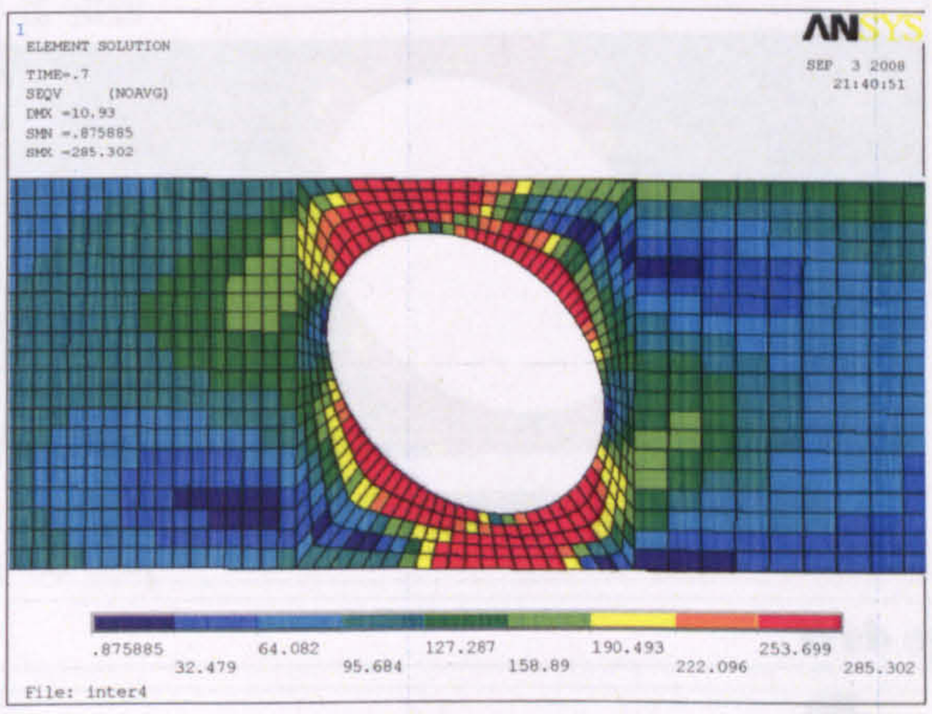

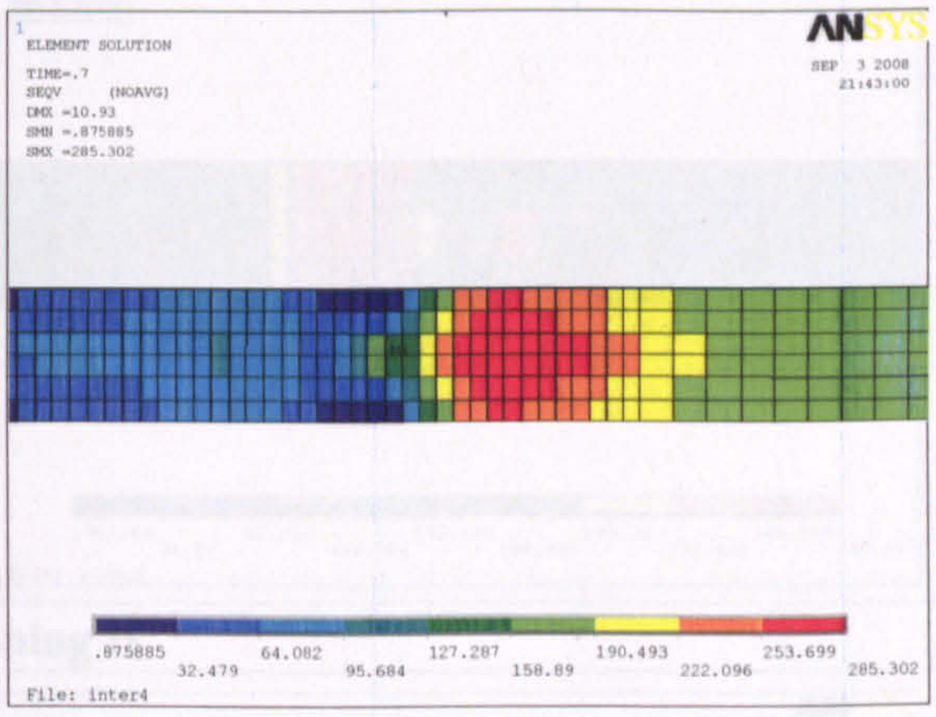

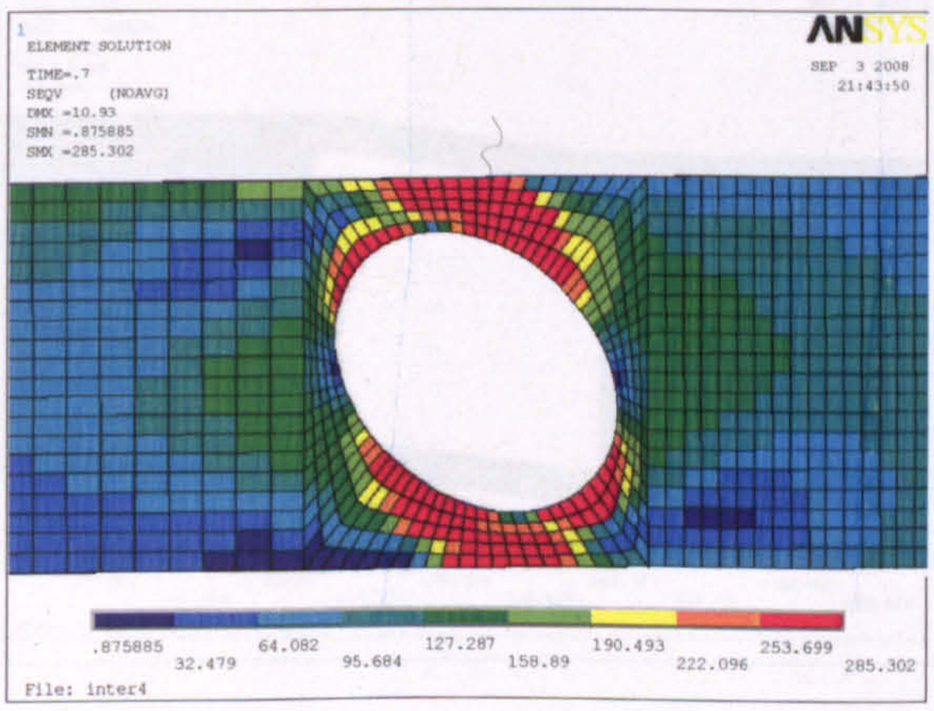

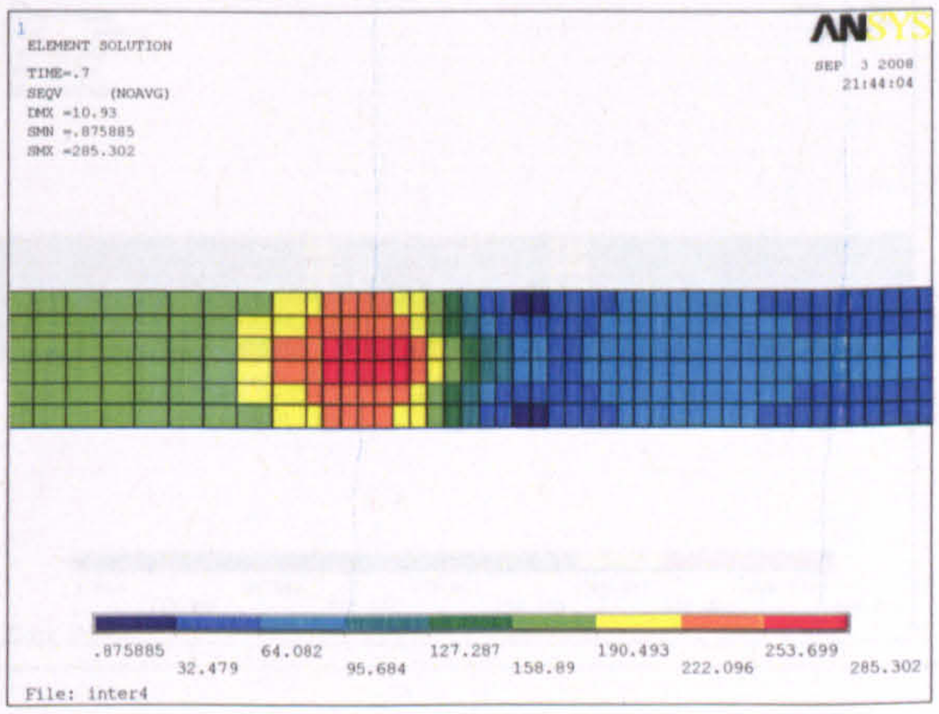

Web opening G

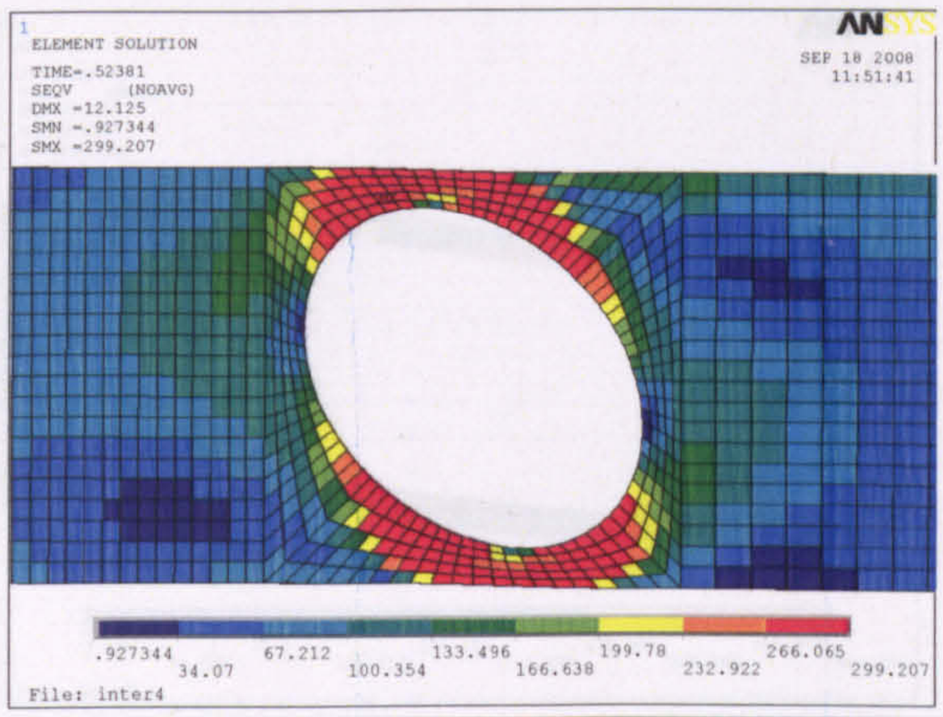

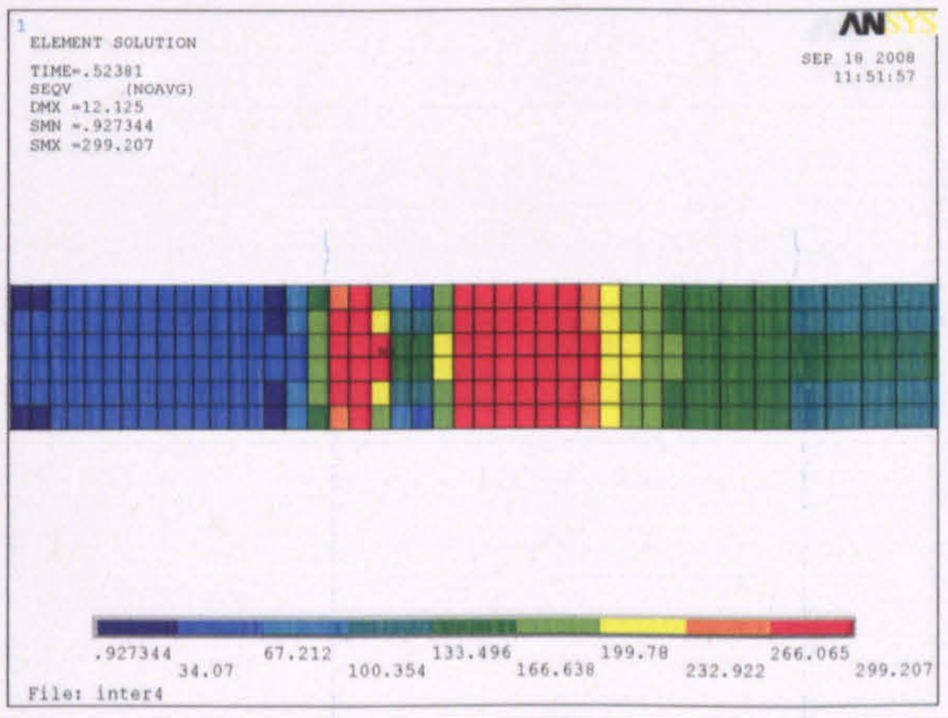

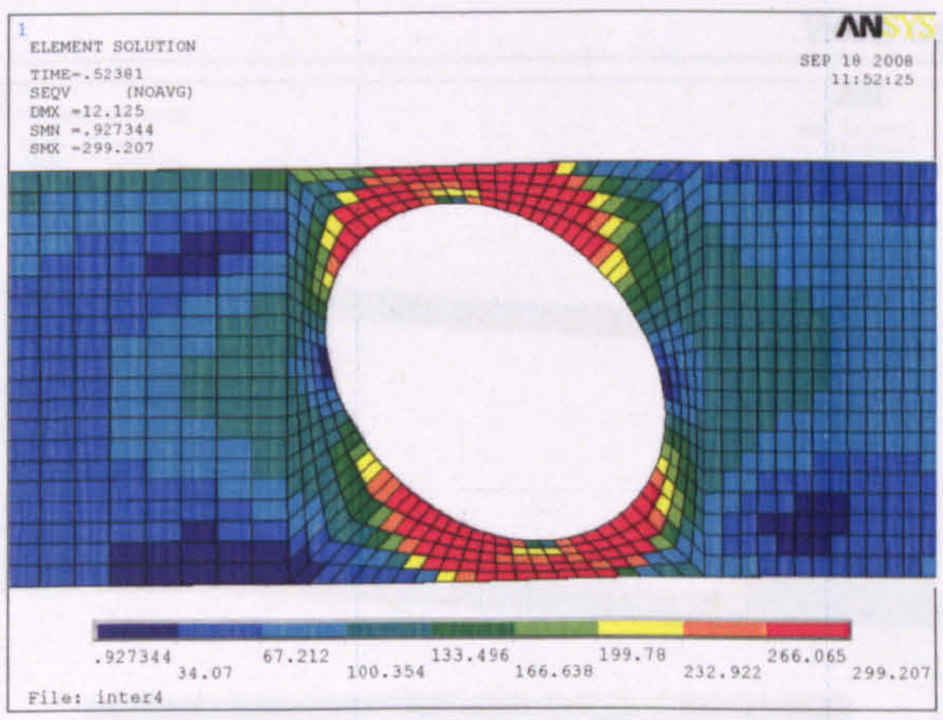

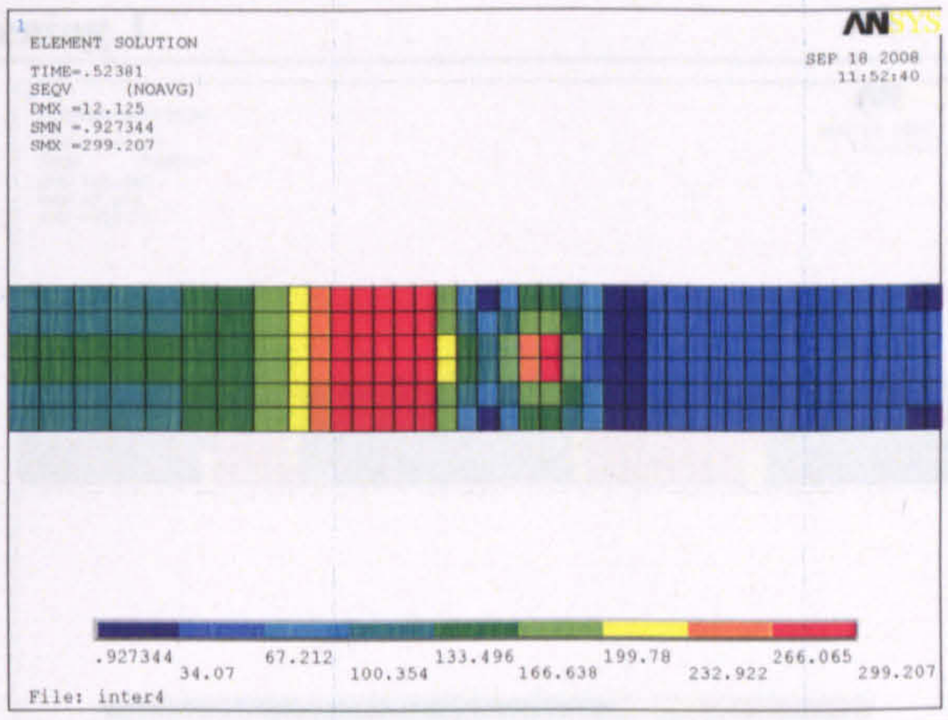

Web opening H

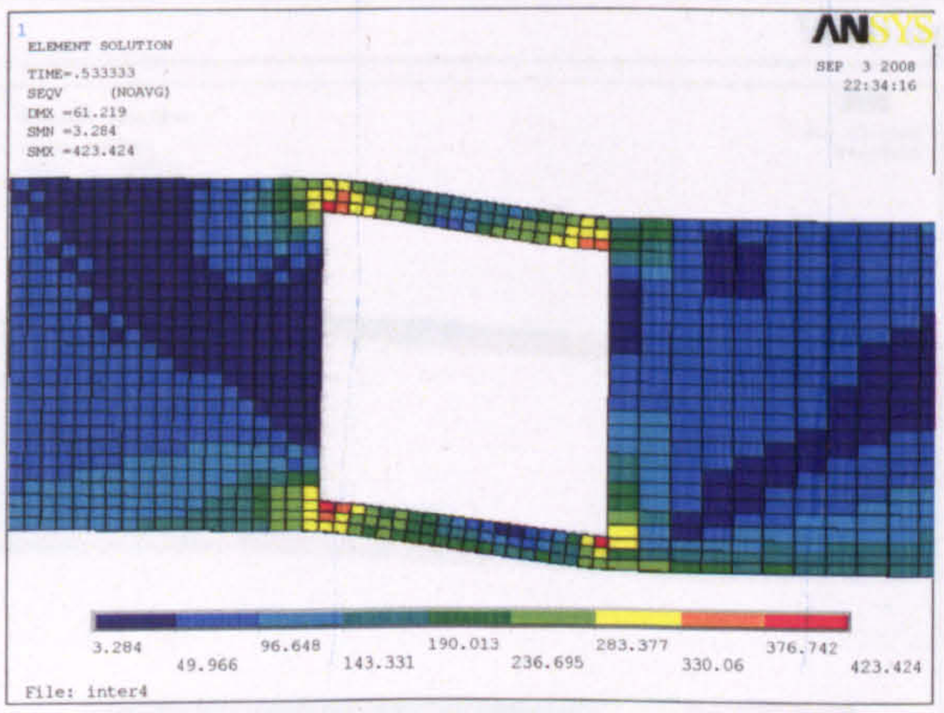

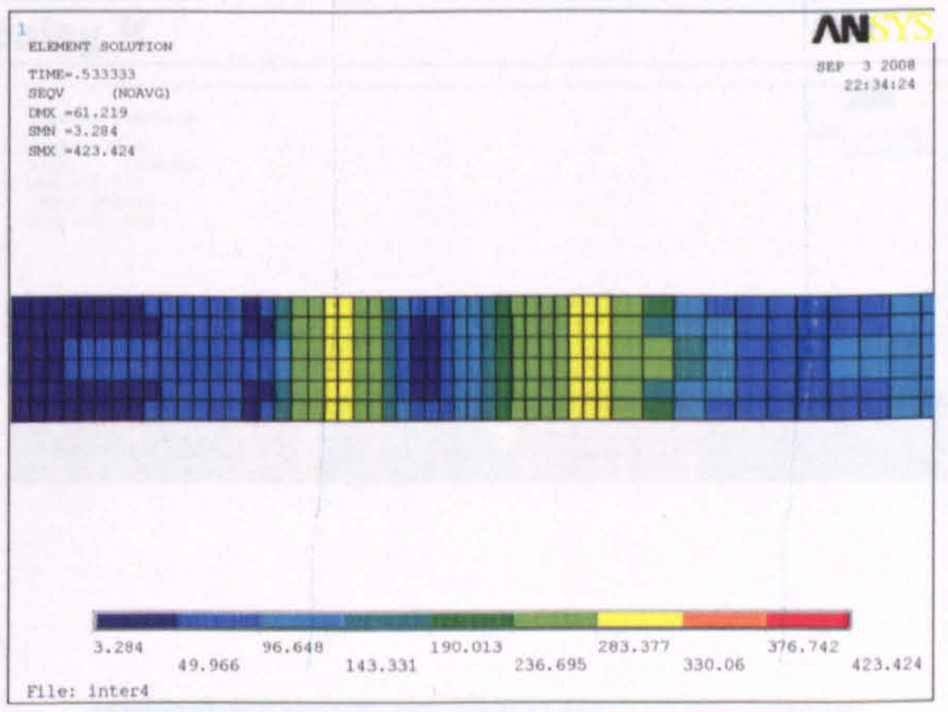

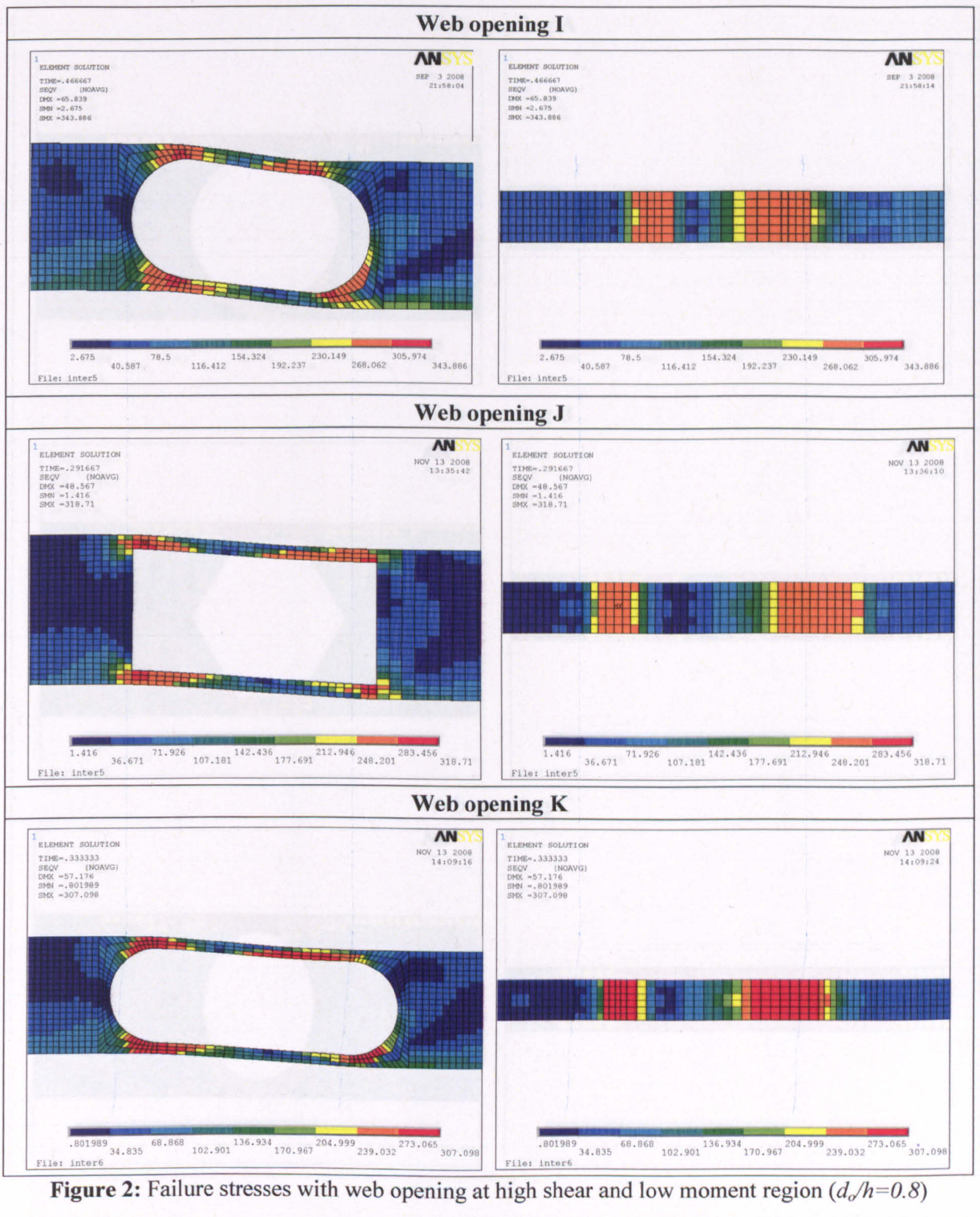

Figure 2: Failure stresses with web opening at high shear and low moment region ($d_o/h=0.8$)

Web opening A

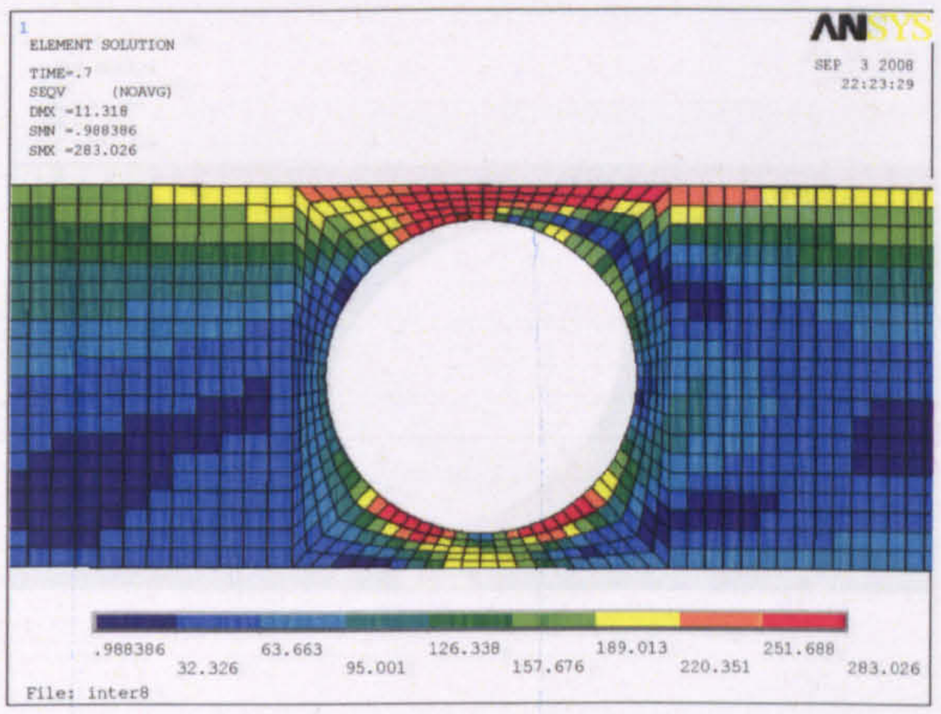

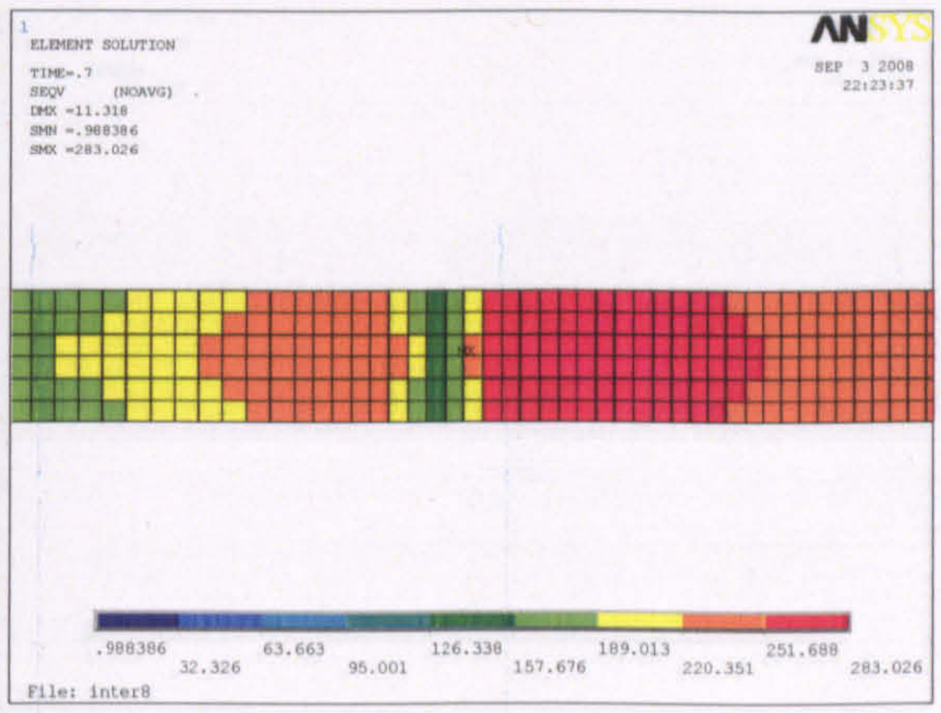

Web opening B

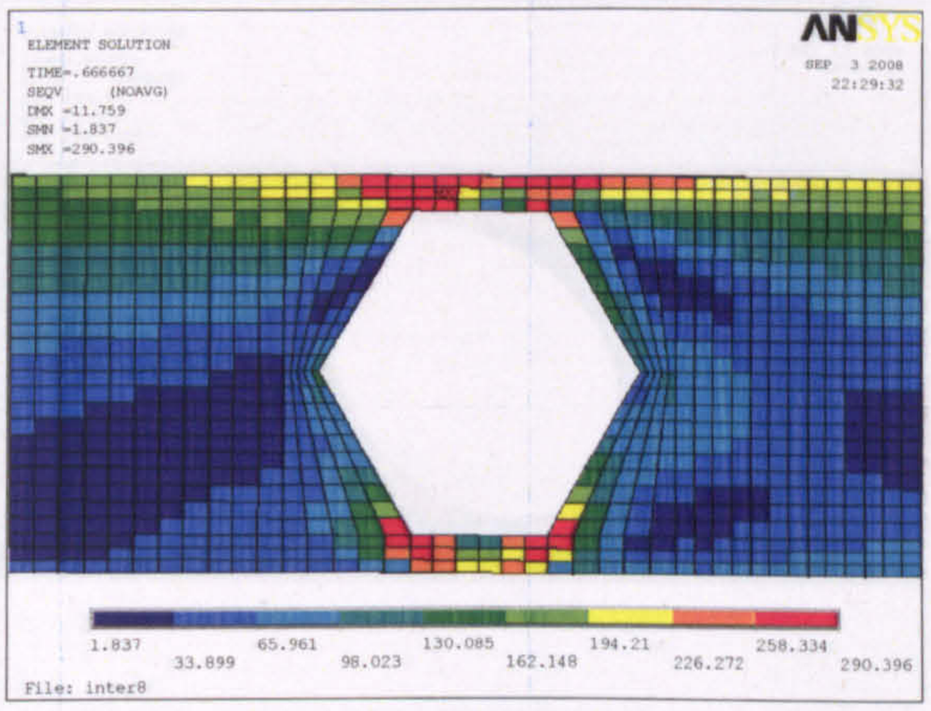

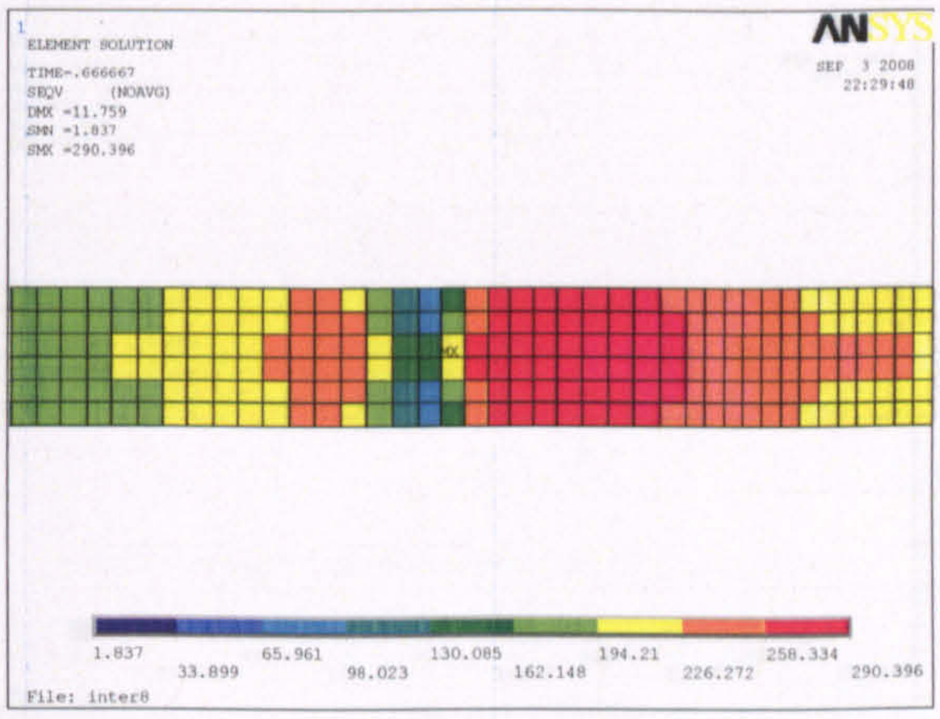

Web opening C

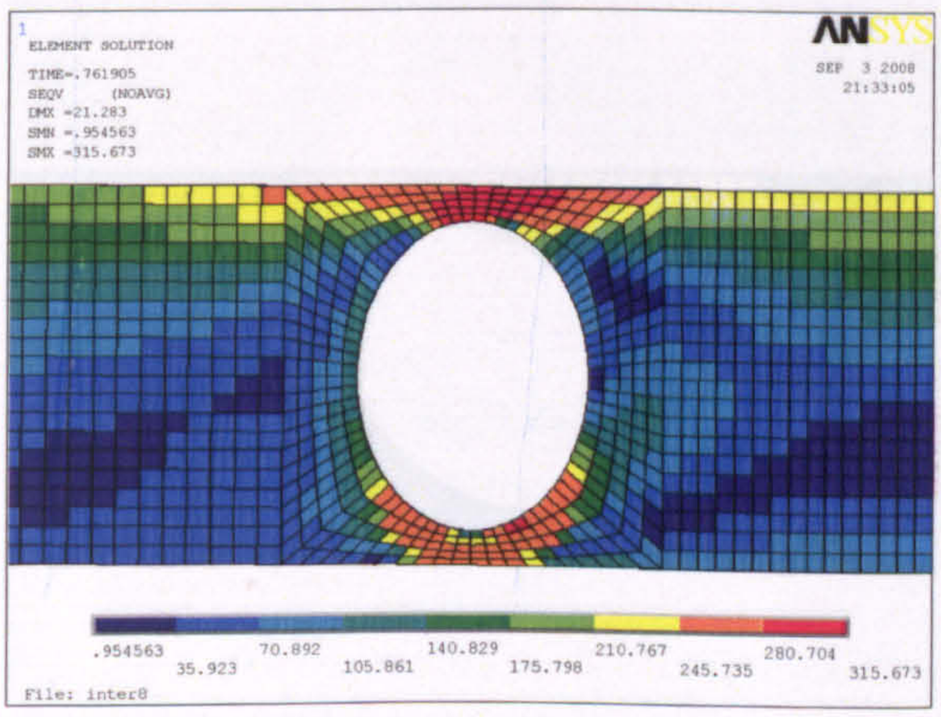

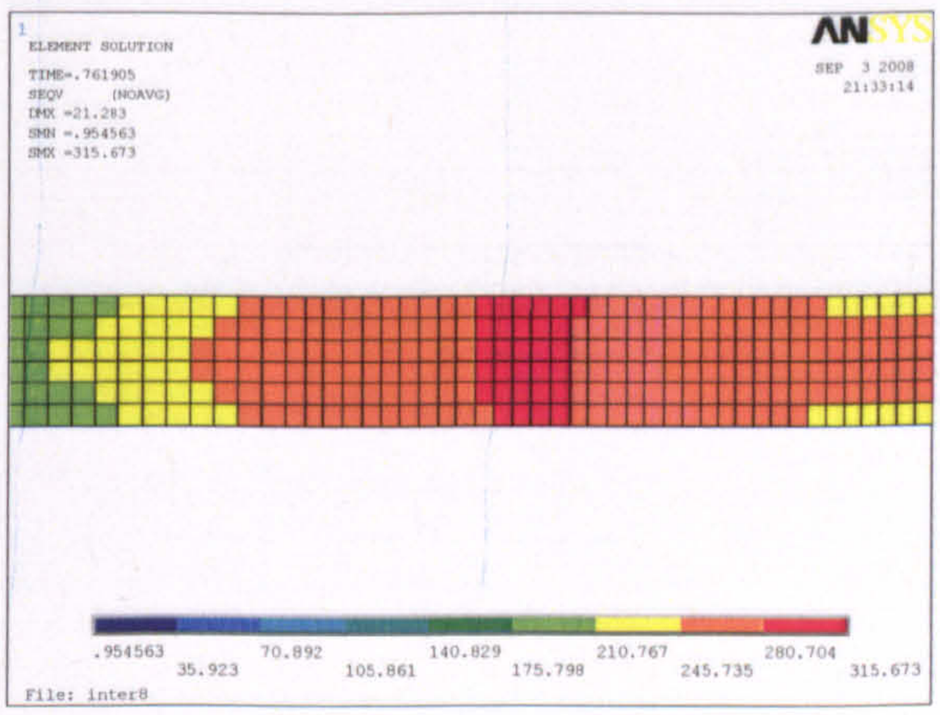

Web opening D

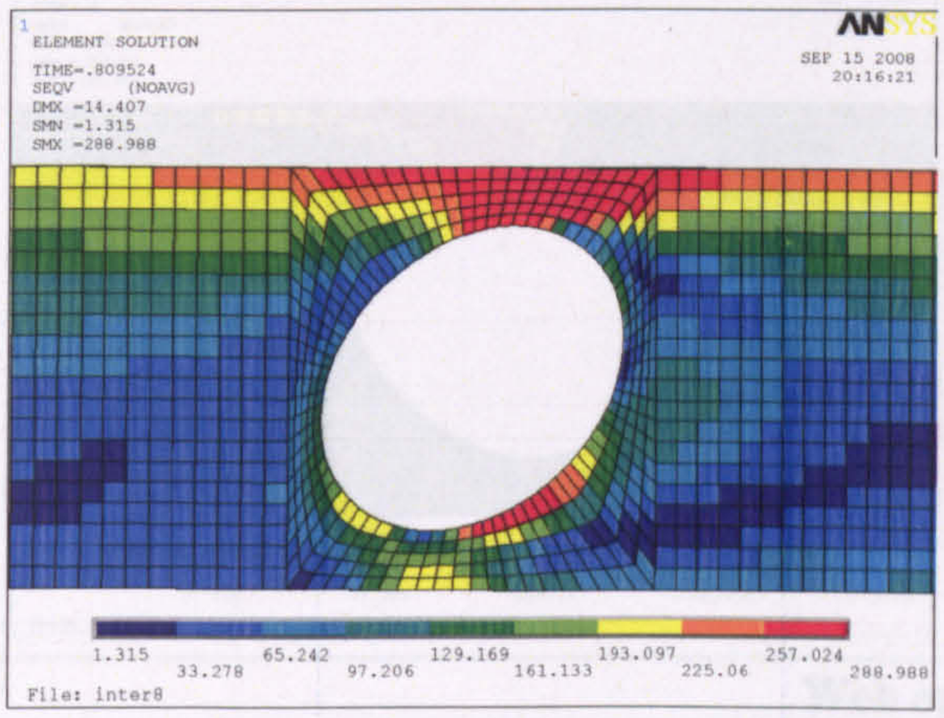

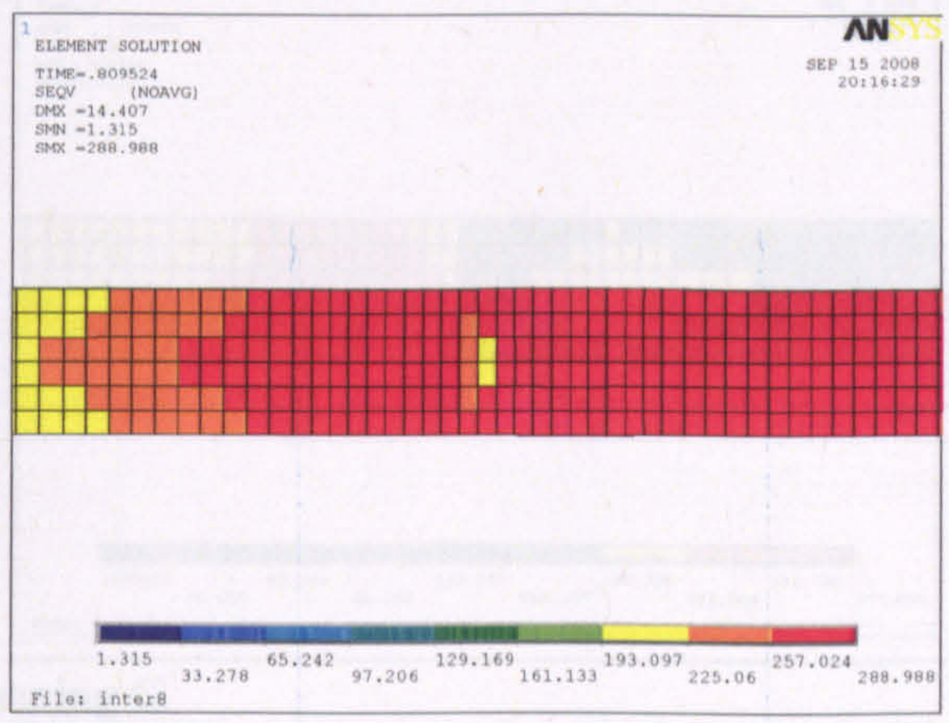

Web opening E

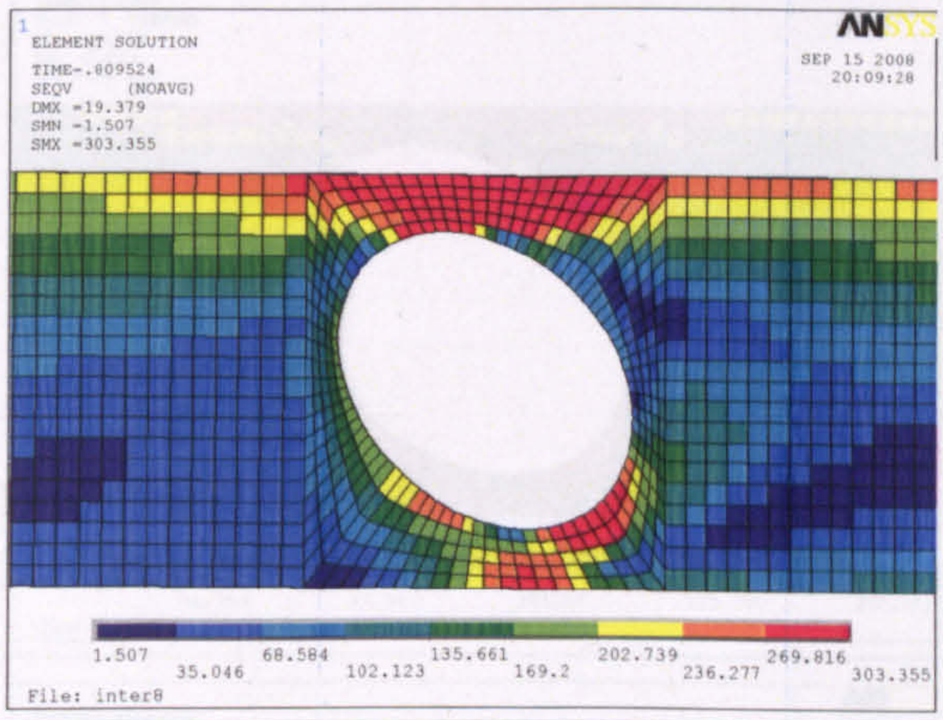

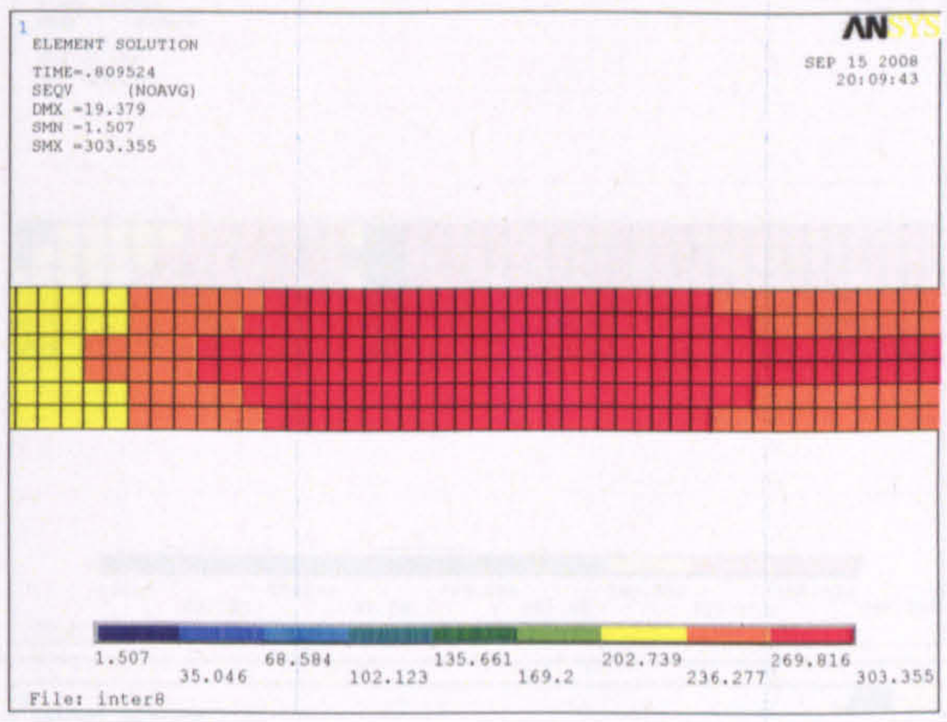

Web opening F

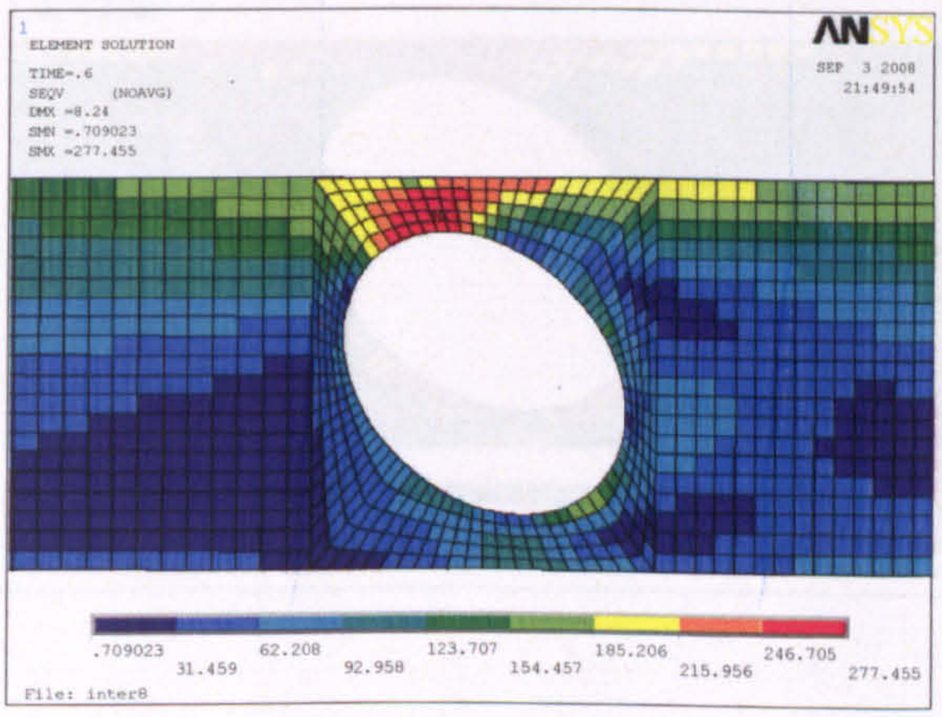

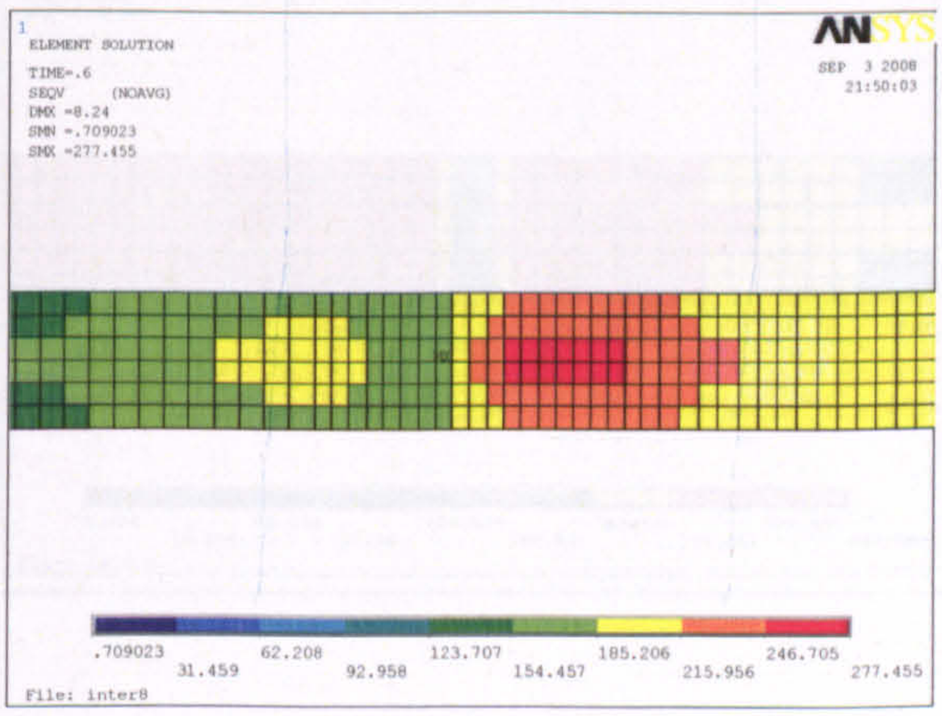

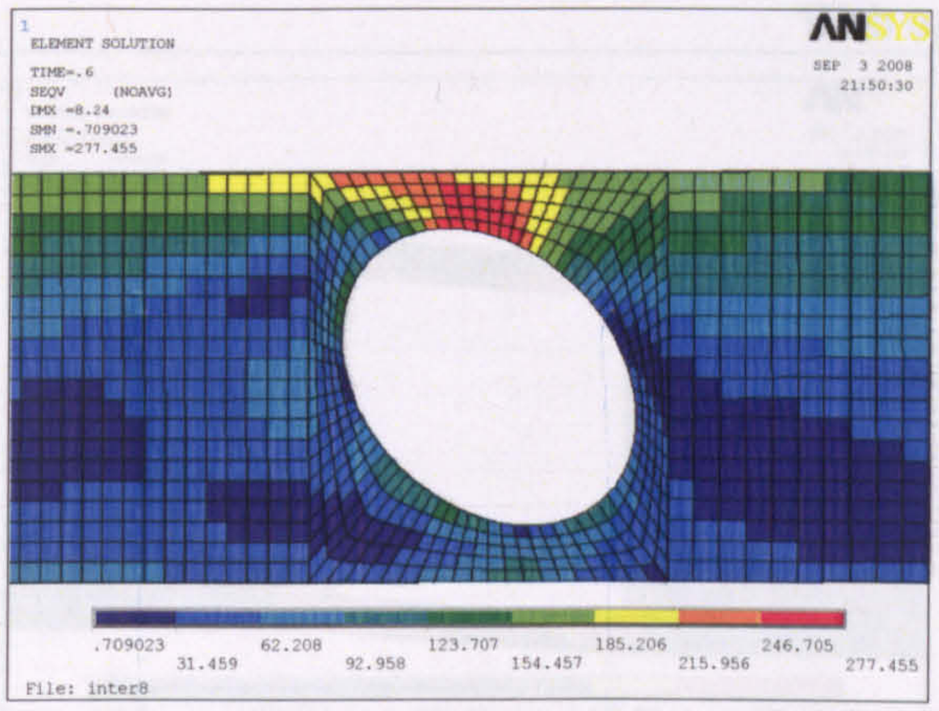

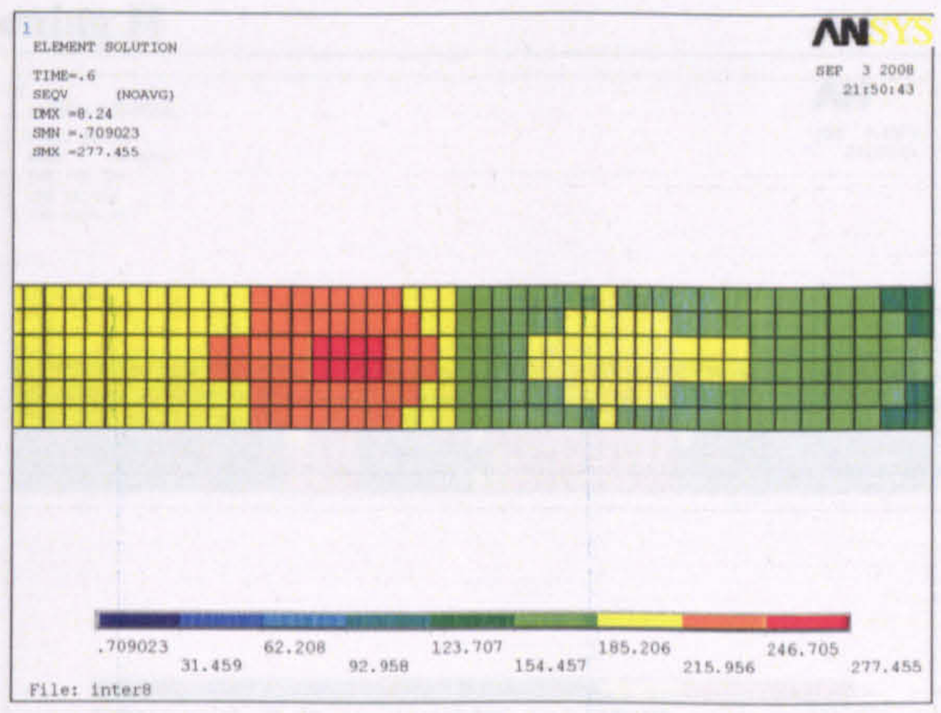

Web opening G

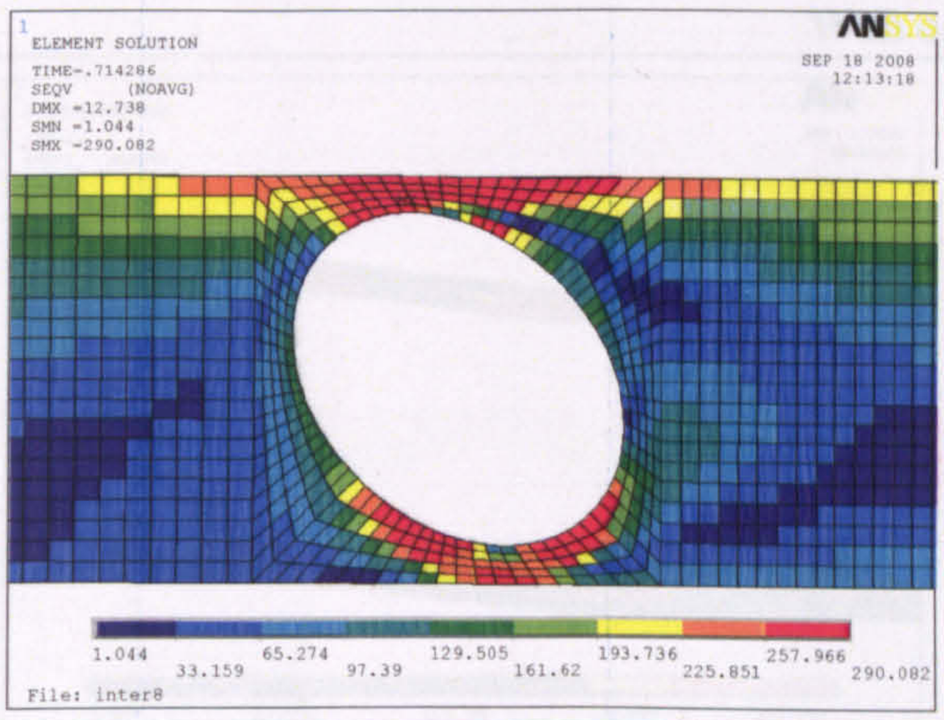

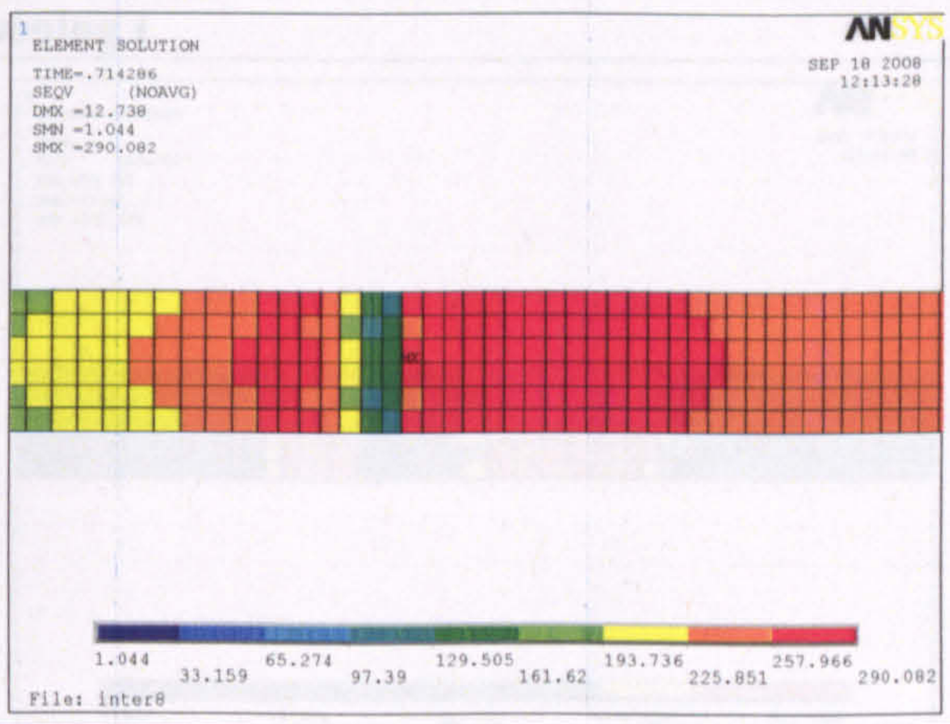

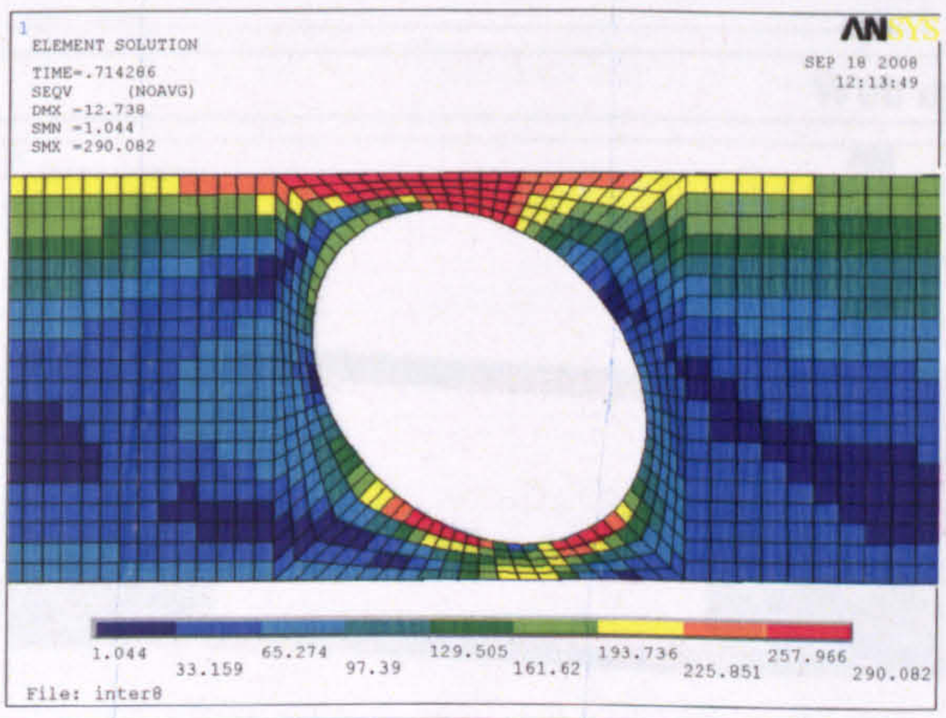

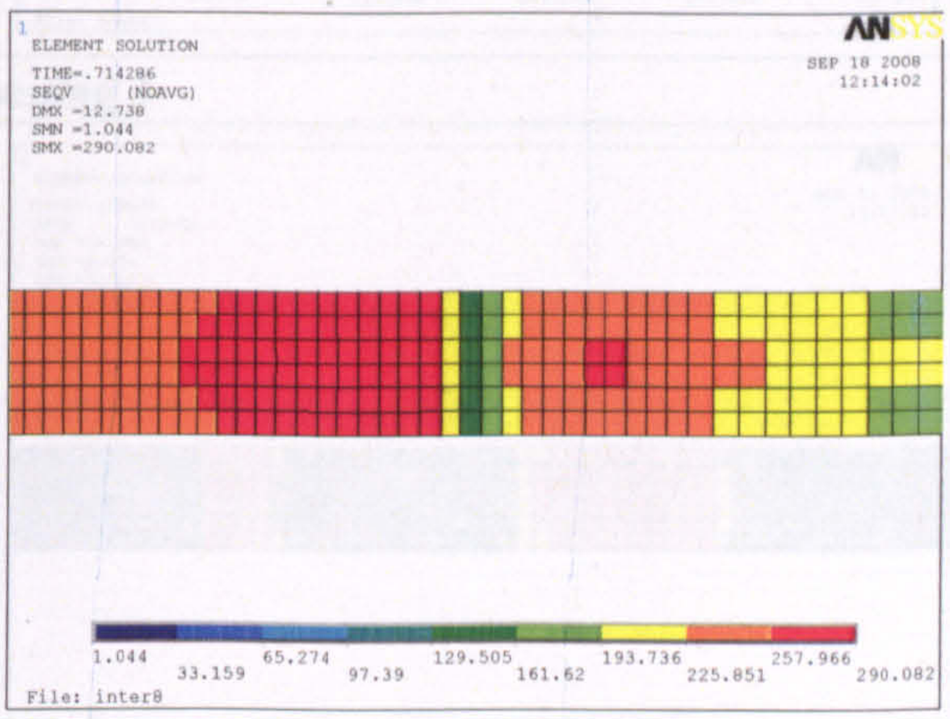

Web opening H

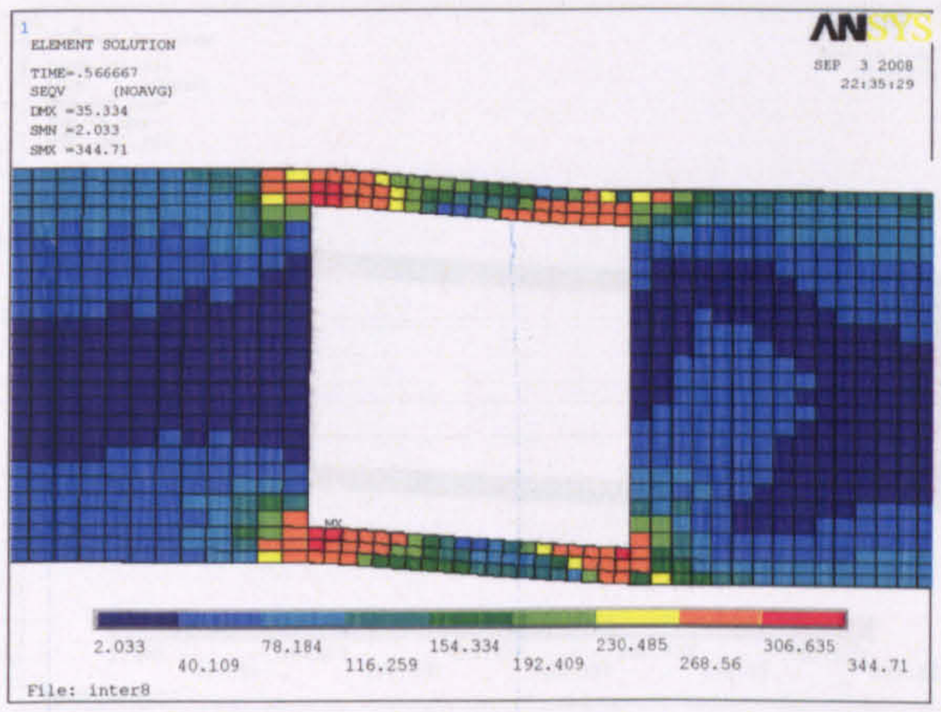

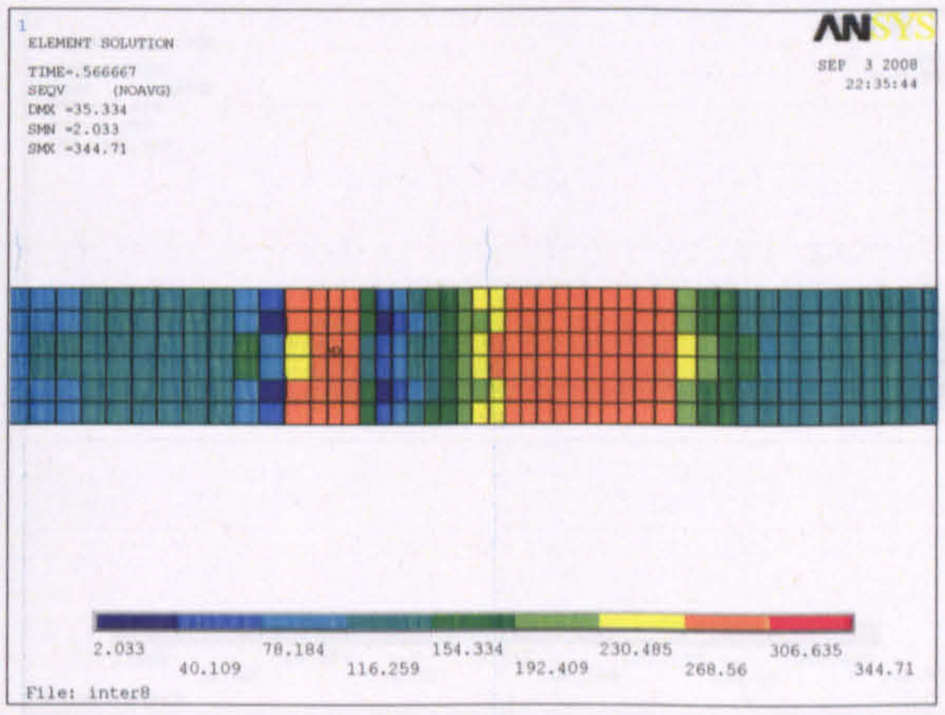

Web opening I

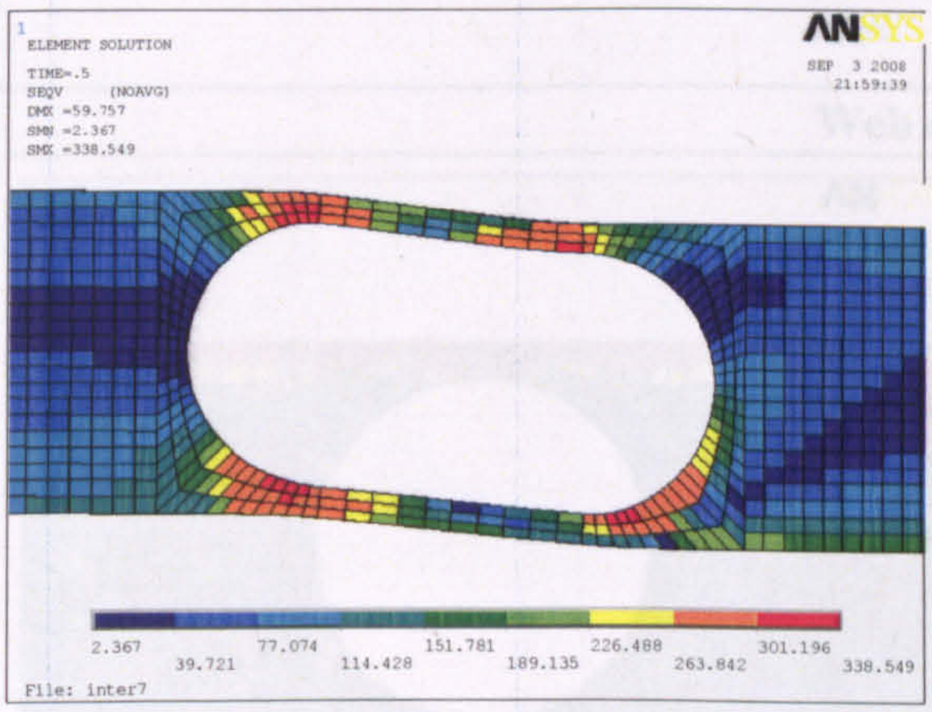

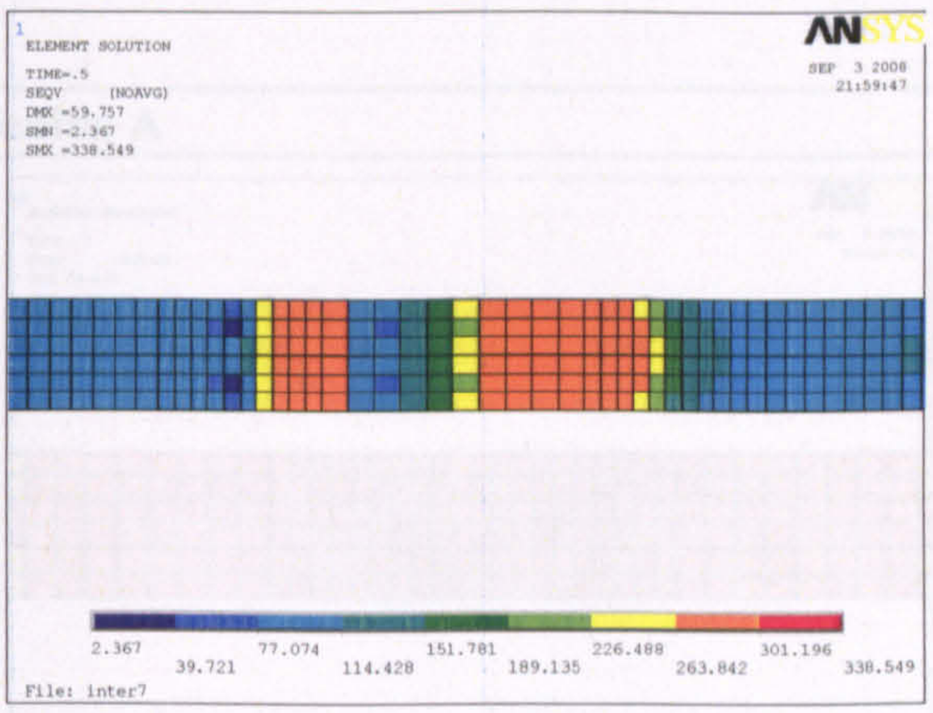

Web opening J

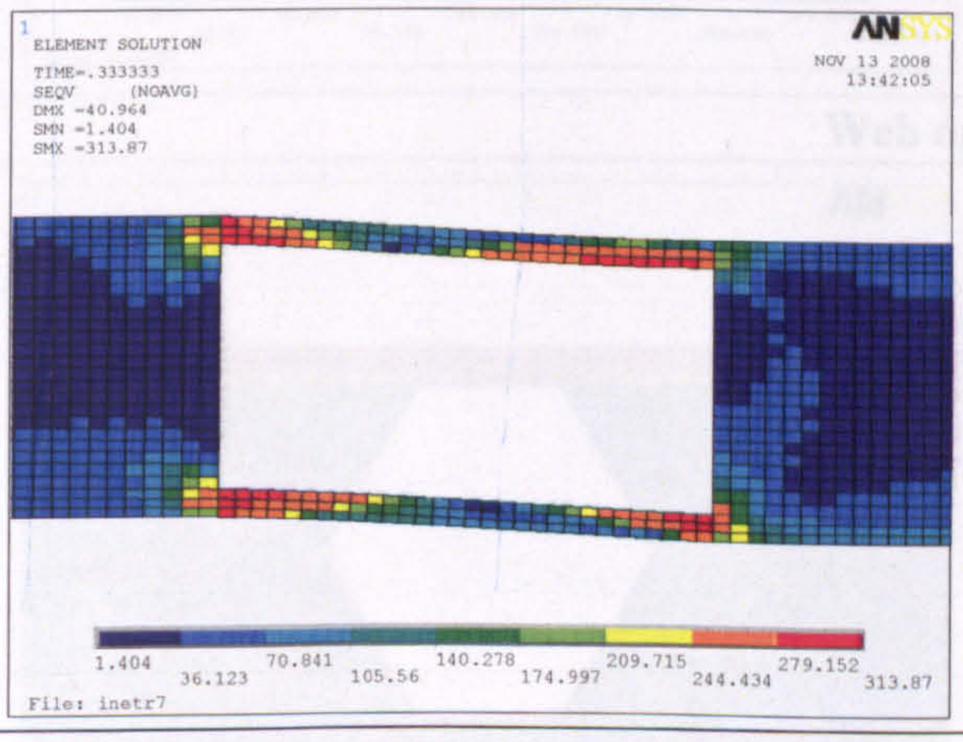

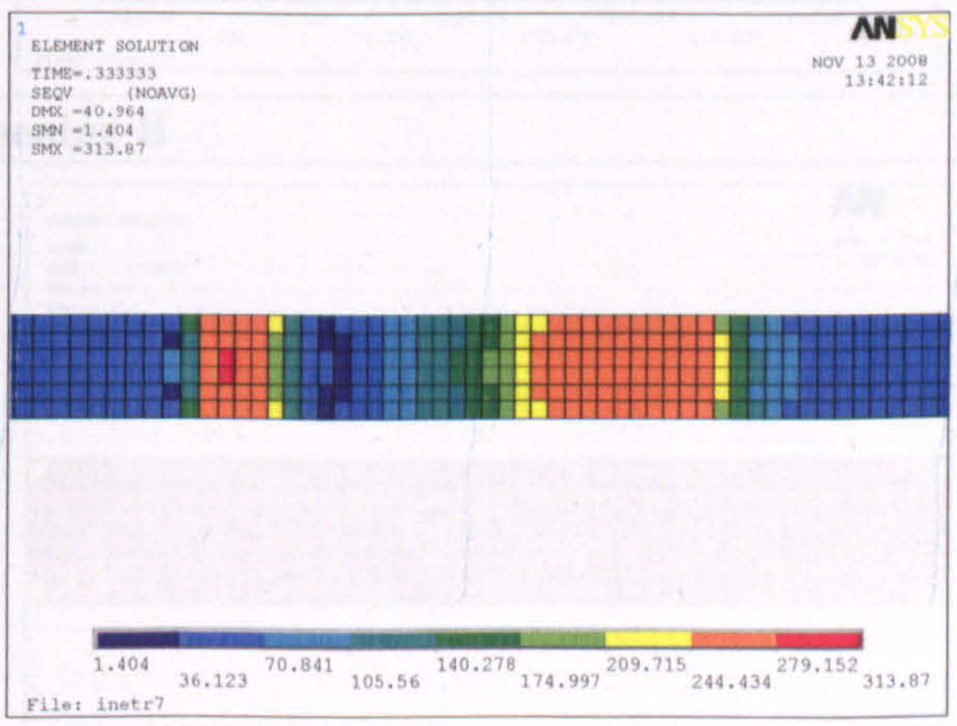

Web opening K

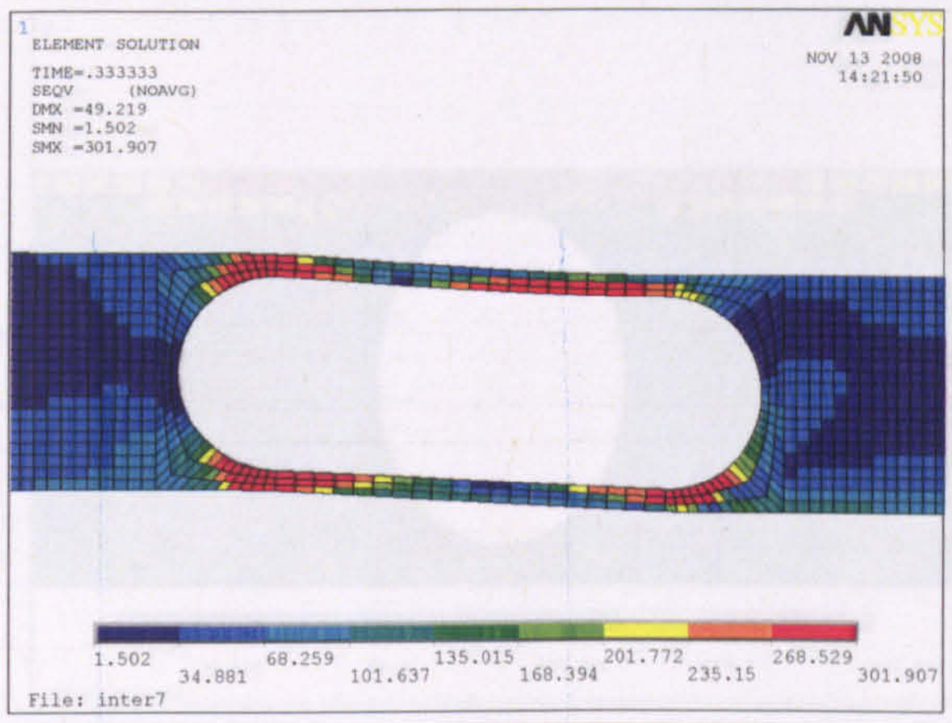

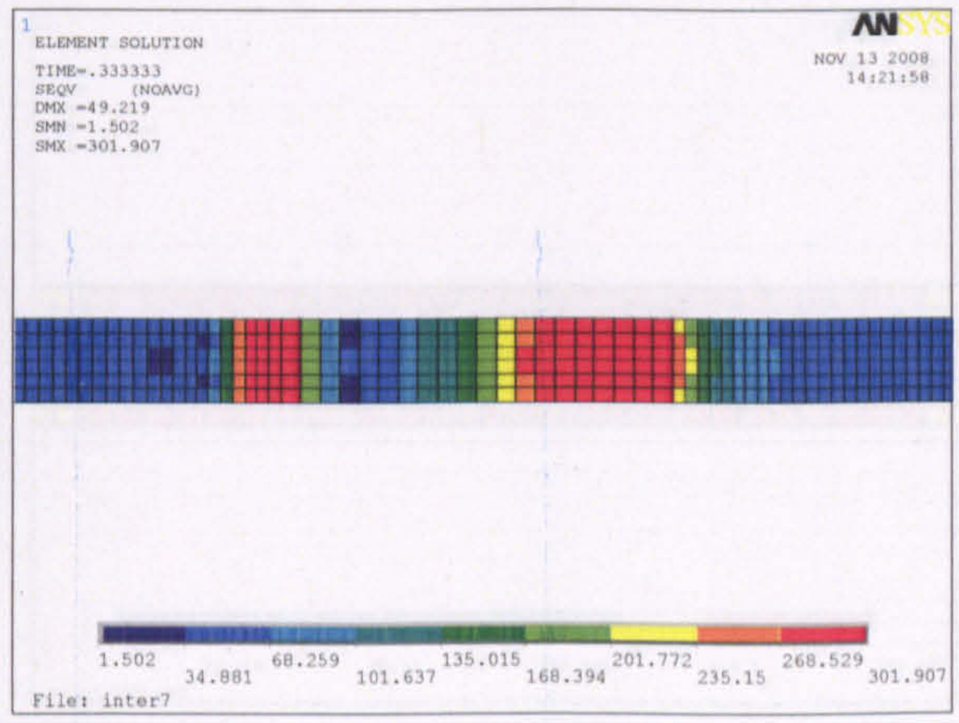

Figure 3: Failure stresses with web opening at high moment and low shear region ($d_o/h=0.8$)

Web opening A

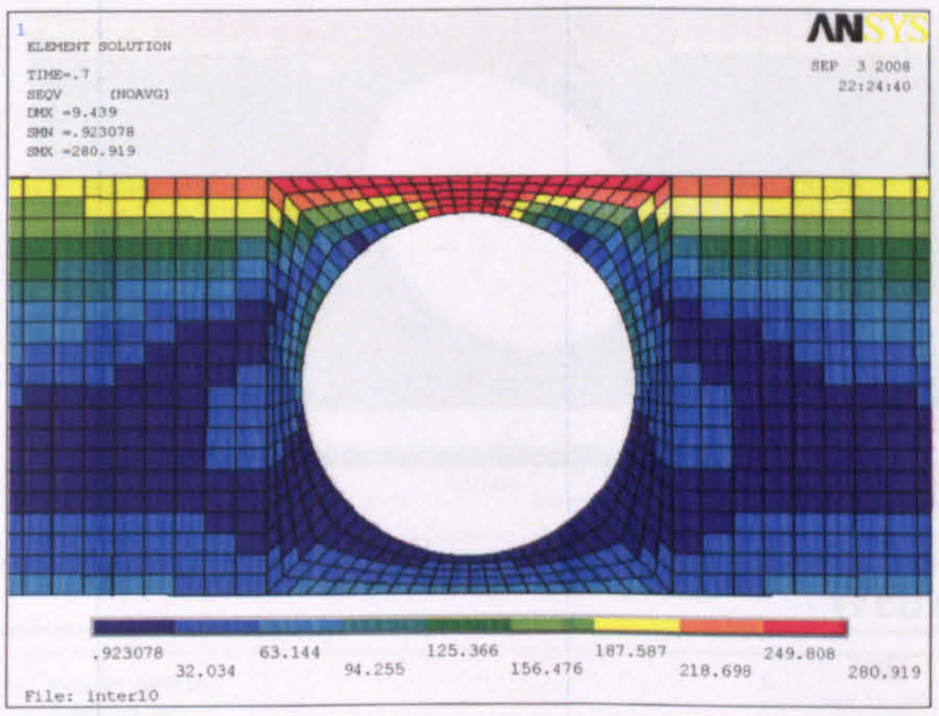

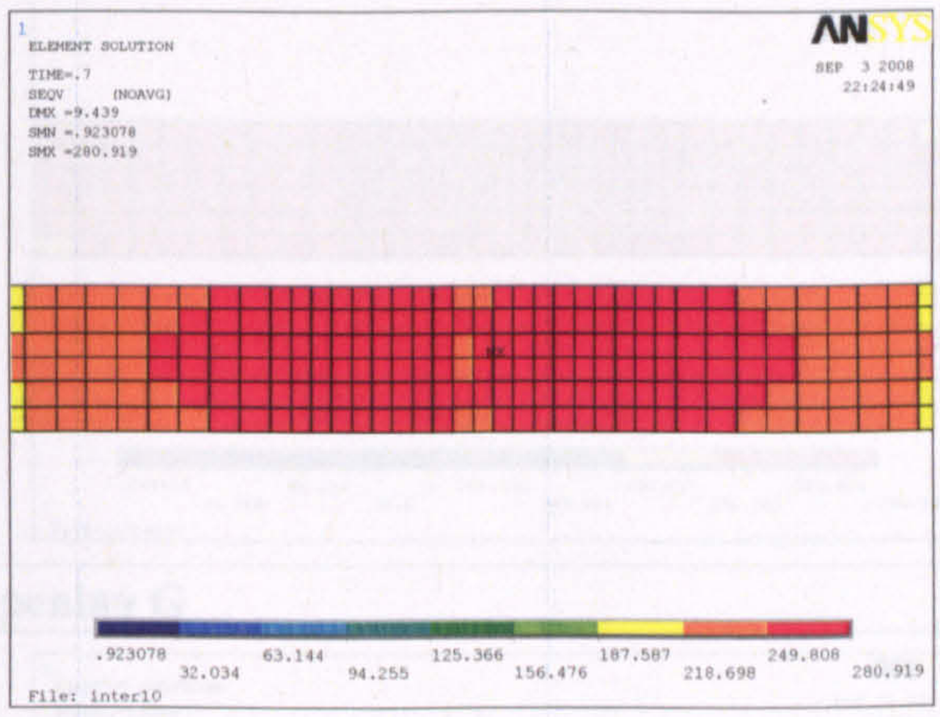

Web opening B

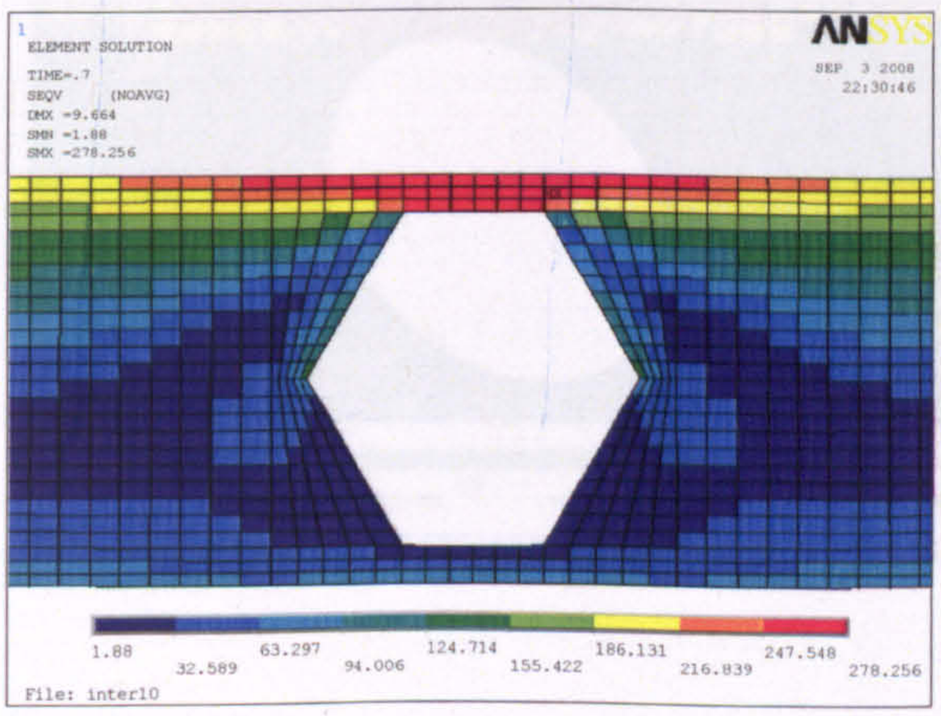

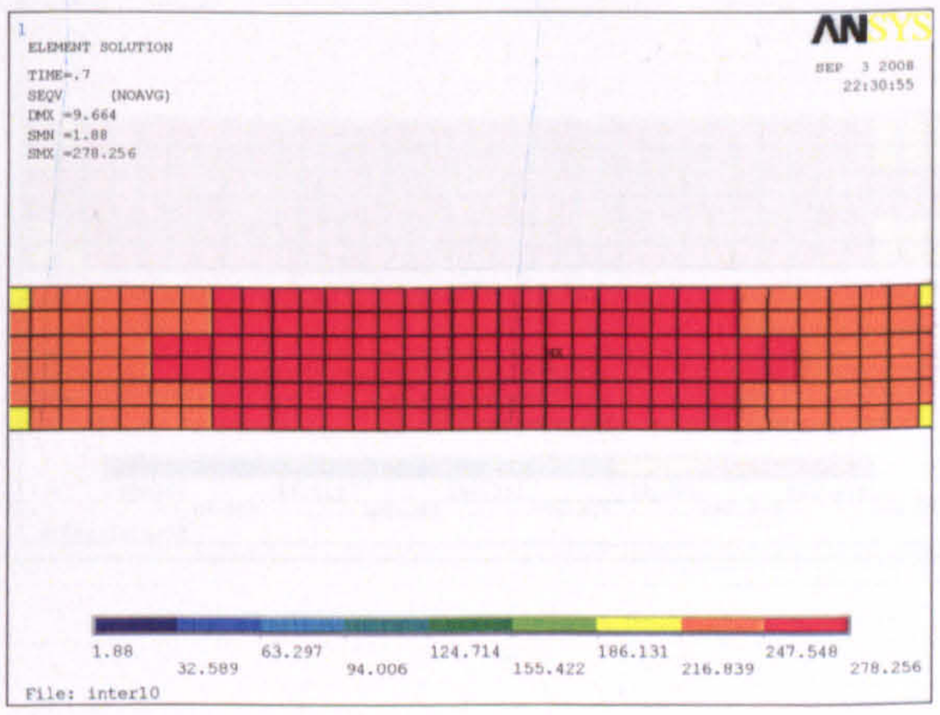

Web opening C

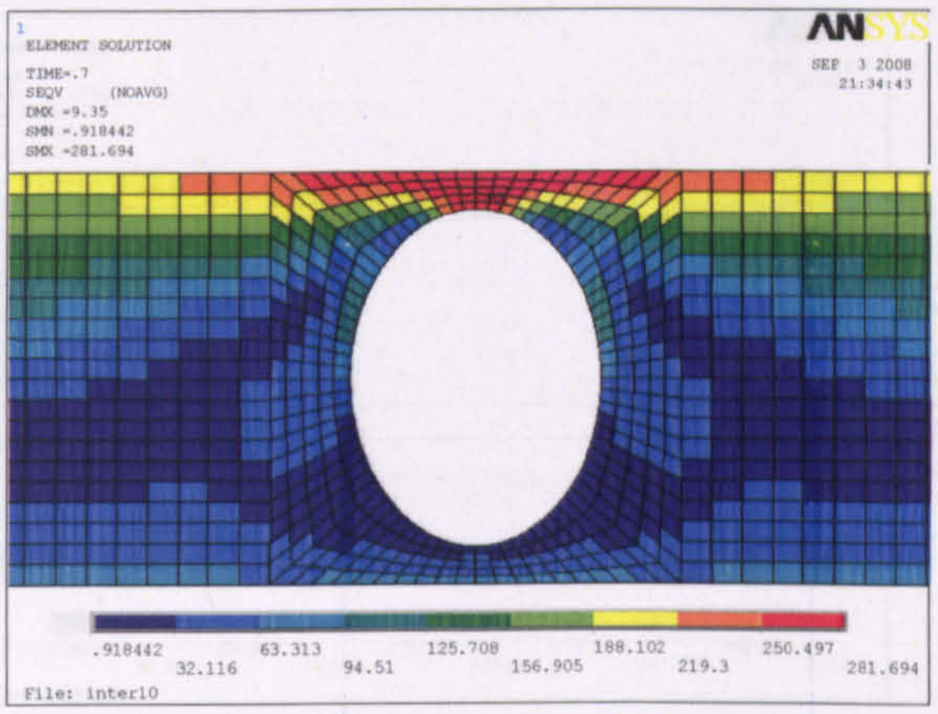

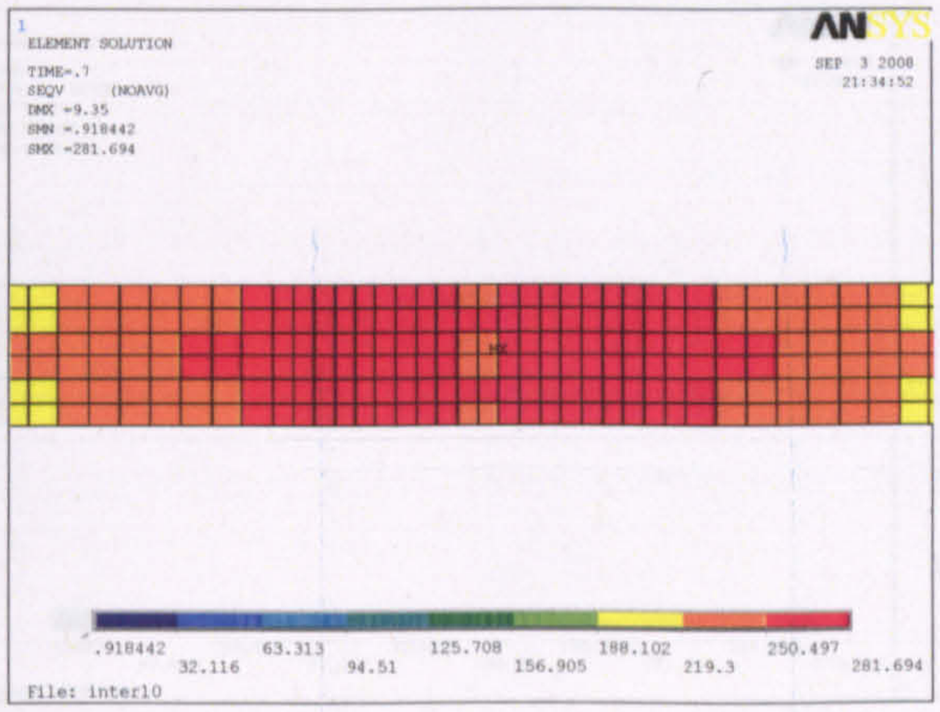

Web opening D-E-F

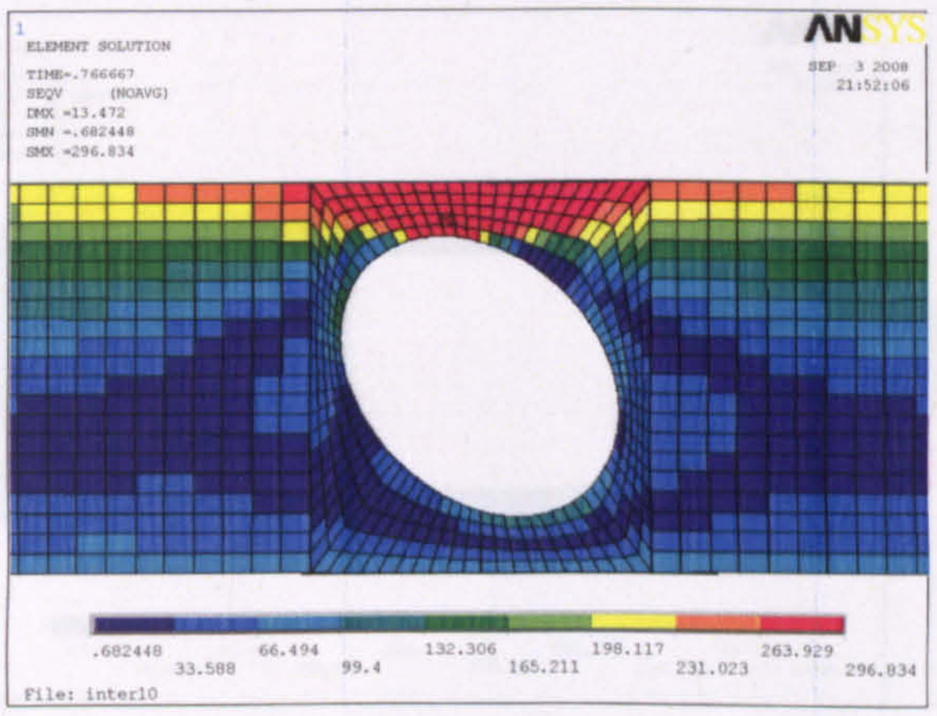

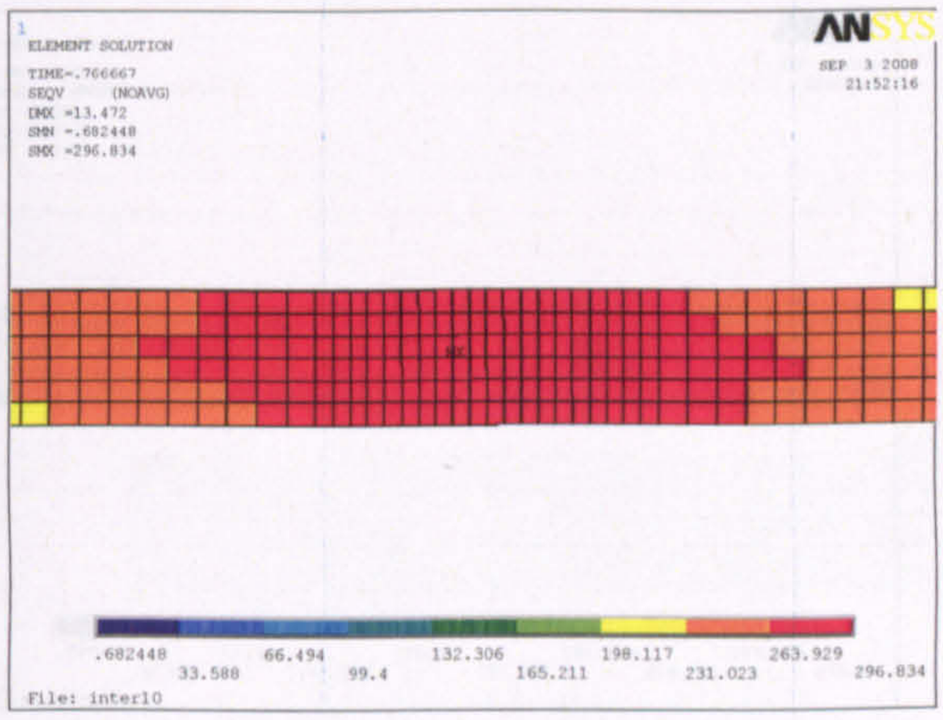

Web opening G

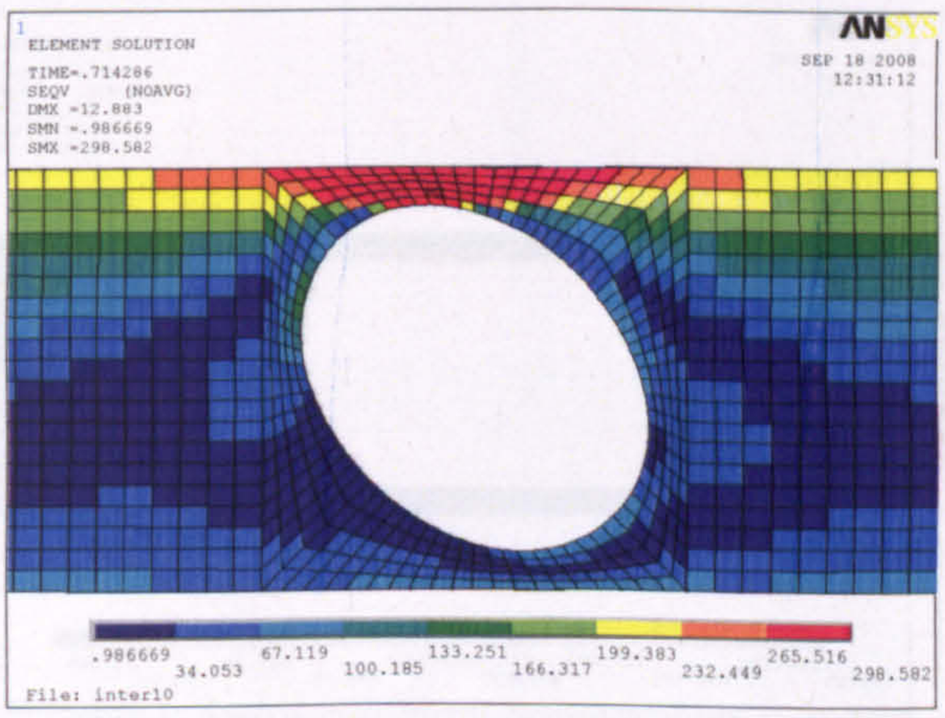

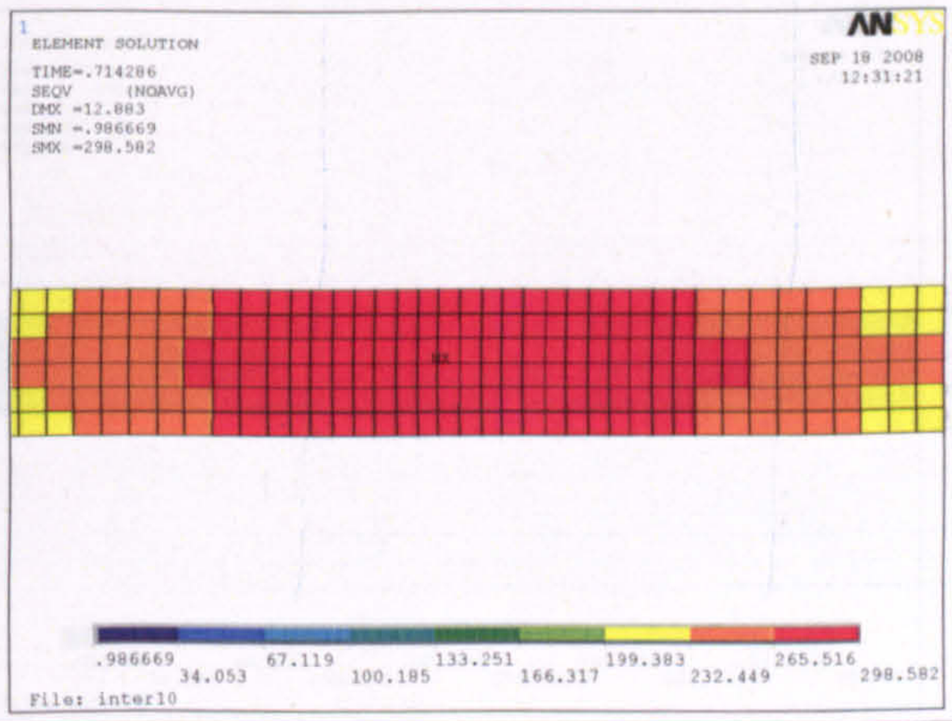

Web opening H

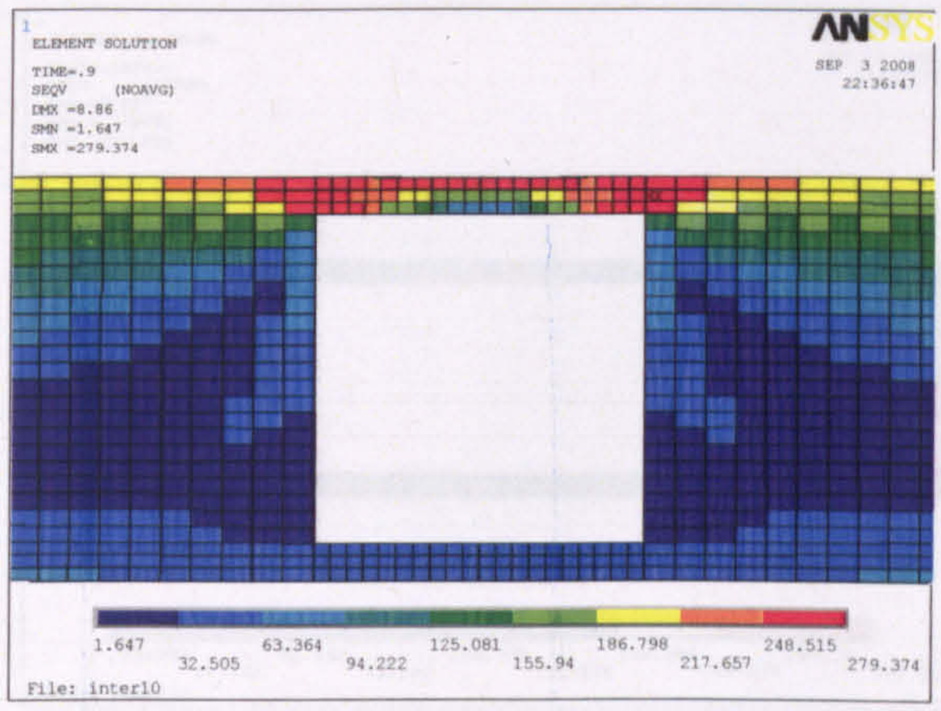

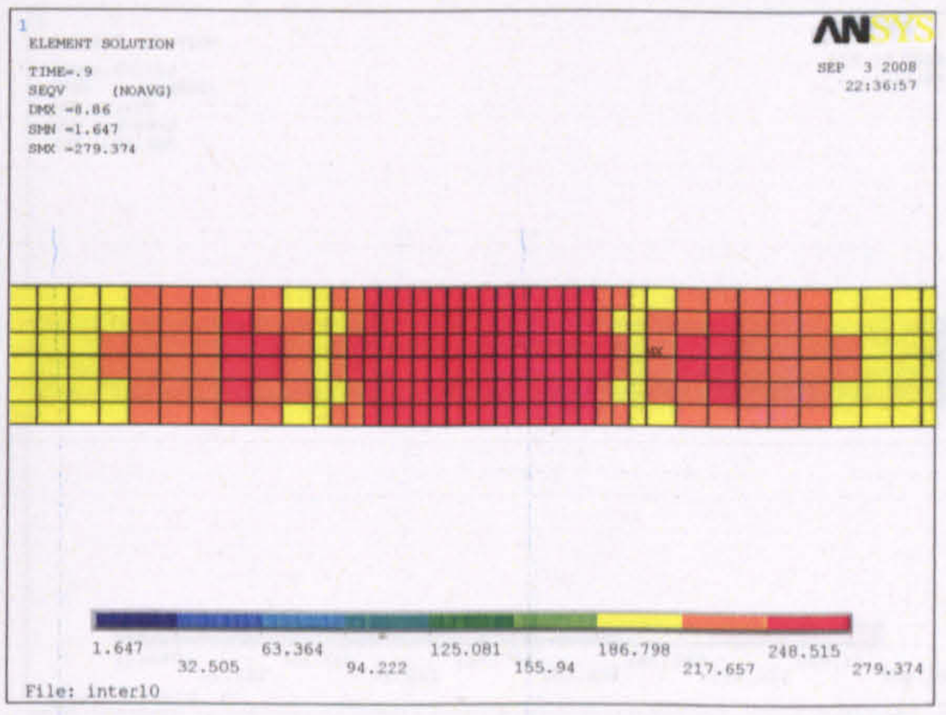

Web opening I

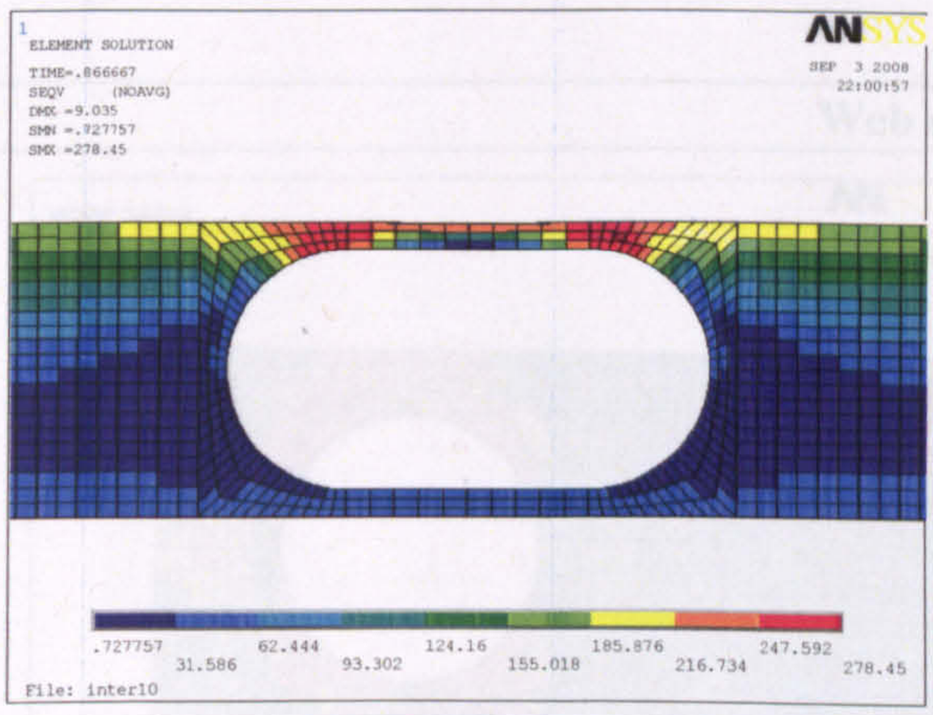

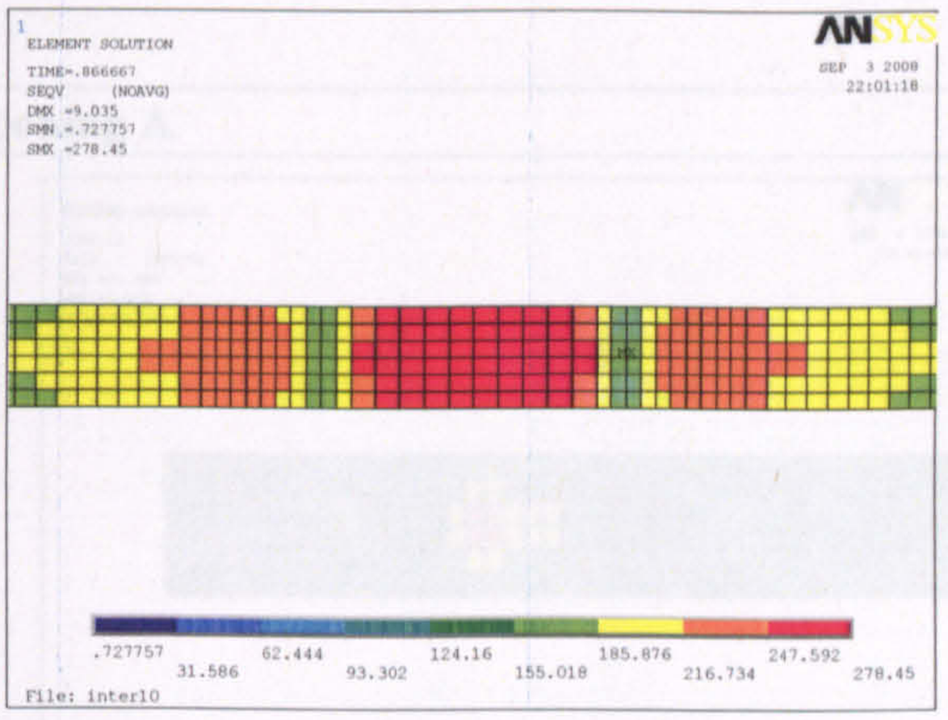

Web opening G

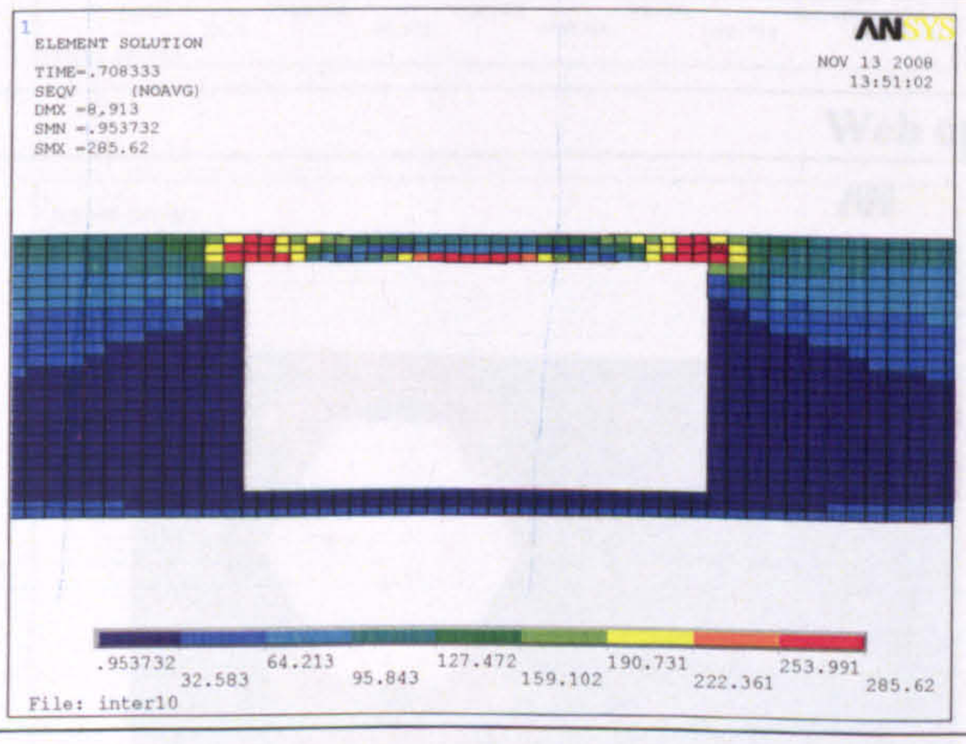

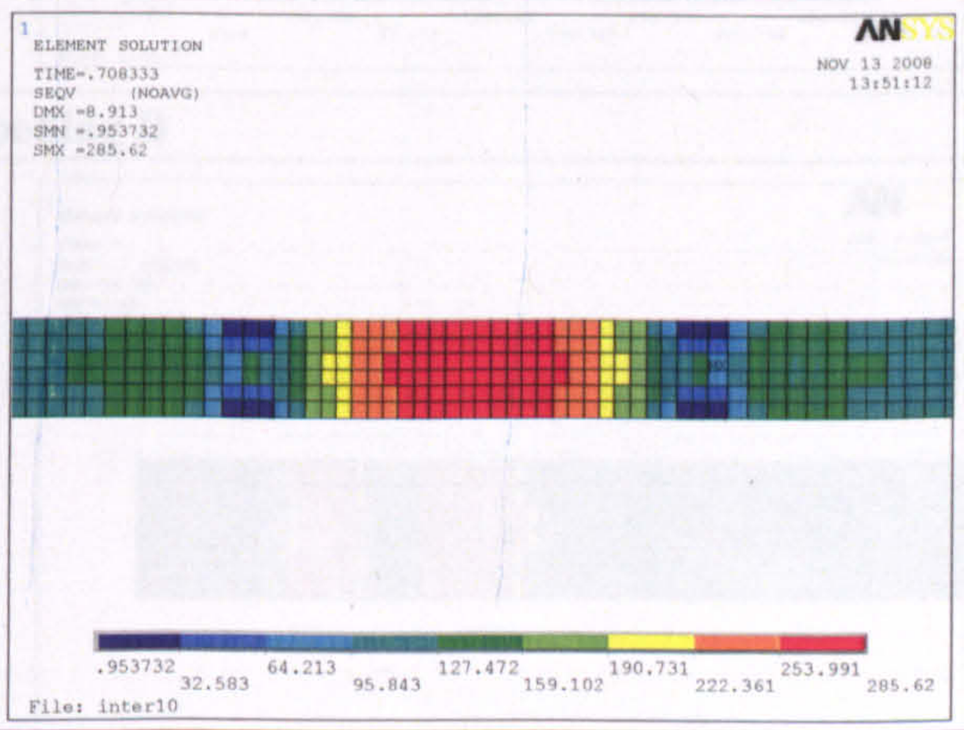

Web opening K

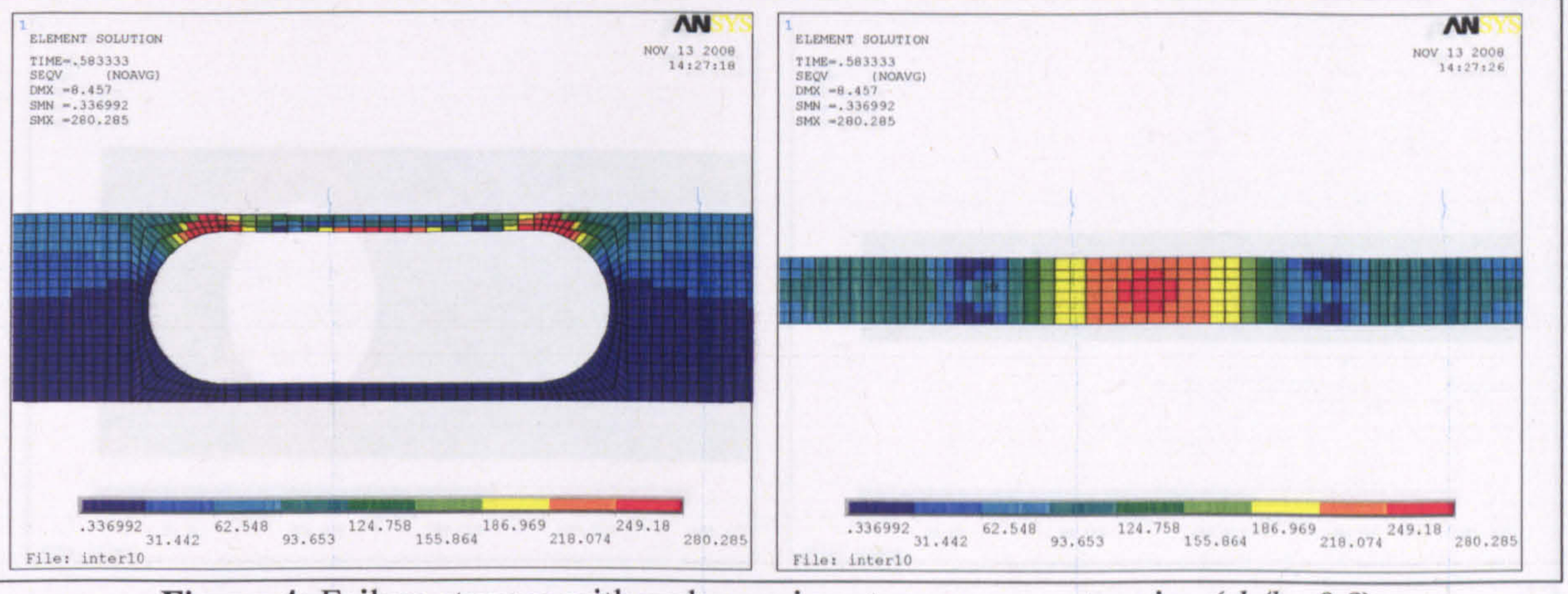

Figure 4: Failure stresses with web opening at pure moment region ($d_o/h=0.8$)

Web opening A

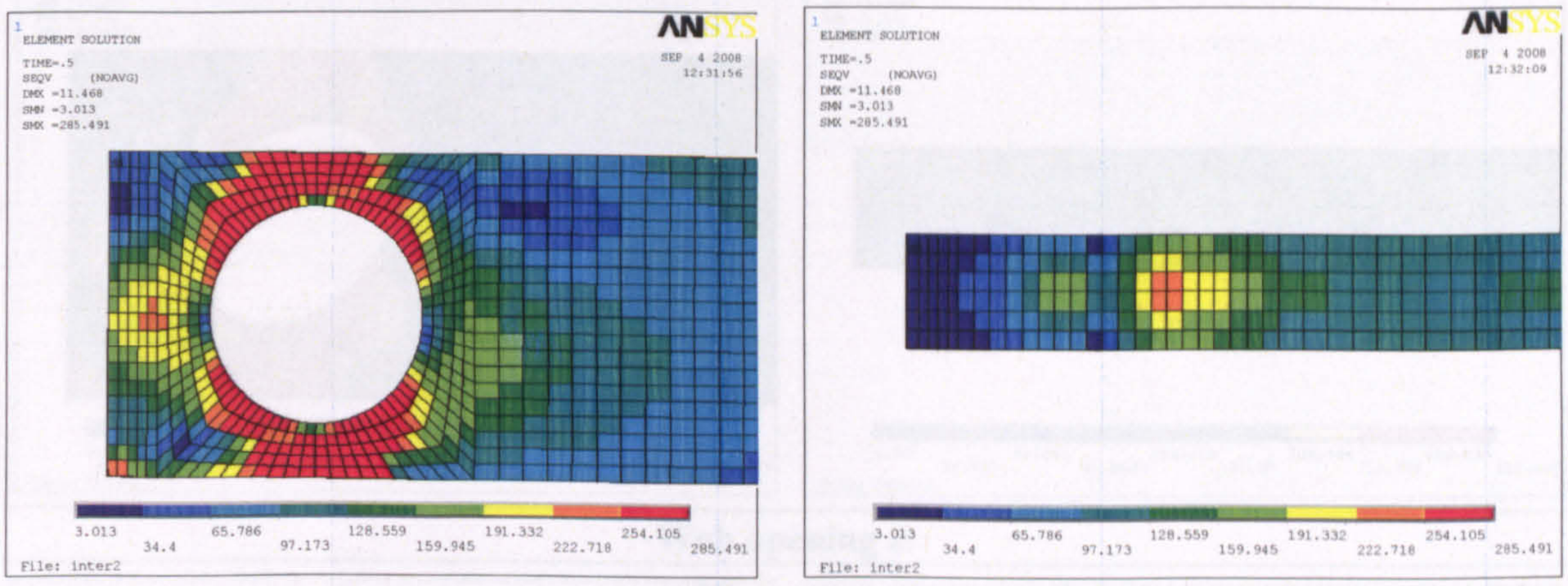

Web opening B

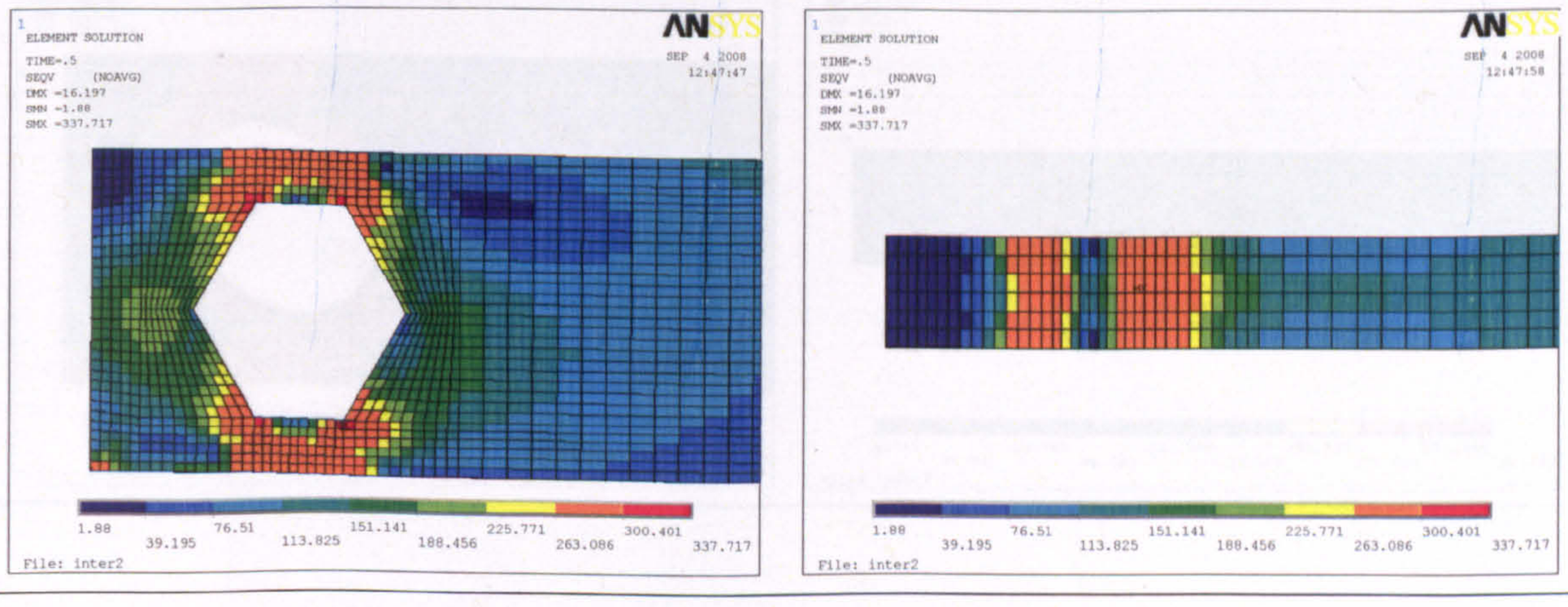

Web opening C

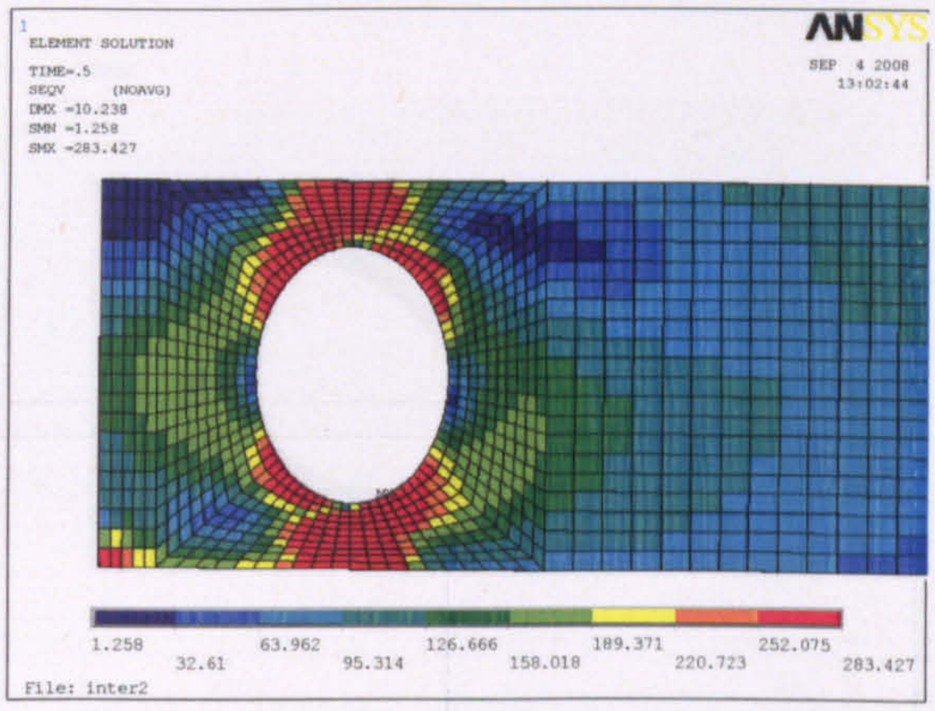

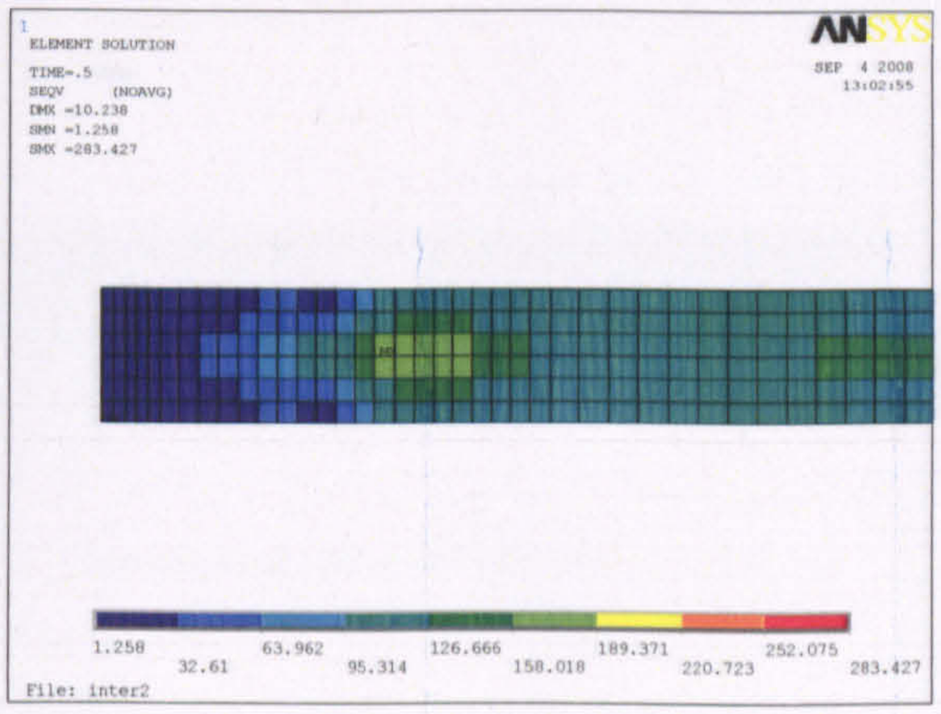

Web opening D

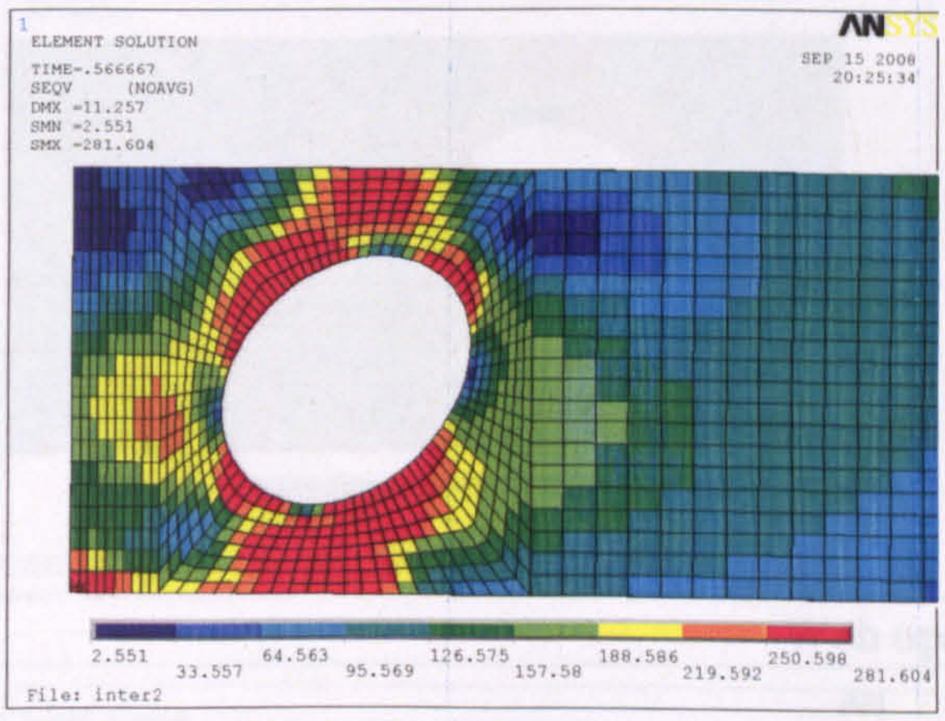

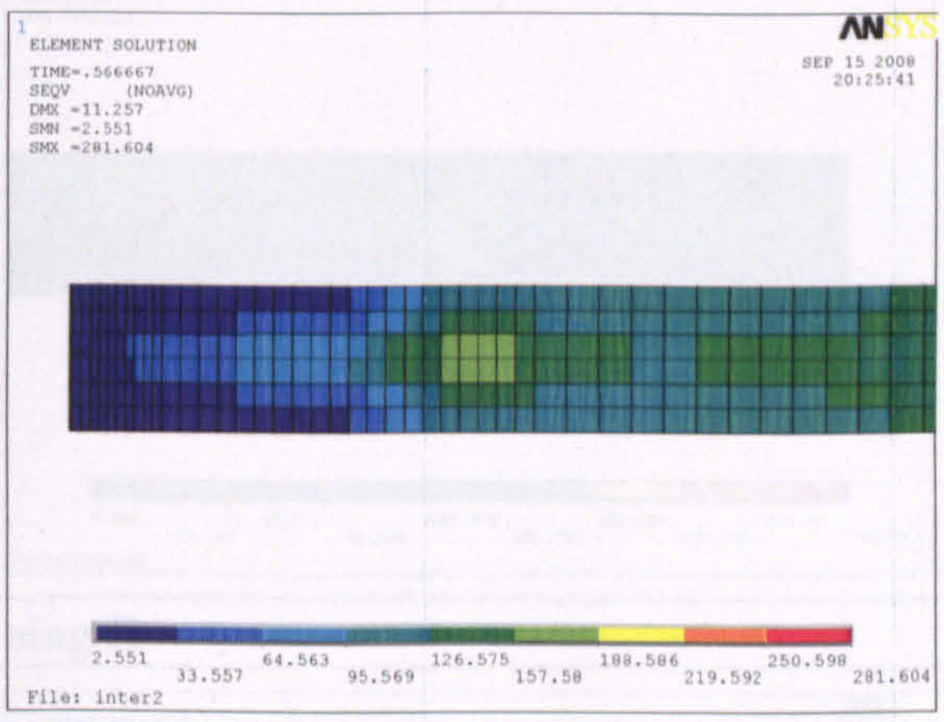

Web opening E

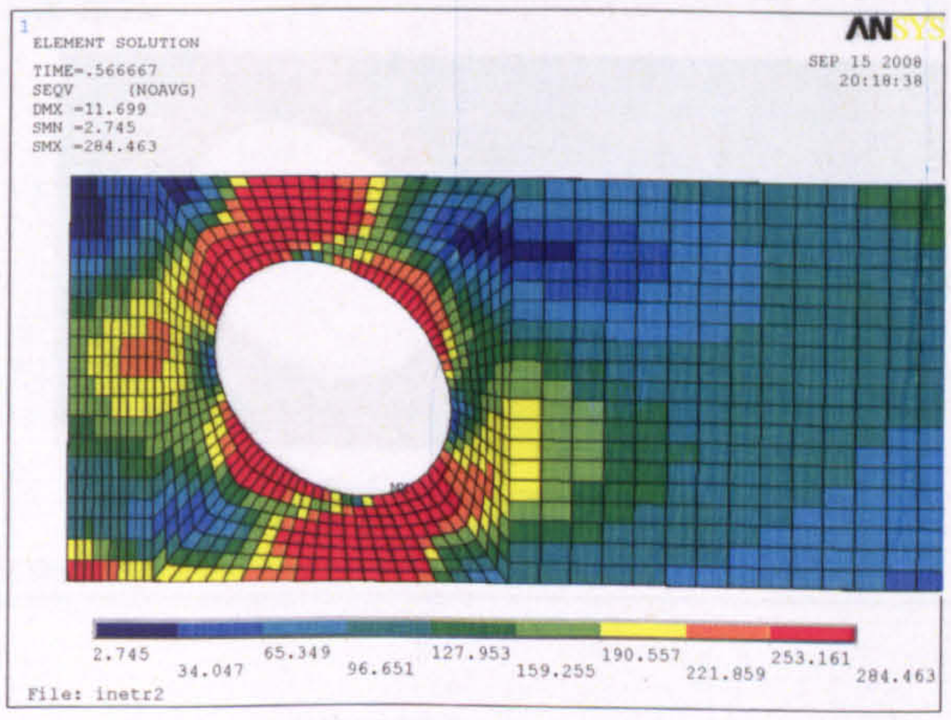

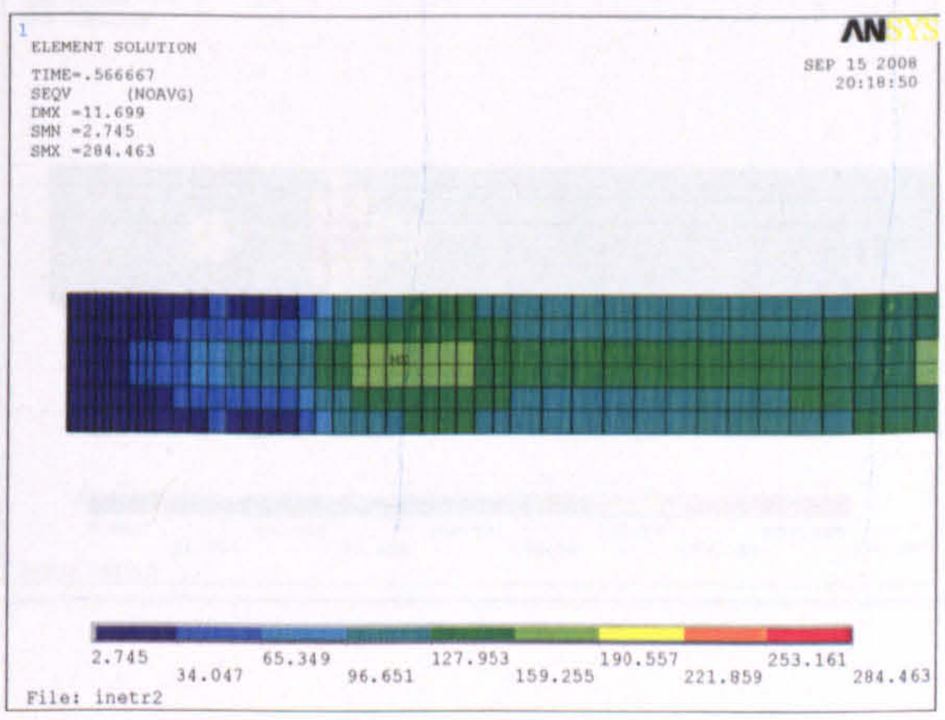

Web opening F

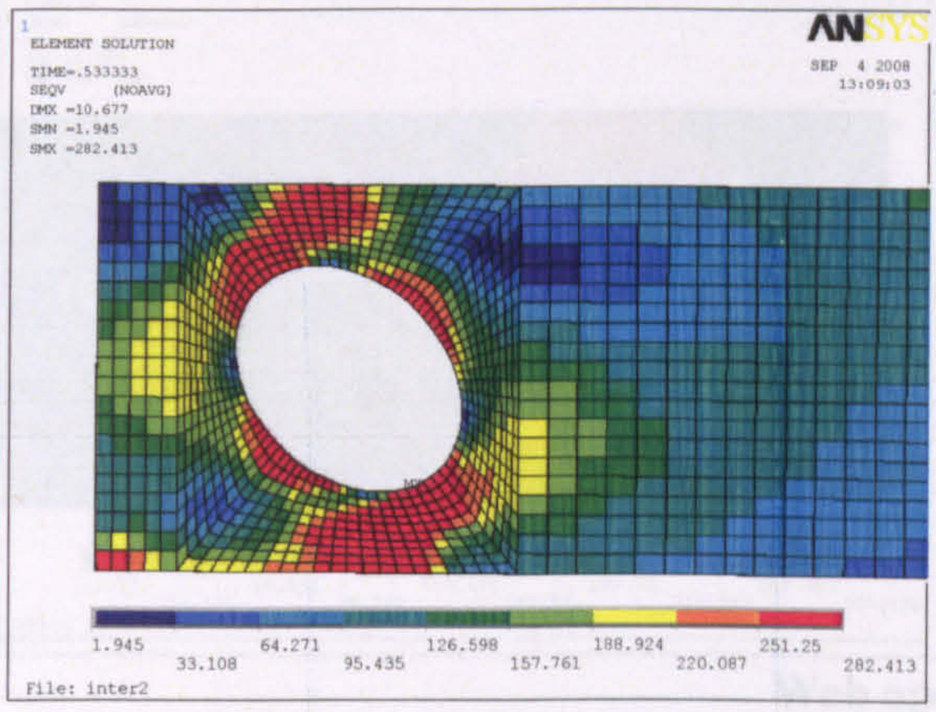

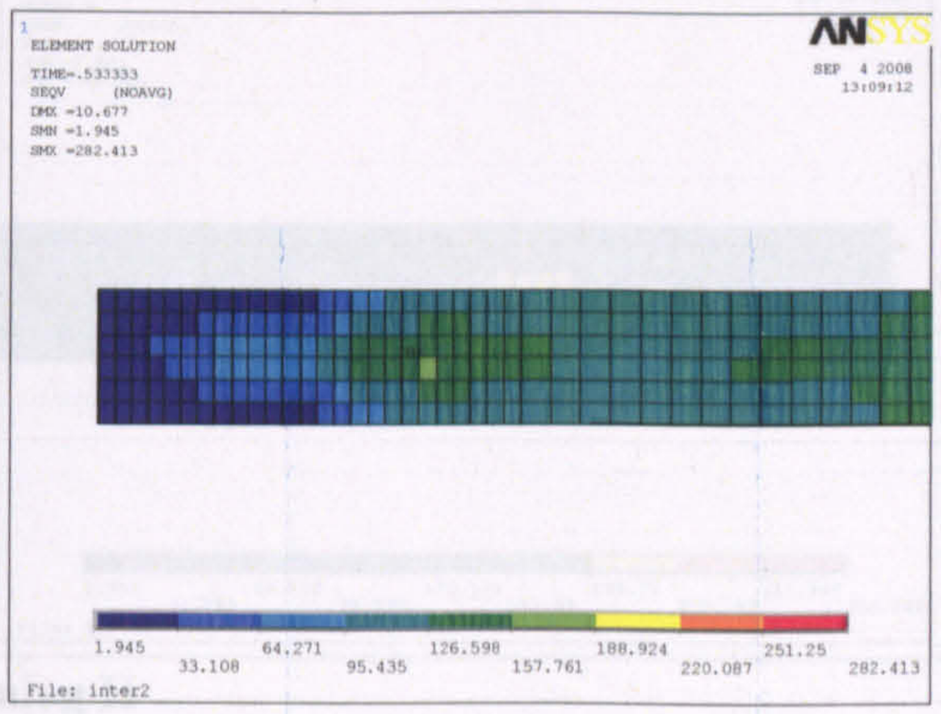

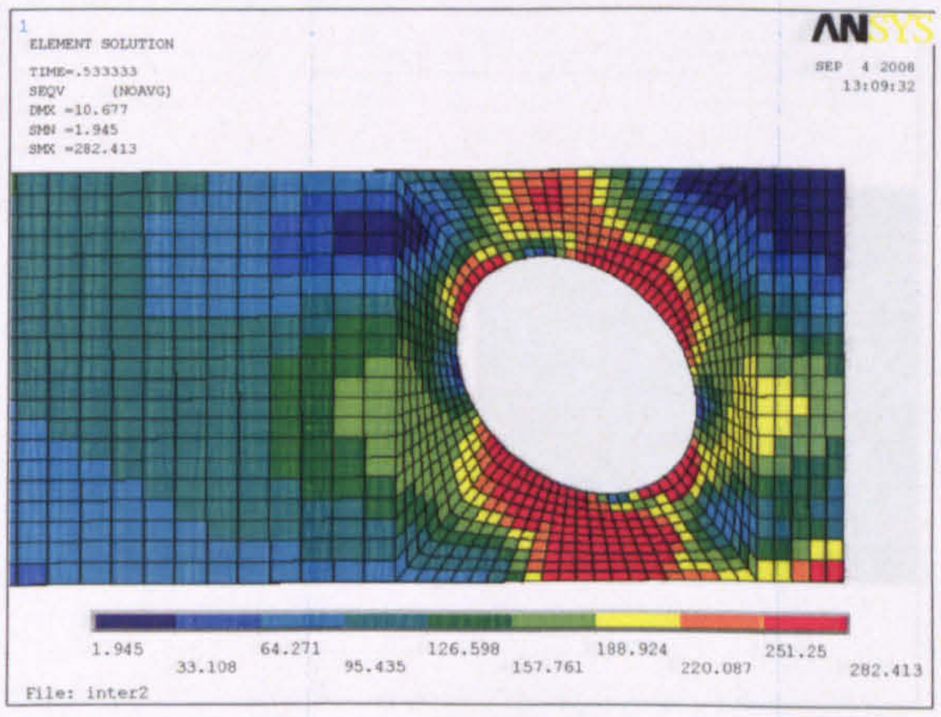

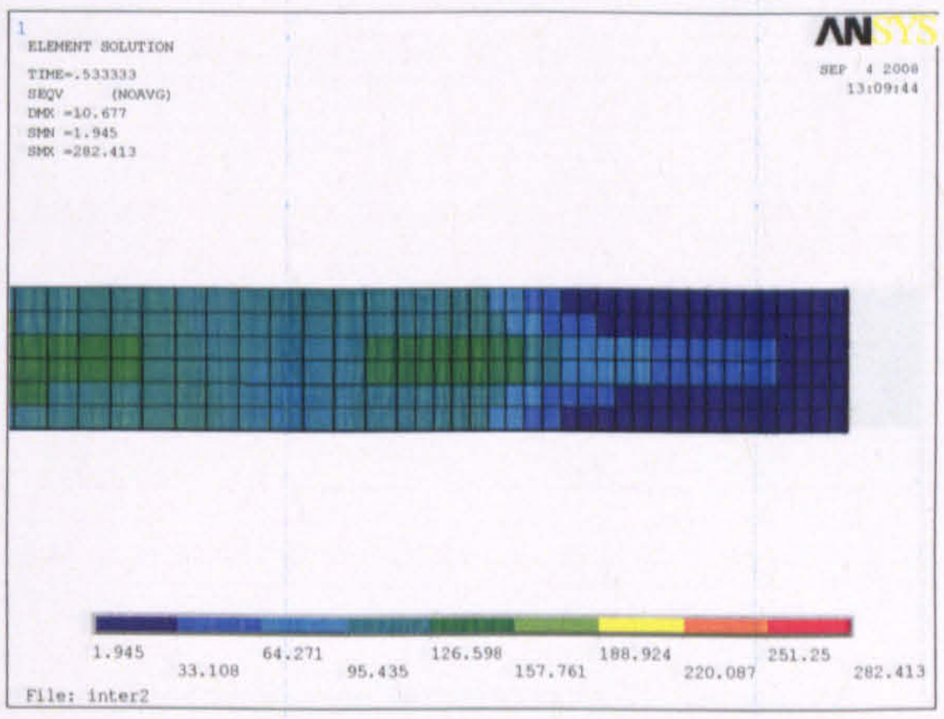

Web opening G

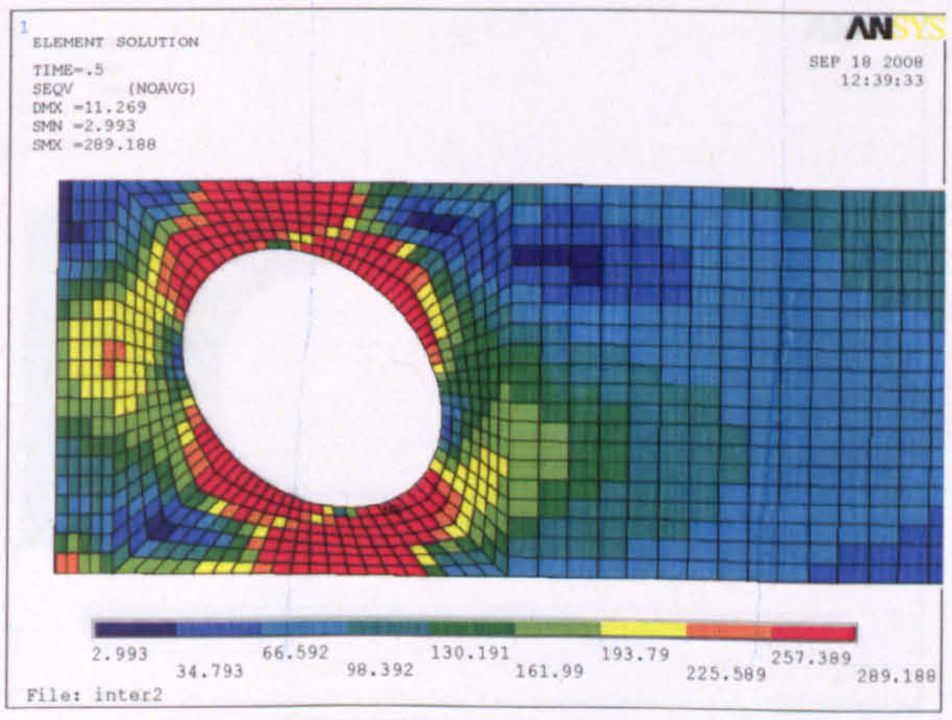

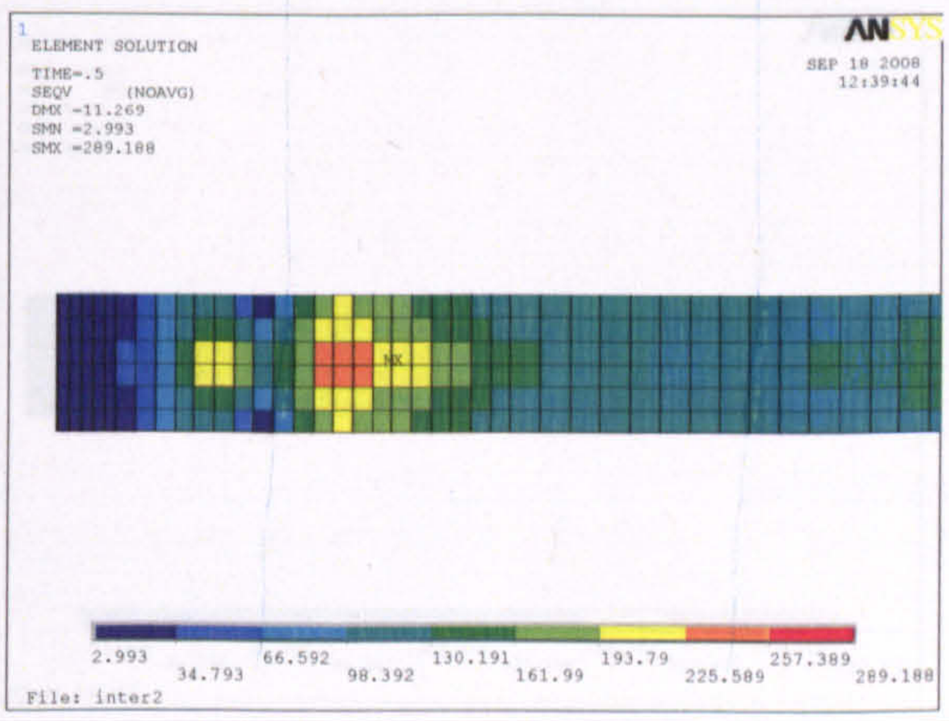

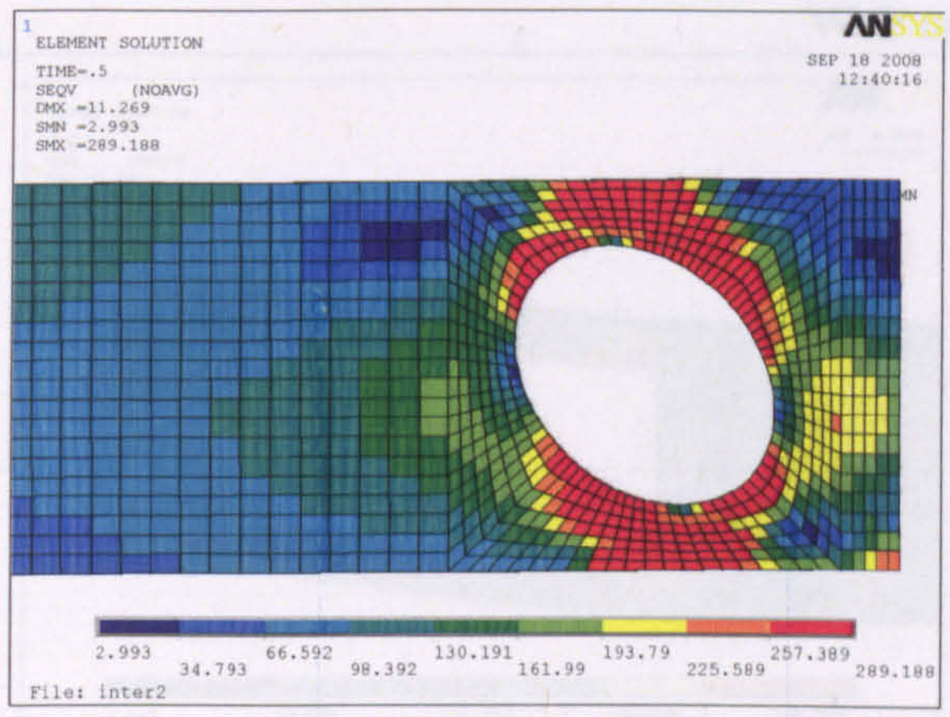

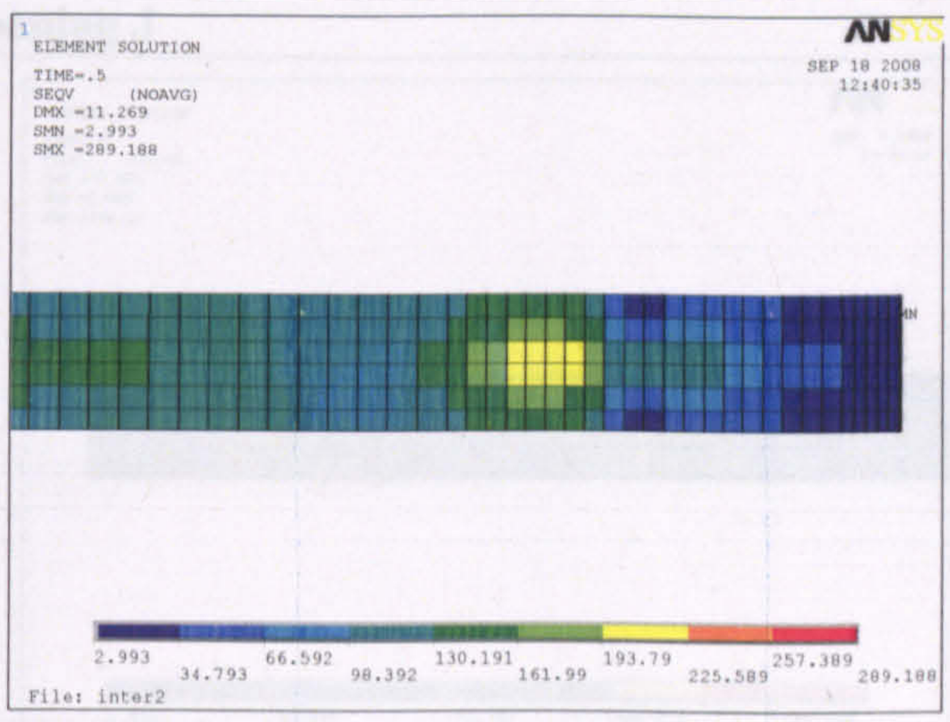

Web opening H

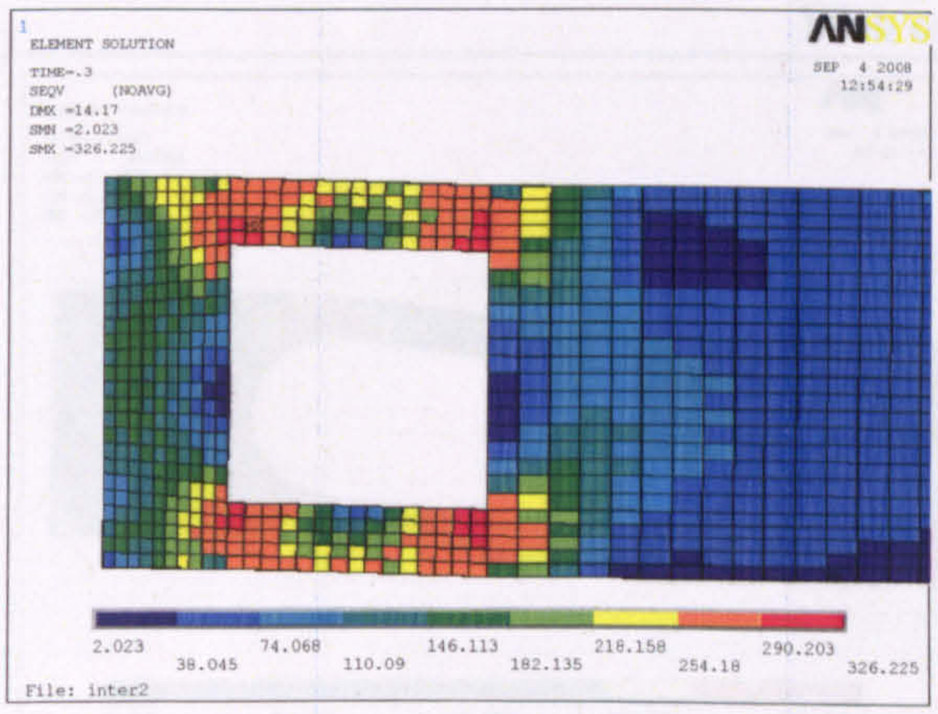

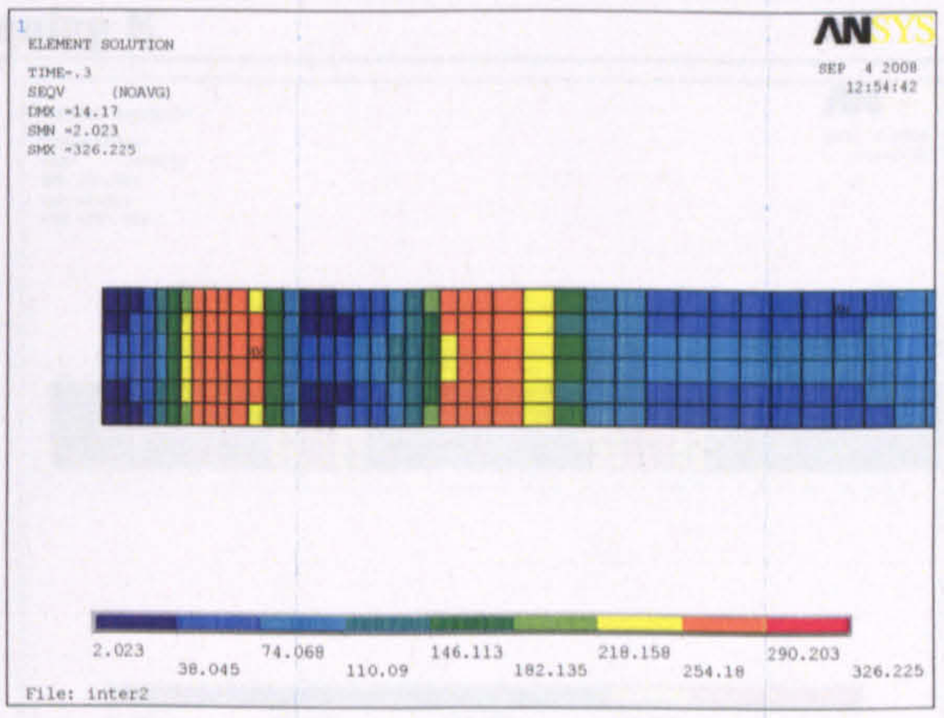

Web opening I

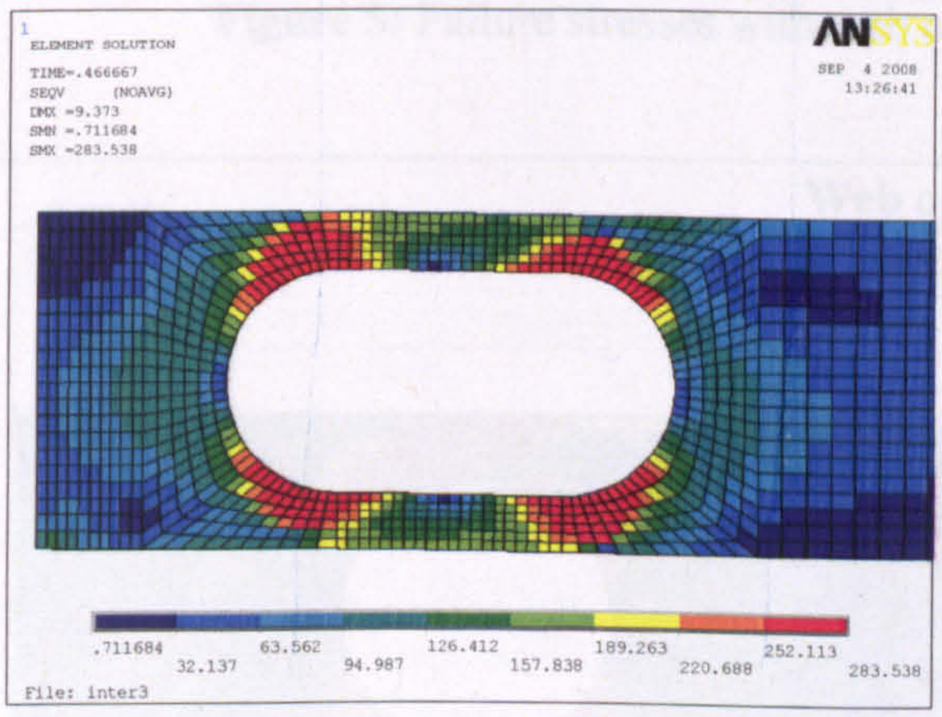

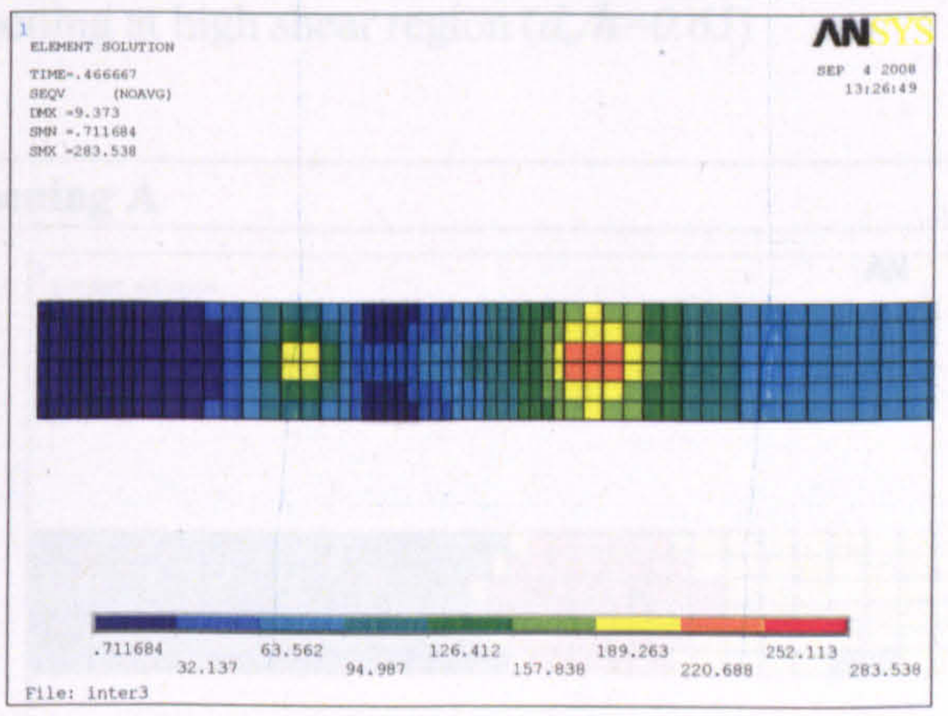

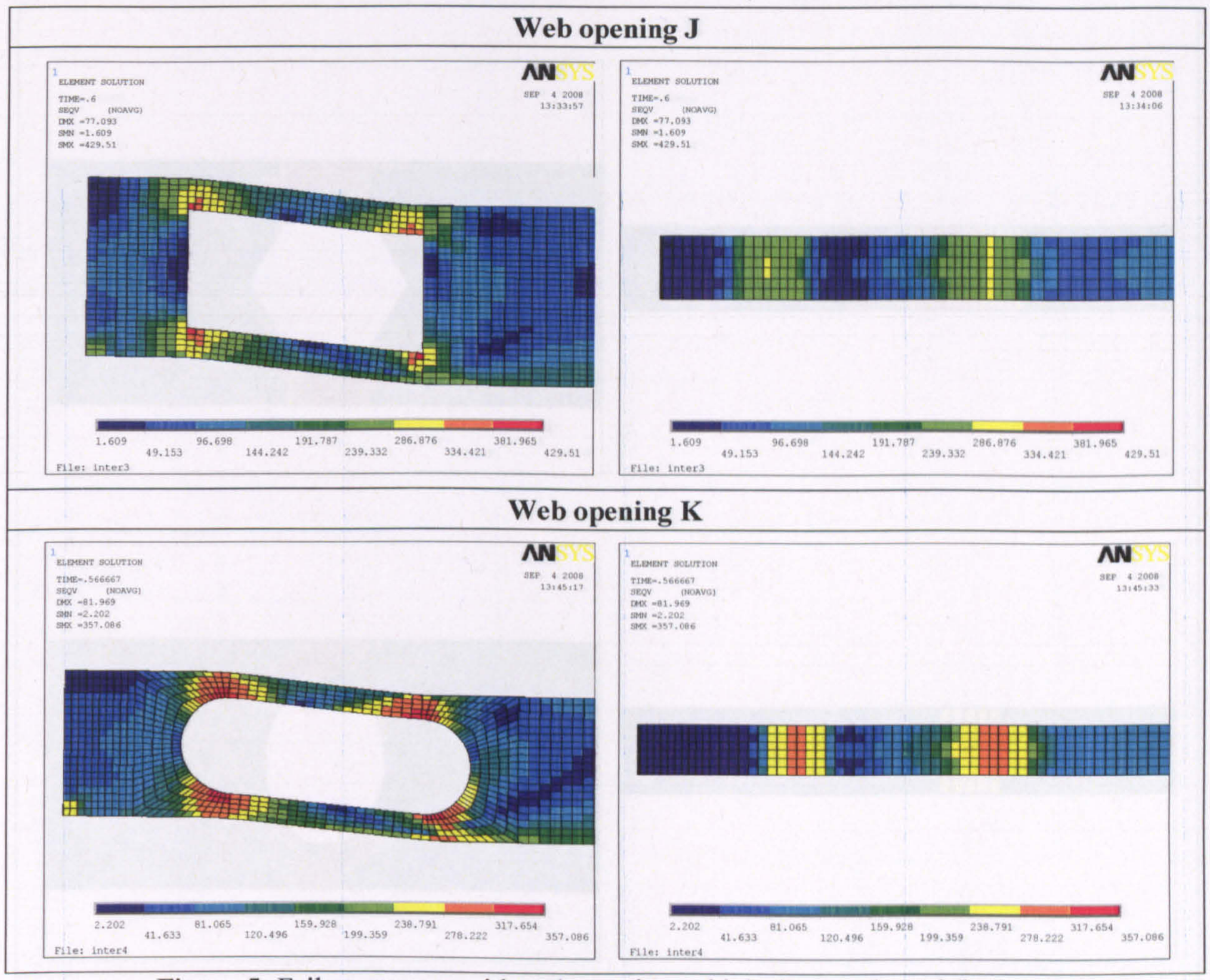

Figure 5: Failure stresses with web opening at high shear region ($d_o/h=0.65$)

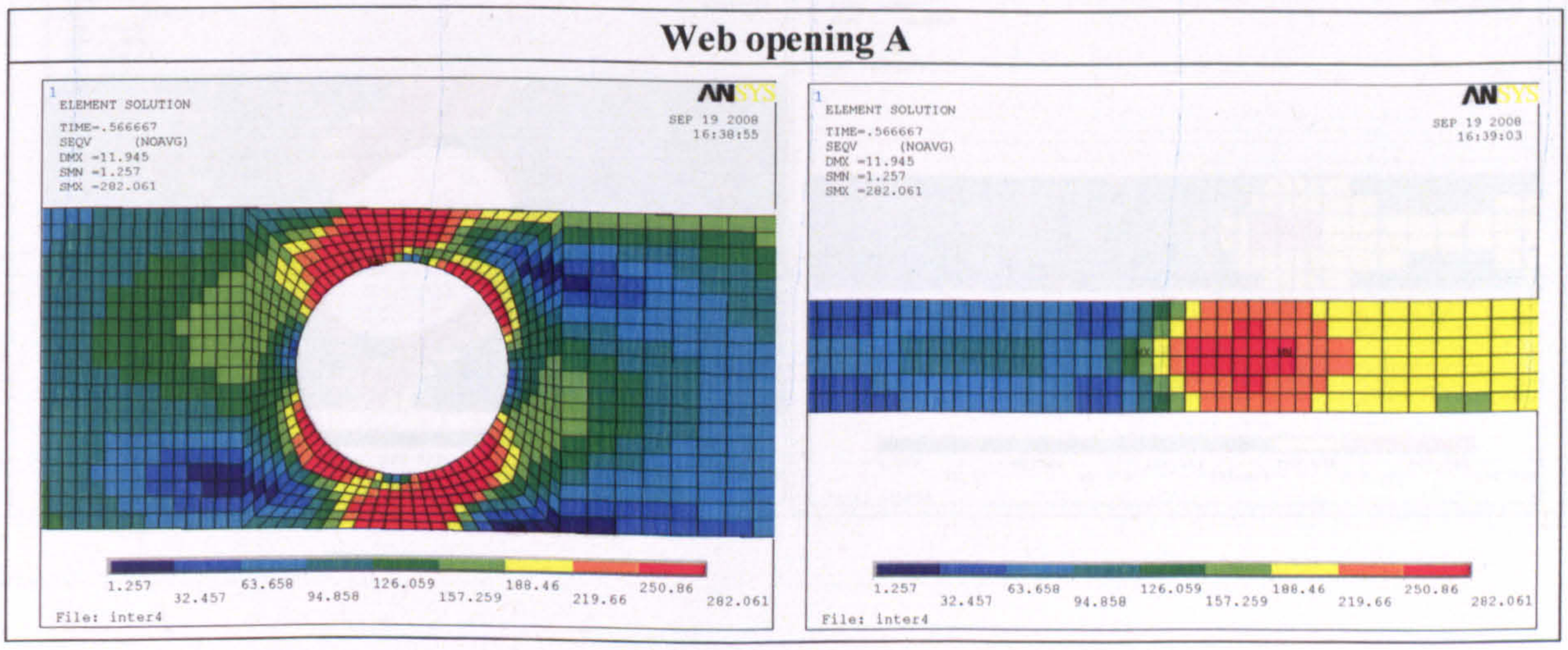

Web opening B

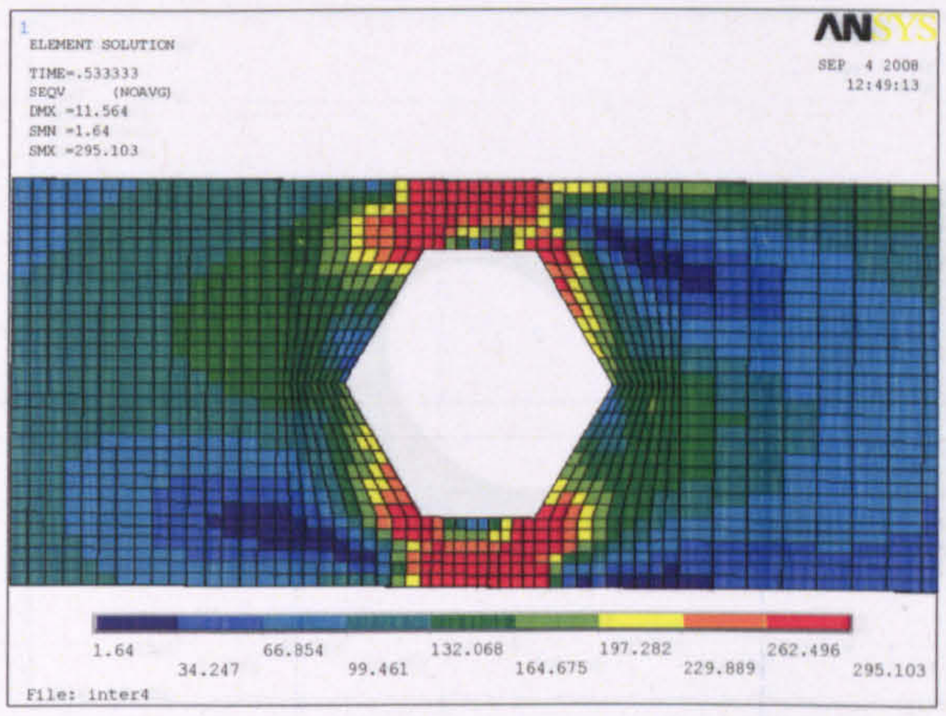

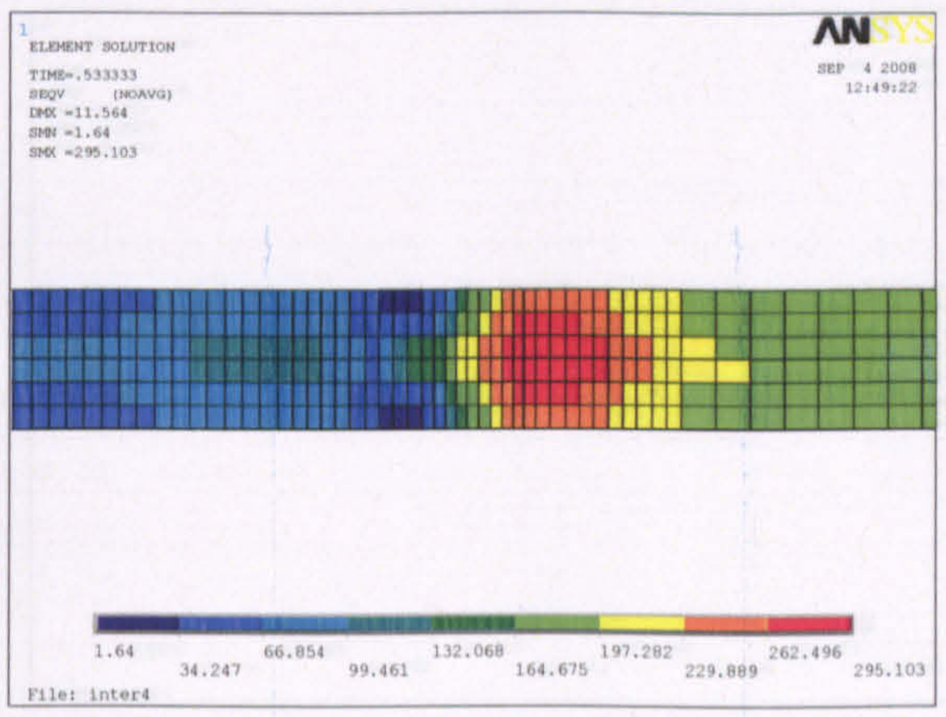

Web opening C

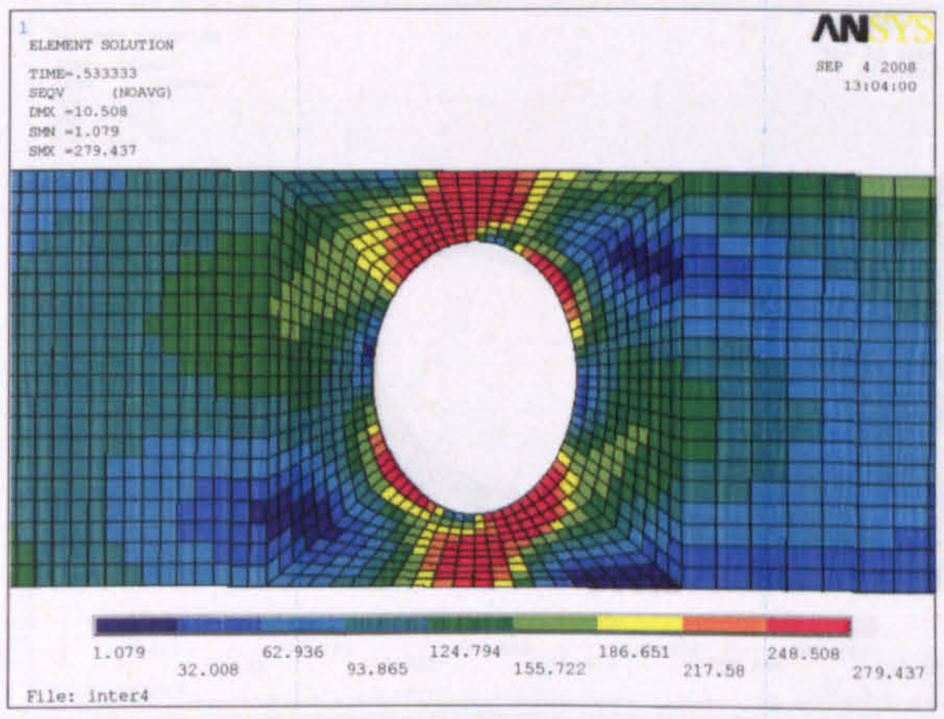

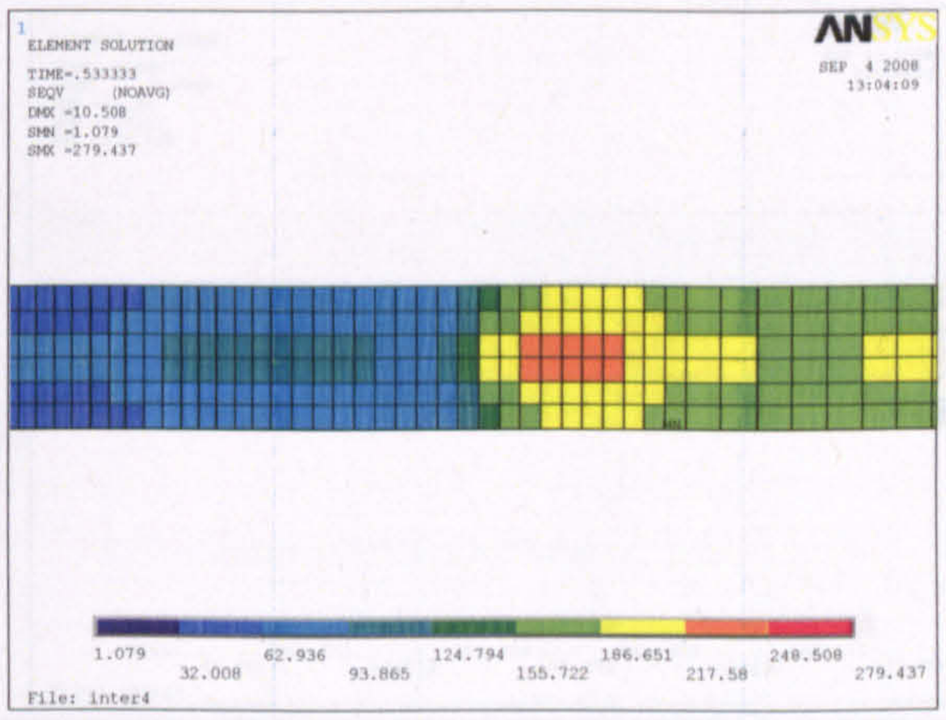

Web opening D

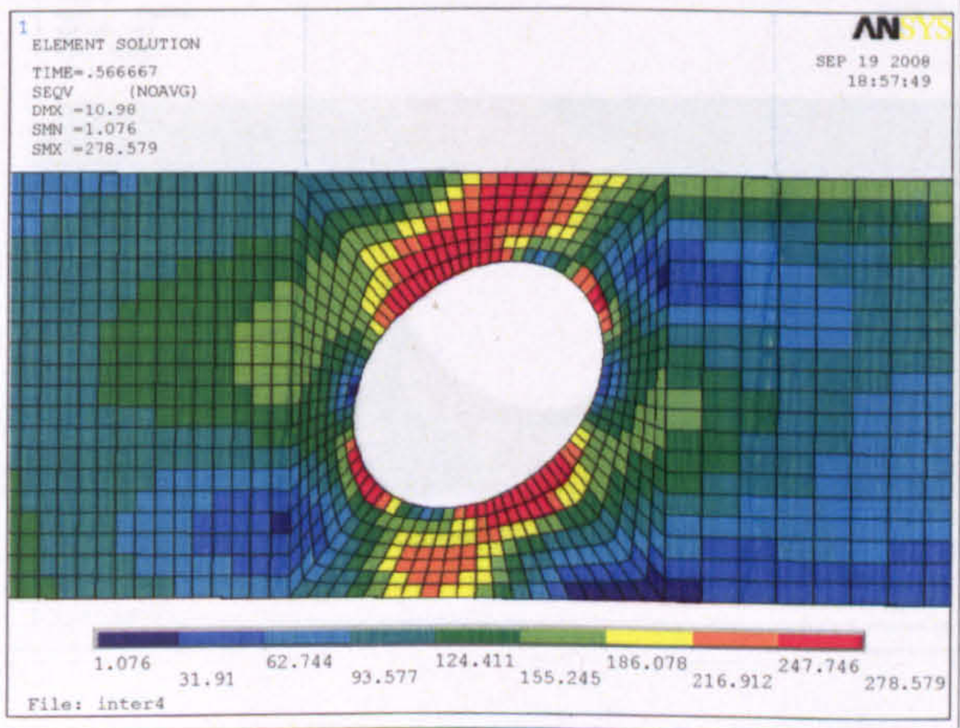

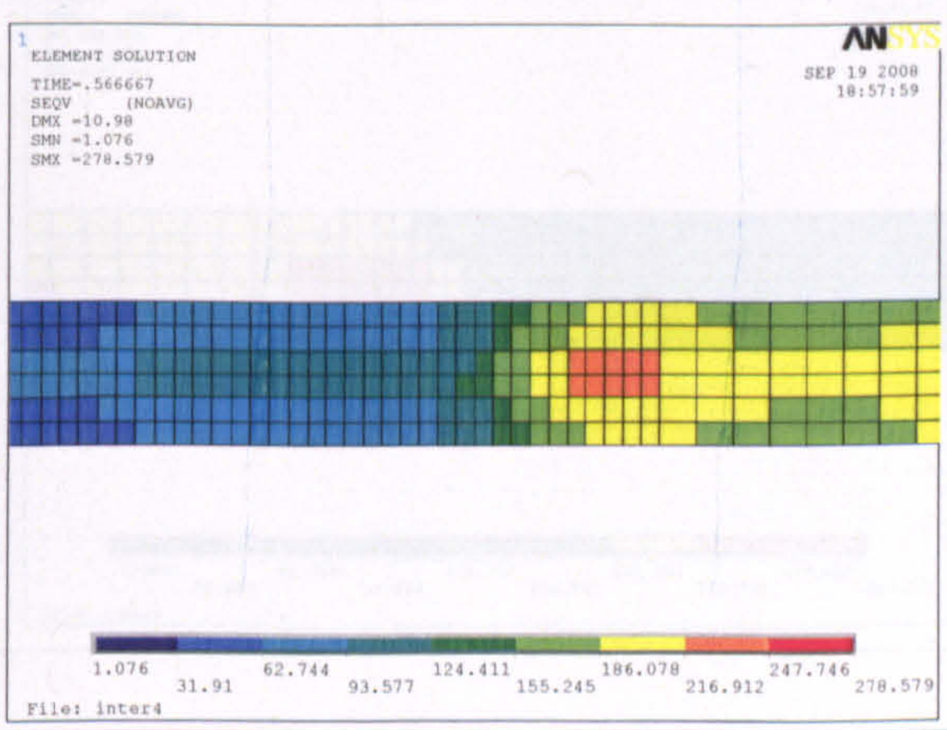

Web opening E

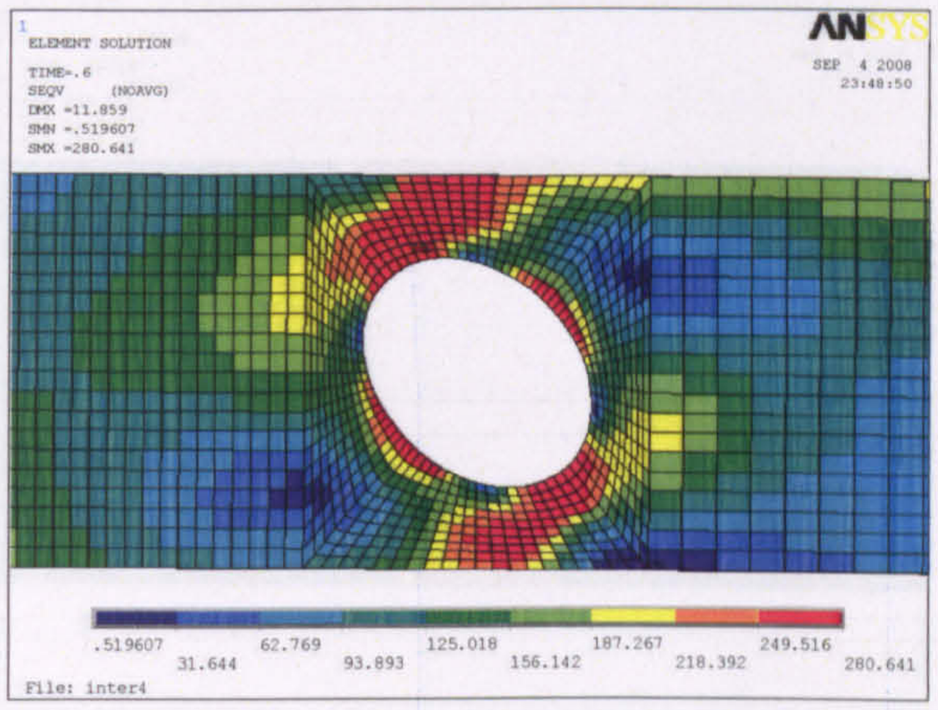

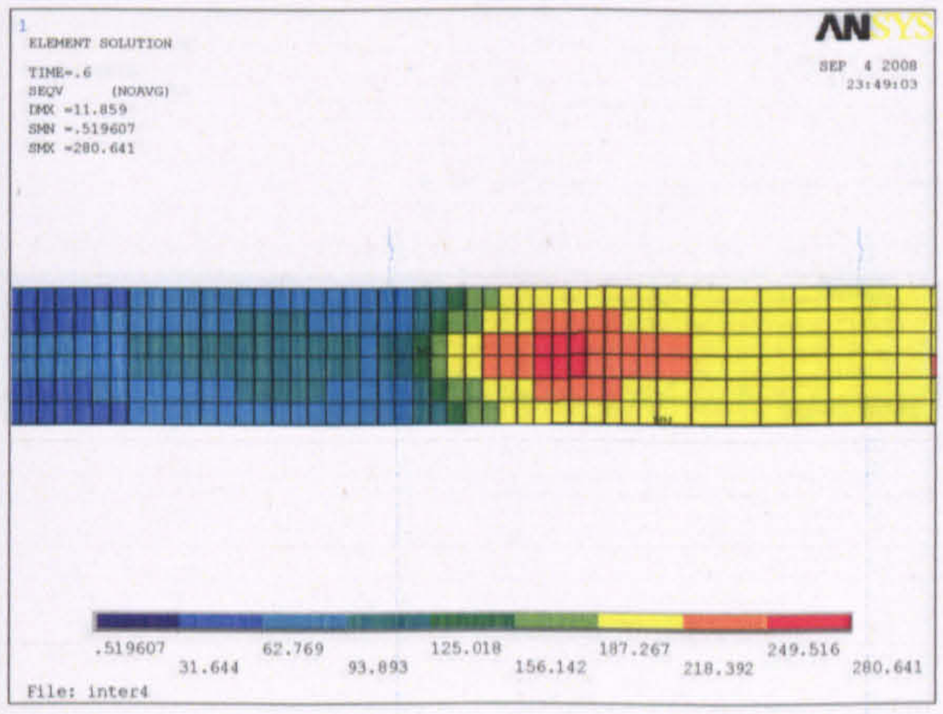

Web opening F

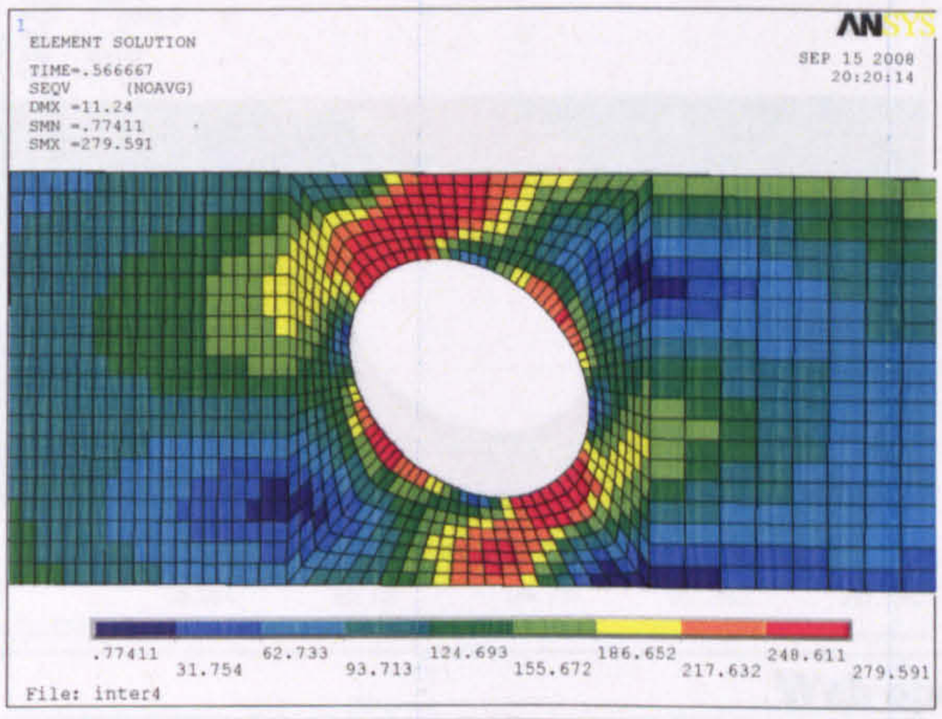

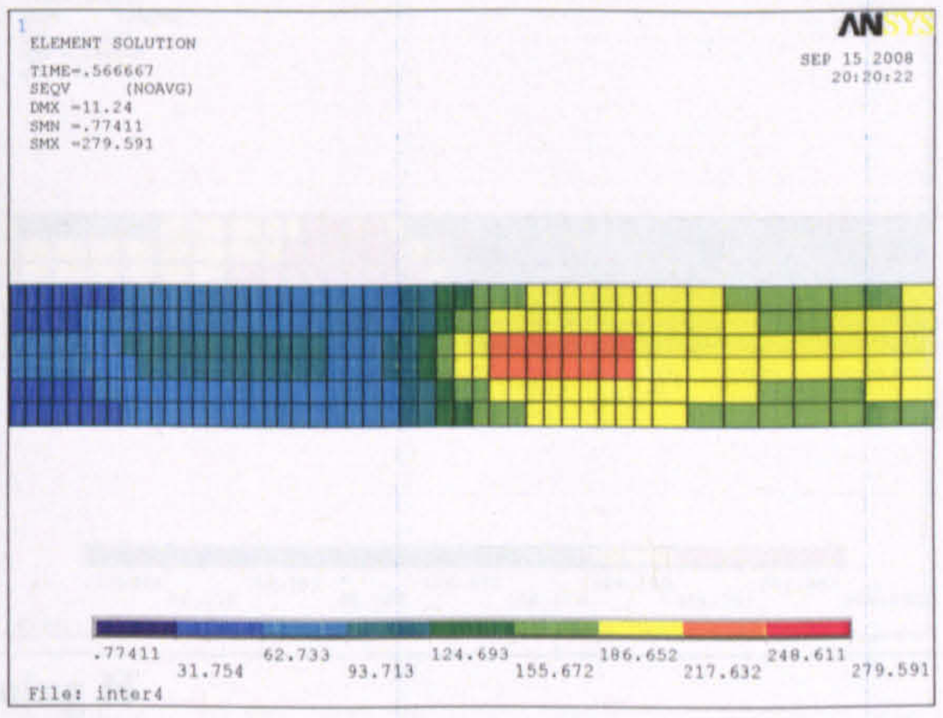

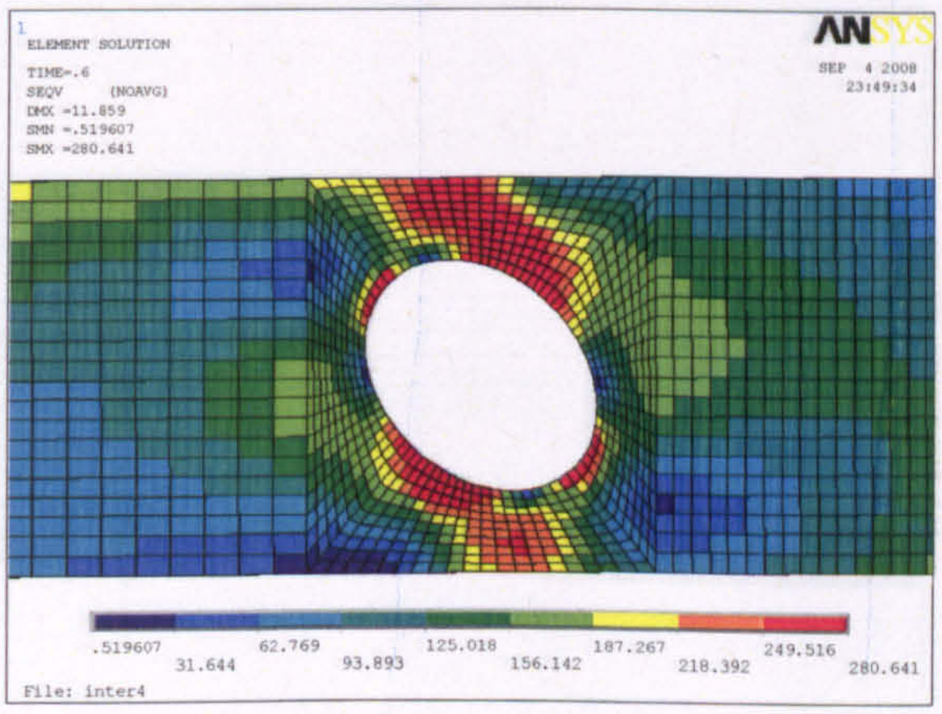

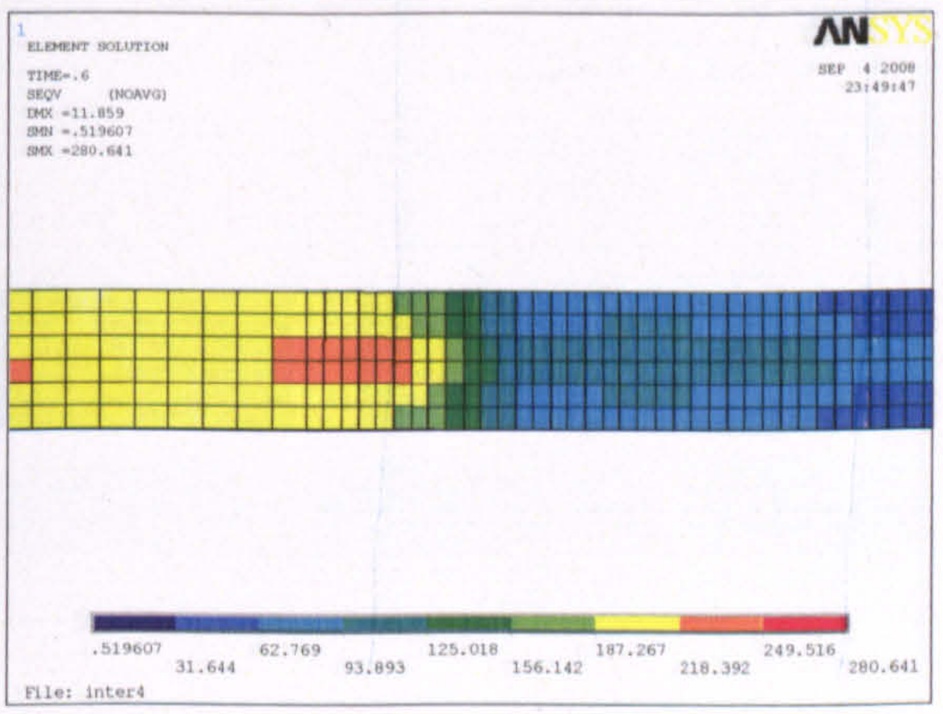

Web opening G

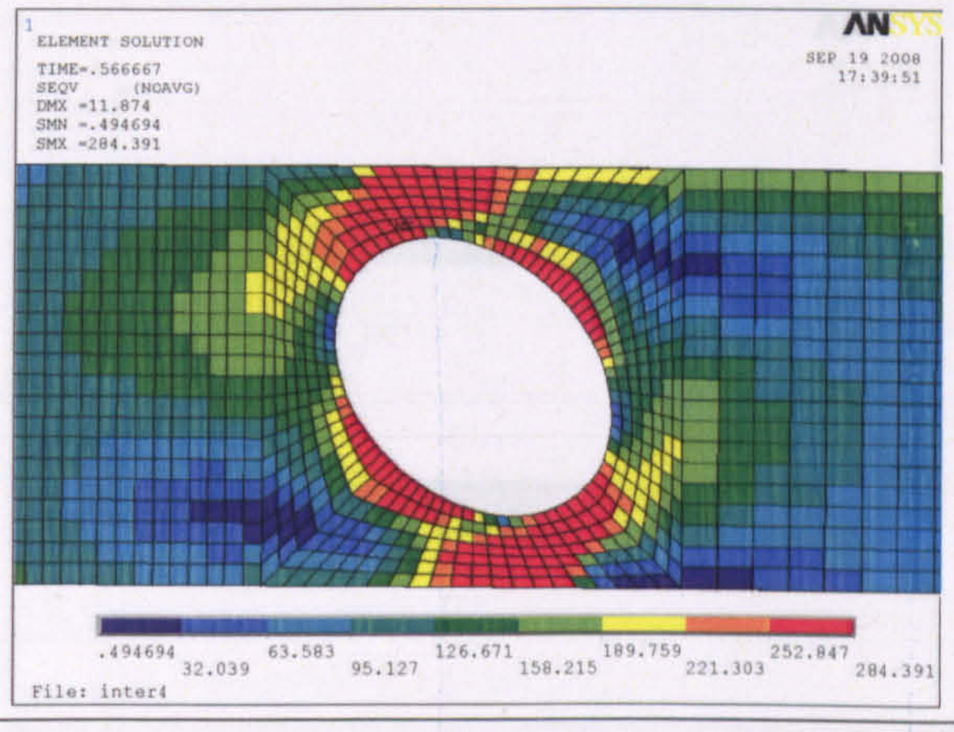

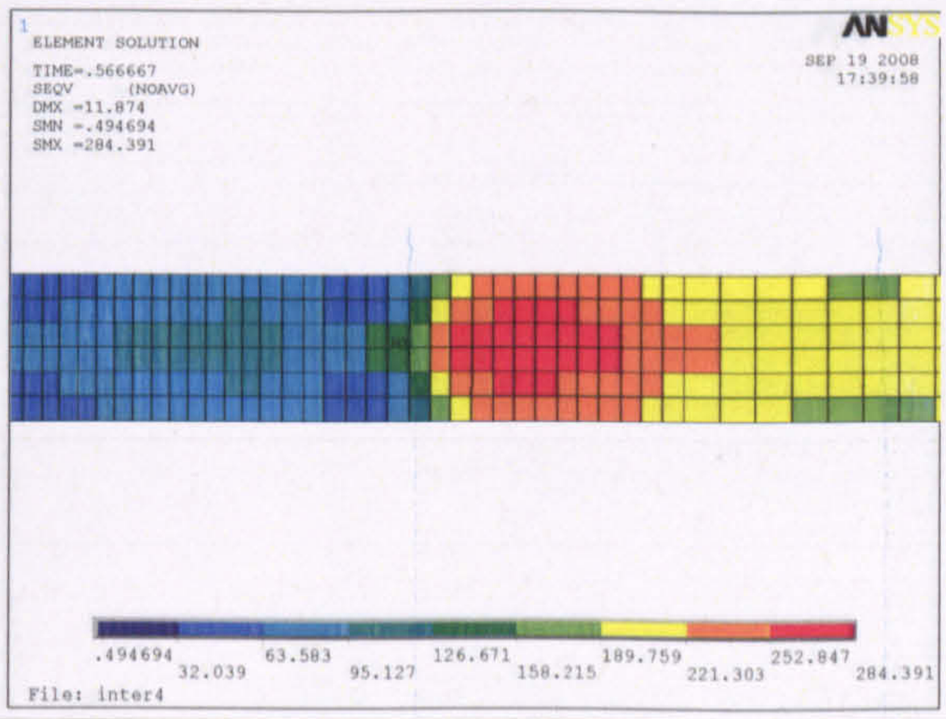

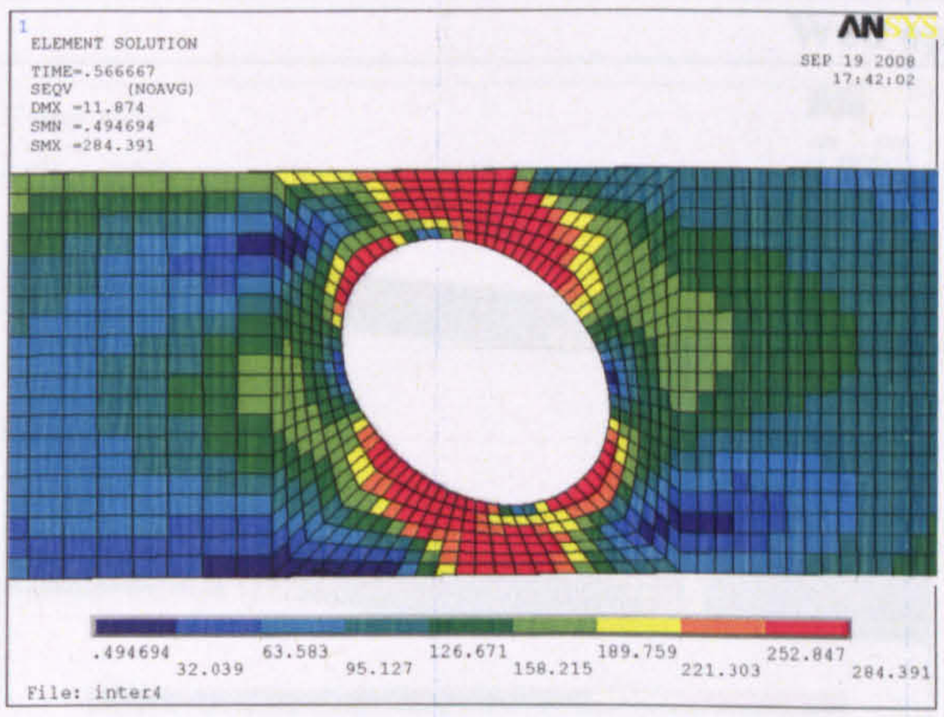

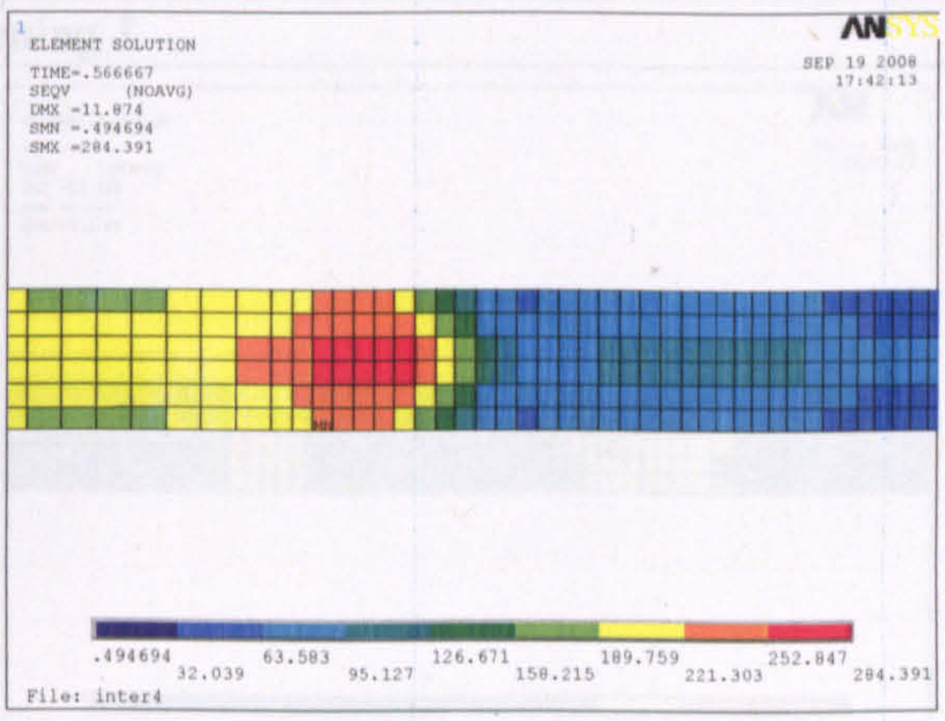

Web opening H

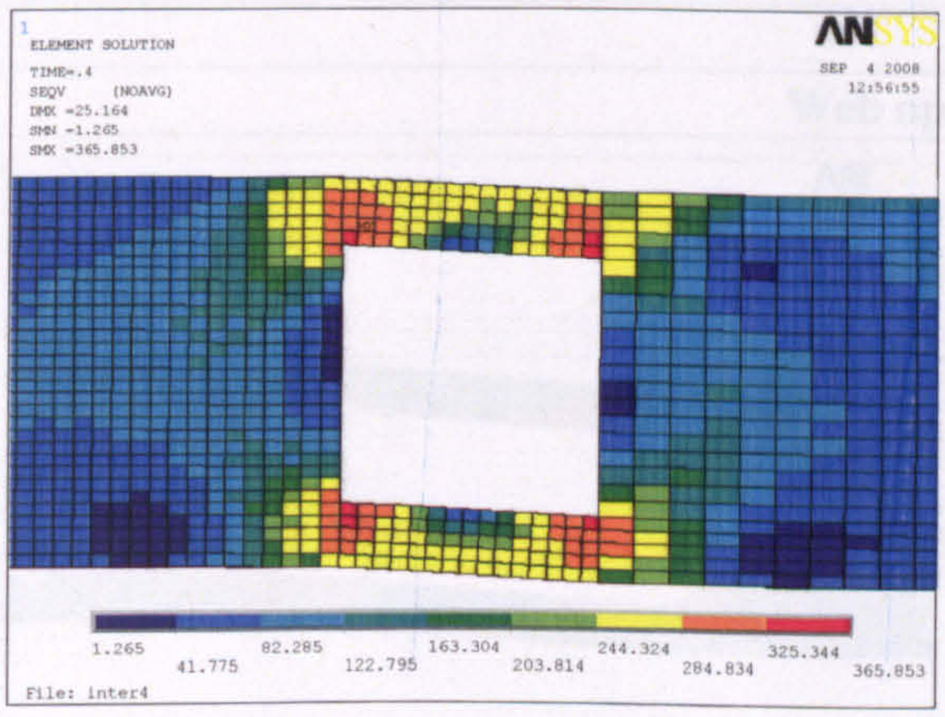

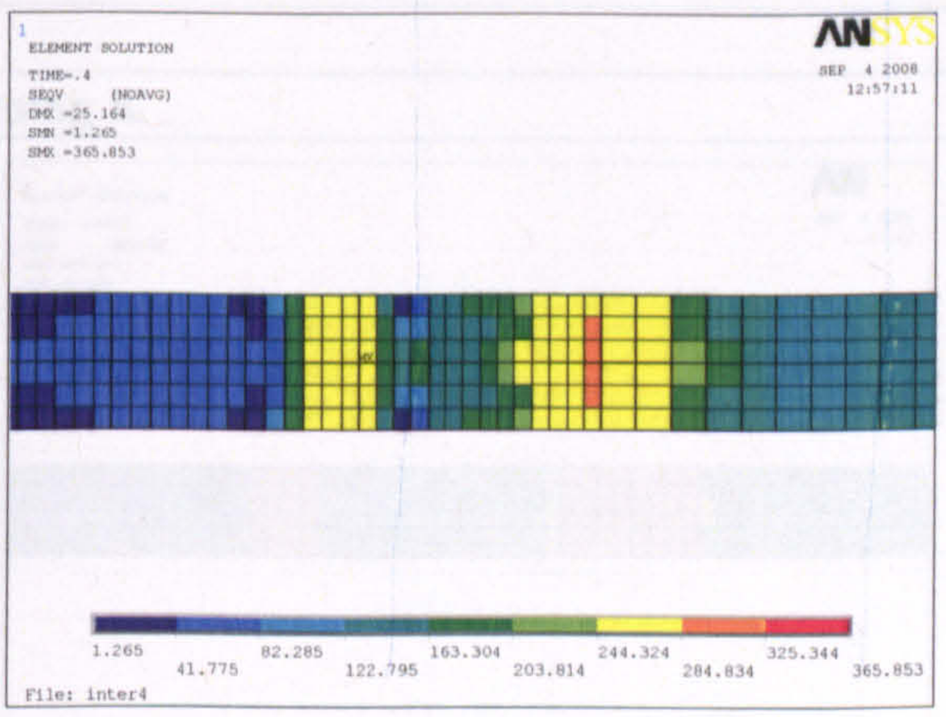

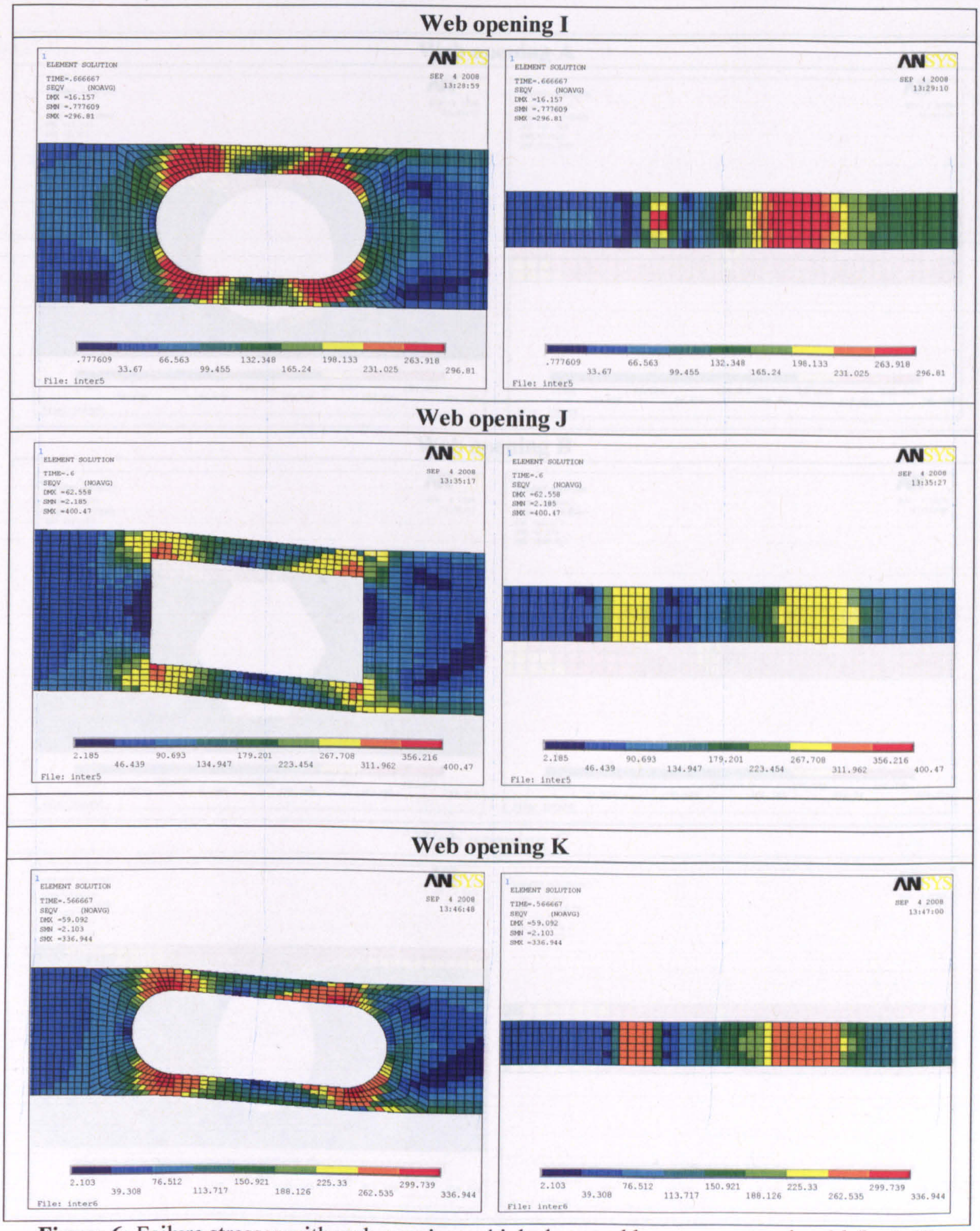

Figure 6: Failure stresses with web opening at high shear and low moment region ($d_o/h=0.65$)

Web opening A

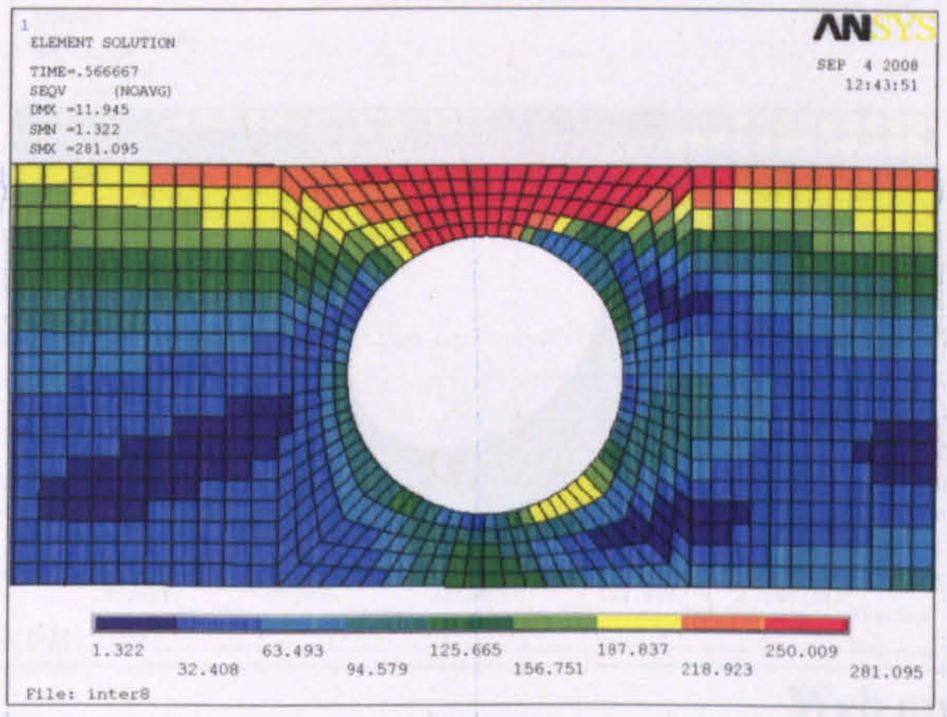

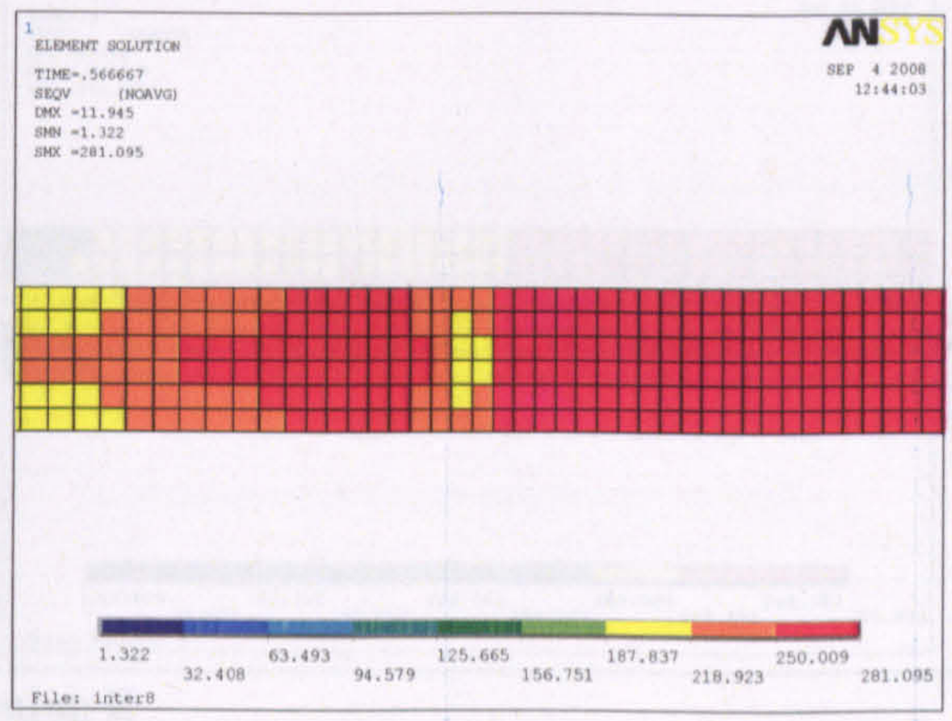

Web opening B

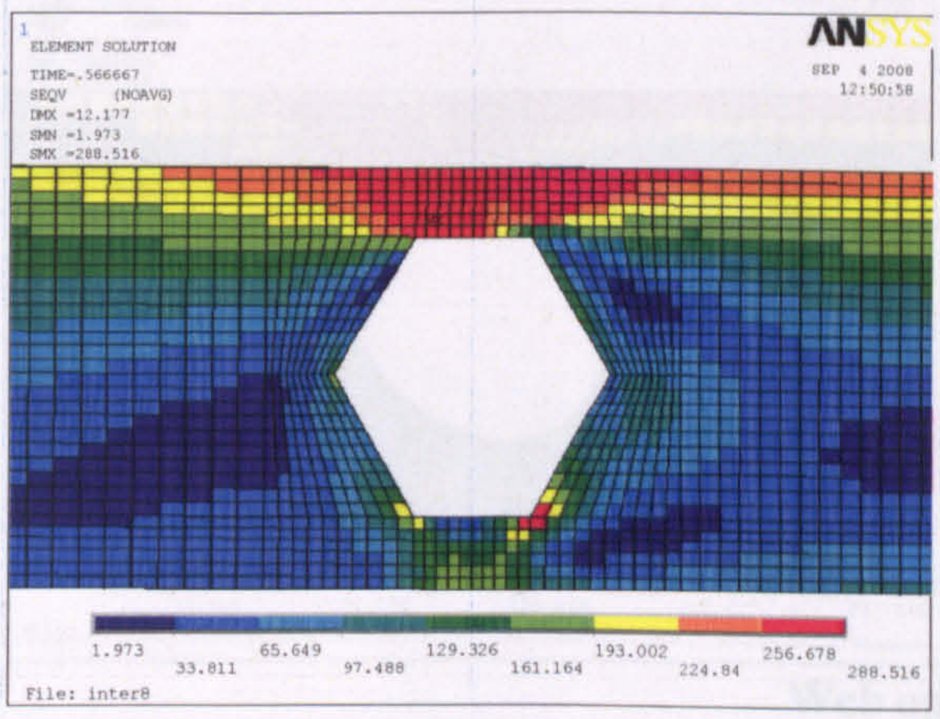

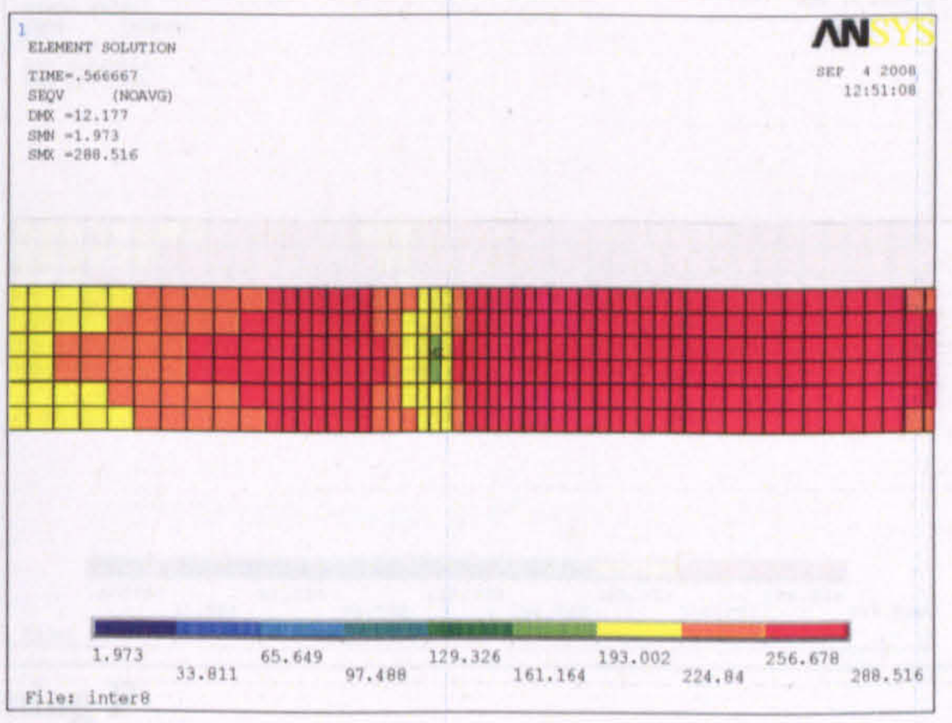

Web opening C

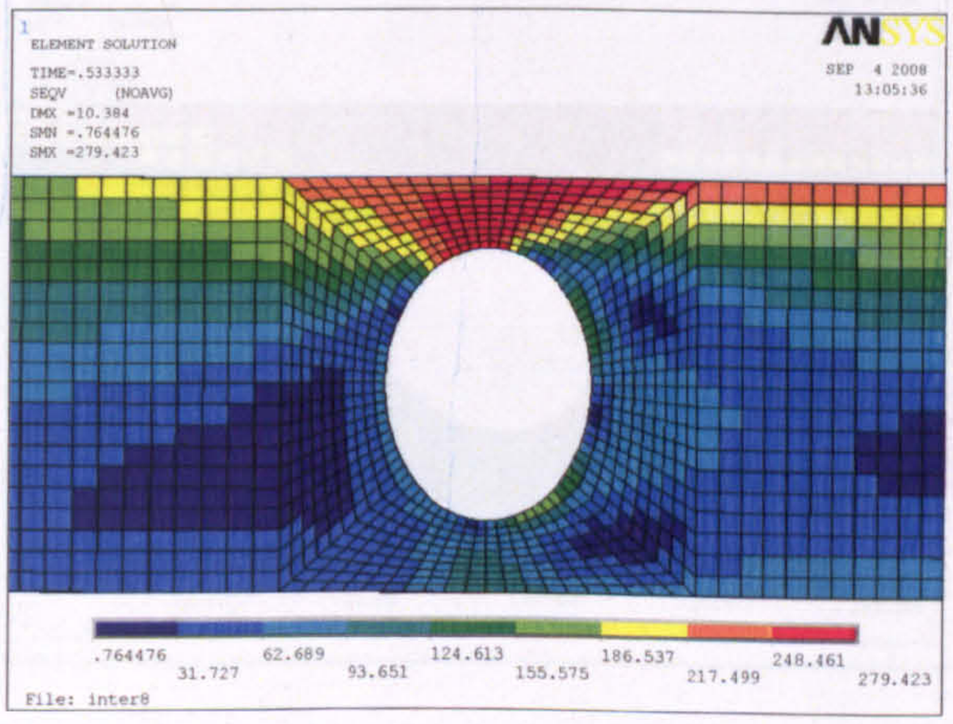

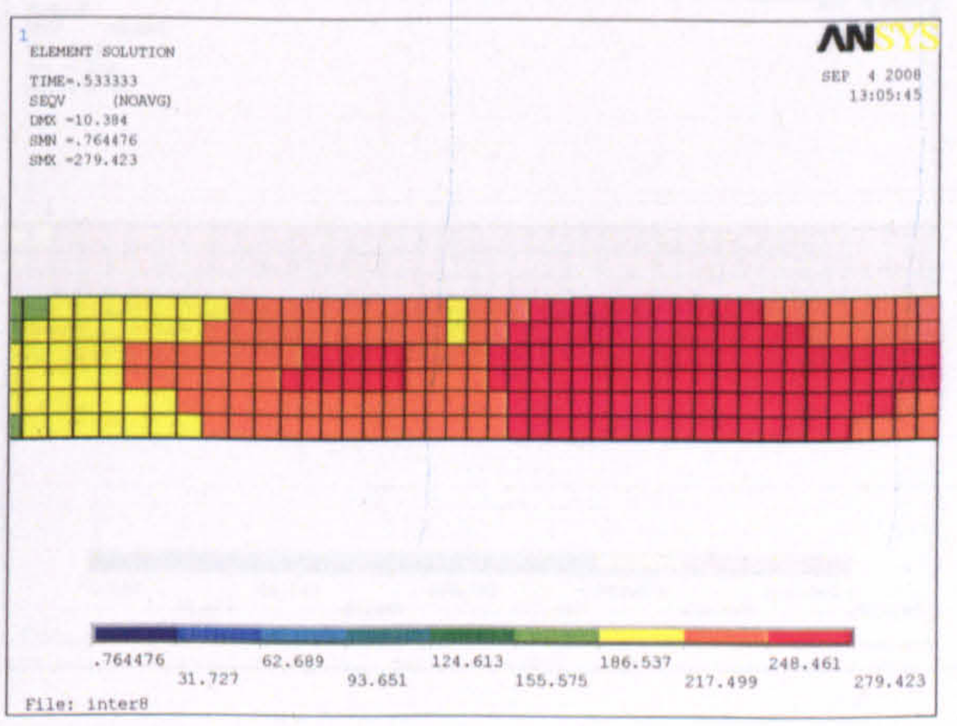

Web opening D

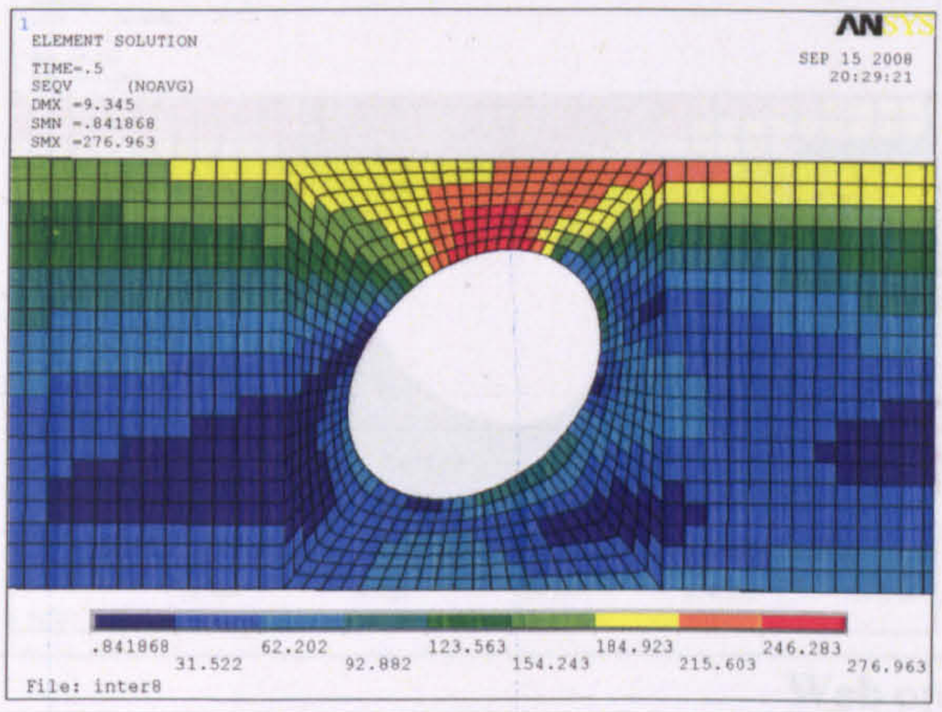

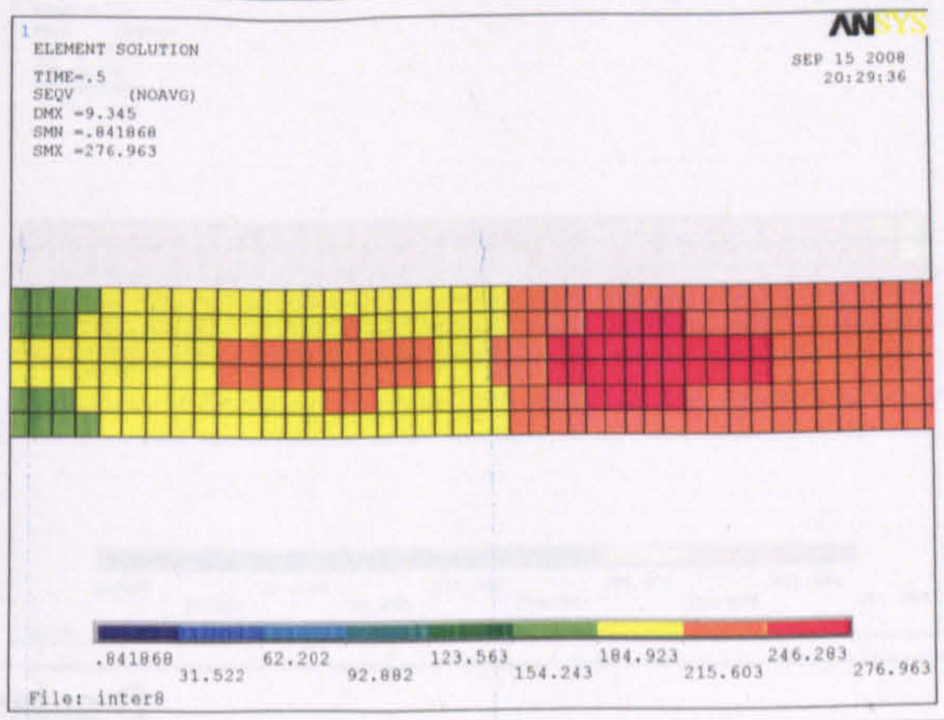

Web opening E

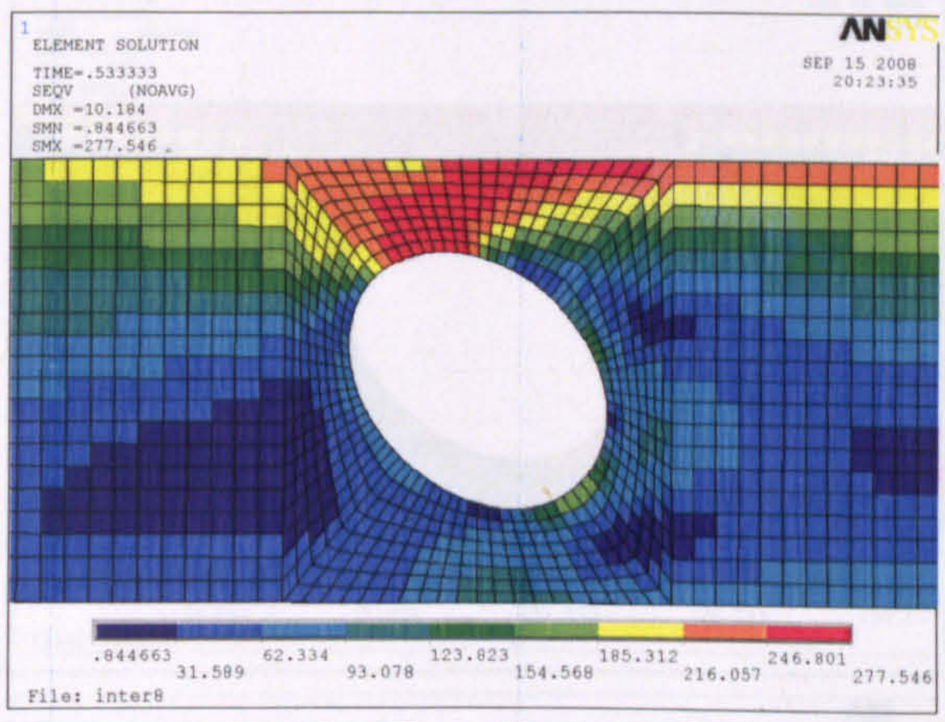

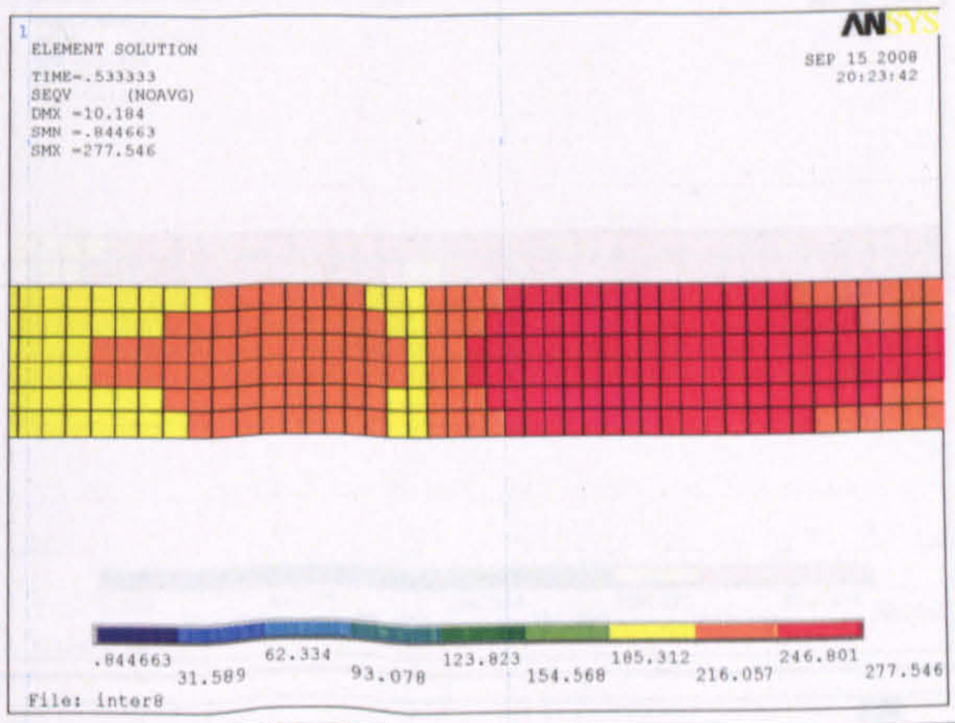

Web opening F

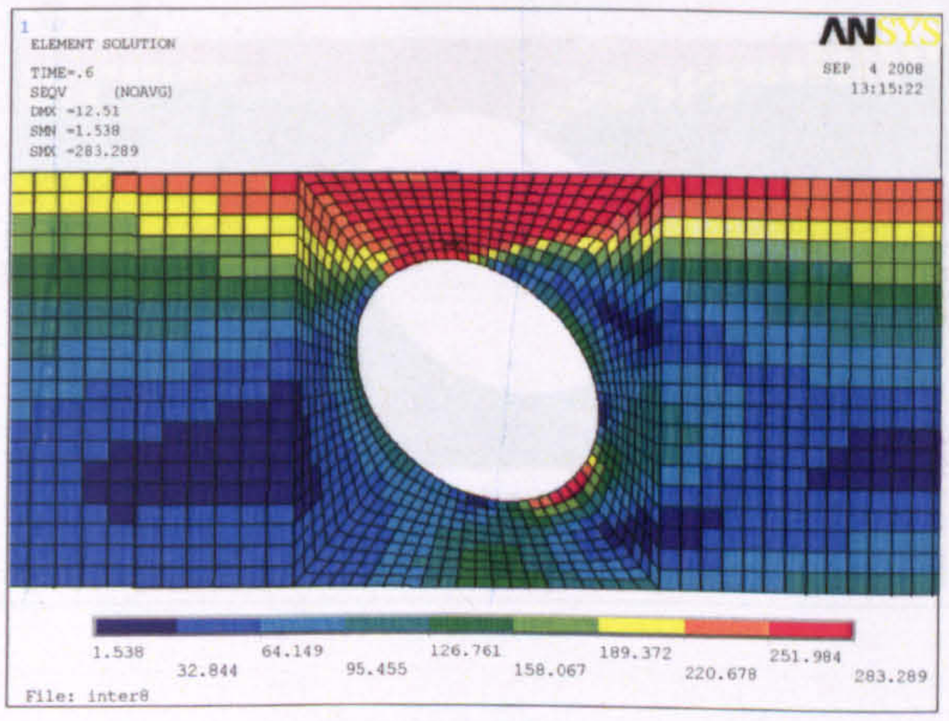

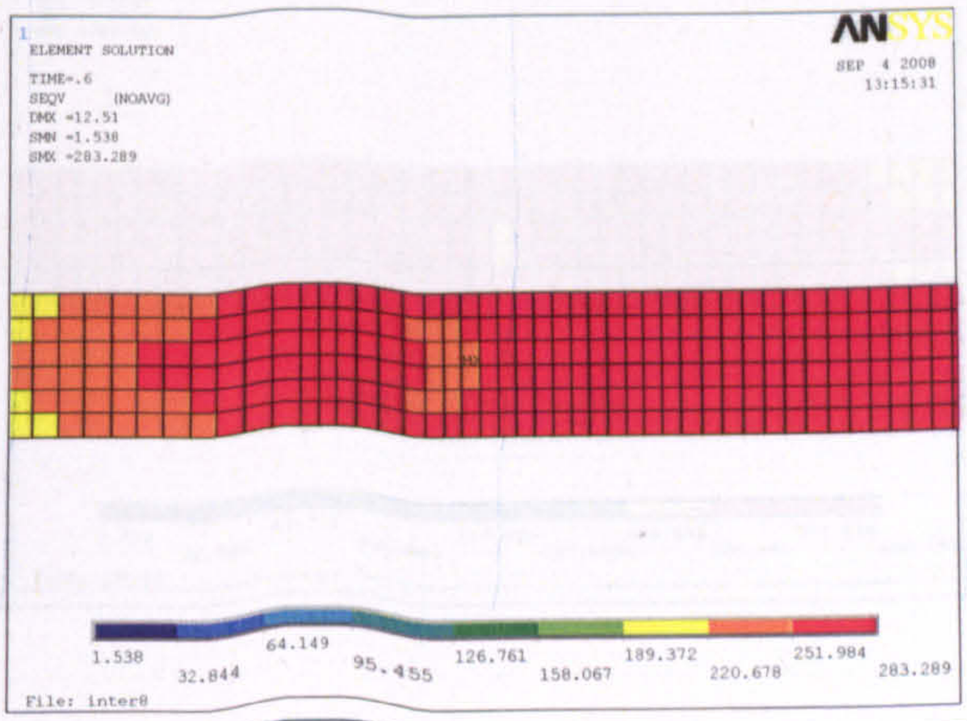

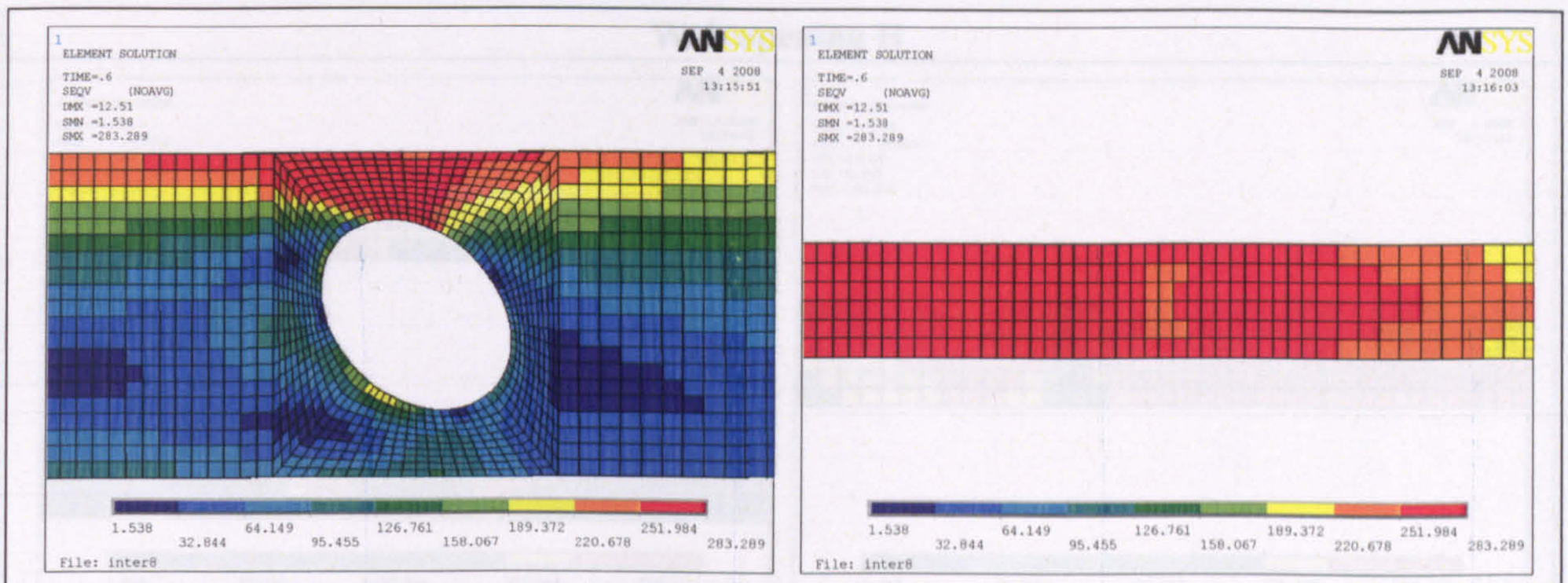

Web opening G

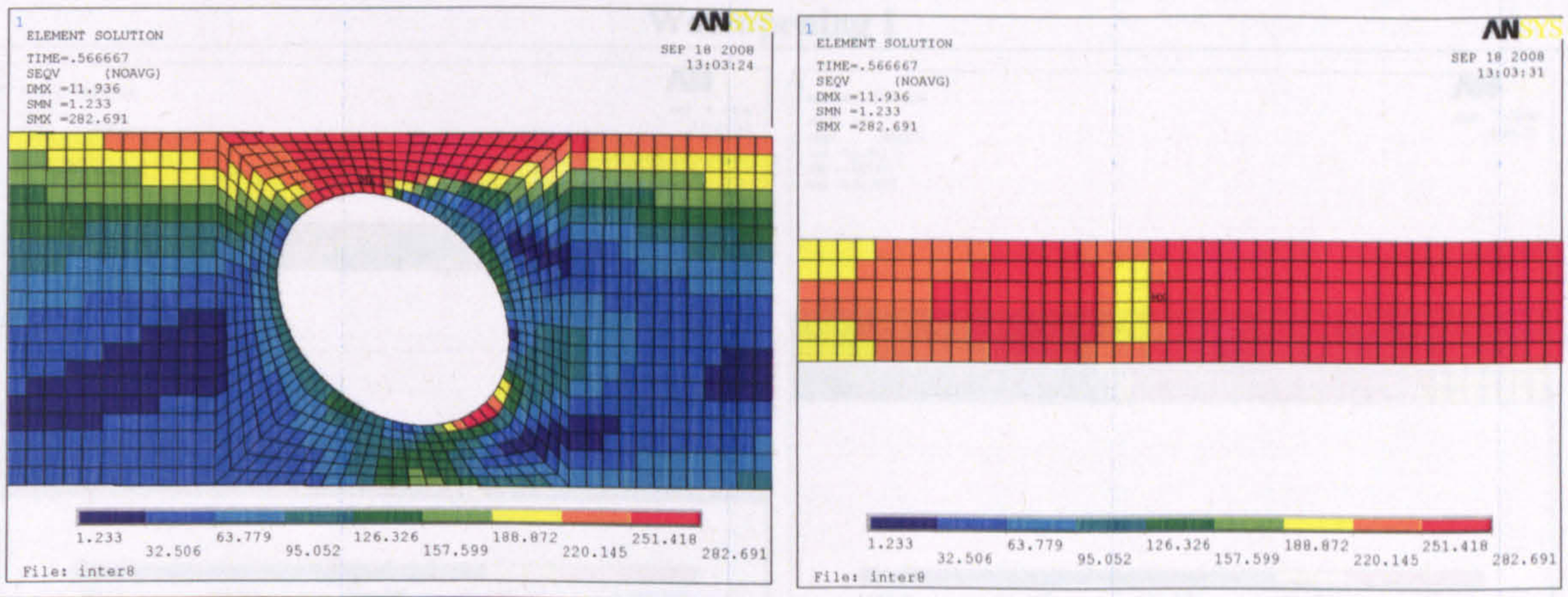

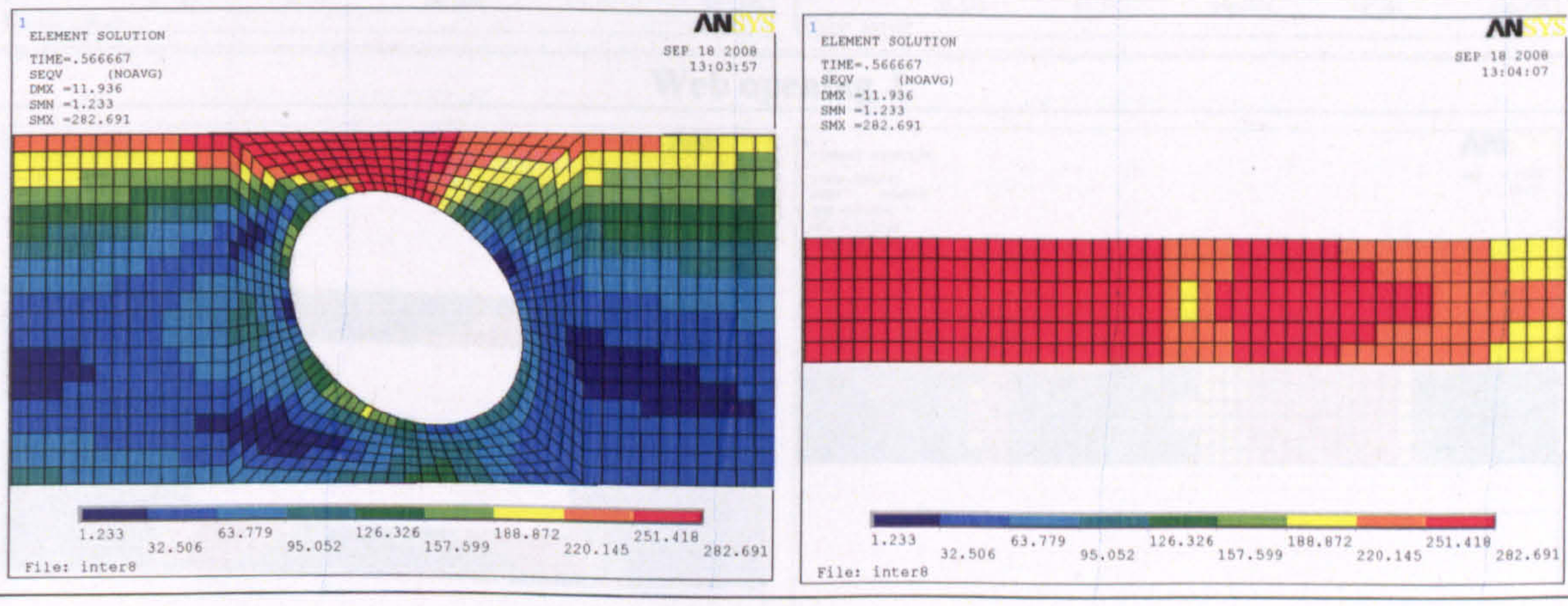

Web opening H

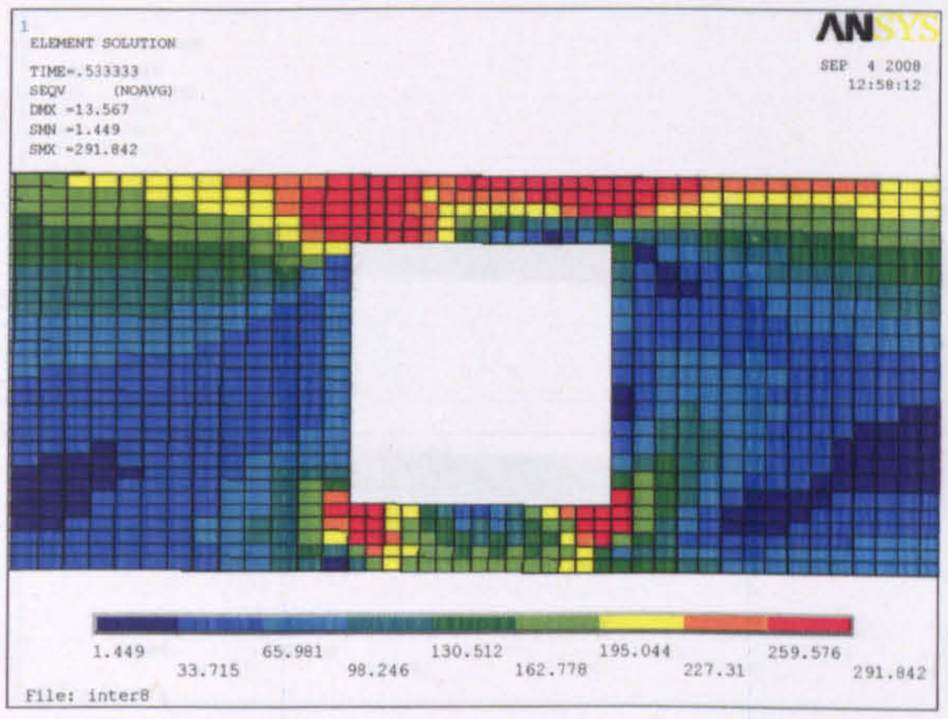

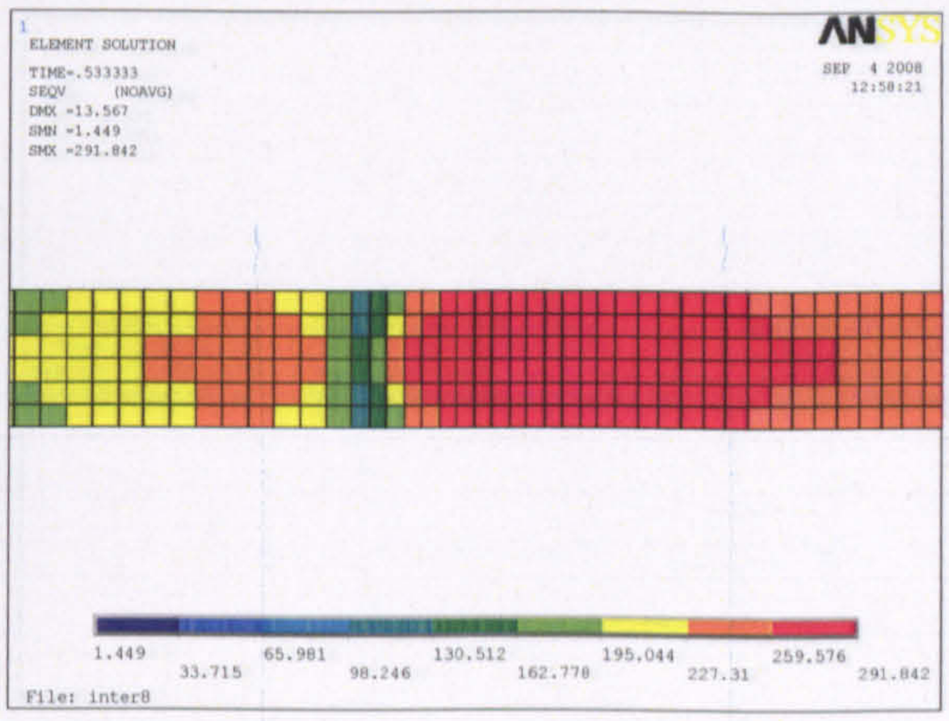

Web opening I

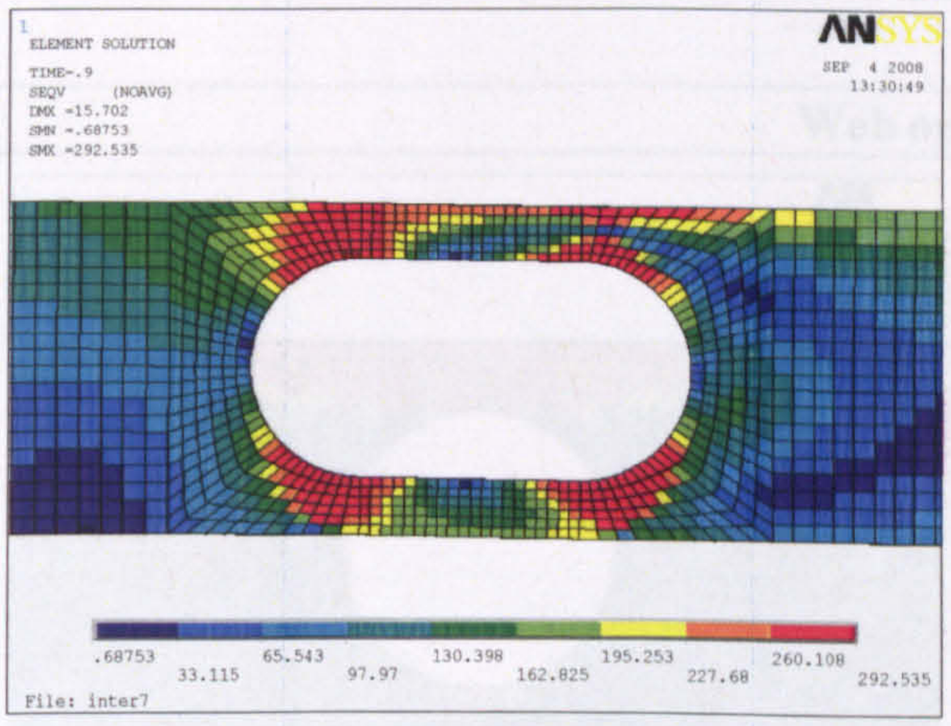

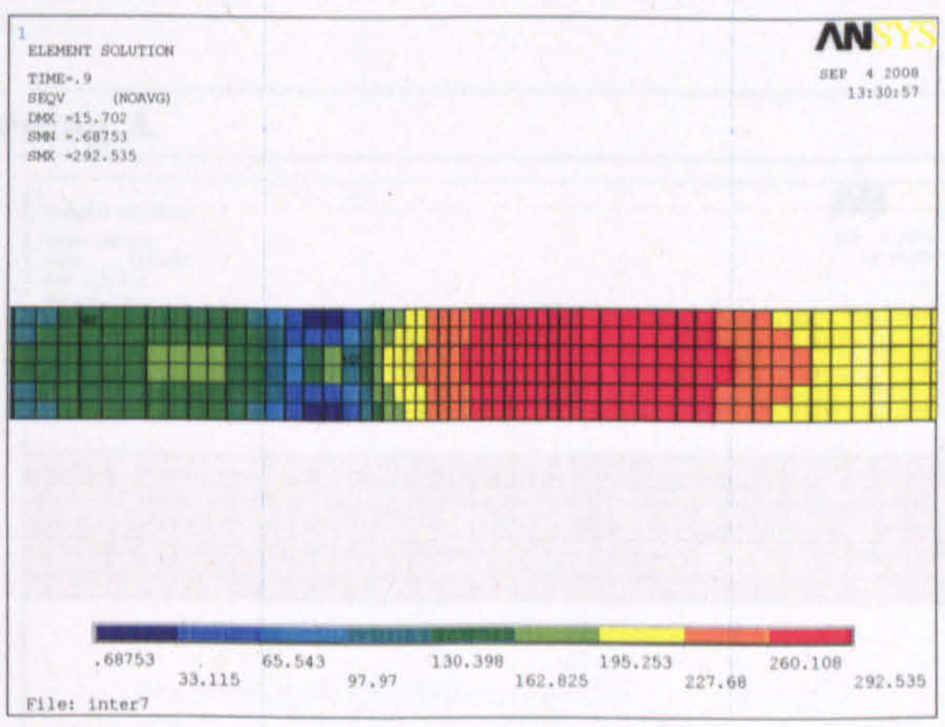

Web opening J

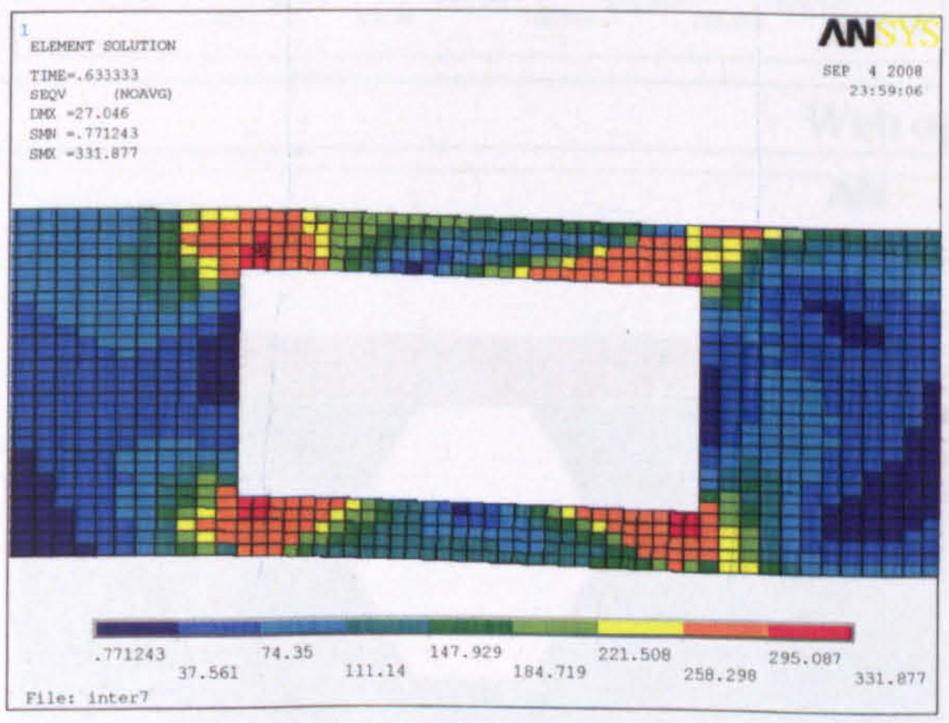

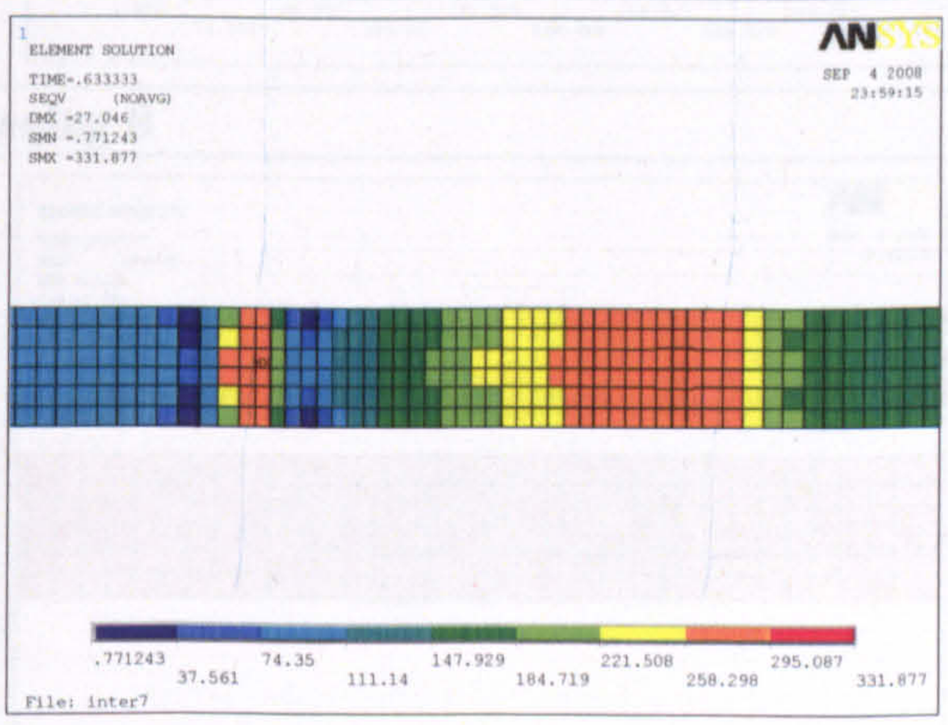

Web opening K

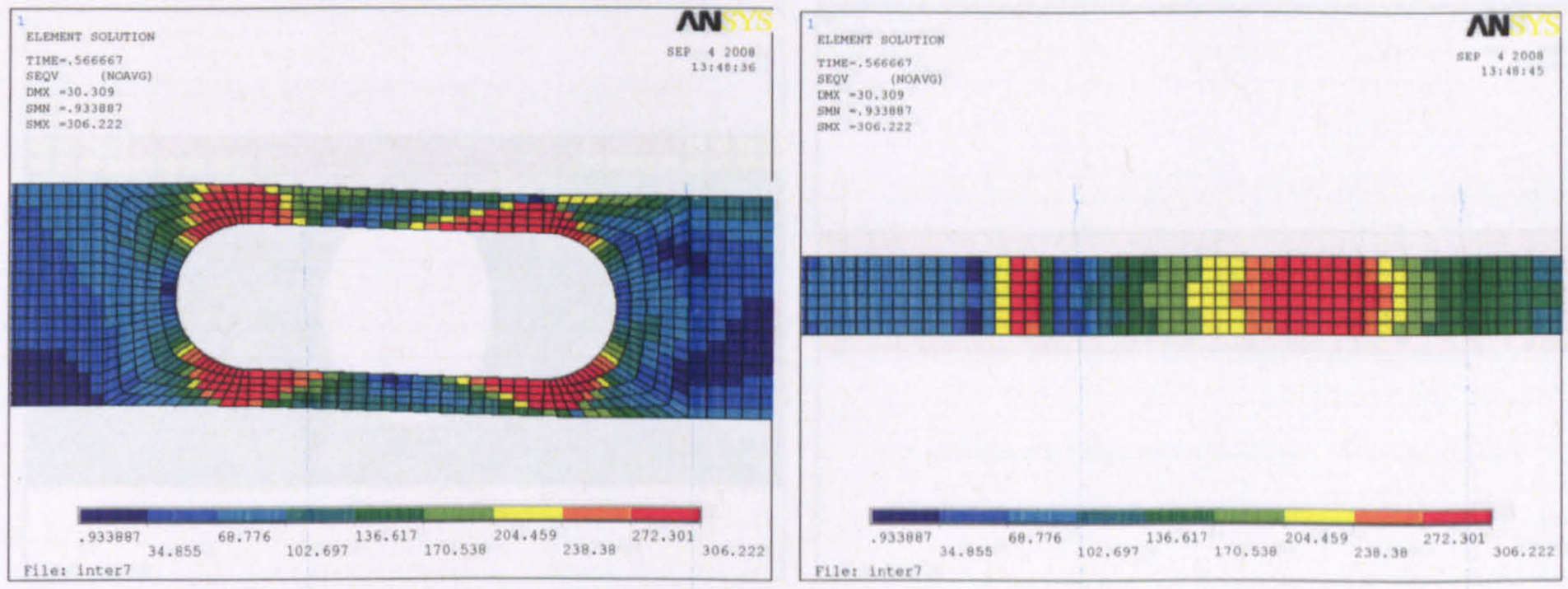

Figure 7: Failure stresses with web opening at high moment and low shear region ($d_o/h=0.65$)

Web opening A

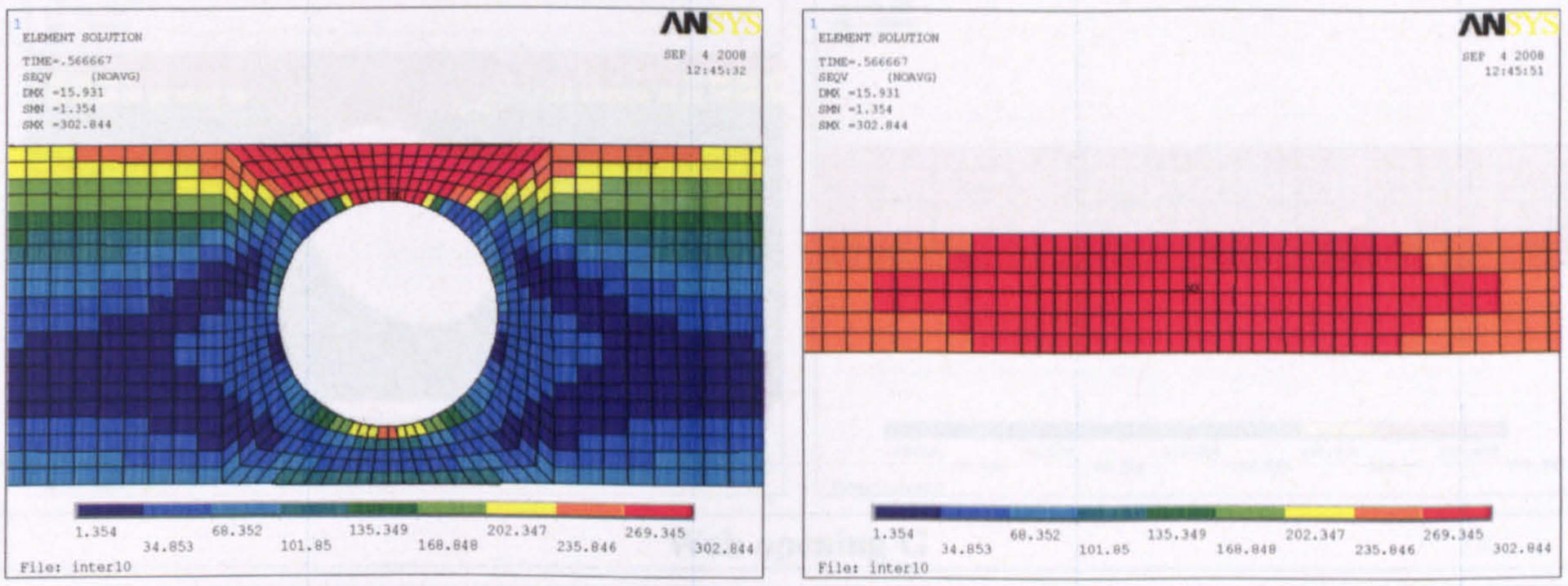

Web opening B

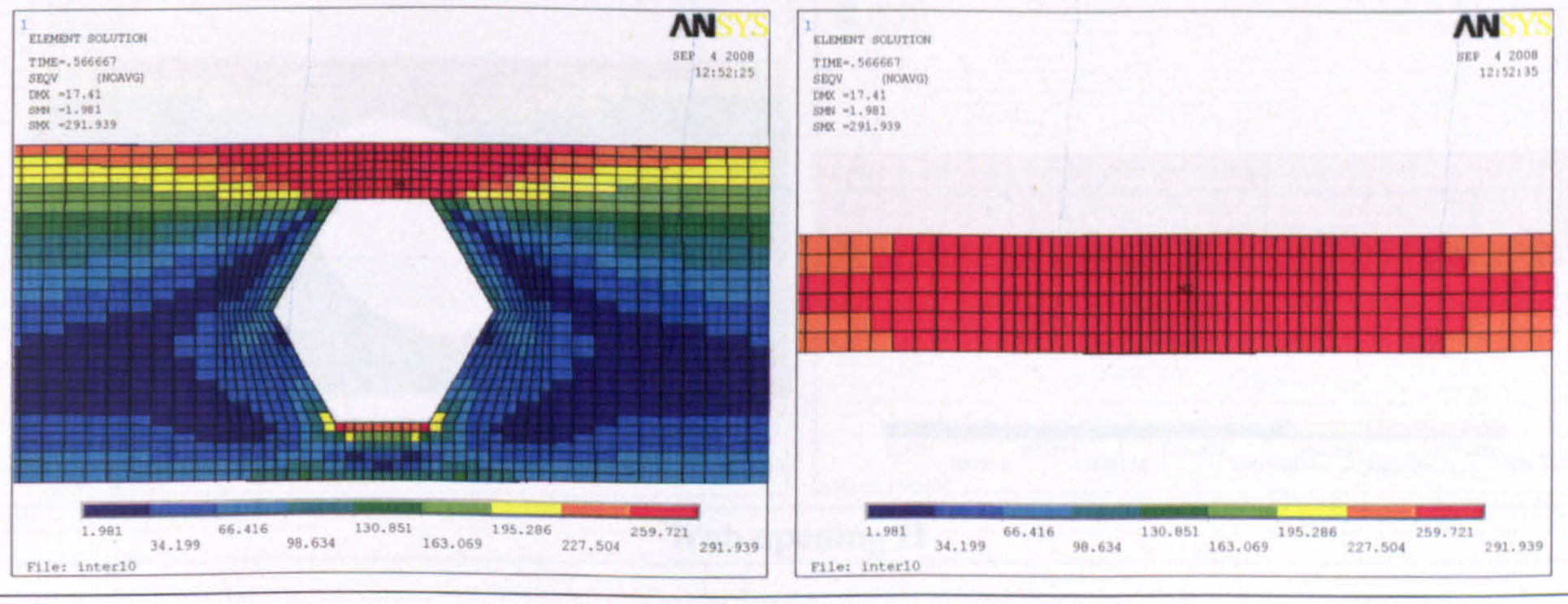

Web opening C

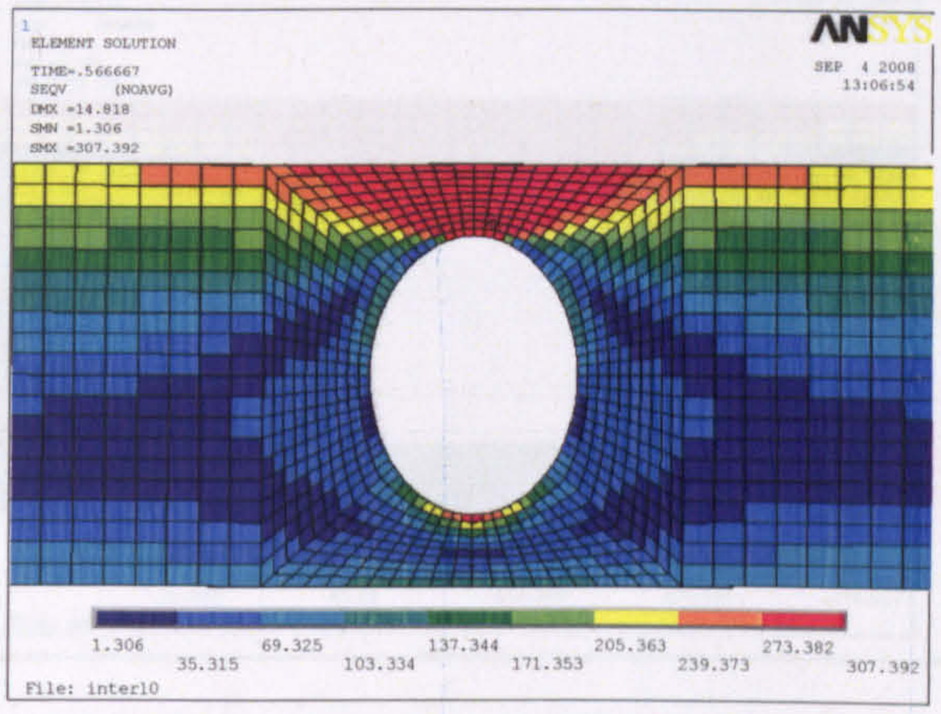

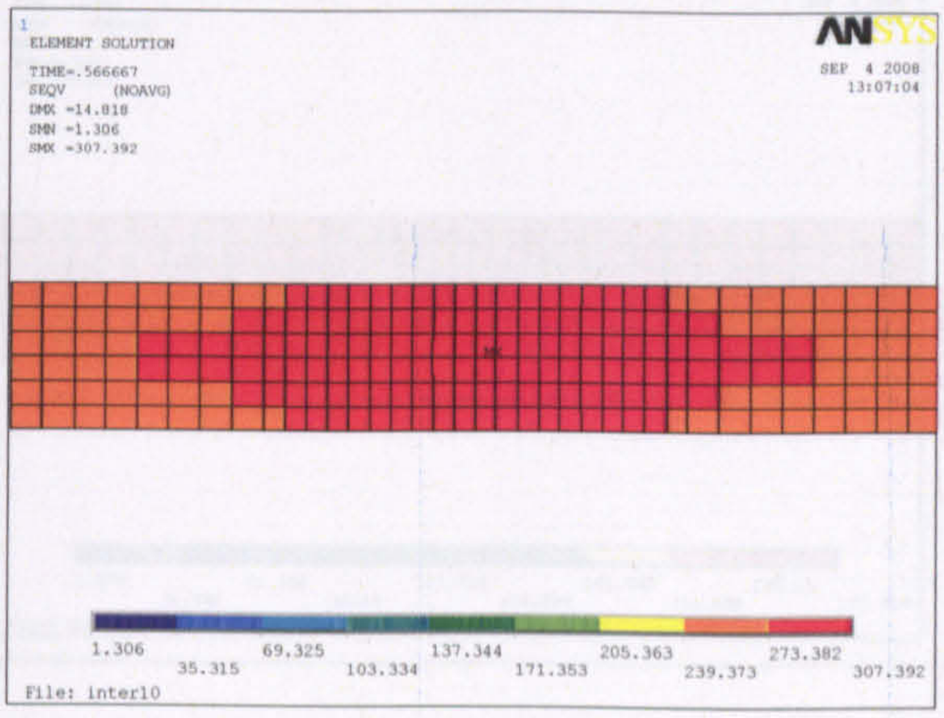

Web opening D-E-F

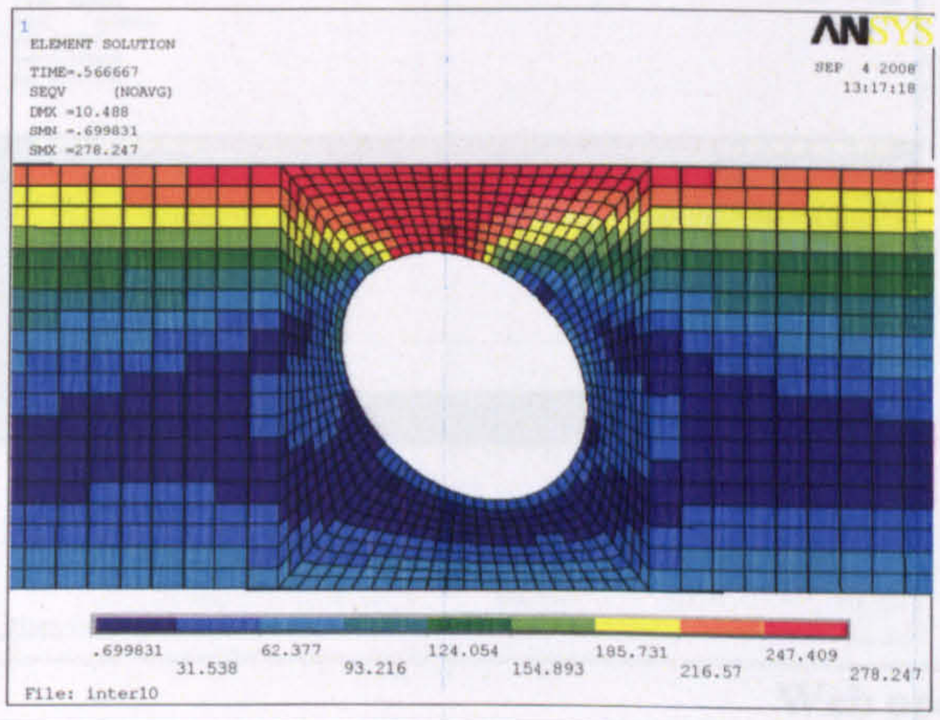

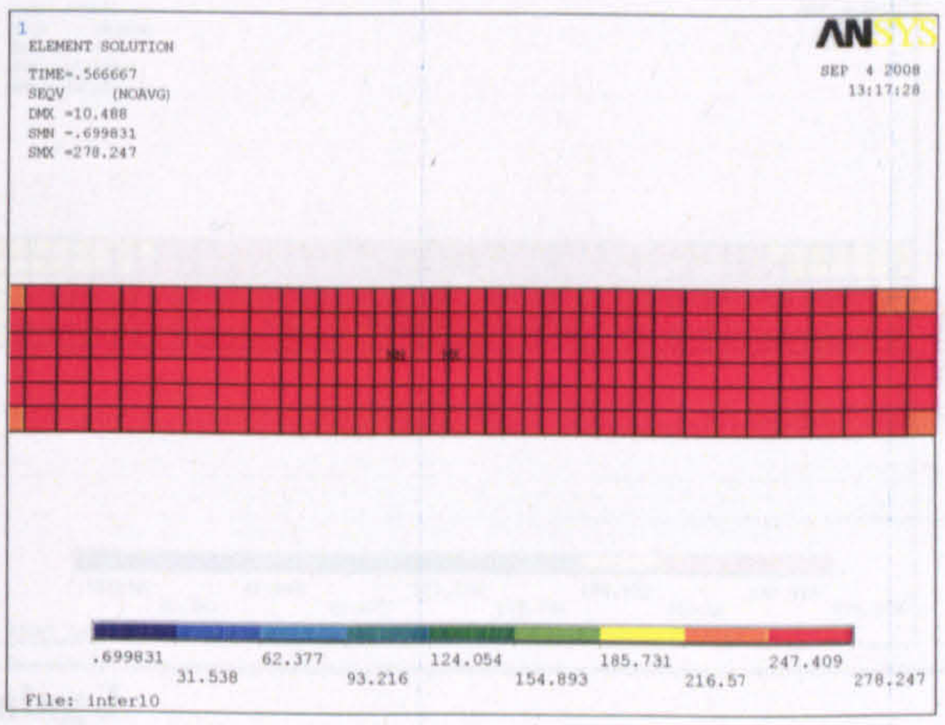

Web opening G

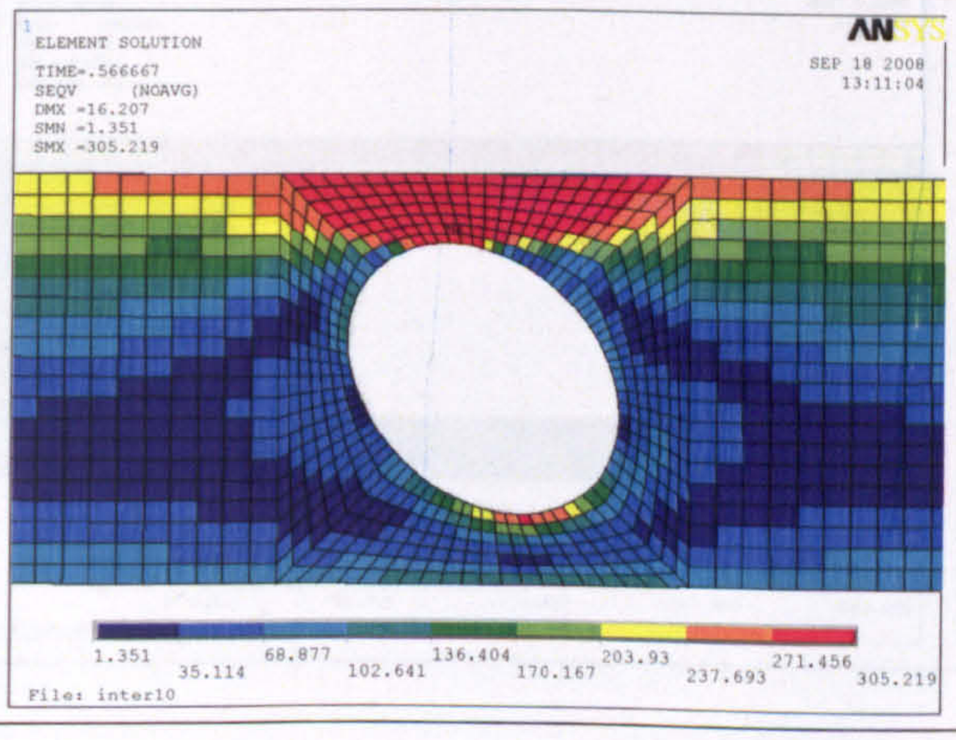

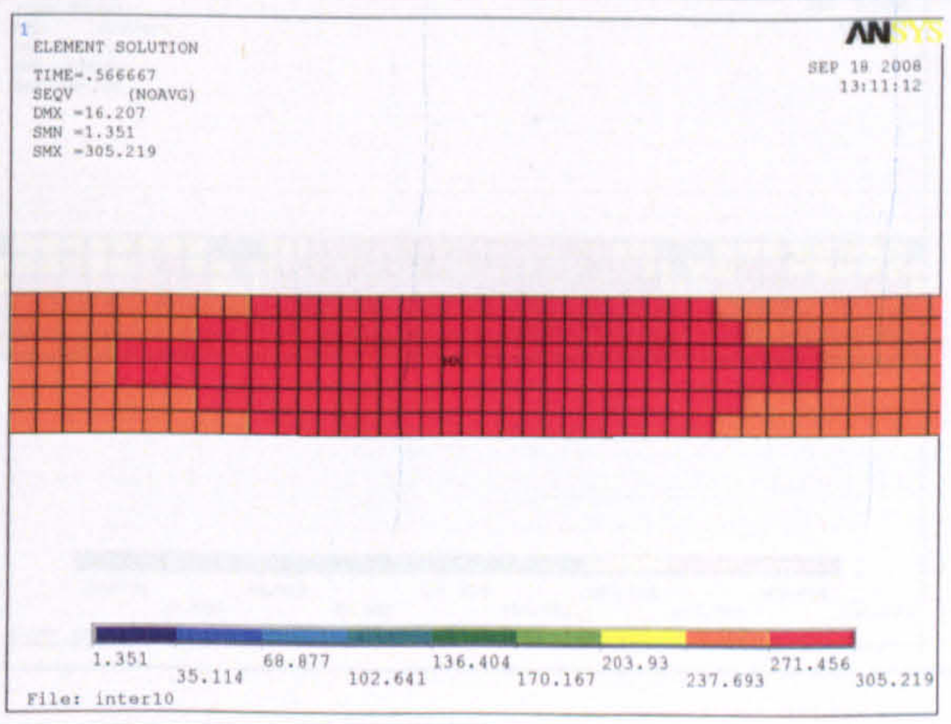

Web opening H

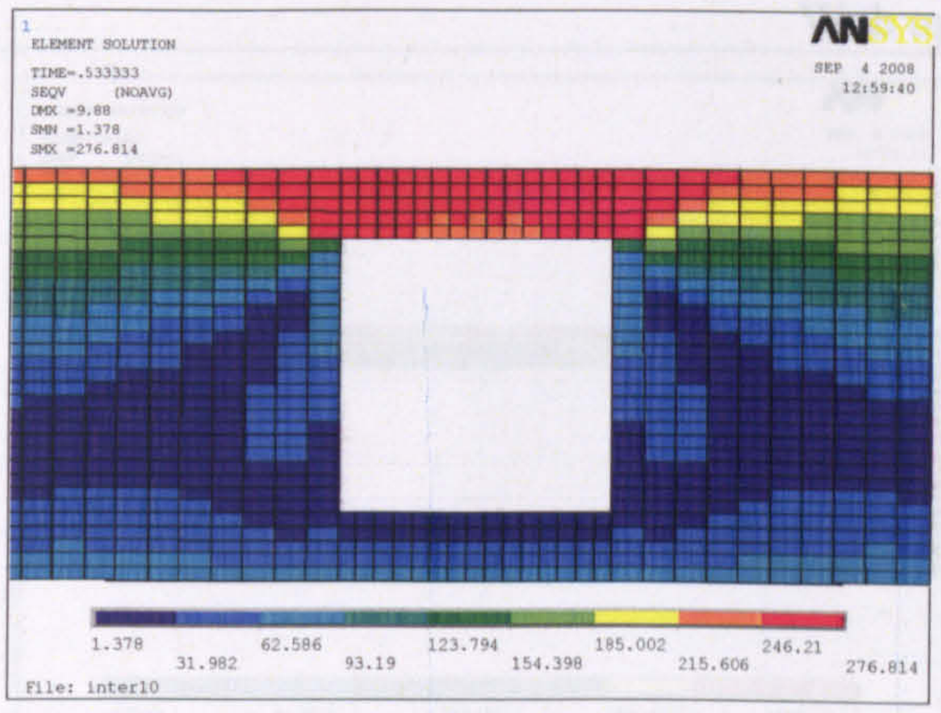

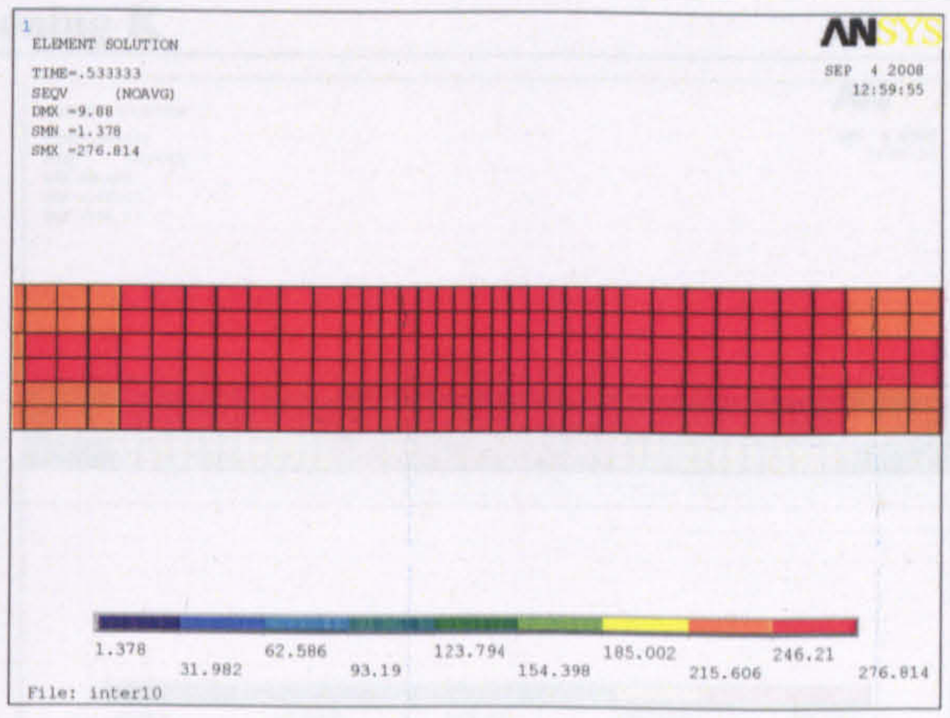

Web opening I

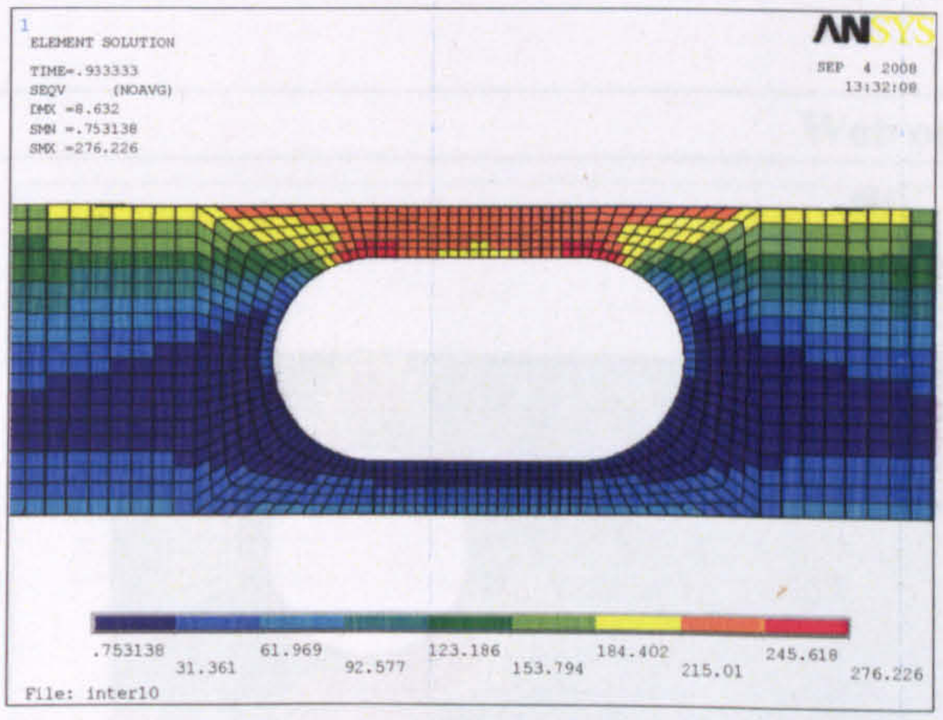

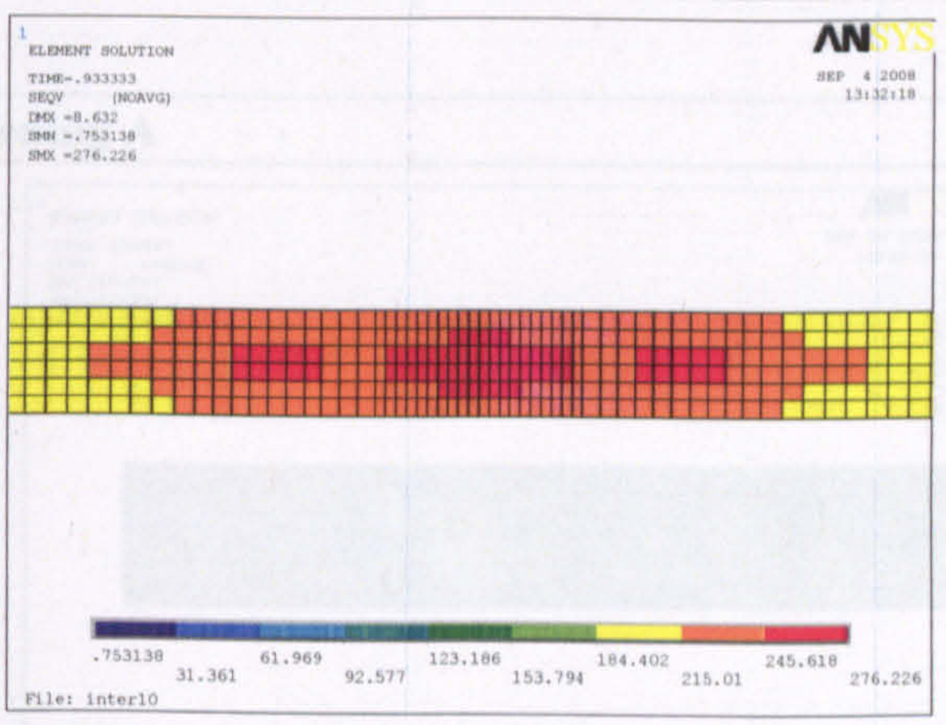

Web opening J

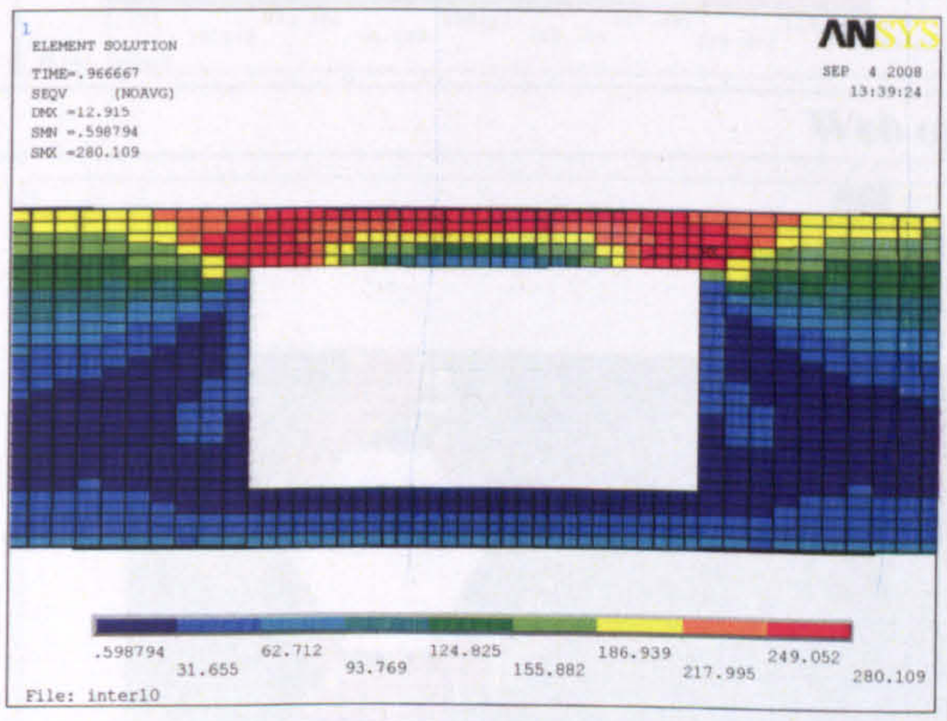

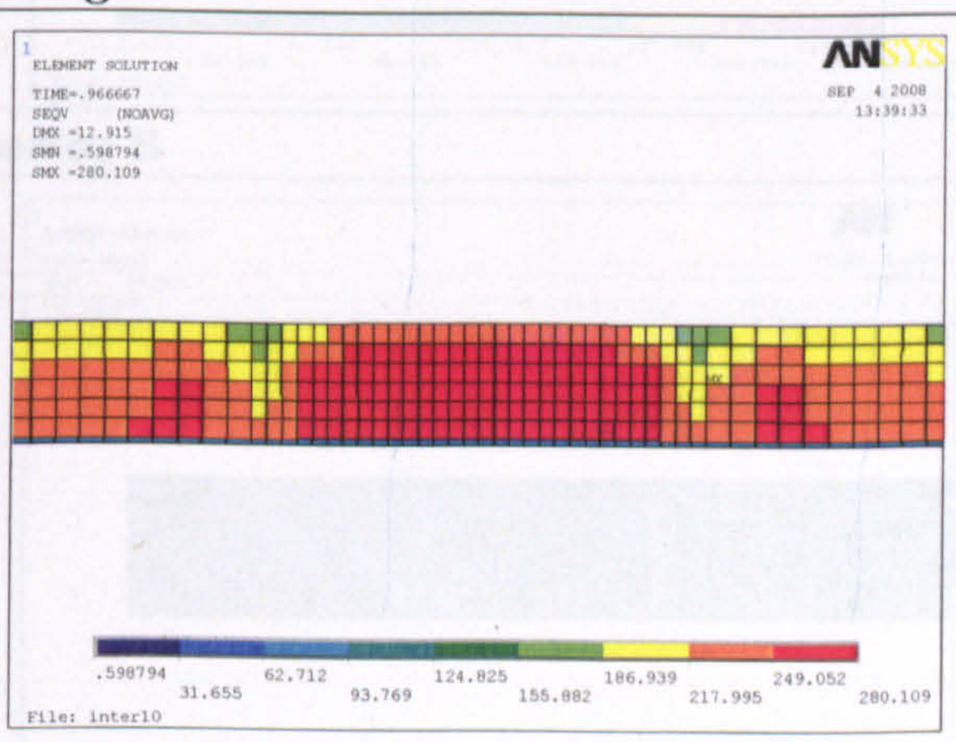

Web opening K

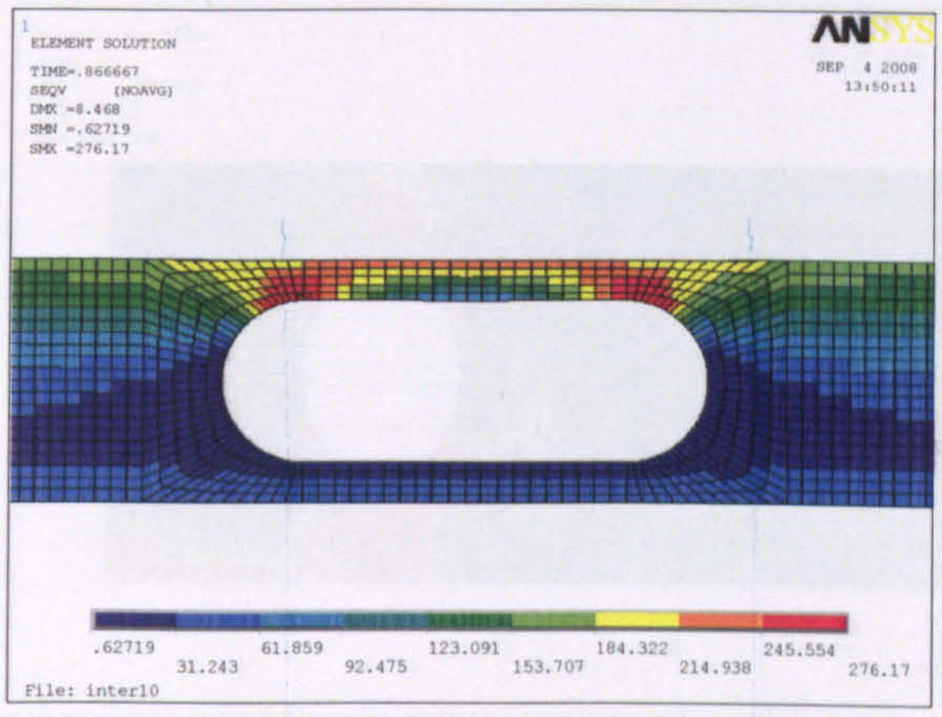

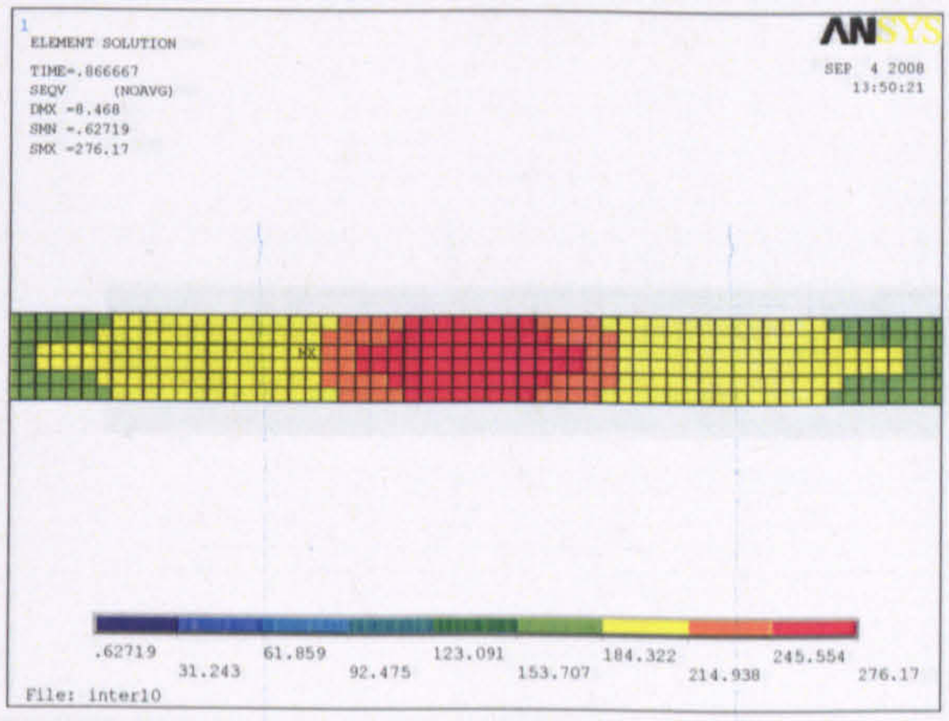

Figure 8: Failure stresses with web opening at high moment region ($d_o/h=0.65$)

Web opening A

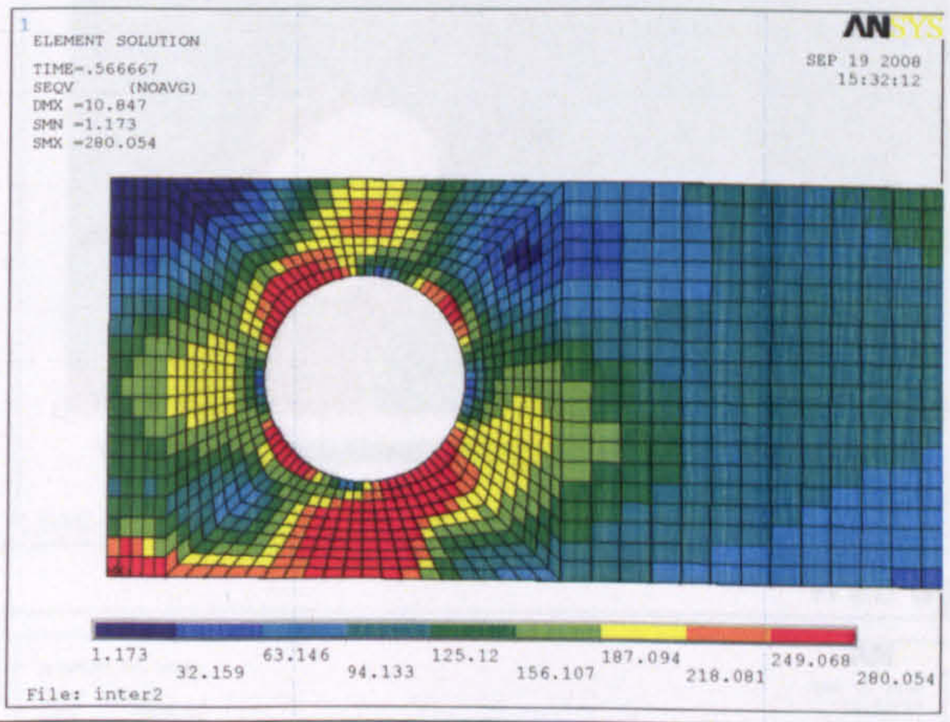

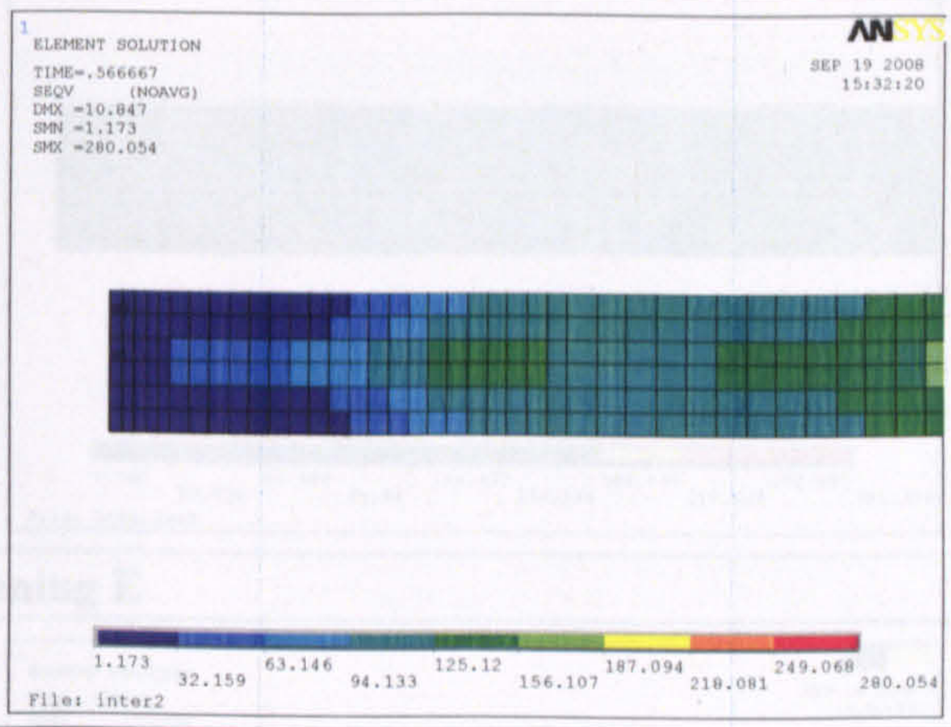

Web opening B

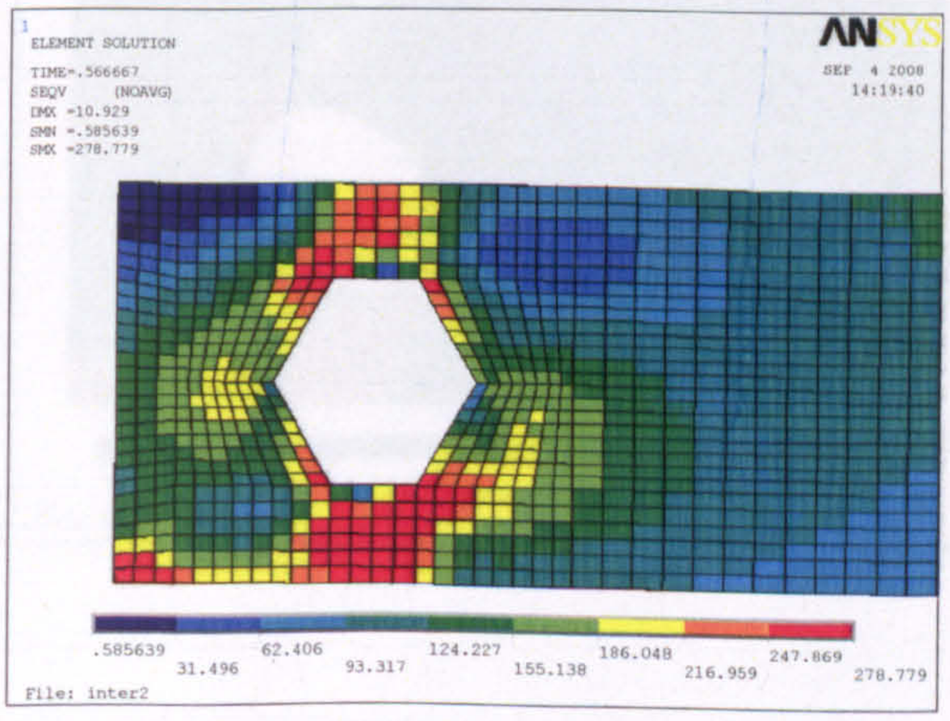

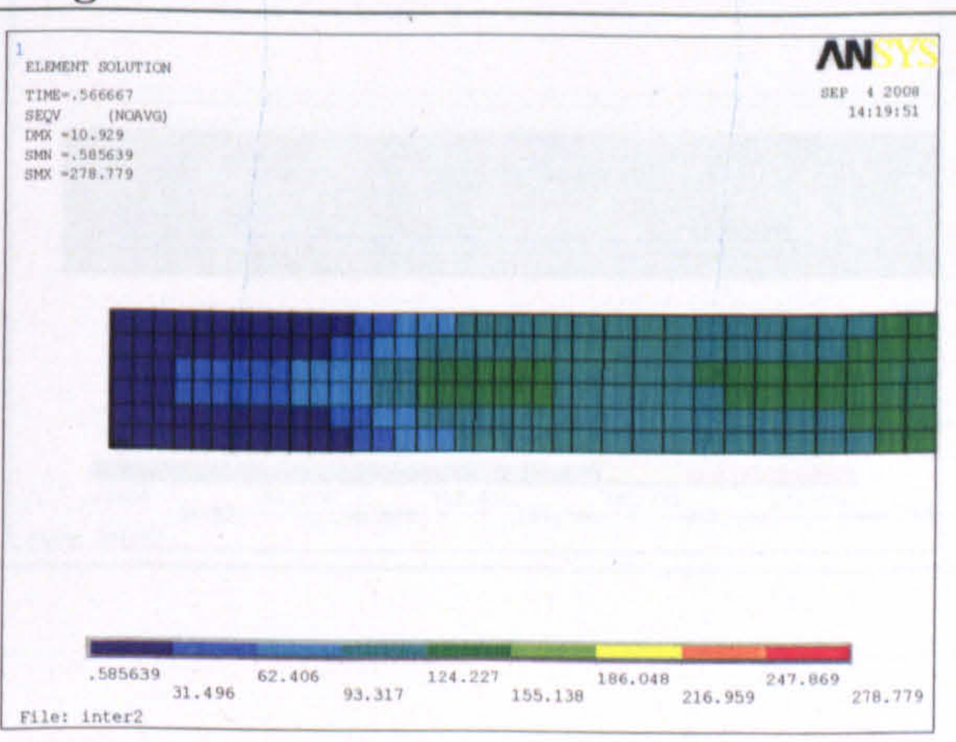

Web opening C

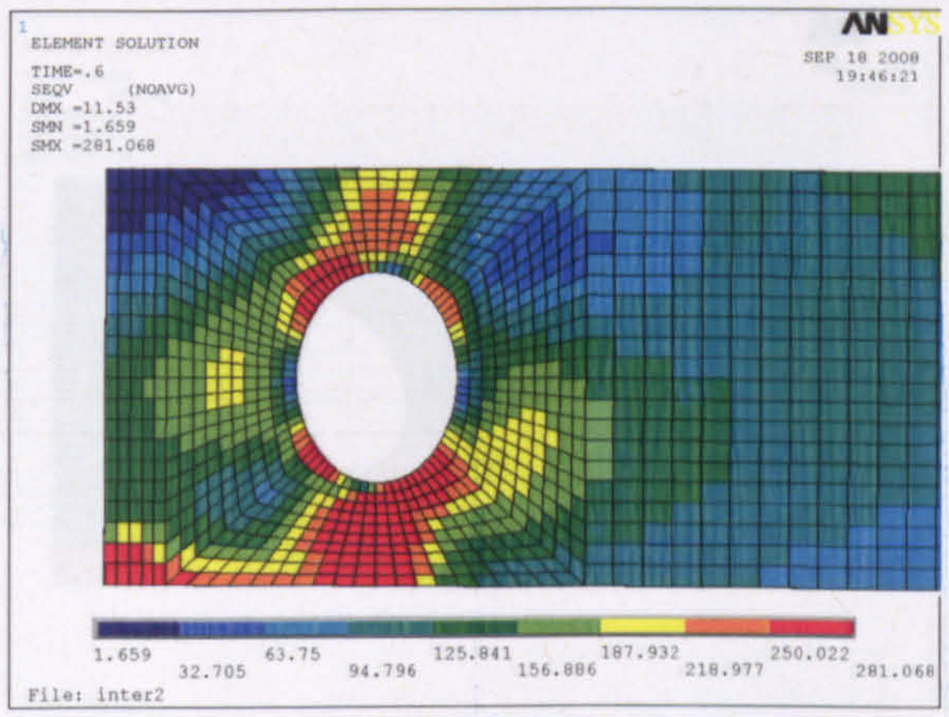

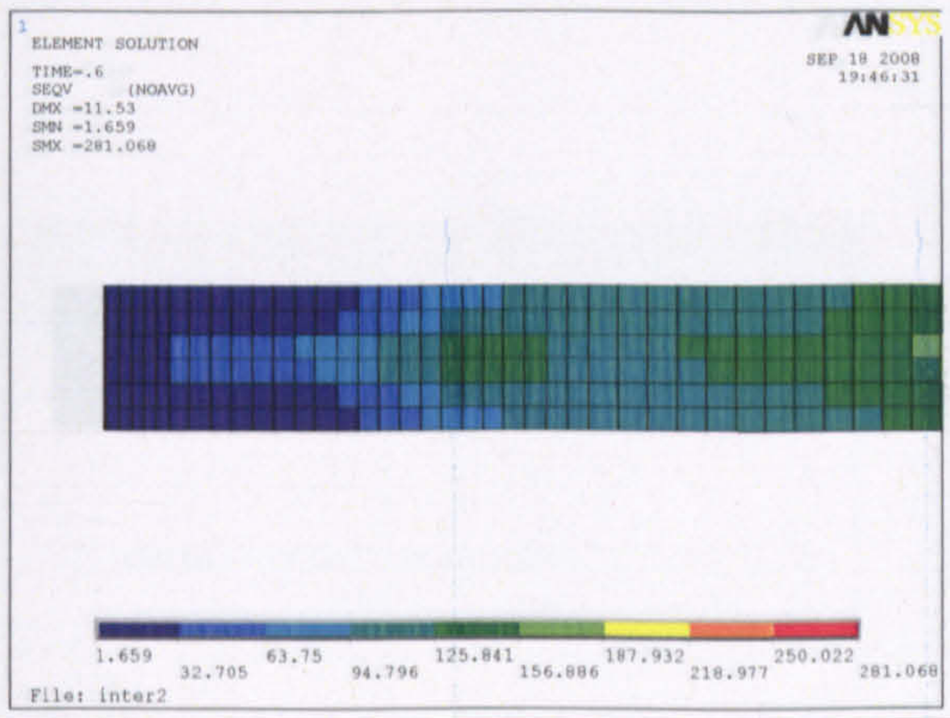

Web opening D

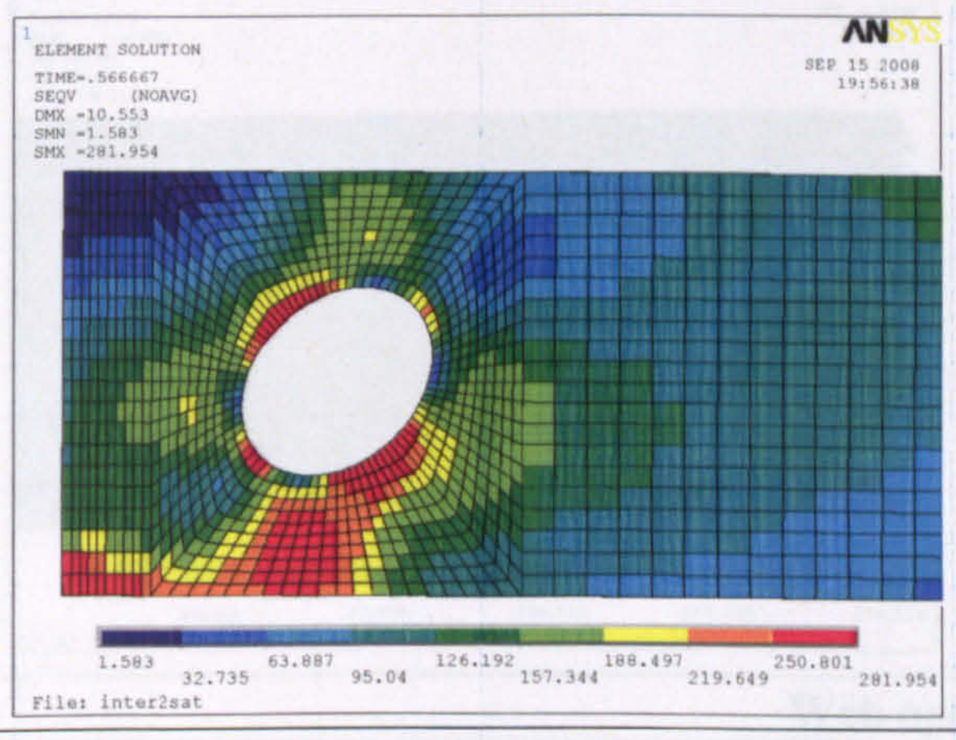

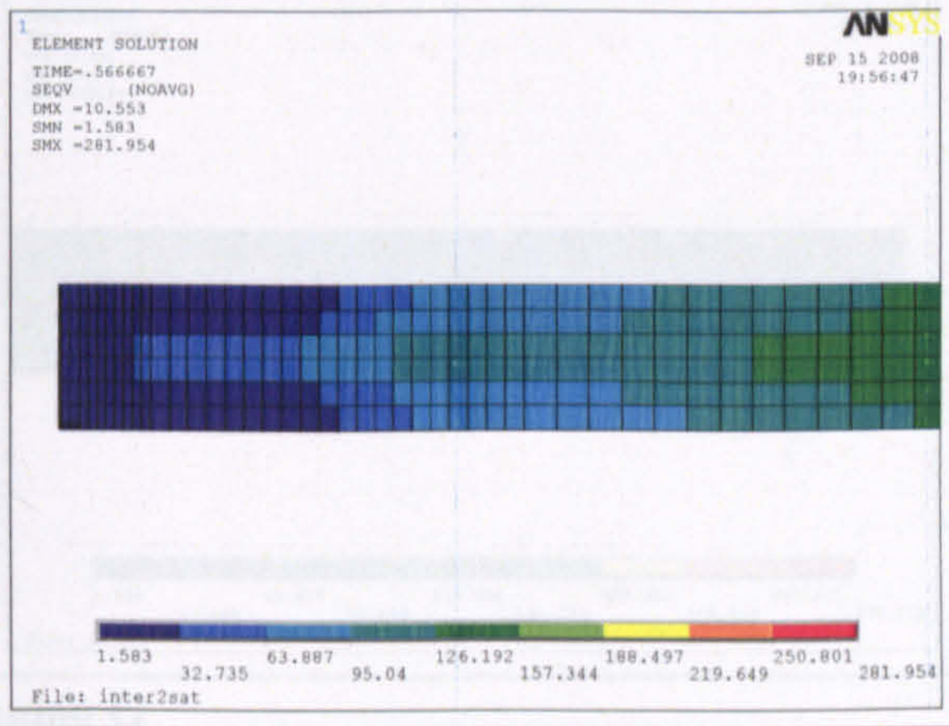

Web opening E

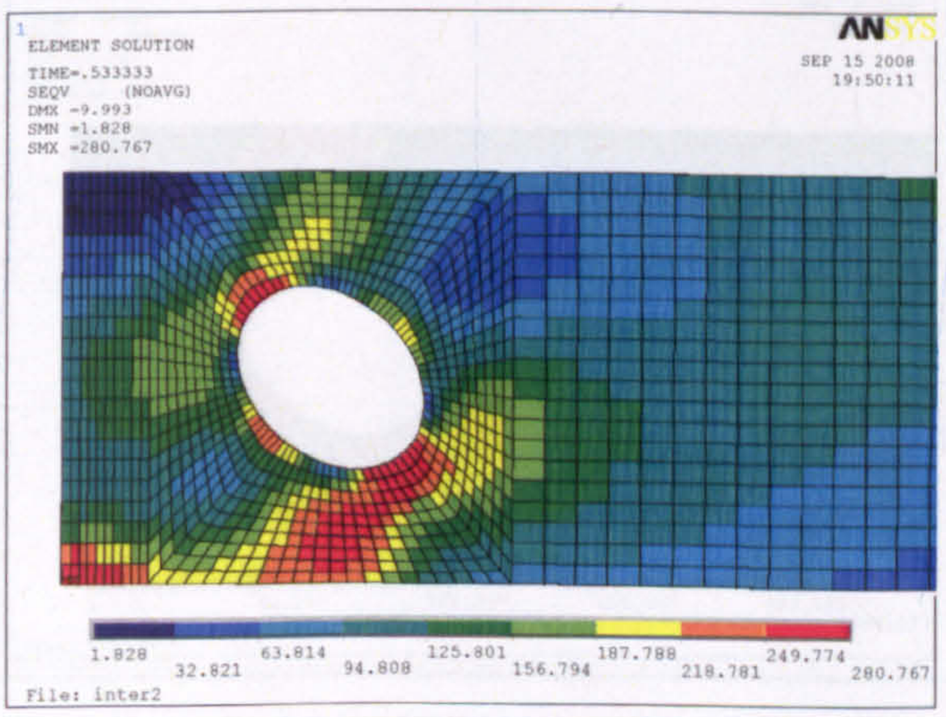

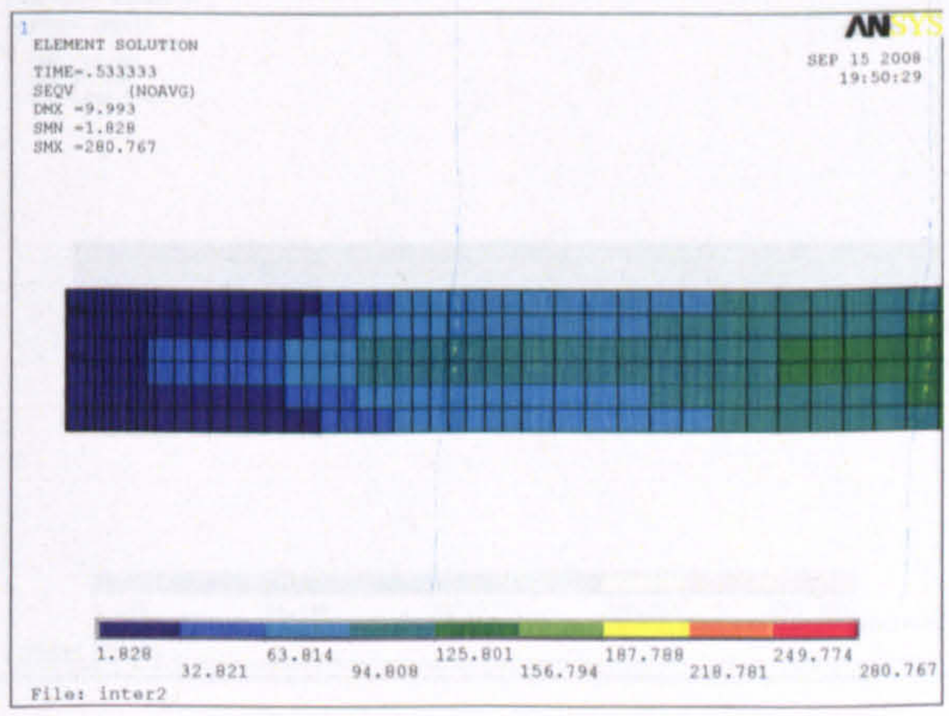

Web opening F

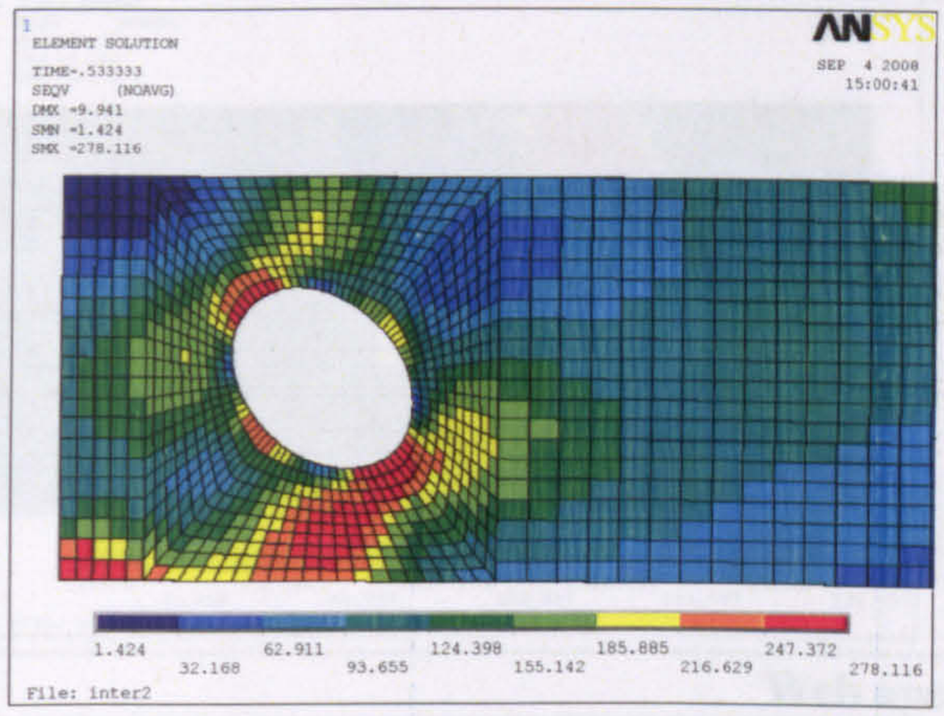

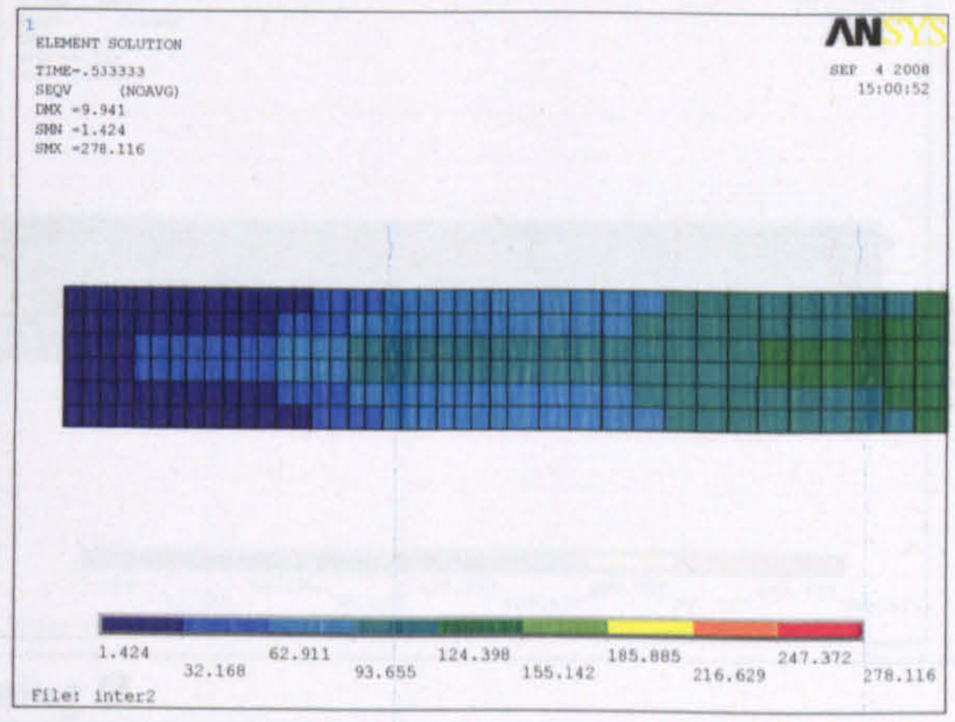

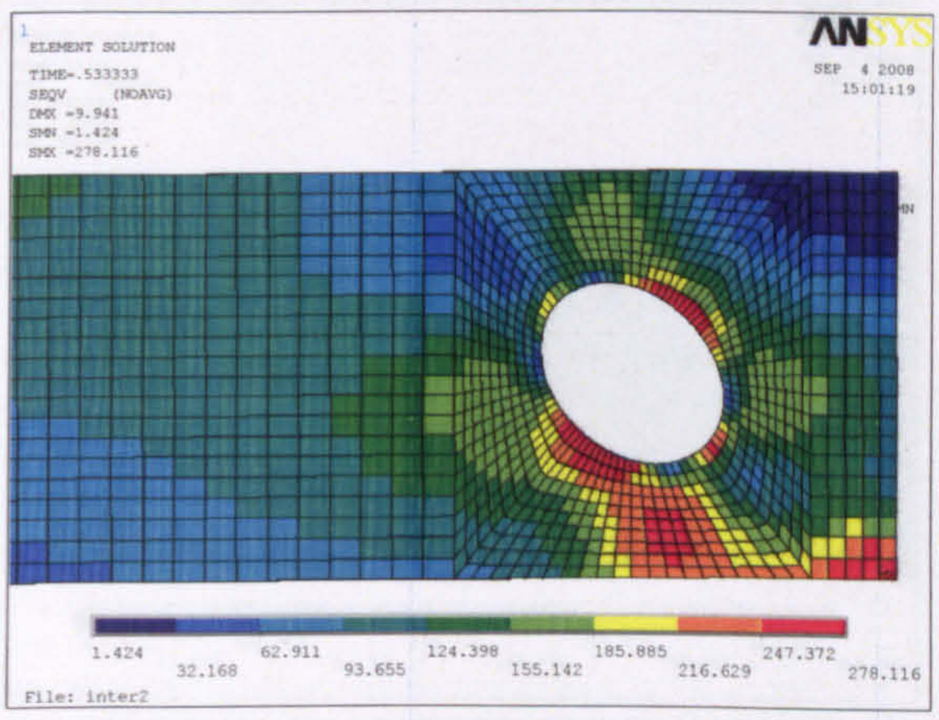

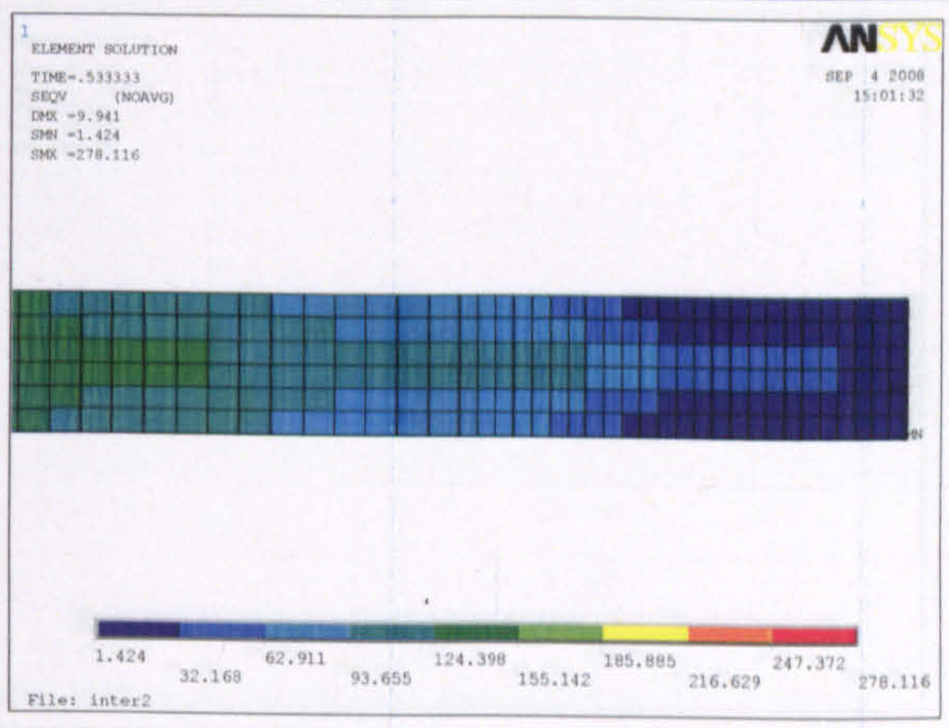

Web opening G

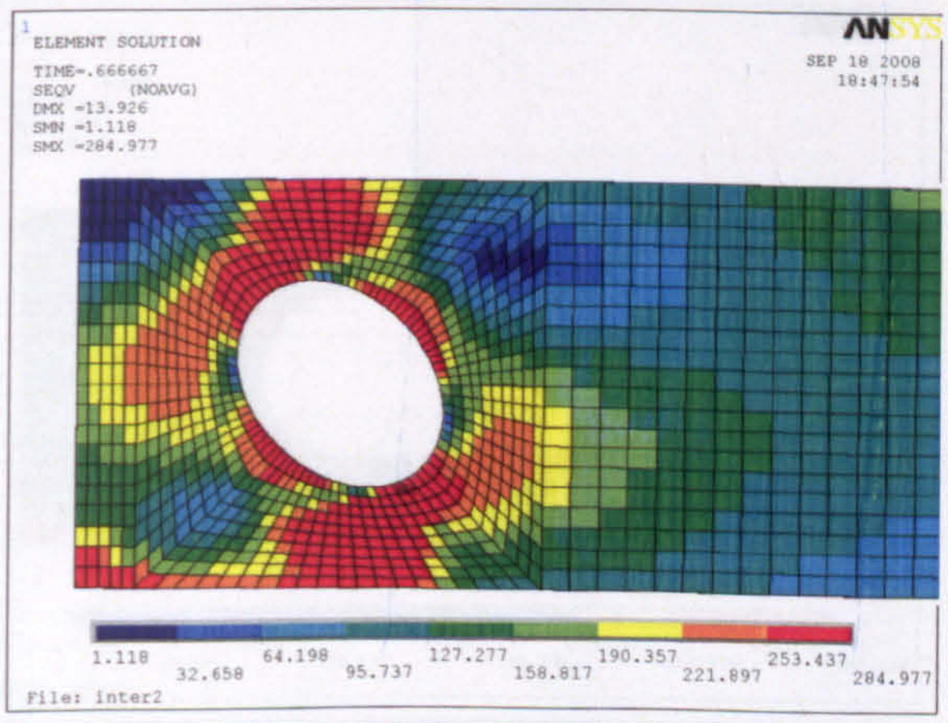

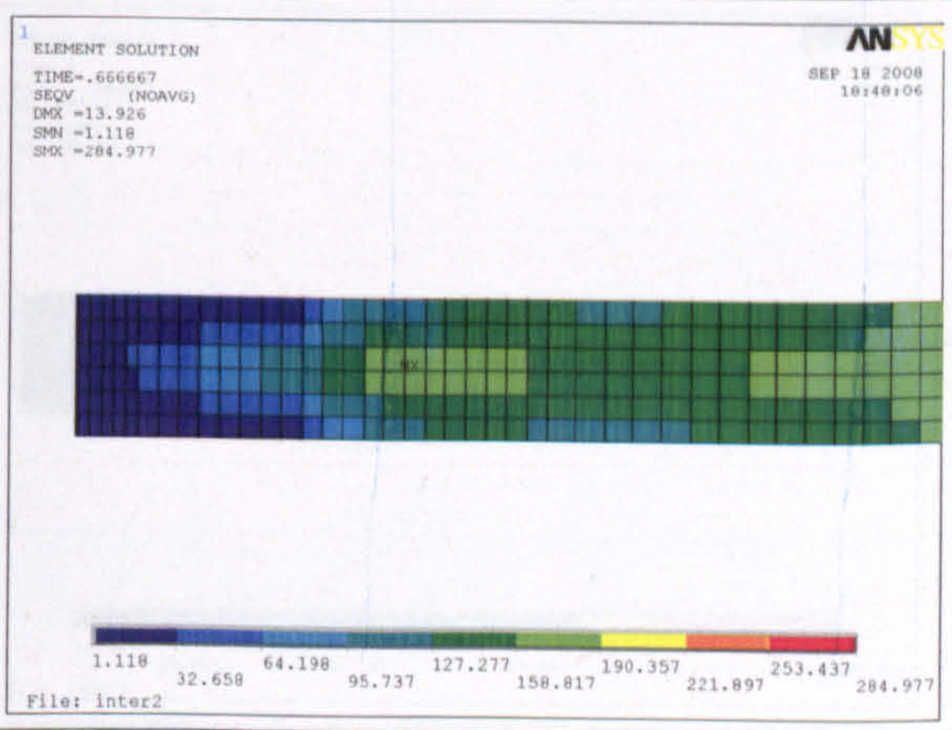

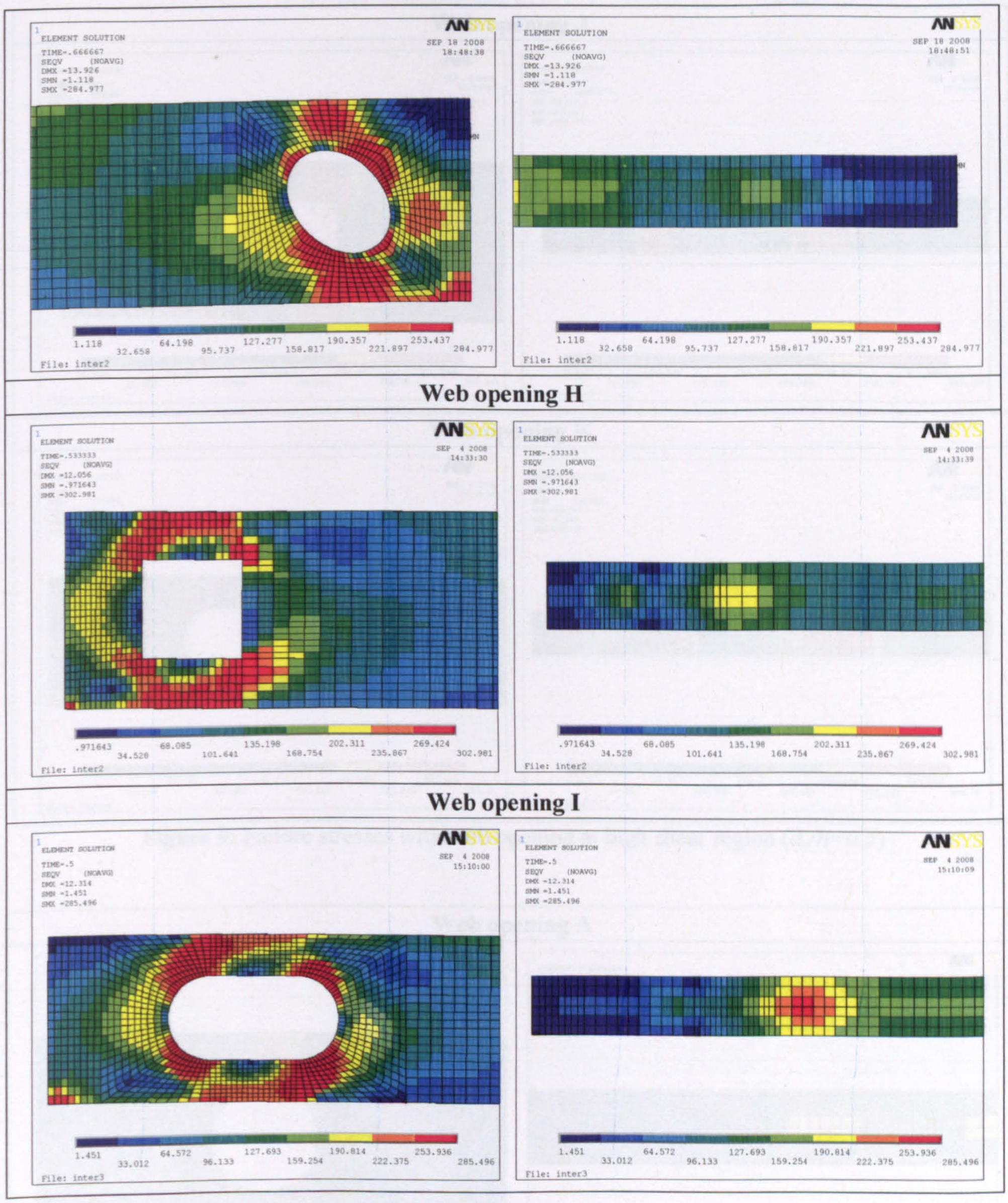
ELEMENT SOLUTION
TIME=.666667
SEQV (NOAVG)
DMX =13.926
SMN =1.118
SMX =284.977
SEP 18 2008
18:48:38
1.118
32.658
64.198
95.737
127.277
158.817
190.357
221.897
253.437
284.977
File: inter2
ELEMENT SOLUTION
TIME=.666667
SEQV (NOAVG)
DMX =13.926
SMN =1.118
SMX =284.977
SEP 18 2008
18:48:51
1.118
32.658
64.198
95.737
127.277
158.817
190.357
221.897
253.437
284.977
File: inter2
Web opening H
ELEMENT SOLUTION
TIME=.533333
SEQV (NOAVG)
DMX =12.056
SMN =.971643
SMX =302.981
SEP 4 2008
14:33:30
.971643
34.528
68.085
101.641
135.198
168.754
202.311
235.867
269.424
302.981
File: inter2
ELEMENT SOLUTION
TIME=.533333
SEQV (NOAVG)
DMX =12.056
SMN =.971643
SMX =302.981
SEP 4 2008
14:33:39
.971643
34.528
68.085
101.641
135.198
168.754
202.311
235.867
269.424
302.981
File: inter2
Web opening I
ELEMENT SOLUTION
TIME=.5
SEQV (NOAVG)
DMX =12.314
SMN =1.451
SMX =285.496
SEP 4 2008
15:10:00
1.451
33.012
64.572
96.133
127.693
159.254
190.814
222.375
253.936
285.496
File: inter3
ELEMENT SOLUTION
TIME=.5
SEQV (NOAVG)
DMX =12.314
SMN =1.451
SMX =285.496
SEP 4 2008
15:10:09
1.451
33.012
64.572
96.133
127.693
159.254
190.814
222.375
253.936
285.496
File: inter3

Web opening J

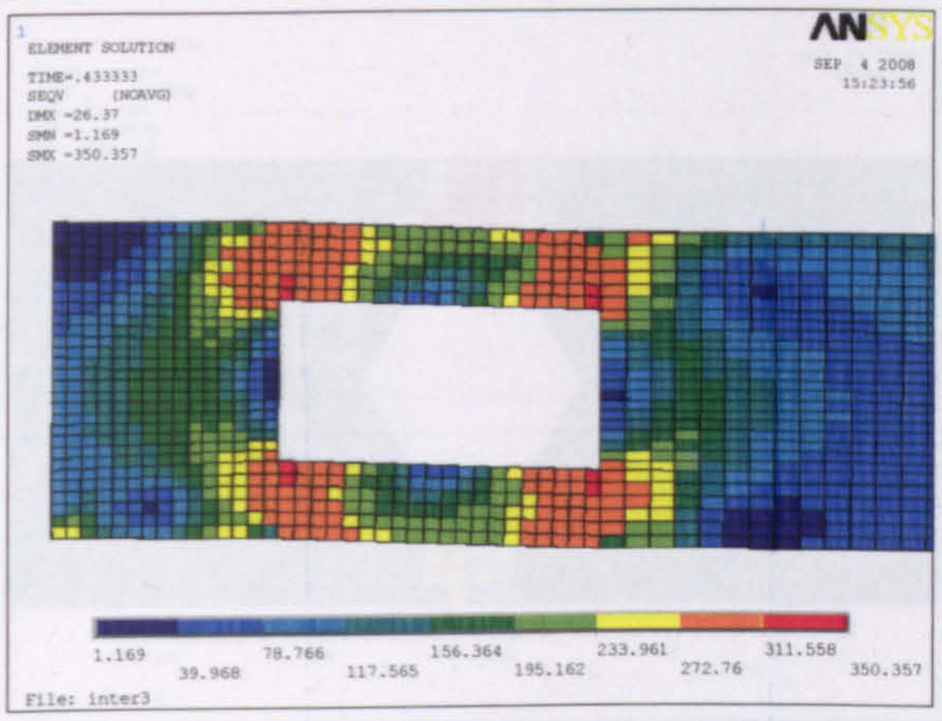

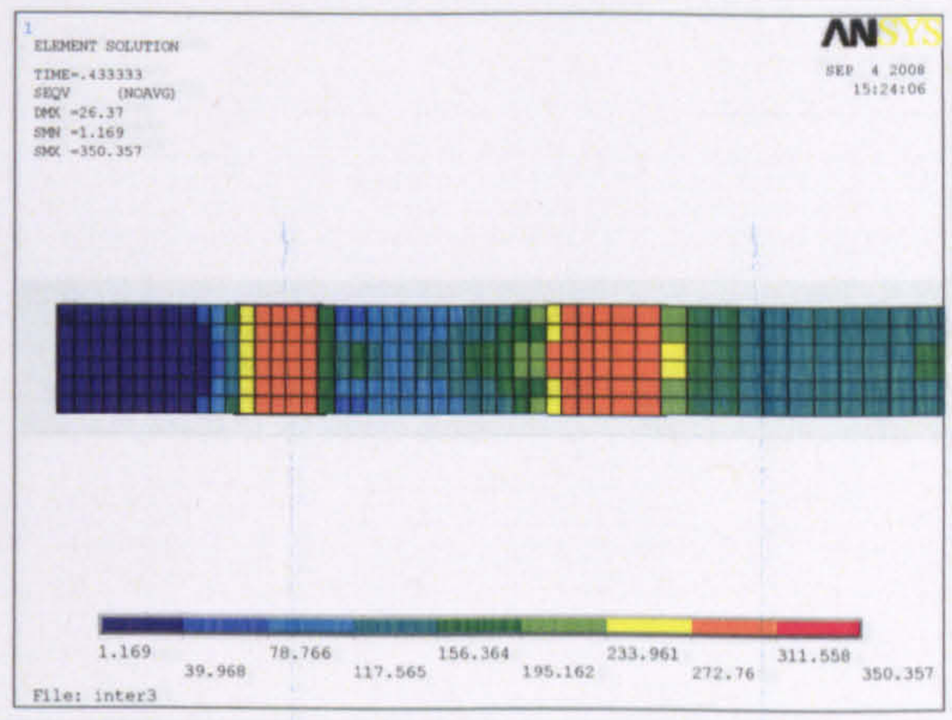

Web opening K

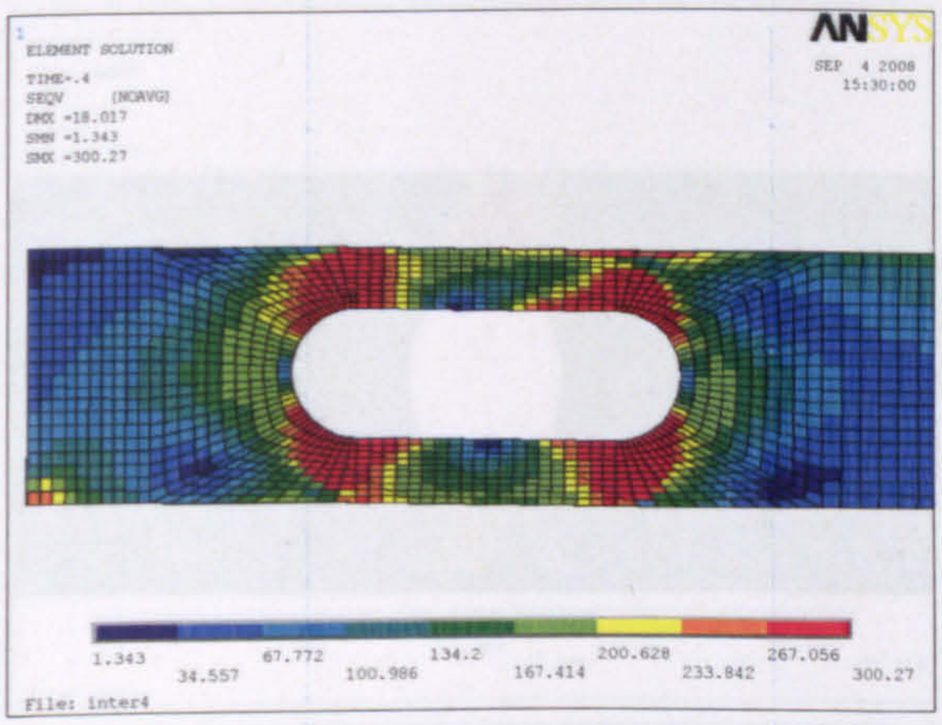

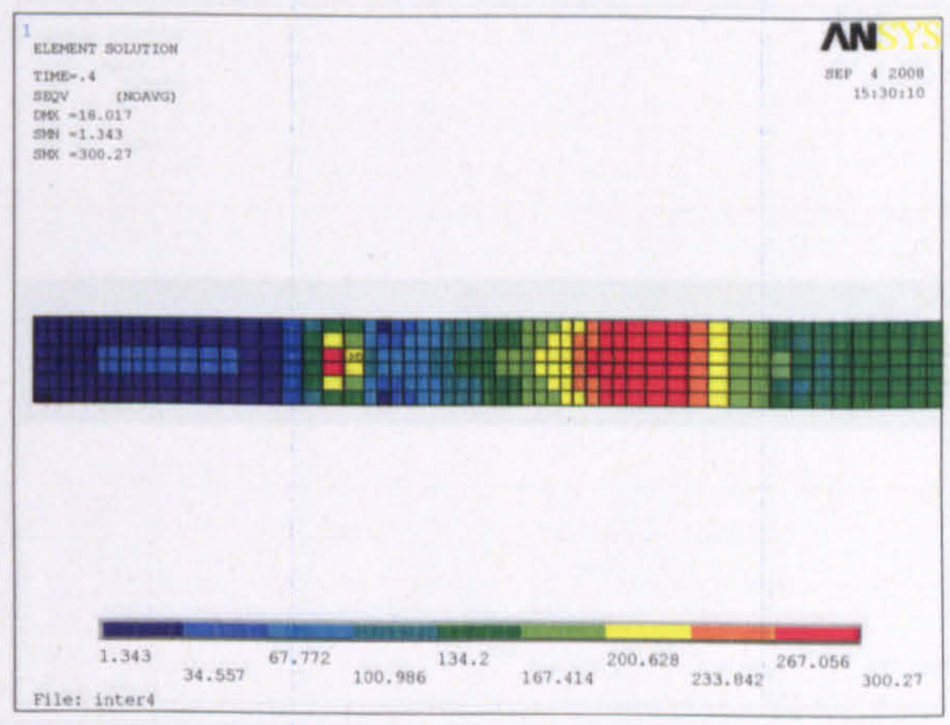

Figure 9: Failure stresses with web opening at high shear region ($d_o/h=0.5$)

Web opening A

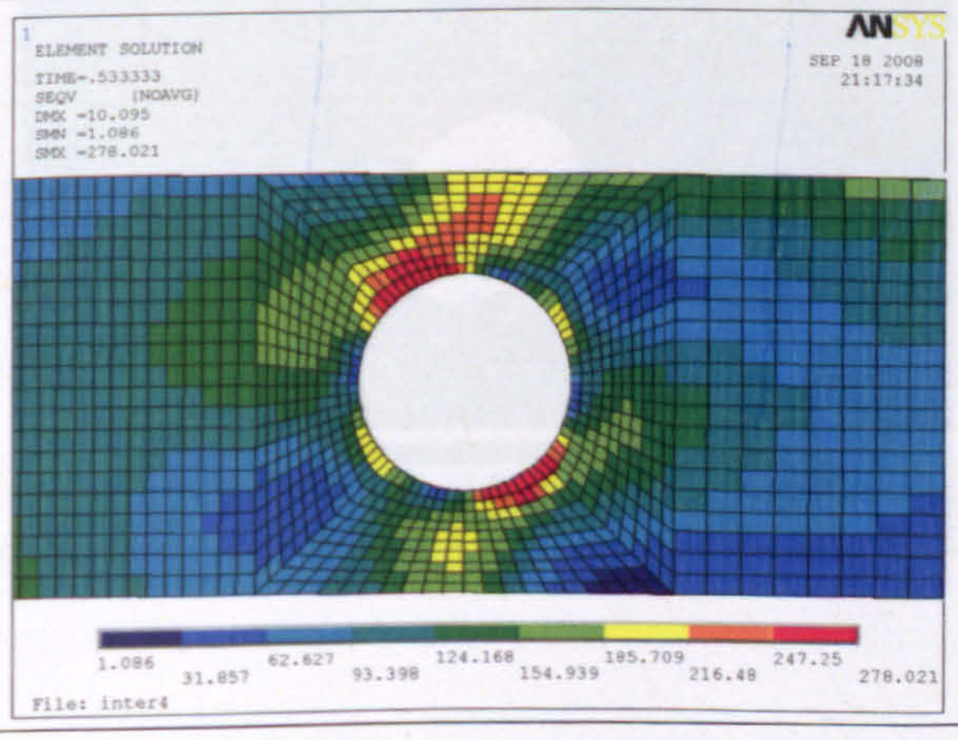

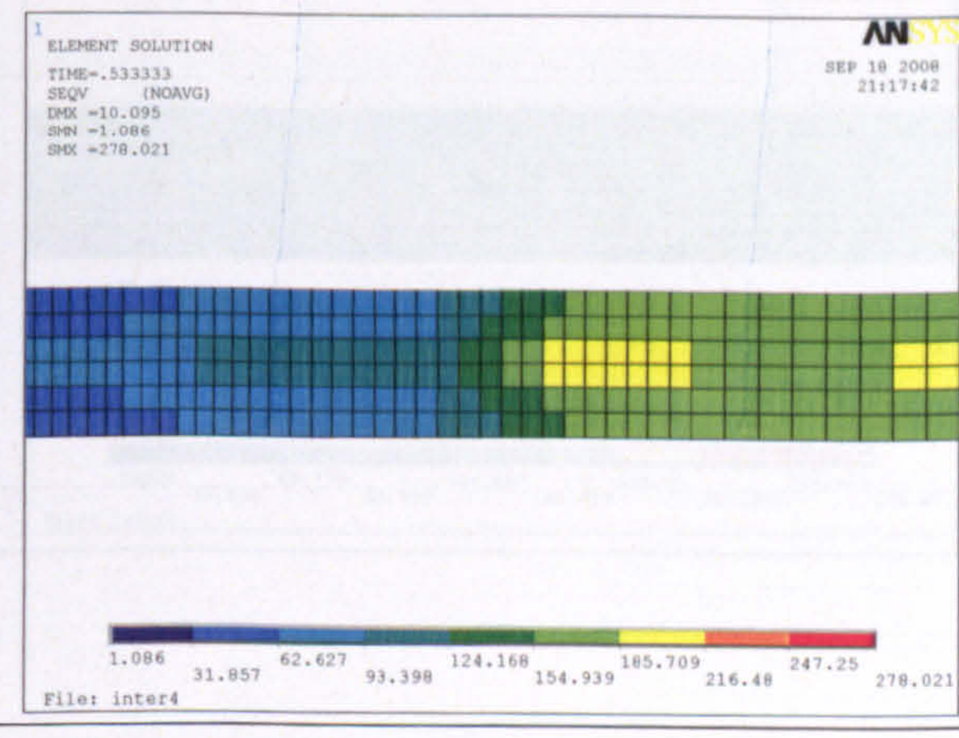

Web opening B

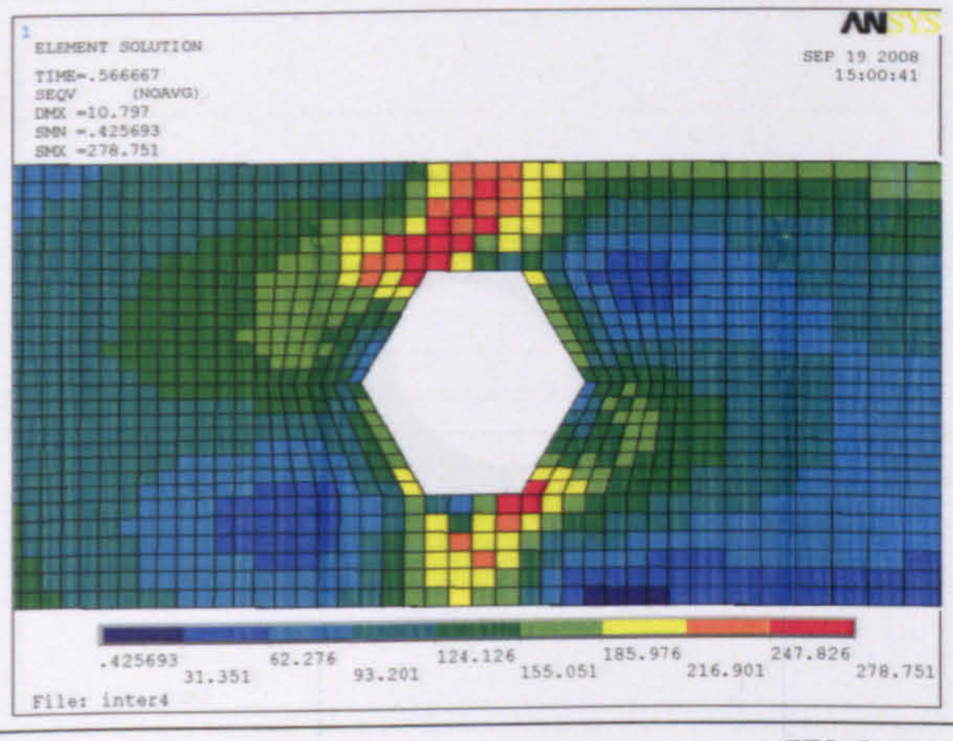

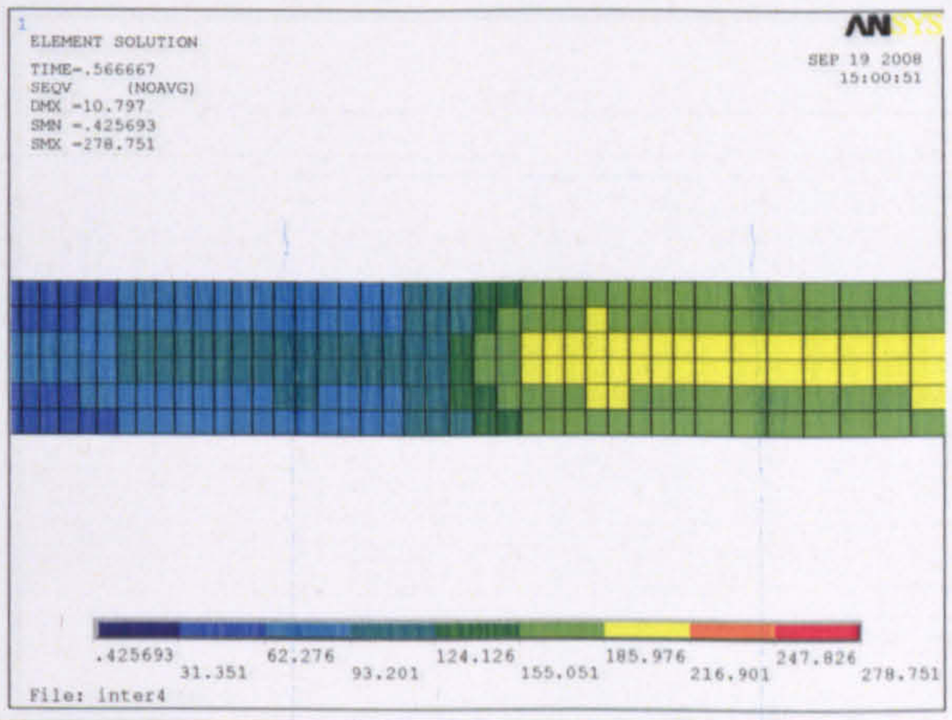

Web opening C

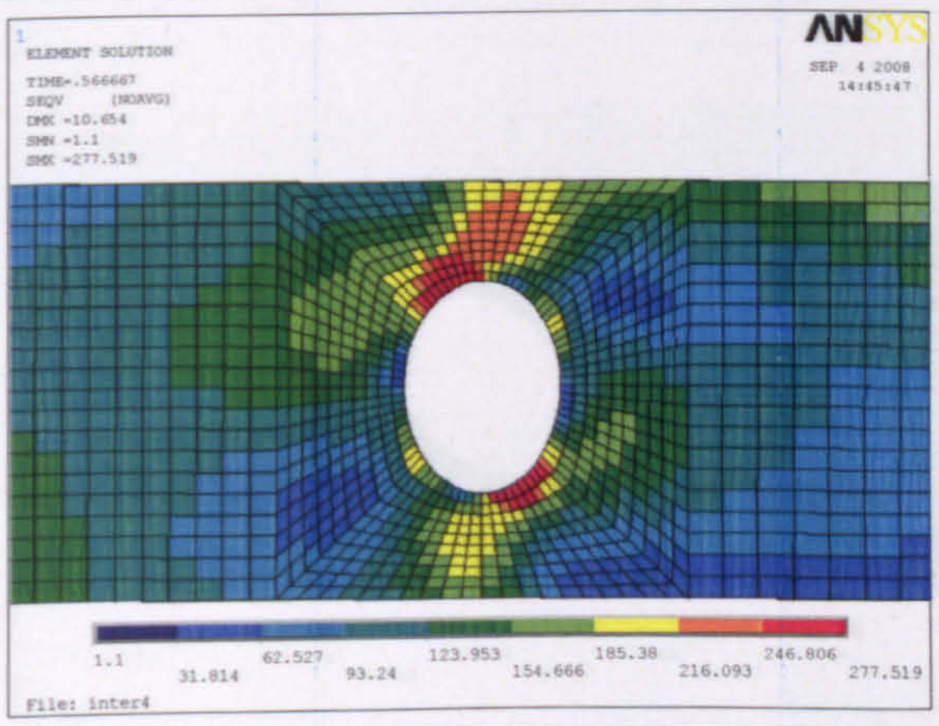

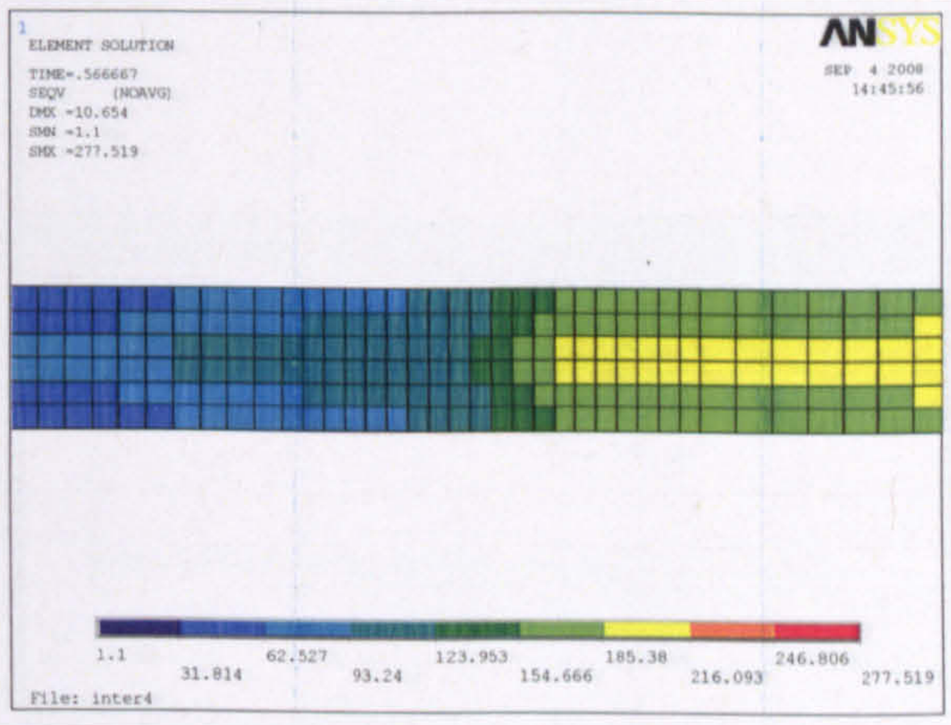

Web opening D

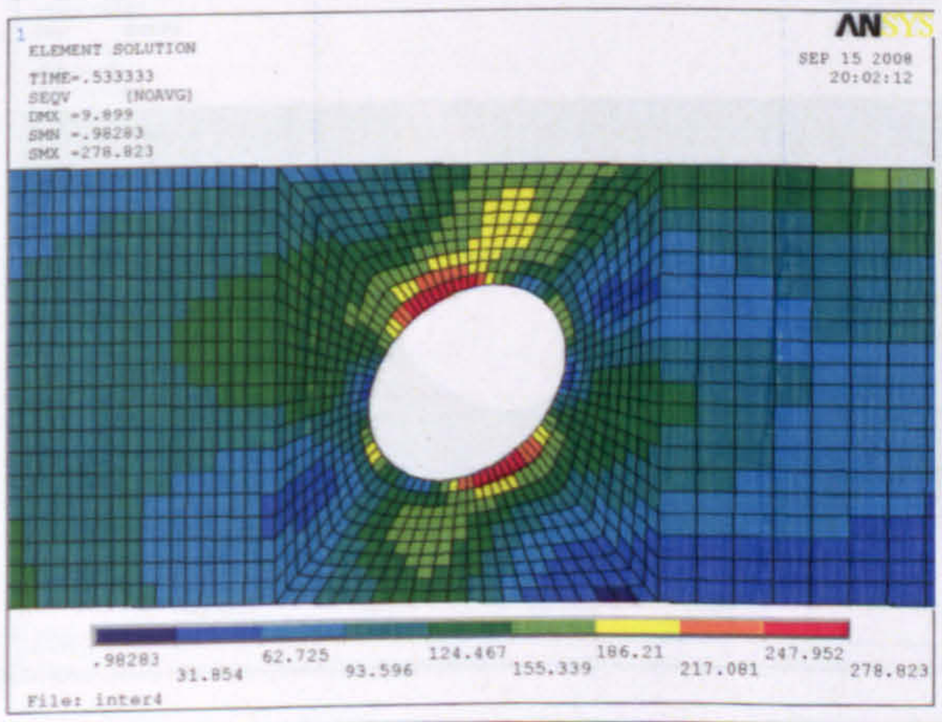

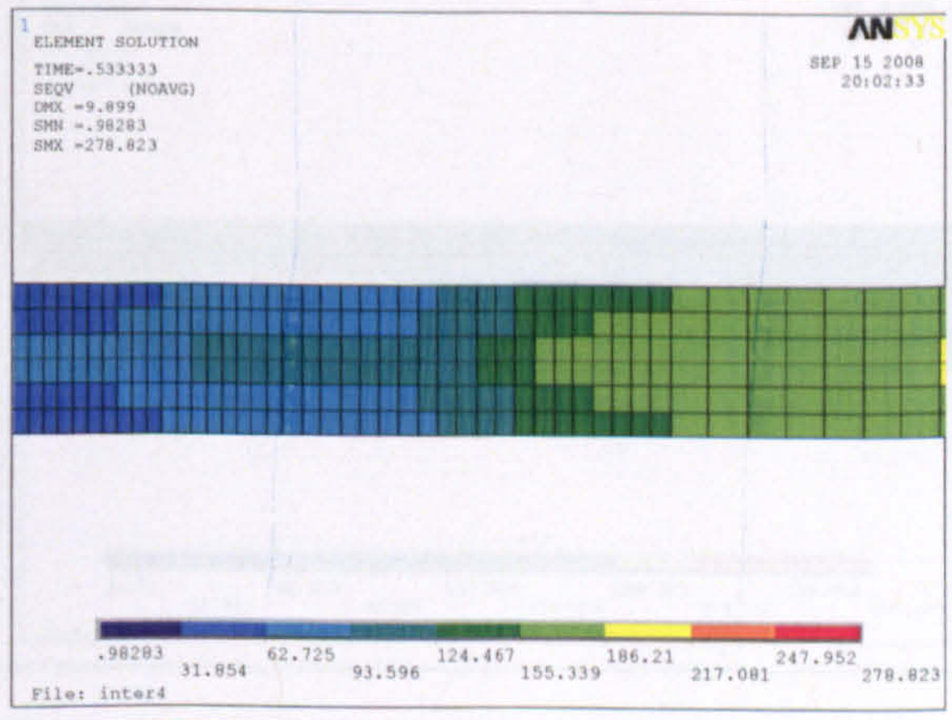

Web opening E

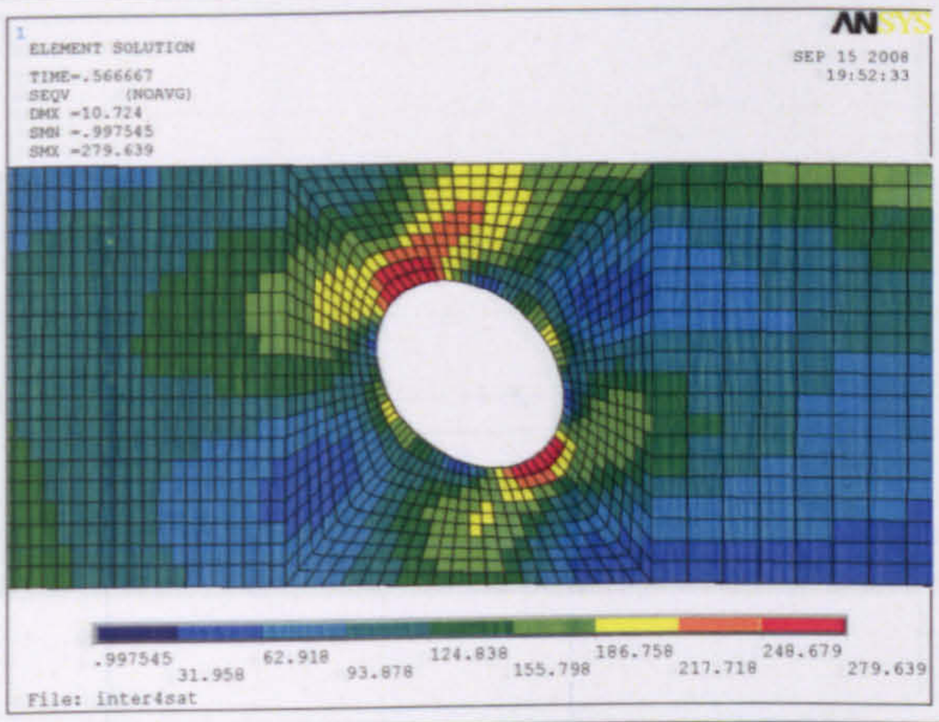

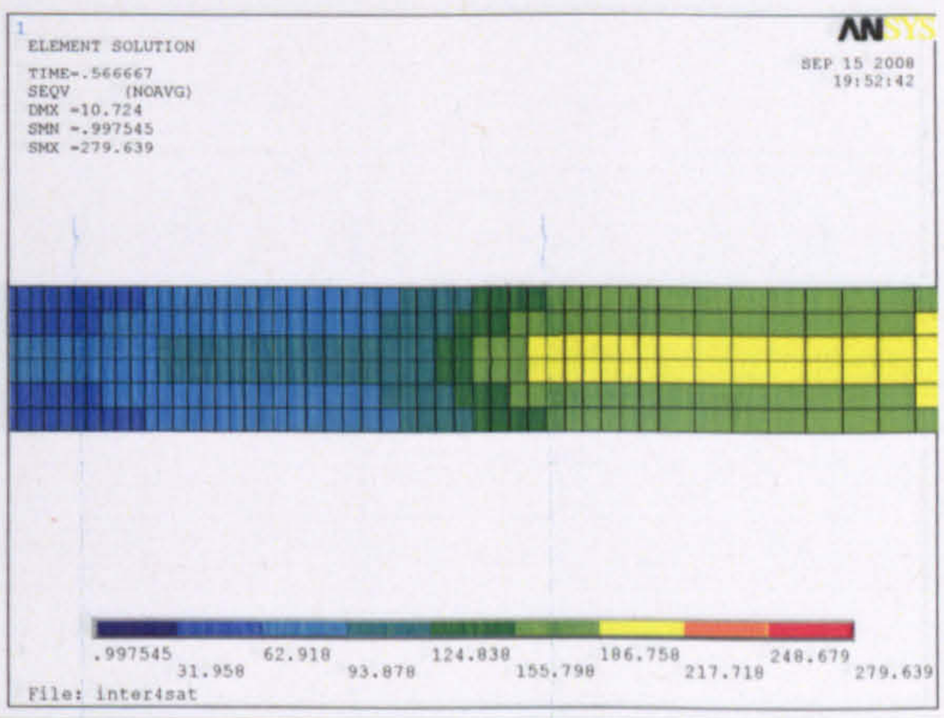

Web opening F

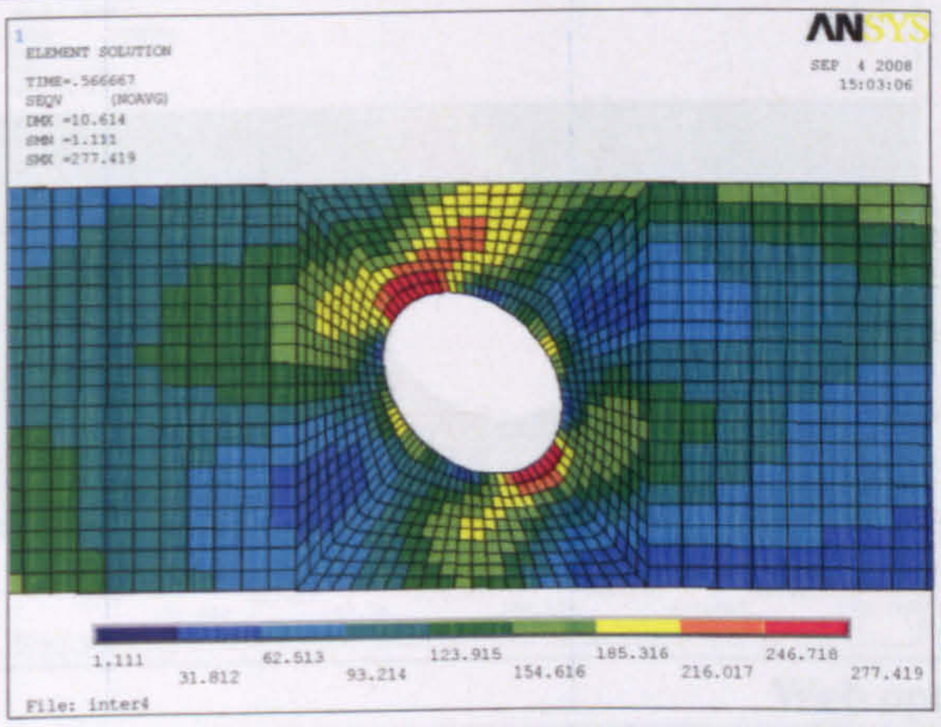

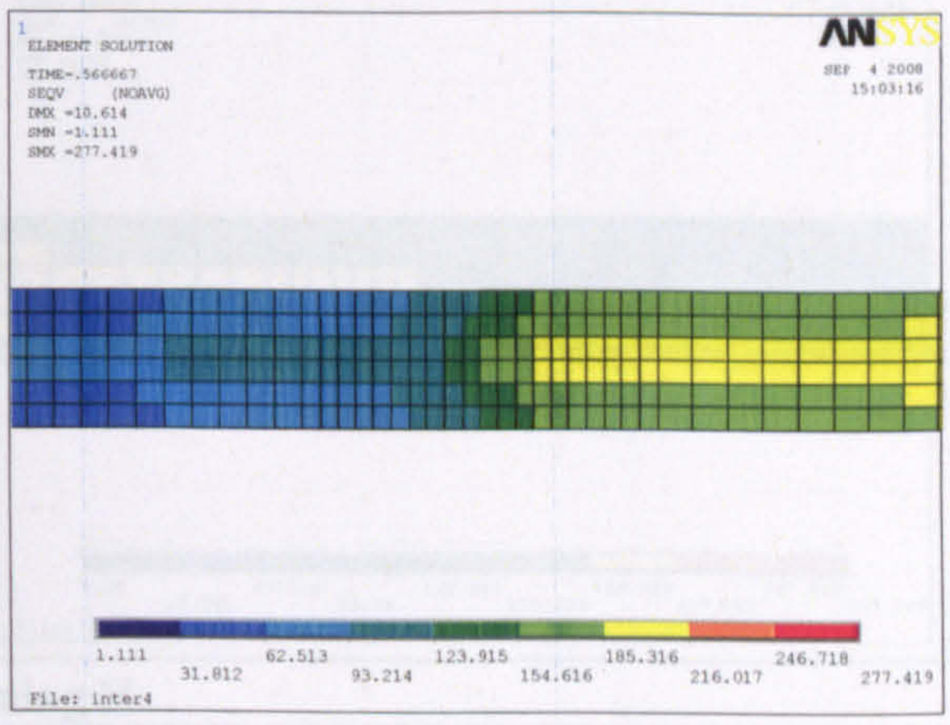

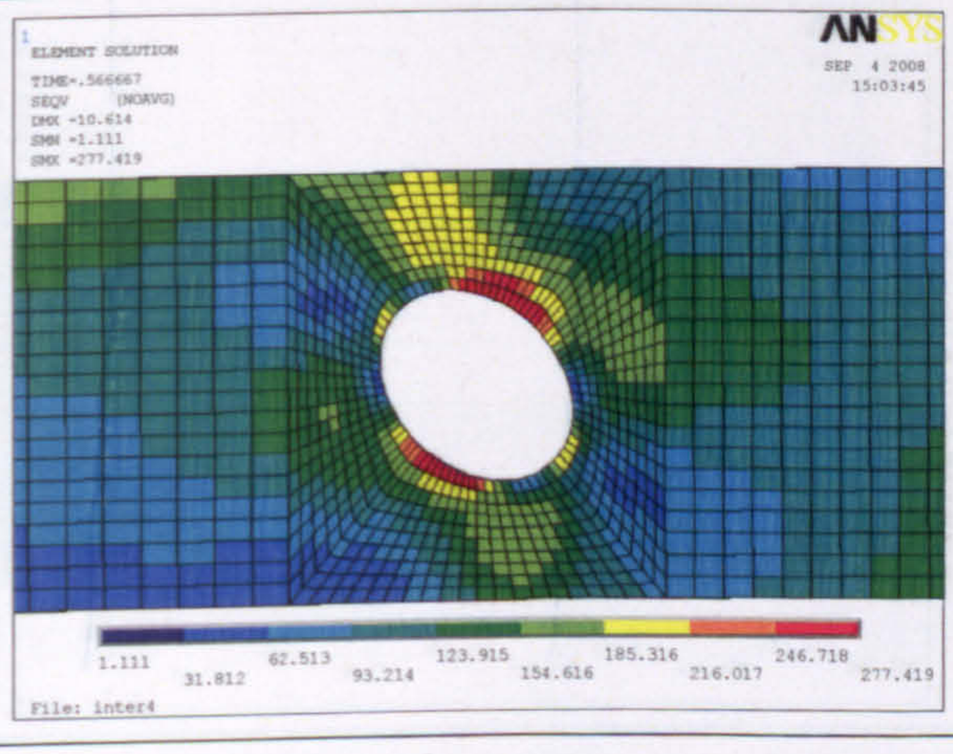

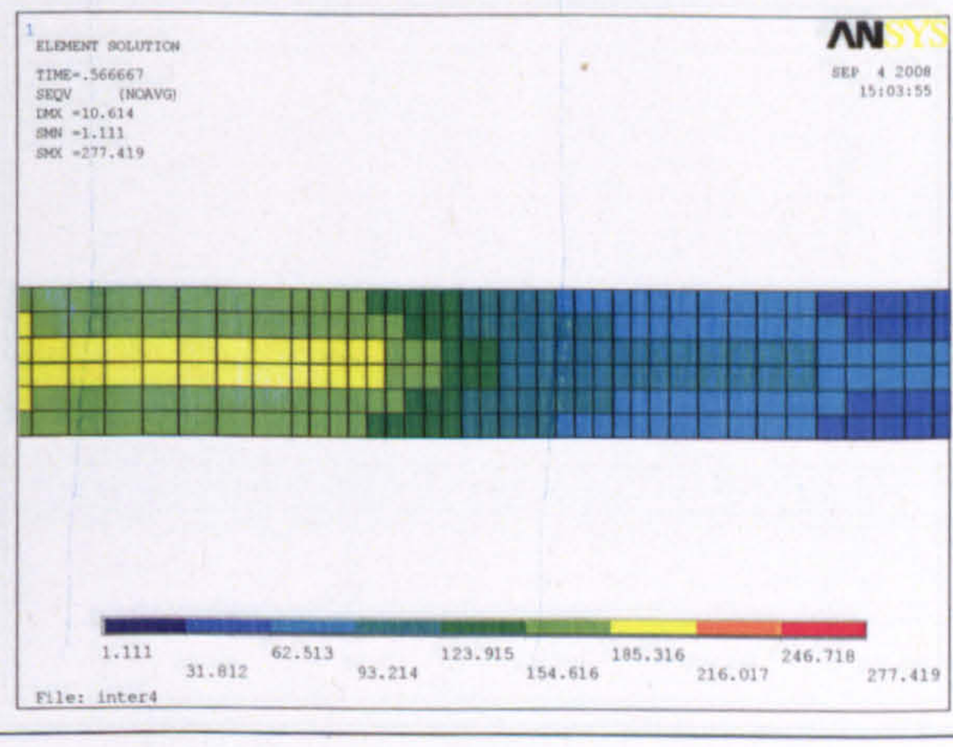

Web opening G

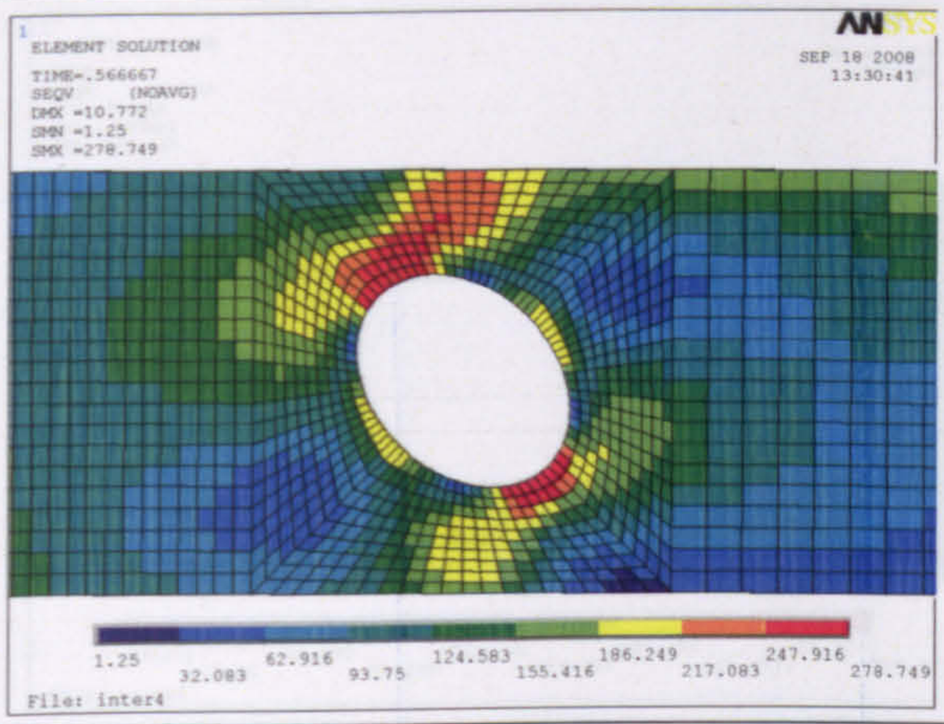

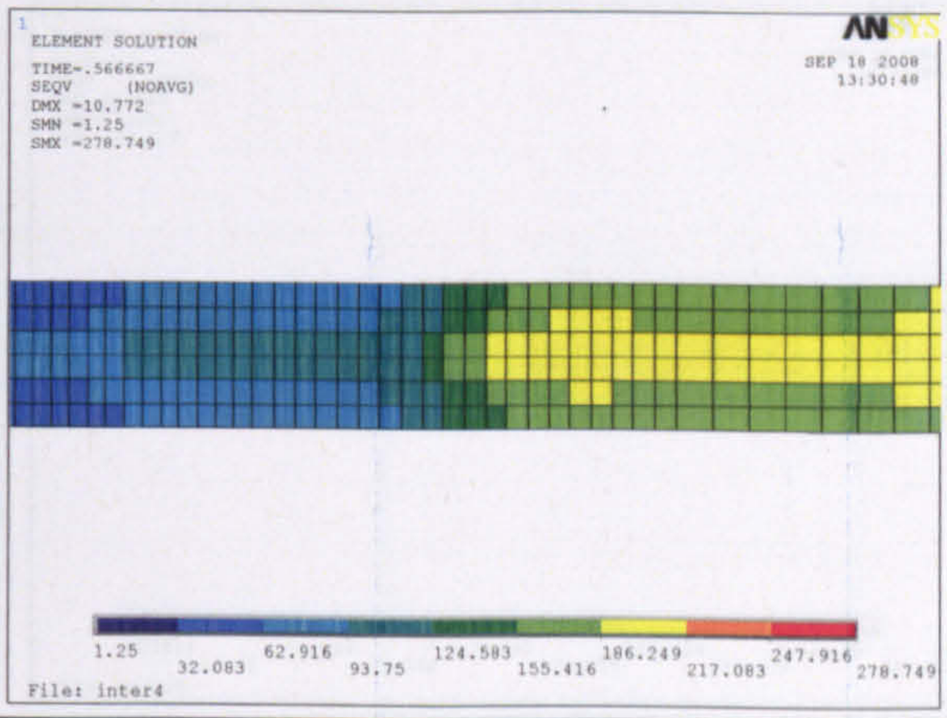

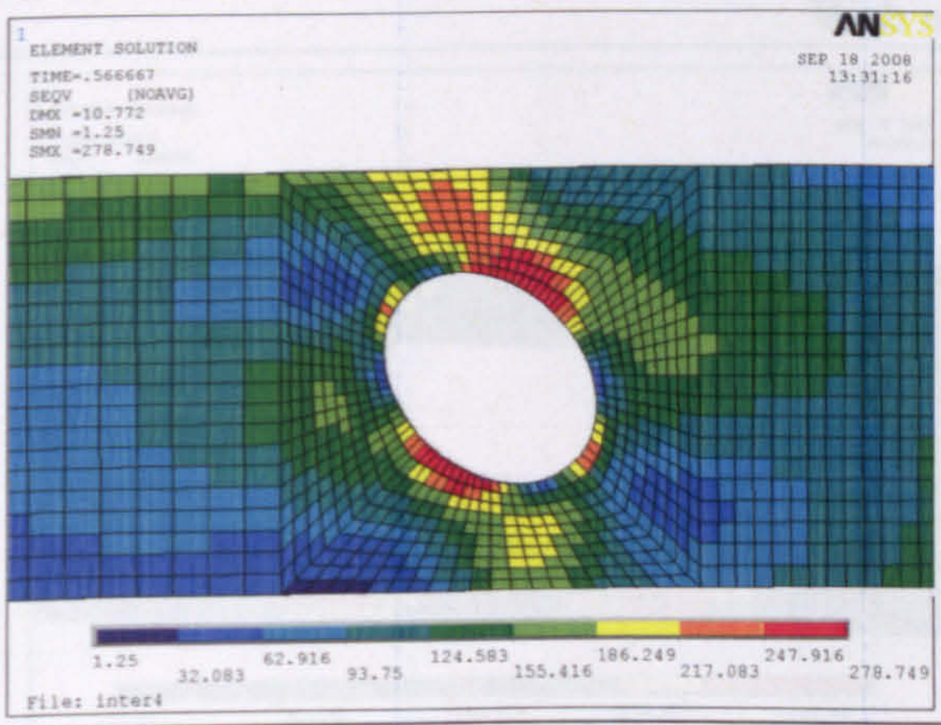

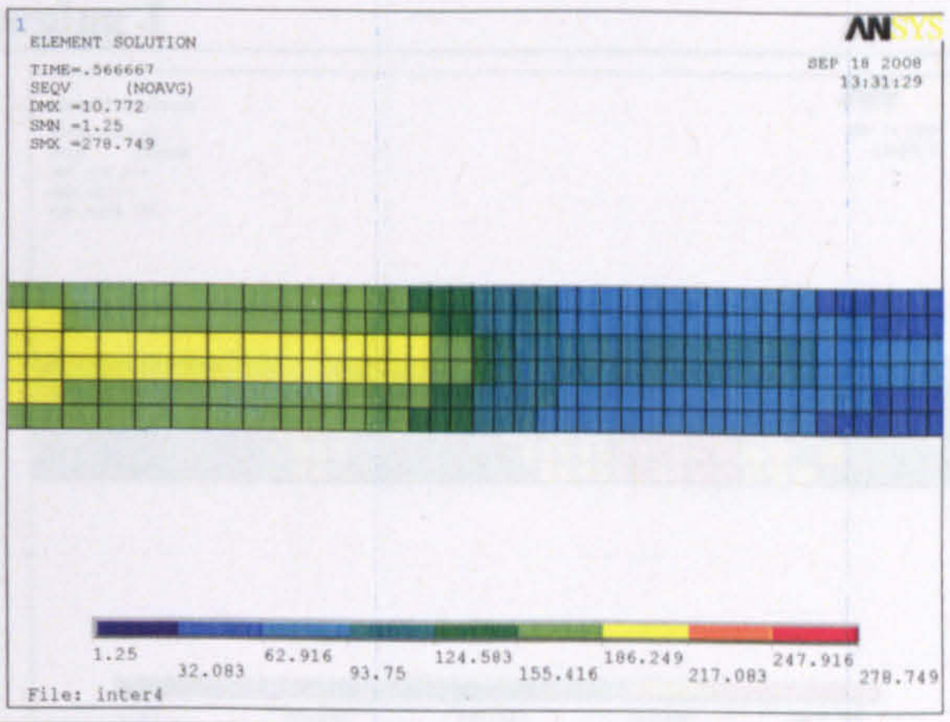

Web opening H

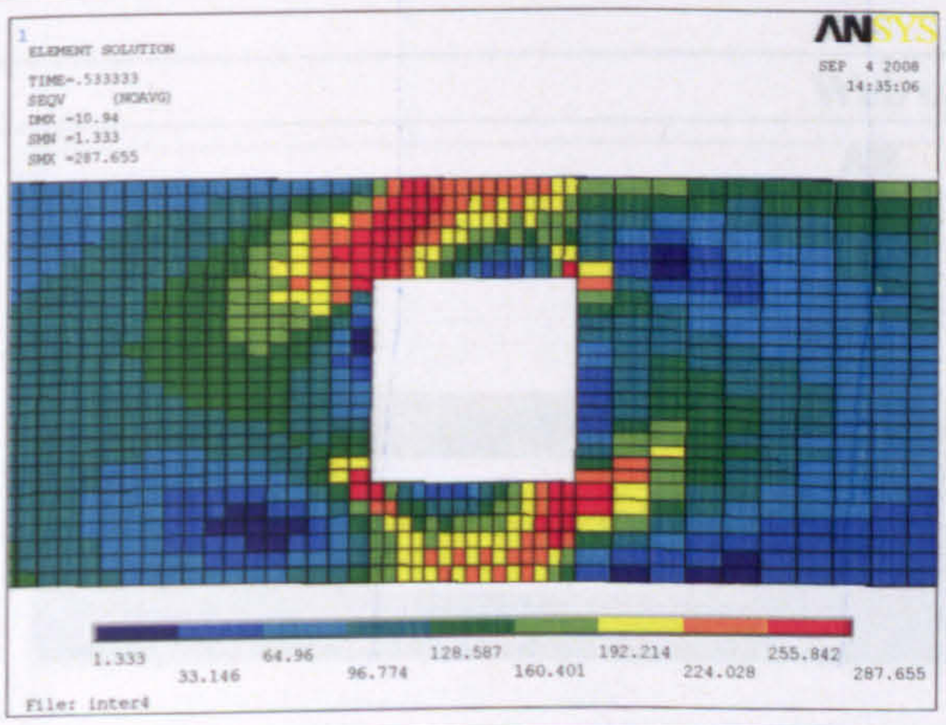

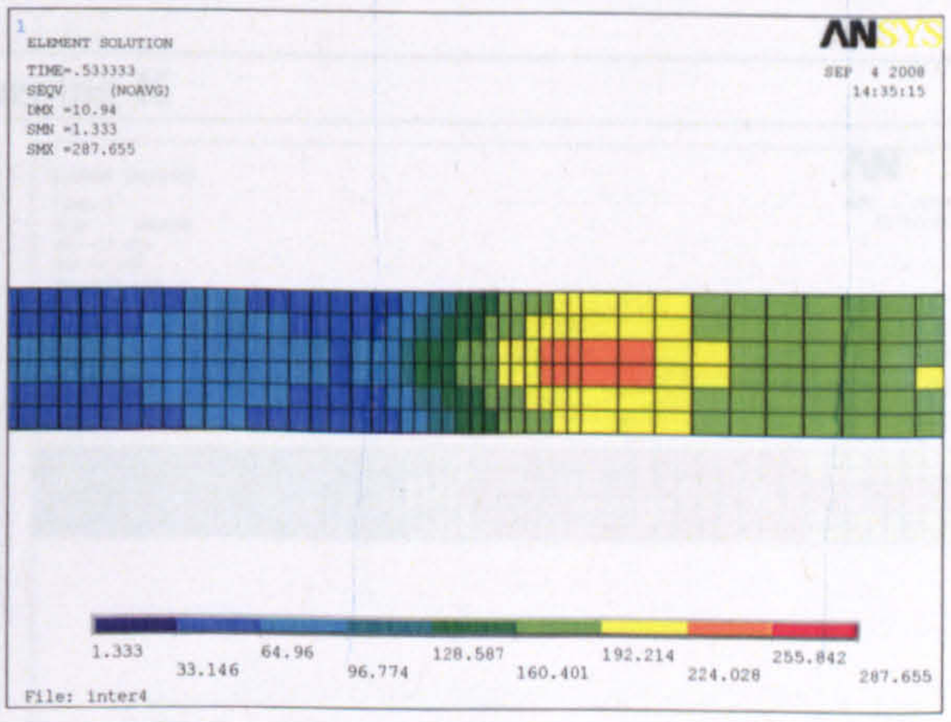

Web opening I

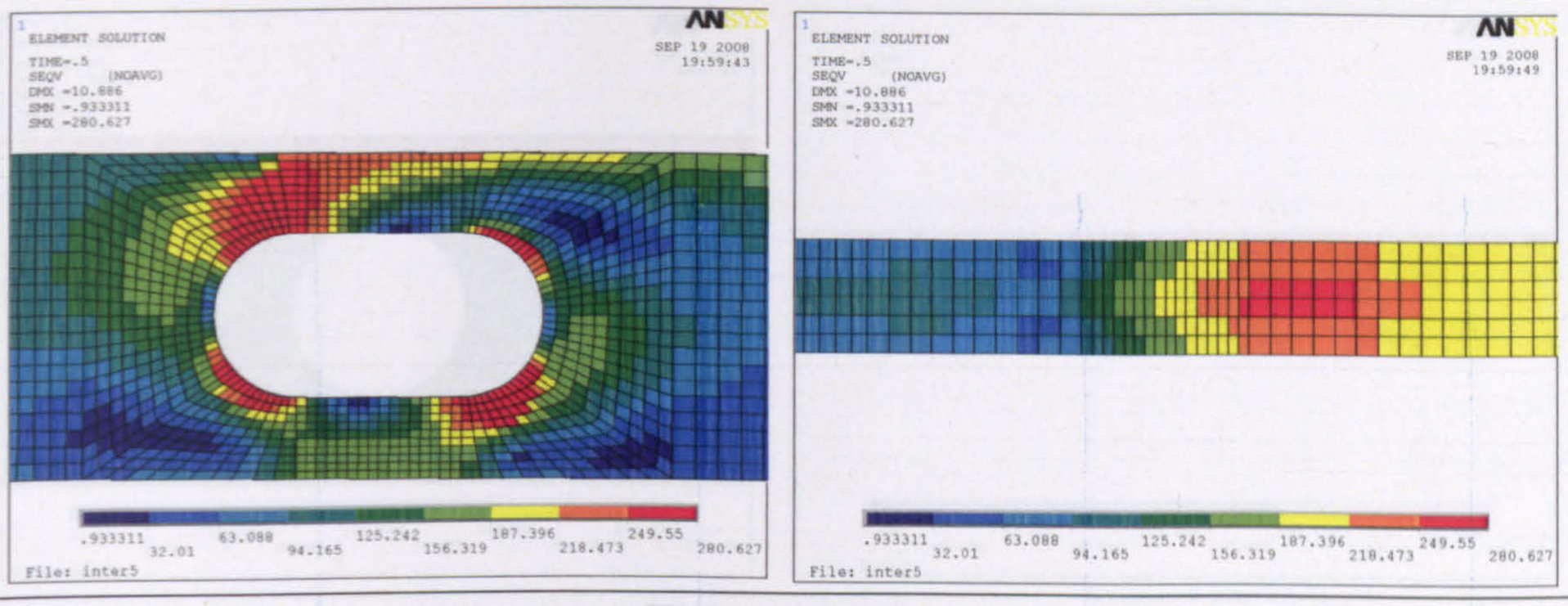

Web opening J

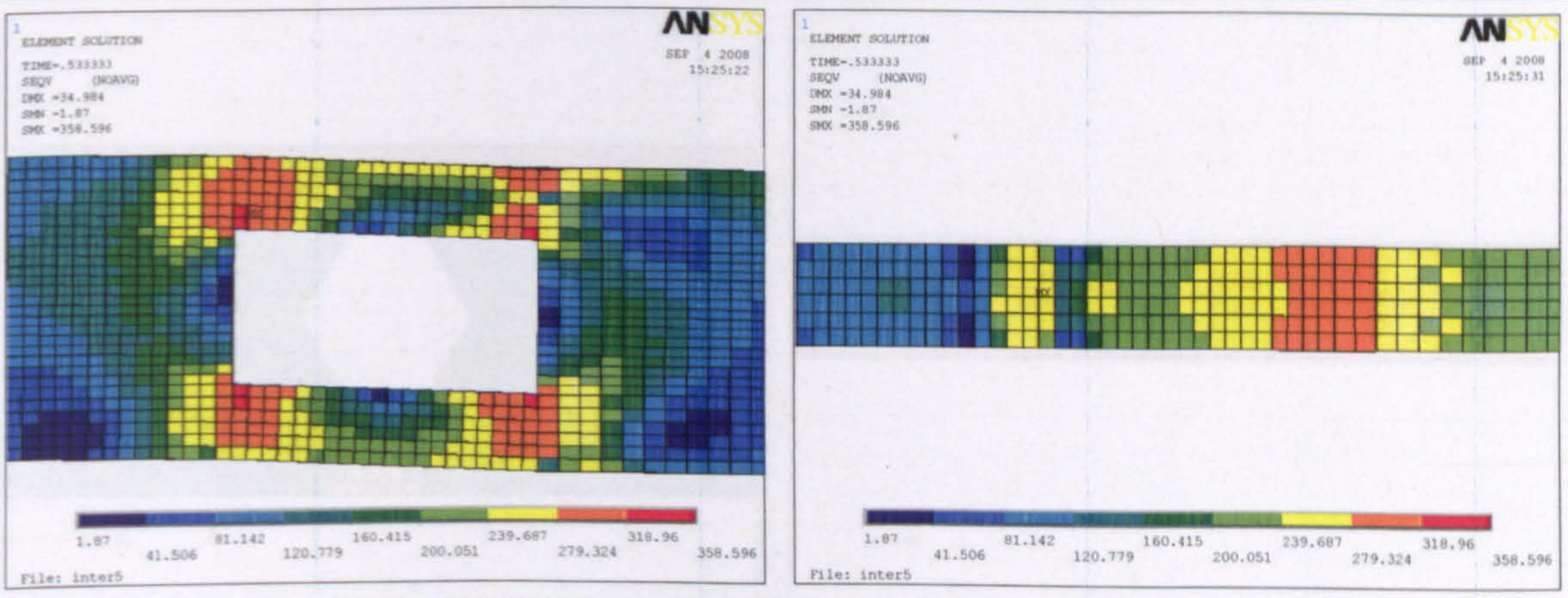

Web opening K

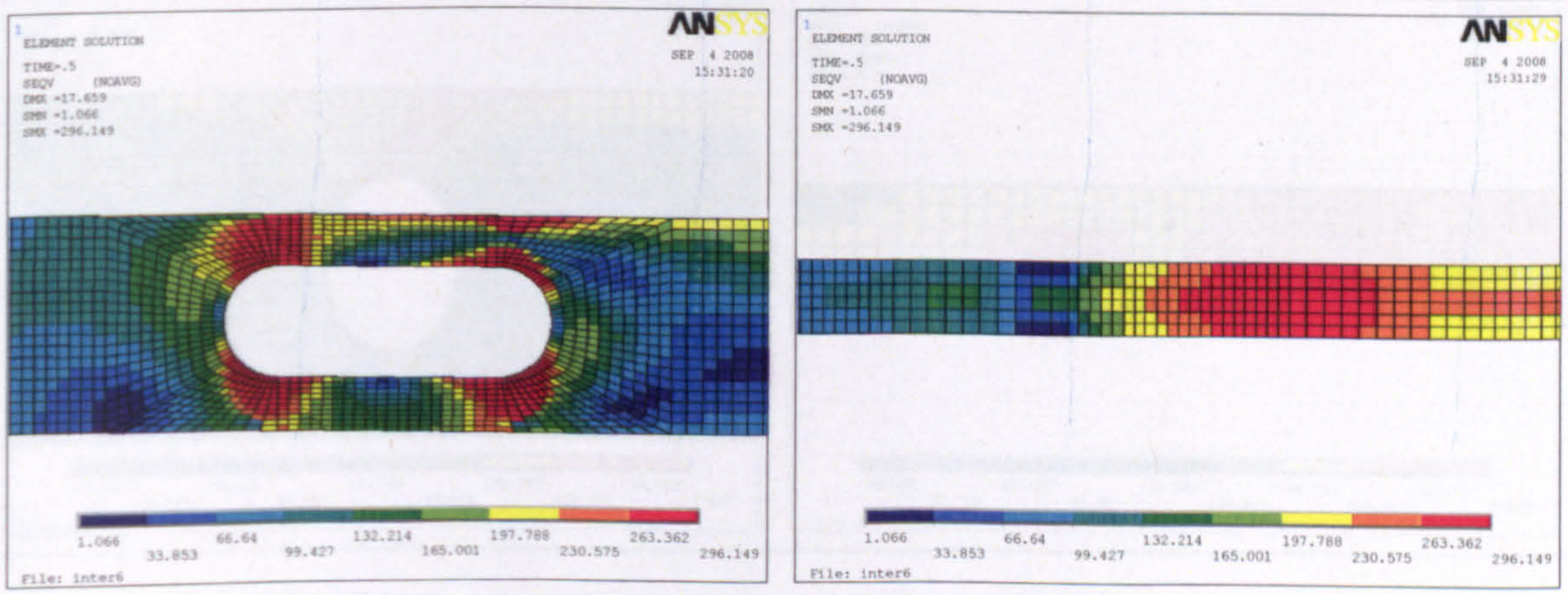

Figure 10: Failure stresses with web opening at high shear and low moment region ($d_o/h=0.5$)

Web opening A

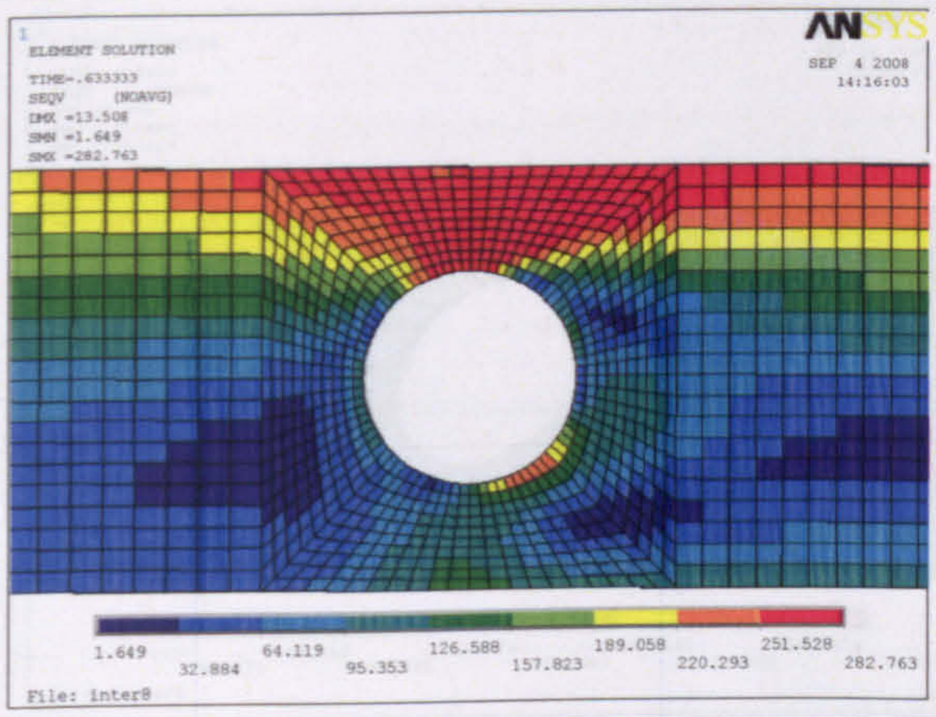

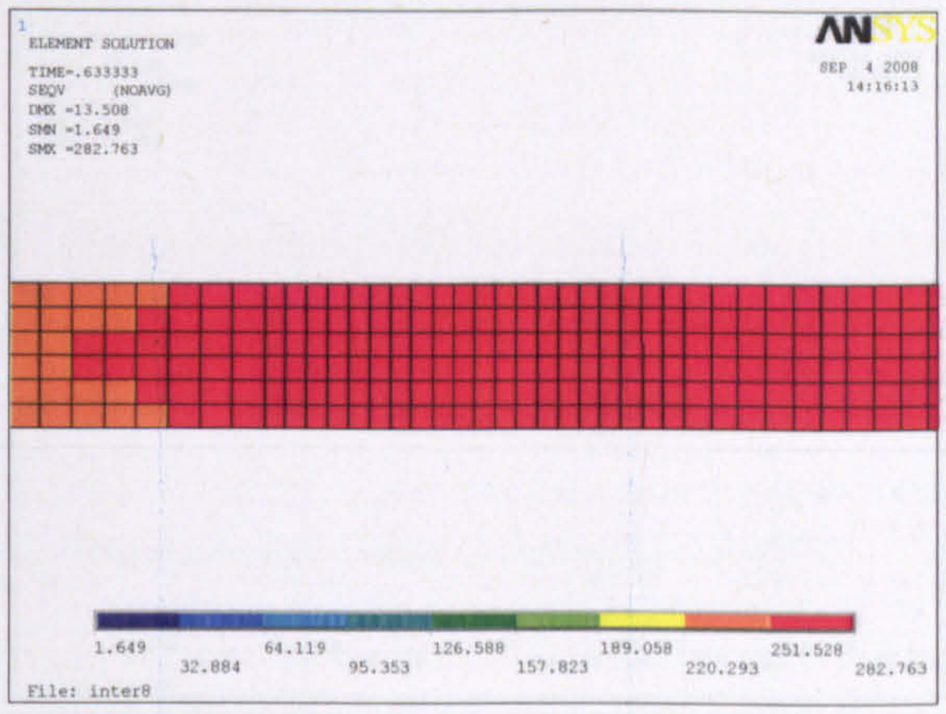

Web opening B

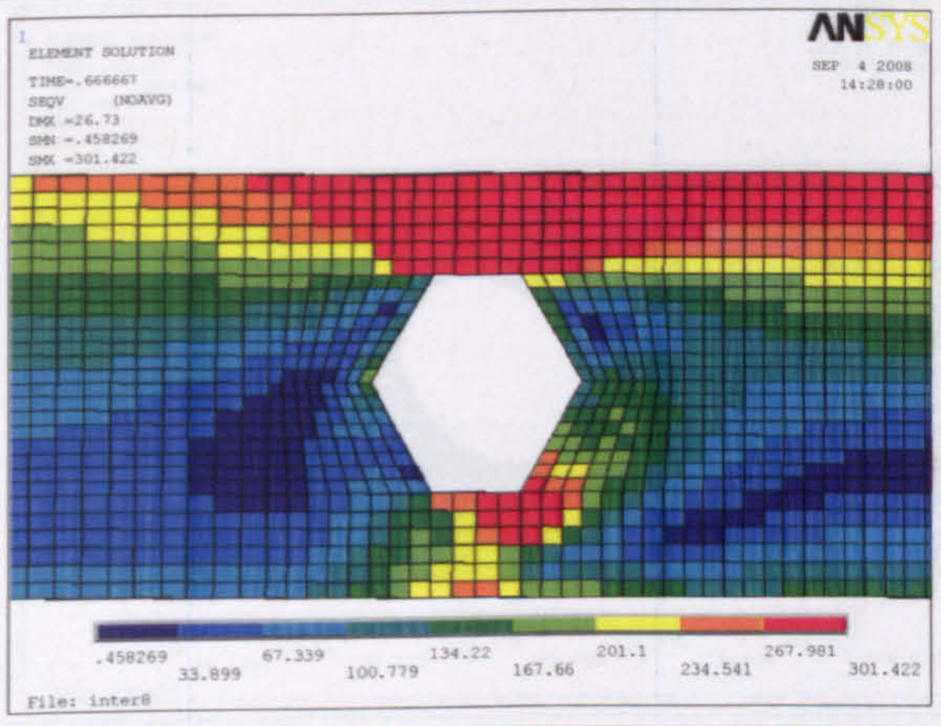

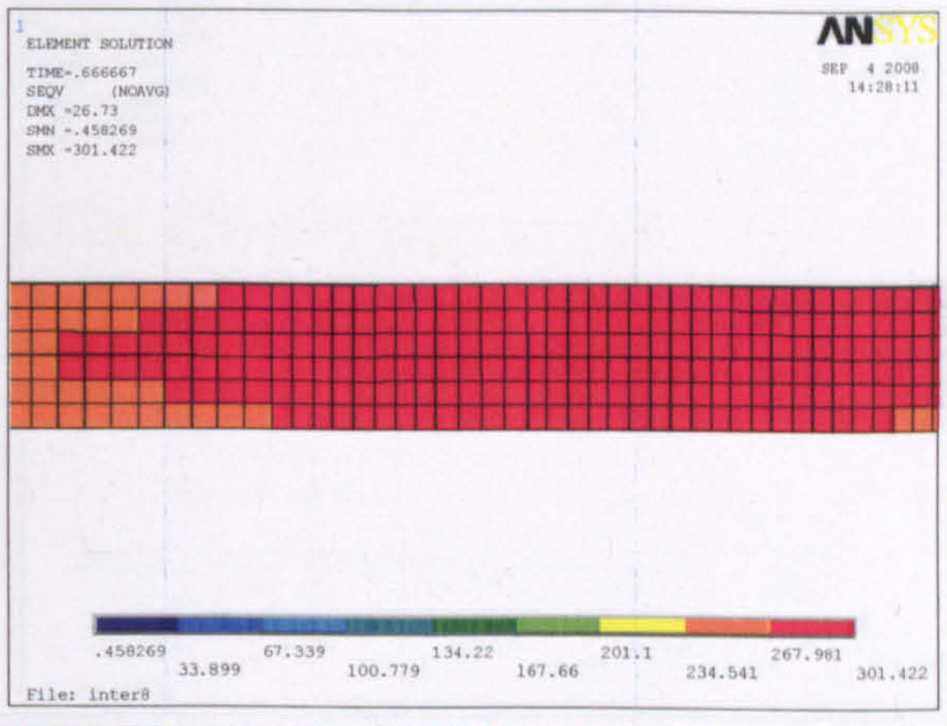

Web opening C

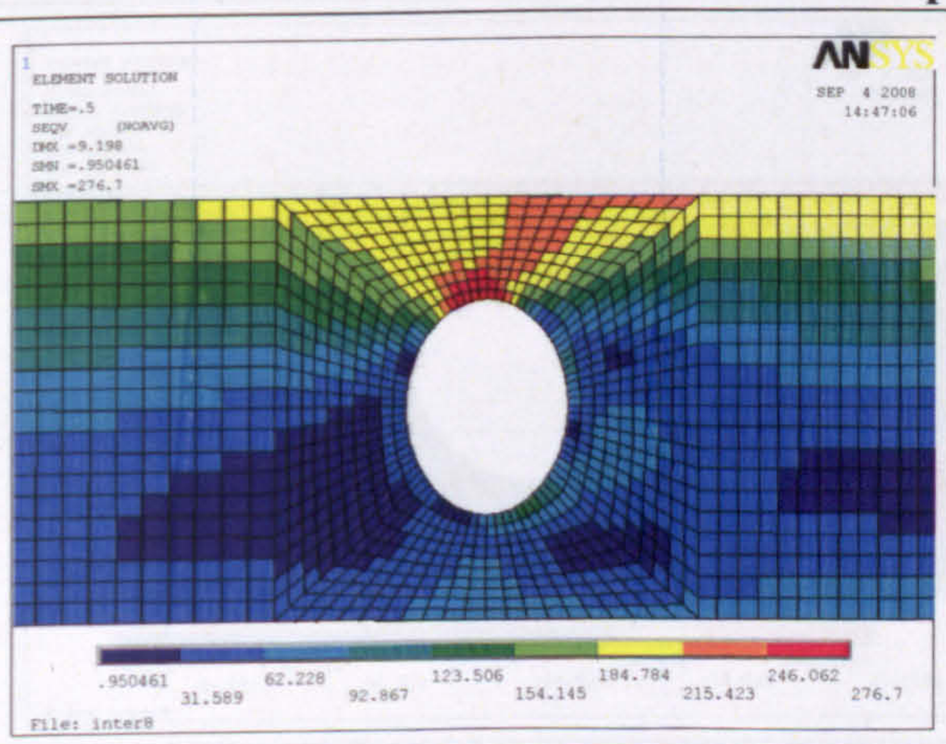

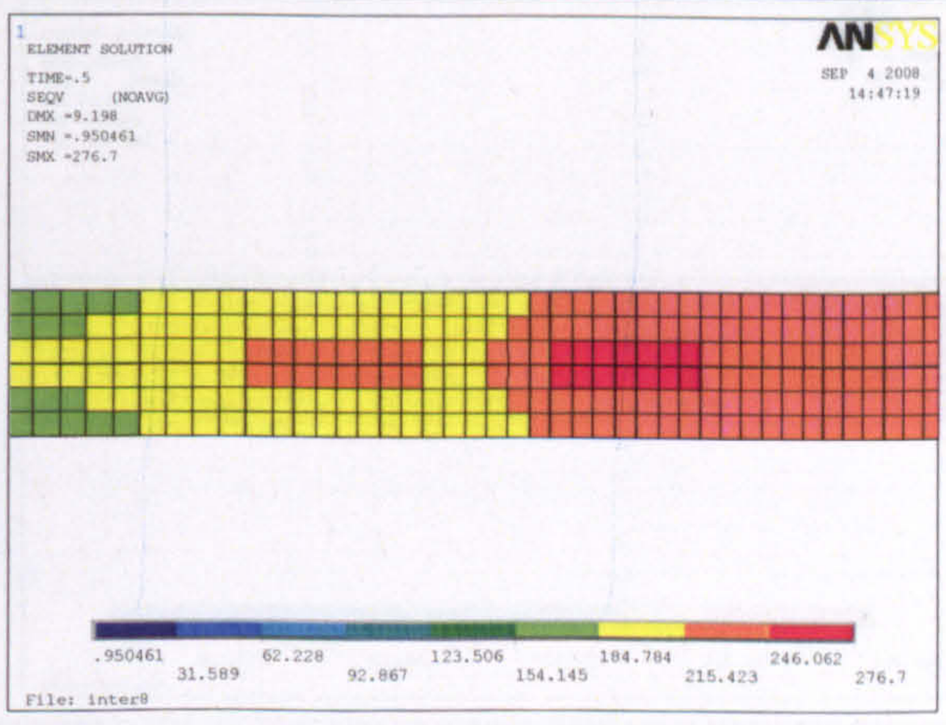

Web opening D

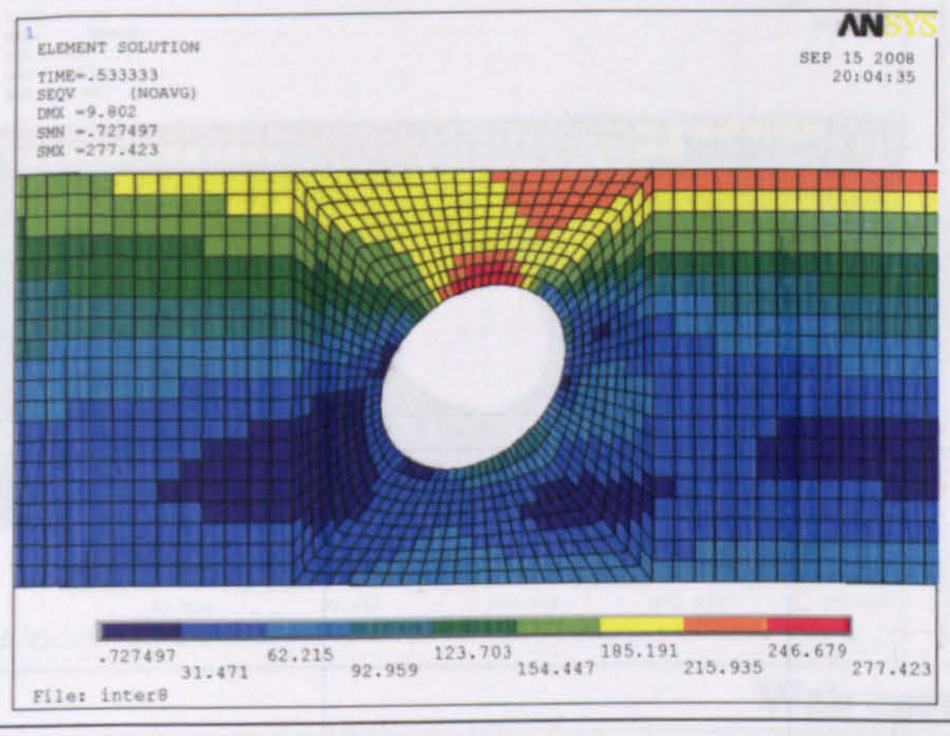

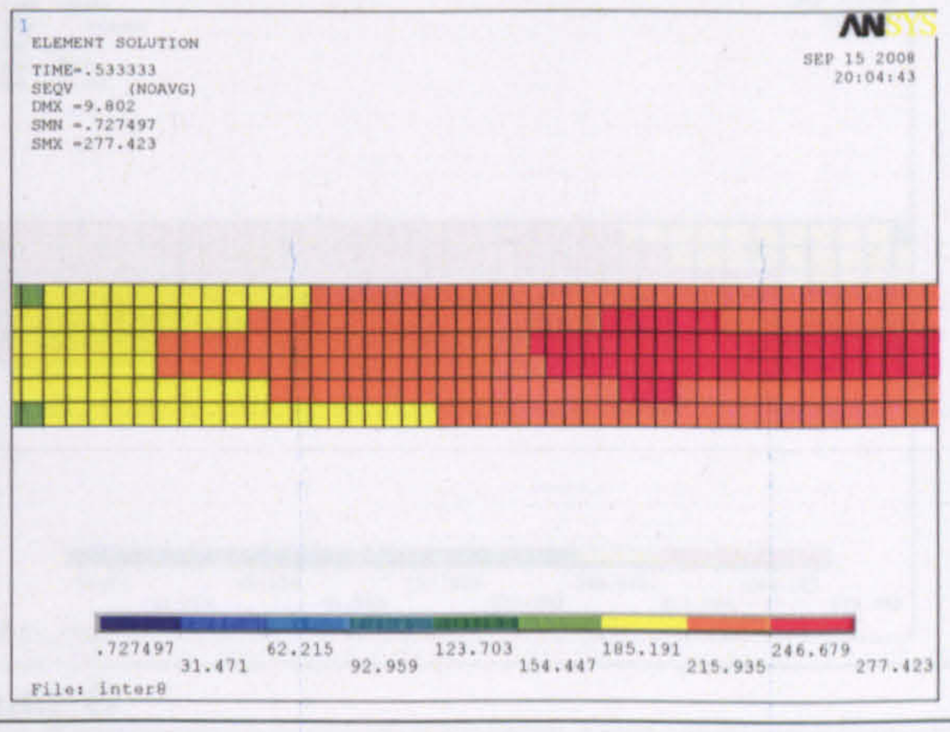

Web opening E

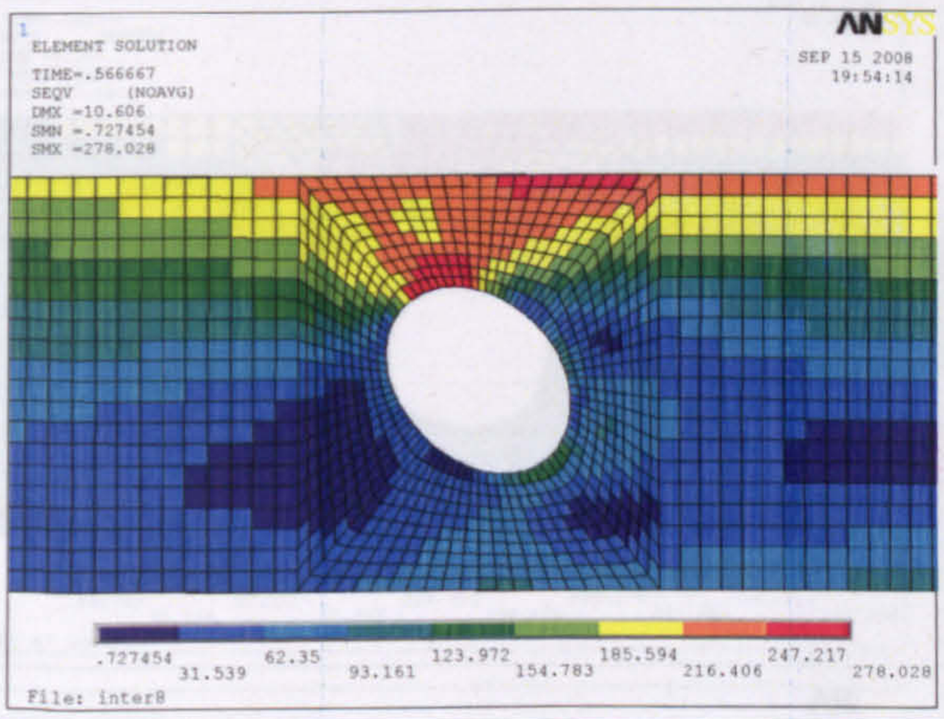

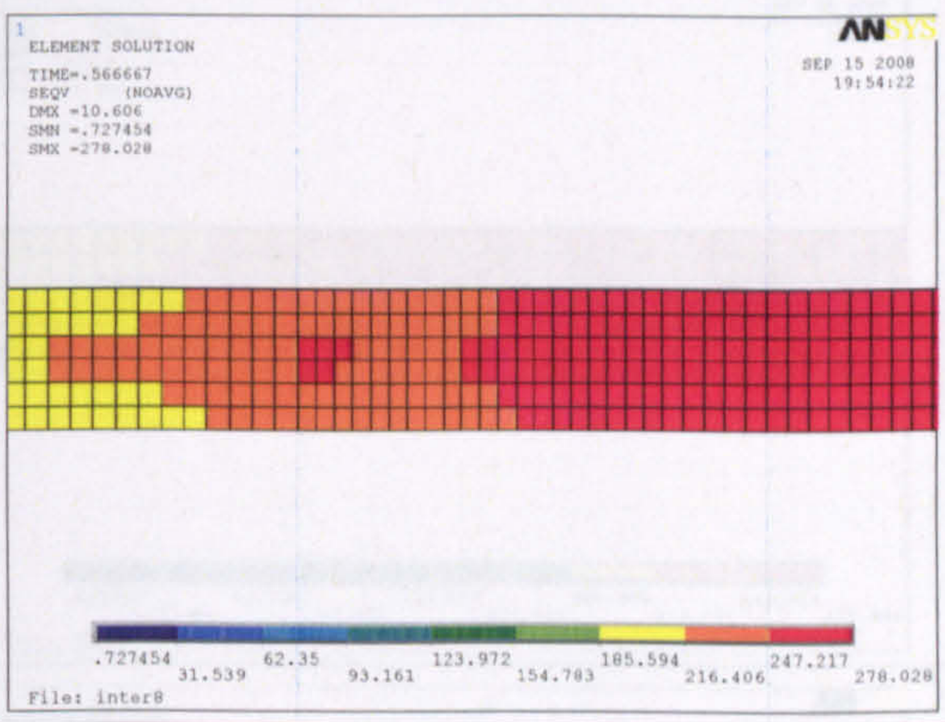

Web opening F

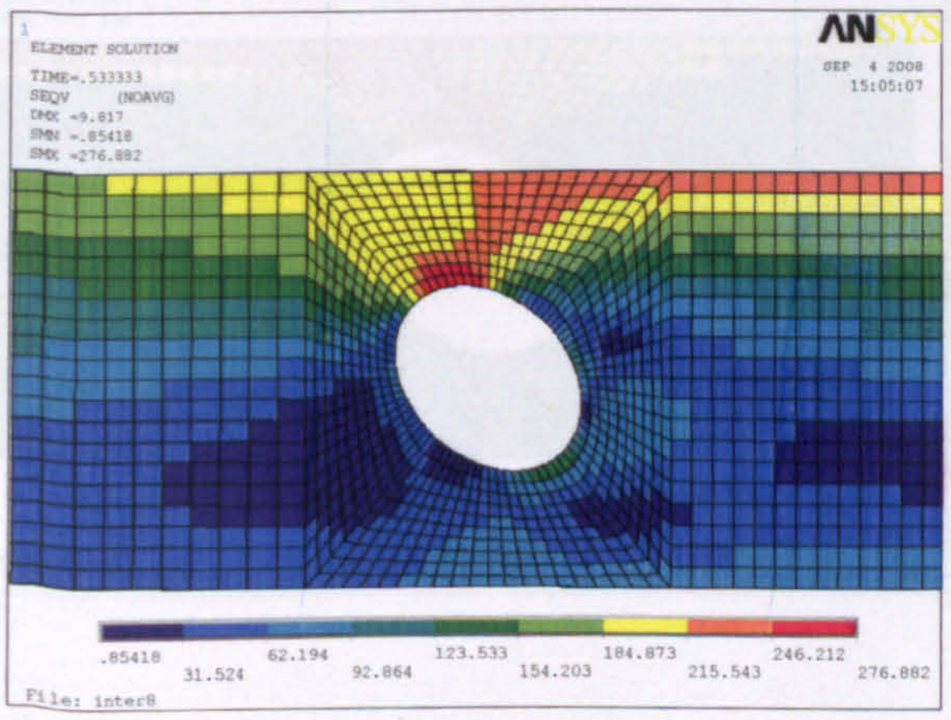

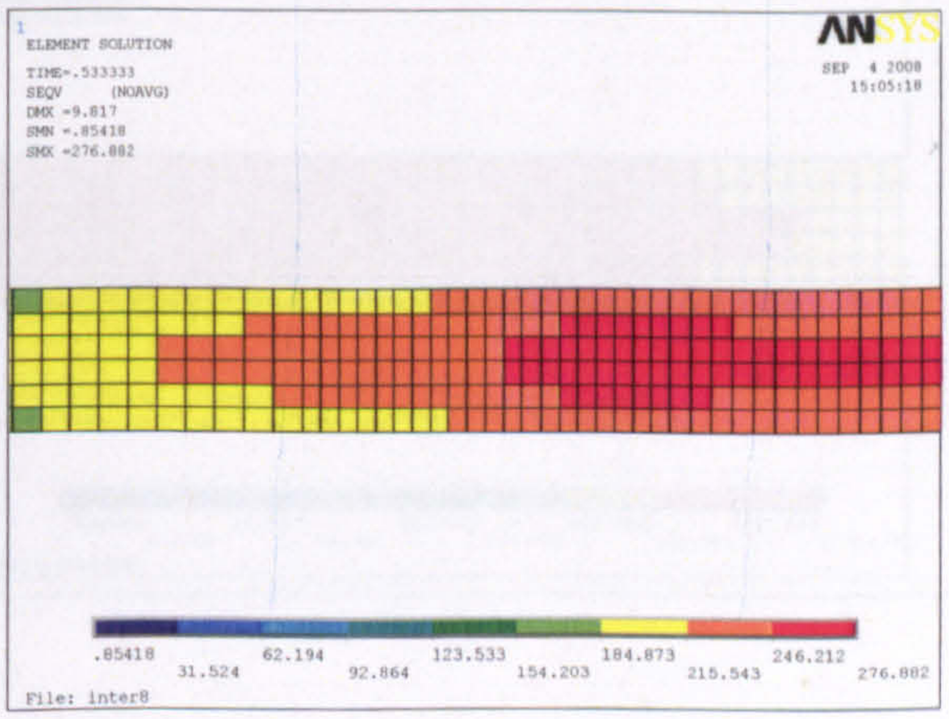

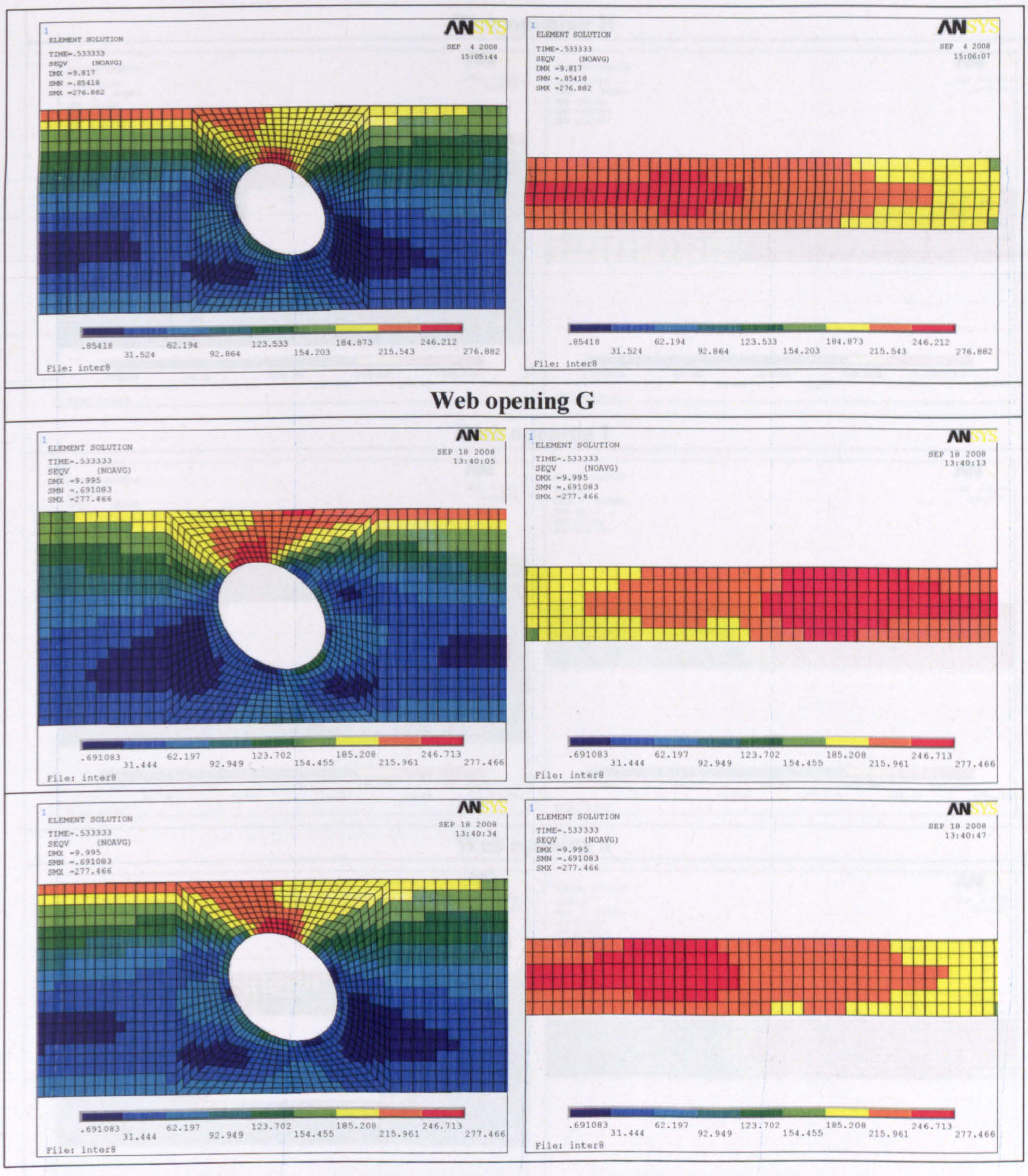
1
ELEMENT SOLUTION
TIME=.533333
SEQV (NOAVG)
DMX =9.817
SMN =.85418
SMX =276.882
ANSYS
SEP 4 2008
15:05:44
.85418
31.524
62.194
92.864
123.533
154.203
184.873
215.543
246.212
276.882
File: inter8
1
ELEMENT SOLUTION
TIME=.533333
SEQV (NOAVG)
DMX =9.817
SMN =.85418
SMX =276.882
ANSYS
SEP 4 2008
15:06:07
.85418
31.524
62.194
92.864
123.533
154.203
184.873
215.543
246.212
276.882
File: inter8
Web opening G
1
ELEMENT SOLUTION
TIME=.533333
SEQV (NOAVG)
DMX =9.995
SMN =.691083
SMX =277.466
ANSYS
SEP 18 2008
13:40:05
.691083
31.444
62.197
92.949
123.702
154.455
185.208
215.961
246.713
277.466
File: inter8
1
ELEMENT SOLUTION
TIME=.533333
SEQV (NOAVG)
DMX =9.995
SMN =.691083
SMX =277.466
ANSYS
SEP 18 2008
13:40:13
.691083
31.444
62.197
92.949
123.702
154.455
185.208
215.961
246.713
277.466
File: inter8
1
ELEMENT SOLUTION
TIME=.533333
SEQV (NOAVG)
DMX =9.995
SMN =.691083
SMX =277.466
ANSYS
SEP 18 2008
13:40:34
.691083
31.444
62.197
92.949
123.702
154.455
185.208
215.961
246.713
277.466
File: inter8
1
ELEMENT SOLUTION
TIME=.533333
SEQV (NOAVG)
DMX =9.995
SMN =.691083
SMX =277.466
ANSYS
SEP 18 2008
13:40:47
.691083
31.444
62.197
92.949
123.702
154.455
185.208
215.961
246.713
277.466
File: inter8

Web opening H

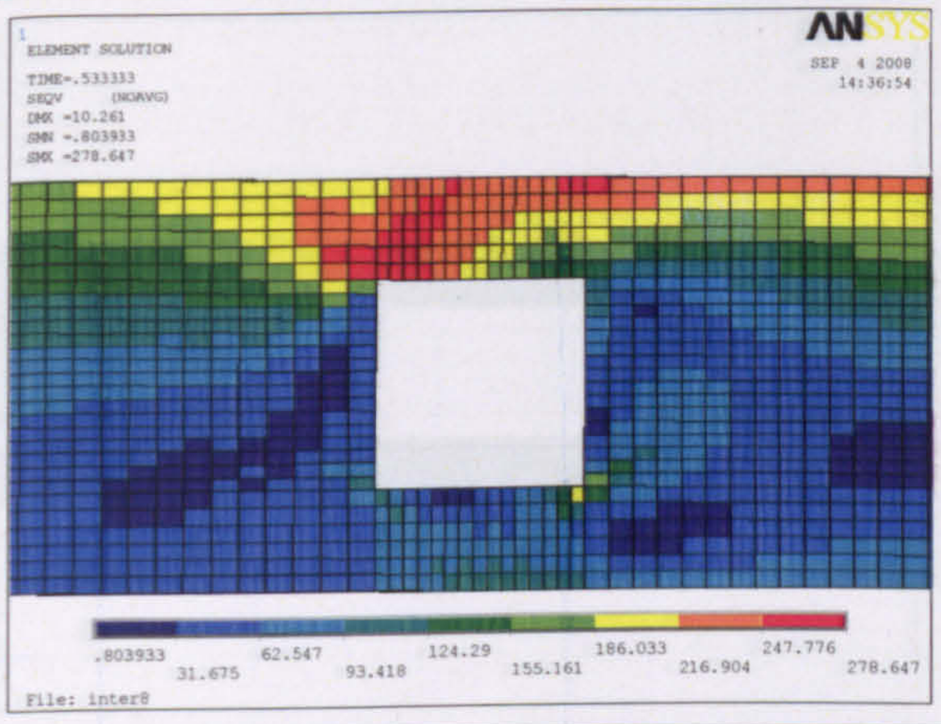

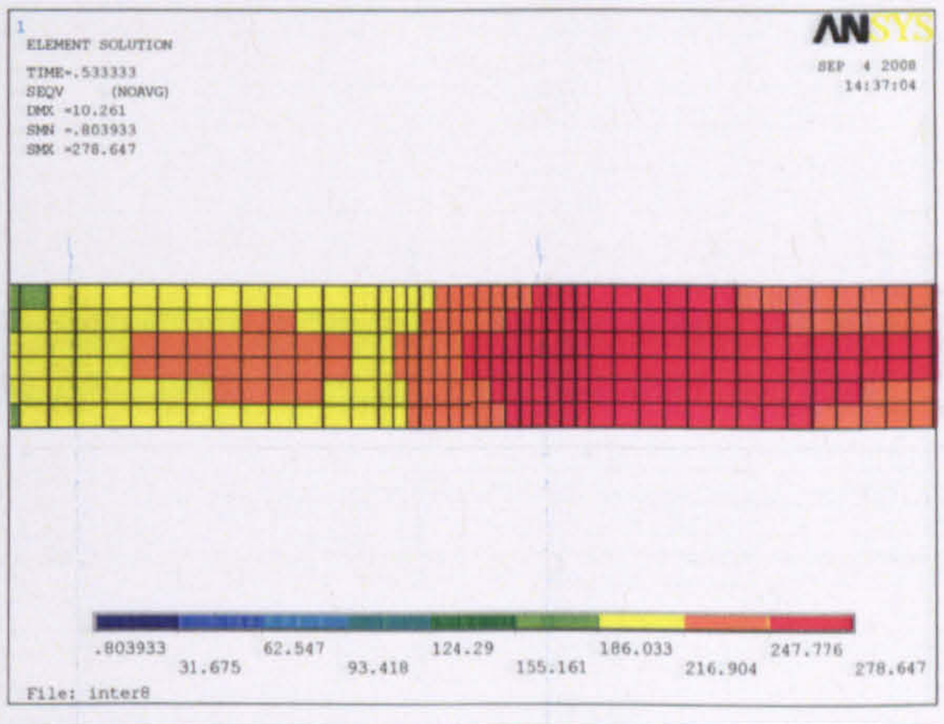

Web opening I

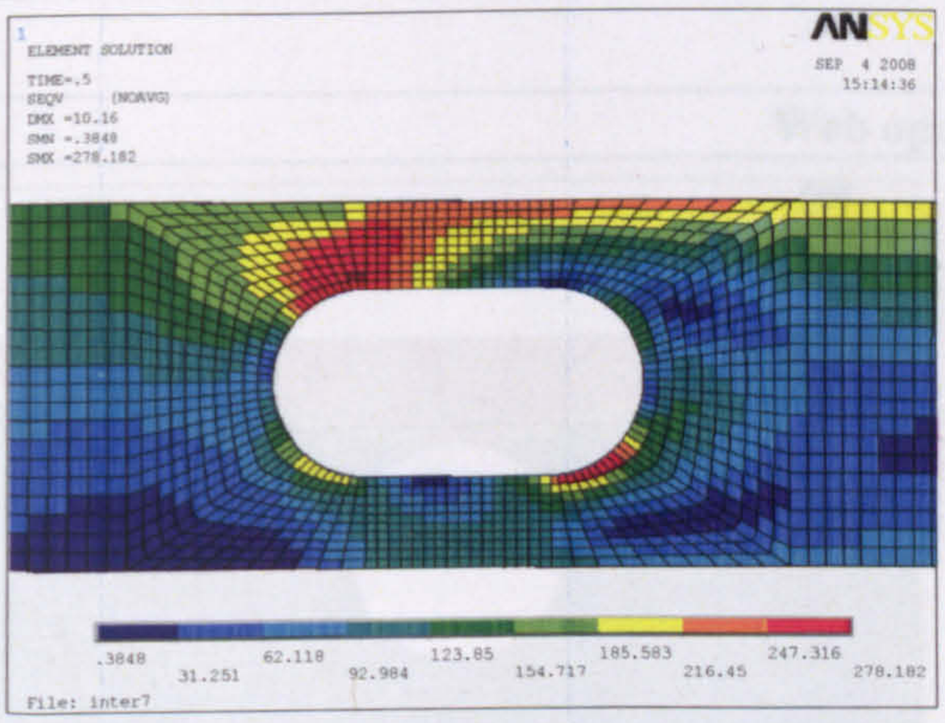

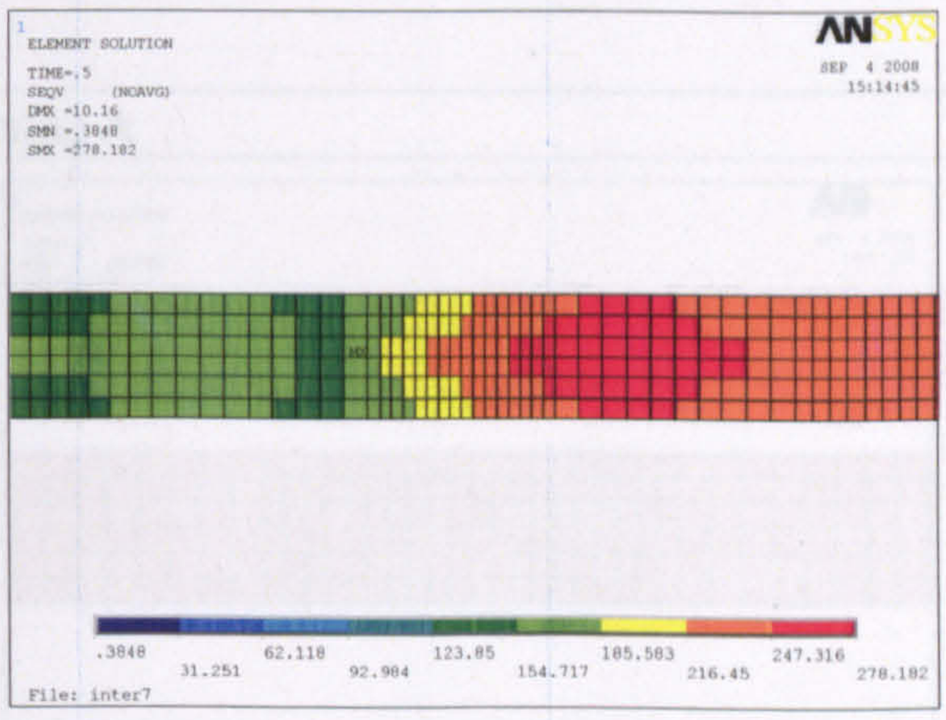

Web opening J

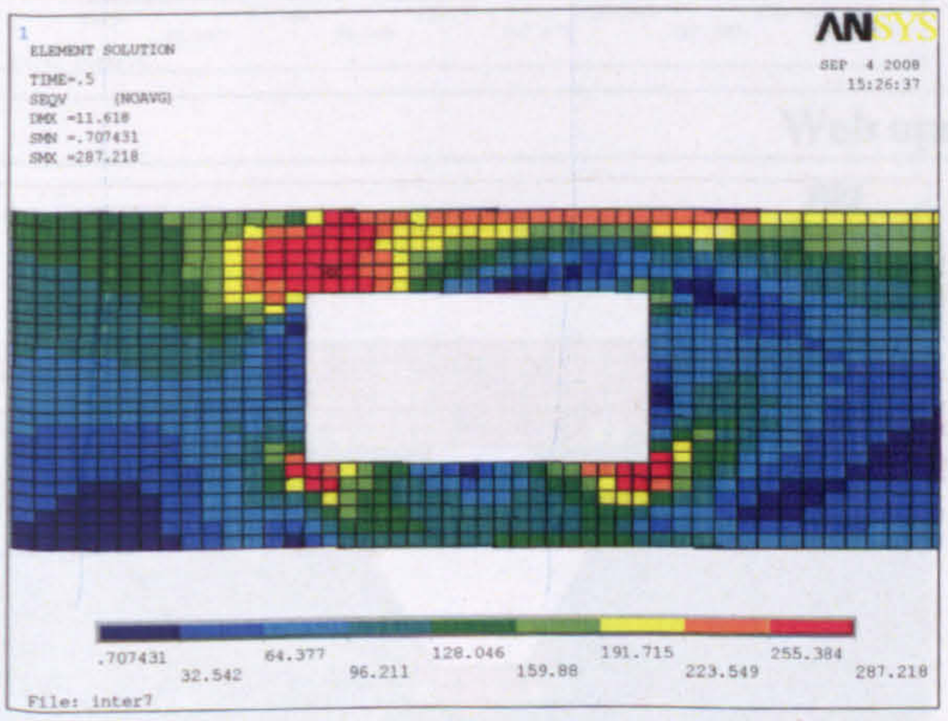

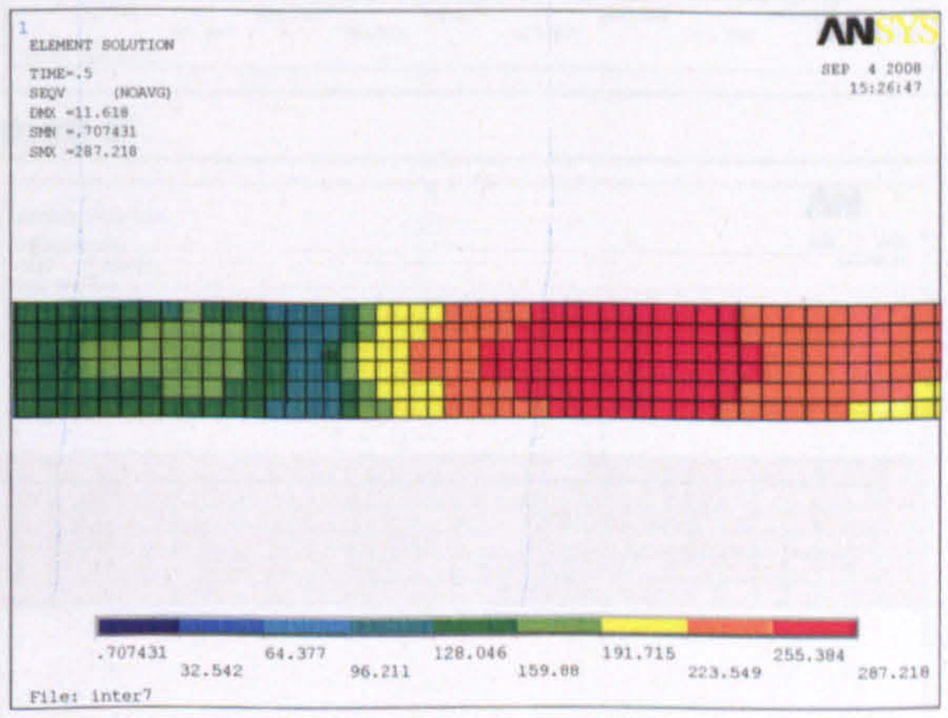

Web opening K

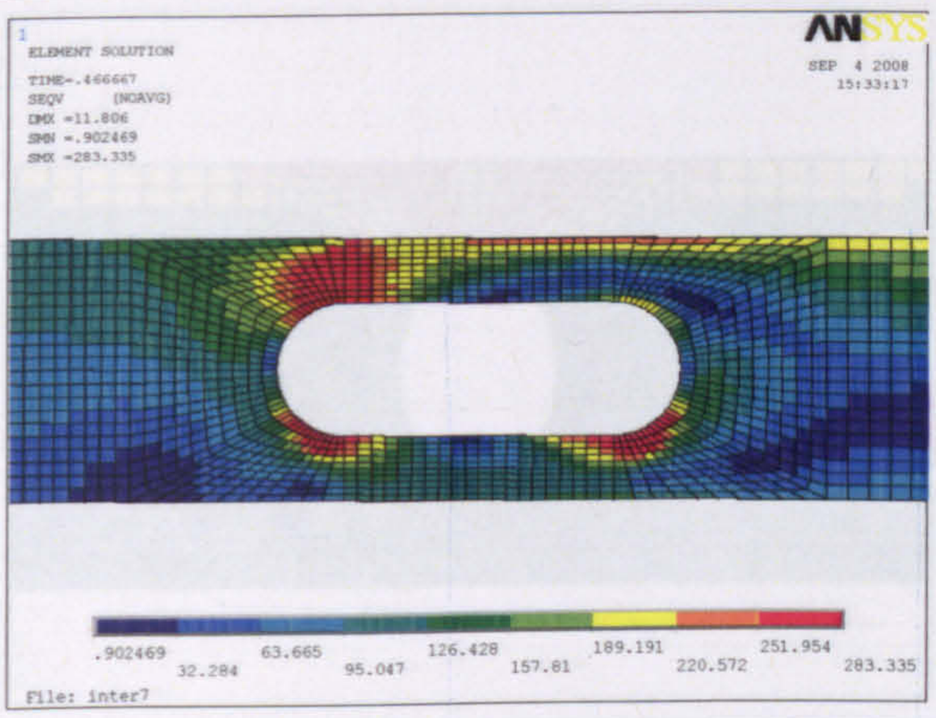

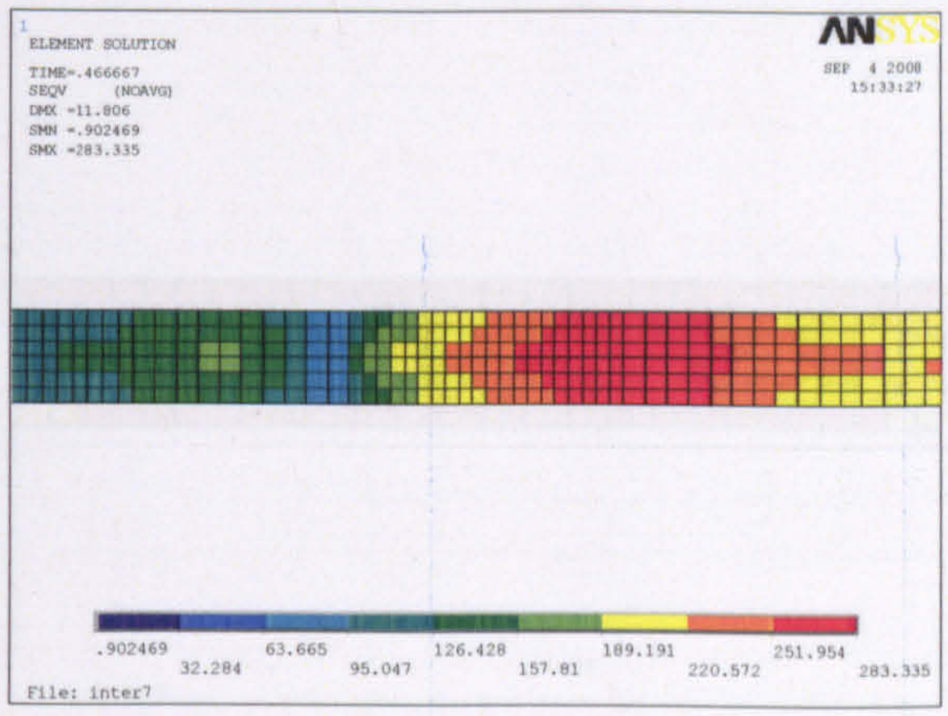

Figure 11: Failure stresses with web opening at high moment and low shear region ($d_o/h=0.5$)

Web opening A

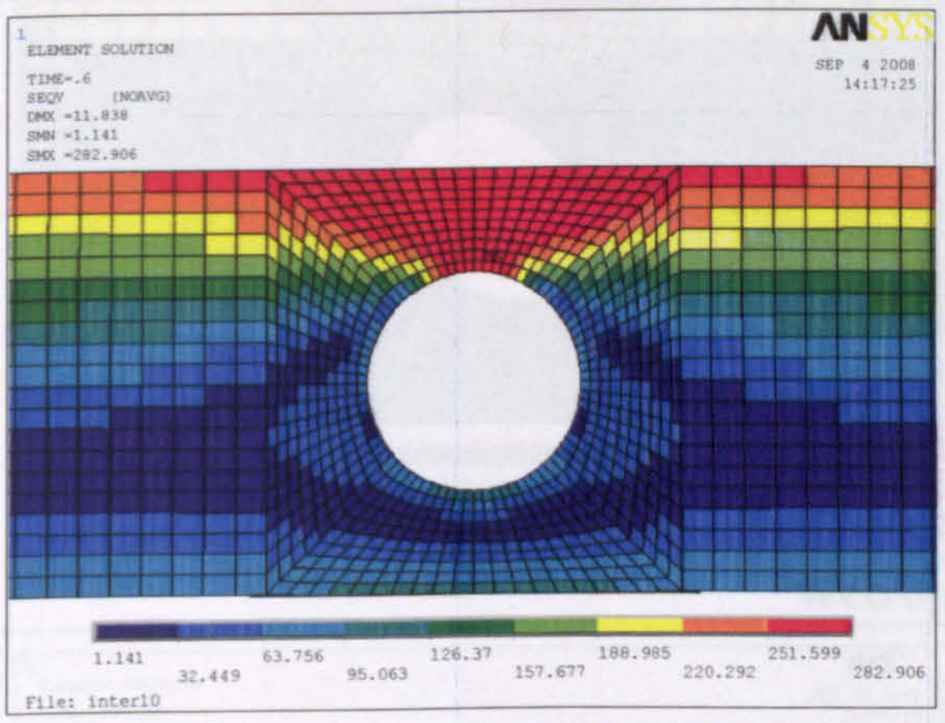

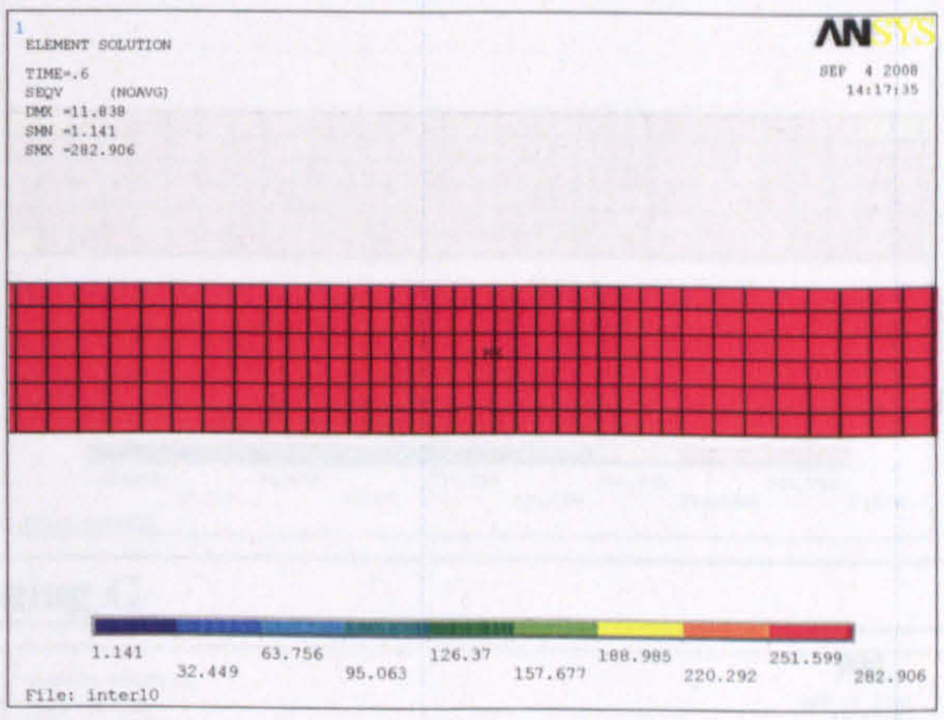

Web opening B

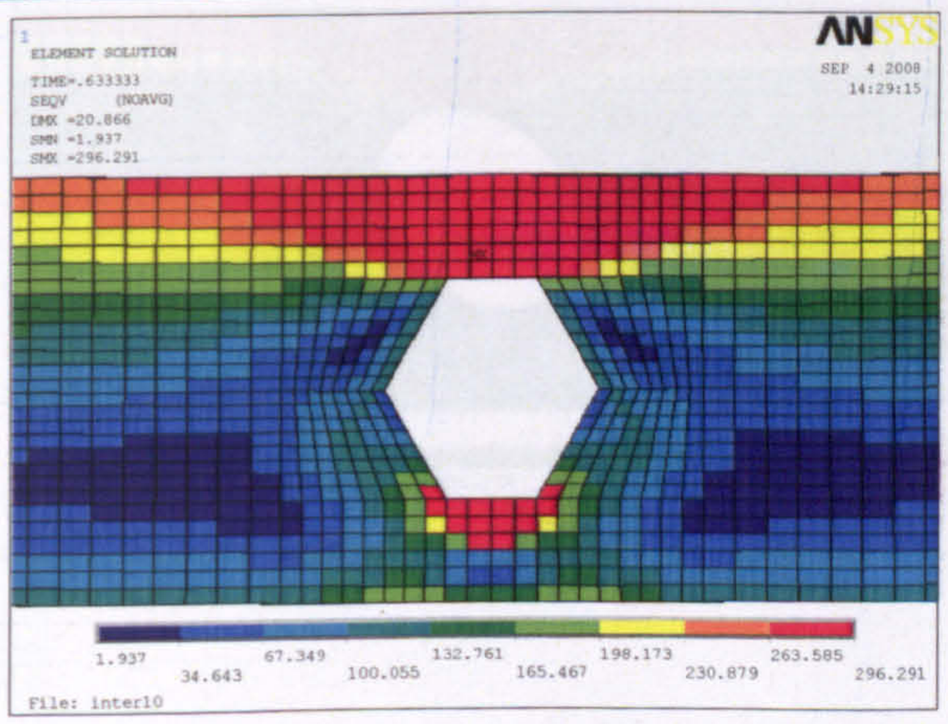

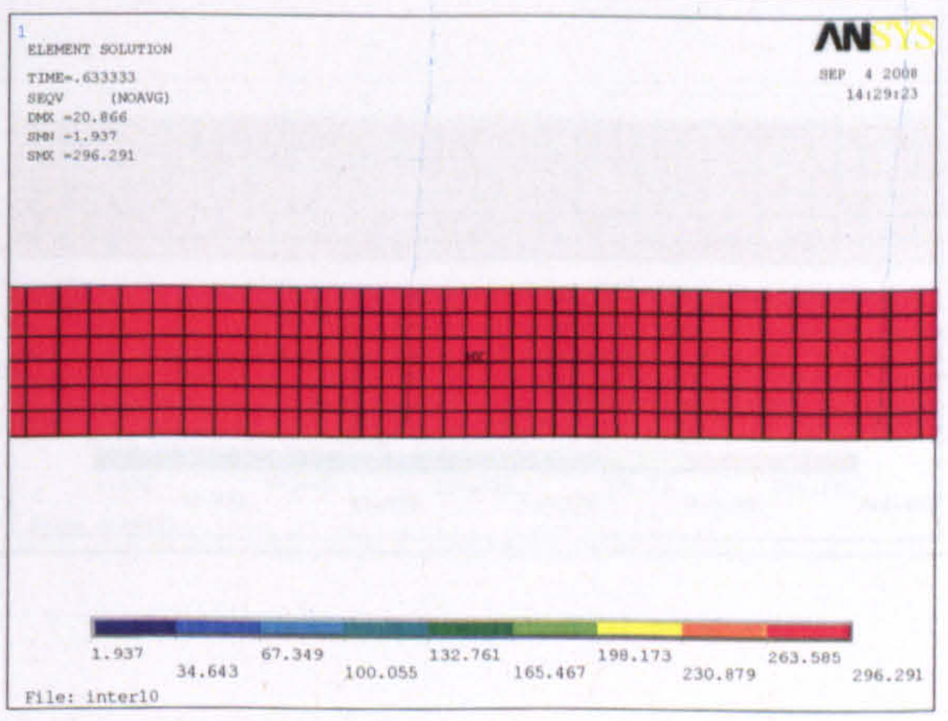

Web opening C

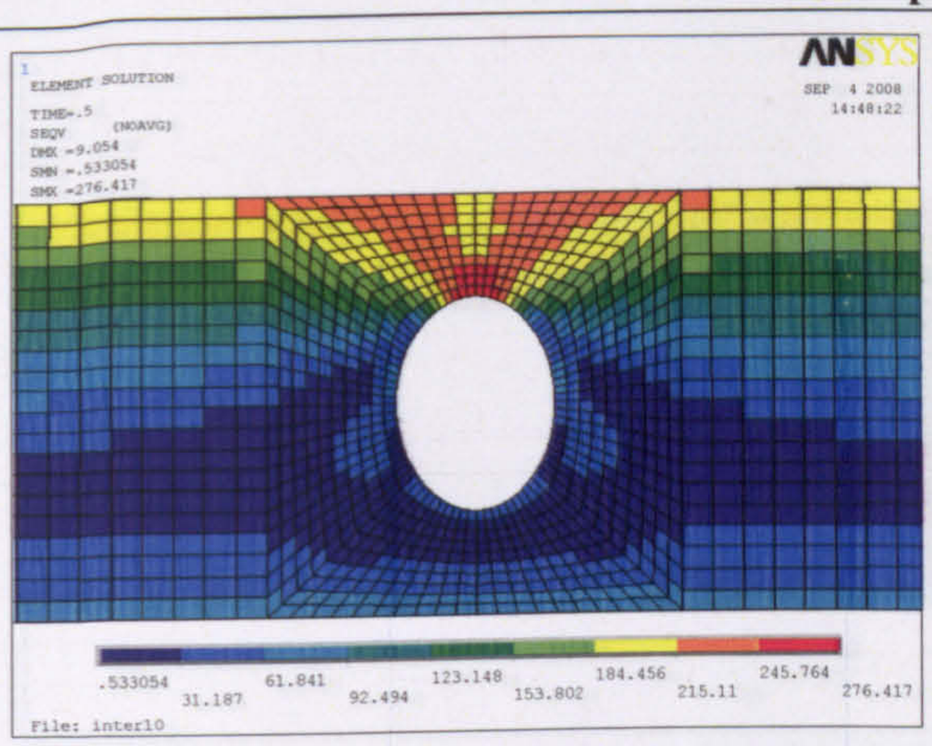

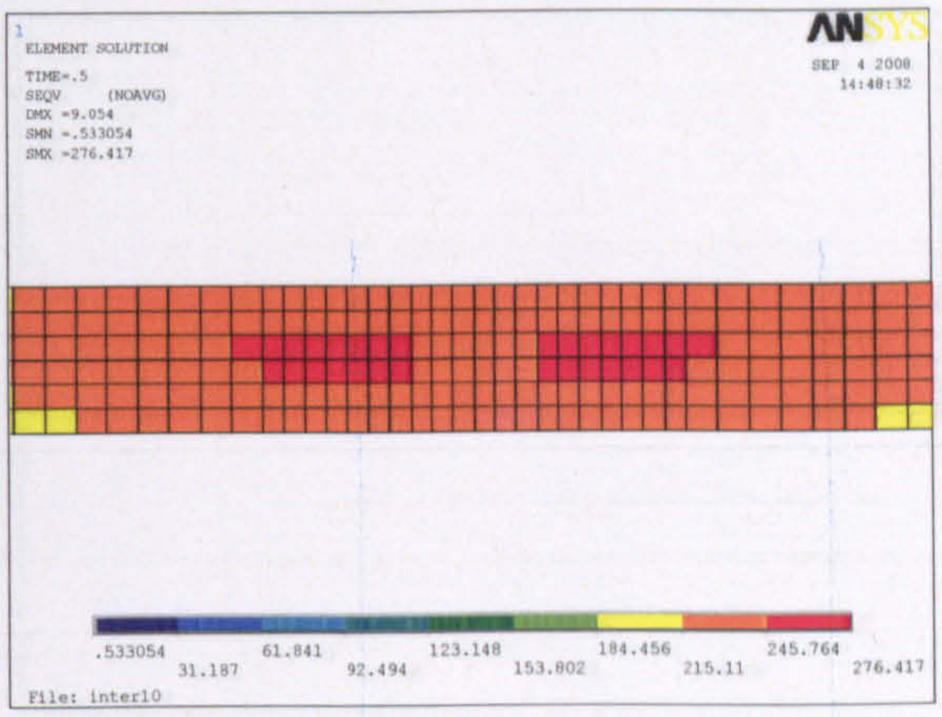

Web opening D-E-F

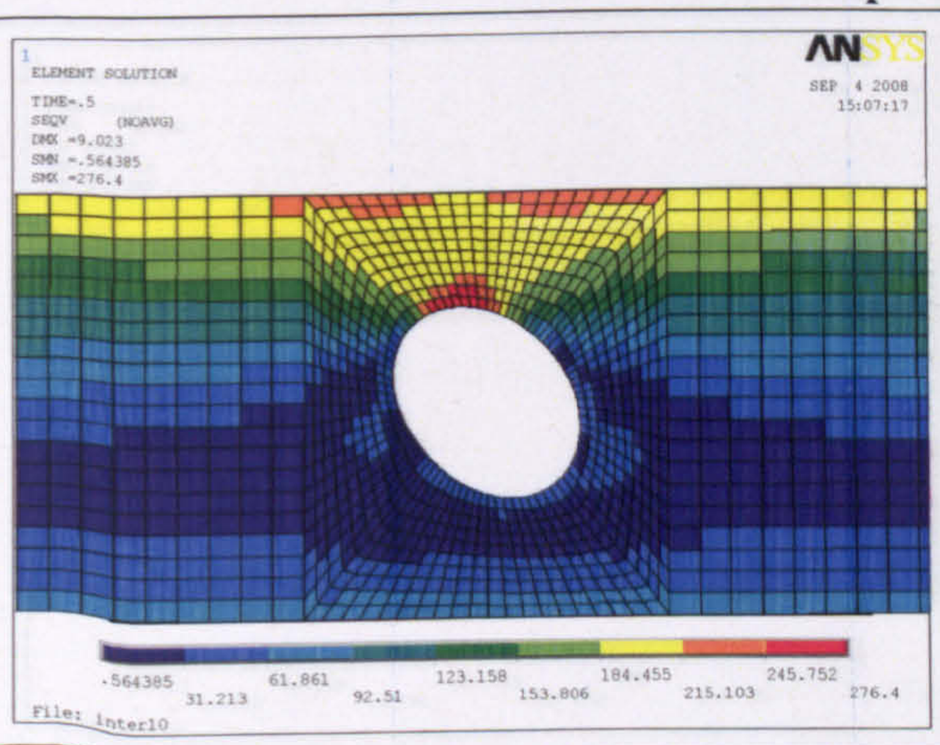

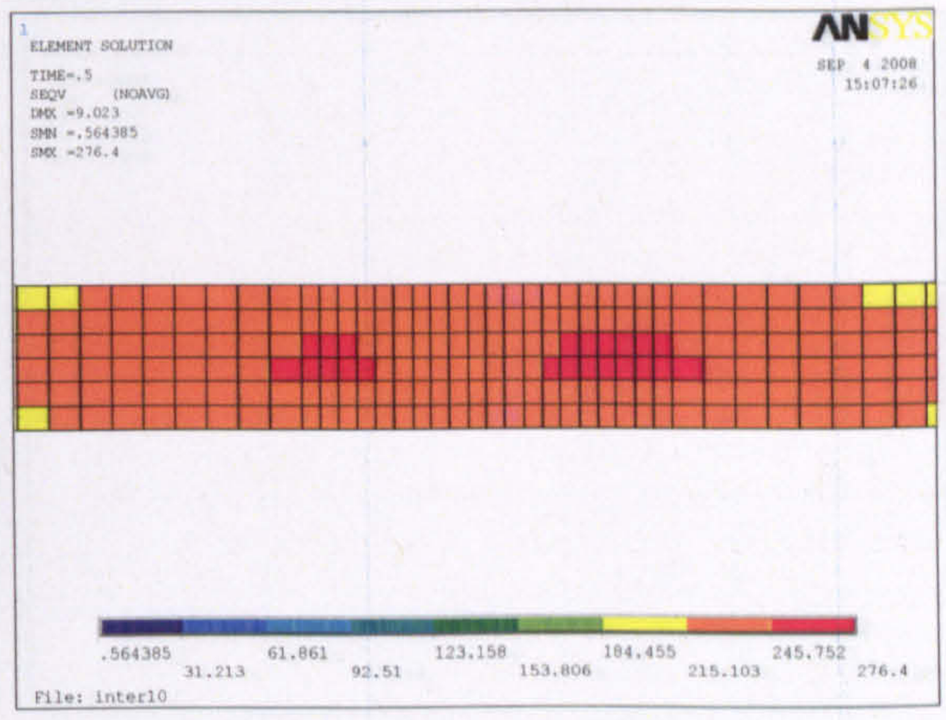

Web opening G

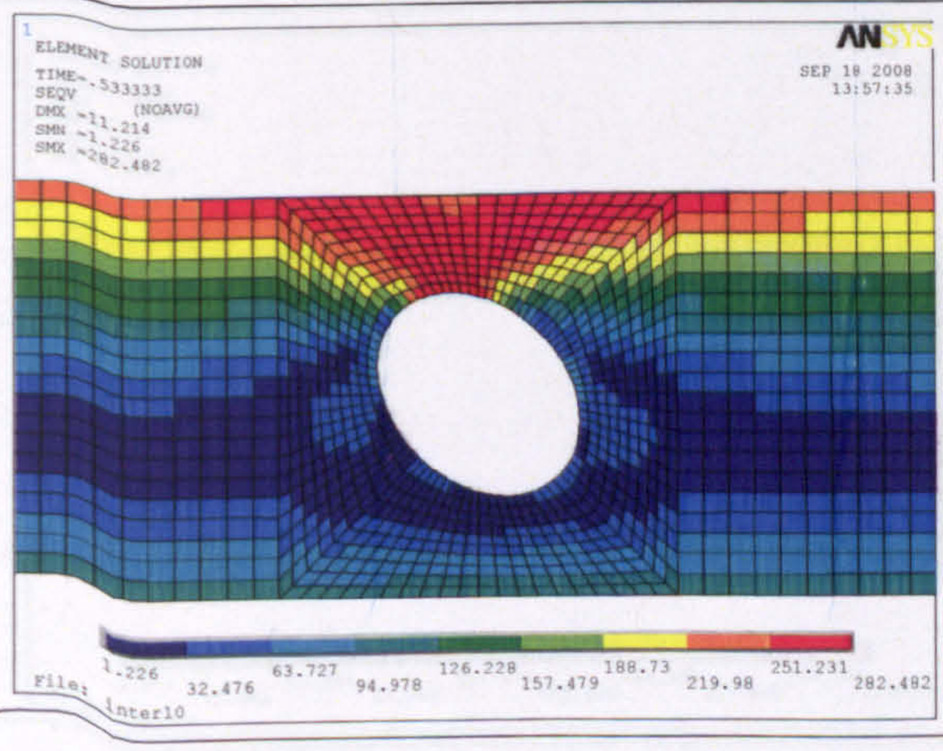

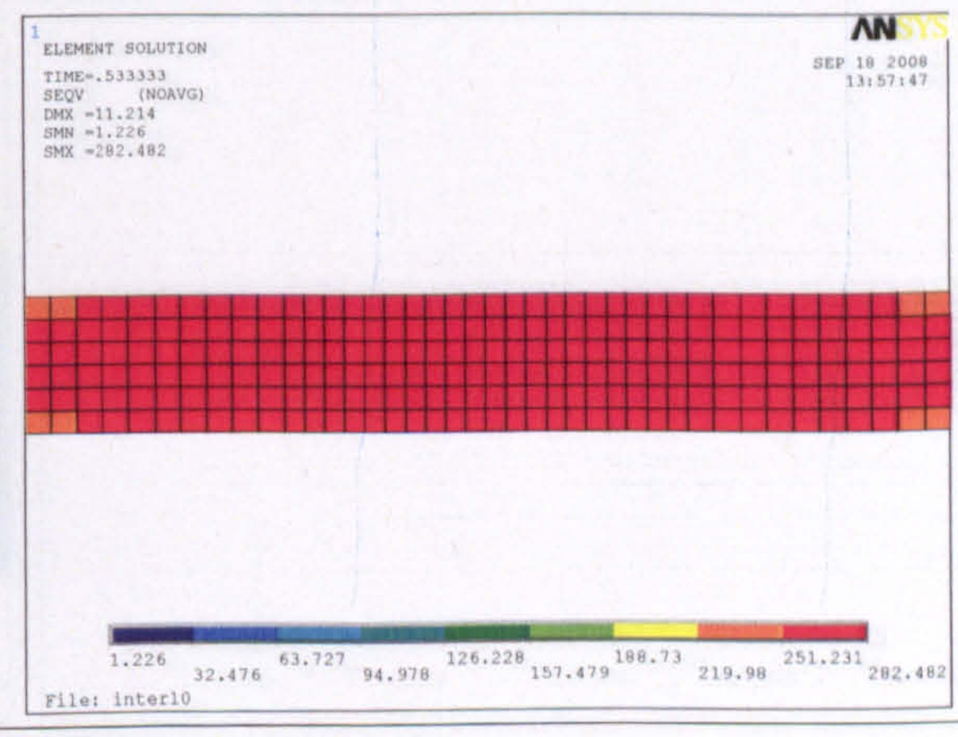

Web opening H

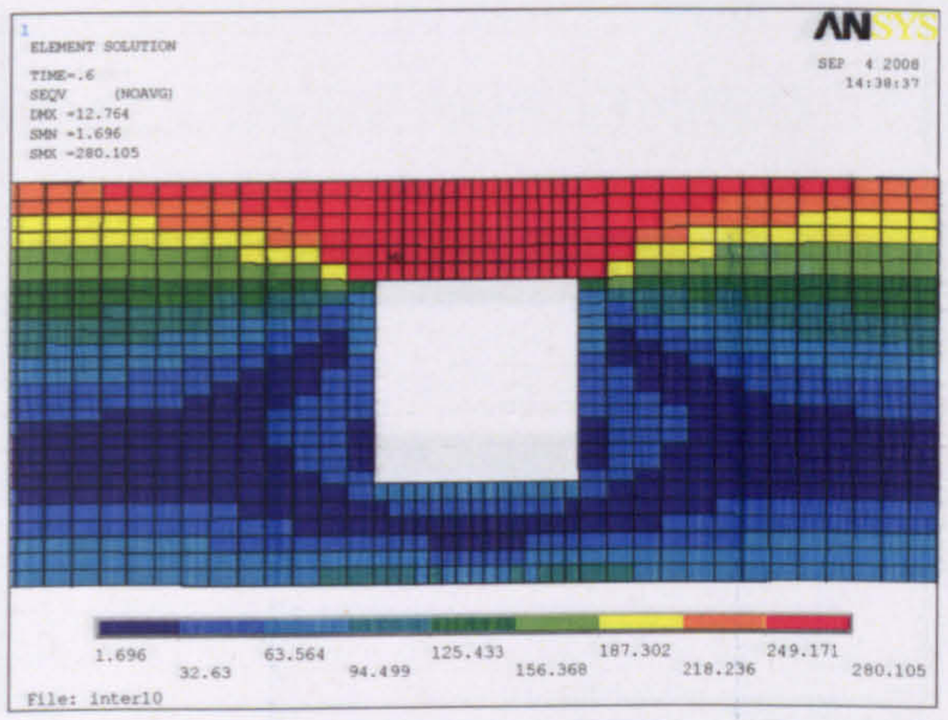

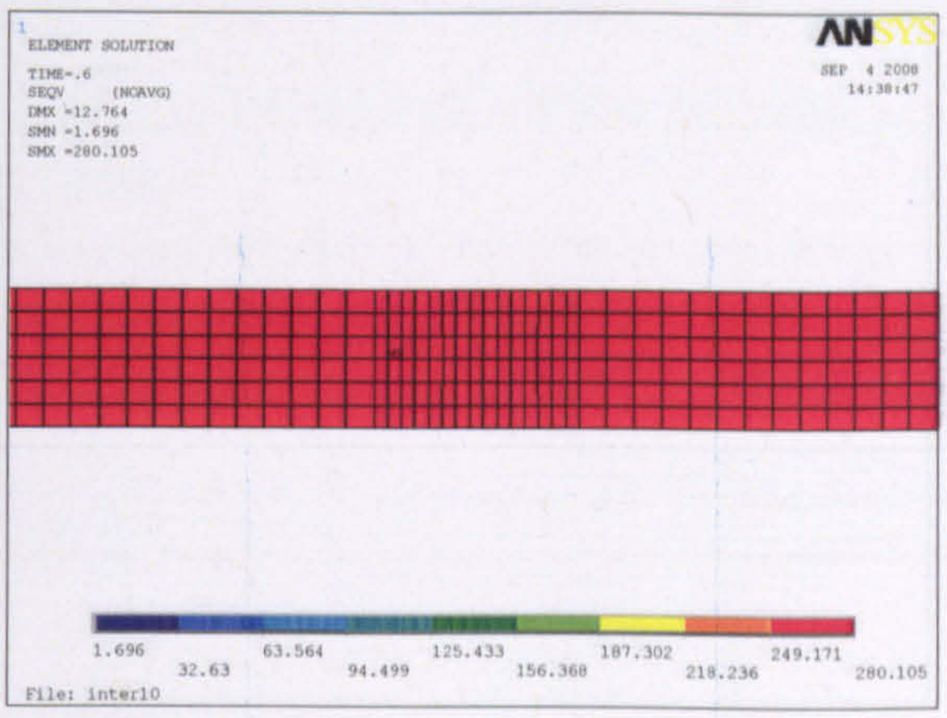

Web opening I

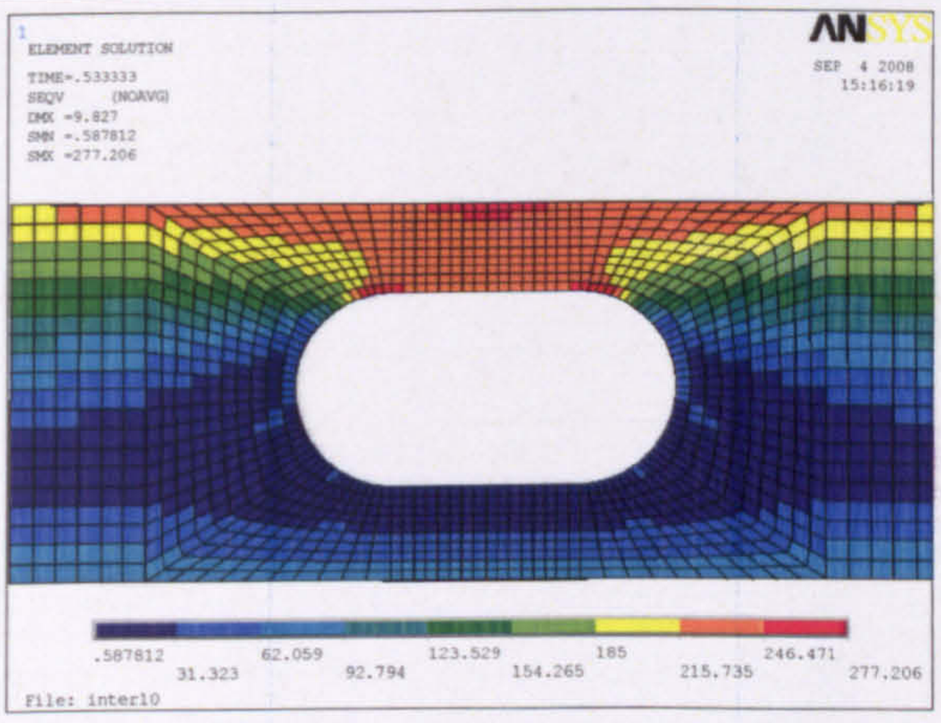

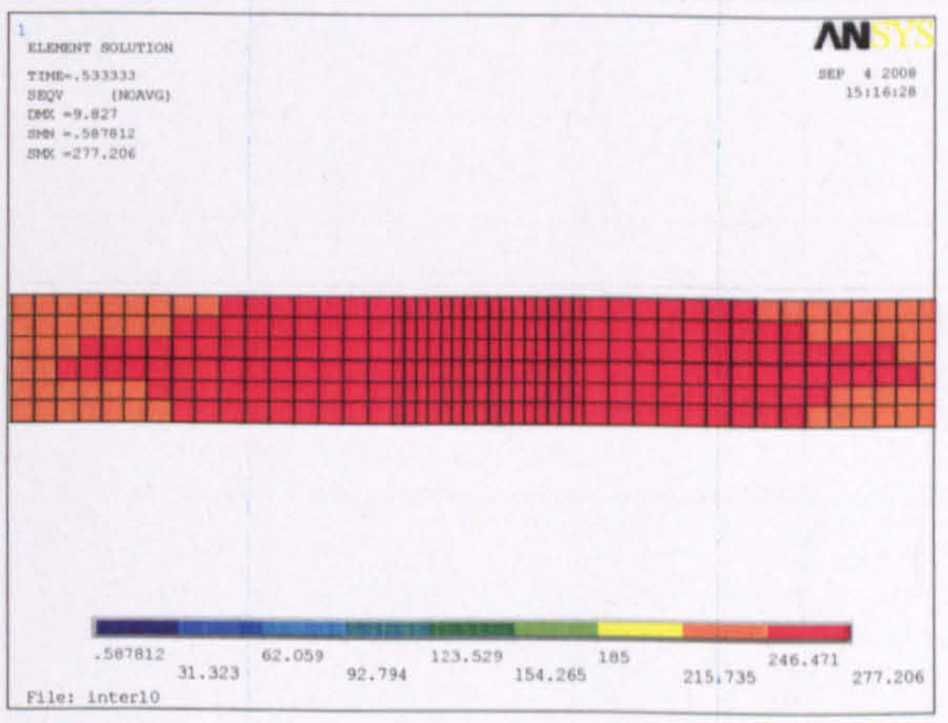

Web opening J

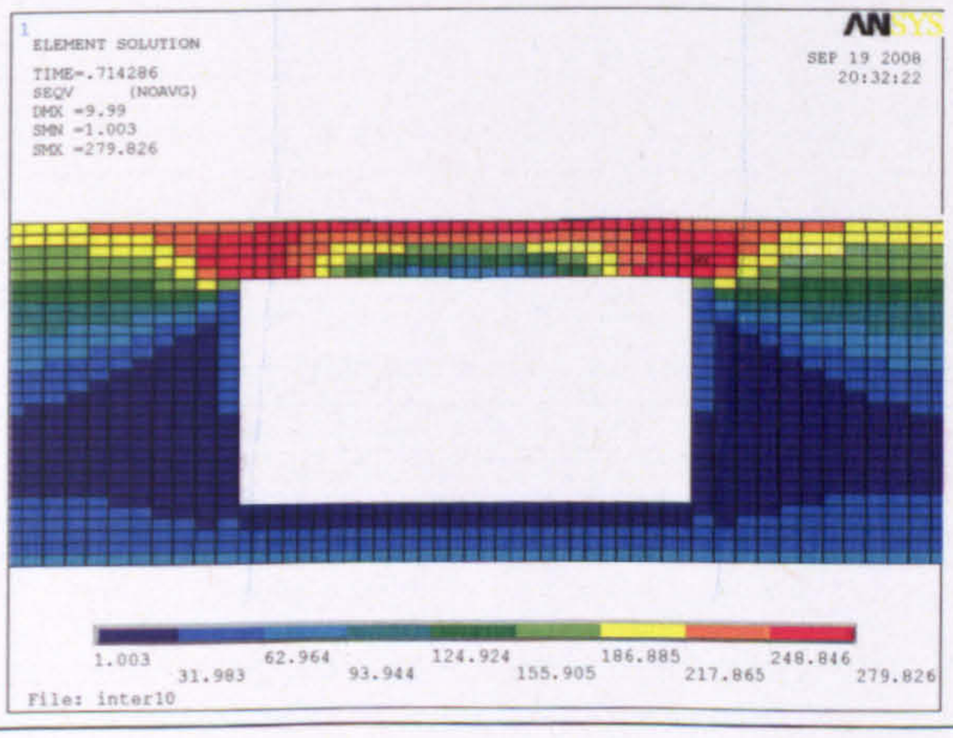

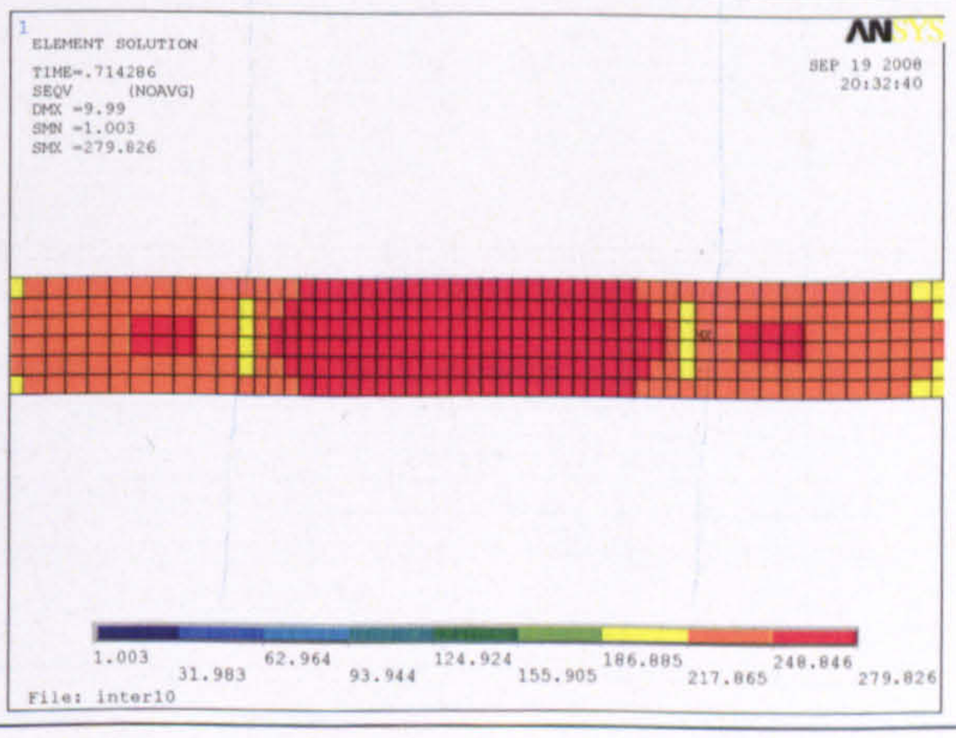

Web opening K

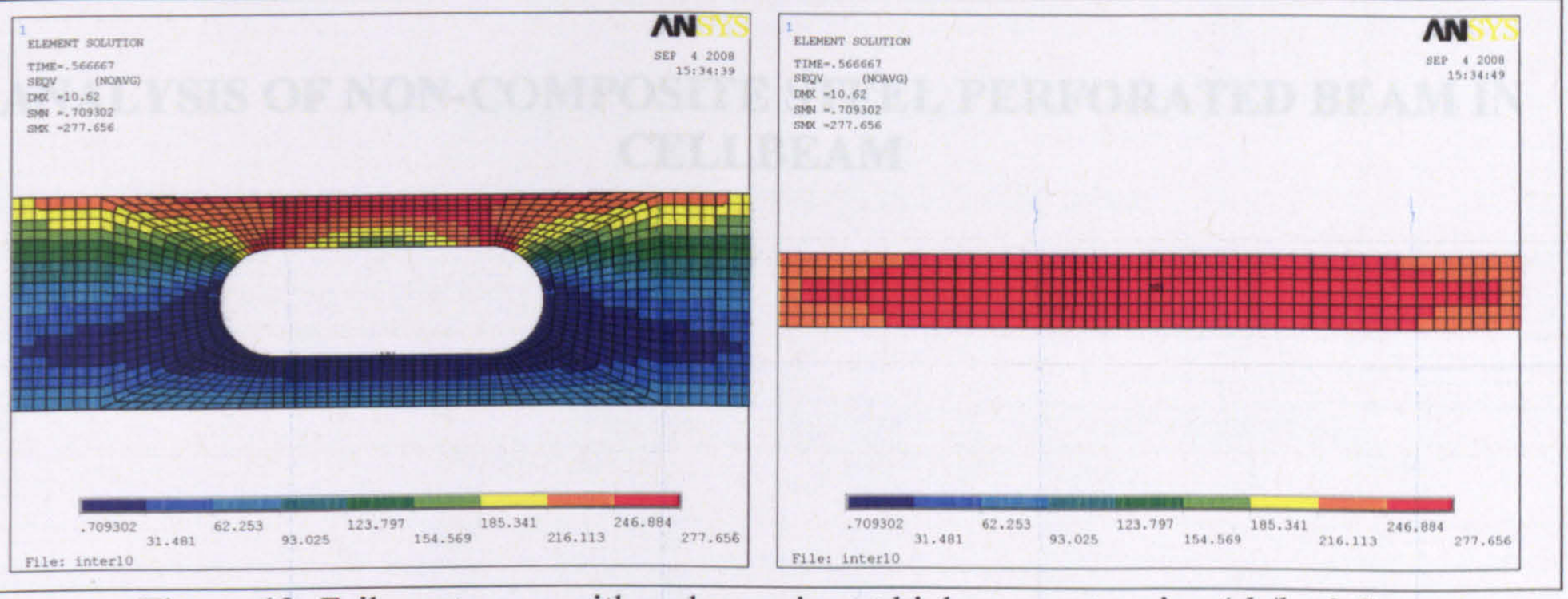

Figure 12: Failure stresses with web opening at high moment region ($d_o/h=0.5$)

APPENDIX 7

ANALYSIS OF NON-COMPOSITE STEEL PERFORATED BEAM IN CELLBEAM

Westok	** C E L L B E A M ** Ver. 6.0 Westok	BS 5950 : Parts 1 & 3
The Steel Construction Institute	Project: Beam Ref.: Company: Westok Limited. Client: Job No.: Calcs by: Revision:	Date: 10/11/2007 Time: 11:05:55 Checked.:

INPUT DATA - FULL OUTPUT

305x165UB40kg/m S355 with x number 230 mm diameter cells @ 900 mm centres.

It is essential that all of the above is on the drawings for tender and construction

Failure Mode	Maximum Unity Factor / Critical Load Combination					
	Normal Stage		Construction Stage		Fire	
Vertical Shear	0.98	(1)	N/A	N/A	-	-
Horizontal Shear	0.25	(1)	N/A	N/A	-	-
Moment-Shear Interaction	0.29	(1)	N/A	N/A	-	-
Vierendeel Bending	**0.98**	(1)	**N/A**	N/A	-	-
Lateral Torsional Buckling	0.25	(1)	N/A	N/A	-	-
Web Post Buckling	0.20	(1)	N/A	N/A	-	-
Steel Stress - TOP	0.28	(6)	N/A	N/A	-	-
Steel Stress - BTM	0.28	(6)	N/A	N/A	-	-
Vibration (Hz)	13.90	(6)	N/A	N/A	-	-
Imposed Load Deflection (mm)	0.00	(6)	N/A	N/A	-	-

GENERAL :
Floor beam construction - NO SLAB
Beam will NOT be propped in construction PARALLEL to beam (SIDE 1)

CELLS DATA : (230 mm diameter cells at 450 mm centres)

Centre of first cell from LHS	300 mm	Number of cells in beam	3
Centre of last cell from RHS	300 mm	Number of cells with infill	1 (see sketch)
Cells with ring stiffeners	NONE		

Infills:

Cell No.	Infill Type	Plate Thickness (mm)
2	FULL	6.0

FLOOR PLAN DATA : [Floor Beam - INTERNAL : SIMPLE SUPPORTS]

Beam span	1.50 m	Beam spacing (SIDE 1)	1.00 m
Beam length	1.50 m	Beam spacing (SIDE 2)	1.00 m

BEAM DATA : [NON STANDARD SECTION Net Mass: 37.7 kg/m]

Overall depth	303.4 mm	Depth between fillets	265.2 mm
TOP TEE		**BTM TEE**	
Tee depth	151.7 mm	Tee depth	151.7 mm
Web thickness	6.0 mm	Web thickness	6.0 mm
Flange width	165.0 mm	Flange width	165.0 mm
Flange thickness	10.2 mm	Flange thickness	10.2 mm
Root radius	8.9 mm	Root radius	8.9 mm
Steel design strength	355.0 N/mm²	Steel design strength	355.0 N/mm²

STEEL SECTION PROPERTIES : (at centrelines of openings)
Section Classification: Normal Stage: Flange - TOP: 2 BTM.: 2 WEB: 1
Elastic neutral axis is in WEB (151.7 mm from beam top flange)
Plastic neutral axis is in WEB (151.7 mm from beam top flange)

2nd moment of area	Ixx = 7894.2 cm4	2nd moment of area	Iyy = 763.9 cm4
Elastic modulus (top)	Zt = 520.4 cm³	Elastic modulus (btm)	Zb = 520.4 cm³
Radius of gyration	rx = 14.5 cm	Radius of gyration	ry = 4.51 cm
Buckling parameter	u = 0.969	Torsional index	x = 27.452
Plastic modulus	Sx = 543.7 cm³	Elastic modulus (minor axis)	Zy = 92.6 cm³
Cross section area	A = 37.5 cm²	Surface area (mean)	1.13 m²/m

Westok BS 5950 : 2000 The Steel Construction Institute

BEAM RESTRAINTS AND EFFECTIVE LENGTHS DATA :

Top:

Top flange laterally unrestrained — Effective length factor 1.00

Bottom:

Bottom flange laterally unrestrained — Effective length factor 1.00

LOADS ACTING ON BEAM :

*** NOTE: Beam subjected to additional point load(s) - see details below

Occupancy imposed loads	0.0 kN/m²	Ceilings, services and finishes	0.0 kN/m²
Partition loads	0.0 kN/m²	Construction load	0.0 kN/m²
Natural frequency limit	4.0 Hz	In-situ concrete	NONE

BS 6399 imposed load reduction is NOT considered

Proportion of imposed load considered as permanent for serviceability calculations = 0.33

TRANSVERSE BEAM DETAILS :

None

ADDITIONAL POINT LOADS :

Load No.	Location (m) - from LHS	Magnitude (kN)	Type
1	0.6	92.0	Dead
2	0.9	92.0	Dead

ADDITIONAL DISTRIBUTED LOADS :

None

END FORCES AND MOMENTS :

None

LOAD COMBINATIONS :

NOTE: MD = Minimum dead load

No.	Dead	Super dead	Live
ULTIMATE			
1	1.0	1.0	1.0
2	0.0	0.0	0.0
3	0.0	0.0	0.0
4	0.0	0.0	0.0
FIRE			
5	0.0	0.0	0.0
SERVICEABILITY			
6	1.0	1.0	1.0
7	0.0	0.0	0.0

NORMAL STAGE - ULTIMATE LIMIT STATE CHECKS - FULL OUTPUT

FLOOR LOADS : (unfactored)

Dead :

Self weight of beam = 37.7 * 9.81 / 1.0 / 1000
= 0.37 kN/m²

Additional point loading (1) = 92.00 kN (at 0.6 m from left support)

Additional point loading (2) = 92.00 kN (at 0.9 m from left support)

Live :

Occupancy load = 0.00 kN/m²

Partitions = 0.00 kN/m²

Total imposed load = 0.00 kN/m² (*** no BS6399 imposed load reduction)

Super-imposed dead :

Ceilings and services = 0.00 kN/m²

Screeds = 0.00 kN/m²

Westok

Load Combination No: 1
BS 5950 : 2000

The Steel Construction Institute

NS: LTB CHECK :
*****NOTE: Lateral torsional buckling check is performed using the 'm' factor approach, as in BS 5950 : Part 1 : 2000, modified for the varying levels of stresses at different sections.**

Top Flange:

Effective length	= 1.00 * 1.50
	= 1.50 m
Maximum applied moment	= 55.30 kNm
Buckling moment m.Mmax	= 0.88 * 55.30
	= 48.39 kNm
Buckling resistance	= 190.67 kNm
UNITY FACTOR	= 48.39 / 190.67
	= 0.25

PASS

Bottom Flange:

Effective length	= 1.00 * 1.50
	= 1.50 m
Maximum applied moment	= 55.30 kNm
Buckling moment m.Mmax	= 0.00 * 55.30
	= 0.00 kNm
Buckling Capacity	= 190.67 kNm
UNITY FACTOR	= 0.00 / 190.67
	= 0.00

PASS

NS: SECTION SHEAR CHECK :

		TOTAL (kN)		TOP (kN)		BTM (kN)			
No.	Dist.(m)	Applied	Resistance	Applied	Resistance	Applied	Resistance	Unity Factor	Remarks
LHS		92.3	387.7	-	-	-	-	0.24	
1	0.30	92.2	93.8	46.1	46.9	46.1	46.9	0.98	
2	0.75	0.0	387.7	0.0	193.9	0.0	193.9	0.00	
3	1.20	92.2	93.8	46.1	46.9	46.1	46.9	0.98	
RHS		92.3	387.7	-	-	-	-	0.24	

NS: INTERACTION OF AXIAL LOAD, VERTICAL SHEAR & BENDING MOMENT :
Maximum moment =55.3 kNm at 0.75 m from LHS (nearest cell position)

			SHEAR (kN)		Effective	AXIAL (kN)			
No.	Dist.(m)		Applied	Resistance	Web Thk.(mm)	Applied	Resistance	Unity Factor	Remarks
LHS			92.3	387.7	6.0	0.0	1797.7	0.00	
1	0.30	TOP	46.1	46.9	0.4	95.5	613.4	0.16	
		BTM	46.1	46.9	0.4	-95.5	613.4	0.16	
2	0.75	TOP	0.0	193.9	6.0	190.8	666.0	0.29	
		BTM	0.0	193.9	6.0	-190.8	666.0	0.29	
3	1.20	TOP	46.1	46.9	0.4	95.5	613.4	0.16	
		BTM	46.1	46.9	0.4	-95.5	613.4	0.16	
RHS			92.3	387.7	6.0	0.0	1797.7	0.00	

NS: HORIZONTAL SHEAR CAPACITY (& WEB-POST BENDING CAPACITY) CHECK :

NOTE: The interaction between the horizontal shear in the web post and the co-existent moment is checked by limiting the applied moment to the elastic moment capacity and applying a reduction of 10% to the shear area

Web Post	Appl. Moment (kNm)	Moment Cap. (kNm)	Appl. shear (kN)	Shear Cap. (kN)	Unity Factor	Remarks
1 / 2	0.0	39.8	95.4	385.3	0.25	
2 / 3	0.0	39.8	95.4	385.3	0.25	

Load Combination No: 1
BS 5950 : 2000

The Steel Construction Institute

NS: WEB POST FLEXURE AND BUCKLING CHECK :

NOTE: Web compression buckling should be checked separately at all point load positions

Web Post	Buck. Force (kN)	Buck. Cap. (kN)	Unity Factor	Remarks
1 / 2	95.4	469.3	0.20	
2 / 3	95.4	469.3	0.20	

NS: VIERENDEEL BENDING CAPACITY CHECK :

No.	Dist. (m)		Critical Angle (°)	Shear (kN) Appl./Cap.	Axial (kN) Appl. / Cap.	Moment (kNm) Appl./Cap.	Eff. Web Thk. (mm)	Unity Factor	Remarks
1	0.30	TOP	20.0	47.8/59.3	73.9/695.5	2.6 / 2.9	3.8	0.98	
		BTM	20.0	47.8/59.3	73.9/695.5	2.6 / 2.9	3.8	0.98	
3	1.20	TOP	20.0	47.8/59.3	73.9/695.5	2.6 / 2.9	3.8	0.98	
		BTM	20.0	47.8/59.3	73.9/695.5	2.6 / 2.9	3.8	0.98	

Load Combination No: 6
BS 5950 : 2000

The Steel Construction Institute

SERVICEABILITY LIMIT STATE CHECKS - FULL OUTPUT

DEFLECTIONS :

	Inertia (cm4)	Maximum Deflection (mm)	Due to openings (mm)
Dead loads (on steel section)	7894	0.6	1.1
Imposed loads (on steel section)	7894	0.0	0.0
Super-dead (on steel section)	7894	0.0	0.0
Totals		**0.6**	**1.1**

Maximum deflection (total) = 0.59 + 1.08
= 1.67 mm

Maximum deflection (imposed) = 0.00 + 0.00
= 0.00 mm **(< SPAN / 500 i.e 3.0 mm)** **SATISFACTORY**

DYNAMIC SENSITIVITY :

*** NOTE: loads are dead + super-imposed dead + 10% imposed
Inertia (steel section) = 7894 cm4 (steel section)
Maximum deflection = 1.67 mm
Frequency = 18 / sqr(1.67)
= 13.9 Hz **(greater than 4.0 Hz)** **SATISFACTORY**

STRESS CHECKS

CONSTRUCTION STAGE : (stresses due to self weight)

Critical cell: Number 2 (at mid-span)
Applied moment = 55.30 kNm (steel section)
Elastic neutral axis is in WEB (151.7mm from beam top flange)
Moment of inertia (steel section) = 8503 cm4
Steel modulus (top) = 560 cm^3
Stress (+ve indicates compression) = 55.3/560.5 * 1000
= 98.7 N/mm^2

Steel modulus (btm) = 560 cm^3
Stress (-ve indicates tension) = -55.3/560.5 * 1000
= -98.7 N/mm^2

NORMAL STAGE :
Applied moment (major axis) = 0.00 kNm
Elastic neutral axis is in WEB (151.7 mm from top of beam)
Moment of inertia (steel section) = 8503 cm4
Steel:
Modulus - top = 560 cm^3
Stress (+ve indicates compression) = 0.0/560.5 * 1000
= 0.00 N/mm^2

Modulus - btm = 560 cm^3
Stress (-ve indicates tension) = 0.0/560.5 * 1000
= 0.0 N/mm^2

STEEL STRESS CHECK : (total stresses)
Top of beam (+ve indicates compression) = 98.67 + 0.00
= 98.67 N/mm^2

UNITY FACTOR = 98.67 / 355.0
= 0.280 **PASS**

Bottom of beam (-ve indicates tension) = -98.67 + 0.00
= -98.67 N/mm^2

UNITY FACTOR = 98.67 / 355.0
= 0.280 **PASS**

Westok

Load Combination No: 6
BS 5950 : 2000

The Steel Construction Institute

BEAM DETAILS AND DIMENSIONS

General:		**Top Tee:**	[NON STANDARD SECTION]	**Bottom Tee:**	[NON STANDARD SECTION]
Beam type:	PRISMATIC	Depth (mm):	151.7	Depth (mm):	151.7
Construction type:	NON-COMPOSITE	Flange thickness (mm):	10.2	Flange thickness (mm):	10.2
Beam span (m):	1.50	Flange width (mm):	165	Flange width (mm):	165
Beam mass (kg/m):	37.68	Web thickness (mm):	6	Web thickness (mm):	6
Cell Data:					
Cell diameter (mm):	230.0	Dist. to 1st Cell (mm):	300.0		
Cell spacing (mm):	450.0	Dist. to last cell (mm):	300.0		

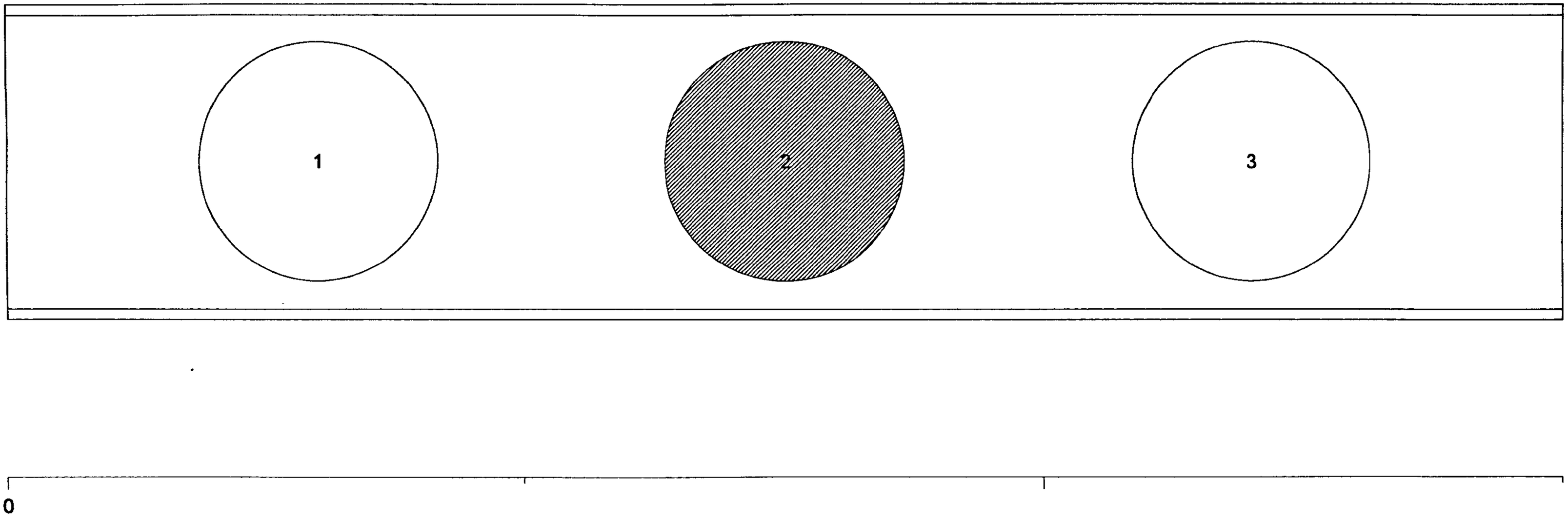

APPENDIX 8

STRESS DISTRIBUTION – NODAL PATH STRESSES

1 Stress distribution in the web at two loading points

In **Figure 1** horizontal 'σ_x', vertical 'σ_y', plane shear 'σ_{xy}', principal 1 'σ_1', principal 2 'σ_2', principal 3 'σ_3', and Von-Mises 'σ_v' stresses generated in the vicinity of the openings are presented in order for both linear elastic (left) and ultimate (i.e. 'failure') (right) loading points.

It is worth noting that in normal stresses σ_x, σ_y and σ_{xy} the stressed areas in the vicinity of the web openings are bigger at 'failure' point compare to those at the linear elastic point. Inversely, principal and Von-Mises stresses present a wider stressed area at the linear elastic point, but a higher stress concentration is found at the 'failure' point due to stress mobilization and load redistribution.

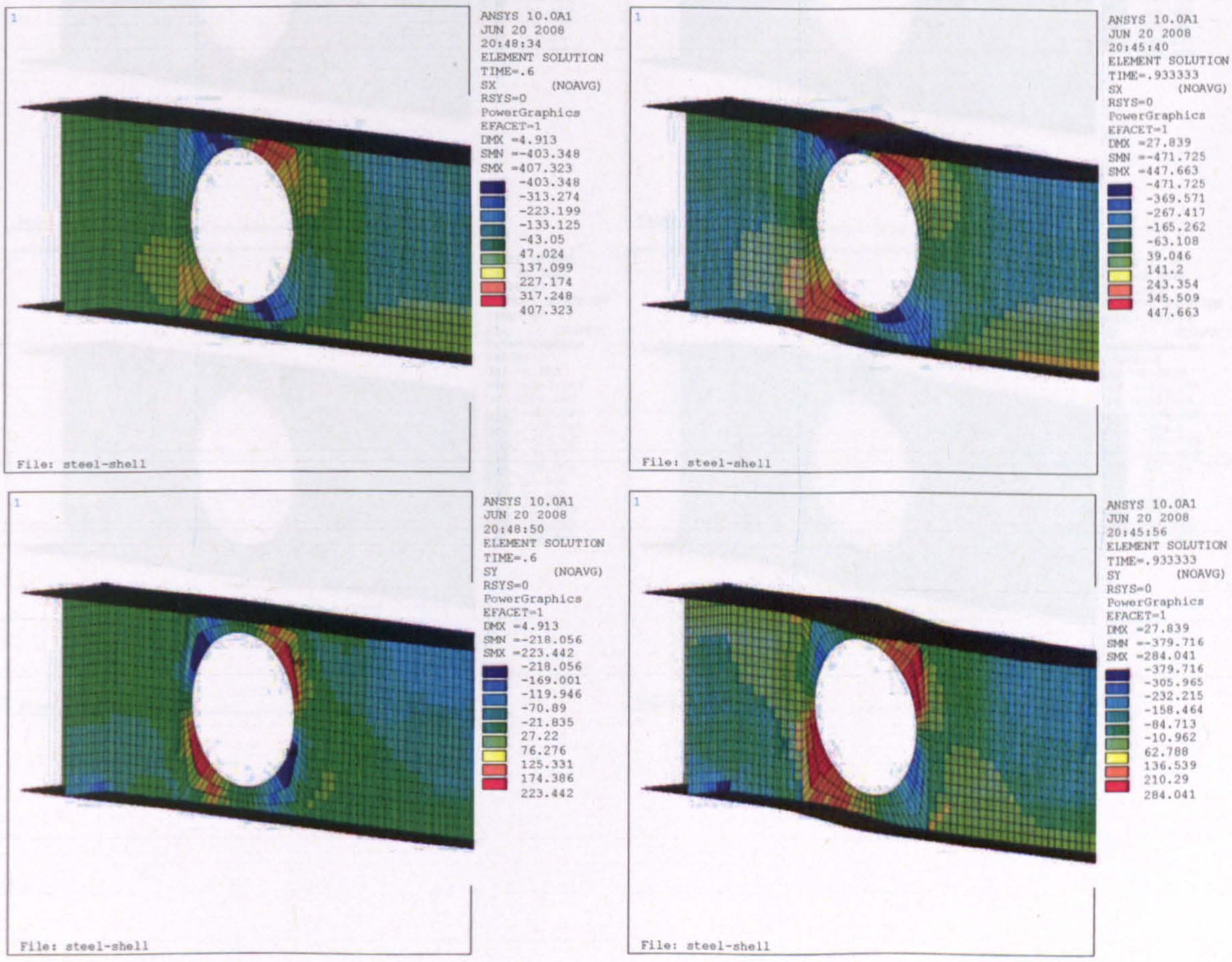

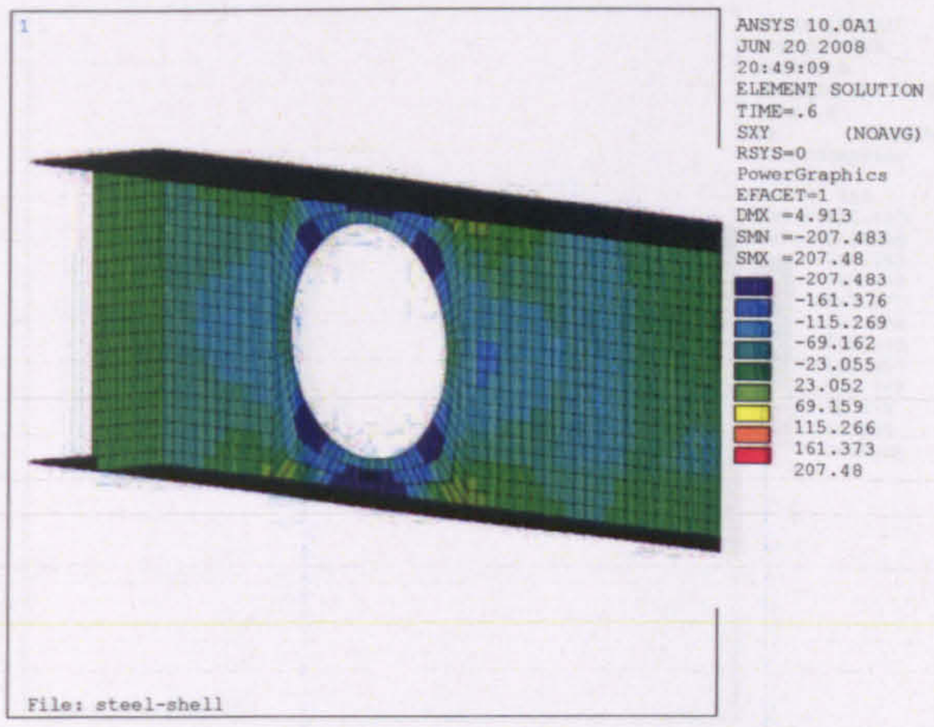
1
ANSYS 10.0A1
JUN 20 2008
20:49:09
ELEMENT SOLUTION
TIME=.6
SXY (NOAVG)
RSYS=0
PowerGraphics
EFACET=1
DMX =4.913
SMN =-207.483
SMX =207.48
-207.483
-161.376
-115.269
-69.162
-23.055
23.052
69.159
115.266
161.373
207.48
File: steel-shell

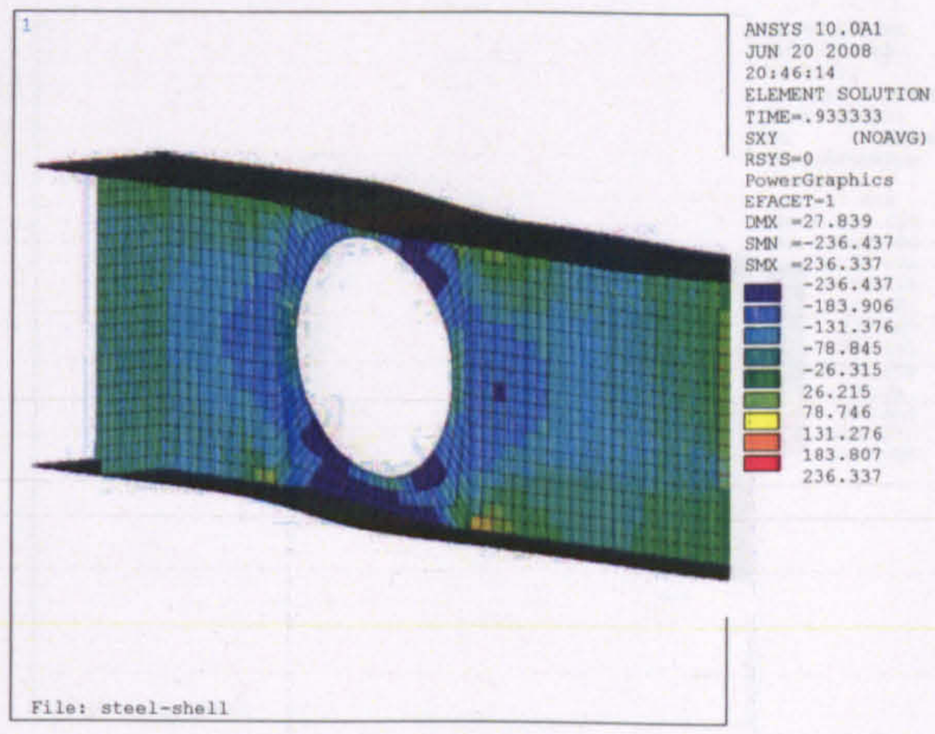
1
ANSYS 10.0A1
JUN 20 2008
20:46:14
ELEMENT SOLUTION
TIME=.933333
SXY (NOAVG)
RSYS=0
PowerGraphics
EFACET=1
DMX =27.839
SMN =-236.437
SMX =236.337
-236.437
-183.906
-131.376
-78.845
-26.315
26.215
78.746
131.276
183.807
236.337
File: steel-shell

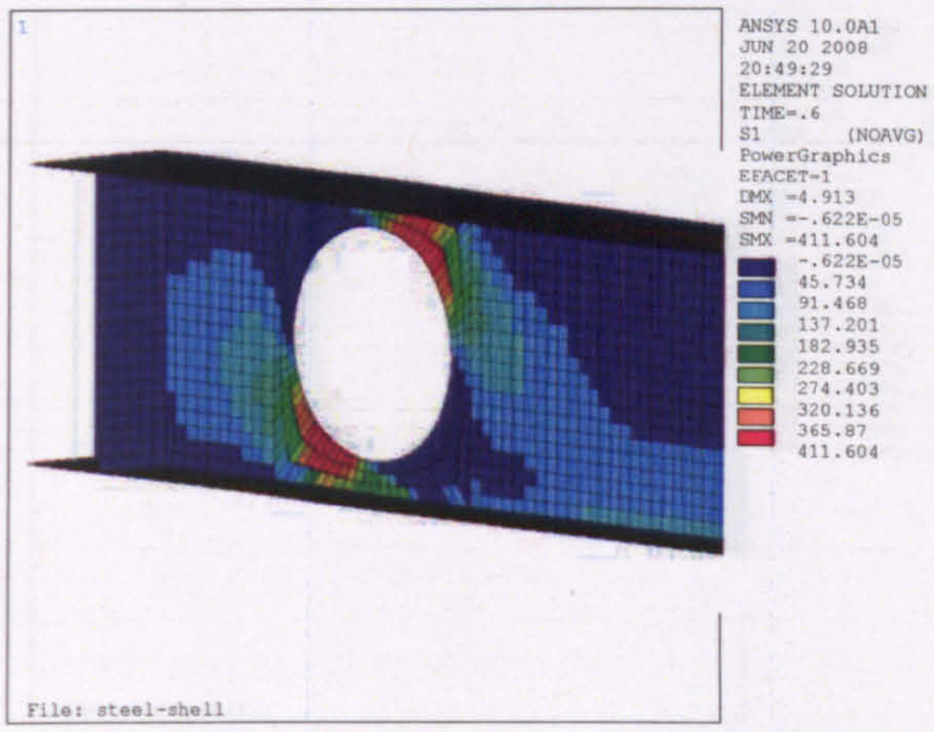
1
ANSYS 10.0A1
JUN 20 2008
20:49:29
ELEMENT SOLUTION
TIME=.6
S1 (NOAVG)
PowerGraphics
EFACET=1
DMX =4.913
SMN =-.622E-05
SMX =411.604
-.622E-05
45.734
91.468
137.201
182.935
228.669
274.403
320.136
365.87
411.604
File: steel-shell

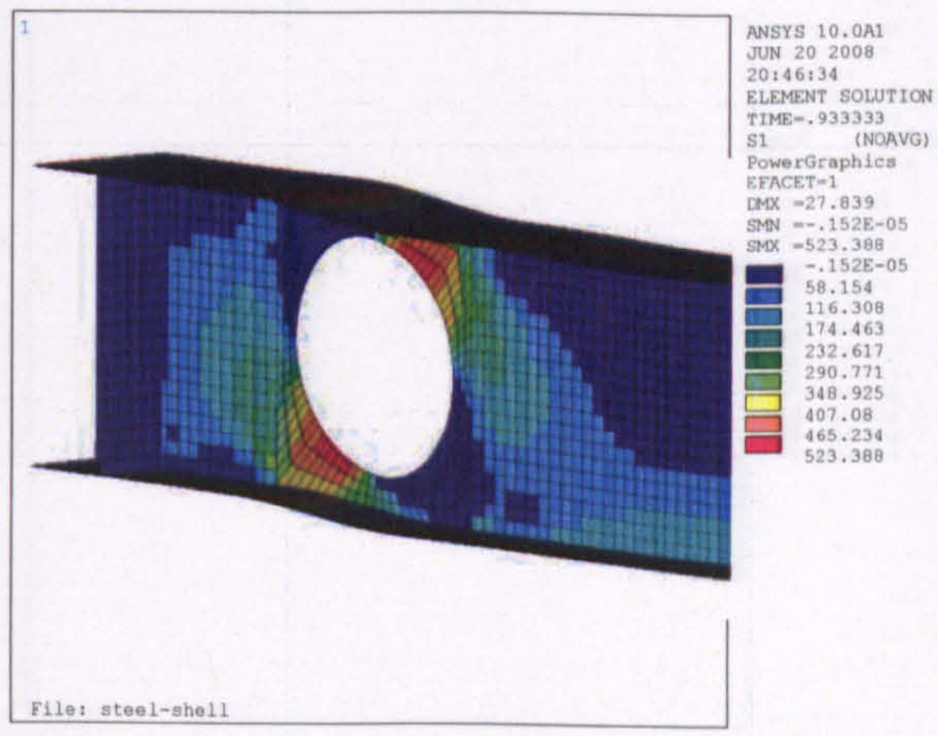
1
ANSYS 10.0A1
JUN 20 2008
20:46:34
ELEMENT SOLUTION
TIME=.933333
S1 (NOAVG)
PowerGraphics
EFACET=1
DMX =27.839
SMN =-.152E-05
SMX =523.388
-.152E-05
58.154
116.308
174.463
232.617
290.771
348.925
407.08
465.234
523.388
File: steel-shell

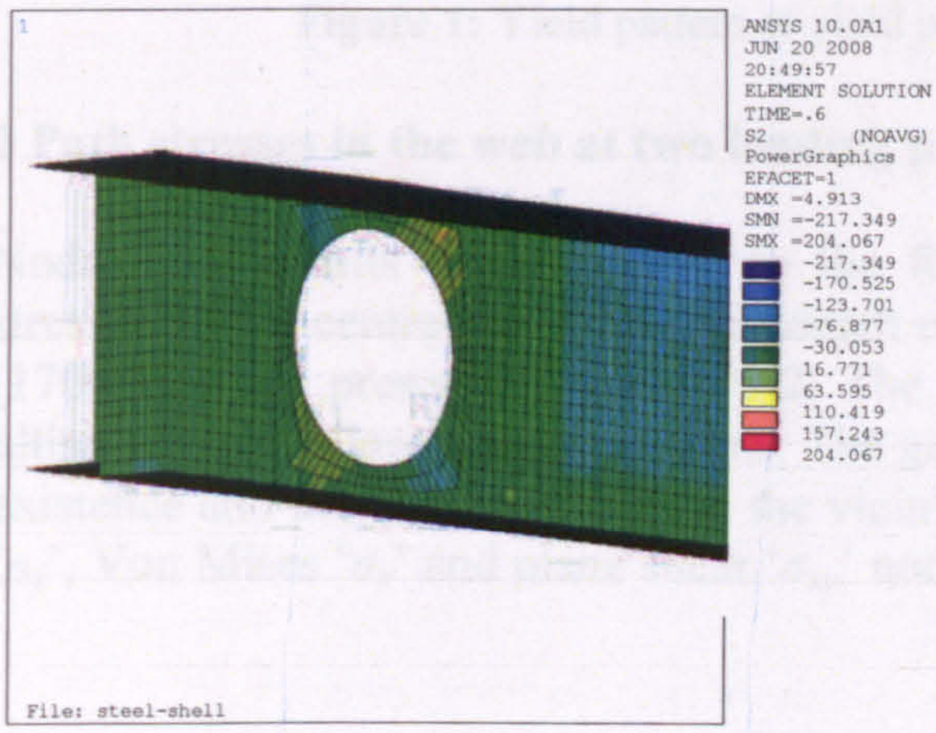
1
ANSYS 10.0A1
JUN 20 2008
20:49:57
ELEMENT SOLUTION
TIME=.6
S2 (NOAVG)
PowerGraphics
EFACET=1
DMX =4.913
SMN =-217.349
SMX =204.067
-217.349
-170.525
-123.701
-76.877
-30.053
16.771
63.595
110.419
157.243
204.067
File: steel-shell

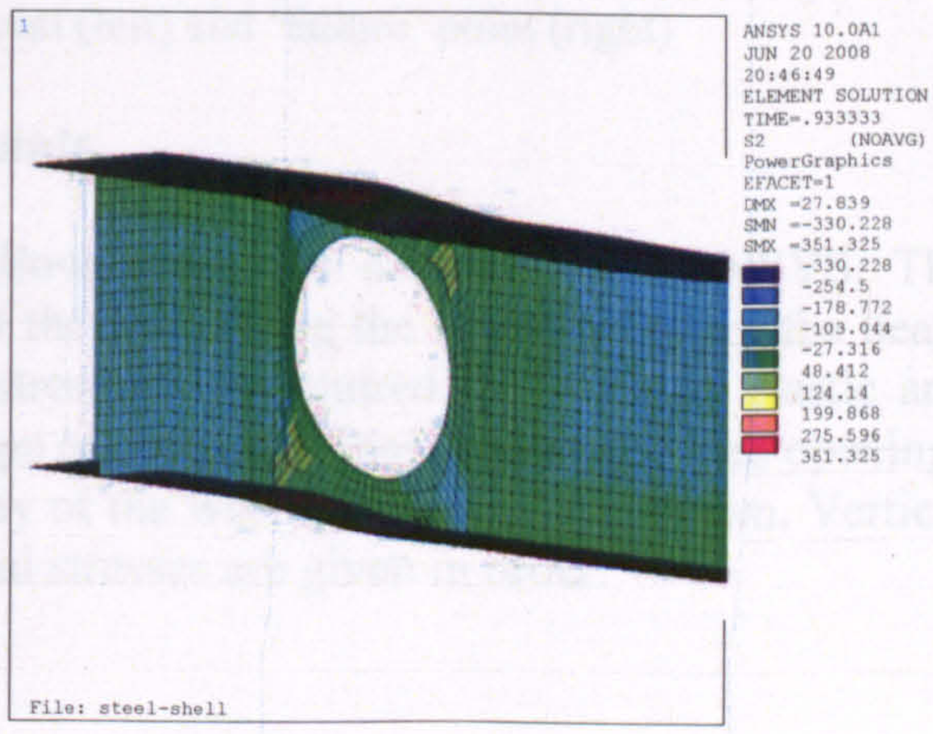
1
ANSYS 10.0A1
JUN 20 2008
20:46:49
ELEMENT SOLUTION
TIME=.933333
S2 (NOAVG)
PowerGraphics
EFACET=1
DMX =27.839
SMN =-330.228
SMX =351.325
-330.228
-254.5
-178.772
-103.044
-27.316
48.412
124.14
199.868
275.596
351.325
File: steel-shell

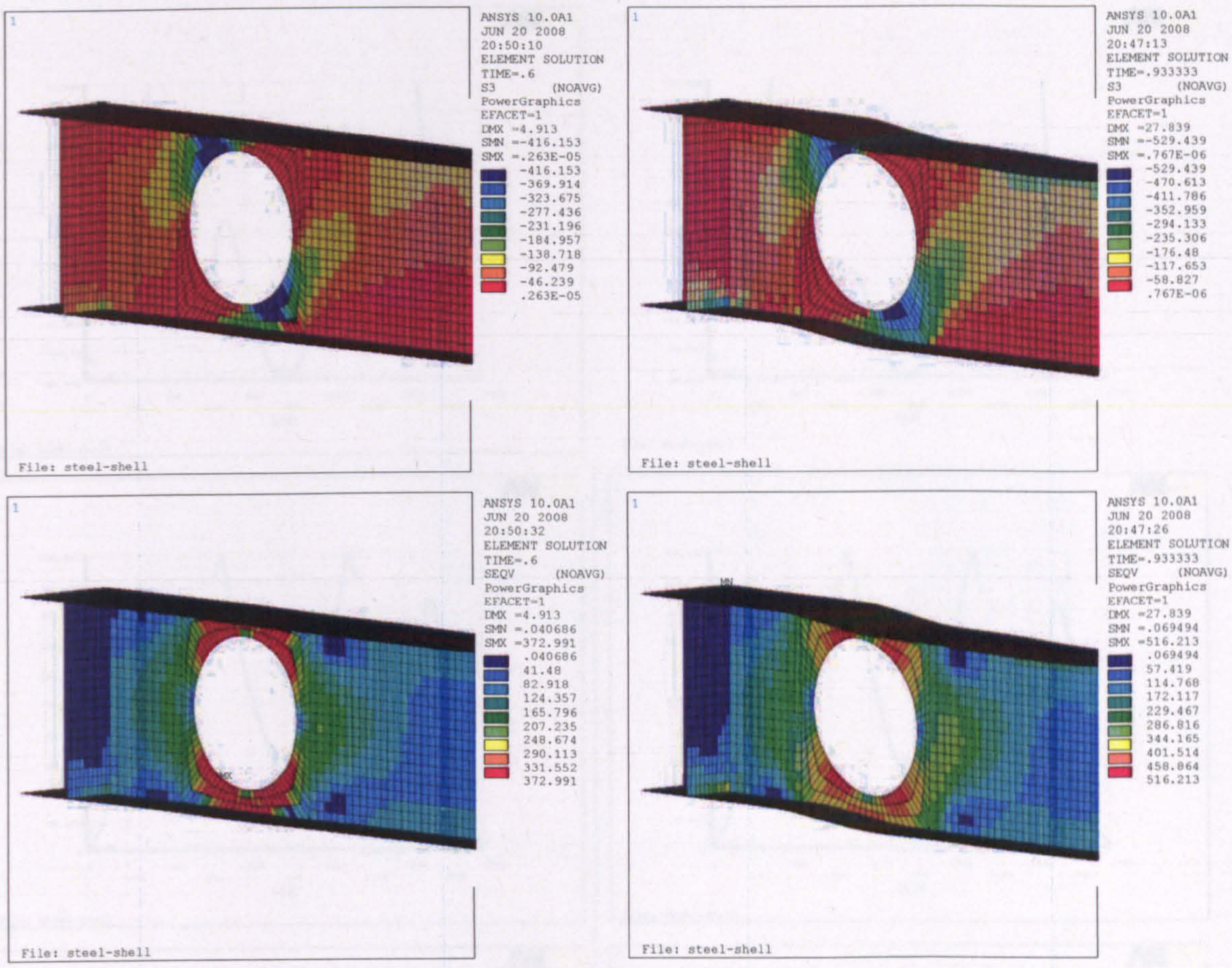

Figure 1: Yield pattern at yield point (left) and 'failure' point (right)

2 Path stresses in the web at two loading points

Nodal path results are presented in the following figures directly from ANSYS. The stresses on the centre-line at the mid-depth of the web, along the whole length of the beam (1700mm), are presented in **Figure 2**. The stresses are acquired at the linear elastic and ultimate (i.e. 'failure') loading points. The gaps of the stress lines present the web openings existence and the stress intensity in the vicinity of the web openings is also shown. Vertical 'σ_y', Von Mises 'σ_v' and plane shear 'σ_{xy}' nodal stresses are given in order.

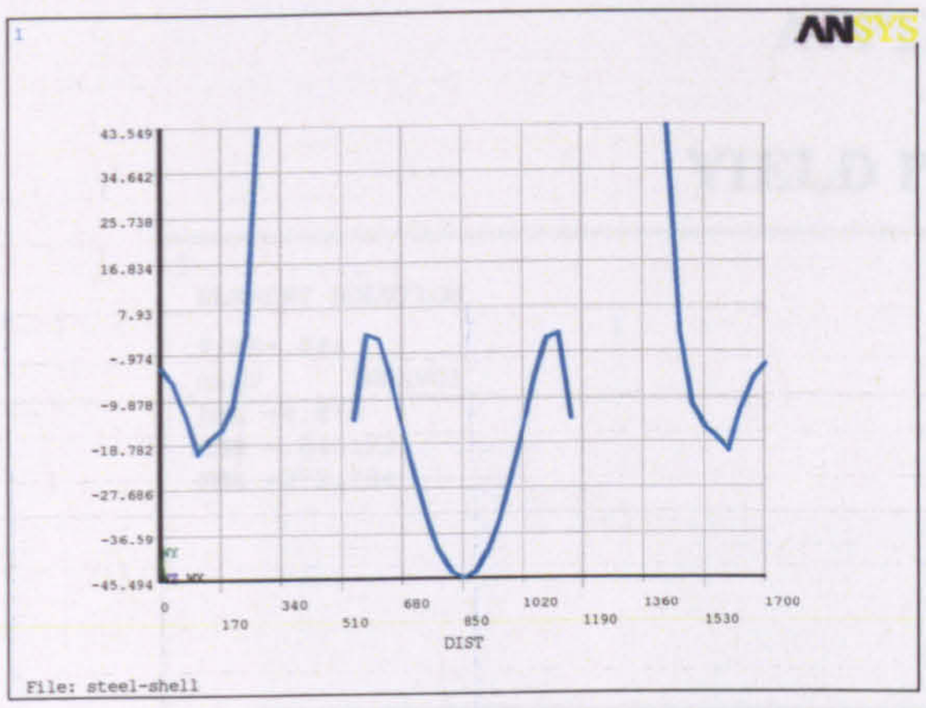

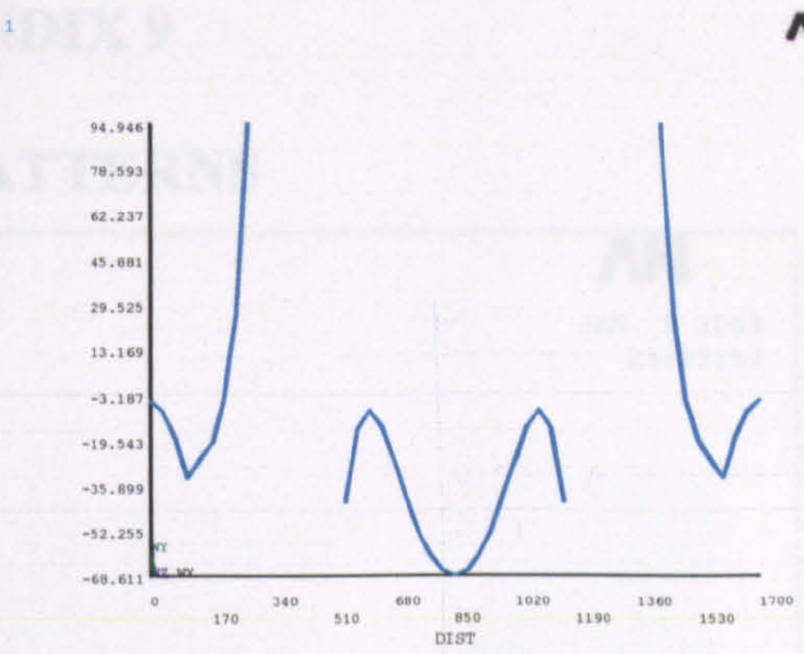

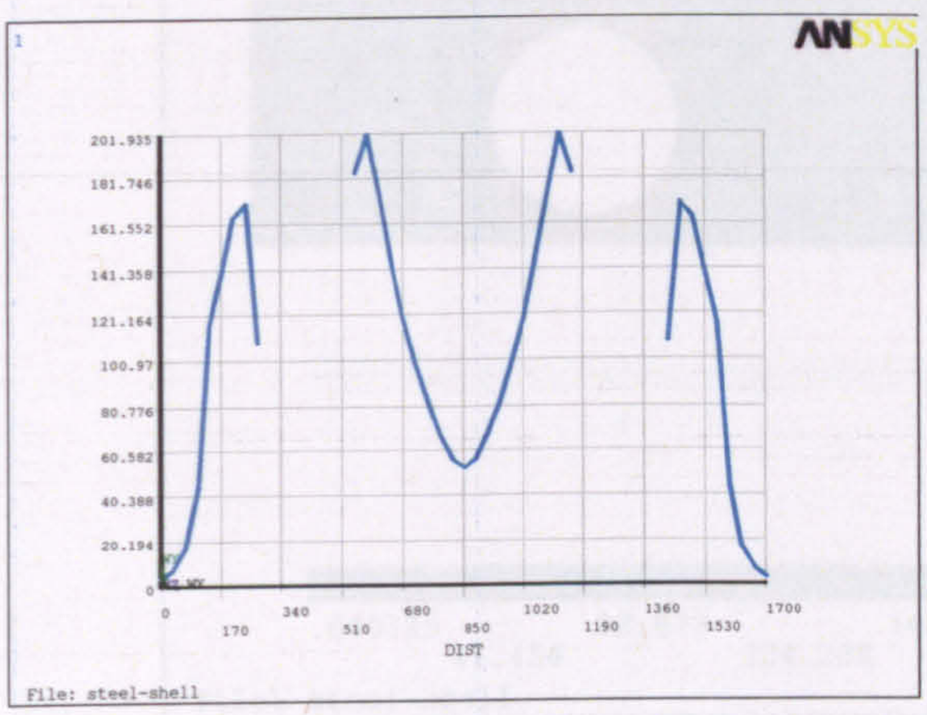

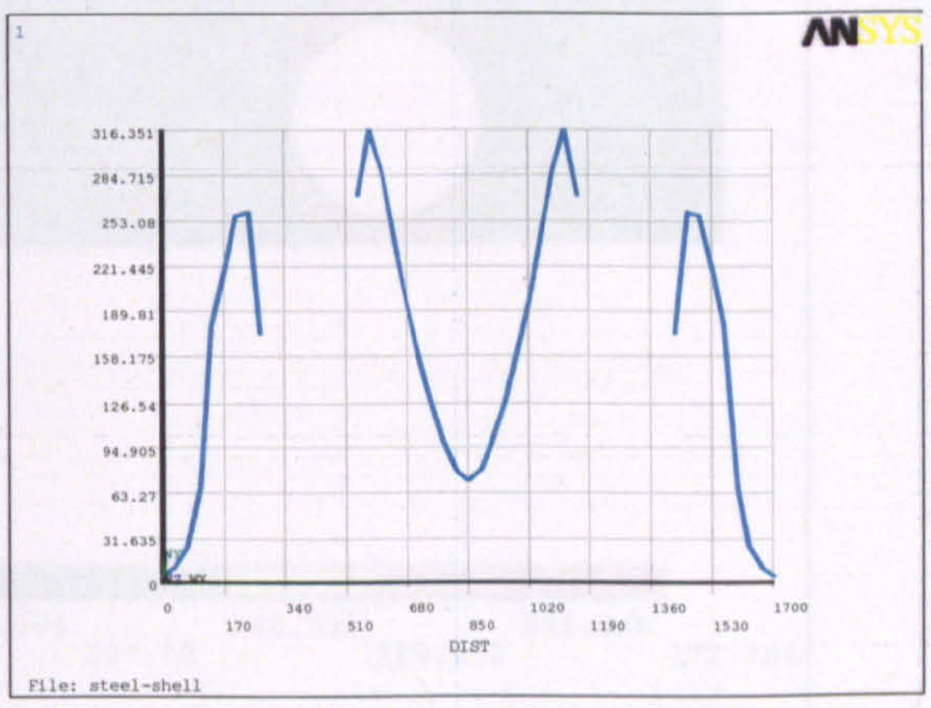

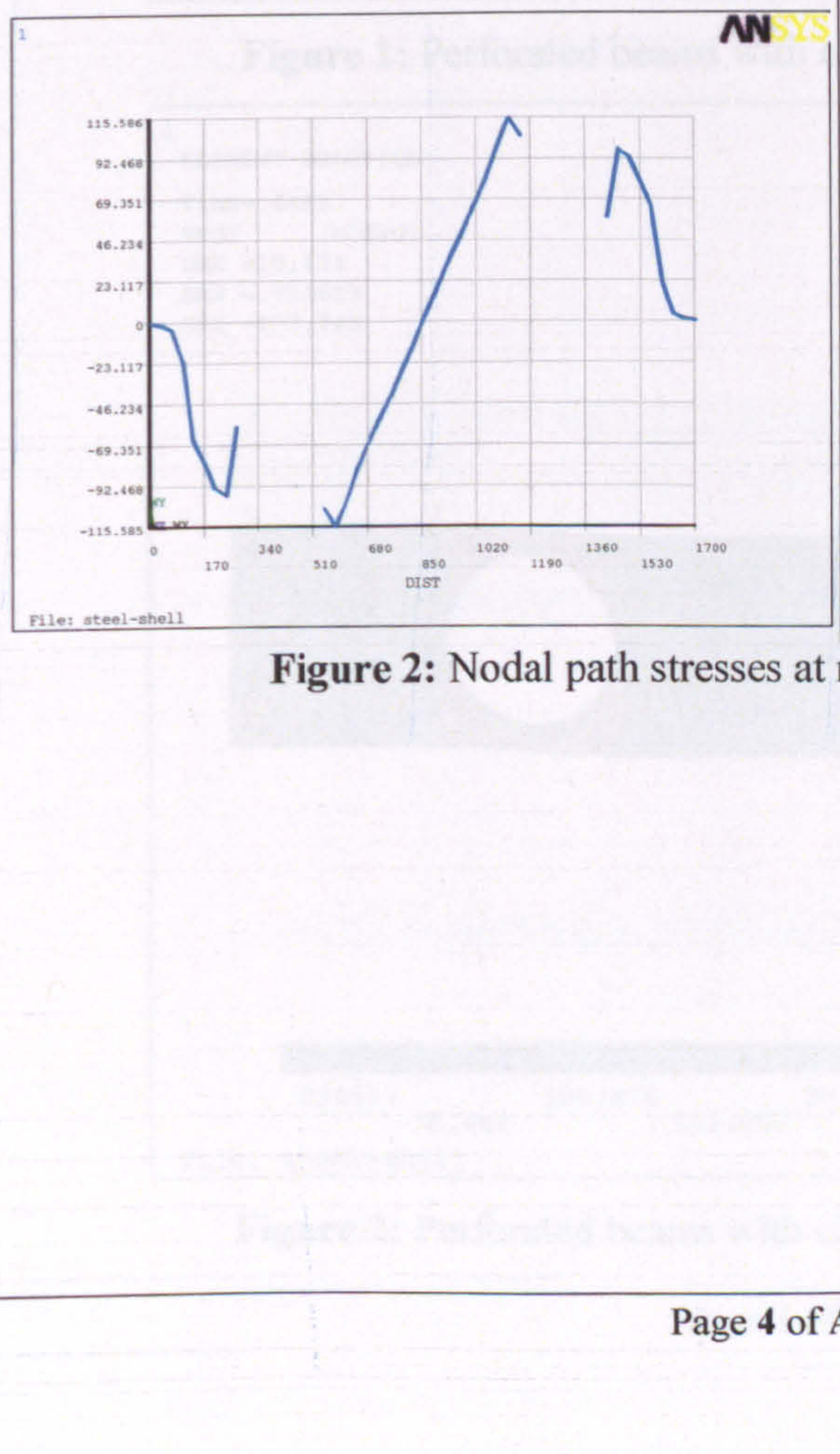

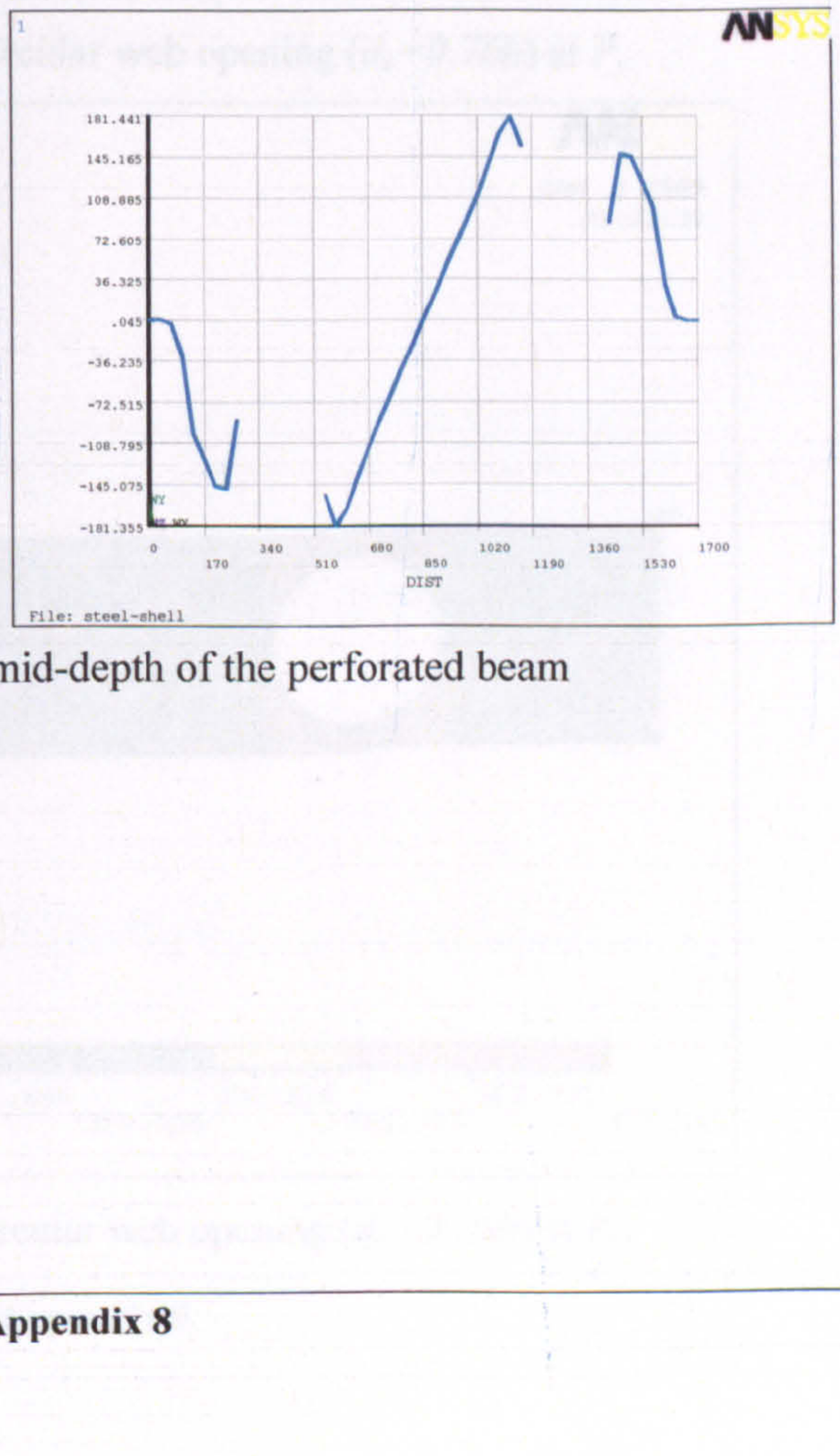

Figure 2: Nodal path stresses at mid-depth of the perforated beam

APPENDIX 9

YIELD PATTERNS

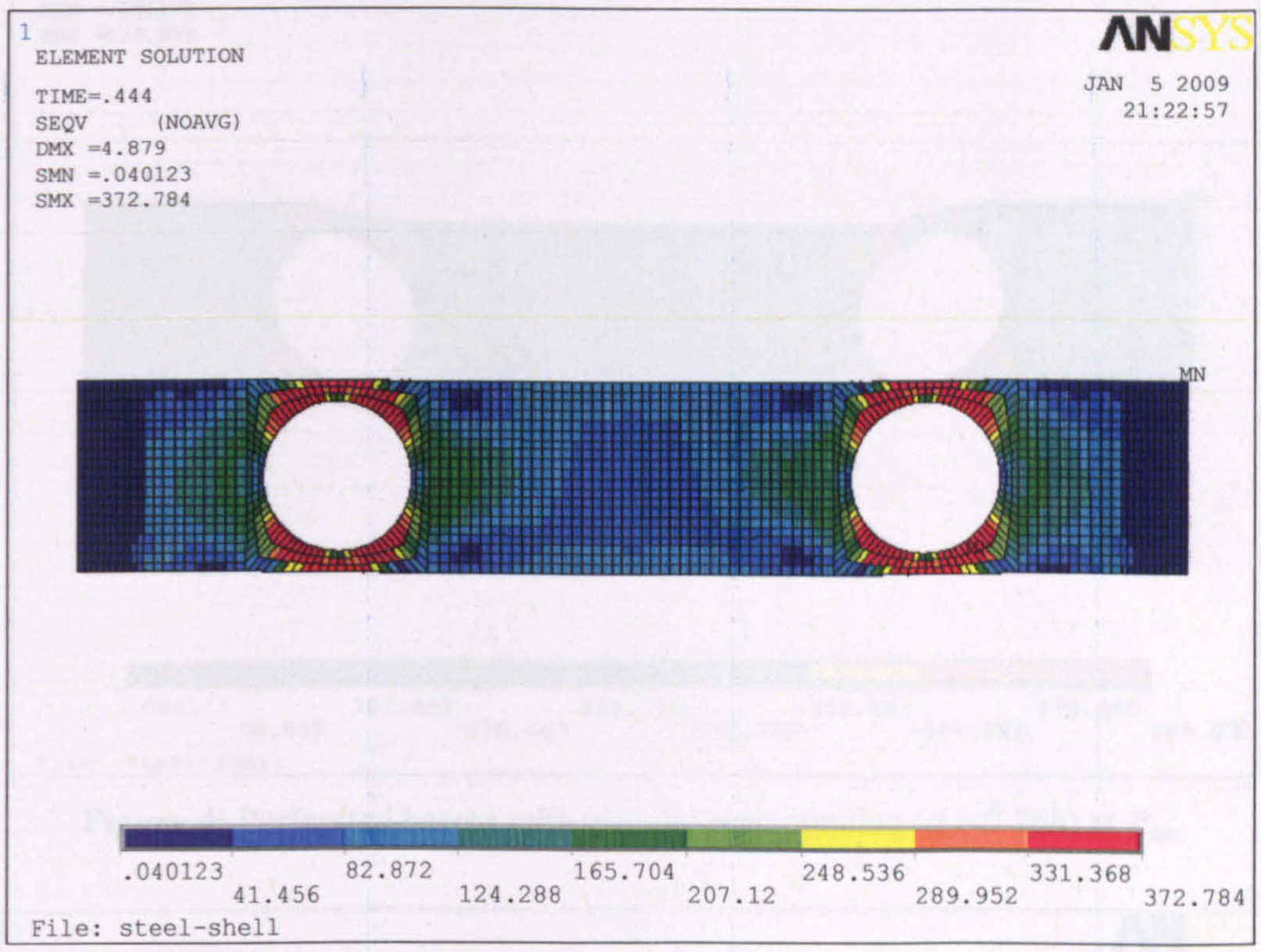

Figure 1: Perforated beams with circular web opening (d_o=*0.76h*) at P_y

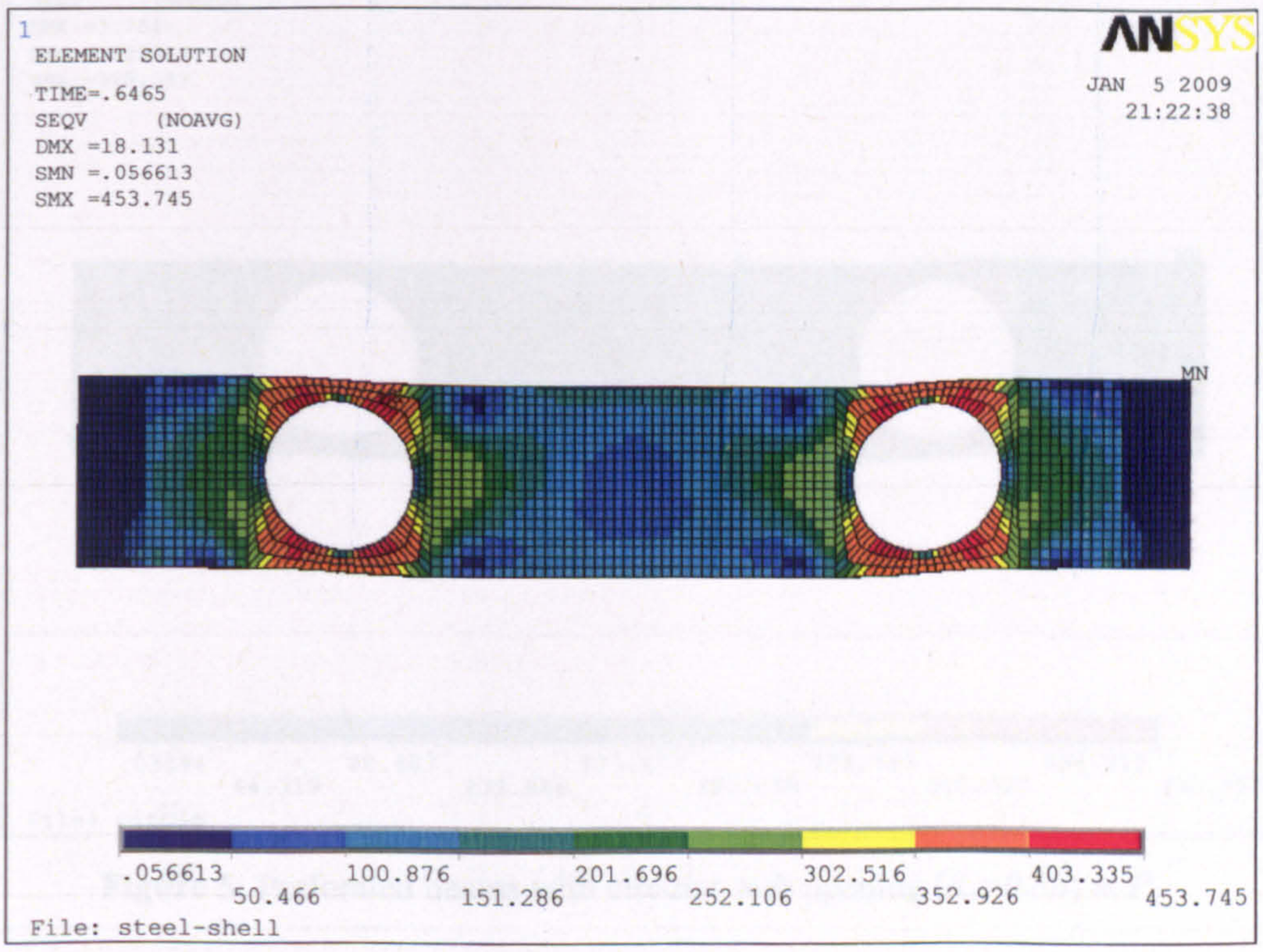

Figure 2: Perforated beams with circular web opening (d_o=*0.76h*) at $P_{cr.}$

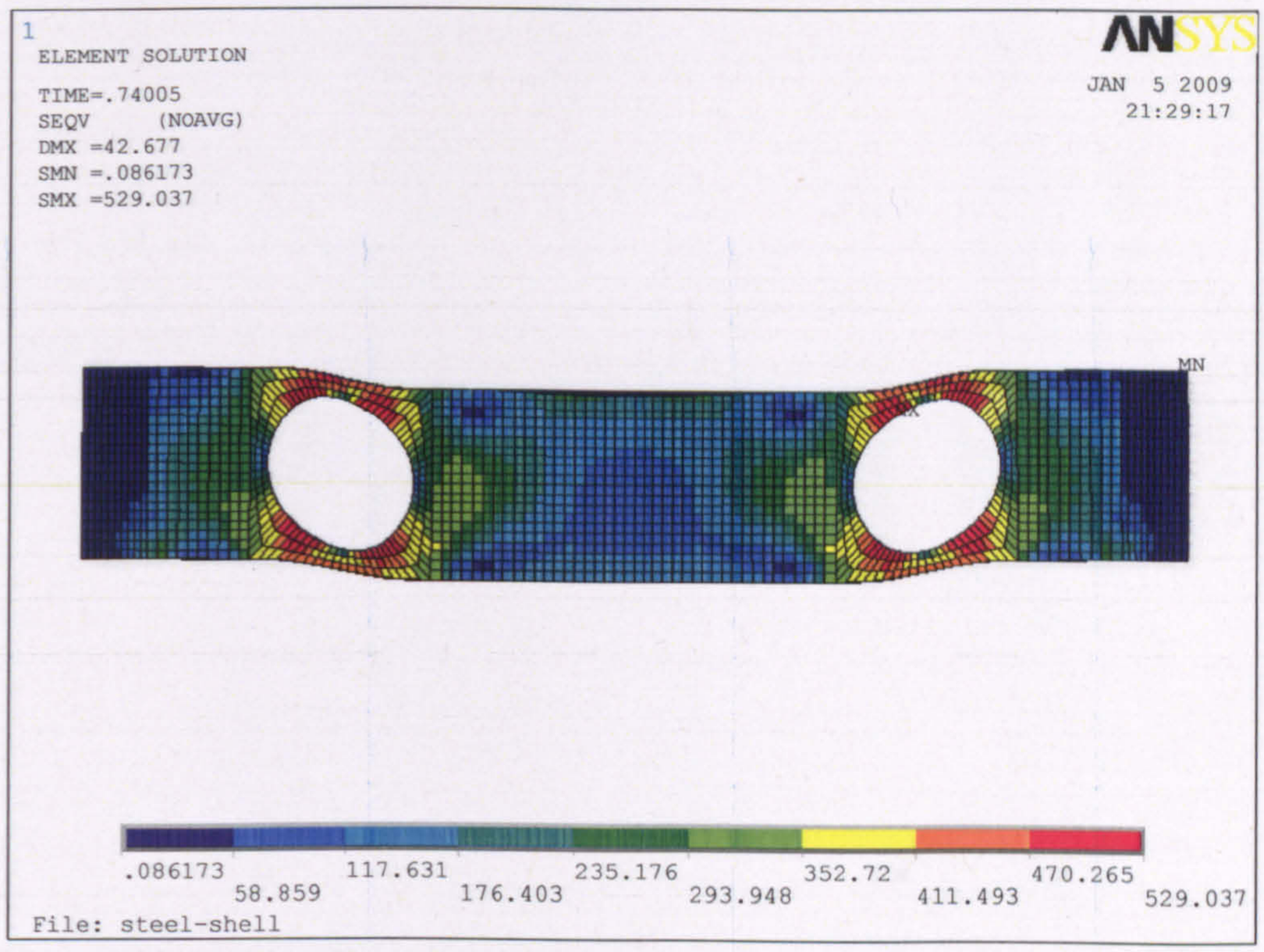

Figure 4: Perforated beams with circular web opening (d_o=*0.76h*) at $P_{ult.}$

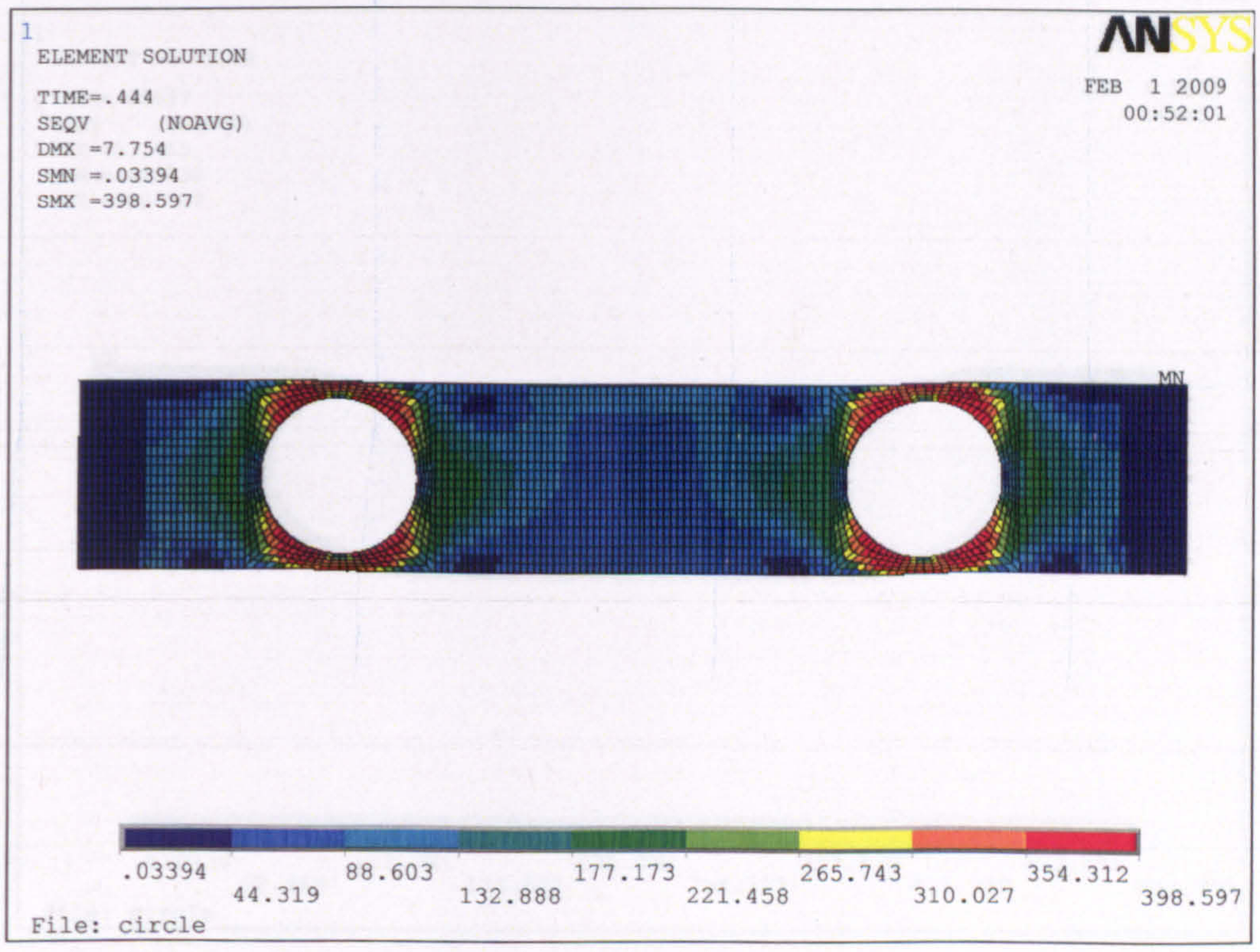

Figure 5: Perforated beams with circular web opening (d_o=*0.8h*) at P_y

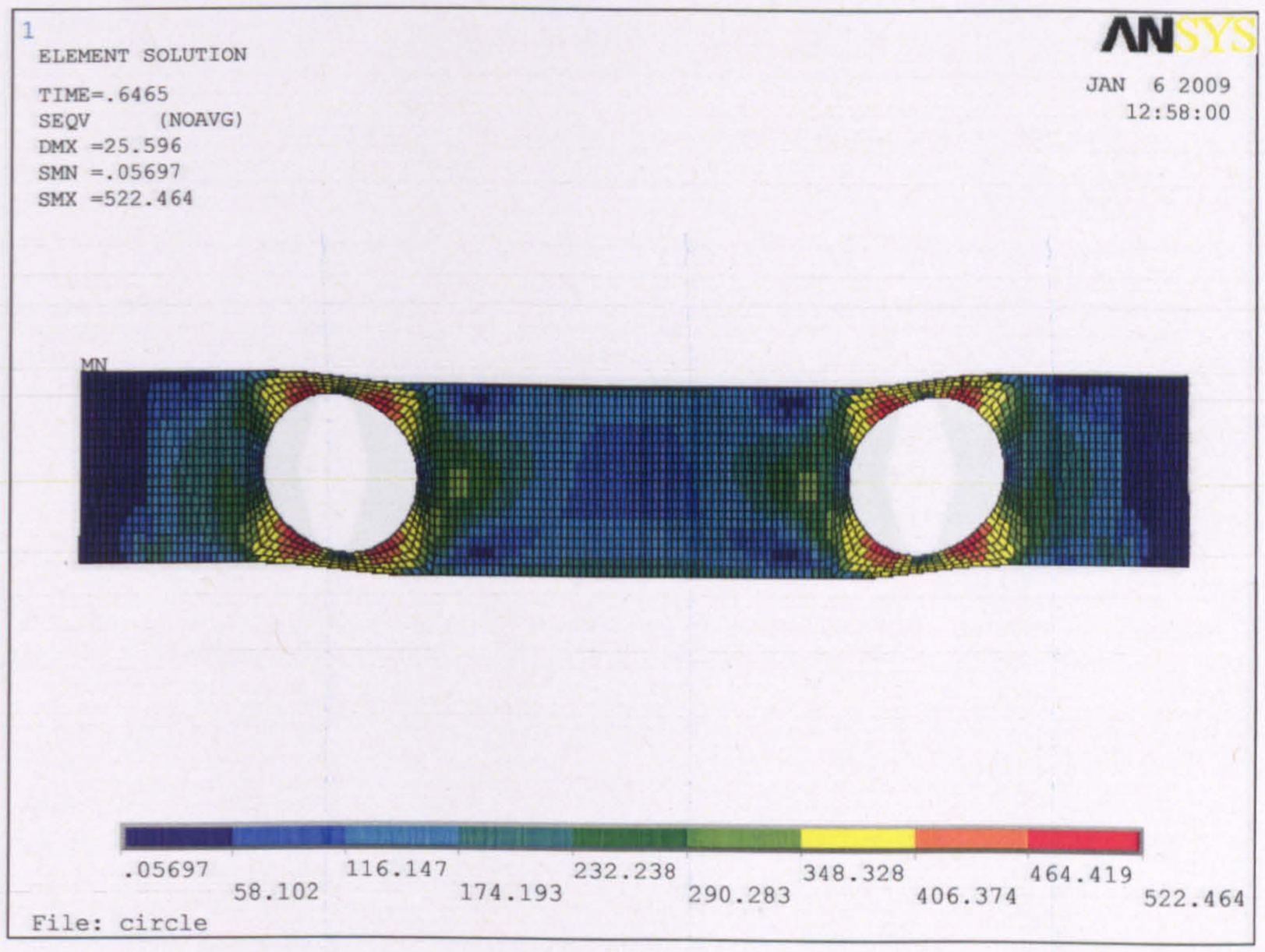

Figure 6: Perforated beams with circular web opening (d_o=*0.8h*) at $P_{cr.}$

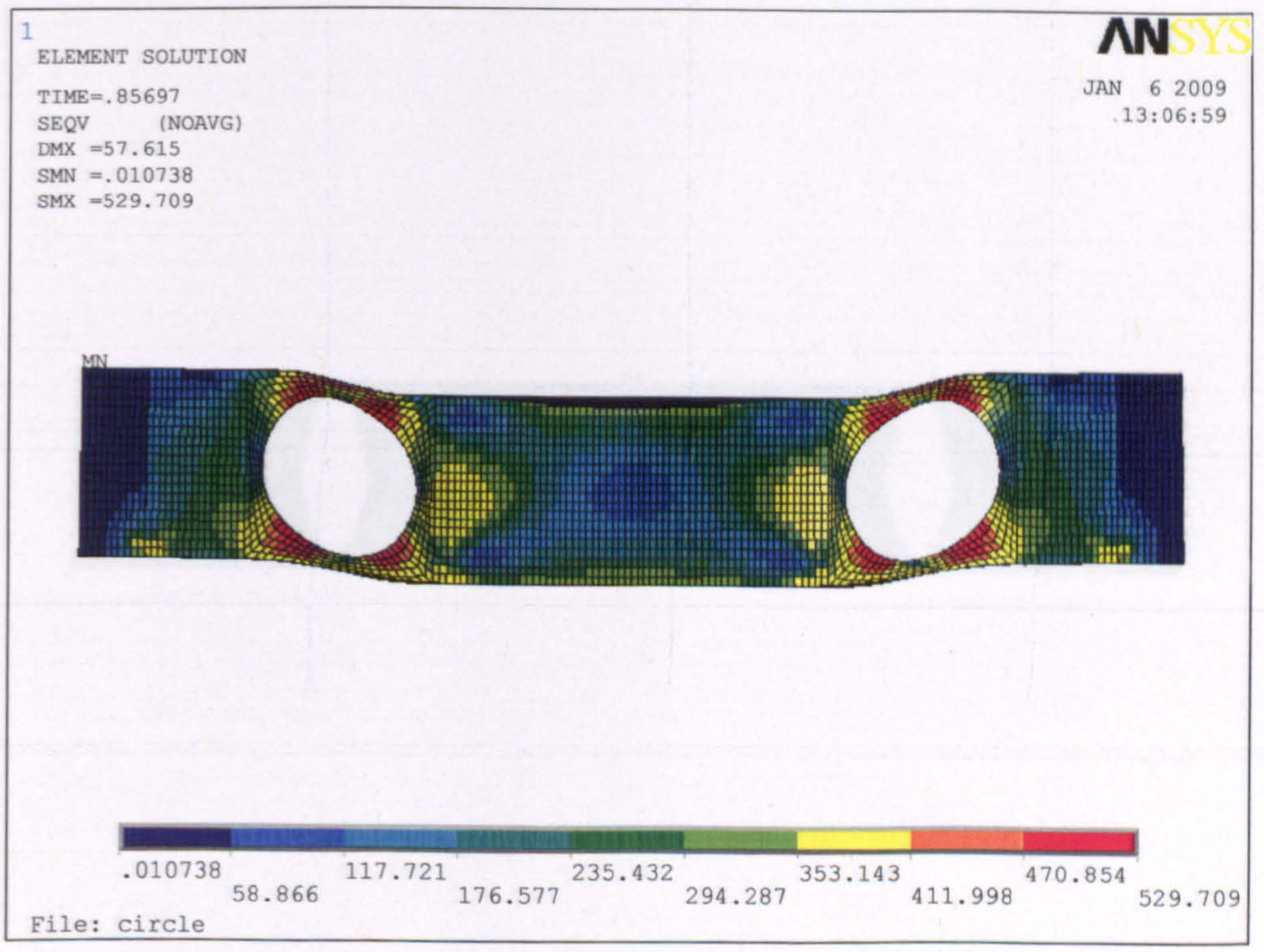

Figure 7: Perforated beams with circular web opening (d_o=*0.8h*) at $P_{ult.}$

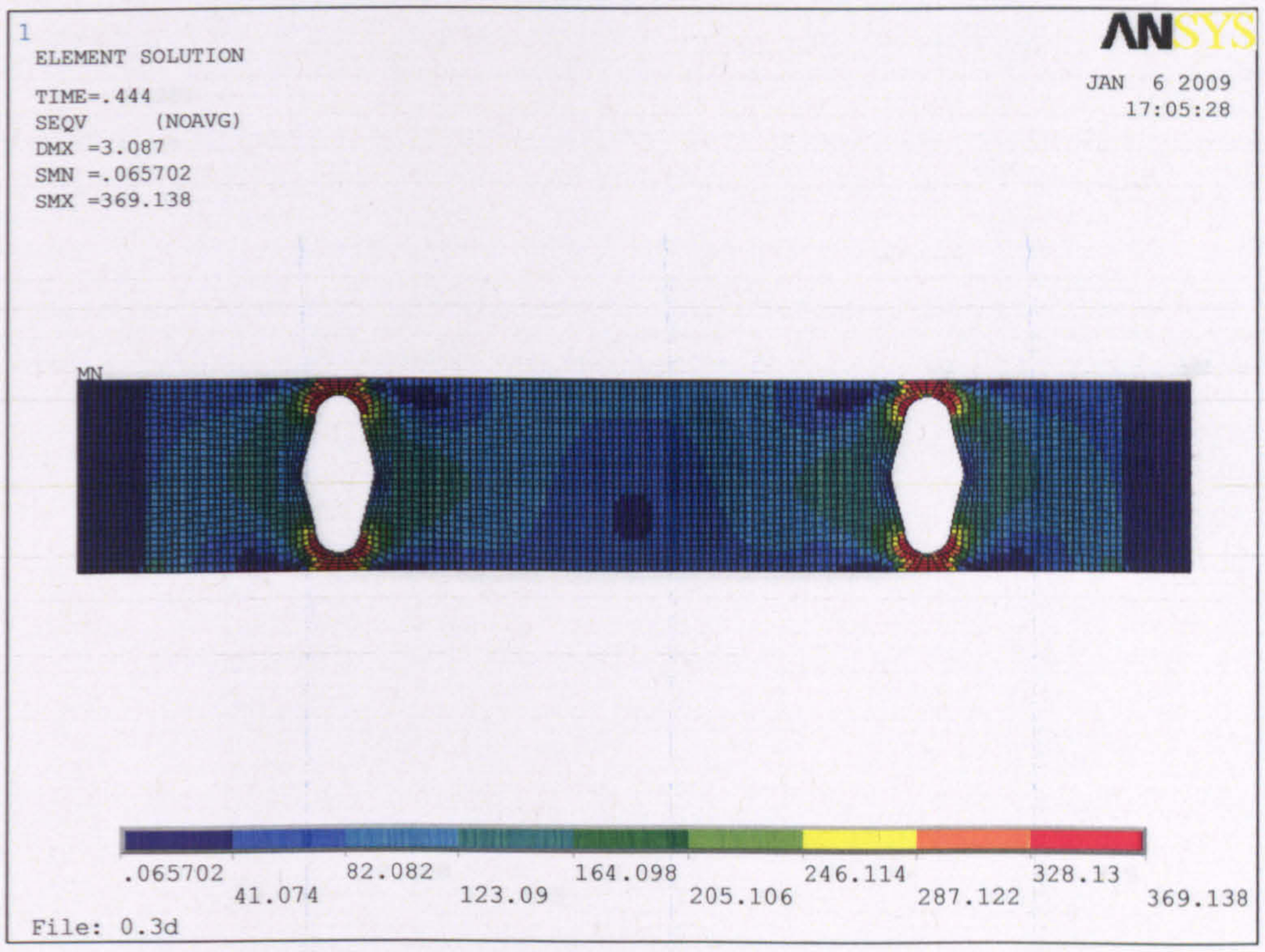

Figure 8: Perforated beams with vertical elliptical web opening (*THETA10,R0.15*) at P_y

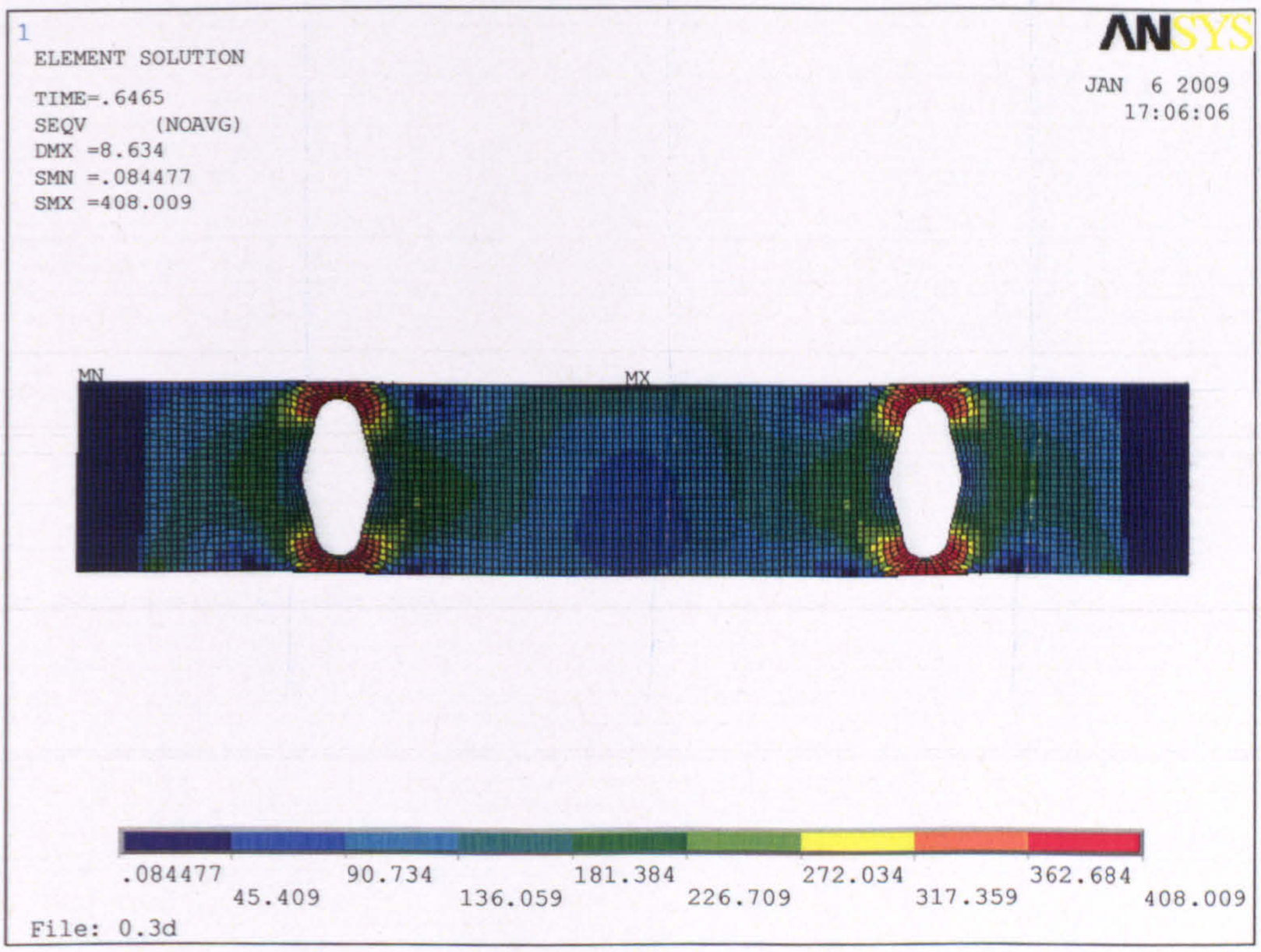

Figure 9: Perforated beams with vertical elliptical web opening (*THETA10,R0.15*) at $P_{cr.}$

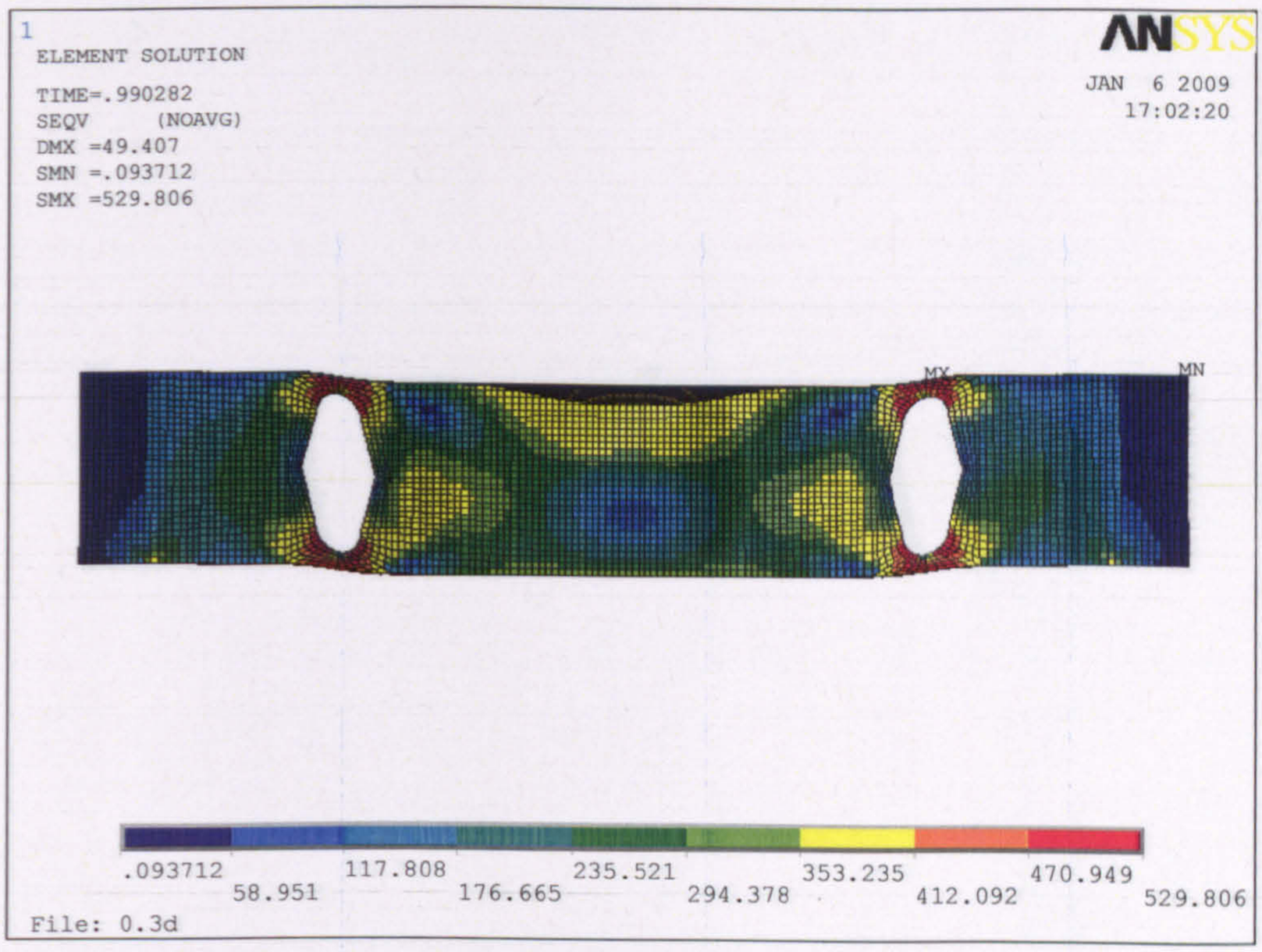

Figure 10: Perforated beams with vertical elliptical web opening (*THETA10,R0.15*) at $P_{ult.}$

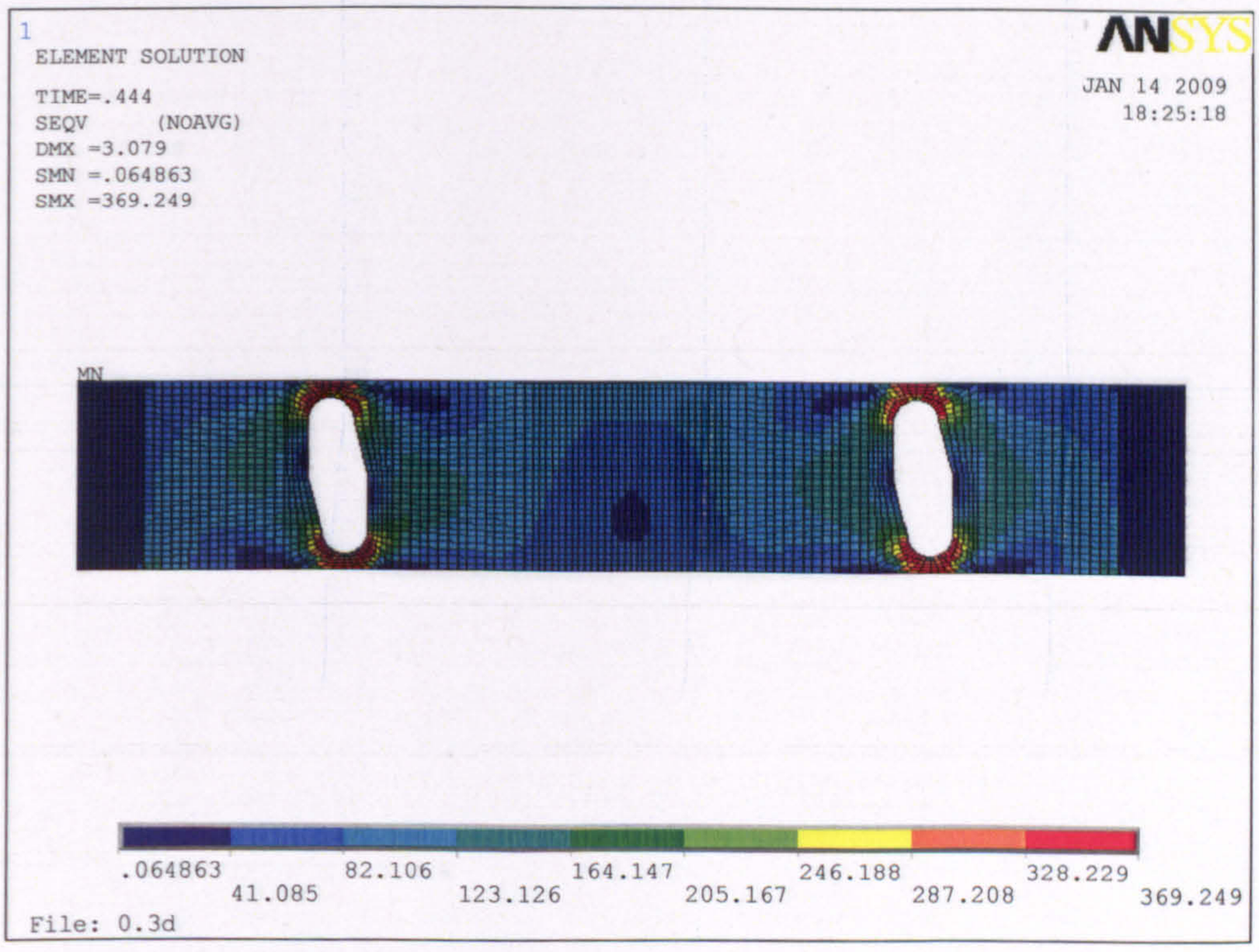

Figure 11: Perforated beams with inclined elliptical web opening (*THETA10,R0.15*) at P_y

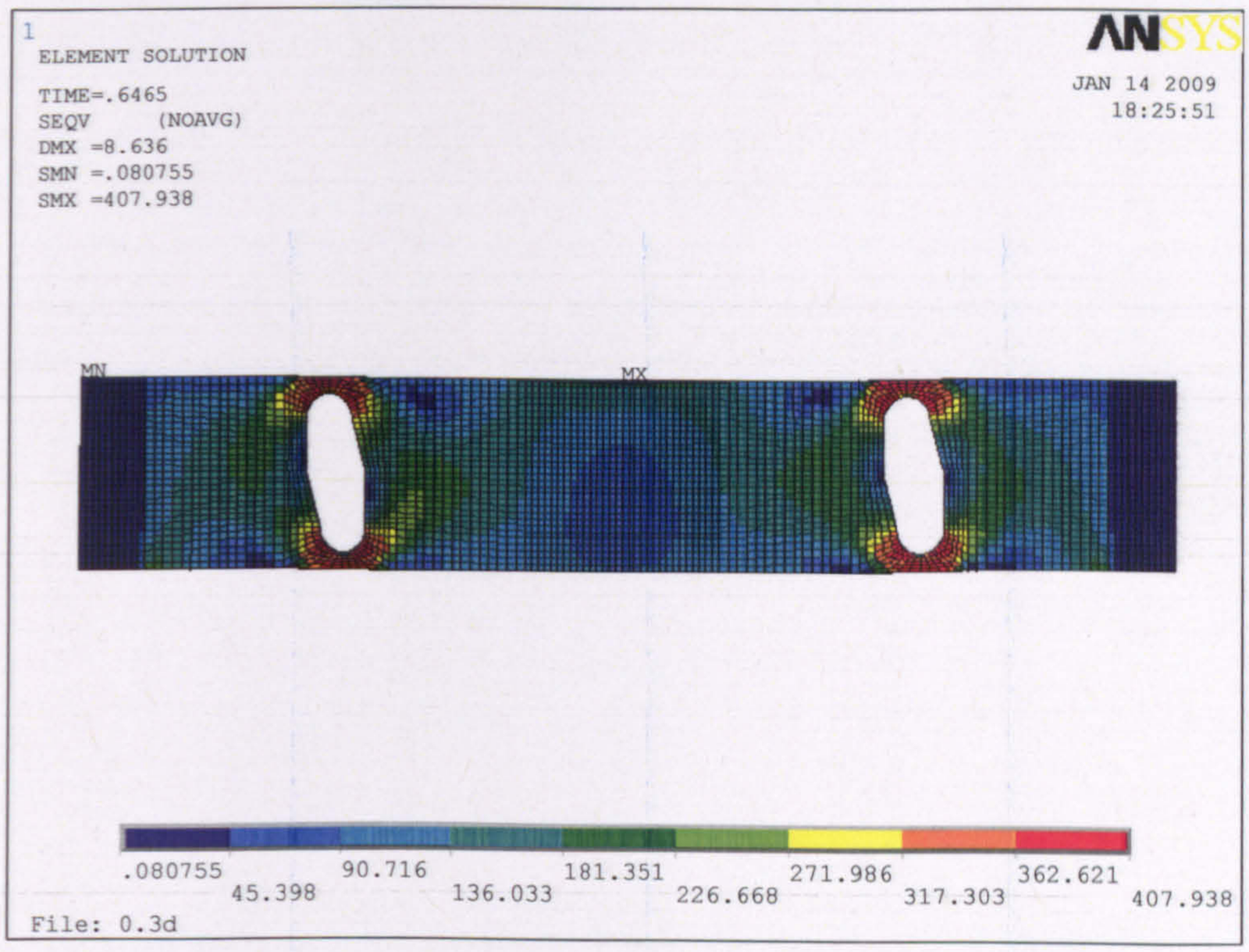

Figure 12: Perforated beams with inclined elliptical web opening (*THETA10,R0.15*) at $P_{cr.}$

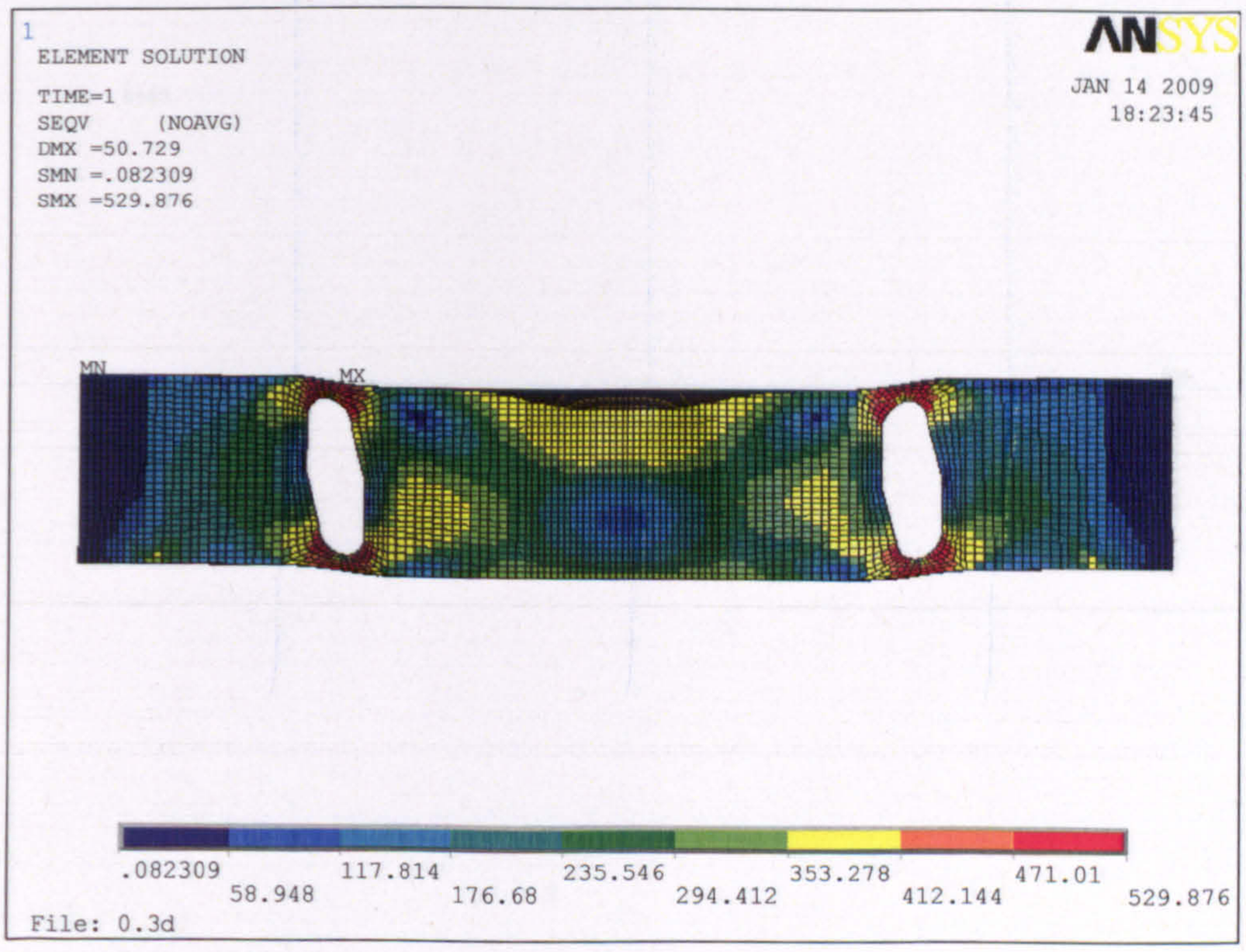

Figure 13: Perforated beams with inclined elliptical web opening (*THETA10,R0.15*) at $P_{ult.}$

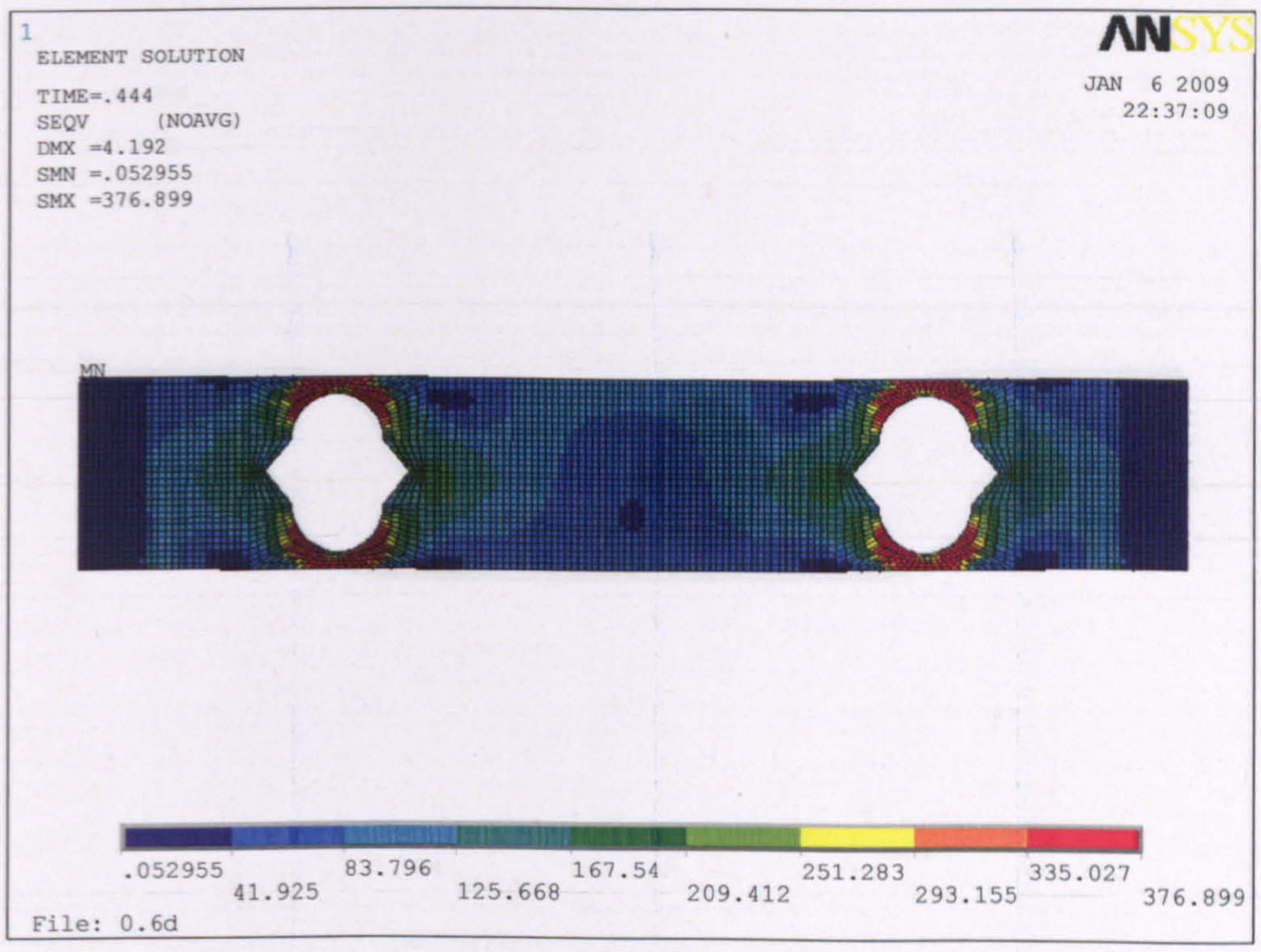

Figure 14: Perforated beams with vertical elliptical web opening (*THETA40,R0.3*) at P_y

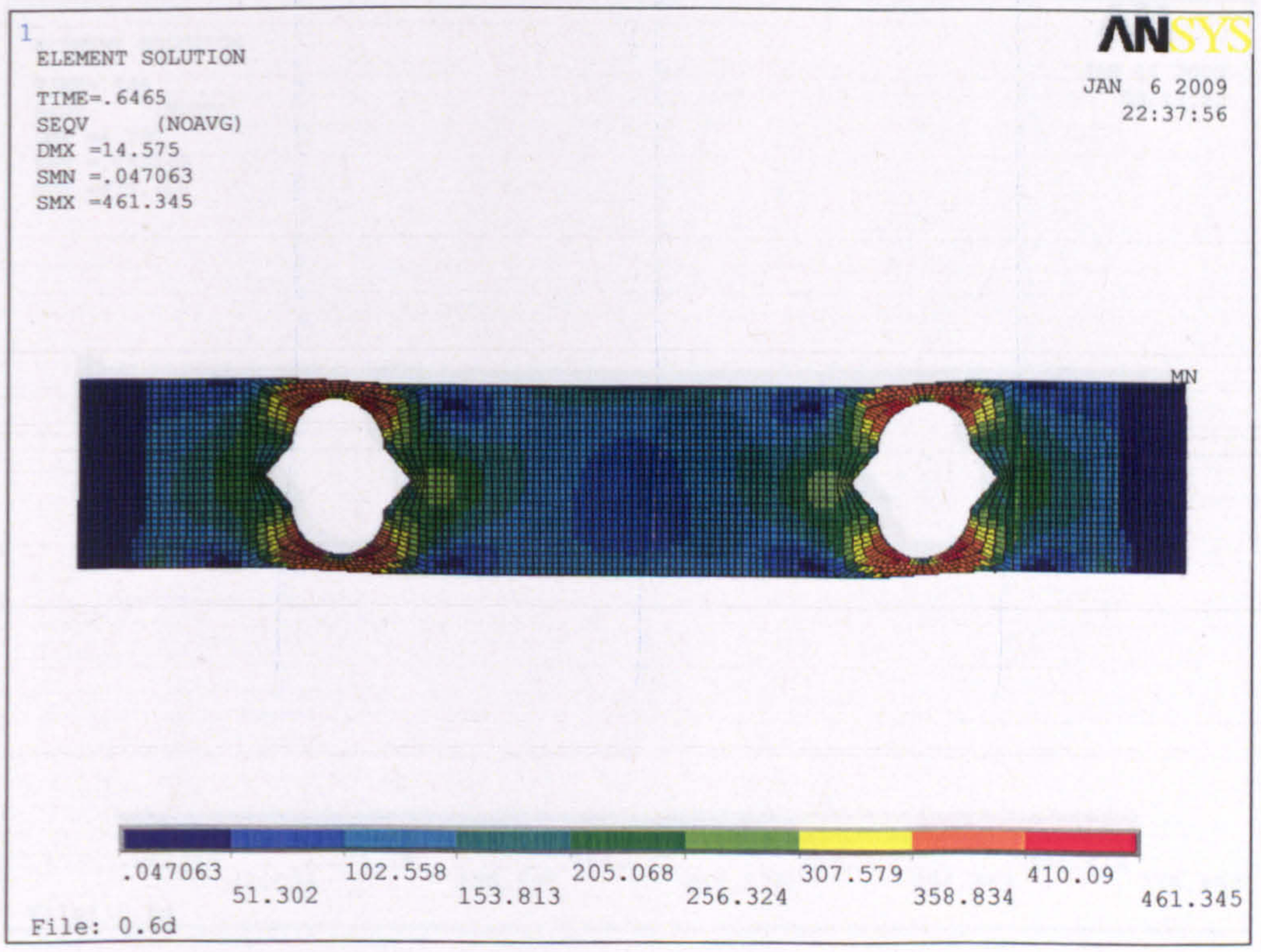

Figure 15: Perforated beams with vertical elliptical web opening (*THETA40,R0.3*) at $P_{cr.}$

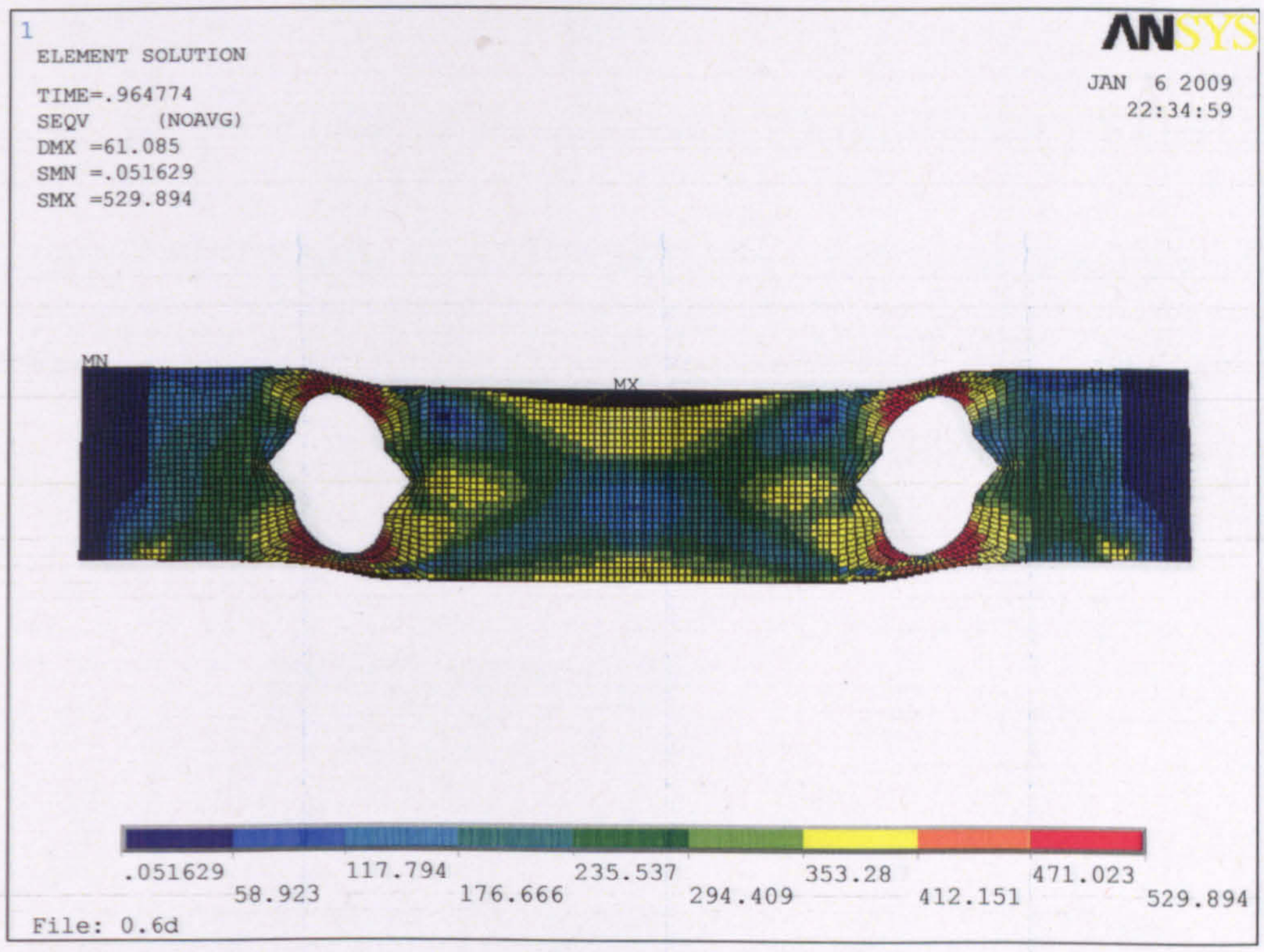

Figure 16: Perforated beams with vertical elliptical web opening (*THETA40,R0.3*) at $P_{ult.}$

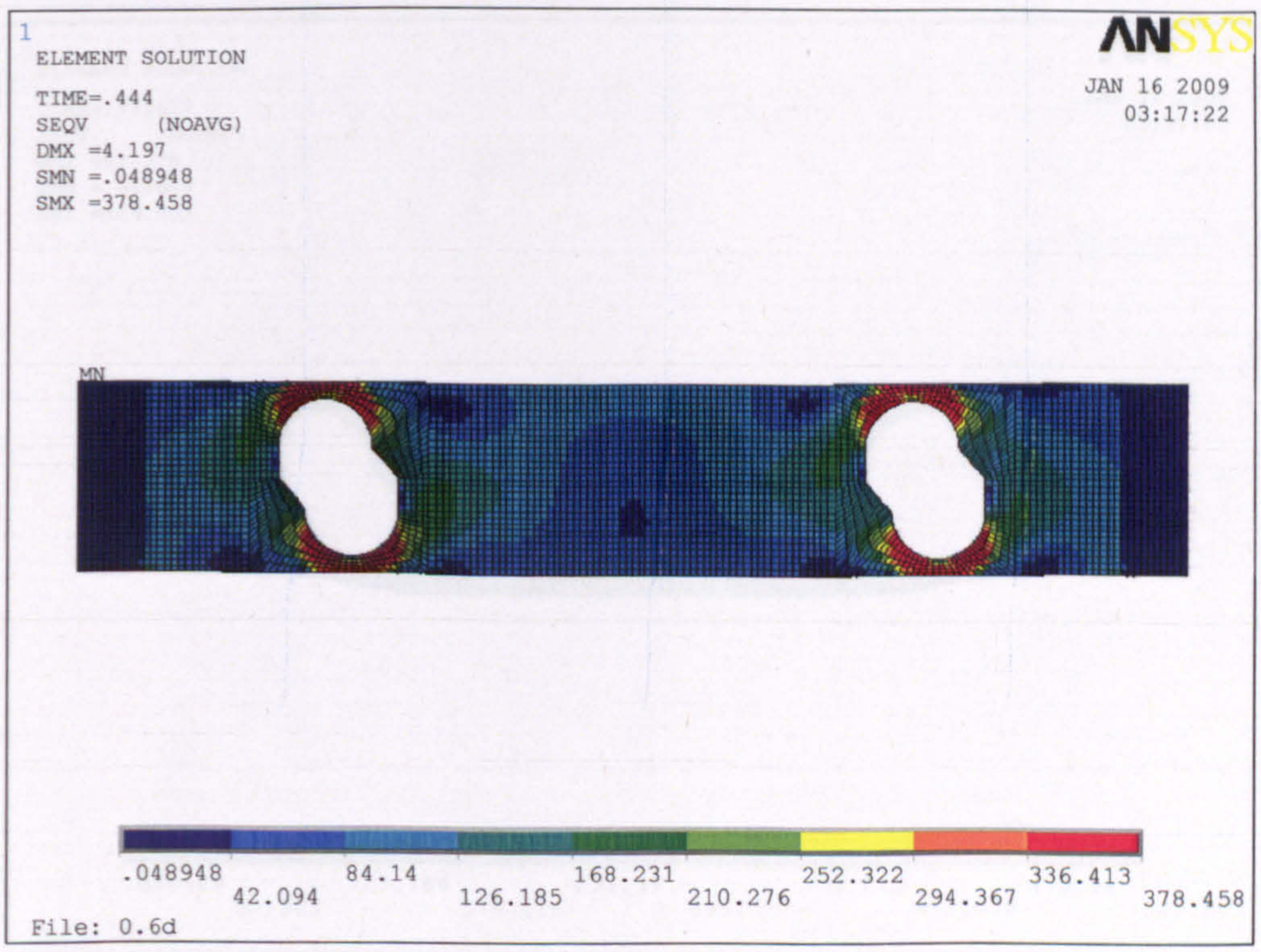

Figure 17: Perforated beams with inclined elliptical web opening (*THETA40,R0.3*) at P_y

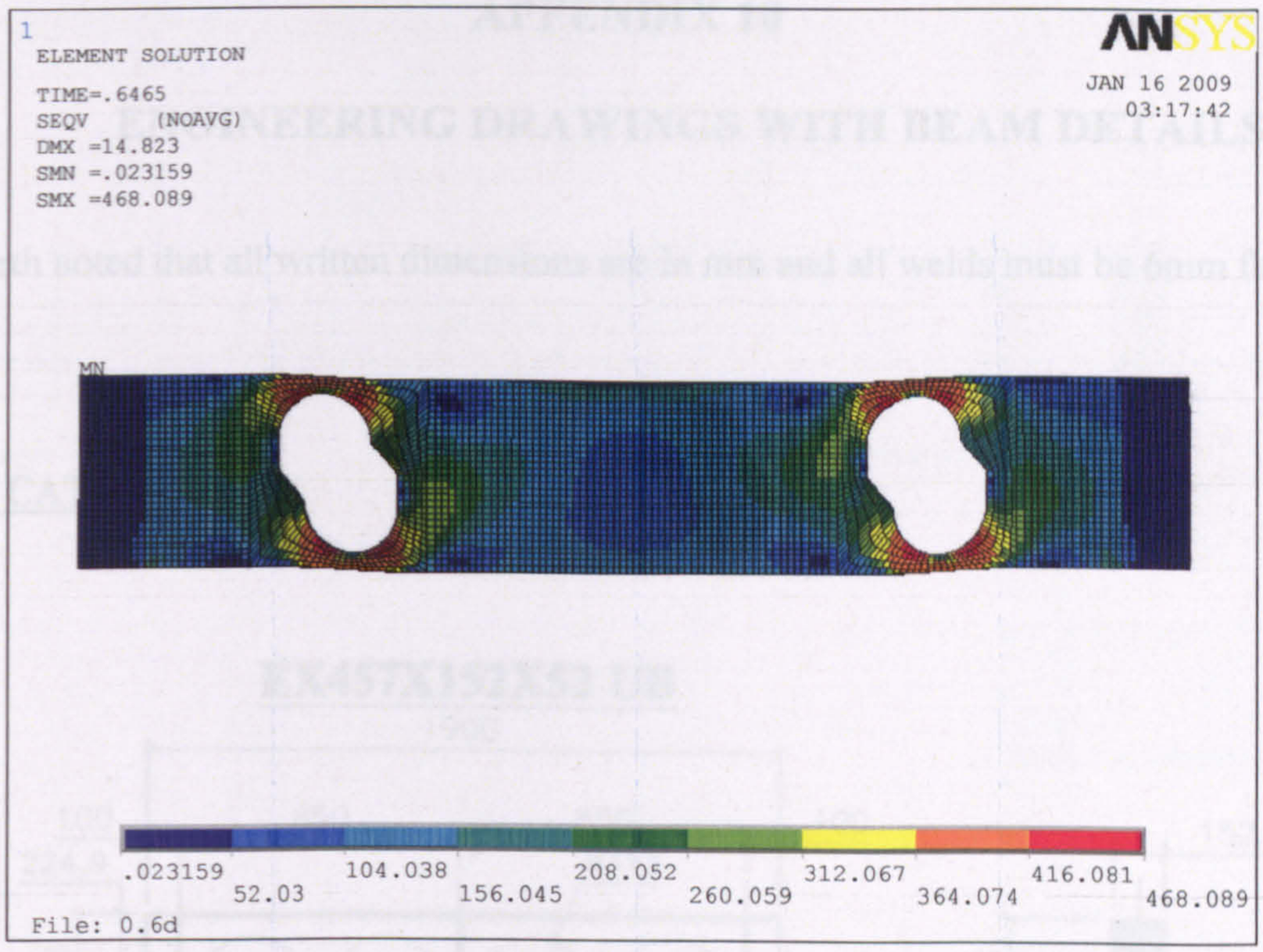

Figure 18: Perforated beams with inclined elliptical web opening (*THETA40,R0.3*) at $P_{cr.}$

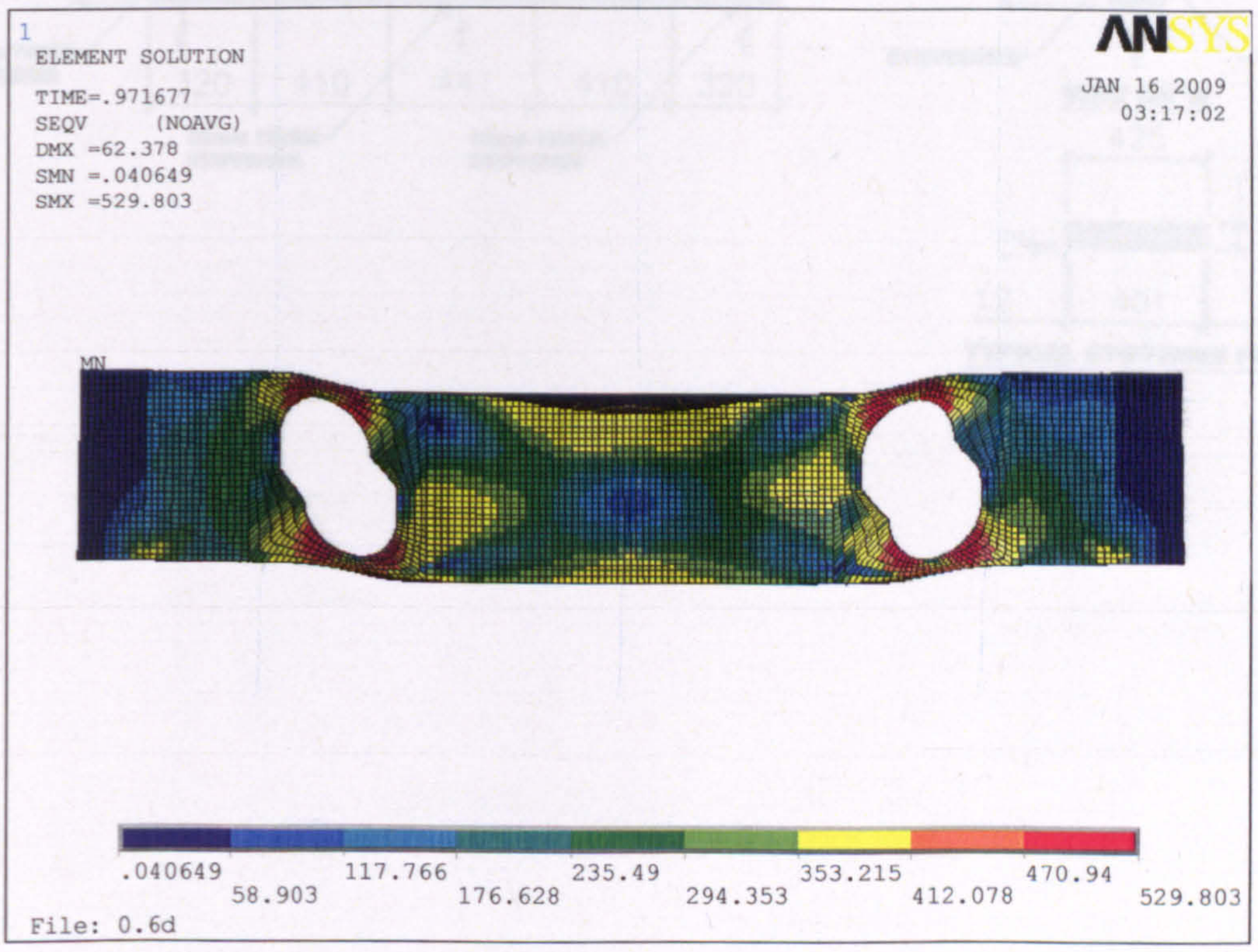

Figure 19: Perforated beams with inclined elliptical web opening (*THETA40,R0.3*) at $P_{ult.}$

APPENDIX 10

ENGINEERING DRAWINGS WITH BEAM DETAILS

It is worth noted that all written dimensions are in mm and all welds must be 6mm full welds.

FIRST CATEGORY

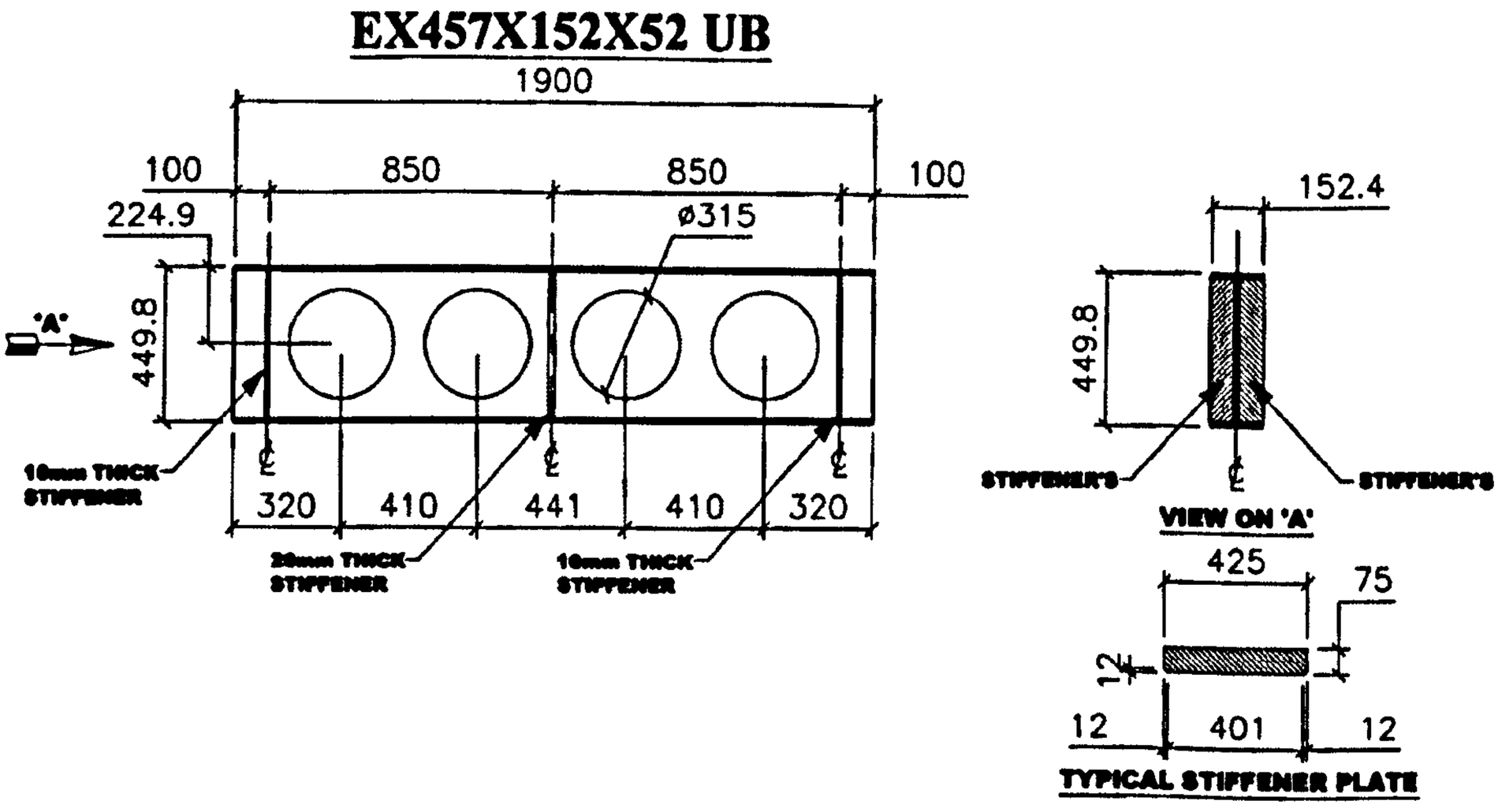

Figure 1: Specimen A-1

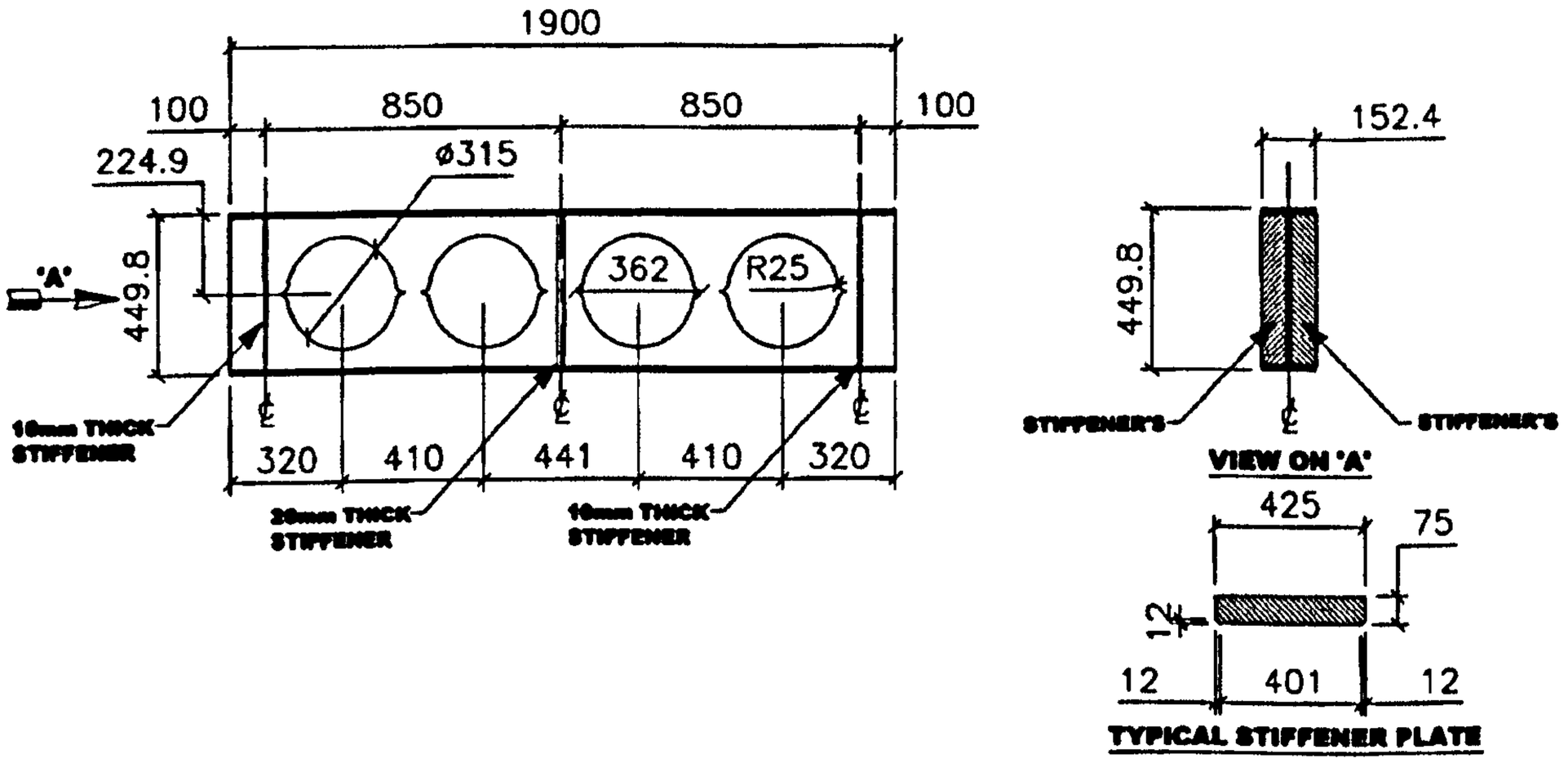

Figure 2: Specimen A-2

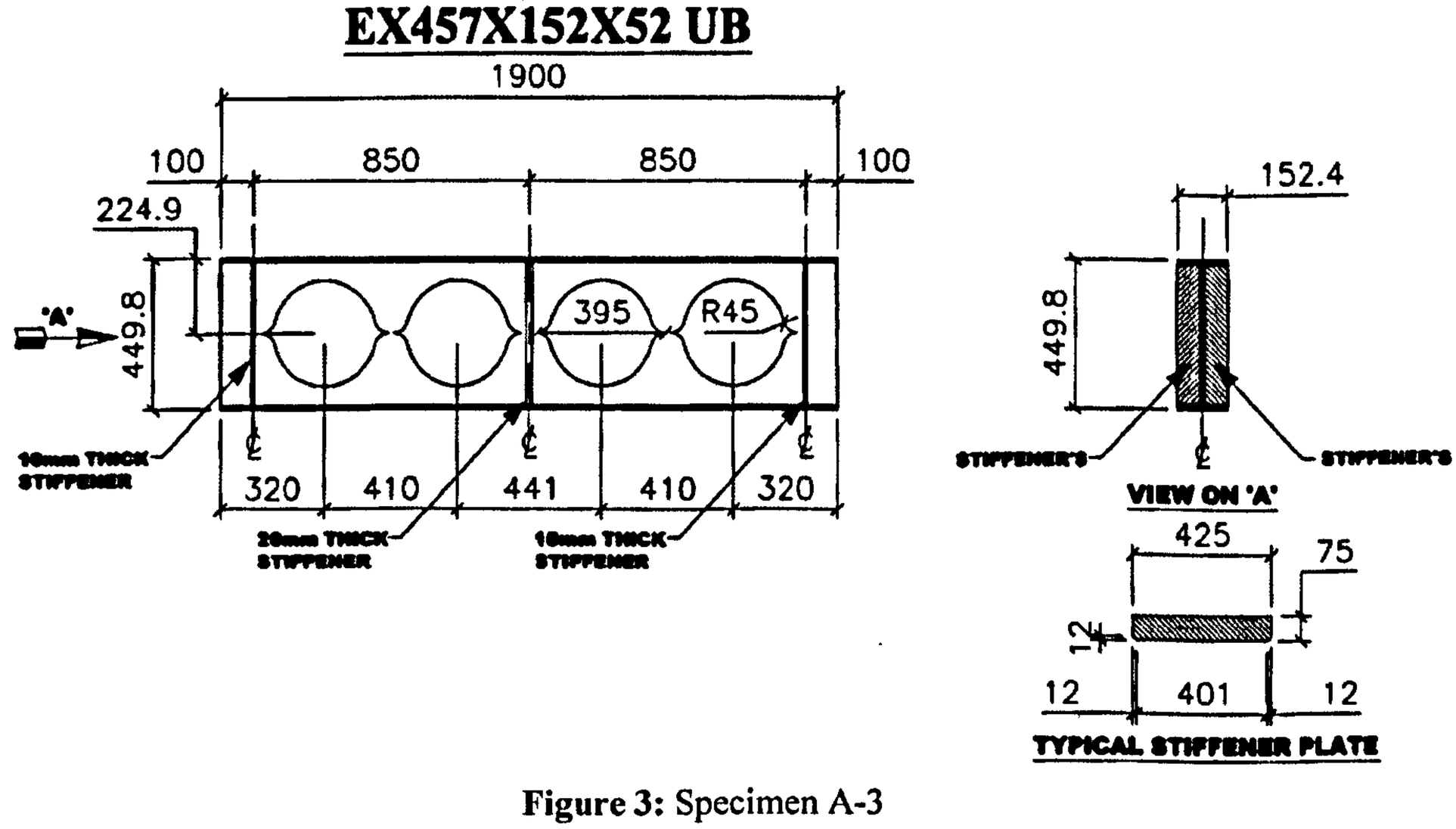

Figure 3: Specimen A-3

SECOND CATEGORY

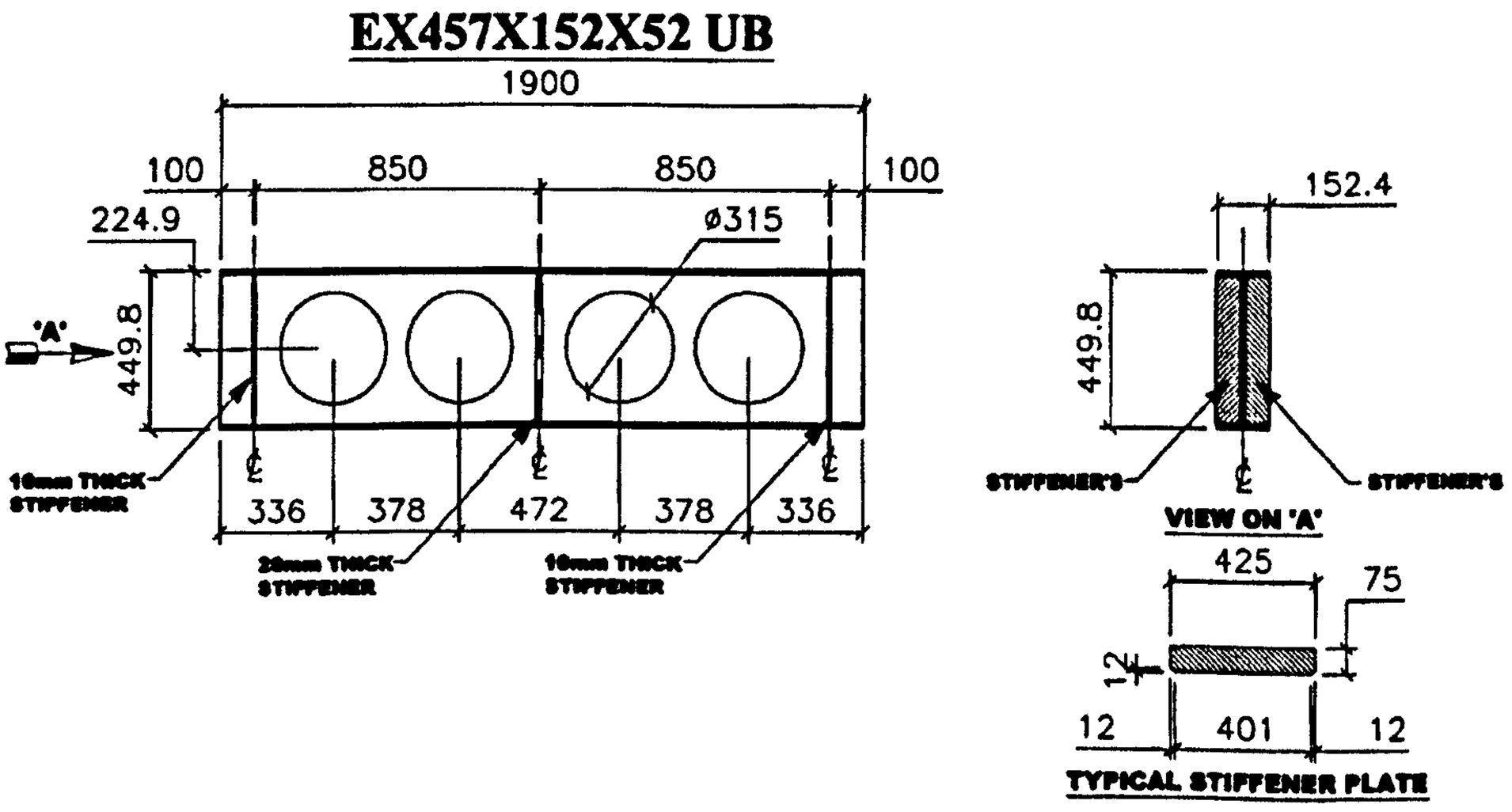

Figure 4: Specimen B-1

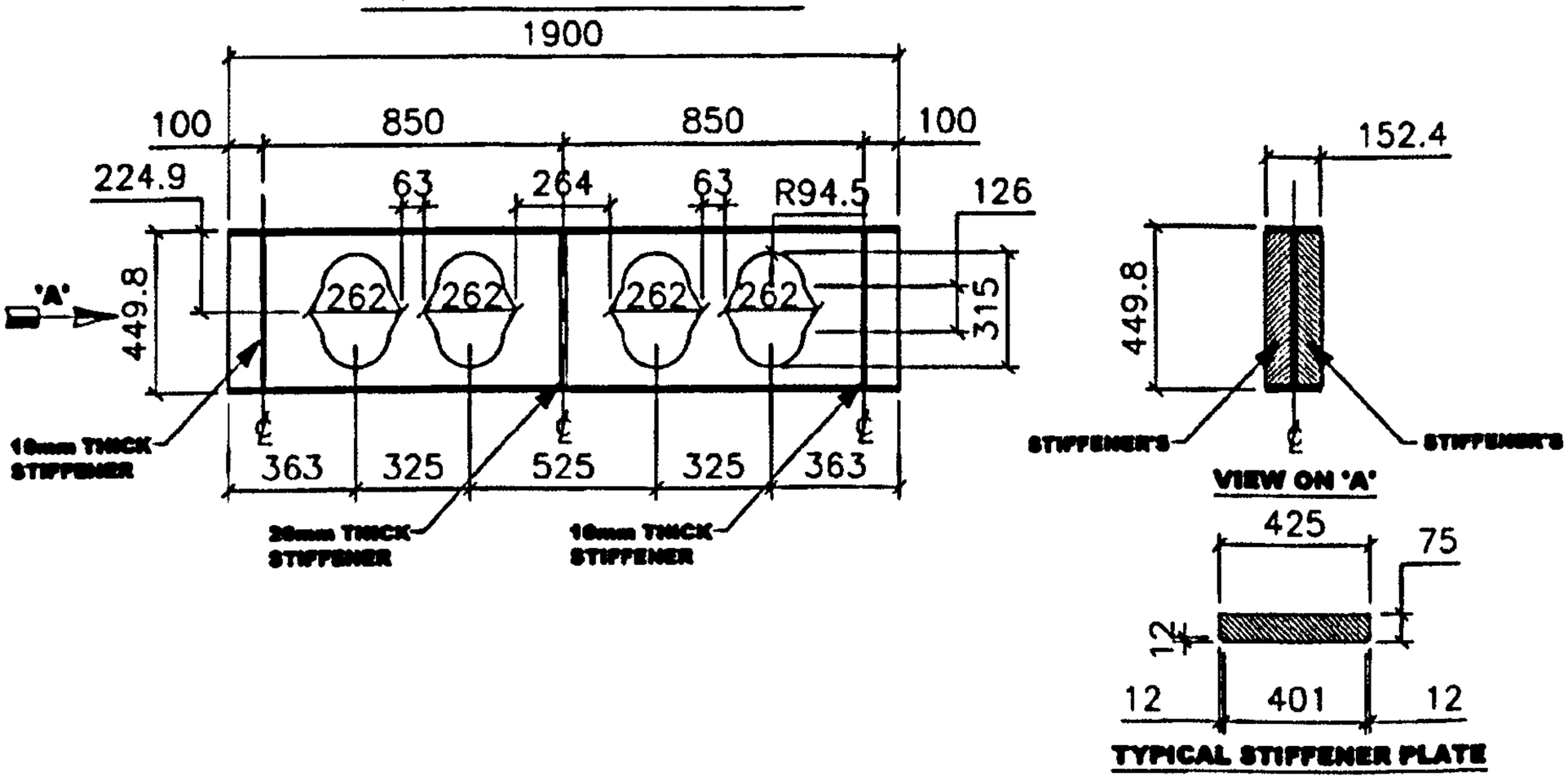

Figure 5: Specimen B-2

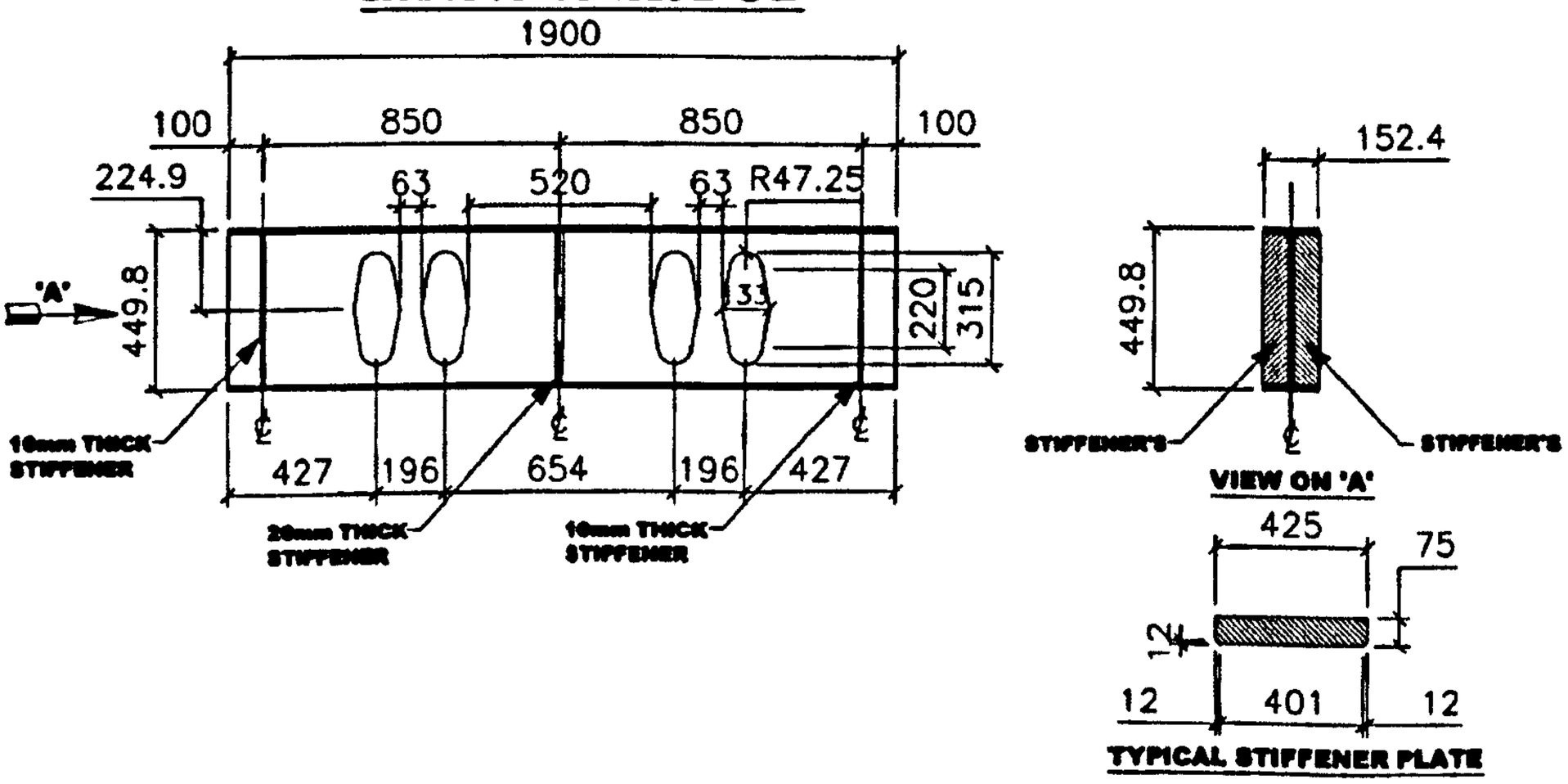

Figure 6: Specimen B-3

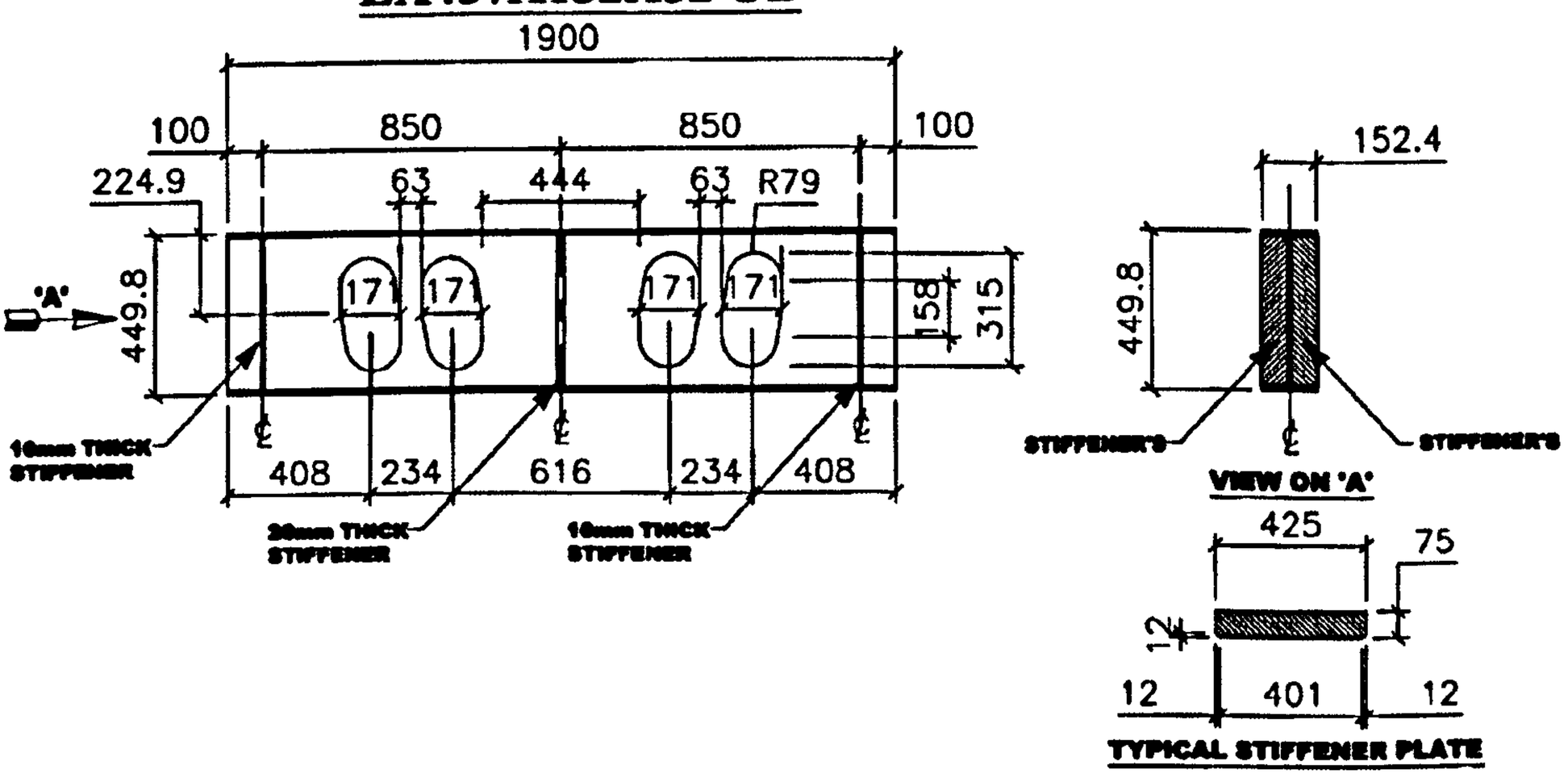

Figure 7: Specimen B-4

APPENDIX 11

WEB STRAIN MEASUREMETNS

The web strain measurements are displayed in tabular forms in this appendix for every load step. The web strains can illustrate the high stressed areas, the web-post buckling, the local flexural strains resulting from local buckling (i.e. membrane strains) and the out-of-plane movement of the web-posts. **Figure 1** (top) shows the strain gauges positions at the front side of the specimens, and the **Figure 1** (bottom) shows the same strain gauges at the back side of the specimen.

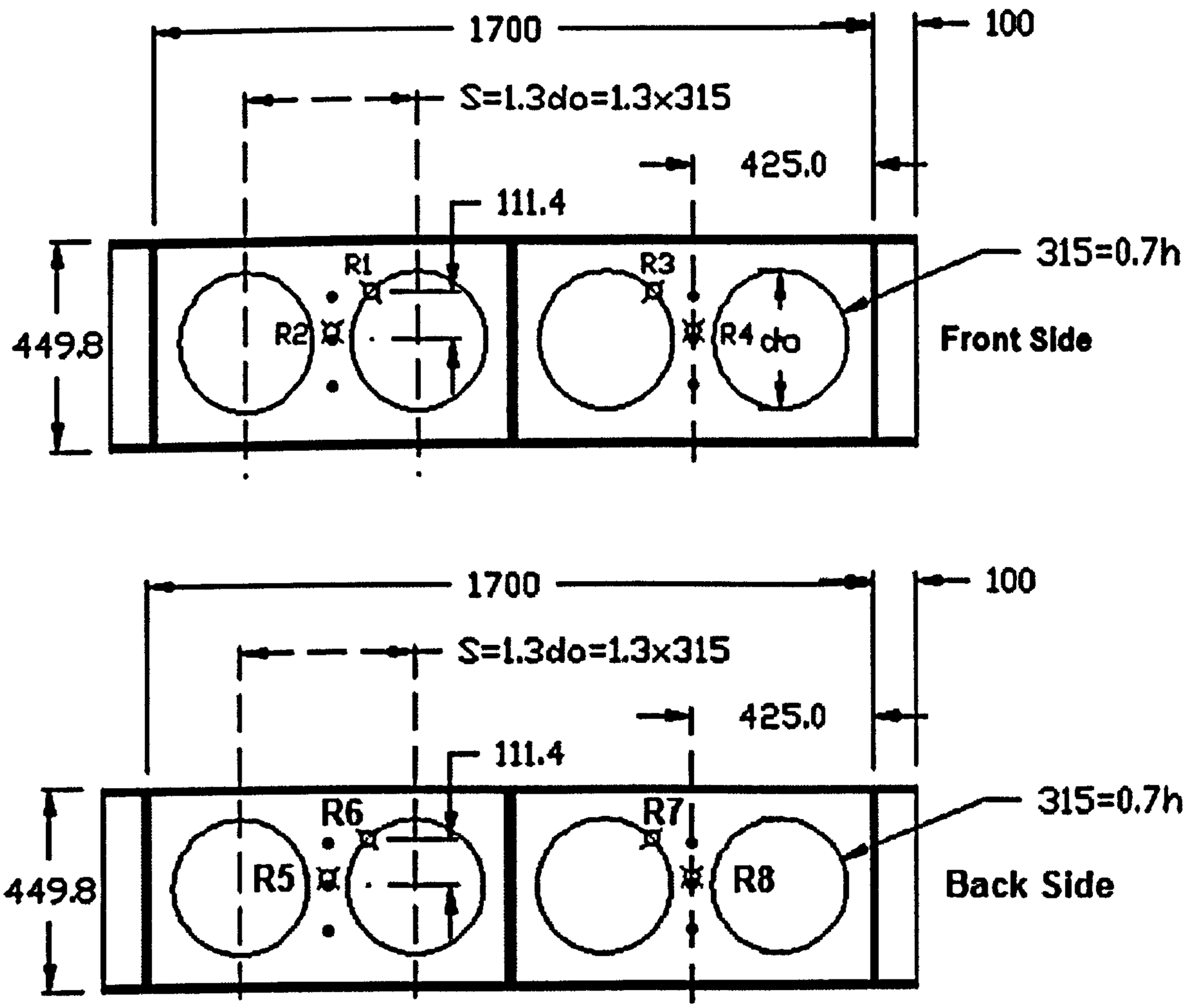

Figure 1: Wed strain gauges at the front and back side of the specimens

In **Figure 9**, strains are not recorded for the Rosette 6 because of a human error. Horizontal, vertical and 2-dimensional plane shear web strains are presented in order.

R1 (microstrain)			R2 (microstrain)			R3 (microstrain)			R4 (microstrain)			Load
R1-εx	R1-εy	R1-εxy	R2-εx	R2-εy	R2-εxy	R3-εx	R3-εy	R3-εxy	R4-εx	R4-εy	R4-εxy	(kN)
0.00	0.96	-1.44	0.00	0.00	0.00	0.96	0.00	0.48	0.96	0 00	-0.48	8.13
-36.52	-43 25	68.72	0 96	0.00	71 61	-43.25	-24.99	58.15	5.77	-10.57	58.15	19.70
-62.48	-74.97	118.71	0.96	1.92	126.40	-75.93	-44.21	101.40	7.69	-16.34	105.25	28.37
-93 23	-111.50	176.38	0.96	5.77	187.91	-113.42	-64.40	150.43	11.53	-20.18	157.15	38 01
-120.15	-146.10	229.24	1.92	8.65	244 62	-145.14	-81.70	192.24	15.38	-22.11	204.25	46.69
-155.71	-190 31	298 93	1.92	10.57	318 63	-187.43	-105.73	249.43	15.38	-24.03	267.69	58.26
-180.70	-220.11	345.55	1.92	12.50	369.58	-217.23	-123.03	289.32	18.26	-24.99	309.98	65.97
-213.38	-259.52	409.46	2.88	14.42	434.45	-255.67	-145.14	342.66	18.26	-25.95	370.06	76.57
-244.14	-296.04	468.10	2.88	15.38	493.57	-292.20	-165.32	392.16	17.30	-22.11	420.52	86.21
-281.63	-335.45	533.46	1.92	14.42	559 89	-328 72	-186.47	444.07	16.34	-22.11	476.75	96.82
-317.19	-377.75	601 22	0.96	14.42	623 81	-367.17	-208 58	496.45	12.50	-19.22	534.90	106 46
-347.95	-411.39	660 33	0.00	14 42	677.15	-401.77	-226.84	542.11	10.57	-16.34	588.24	115.13
-381.59	-448 87	722 81	-1.92	14.42	735.79	-436.38	-244.14	588 24	11.53	-12.50	635.82	123 81
-416.19	-487.32	788.17	-2.88	13.46	796.34	-473.86	-263.36	641.59	9.61	-9.61	691.09	133.45
-452.72	-526.73	857.86	-3.84	13.46	857.38	-512.31	-283.55	693.01	5.77	-9.61	752.61	143.09
-491.16	-569.02	928 02	-5.77	12.50	916.49	-550.76	-300.85	744.92	1.92	-7.69	805.47	152.73
-534.42	-614.20	1013.57	-8 65	9 61	980 89	-590.17	-318.15	805.95	4.81	-2.88	862.18	162.37
-572.87	-653.60	1084 21	-11.53	8.65	1040.48	-627.65	-333.53	859.30	1.92	4.81	920.33	172.01
-619.00	-703.59	1181.29	-14.42	8 65	1118.82	-674.75	-353.72	922.74	-0.96	13.46	989.54	183.58
-652.64	-735.31	1248.58	-7 69	0.96	1187.54	-708.39	-365.25	969.35	-2.88	19.22	1033.75	191.29
-693.97	-771.83	1330.76	-6.73	-13 46	1252.90	-743.96	-375.82	1018.37	-4.81	24.03	1079.41	200.93
-735.31	-806.43	1411.98	-109 57	-98 04	1524.44	-786.25	-383.51	1076.05	-7.69	52.87	1140.44	209.60
-792.02	-835.27	1514.34	-115.34	-173.97	1869.98	-838.15	-382.55	1131.31	140.33	57.67	1229.35	220.21
-845.84	-856.41	1607.58	-59.59	-297.97	2410.65	-878.52	-387.36	1179.85	281.63	49 02	1364 88	229.85
-914.09	-863.14	1703.70	74 97	-510.39	3496.31	-921.77	-386.40	1225.03	470.02	-98 04	1803.66	239.49
-1020.78	-833.35	1816.16	829.50	-873.72	5638.30	-967.91	-374.86	1266.36	1099.59	-613.24	2556.75	250.09
-1121.70	-768.95	1866.14	1825 29	-1287.03	7716.38	-1001.55	-364.29	1289.43	1758.01	-1064.99	3813.50	256.84
-1370.65	-487.32	1865.18	3108.47	-2093.46	11787.00	-1034.23	-337.38	1306.73	2275.12	-1061.15	4766.99	266.48
-2122.29	1193.79	1091 90	3269.95	-2773.01	13756.94	-1005.40	-326.80	1273.57	2607 69	-1095.75	5360.04	267.44
-3073.87	3795.71	-527.21	3396.82	-2841.26	13838.16	-997.71	-334.49	1274.53	2758.60	-1056.34	5881.00	269.37
-3620.78	5018.34	-1305 29	3417.97	-2831.65	13837.20	-1006.36	-331.61	1282.22	3030.61	-1208.21	6872.46	272.26
-4101.37	6072.76	-1980.52	3413.16	-2800.89	13827.10	-1011.17	-316.23	1275.01	3353.57	-1438.89	8144.11	275.15
-4506.03	6945.51	-2532.72	3405.47	-2773.98	13825.18	-1021.74	-300.85	1266.84	3535.23	-1558.08	9209.58	278.05
-4903.00	7799.04	-3077.23	3387.21	-2738.41	13819.42	-1032.31	-268.17	1248.10	3764.00	-1688.80	10649.43	281.90
-5209.62	8467.06	-3503.99	3369 91	-2712.46	13820.86	-1048.65	-241.26	1237.04	3862.04	-1762.81	11826.40	284.79
-5578.71	9270.61	-4021.11	3343.00	-2682.66	13830.95	-1080.37	-188.39	1213.01	3953.35	-1878.15	13408.99	287.69
-6020.85	10241.41	-4653.57	3316.08	-2649.98	13843.45	-1104.40	-149.94	1191.39	4047.54	-1917.56	14482.15	287.69
-6364.00	11010.36	-5156.75	3288 21	-2626.92	13850.65	-1135.16	-109.57	1182.74	4080.22	-1950.24	15169.40	288.65
-6889.76	12198.38	-5943.48	3263.22	-2608 65	13805.00	-1214.94	-4 81	1146.21	4187.88	-2052.13	16129.63	284.79
-7238 67	13038.46	-6518.75	3246.88	-2576.93	13741.56	-1283.18	75.93	1128.43	4235.94	-2122.29	16460.75	280.94
-7494 35	13675.72	-6966.18	3222.85	-2528.87	13690 13	-1386 03	189.35	1101 04	4312.83	-2206.88	16843.30	279.01
-7703 89	14197.64	-7330.95	3196 90	-2463.51	13637.75	-1784 92	929.46	728 58	4556.97	-2503.88	17928 96	276.12
-7730.80	14287.99	-7398 23	3186.32	-2448.14	13631.51	-4152.31	6561.04	-3439.12	4688.65	-2800.89	18229.81	266.48
-7787.51	14437.94	-7500.60	3168.06	-2424.11	13631.50	-4833.79	8109.51	-4618.49	4663.66	-2799.93	18252.39	265.52
-7841.34	14563.85	-7581.81	3167.10	-2394.31	13621.89	-5329.76	9291.76	-5530.65	4630.98	-2778.78	18277.39	264.55
-7899.97	14707.07	-7675.05	3151.72	-2354.90	13600.27	-5775.75	10400.00	-6402.92	4579.08	-2735.53	18300.93	262.62
-7941.30	14803.19	-7735.13	3141 15	-2320.30	13588.25	-6051.61	11137.23	-6997.90	4557.93	-2713.42	18302.37	261.66
-7968.21	14862.78	-7772.61	3129 61	-2294.35	13570.47	-6329.39	11930.21	-7664.00	4542.55	-2696.12	18216.83	254.91
-7988.40	14911.80	-7800.48	3120.96	-2268.39	13572.40	-6482.22	12410.80	-8073.94	4531.02	-2666.32	18168.29	253.95
-8012.43	14948.33	-7814 42	3110.39	-2231.87	13566.15	-6586 03	12761.63	-8381.04	4511.80	-2626.92	18124.56	252.02
-7983 59	14188 99	-7209.84	2918 15	-2080.00	12080.15	-6503.37	12026.33	-7784.63	4144.62	-2183.81	16637.13	1.38

Figure 2: 2D web strains at the front side for Specimen A-1

R5 (microstrain)			R6 (microstrain)			R7 (microstrain)			R8 (microstrain)			Load
R5-εx	R5-εy	R5-εxy	R6-εx	R6-εy	R6-εxy	R7-εx	R7-εy	R7-εxy	R8-εx	R8-εy	R8-εxy	(kN)
0 00	0 00	2 88	0.00	0.00	0.00	0.00	0.00	-0.96	0.96	0.96	-0.96	8.13
-0 96	3 84	74 49	-29 80	-44.21	62.96	-40.37	-34.60	63.44	0.00	-0.96	64.88	19.70
0 00	6.73	132.16	-49.98	-76.89	107.65	-72.09	-61.52	111.98	-1.92	-1.92	115.34	28.37
4 81	7.69	190.79	-74.01	-112 46	159.56	-105.73	-90.35	167.25	-2.88	-1.92	173.49	38 01
12.50	8 65	245.10	-95.16	-143 22	203.77	-137.45	-115 34	215.79	-3.84	-0.96	225.40	46 69
14.42	10 57	314 31	-122.07	-184 55	261.92	-179.74	-150.91	281.63	-6.73	0.00	294.60	58.26
13.46	14 42	365.73	-141.29	-213 38	303 25	-207 62	-174.94	325.84	-6.73	0.96	342.18	65.97
17.30	18.26	430.13	-166.28	-250 87	356 60	-246.06	-205.69	385.43	-6.73	2.88	403.70	76.57
10.57	23.07	496.45	-188.39	-287.39	407 06	-280.67	-235.49	440.70	-8 65	4 81	462.33	86.21
10.57	29 80	558.45	-212.42	-323.92	460 41	-319.11	-269.13	500.78	-10.57	7.69	522.40	96.82
0.00	39.41	617.56	-235 49	-362.37	512.31	-358.52	-304.70	564.21	-15.38	10.57	583.92	106.46
5.77	43.25	681.96	-255.67	-396 97	558.93	-392.16	-335.45	619.48	-19 22	13 46	637.26	115.13
-0.96	48.06	753.09	-275.86	-431.57	608.43	-427.73	-367.17	677.15	-22.11	16.34	692.05	123 81
-1.92	54.79	811.72	-297.97	-469 06	660.33	-465.21	-401.77	737.23	-27.87	21.15	749.24	133.45
-7.69	67.28	873.72	-320.07	-509.43	714.64	-504 62	-438.30	799 22	-31.72	25.95	807.39	143.09
-1.92	72.09	941.48	-342.18	-546 91	767.51	-542.11	-474.82	862.18	-38.45	30.76	865.07	152.73
2.88	80.74	1004.92	-365.25	-588 24	825.66	-587.28	-517.12	935.71	-45.18	37.49	929.46	162.37
-19.22	79.78	1060.67	-383.51	-625.73	880.44	-625.73	-554.60	998.67	-52.87	44.21	984.73	172.01
-29 80	94 20	1137.56	-408.50	-670.91	944.36	-671.87	-602.66	1080.37	-69.21	52.87	1061.63	183.58
-30.76	95.16	1192.35	-422.92	-700.70	990.50	-701.66	-635.34	1136.60	-72.09	58.63	1129.39	191.29
-36.52	115.34	1249.54	-440.22	-738.19	1042.88	-734.34	-675.71	1204.84	-75.93	56.71	1197.63	200.93
-19.22	127.84	1356.71	-455.60	-776 64	1099.59	-761.26	-717.04	1270.68	-143.22	127.84	1197.63	209.60
98 04	117.26	1424.47	-470.98	-812.20	1152.94	-790.09	-766.06	1349.02	-163.40	217.23	1247.62	220.21
200 89	77 86	1499 45	-483.48	-853.53	1208.69	-809.32	-813.16	1417.75	-134.57	285.47	1285.58	229.85
366.21	79.78	1598 45	-488.28	-894.86	1261.55	-813.16	-871.79	1487.43	-56 71	224.92	1930.54	239.49
949 65	-316 23	2115.08	-484 44	-941.96	1313.94	-765.10	-970.80	1551.35	202 81	68.24	3623.66	250.09
1532.13	-617 08	3467.95	-481.55	-977.52	1348.54	-692.05	-1057.30	1566.73	864.10	-166.28	5619.08	256.84
2083 85	-829 50	4739.12	-463.29	-1024 62	1388 91	-411.39	-1299.52	1534.05	2102.11	-374.86	9495.05	266.48
2460.63	-1033 27	5397.53	-445.03	-998 67	1354.31	877.56	-2533 68	1558.56	2303.00	76.89	11544.77	267.44
2700.93	-1089.02	5923.29	-442.14	-985.21	1340.37	2265.51	-4391 65	2308.76	2259.74	306.62	11333.32	269.37
3055.60	-1230.32	6727 81	-432.53	-995.79	1342.77	2891.24	-5143.29	2580 30	2267.43	365.25	11286.70	272.26
3481.41	-1501.37	7905.74	-414.27	-1009.24	1336.53	3415.09	-5737.31	2771.09	2281.85	400.81	11255.94	275.15
3715.94	-1601.33	8846.73	-392.16	-1025 58	1331.72	3852.42	-6203.48	2900.85	2297.23	436.38	11231.43	278.05
3886.07	-1711 87	10295.24	-361.41	-1054 42	1325.95	4278 23	-6632.17	2998.41	2304.92	462.33	11210.77	281.90
3940.85	-1779.15	11464.52	-333.53	-1079.41	1324.51	4611.76	-6946.47	3051.28	2314.53	486.36	11191.06	284.79
3920.67	-1814.71	13101.41	-288.36	-1124.59	1331.24	5025.07	-7306.92	3081.55	2325.10	509.43	11163.66	287 69
3838.01	-1817.60	14249.55	-249.91	-1159.19	1317.78	5563.33	-7721.19	3055.12	2343.37	547.87	11110.32	287.69
3813.02	-1786 84	15014.65	-216.27	-1203.40	1327.88	6030 47	-8039.34	2974.86	2358.75	578.63	11062.26	288.65
3755.34	-1752.24	16096.94	-130.72	-1311.05	1347.58	6834.02	-8529.54	2742.26	2365.47	636.30	11022.37	284.79
3761.11	-1739.74	16494.39	-67.28	-1398.52	1373.05	7443.41	-8870.76	2498 60	2358.75	683.40	11009.88	280.94
3740.93	-1715.71	16934 61	35.56	-1524.44	1399.00	7955.72	-9133.17	2247.73	2351.06	724.73	11007.48	279 01
3614.05	-1452.35	17896.76	692.05	-2201.11	1460.04	8417.08	-9360.97	1990.61	2332.79	762.22	11002.66	276.12
3694.79	-853 53	17267.66	4084 07	-6183.29	2510.61	8490.13	-9401.34	1952.16	2332.79	766.06	11004.59	266.48
3719.78	-757.41	17148.48	4965.47	-6975.31	2518.78	8627.58	-9471.50	1871.43	2324.14	786.25	11012.27	265.52
3701.52	-669 94	17094.65	5733 46	-7567.40	2396.23	8764 07	-9533.98	1788.28	2317.41	801.63	11013.72	264.55
3709.21	-562 29	16989.88	6554.31	-8124.89	2141.52	8927.47	-9609.91	1683.03	2311.65	822.77	11010.84	262.62
3692.87	-484.44	16953.35	7127.18	-8478.60	1897.38	9046.66	-9665.66	1607.10	2303.00	840.07	11017 08	261 66
3654.42	-408.50	16953.83	7738 49	-8834.24	1585.95	9122.59	-9703.15	1559 04	2295.31	842.00	11019.01	254.91
3641.92	-348 91	16959.12	8122.96	-9036.09	1358.15	9186.03	-9733.91	1519 63	2290.50	860.26	11033.42	253.95
3615.01	-317.19	16985.55	8424.77	-9186.03	1159.19	9254.28	-9766.59	1473.01	2283.77	870.83	11038.23	252 02
3432.39	-1505.21	15752.35	7546.25	-8942.85	1722.92	8419.01	-9517.64	1969.95	2103.07	-338.34	9936.71	1.38

Figure 3: 2D web strains at the back side for Specimen A-1

R1 (microstrain)			R2 (microstrain)			R3 (microstrain)			R4 (microstrain)			Load
R1-εx	R1-εy	R1-εxy	R2-εx	R2-εy	R2-εxy	R3-εx	R3-εy	R3-εxy	R4-εx	R4-εy	R4-εxy	(kN)
0 96	0.96	-0 96	0.00	0.96	-0.48	0.97	0.00	-0.48	0.00	0.00	0.00	12.95
-52.11	-41 49	80.58	4 81	-15.38	96.60	-59 83	-39.56	83.47	-7.72	10 61	93.12	27.41
-90.71	-72.37	141 37	9 61	-24 99	168.21	-103.25	-68.51	144.75	-13 51	22.19	162.60	38 01
-123.52	-98 43	193 96	13.46	-33.64	231.16	-139.92	-91.67	194.93	-16.40	32.81	217.60	46.69
-167.91	-135.10	264.41	18.26	-46.14	315.75	-188.17	-125 45	262.96	-22.19	46.32	296.73	59.22
-203.61	-163 08	319.41	22.11	-57 67	380 15	-222.91	-150.54	312.17	-26.05	56.93	355.11	67.90
-236.42	-190.10	371.52	24.99	-68.24	440.70	-255.72	-173.70	359.46	-30.88	67.55	409.15	75.61
-273.09	-221 95	430 86	27.87	-79.78	507.50	-290.46	-198.79	410.60	-35.70	77.20	468.50	85.25
-315.55	-257.65	499.86	30.76	-96.12	590.17	-332.92	-230.63	473.81	-44.39	89.74	537.01	95.85
-359.94	-296 25	573 20	33.64	-114.38	671.87	-374.41	-262.48	536.53	-53.07	99.39	604 08	106.46
-399.50	-330.99	637.37	34.60	-131.68	746.36	-411.08	-291.42	592.50	-61.76	108 08	662.94	115.13
-440.03	-365.73	703.96	34.60	-151.87	824.70	-448.72	-321.34	650.40	-48.25	111.94	712.16	124.77
-487.32	-407.22	785.01	35.56	-181.66	922.74	-491.18	-356.08	716.98	-66.58	129.31	777.29	135.38
-524.95	-439 07	849.67	35.56	-205.69	1026.06	-525.92	-384 06	771.50	-82.02	151.50	814.45	144.05
-566.44	-475 74	924.45	20.18	-240.30	1149.09	-563.55	-419.77	836.16	-22.19	141.85	826.03	153 69
-605.04	-507.58	994.41	10.57	-258.56	1265.88	-600.22	-452.58	896.95	26.05	158.26	851.60	163.33
-637.85	-524 95	1050 38	45.18	-229.72	1428.32	-635.92	-490.21	960.64	71.41	184.31	864.14	172.97
-672.59	-538 46	1104.42	126.88	-299 89	1610.94	-671.63	-531.71	1033.01	118 69	247.04	900.81	184.54
-702.51	-550.04	1154.12	260.48	-508.47	1851.24	-696.72	-565 48	1088.50	131.24	304.93	947.61	192.25
-732.42	-559.69	1200.92	377.75	-817 01	2151 61	-721.81	-602.15	1147.36	919 63	-65.62	2057.83	201.89
-764.27	-568 37	1252.07	555.56	-1395.64	2758.60	-749.79	-645.57	1217.81	1814.17	-523 02	3680.44	211.53
-791.29	-576.09	1295.49	835.27	-2096 34	3596.75	-771.99	-682.24	1275.22	2270.60	-890.68	4732.27	221.17
-817.34	-580.92	1337.95	1505 21	-3126.73	5392.72	-791.29	-719.88	1334.57	2483.87	-1245.79	5766.26	229.85
-846.29	-583.81	1380.89	2500.04	-4329 17	7965.81	-811.55	-763.30	1402.12	2458.78	-1664.60	7315.05	239.49
-873.31	-581.88	1415.63	3349.73	-5472.02	10740.26	-827.96	-804.80	1462 91	2370.96	-1848.91	9285.55	248.16
-911.91	-575.13	1457.61	4228 25	-6680.23	13682.93	-846.29	-860.76	1543 49	2497.38	-1803.55	11799.33	259.73
-936 03	-561 62	1476.42	4853 02	-7518.38	15881 15	-853 04	-905.15	1598.98	2514.75	-1543.01	14136.51	267.44
-962.09	-544.25	1491.38	5670.02	-8569.91	18589.77	-844.36	-963.05	1655.43	2537.91	-1171.49	16581.29	277.08
-992.00	-511.44	1493.79	6495.68	-9590.69	21145.08	-821.20	-1030.60	1708.50	2633.44	-881.99	18657 46	285.76
-1068 24	-388.89	1453.26	7651.98	-11109.36	24468.37	-757.51	-1153.15	1776.53	2719.32	-532.67	20906.34	295.40
-1526 60	707.33	906 60	10115.50	-14678.24	29112.81	-656.19	-1186.93	1730.21	2743.45	-318.44	21965.42	286.72
-2373.86	3682.37	-1165.70	11468 84	-15591 36	30420.98	-648.47	-1165.70	1707.05	2733.80	-277.92	22032.97	280.94
-3112 07	5449.26	-2355.52	11621 67	-15483.71	30354.18	-651.36	-1182.10	1723.46	2727.04	-244.14	22129.46	280.94
-4342.42	8105.85	-4024 94	11646 66	-15206.89	30182.13	-623.38	-1253.51	1763.51	2718.36	-147.64	22538.13	280.94
-5135 64	9670.09	-4936.37	11607.25	-15006.96	30024.98	-552.94	-1335.54	1779.91	2726.08	-91.67	22951.15	278.05
-5556.37	10483 57	-5405 83	11567.84	-14882.96	29907.70	-527.85	-1269.92	1701.75	2721.25	-97.46	22962.25	268.41
-6035.97	11397.41	-5914.38	11510.17	-14703.23	29832.26	-532.67	-1339.40	1767.85	2716.43	-92.64	23015.32	267.44
-6648.73	12589.16	-6579 25	11405 40	-14383.15	29772.67	-253.79	-1636.61	1818.51	2684.58	-7.72	23595.76	268.41
-7074 29	13441.24	-7054.02	11294.87	-14042.89	29752.95	2495.45	-5020.81	3224.49	2460.71	329.06	23887.67	261.66
-7289 48	13886 10	-7300 09	11217.97	-13799.71	29779 39	4330.84	-6967.18	3950.64	2554.31	486.35	23708.18	260.70
-7472.83	14257.62	-7498.40	11113.20	-13512.32	29809.19	5639.36	-8109.72	4183.20	2603.52	595.39	23570.18	260.70
-7555.81	14442.89	-7603.58	11046 88	-13327.77	29830.82	6522.32	-8790.99	4209.74	2651.77	670 66	23449.56	258.77
-7325.18	13731.70	-7219.52	10406.73	-13875.65	28528.41	5414.52	-7925.40	4316.37	2275.43	-469.95	21985.68	1.38

Figure 4: 2D web strains at the front side for Specimen A-2

R5 (microstrain)			R6 (microstrain)			R7 (microstrain)			R8 (microstrain)			Load
R5-εx	R5-εy	R5-εxy	R6-εx	R6-εy	R6-εxy	R7-εx	R7-εy	R7-εxy	R8-εx	R8-εy	R8-εxy	(kN)
0.00	-0.96	0.48	-0.97	0.97	0.00	0.00	0.00	0.96	0.00	0.00	0.00	12.95
8.68	-11.58	97.95	-43.42	-56.93	82.99	-35.70	-46.32	70.93	-0.96	9.65	91.19	27.41
15.44	-16.40	170.32	-74.30	-96.50	140.40	-62.72	-81 06	123.04	-1.93	19.30	161.15	38.01
22.19	-18.33	227.74	-97.46	-126.41	188.17	-83.95	-108.08	167.42	0.00	29.91	218.57	46.69
28.95	-24.12	311.21	-134.13	-169.84	252.34	-119.66	-146.68	229.67	-1.93	40.53	299.14	59.22
33.77	-27.02	372.97	-161.15	-201.68	300.11	-143.78	-177.56	275.50	-3.86	50.18	359.94	67.90
37.63	-27.98	430.38	-185.28	-229.67	344.50	-166.94	-203.61	319.41	-4.82	58.86	414.94	75.61
42.46	-28.95	494.07	-212.30	-262.48	394.68	-192.03	-235.46	370.07	-8.68	70.44	476.70	85.25
47.28	-28.95	567.89	-245.11	-299.14	452.58	-221.95	-272.13	428.45	-13.51	83.95	549.56	95.85
50.18	-27.98	643.16	-277.92	-335.81	512.41	-251.86	-310.72	487.80	-18.33	98.43	621.93	106.46
52.11	-27.02	710.23	-306.86	-368.62	563.55	-277.92	-343.53	540.39	-24.12	111.94	686.59	115.13
46.32	-25.09	773.92	-335.81	-402.40	617.11	-303.97	-377.31	594.43	-28.95	126.41	751.24	124.77
42.46	-9.65	848.22	-370.55	-440.03	680.31	-333.88	-418.80	661.01	-34.74	144.75	828.92	135.38
36.67	4 82	923.97	-397.57	-469.95	729.04	-358.97	-451.61	714.09	-36.67	173.70	905.15	144.05
55.97	-85 88	932.66	-430.38	-503.72	786.46	-385.99	-490.21	777.78	-53.07	214.23	981.87	153.69
82.02	-92.64	931.69	-462.23	-533 64	840.50	-410.12	-526.88	837.12	-64.65	291.42	1041.70	163.33
118.69	-122.55	940.86	-494.07	-563.55	896.47	-427.49	-567.41	896.95	-52.11	437.14	1066.79	172.97
169.84	-167.91	1039.29	-526.88	-591.53	952.92	-444.86	-612.76	963.05	-36.67	538.46	1088.50	184.54
200.72	-340.64	1382.34	-551.97	-606.01	991.04	-458.37	-650.40	1020.47	27.02	517.23	1149.29	192.25
579.95	-1087.54	2778.19	-579.95	-620.48	1030.60	-471.88	-689.96	1079.82	120.62	425.56	1295.97	201.89
1227.46	-1796 80	4112.76	-609.87	-635.92	1074.51	-487.32	-736.28	1150.26	262.48	182.38	1765.44	211.53
1645.30	-2521.50	5313.20	-635.92	-646.54	1111.18	-499.86	-773.92	1211.05	404.33	-87.81	2350.70	221.17
1997.51	-3310.86	6985.99	-661.98	-652.33	1143.50	-512.41	-813.48	1275.71	604.08	-409.15	3335.95	229.85
2451.06	-4013.36	9193.87	-690.93	-657.15	1178.73	-525.92	-857.87	1348.08	1104.91	-794.18	4937.82	239.49
3130.40	-4577.88	11282.58	-719.88	-655.22	1207.68	-534.60	-900.33	1415.15	1546 87	-1151.22	7194.91	248.16
3981.52	-5112.48	13685.38	-755.58	-652.33	1243.38	-544.25	-959.19	1502.48	2194.37	-1542.04	10182.50	259.73
4508.40	-5489.79	15666.01	-785.50	-639.78	1262.68	-549.08	-1005.51	1570.51	2599.66	-1634.68	12367.22	267.44
5057.47	-5850.69	17882.10	-824.10	-617.59	1280.53	-553.90	-1061.48	1651.09	3084.09	-1661.70	14917.67	277.08
5661.55	-6220.28	19984.31	-869.45	-579.95	1293.08	-547.15	-1125.17	1730.70	3519.29	-1548.80	17152.56	285.76
6401.69	-6508.81	22245.27	-941.82	-491.18	1279.08	-461.26	-1267.02	1812.72	3872.48	-931.21	19694.33	295.40
6724.00	-6442.23	23148.00	-949.54	-380.20	1196.58	507.58	-2122.00	1773.16	2877.58	2522.47	21517.19	286.72
6699.88	-6211.59	23059.23	-934.10	-380.20	1183.07	2013.92	-4323.12	2782.53	2284.11	3787.56	21011.53	280.94
6705.67	-6173.96	23113.75	-951.47	-383.10	1200.92	2812.93	-5390.39	3229.31	2290.87	3808.79	21004.30	280.94
6806.02	-6192.29	23521.46	-1011.30	-348.36	1224.08	4136.88	-6801.20	3556.44	2399.91	3676.58	21098.86	280.94
6945.94	-6220.28	23934.47	-1070.17	-260.55	1204.78	5067.12	-7600.20	3554.51	2467.46	3567.54	21190.06	278 05
6935.33	-6162.38	23909.85	-996.83	-236.42	1120.34	5595.94	-8015.15	3492.75	2491.59	3489.38	21230.58	268.41
6955 60	-6207.73	23933.98	-1069.20	-233.53	1180.17	6292.65	-8521.76	3343.67	2537.91	3401.56	21290.90	267.44
7283.69	-6313.88	24546.75	-1310.45	95.53	1118.90	7343.52	-9229.10	2993.38	2606.42	3247.17	21344.46	268.41
8175.33	-6400.73	25550.33	-3157.42	4414.80	-1132.41	8213.93	-9781.06	2605.45	2662.39	3090.84	21381.12	261.66
8206.21	-6266.60	25649.23	-4767.02	7623.36	-2894.95	8719.58	-10081.17	2338.63	2707.74	2991.45	21396.57	260.70
8137.70	-6131.50	25724.03	-5853.59	9687.46	-3980.07	9209.80	-10356.19	2045.76	2755.99	2861.17	21389.33	260.70
8082.70	-6050.44	25823.90	-6479 86	10920.71	-4640.60	9452.97	-10495.15	1901.98	2789 77	2786 87	21398.01	258.77
7097.45	-5875.78	23948.94	-5770 60	9784.93	-4339.53	8458.07	-10163.20	2466.98	2214.64	1812.24	19869.47	1.38

Figure 5: 2D web strains at the back side for Specimen A-2

R1 (microstrain)			R2 (microstrain)			R3 (microstrain)			R4 (microstrain)			Load
R1-εx	R1-εy	R1-εxy	R2-εx	R2-εy	R2-εxy	R3-εx	R3-εy	R3-εxy	R4-εx	R4-εy	R4-εxy	(kN)
0 00	0.00	0.00	-0.96	-0.96	0.96	-0.96	-1.93	1.45	-0.96	-0.96	0.00	0.00
-14 47	-23.16	34 26	-6.73	2.88	100.92	-34.74	-17.37	40.53	-8.65	-3.84	41.81	0.00
-30 88	-44 39	66.58	-10.57	5.77	180.22	-74 30	-42.46	93.12	-11.53	-11.53	109.57	4.27
-52.11	-72.37	108.56	-14 42	8 65	289.32	-126.41	-72.37	160.19	-14.42	-13.46	198.48	13 91
-66.58	-90.71	137.51	-16.34	7.69	353.23	-154.40	-91.67	198.30	-20.18	-2.88	241.26	23.55
-81.06	-113 87	168 87	-11.53	-9.61	438.30	-183.35	-111.94	237.39	10.57	-49.02	303.73	37.05
-97.46	-132.20	198.79	15 38	-60.55	543.55	-203 61	-130.27	272.13	52.87	-365 25	329.21	45.73
-111.94	-152 47	230.63	131.68	-288.36	669.46	-222.91	-151.50	301.07	37.49	-544.03	306.14	55.37
-127.38	-159 22	249.45	323.92	-914.09	858.34	-238.35	-160.19	325.68	-4.81	-659 37	267.69	65.01
-135 10	-161.15	259.10	499.82	-1723.40	1012.61	-245.11	-167.91	336.78	-36.52	-773.75	229.24	74 65
-147.64	-165 01	274 06	832.38	-3009.47	1354.79	-253.79	-178.52	353.18	-76.89	-918.89	182.62	85.25
-151.50	-166.94	279.85	1284.14	-4244.59	1683.03	-256.69	-183.35	360.90	-97.08	-1047.69	160.04	92.96
-157.29	-167.91	287.08	1853.16	-5685.40	2174.68	-259.58	-188.17	368.62	-115.34	-1178.41	159.56	104 53
-160.19	-171 77	291.42	2240.52	-6541.82	2458.23	-256.69	-196.86	370.55	-121.11	-1255.31	170.13	113.20
-161.15	-172.73	294.32	2979.67	-7831.72	3020 04	-254.76	-199.75	371.04	-115.34	-1320.67	212.42	123.81
-161.15	-174 66	296.25	3446.80	-8540.12	3330.02	-253.79	-195.89	368.62	-123.03	-1339.89	239.33	131.52
-158.26	-172.73	292.87	3921.63	-9178.34	3702.00	-211.33	-173.70	311 21	-103.81	-1049.61	63.44	143.09
-154.40	-168 87	288 05	4440 67	-9789.65	4147.99	-21.23	-46.32	51.14	55.75	-560.37	-319.59	151.76
-160.19	-178.52	296.73	4816.49	-10216.42	4468.54	-19.30	-31.84	41.01	167.25	-657.45	-347.95	160.44
-57 90	-50.18	100.36	5193.28	-10966.14	3388.17	115.80	162.12	-233.53	-110.54	-690.13	-657.93	164.30
-66.58	-57.90	117.25	5237.49	-10903.67	3391.54	213.26	218 09	-355.60	-247.99	-648.80	-701.18	170.08
-85 88	-86.85	156.81	5281.70	-10834.46	3438 63	248.00	140.89	-318.93	-198.00	-668.98	-743.96	155.62
-90.71	-97.46	168.39	5310.54	-10697.97	3369.43	242.21	135.10	-306.38	-199.93	-677.63	-736.75	157.55
-86 85	-98.43	170.80	5262 48	-10298.12	3371.35	237.39	137.99	-300.59	-198.97	-677.63	-739.15	167.19
-78.16	-97.46	161.15	5222.11	-10057.82	3470.35	228.70	134.13	-294.32	-198.00	-683.40	-736.75	172.01
-63.69	-113.87	162.12	4892.42	-9509 95	3479.49	222.91	128.34	-284.67	-198.97	-685.32	-737.23	177.79
-53.07	-119 66	157.77	4725.18	-9015.90	3659.23	222.91	126.41	-283.70	-198.97	-687.25	-737.23	180 68
-42.46	-113.87	142.82	4693.46	-8871.73	3734.68	232.56	130.27	-289.49	-201.85	-688.21	-736.27	184.54
-34.74	-101.32	127.86	4701.15	-8900.56	3720.26	248.00	135.10	-304.45	-201.85	-691.09	-734.83	186.47
-28.95	-93 60	114.35	4704 99	-8928 43	3704.40	249.93	127.38	-310.24	-203.77	-694.94	-734 82	186.47
199.75	273.09	-395.64	5522.00	-10813.32	2880.19	82.99	110.01	-163.08	-201.85	-696.86	-734.82	181.65
57.90	124.48	-143.30	5421.08	-10506.70	2851.35	94.57	112.90	-174.18	-201.85	-697.82	-734.34	177.79

Figure 6: 2D web strains at the front side for Specimen A-3

R5 (microstrain)			R6 (microstrain)			R7 (microstrain)			R8 (microstrain)			Load
R5-εx	R5-εy	R5-εxy	R6-εx	R6-εy	R6-εxy	R7-εx	R7-εy	R7-εxy	R8-εx	R8-εy	R8-εxy	(kN)
-0.96	0.00	0 48	0.00	-1.92	0.96	-0.96	0.00	0.48	2.88	-2.88	2.88	0.00
3.84	-26 91	90.35	-22.11	-40.37	56.23	-10.57	-25 95	28.84	4.81	20.18	42.29	0.00
4.81	-47 10	162.44	-46 14	-74.01	106.21	-22.11	-62.48	66.32	7.69	36.53	117.26	4.27
6.73	-63.44	257.12	-79.78	-120.15	173.97	-38.45	-111.50	117.26	11.53	63.44	222.03	13 91
4.81	-70.17	308.54	-96.12	-144.18	208.58	-47.10	-141.29	148.02	16.34	69.21	282.11	23.55
-10.57	-131 68	381.59	-114.38	-171 09	246.54	-59.59	-178.78	188.39	28.84	85.55	333.05	37.05
2.88	-344.10	418 60	-126.88	-187.43	272.50	-71.13	-213.38	223.96	43.25	86.51	402.26	45.73
-7 69	-474 82	365 25	-138.41	-207.62	298.93	-82.66	-253.75	264.33	50.94	24.99	498.37	55.37
-51.90	-546.91	306.14	-145.14	-224.92	319.59	-85.55	-296 04	298.45	84.58	-141.29	608.91	65.01
-86.51	-582.48	264.33	-146 10	-234.53	331 61	-84.58	-325.84	320.55	147.06	-278.74	661.77	74.65
-123 03	-596 89	232.13	-148 98	-249.91	344.58	-82.66	-364.29	345.55	232.61	-443.11	674.27	85.25
-142.26	-592 09	217.23	-148 02	-257.60	350.83	-80.74	-389.28	360.92	305.66	-599.78	670.91	92.96
-152.83	-560 37	210.50	-145.14	-268.17	356.60	-76.89	-414.27	375.34	364.29	-744.92	623.81	104.53
-154.75	-539 22	212 42	-143 22	-275.86	361.41	-76.89	-430.61	387.36	393.12	-844.88	611.31	113.20
-142.26	-469 06	227.80	-138 41	-283.55	363.81	-68.24	-445.99	391.68	438.30	-970.80	577.67	123.81
-132.64	-431.57	221.55	-132.64	-287.39	361.89	-65.36	-457.52	396.97	469.06	-1058.26	586.80	131.52
-99.00	-69 21	86 99	-105.73	-268.17	319.59	-60.55	-464.25	396.01	497.89	-1114.97	609.39	143.09
95.16	372 94	-124 47	21.15	-117.26	80.74	-53.83	-468.10	392.64	532.50	-1238 97	668.50	151.76
238.37	307.58	-100.92	32.68	-128.80	83 62	-54.79	-482.51	404.18	558.45	-1380.26	747.32	160.44
86.51	362.37	-297.49	193.20	-105.73	-85 06	20.18	-262.40	173.01	550.76	-1436.01	-0.48	164.30
14 42	343 14	-409 46	259.52	-36 52	-201.85	14.42	-277.78	188 39	537.30	-1376.42	6 25	170 08
-40.37	368.13	-378.23	227.80	48 06	-241.74	0.96	-327.76	239.33	556.53	-1305.29	86.03	155.62
-41.33	367.17	-373.42	221.07	47.10	-235.97	-6.73	-333.53	247.99	550.76	-1213.98	92.27	157.55
-39.41	366 21	-373.90	221.07	45 18	-231.16	-9 61	-330.65	249.91	586.32	-1053 46	168.21	167.19
-38.45	366 21	-374.38	217.23	45.18	-227.32	-6.73	-318.15	240.30	708.39	-1117.86	225.88	172.01
-39.41	365 25	-373.42	212.42	43.25	-222.99	-16.34	-296.04	234.05	802.59	-1190.91	241.26	177.79
-38 45	365 25	-373.90	213.38	46 14	-226.84	-20.18	-277.78	223 96	820 85	-1149.58	303.73	180.68
-38.45	364 29	-374.38	221 07	50 94	-237.89	-16.34	-255.67	203.29	821.81	-1157.27	302.29	184.54
-39.41	365.25	-373.42	232.61	58 63	-257.12	-7.69	-237.41	182.14	808.36	-1158.23	264.33	186.47
-39.41	364 29	-373.90	240.30	62 48	-265.77	-3.84	-223.96	167.73	780.48	-1190.91	243.66	186.47
-44 21	366 21	-373.42	89.39	43.25	-116.30	260.48	248 95	-396.97	606.51	-2633.64	-2014.16	181.65
-45.18	367.17	-374.38	99.00	47.10	-127.84	127.84	-7.69	-81.22	650.72	-2470.24	-1894.01	177.79

Figure 7: 2D web strains at the back side for Specimen A-3

R1 (microstrain)			R2 (microstrain)			R3 (microstrain)			R4 (microstrain)			Load
R1-εx	R1-εy	R1-εxy	R2-εx	R2-εy	R2-εxy	R3-εx	R3-εy	R3-εxy	R4-εx	R4-εy	R4-εxy	(kN)
-859 30	-656.49	119 67	-482 51	-907.36	476.75	-1101.52	-656.49	610.83	-951.57	-162.44	234.05	0.00
-859.30	-656 49	118.71	-483.48	-908.32	477.71	-1102.48	-656 49	610.35	-951.57	-162.44	233.09	18.73
-891.02	-713.20	185.03	-481.55	-909 28	558.93	-1147.65	-713.20	694 94	-945.80	-166 28	338.82	31.27
-937.15	-796 82	282.59	-477.71	-901.59	682.92	-1216.86	-796 82	824 21	-934 27	-170.13	503.18	49.58
-987.14	-885 25	388.32	-475.79	-890.06	807.87	-1287.99	-885.25	959.74	-931.39	-166.28	680.52	68 86
-1040 00	-979 45	500.30	-474 82	-879.48	933 79	-1364.88	-979.45	1104.88	-929.46	-163.40	880.92	88.14
-1112.09	-1072 68	636.78	-474 82	-877.56	1095.27	-1437.93	-1072.68	1252.42	-926.58	-151.87	1101.52	110.31
-1163.03	-1129 39	730.02	-474 82	-874 68	1207.25	-1477.34	-1129.39	1339.89	-914.09	-151.87	1247.14	125.74
-1227.43	-1201 48	851.13	-478.67	-862.18	1353.83	-1523.48	-1201.48	1451.87	-835.27	-158 60	1411.02	145.98
-1289.91	-1262 03	970.31	-488.28	-827.58	1495 12	-1560.00	-1262.03	1549 43	-222.03	-522.88	3214.68	166.22
-1338.93	-1317.78	1078 45	-492.13	-767 02	1647.47	-1566.73	-1317.78	1616.23	477.71	-913.12	5410.98	185.50
-1325.47	-1393.72	1144.29	-505.58	-536.34	1663.81	-1518.67	-1393.72	1649.39	1438.89	-1244.73	8635.27	202.86
-1213.98	-1520.59	1156.78	-795 86	84.58	2867.21	-1397.56	-1520.59	1658.04	2003.11	-1316 82	12879.86	219.24
-1042.88	-2187.65	1404.77	-625.73	-133.60	12110.92	-799.70	-2187.65	1737.82	2083.85	-622.85	16306.48	240.45
-350.83	-4894 35	2454.38	407.54	-214.34	17306.59	469 06	-4894.35	3492.94	1699.37	324.88	16021.00	245.27
928 50	-6482.22	3581.37	0.00	710.31	17088.40	1238 00	-6482.22	4543.51	1635.93	532.50	15952.77	251.06
1444 66	-7276.16	4227.77	-85.55	910.24	17027.36	1679.19	-7276.16	5004.40	1609.02	606.51	15921.53	254.91
1976.19	-8276.75	4879.45	-150.91	1057.30	16999.01	2381.81	-8276.75	5441.74	1598.45	686.29	15867.70	255.88
2340.48	-9345.59	5479.71	-189.35	1131.31	16979.31	3355.49	-9345.59	5712.31	1606.14	740.11	15816.76	251.06
2406.80	-10686.44	6162.15	-198.97	1129.39	16959.12	4895.31	-10686.44	5736.83	1628.25	789.13	15785.04	246.24
2405.84	-11985.00	6825.37	-200.89	1118 82	16943.26	6669 65	-11985.00	5375.90	1644.59	809.32	15758.12	245.27
2420.26	-12466.55	7064 70	-200.89	1132.27	16950.00	7393.42	-12466.55	5122.15	1646.51	815.08	15745.62	244.31
2426.03	-12730 88	7196.86	-201.85	1133.24	16949 03	7819.23	-12730.88	4943.37	1645.55	807.39	15734.57	245.27
1207 25	-12294.50	7560.19	-210.50	-506.54	15271.28	6605.25	-12294.50	5610.91	1655.16	-680.52	14294.72	1.38

Figure 8: 2D web strains at the front side for Specimen B-1

R5 (microstrain)			R6 (microstrain)			R7 (microstrain)			R8 (microstrain)			Load
R5-εx	R5-εy	R5-εxy	R6-εx	R6-εy	R6-εxy	R7-εx	R7-εy	R7-εxy	R8-εx	R8-εy	R8-εxy	(kN)
-346.99	-960.22	-28 84	NA	NA	NA	-5289.39	-3876.45	2403.92	-5895.90	-8207.55	10803.22	0.00
-346 99	-961.18	-28.35	NA	NA	NA	-5085.62	-2441.41	4518 04	-3283.40	-8380.56	9353.76	18 73
-348 91	-964 07	77.86	NA	NA	NA	-4875.12	-4719.41	-496.93	-5728 65	-6833 05	3832.72	31.27
-352.75	-962.14	246.06	NA	NA	NA	-4893.39	-4407.99	656.01	-7048.36	-6993.57	6897.93	49.58
-367.17	-957.34	424.84	NA	NA	NA	-5407.62	-4710.76	532.02	-7242.52	-7027.21	6623.52	68.86
-385.43	-950.61	625.73	NA	NA	NA	-5769.02	-4978.93	-71.13	-7170.43	-7003.18	4580.04	88.14
-401.77	-940.04	852.57	NA	NA	NA	-5850.72	-4964 51	226.84	-7553 94	-7213.68	5492.20	110.31
-391.20	-938.12	994.34	NA	NA	NA	-5638.30	-5259.60	-76 89	-7198.30	-7140.63	5012.57	125.74
-297.97	-931.39	1141.41	NA	NA	NA	-5731.54	-5331 69	92.27	-7457.82	-7366.51	5487.88	145.98
802 59	-1332 20	2819 63	NA	NA	NA	-6049.69	-4798.23	191.28	-7197.34	-7601.04	5928.58	166.22
1809 91	-1792.61	5305.73	NA	NA	NA	-5852.65	-5171.17	104 29	-7618.34	-7140.63	5151.46	185.50
2272.24	-2247.25	9378.27	NA	NA	NA	-6001.63	-5259.60	603.62	-7759.63	-7349.21	6514.42	202.86
2374.12	-2543 29	13149.95	NA	NA	NA	-6093.90	-5372.06	396.49	-7675.05	-7323.26	5579.67	219.24
1584.99	-2325.10	10133.76	NA	NA	NA	-6073.72	-5087.55	215.30	-7569.32	-7379.97	5837.75	240.45
2444.29	-1946.40	8961.11	NA	NA	NA	-5621.96	-5270.17	577.67	-7695 24	-7632 76	7135.35	245.27
2468.32	-1847 40	8782.34	NA	NA	NA	-5896.86	-5042.37	246.54	-7512.61	-7674.09	6788.84	251.06
2504.84	-1787 80	8590.10	NA	NA	NA	-6972.43	-4443.55	757.89	-7168.51	-8135.46	8170.06	254.91
2505.81	-1778.19	8543.48	NA	NA	NA	-5838.23	-5197.12	421.48	-7580.86	-7345.37	6262.59	255.88
2501.00	-1769.54	8489 65	NA	NA	NA	-5770.95	-5437.42	213.86	-7452.06	-7550.10	6168.88	251.06
2450.06	-1710.91	8423.33	NA	NA	NA	-5722.89	-5271.13	775.68	-7743.29	-7665.44	7597.68	246.24
2350.09	-1587.88	8356.05	NA	NA	NA	-6048.73	-4370.50	1115.93	-7113.72	-8226.77	9469.58	245.27
2293.38	-1536.93	8305.11	NA	NA	NA	-5340.34	-4704.03	1676.30	-6857.08	-8553.57	11035.83	244.31
2258.78	-1501.37	8287.32	NA	NA	NA	-5957.42	-4950.10	722.81	-7533.76	-7877.86	7885.55	245.27
2162.66	-1709.95	7628.43	NA	NA	NA	-5640.23	-5069.28	260.48	-7346.33	-7638.53	6974.35	1.38

Figure 9: 2D web strains at the back side for Specimen B-1

R1 (microstrain)			R2 (microstrain)			R3 (microstrain)			R4 (microstrain)			Load
R1-εx	R1-εy	R1-εxy	R2-εx	R2-εy	R2-εxy	R3-εx	R3-εy	R3-εxy	R4-εx	R4-εy	R4-εxy	(kN)
0 00	-0 96	0 48	-0 96	-0.96	0.96	0.00	0.00	0 00	0 00	-0.96	0.48	3.31
-4 81	-93 23	63 44	-3.84	0.00	68 24	-13.46	-59.59	53.83	1.92	2.88	47.58	14.88
-6.73	-155.71	107.17	-5.77	0.00	115 34	-24.03	-104.77	96.12	3.84	2.88	83.14	24.52
-10.57	-245.10	167.25	-7.69	0.96	180.22	-39.41	-172 05	156.67	7.69	3.84	134.57	37.05
-13.46	-316.23	215.79	-10.57	0.96	233.57	-51.90	-225 88	205.21	10.57	4.81	175.90	46.69
-16.34	-375.82	256.64	-12.50	1.92	275.38	-61.52	-271.05	246.06	13.46	4.81	210.02	55.37
-17.30	-443.11	301.33	-13 46	1.92	323.92	-70.17	-322.00	290.28	16.34	5.77	247.50	65.01
-20.18	-519 04	352.27	-15.38	2.88	377.26	-81.70	-379 67	341.22	20.18	7.69	288.84	74.65
-21.15	-592.09	400.81	-18.26	3.84	427.25	-91.31	-434 46	388.80	23.07	11.53	329.69	84.28
-22.11	-665 14	448.39	-22.11	5.77	475.31	-99.96	-490.20	436.38	24.99	18.26	367.65	93.92
-23.07	-749.72	504.62	-24.99	8 65	531.05	-111.50	-554 60	493.57	27.87	25.95	414.27	103.56
-23 07	-831.42	557.97	-28.84	10.57	584.88	-121.11	-616 12	546.43	30.76	34 60	457.52	114.17
-24.03	-990.98	660.33	-33.64	20.18	700.70	-142.26	-740.11	653.60	32.68	50.94	541.63	122.84
-24.03	-990.02	659.85	-33.64	22.11	700.70	-142.26	-740.11	653.60	32.68	52.87	541.63	133.45
-24.03	-1067.88	709.35	-36.52	25.95	759.82	-151.87	-800 67	707.91	33 64	61.52	583.92	142.12
-24.03	-1148 61	760.30	-38.45	30.76	826.62	-162.44	-865.07	762.70	33.64	72.09	628.61	151.76
-23.07	-1225.51	808.84	-40.37	43.25	906 88	-173.01	-926.58	817.01	34.60	81.70	670.43	161.40
-23.07	-1300.48	855.93	-40.37	52.87	985.69	-182 62	-988.10	869.87	33.64	94.20	714.64	171.04
-21.15	-1382.18	905.43	-41.33	63.44	1073.16	-192.24	-1053.46	928.50	33 64	104.77	761.26	180.68
-20.18	-1461.00	953.97	-41.33	79.78	1172.64	-201.85	-1119.78	984.73	31 72	118.23	806.43	190.32
-17.30	-1539.82	1000.59	-46.14	100 92	1281.74	-211.46	-1183.22	1041.44	28 84	131.68	853.05	199.96
-15.38	-1618.63	1047 69	-54.79	122.07	1402.37	-220.11	-1250.50	1099.59	24.03	147.06	900 63	208 64
-10 57	-1703.22	1097.19	-71.13	167.25	1548.47	-231.65	-1316.82	1165.43	40.37	198.97	953.97	219.24
-6.73	-1774.35	1139 48	-85.55	196.08	1656.60	-240.30	-1374.49	1221.66	48.06	226.84	992.90	227.92
-2.88	-1847.40	1185.62	-116 30	267 21	1784.44	-249.91	-1434.09	1284.14	72.09	261.44	1027.99	237.56
0.96	-1919 48	1231.28	-147.06	359.48	1900.74	-261.44	-1487.91	1344.70	55.75	318.15	1027.99	248.16
5.77	-1981.96	1271.65	-146.10	449.83	2026.18	-272.01	-1523.48	1391.79	99.00	374.86	1040.48	256.84
11.53	-2056.93	1321.63	-119.19	518.08	2197.75	-283.55	-1560.00	1440.81	70.17	404.66	1050.57	267.44
19.22	-2125.18	1367.28	-148.02	630 54	2408.73	-292.20	-1587.88	1483.11	518.08	205.69	1981.48	276.12
28.84	-2206.88	1422.55	-151.87	668.02	2908.06	-297.97	-1635.93	1536.93	1096.71	-54.79	3186.32	285.76
46.14	-2323.18	1500 89	-203.77	667.06	3541.96	-302.77	-1689.76	1597.97	1648.43	-346.99	4464.70	296.36
59 59	-2421.22	1568.17	-261.44	694.94	6386.58	-306.62	-1745.51	1658.52	1804.14	-484.44	4891.94	305.04
78.82	-2539.45	1649.39	130.72	800.67	12301.71	-305.66	-1818.56	1733.01	2137.67	-927.54	6564.40	314.68
108 61	-2719.19	1772.42	479.63	676.67	15403.45	-305.66	-1901.22	1816.64	2895.09	-1801.26	11937.90	324.32
141.29	-2924 88	1917.56	668.98	705.51	17485.85	-304.70	-2031.94	1916.12	3131.54	-2017.52	14528.76	333.96
177.82	-3186.32	2104.99	889.09	720.89	19532.69	-303.73	-2130.94	2001.66	3322.81	-2043.48	16024.37	342.63
221.07	-3514 09	2353.94	1108 25	752.61	21649.70	-305.66	-2226.10	2110.76	3501.59	-2000.22	17503.16	351.31
302.77	-4117.71	2836.93	1394.68	858.34	24686.07	-306.62	-2352.98	2246.77	3741.89	-1907.95	19370.73	360.95
381.59	-4731.91	3377.60	1595.57	1031.35	26587.78	-311.42	-2460.63	2369.32	3951.43	-1817.60	20891.33	367.70
479 63	-5639 26	4262 85	1818.56	1223.59	26372 47	-317.19	-2610.57	2547.14	4245.55	-1632.09	22980.46	376.37
579.59	-6950.32	5712.31	1386 03	1548.47	24963.37	-348.91	-2846.06	2885.47	4733.83	-1194.75	26320.09	386.98
667 06	-7998.01	6929.65	1682.07	1471.57	22966 04	-366.21	-3063.29	3188.25	5067.36	-715.12	28642.31	394.69
616.12	-9869 43	9295.13	3764.96	785.29	18405.70	-329.69	-3526.58	3722.66	2674.97	743.96	8703.03	402.40
495.97	-10347.14	10294.76	3830.32	660.33	17212.87	1653.24	-6552.39	4179.71	1325.47	-263.36	7789.91	372.52
502.70	-10227 96	10203.93	3822 63	583.44	16519.86	3557.34	-10098.19	5452.31	1218.78	-236.45	7761.56	361.91
514.23	-10051.10	10067.44	3806.29	601.70	16416 06	5404.74	-12994.24	6058.34	1204.36	-211.46	7730.32	348.42
525.77	-9829 06	9898.75	3793.79	587 28	16306.48	7415.53	-15379.90	5976.64	1192.83	-197.04	7725.03	332.99
534 42	-9636 83	9752.17	3784 18	570.94	16216.61	9042.81	-16747.66	5401.85	1191.87	-195.12	7712.06	319.50
540.19	-9501.30	9649.80	3776.49	560.37	16107.51	10125.11	-17432.98	4796.78	1184.18	-189.35	7687.06	310.82
544 99	-9399 41	9574.35	3771 68	552 68	16062.82	10829 65	-17798.24	4307.07	1182.26	-188.39	7674.09	304.07
546 91	-9304.26	9501.78	3764.96	545.95	16009.00	11444.81	-18079.86	3812.53	1170.72	-175.90	7641.89	298.29
548.84	-9239.86	9453.24	3760.15	541.15	15946.52	11831 21	-18245.19	3477.08	1168.80	-178.78	7620.26	294.43
549.80	-9182.19	9408.55	3755.34	536.34	15909.99	12129.17	-18366 29	3200.26	1169.76	-180.70	7604.40	291.54
552.68	-9112.02	9355.68	3751.50	533 46	15873.95	12384 85	-18463.38	2950.84	1169.76	-181.66	7593.35	286.72
553.64	-9058.19	9311.95	3745.73	529.61	15822.04	12551.13	-18529.70	2785.51	1166.88	-183.59	7571.72	283.83
556.53	-8984.18	9256.20	3741.89	526.73	15788.88	12735 68	-18598.90	2596.16	1167.84	-185.51	7558.75	279.97
556.53	-8931.32	9215.35	3737.08	524.81	15755.73	12831.80	-18640.23	2500.52	1166.88	-186.47	7541.45	277.08
395.05	-5241.33	5957.42	3504.48	457.52	15127.11	11894.65	-18171.18	3247.84	1156.30	-156.67	7509.73	1.38

Figure 10: 2D web strains at the front side for Specimen B-2

R5 (microstrain)			R6 (microstrain)			R7 (microstrain)			R8 (microstrain)			Load
R5-εx	R5-εy	R5-εxy	R6-εx	R6-εy	R6-εxy	R7-εx	R7-εy	R7-εxy	R8-εx	R8-εy	R8-εxy	(kN)
0.00	0.00	0 96	0.00	-0.96	0.48	0.00	0.00	0 00	0.00	0.00	0.00	3.31
9 61	-14 42	69.69	-7 69	-73 05	56.71	-18.26	-57.67	62 00	3.84	-2.88	64.88	14.88
16.34	-24 03	123.03	-13.46	-125.92	98.52	-30.76	-97.08	104.29	5.77	-4.81	112.94	24.52
25 95	-39 41	198.96	-23.07	-202.81	160.04	-48.06	-151.87	161.48	8 65	-5.77	176.38	37.05
33 64	-50.94	257.60	-29.80	-262.40	206.65	-62.48	-195.12	209.54	11.53	-7.69	228.76	46.69
39 41	-59 59	307.10	-35.56	-308.54	244.14	-74.97	-230.68	247.99	12.50	-8 65	272.98	55.37
46.14	-68.24	359.00	-41.33	-359.48	284.99	-87.47	-269.13	289.80	15.38	-9.61	320.07	65.01
52.87	-78 82	421.48	-49.98	-416.19	332 09	-103.81	-312.38	338.82	17.30	-10.57	375.34	74.65
59.59	-88.43	477.71	-55.75	-469.06	375.82	-119.19	-354.68	386.88	20.18	-9.61	425.32	84.28
65.36	-99.96	531.53	-63.44	-521.92	418.60	-135.53	-396.01	433.97	21.15	-8.65	474.34	93.92
72.09	-111 50	595.45	-70.17	-582.48	469.54	-153.79	-444.07	489.24	23.07	-6.73	531.05	103.56
78.82	-123 03	654.57	-76.89	-639.19	517.60	-171.09	-489 24	542.59	24.99	-4.81	584.88	114.17
89.39	-147.06	770.87	-91.31	-753.57	611.79	-207.62	-576.71	644.95	25.95	-0.96	708.39	122.84
89.39	-146.10	768.47	-91.31	-751.65	610.83	-206.65	-575.75	643.99	25.95	0.00	709.83	133.45
94.20	-157.63	826.62	-97.08	-807.39	656.97	-224.92	-617.08	694.94	27.87	2.88	769.91	142.12
98 04	-170.13	887.65	-103 81	-866.03	705.03	-244.14	-661.29	746.84	30.76	4.81	836.71	151.76
101.89	-180.70	944 84	-108 61	-921.78	751.65	-262.40	-701.66	796.34	30.76	13.46	921.78	161.40
103.81	-192.24	1001.55	-114 38	-976.56	797.30	-281.63	-742.03	846.32	34.60	16.34	1001.07	171.04
105.73	-201 85	1064 03	-119.19	-1036.16	846.80	-301.81	-783.36	899.19	42.29	18.26	1089.50	180 68
105.73	-211.46	1123.62	-123 99	-1090.94	893.90	-322.00	-823.73	949.65	47.10	24.03	1186.10	190.32
105.73	-222.03	1185.62	-126.88	-1148.61	942.44	-343.14	-864.10	1001.55	45.18	35.56	1291.83	199.96
103.81	-232 61	1247.62	-131.68	-1207.25	991.46	-364.29	-903.51	1052.02	48.06	40.37	1407.17	208.64
111.50	-250.87	1323 07	-129.76	-1271.65	1045.77	-387.36	-944.84	1106.32	35.56	66.32	1538 86	219.24
125.92	-261.44	1383.62	-128.80	-1326.43	1090.94	-405.62	-979.45	1151.02	32.68	84.58	1630.17	227.92
150.91	-271.05	1445 14	-125.92	-1389.87	1143.33	-423.88	-1013.09	1195.23	16.34	138.41	1733.49	237.56
196.08	-332.57	2051.17	-118.23	-1460.04	1196.67	-442.14	-1044.81	1236.56	25.95	192.24	1833.46	248.16
222.03	-346.99	2339.52	-108 61	-1524.44	1243.29	-455.60	-1070.76	1269.72	14.42	222.03	1949.28	256.84
478.67	-447.91	3484.29	-98.04	-1595.57	1296.64	-471.94	-1098 63	1307.21	44.21	258.56	2152.57	267.44
646.88	-507.50	3823.11	-88.43	-1653.24	1340.85	-483.48	-1117.86	1333.16	14.42	283.55	2460.63	276.12
749.72	-619 00	4383.00	-72.09	-1732.05	1400.93	-497.89	-1139.96	1363.92	-79.78	236.45	2948.43	285.76
1105.36	-898.71	5990.58	-53.83	-1813.75	1465.32	-514.23	-1159.19	1396.12	-223.96	284.51	3551.09	296.36
1537.89	-1276.45	8374.79	-38.45	-1880.08	1515.79	-526.73	-1170.72	1417.75	-8.65	238.37	5515.75	305.04
2270.32	-1857.97	12229.62	-18.26	-1957.93	1576.34	-539.22	-1177.45	1436.01	449.83	309.50	11513.05	314.68
2871.06	-2260.70	15851.35	2.88	-2039 63	1638.34	-555.56	-1184.18	1459 08	903.51	328.72	16208.44	324.32
3094.05	-2390.46	17601.20	44 21	-2134.79	1707.54	-571.90	-1182.26	1475.90	1118.82	442.14	18579.68	333.96
3320.89	-2531.76	19252.98	74 01	-2215.53	1767.62	-585.36	-1167.84	1485.03	1360.08	516.16	20827.88	342.63
3574 64	-2685.55	21046.55	80.74	-2340.48	1881.52	-603.62	-1142.85	1493.20	1598.45	600.74	23152.03	351.31
3944.70	-2924.88	23513.91	104.77	-2486.58	1993.49	-627.65	-1091.91	1497.04	1921 41	768.95	26471.47	360.95
4238.82	-3120.96	25497.80	120.15	-2596.16	2081.92	-642.07	-1038 08	1492.72	2159.78	968.87	29194.50	367.70
4613 68	-3401.63	28197.76	163 40	-2802.81	2234.75	-691.09	-966.95	1530.68	2501.00	1234.16	29539.09	376.37
5230.76	-3889.91	31212.03	256.64	-3110.39	2439 00	-794 90	-885.25	1629.21	3021.00	1649.39	29071.47	386.98
5582.55	-4360.89	31271.63	335.45	-3351.65	2596.16	-748.76	-839.11	1593.64	3434.31	1882.00	28748.52	394.69
5796.90	-5574.87	31771.44	390.24	-3516.97	2704.29	-500.78	-740.11	1251.94	852.57	837.19	12502.11	402.40
4626.18	-3047.91	17053.32	-899.67	-348 91	1902.66	-301.81	-708.39	972.24	777.60	743.96	12282.48	372.52
4489.69	-2732.65	15113 65	-2336 64	3050.80	765.58	-298.93	-726.65	983.77	754.53	707.43	12044.11	361.91
4480.08	-2752.83	14671.99	-4039 85	6276.53	64.88	-295.08	-743.96	990.50	745.88	702.63	11940.30	348.42
4452.20	-2715 34	14389 40	-5984.33	9385.96	-229.24	-288.36	-762.22	991.46	738.19	698.78	11864.37	332.99
4384.92	-2609 61	14170 25	-7544.33	11477.49	-101.88	-279.70	-774.71	987.62	734.34	695.90	11790.84	319.50
4294.57	-2451.02	13975 61	-8471 87	12551.13	140 34	-272 02	-782.40	983.77	727.62	693 01	11692.80	310 82
4225.36	-2298.19	13876.12	-8974.57	13051.91	347.95	-266.25	-786.25	979.93	726.65	691.09	11650.99	304.07
4141.74	-2130.94	13759.34	-9324 44	13358.53	533.94	-262.40	-791.05	975 60	722.81	688.21	11603.41	298 29
4071.57	-2005.99	13640 64	-9513.80	13520 01	647.84	-258.56	-793.94	973.20	716.08	690.13	11547.18	294.43
4014.86	-1917.56	13548 85	-9648.36	13624.78	742.51	-255.67	-795.86	970.80	713.20	690.13	11509.22	291.54
3950.46	-1821.44	13469.55	-9759.86	13704 55	831.43	-251.83	-796.82	966.47	711.28	689.17	11477.01	286.72
3895 68	-1758.01	13366.21	-9841.56	13765.11	892.94	-248.95	-797.78	963.59	709.35	688.21	11425.59	283.83
3792.83	-1545.58	13261.45	-9949.21	13835.28	988.58	-244.14	-797.78	956.38	707.43	686.29	11397.71	279.97
3727 47	-1425.44	13167.73	-10022.26	13884.29	1050.58	-241.26	-798.74	954.46	706.47	686.29	11360.71	277 08
3732.28	-1792.61	12950.99	-9502.26	13254.72	777.60	-16.34	-233 57	263.36	707.43	696.86	11316.50	1.38

Figure 11: 2D web strains at the back side for Specimen B-2

R1 (microstrain)			R2 (microstrain)			R3 (microstrain)			R4 (microstrain)			Load
R1-εx	R1-εy	R1-εxy	R2-εx	R2-εy	R2-εxy	R3-εx	R3-εy	R3-εxy	R4-εx	R4-εy	R4-εxy	(kN)
0 00	0.00	0.00	-0.96	0 96	0 00	-0.96	-0.96	0.96	-0.96	-0.96	0.00	3.31
12.50	-60.55	22.11	0.00	1.92	25.95	18.26	-76.89	22.59	-3.84	4.81	31.24	12.95
24 99	-121.11	43.25	0 00	3.84	52.87	37.49	-151 87	43.73	-5.77	10.57	62.96	21.63
41.33	-197.04	72.09	0.00	5.77	86 51	61.52	-248.95	70.65	-9 61	19 22	102.85	34.16
51.90	-250.87	91 79	-0 96	7.69	109.09	77.86	-318.15	90.35	-12.50	24.03	130.72	42.83
69.21	-331.61	120 63	-1.92	12.50	143.70	104.77	-421.96	119.19	-15.38	34.60	171.09	54.40
78.82	-382.55	139.37	-3.84	16.34	165 80	120.15	-487.32	138.41	-17.30	39.41	193.68	62.11
91.31	-448 87	163.40	-4 81	20.18	193.20	143.22	-572.87	161.00	-20.18	45.18	223.96	71.75
105 73	-518.08	188.87	-6.73	24 03	222.03	165.32	-661 29	186.47	-23 07	49 98	254 71	81.39
119.19	-584.40	211.46	-7.69	29 80	248.47	185.51	-743.96	210.98	-24.99	55.75	282.59	91.03
132.64	-653.60	236.45	-10.57	34.60	275.38	207.62	-829.50	235.01	-26.91	61.52	310.46	100.67
148 98	-740.11	265.77	-13 46	40.37	309 50	234.53	-937.15	265.77	-30.76	66.32	346.51	112.24
160.52	-804.51	288.36	-16 34	45.18	333.53	253.75	-1014 05	287.87	-33.64	71.13	372.46	120.92
172.05	-867.95	311.42	-18.26	49.98	358.04	272.98	-1089.98	310.46	-36.53	75.93	397.45	128.63
186.47	-949.65	340.26	-21.15	54.79	389.76	297.01	-1188 02	338.82	-40.37	82.66	428 69	139.23
200.89	-1032.31	369.57	-24.03	60.55	420 04	321.04	-1284.14	366.21	-44.21	88.43	460.41	148.87
214.34	-1111 13	397.45	-26.91	64.40	448.39	343.14	-1375.45	393.12	-48.06	93.23	488.76	158.51
226.84	-1188 98	426.28	-30 76	70.17	475.31	364.29	-1462.92	418.60	-51.90	99 00	516.64	168.15
241.26	-1277 41	459.45	-33.64	74.97	506.06	391.20	-1558.08	444.07	-55.75	105.73	546.91	177.79
254.71	-1359 11	489.72	-37.49	79.78	534.42	414.27	-1646.51	469.06	-59.59	111.50	574.79	187.43
269.13	-1453 31	524.81	-40.37	83 62	565.66	438 30	-1744.55	496.45	-64 40	117.26	606.03	197.07
283.55	-1553 27	561.81	-43.25	88.43	596.41	465.21	-1845.47	523.84	-69.21	123 03	634.38	207.68
297.97	-1646 51	597.38	-47.10	93.23	624.77	492.13	-1942 55	549.32	-73.05	127.84	662.74	216.35
312.38	-1739.74	631 02	-50 94	97.08	652.64	517.12	-2034.83	572.38	-77.86	132.64	689.65	225.99
329 69	-1847.40	675.23	-54.79	100.92	683.40	547.87	-2143.44	598.82	-83.62	136 49	720.41	236 60
344.10	-1934 86	712.72	-57 67	104.77	709.83	577 67	-2240.52	618 04	-87.47	141.29	745.88	245.27
357.56	-2027.14	759.82	-60.55	106.69	739.15	612.27	-2346.25	637.26	-96.12	146.10	776.64	254.91
363.33	-2104 99	816 04	-64 40	109 58	767.50	645.92	-2443.33	652.64	-101.89	148.98	802.11	263.59
348 91	-2176 12	879 96	-68 24	111.50	798.26	693 01	-2556.75	656.97	-110.54	152.83	832.38	274.19
339.30	-2243.40	943 40	-72.09	112.46	824 70	718.97	-2630.76	665.62	-116.30	155.71	857.86	283.83
327.76	-2291 46	1003.00	-74 97	110.54	851.13	723.77	-2643.26	658.89	-123.03	159.56	880.44	292.51
299.89	-2311.65	1101.04	-78.82	108 61	880 92	723.77	-2674 01	660.81	-130.72	161.48	907.36	303.11
272.02	-2314.53	1201.00	-80.74	106.69	905.92	699.74	-2657.67	654.09	-136.49	163.40	928.50	312.75
249.91	-2339 52	1296 64	-84.58	99.96	932.35	669.94	-2673.05	657.45	-141.29	161.48	949.17	322.39
226.84	-2361.63	1385.55	-86.51	94.20	956.38	712.24	-2693.24	674.27	-146.10	162.44	966.47	331.07
177.82	-2462.55	1448.98	-89.39	87.47	982.33	1460.04	-3744.77	937.63	-150.91	162.44	985.21	340.71
236.45	-2499 08	1446.58	-91.31	79.78	1002.51	2647.10	-5476.82	1156.30	-154.75	160.52	997.71	350.35
259.52	-2557.71	1500.89	-94.20	74.01	1025.10	4548.32	-8016.27	1484.07	-158 60	161.48	1013.57	359.99
278.74	-2636.53	1580.67	-97.08	65.36	1045.29	5635.42	-10291.39	2095.38	-163.40	166.28	1025.10	369.63
328 72	-2805 70	1721.96	-100.92	58.63	1057.30	6250.58	-11908.10	2577.89	-170.13	170.13	1038.08	378.30
700.70	-3461.22	2143.44	-103.81	60.55	1059.70	7314 61	-14017.90	3181.52	-177.82	185 51	1048.65	386 98
1108.25	-4798.23	2909.98	-107.65	66.32	1047.21	8687.18	-16355.50	3822.63	-186.47	200.89	1059.71	395.65
1497.52	-6385.14	4254.68	-114 38	85.55	1030.39	9880.97	-18335.54	4379.15	-194.16	215.31	1069.80	403.37
2066.55	-8979.38	7718.30	-138.41	123 99	989.54	11577.46	-21169.11	5104.36	-205.69	231.65	1077.01	409.15
1963.70	-9068.77	11291.02	-182.62	258 56	906.88	13029.80	-23744.12	5746.44	-214.34	249.91	1087.58	413.97
1227.43	-9152.39	14443.23	-213.38	371.98	845.36	13881.41	-25278 17	6158.79	-222.99	264 33	1094.31	415.90
3752.46	-7648.14	12150.80	-223.96	428.69	721.37	14247 62	-25882.75	6329.88	-227.80	276.82	1066.43	402.40
4307.06	-7025.29	12101.30	-228.76	454 64	645.43	14229.36	-25804.90	6309.69	-230.68	292.20	1044.81	391.80
5621.00	-6299.60	8957.27	-235 49	483 48	584.40	14201.49	-25710.70	6281.33	-235.49	313.35	1024.14	380.23
5951.65	-6075.64	8462.74	-237.41	486.36	555.08	14181.30	-25647.26	6262.59	-238.37	327.76	1009.72	374 45
6037.19	-5838.23	7677.45	-235.49	489.24	515.19	14150.54	-25545 38	6232.80	-240.30	342.18	979.45	365.77
6080 45	-5681.56	7377.56	-239.33	494.05	473.38	14114.02	-25425.23	6198.67	-241.26	354.68	946.77	358.06
6103.52	-5612.35	7323.74	-241 26	508.47	442.14	14113.06	-25429 07	6198.19	-246.06	372.94	955.42	356.13
5828.62	-5341.30	6934.46	-198.97	13.46	-93.72	12703.96	-21704.49	5306.70	-117.26	-21.15	-185.51	1.38

Figure 12: 2D web strains at the front side for Specimen B-3

R5 (microstrain)			R6 (microstrain)			R7 (microstrain)			R8 (microstrain)			Load
R5-εx	R5-εy	R5-εxy	R6-εx	R6-εy	R6-εxy	R7-εx	R7-εy	R7-εxy	R8-εx	R8-εy	R8-εxy	(kN)
0 00	0 00	0.96	0.96	0.96	0 96	0 00	0.00	0 96	0 00	0.96	0.48	3 31
1.92	-2.88	37.01	17.30	-82.66	24 99	11.53	-57.67	20.18	0.00	0.96	28.35	12.95
2.88	-6.73	72.09	32.68	-162.44	48.54	22.11	-116.30	41.33	0.00	0.96	58.15	21 63
3 84	-9 61	119 19	51.90	-265.29	79.78	35.56	-189.35	68.24	0.00	1.92	94.20	34.16
4.81	-12 50	150 91	65.36	-335.45	100 44	45.18	-240.30	85.06	0.00	0.96	120.63	42.83
6 73	-16.34	198 00	85.55	-441.18	134.57	60.55	-318.15	114.38	-0.96	0 96	159.56	54.40
7.69	-19 22	225 88	98 04	-505.58	154.75	69.21	-366.21	133.12	-1.92	0.96	184.07	62.11
9.61	-22.11	260.00	113.42	-589 21	183.11	81.70	-429 65	157 63	-2.88	0.96	215.31	71.75
10.57	-26.91	296.53	128 80	-674.75	211.46	95.16	-495.97	184 07	-3.84	0.96	248.47	81.39
11.53	-28 84	327.76	144.18	-753.57	237.41	107.65	-558.45	210.02	-4.81	2.88	280.67	91.03
11.53	-31.72	360.92	158 60	-835.27	265.29	120.15	-623.81	238.37	-6.73	1.92	313.83	100.67
11.53	-36.52	402 74	176.86	-935.23	296.53	136.49	-706 47	274 42	-8 65	2.88	354.68	112 24
11.53	-38 45	431 57	191.28	-1009 24	320.55	148 02	-766.06	301.33	-10.57	2.88	386.40	120.92
12.50	-40.37	458.97	204.73	-1080.37	344.58	160.52	-825.66	328.72	-11.53	2.88	415.71	128.63
11 53	-44.21	495 01	222.99	-1173.61	375.34	175.90	-901.59	362.85	-13.46	2.88	453.20	139.23
11.53	-48.06	529.61	239.33	-1264.92	405.14	191.28	-978.48	398.41	-16.34	2.88	491.16	148.87
10.57	-51.90	560.85	255 67	-1351.42	432.53	204.73	-1049.61	432.05	-18.26	1.92	524.33	158.51
9 61	-55.75	592.09	272.02	-1435 05	460.41	219.15	-1120.74	465.21	-20.18	1.92	558.93	168.15
9 61	-59 59	625.73	290 28	-1527.32	488.76	234.53	-1196.67	502.22	-22.11	1.92	594.49	177.79
8 65	-63.44	656 01	307.58	-1613.83	515.67	249.91	-1269.72	537.78	-24.99	0.96	629.09	187.43
7.69	-69.21	690.13	325.84	-1707.06	543.55	266.25	-1349.50	577.19	-27.87	0.96	666.10	197.07
7 69	-74 01	722.33	346 03	-1805.10	572.87	283.55	-1430.24	619.48	-30.76	0.00	702.63	207.68
7.69	-80.74	752 61	367.17	-1902.18	600.26	299.89	-1504.25	657.93	-32.68	-0.96	737.71	216.35
6.73	-87.47	784.33	387.36	-1993.50	624.29	314.31	-1576.34	696.38	-35.56	-1.92	771.35	225.99
4.81	-95.16	817.01	412.35	-2103.07	652.16	331.61	-1657.08	743.48	-38.45	-3 84	808.36	236.60
4.81	-101.89	845.36	437.34	-2201.11	673.31	345.06	-1725.32	783.36	-39.41	-4.81	840.07	245.27
-0.96	-108 61	878.52	466.17	-2311.65	697.82	360.44	-1802.22	829.50	-42.29	-7.69	875.64	254.91
-4.81	-115.34	907.84	494.05	-2417.38	720 41	371.98	-1874.31	876.12	-45.18	-10.57	910.24	263.59
-10.57	-127.84	941.96	526.73	-2556.75	755.49	384.47	-1966.58	942.92	-48.06	-16.34	948.21	274.19
-13 46	-138 41	970 80	533.46	-2622.11	789.61	396.01	-2043.48	992.90	-49.98	-21.15	979 45	283.83
-16.34	-149.94	997.23	560 37	-3120.00	792.50	409.46	-2123.25	1037.60	-52.87	-29.80	1013.09	292.51
-18.26	-163.40	1026 06	624 77	-3572.72	856.90	420.04	-2207.84	1083.25	-53.83	-39.41	1049.13	303.11
-20.18	-177.82	1049.61	739.15	-4146.55	919.37	446.95	-2275.12	1116.90	-54.79	-48.06	1081.81	312.75
-21.15	-196 08	1071.72	904.47	-4929.91	1100.56	471 94	-2309.72	1141.89	-57.67	-60.55	1114.49	322.39
-19.22	-214.34	1088.54	1405.25	-6191 95	1399.48	501.74	-2335.68	1131.31	-59.59	-73.05	1145.73	331.07
-16.34	-236 45	1105.84	2633 64	-8403.63	1996.86	514.23	-2338.56	1108.24	-61.52	-84.58	1178.41	340.71
-11.53	-258.56	1116.41	3697 67	-10414.42	2629.80	549.80	-2341.44	1112.09	-63.44	-97.08	1206.77	350.35
-5.77	-279.70	1127.95	4346.47	-12165.70	3337.71	602.66	-2439.48	1179.85	-64.40	-108.61	1237.04	359.99
-0.96	-304.70	1135.16	4835.71	-13457.53	4132.13	650.72	-2558 67	1246.17	-69.21	-117.26	1263.96	369.63
4 81	-327.76	1140.92	5352.83	-14528 29	4791.50	701.66	-2864.33	1341.81	-72.09	-126.88	1285.58	378.30
11.53	-356.60	1150 06	6228 47	-16064.26	5523.44	1329.32	-4289.76	1878.15	-73.05	-140.33	1308.17	386.98
17.30	-383.51	1161.59	7108.91	-17723.26	6183.77	2199.19	-5892.06	1832.98	-80.74	-140.33	1322.59	395.65
22.11	-404.66	1171.68	7776.94	-19053.54	6687.91	3533.31	-8116 23	1260.11	-95.16	-123.99	1328.36	403.37
26.91	-421.96	1173.12	8503 59	-20511.66	7232.43	5281.70	-10647.03	-750.68	-146.10	-2.88	1264.44	409.15
30.76	-436.38	1174.57	9245.63	-21925.56	7750.99	7467.44	-12036.90	-5548.91	-245.10	297.97	1075.08	413.97
30.76	-444 07	1171.68	9657.01	-22689.70	7991.76	8959.19	-12396.38	-9800.23	-287.39	483.48	963.11	415.90
29.80	-435 42	1139.96	9839.64	-22993 43	8074.42	10765.26	-12676.09	-15402 01	-311.42	606.51	923.22	402.40
26.91	-422.92	1120.74	9842.52	-22976.13	8072.02	11670.69	-12740.49	-18417.72	-312.38	646.88	923.70	391.80
24.03	-408.50	1105 36	9837.71	-22947.30	8066.74	12406.00	-12753.94	-20998.98	-310.46	681.48	925.62	380.23
24.03	-401.77	1094.31	9837.71	-22926.15	8060.00	12750.10	-12765.48	-22249.48	-306.62	691.09	917.93	374.45
21.15	-387.36	1073.16	9940.56	-18670.03	6141.00	13012.50	-12767.40	-23238 05	-305.66	699.74	918 89	365.77
18.26	-371.98	1046.73	9922.30	-18267.29	6008.36	13220.12	-12761.63	-24044.49	-304.70	706.47	924.66	358.06
17.30	-365.25	1060.19	9924.22	-18217.31	5985.29	13356.61	-12742.41	-24580.83	-306.62	719.93	947.73	356.13
-24.99	-233.57	-188.87	9175.46	-16207.48	5270.17	13053.83	-13754.54	-22925.67	-123.03	-179.74	258.08	1.38

Figure 13: 2D web strains at the back side for Specimen B-3

R1 (microstrain)			R2 (microstrain)			R3 (microstrain)			R4 (microstrain)			Load
R1-εx	R1-εy	R1-εxy	R2-εx	R2-εy	R2-εxy	R3-εx	R3-εy	R3-εxy	R4-εx	R4-εy	R4-εxy	(kN)
0.00	0 00	-0.96	0 00	0.96	-0 48	0.96	0.00	-0.48	-0.96	0.96	0.00	12.95
6.73	-66.32	27.87	3 84	-1.92	29 80	7 69	-63.44	24 99	2.88	-1.92	26.43	19.70
17 30	-166 28	71.61	10.57	-3.84	73.53	15.38	-158 60	66.80	7.69	-5.77	67.28	29.34
28 84	-260.48	111.98	15.38	-4.81	114.86	24.03	-246.06	104.29	11.53	-7.69	106 69	38.01
47.10	-403.70	174.45	24 03	-4 81	170.13	36.52	-372.94	159.56	18.26	-9.61	158.11	50.55
56 71	-488 28	210.98	26.91	-4.81	203.29	43.25	-449.83	193.68	21.15	-11.53	187.43	58.26
69 21	-589 21	255.19	30.76	-4.81	243.66	50.94	-544 03	235.97	24 99	-13 46	223.96	66.93
85.55	-735 31	320.07	34.60	-2.88	301.33	62.48	-683.40	298.93	32.68	-18.26	274.42	79.46
96.12	-818.93	356 60	37.49	-0.96	336.41	71.13	-768.95	337.38	36.52	-19.22	304.70	87.18
109.58	-947.73	414.27	40.37	1.92	388.32	81.70	-900.63	396.97	41.33	-24.03	349.87	98.74
118.23	-1029 43	452.72	41.33	3 84	423 40	89.39	-990.02	435.90	45.18	-27.87	378.71	105.49
129.76	-1142 85	506.54	43 25	6 73	470.98	99.00	-1114.97	492.61	49.02	-31.72	417.15	116.10
145.14	-1258 19	565.18	45.18	11.53	521.44	109.58	-1246.66	551.24	53.83	-35.56	457.04	126.70
159.56	-1353.35	616.12	46.14	15.38	561.33	118.23	-1354.31	598.82	57.67	-38.45	489.24	135.38
177 82	-1462.92	679 08	47.10	20.18	606.51	126.88	-1477.34	653.12	61.52	-44.21	524.81	145.02
202 81	-1588.84	750 68	47.10	24.99	653.12	136.49	-1609.02	712.24	65.36	-49.02	562.77	154 66
234.53	-1725.32	828 06	48 06	28.84	700.70	147.06	-1743.59	775.19	69.21	-54.79	599.30	164.30
270.09	-1867.58	904.47	49.98	32.68	742.99	162.44	-1878.15	838.63	71.13	-59.59	632.46	173.94
315.27	-2026.18	977.52	52 87	34.60	787.69	184.55	-2037.71	919.85	74.01	-65.36	669.46	183.58
364.29	-2195.34	1050.09	56.71	35.56	833.35	218.19	-2221.30	1015.97	76.89	-70.17	705.03	194.18
415.23	-2352.98	1112.09	59 59	35.56	869.39	256.64	-2392.39	1110.17	79.78	-74.01	732.42	202.86
478.67	-2540.41	1176.97	63.44	33.64	907.84	310.46	-2609.61	1232.24	79.78	-80.74	764.62	212.50
569.98	-2796.08	1256 27	69 21	31.72	950.13	386.40	-2886.43	1387.47	81.70	-84.58	797.30	223.10
678 60	-3082.52	1333 64	74 01	24.99	976 08	460.41	-3150.76	1538.37	82.66	-89.39	824.21	231.78
832.39	-3474 68	1450.91	77.86	19.22	1003.00	605.55	-3548 69	1733 01	83.62	-92 27	849.21	240.45
1068 84	-4065.81	1671 50	81.70	10.57	1030.39	742.03	-3942.78	1901.22	82.66	-93.23	872.27	251.06
1378.34	-4843.40	2037.23	85.55	0 96	1050.57	889.09	-4358.01	2094.90	81.70	-91 31	889.09	259.73
1896 42	-5991.06	2624.03	88.43	-11 53	1073.64	1143.81	-5100.04	2524.07	79.78	-91.31	906.40	270.34
2441.41	-7227.14	3291.57	92.27	-24.99	1098 63	1403.33	-5877.64	3041.67	77.86	-87.47	921.78	279.97
3065.21	-8723.70	4064.37	98 04	-40.37	1124.58	1762.81	-6904.18	3708.73	77.86	-87 47	934.27	288 65
3802.44	-10592.24	4977.01	102.85	-54.79	1154.38	2198.23	-8072.02	4493.05	79.78	-87.47	948.69	298.29
4573.31	-12768 36	5947.80	107 65	-72.09	1192.35	2795.12	-9660.86	5587.84	84.58	-98 04	971.76	307.93
5219 23	-14615.76	6761.93	113.42	-89.39	1228 87	3214.20	-10978 64	6688 88	92.27	-112.46	992.42	316.61
5855.53	-16561.19	7701 00	120.15	-116 30	1268.76	3432.39	-12134.94	8107.58	102.85	-139.37	1011 17	326.25
6176.57	-17813.61	8622.29	134.57	-159.56	1300.48	3041.19	-12275.28	9730.54	125.92	-174.94	1003.96	334.92
5566 21	-17248.44	9651.25	180.70	-242.22	1295.68	1619.59	-10853.68	12179.64	153.79	-203.77	957.34	344.56
2022 33	-12088 80	12344.00	264.33	-322.96	1126 99	-140.33	-8894.79	14660.93	172.05	-198.97	893.90	345.53
-2355.86	-6437.05	15973.90	280.67	-288.36	965.03	-491.16	-8447.84	15105.96	168.21	-183.59	867.95	336.85
-7180.04	-285 47	20507.34	249.91	-185.51	802.11	-520.00	-8395.94	15129.99	163.40	-171.09	863.14	327.21
-9978 05	2529.84	23218 84	207.62	-67 28	691 09	-554.60	-8370 95	15185.73	163.40	-168 21	871.31	322.39
-4631.94	2407.77	17398.38	134 57	132 64	558.45	-746 84	-8181.59	15462 08	164.36	-171 09	875.16	321.43
672 83	106.69	4924 62	90 35	250 87	485.88	-1134 20	-7775.97	15998 90	169.17	-172.05	870.35	321.43
585.36	26 91	4643 00	44 21	368.13	399.37	-2367.40	-6385.14	17624.26	173.01	-156.67	831.90	321.43
515.19	0 96	4533.42	-2.88	493.09	313.35	-3513.13	-5077.93	19119.86	172.05	-137.45	803.55	319.50
469 06	-21.15	4526 21	89.39	-195.12	-164 36	-2389 50	-4501.22	16083.00	-3 84	58 63	-150.43	1.38

Figure 14: 2D web strains at the front side for Specimen B-4

R5 (microstrain)			R6 (microstrain)			R7 (microstrain)			R8 (microstrain)			Load
R5-εx	R5-εy	R5-εxy	R6-εx	R6-εy	R6-εxy	R7-εx	R7-εy	R7-εxy	R8-εx	R8-εy	R8-εxy	(kN)
0 96	-0 96	0.96	0 00	0 00	0.00	0.00	0.96	0.48	0.00	0.00	0.00	12.95
3 84	-0.96	21 63	0.96	-53 83	30.28	1.92	-64.40	37.97	3 84	-2 88	24.51	19 70
7.69	-2 88	55.27	3 84	-138 41	76.89	5.77	-161.48	92.27	8 65	-8.65	60.55	29.34
10.57	-1.92	86 03	6.73	-216.27	120.15	9.61	-254.71	144.66	14.42	-10.57	92.27	38.01
17.30	0 00	127 84	10.57	-325.84	183.59	18.26	-392.16	219.63	20.18	-12.50	136.49	50.55
20.18	0.00	153.31	11.53	-393.12	222.51	22.11	-474.82	265.77	22.11	-13.46	161.96	58.26
24.99	0.96	182.14	13.46	-476.75	270.09	27.87	-572.87	319.59	24.03	-13.46	193.68	66.93
30.76	2.88	224 44	17.30	-598.82	340.74	36.53	-714.16	397.45	25.95	-11.53	239.82	79.46
34 60	4 81	249.43	21.15	-672.83	384.47	42.29	-792.02	441.18	26.91	-8 65	265.77	87.18
39 41	5.77	286.91	24.99	-788.17	450.80	47.10	-910.24	510 39	27.87	-5.77	308.06	98.74
41.33	6.73	311.42	26.91	-866.03	494.53	49 02	-983.29	556.53	26.91	-3.84	336.41	105.49
45.18	8 65	344.10	32.68	-975.60	557.01	51.90	-1084.22	620.92	26.91	0.96	372.46	116.10
49 02	10.57	377.75	37.49	-1089.02	622.85	54.79	-1187.06	692.05	25.95	5.77	410.91	126.70
51.90	11.53	405.62	44 21	-1183.22	676.19	57.67	-1270.69	750 68	24.99	10.57	441.66	135.38
54.79	13.46	433.97	49 98	-1287.99	735.31	63.44	-1366.80	821.81	23 07	15.38	475.79	145.02
56.71	16.34	464.25	56.71	-1399.48	800.19	72.09	-1474.46	903.99	21.15	21.15	510.39	154.66
59.59	19 22	495 97	65.36	-1510.02	866.51	86.51	-1588.84	992.42	19.22	28.84	544 03	164.30
60.55	23 07	522.40	74.01	-1616.71	934.75	102.85	-1698.41	1080.37	17.30	35.56	575.27	173.94
61.52	26.91	552.68	84.58	-1736.86	1016.45	123.03	-1813.75	1166 40	15.38	44.21	605.55	183.58
63.44	30.76	580.55	99.96	-1864.70	1109.21	148.98	-1936.79	1251.46	14.42	52.87	635.34	194.18
64 40	33.64	602 66	115.34	-1979.08	1197.15	176.86	-2042.52	1316.34	12.50	60.55	658.41	202 86
62 48	36.52	627.17	136.49	-2124.22	1309.13	206.65	-2157.86	1381.22	11.53	68.24	679.08	212.50
62.48	39.41	652.64	173.01	-2308.76	1448.50	248.95	-2299.15	1442.26	11.53	74.97	701.66	223.10
62.48	43.25	670.91	213.38	-2490.43	1582.59	291.24	-2436.60	1485.99	6.73	88.43	711.76	231.78
61.52	45 18	687.73	289.32	-2766 29	1728 69	336.41	-2585.58	1529.24	2 88	99.96	720.41	240.45
59.59	48 06	705.51	367 17	-3055.60	1872.87	421.00	-2823 96	1614.79	-1.92	113.42	726.65	251.06
56.71	51.90	716.56	450 80	-3346.84	2018 00	594.01	-3214.20	1824.33	-6.73	125.92	724.73	259.73
52.87	60.55	726 65	596.90	-3788.99	2265.99	921.78	-4011.98	2393.83	-10.57	135.53	723.77	270.34
48.06	71.13	734.34	788.17	-4386 84	2656.71	1260.11	-5028.91	3184.88	-15.38	149.94	724.73	279.97
43.25	81.70	739.15	1015 01	-5269 21	3303.59	1660 93	-6159.27	4082.15	-20.18	163.40	723.29	288.65
35.56	87.47	747.80	1396 60	-6544.70	4104.25	2142.48	-7585.66	5233.16	-24.99	175.90	725.21	298.29
27.87	97.08	756 45	2067 51	-8561.26	5280.74	2761.48	-9471.50	6556.71	-32.68	197.04	727.14	307.93
12.50	116 30	763.18	2944.11	-10904.63	6512 02	3318.97	-11238.16	7655.35	-43.25	222.99	729.06	316.61
-18.26	165.32	765.58	4355.12	-14456.20	8088.84	4082.15	-13605.55	8958.23	-60.55	269.13	729.06	326.25
-78 82	268 17	767.51	6572.57	-19568.73	9782.44	5200.96	-16601.56	10293.79	-95.16	354 68	727.62	334.92
-181 66	455 60	767.51	10613 39	-27232.25	11049.76	7831.72	-22363.86	11959.53	-217.23	589.21	732.90	344.56
-269 13	618 04	750 20	14256 28	-31411.48	10163.55	14951.21	-30184.05	10109.73	-439.26	1032.31	730.98	345.53
-281.63	633.42	725.69	14902.19	-31411.48	9601.26	20717.35	-30184.05	4108.58	-521.92	1235.12	742.03	336.85
-285.47	634.38	715 60	14961.78	-31411.48	9554.17	26194.17	-30184.05	-2260.22	-555.56	1367.76	783.85	327.21
-286.43	645.92	718 00	15029.07	-31411.48	9493.61	29730.37	-30184.05	-6755.20	-557.49	1431.20	833.83	322.39
-294.12	666.10	724 25	15375.09	-31411.48	9177.38	32253.47	-30184.05	-11423.18	-550.76	1462.92	929 95	321.43
-306 62	698.78	729.54	16046.00	-31411.48	8553.57	32253.47	-30184.05	-13097.56	-542.11	1460.04	991.46	321.43
-339.30	766 06	724.73	18078.90	-31411.48	6612.46	32253.47	-30184.05	-14706.59	-529 61	1434 09	1059.71	321.43
-363.33	822.77	722.81	19838.83	-31411.48	4857.82	32253.47	-30184.05	-16149.32	-516.16	1402.37	1137 08	319.50
-220.11	-268.17	-259 52	17782.86	-31411.48	7217.05	32253.47	-30184.05	-15190.06	-397.93	296 04	171.09	1.38

Figure 15: 2D web strains at the back side for Specimen B-4

APPENDIX 12

PRELIMINARY FE BUCKLING STUDY OF EXPERIMENT

1 Introduction to the model

A FE study is conducted investigating the behaviour of thin webs, with particular attention paid to the buckling of the web-posts. One specimen (10-3) out of fourteen non-composite castellated beams with mid-depth web openings, which was tested by Zaarour and Redwood (1996), it is now modelled with the use of ANSYS v11.0.

Zaarour and Redwood (1996) mentioned that a single point load was applied with a slight offset from the centre of 25.4mm (1in). It should be noted that the web opening depth is equal to *0.7h* and the inclined side of the web opening has an angle of 45.5°. The yield and ultimate steel strength for web and flanges were taken from coupon tensile tests and they are approximately f_y=*357MPa*, f_y=*342MPa* and $f_{ult.}$=*501MPa*, $f_{ult.}$=*505MPa*. The Young's and Tangent Modulus are assumed as *200GPa* and *2000MPa* respectively and the Poisson's Ratio is equal to *0.3*. The span of the specimen was *3048mm* and four web openings were positioned at each side.

A sensitivity study is performed regarding the element size. A FE model containing approximately 8,980 elements, with an element side length of approximately 15mm is incorporated (**Figure 1**).

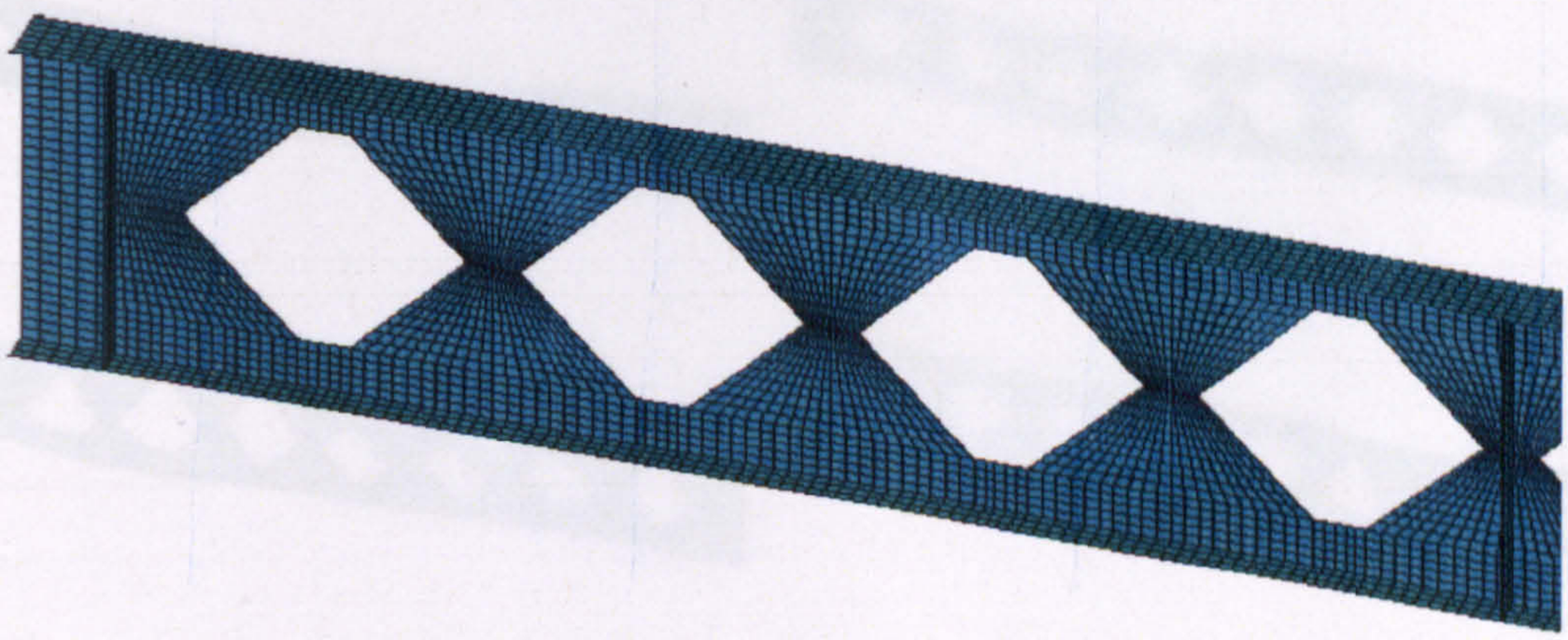

Figure 1: Half span mapped mesh model of specimen 10-3

2 Method of study

Similarly, applying an eccentric load in the FE model, an overall lateral torsional buckling (LTB) is obtained, instead of the double curvature web-post buckling. So, eigenvalue buckling analysis is then performed to obtain the buckling mode shapes. Applying a point load at mid-span without eccentricity, four failure modes are extracted by 'Block Lanczos' method, as shown in **Figure 2**. **Figure 3** shows the vector-loads the castellated beam experiences after the eigenvalue buckling analysis.

The next step is to update the geometry of the beam applying the previously taken vector-loads on the nodes of the FE model. The first failure mode shape with maximum amplitude of $t_w/200$ (usually maximum of 1-10% of the thickness) is incorporated. Once all boundary conditions are specified, the model is solved using large displacement static analysis, while the loading is applied incrementally until the model becomes unstable.

Summarizing the buckling analysis conducted as follows:

- Perform a static analysis with pre-stress effects on.
- Perform an eigenvalue buckling analysis.
- Update the geometry by scaling one failure mode obtained from the eigenvalue buckling analysis.
- Perform a non-linear buckling analysis with an applied load of approximately 75% of the eigenvalue buckling load.

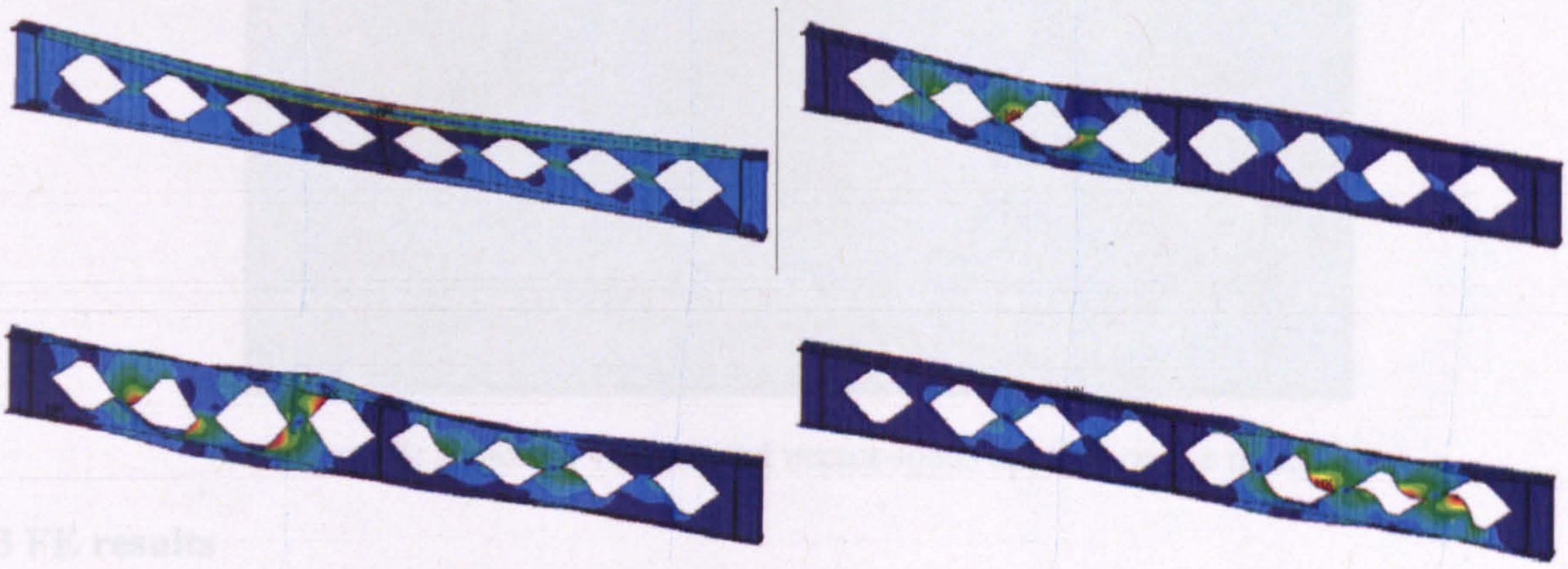

Figure 2: Four buckling modes extracted by 'Block Lanczos' method

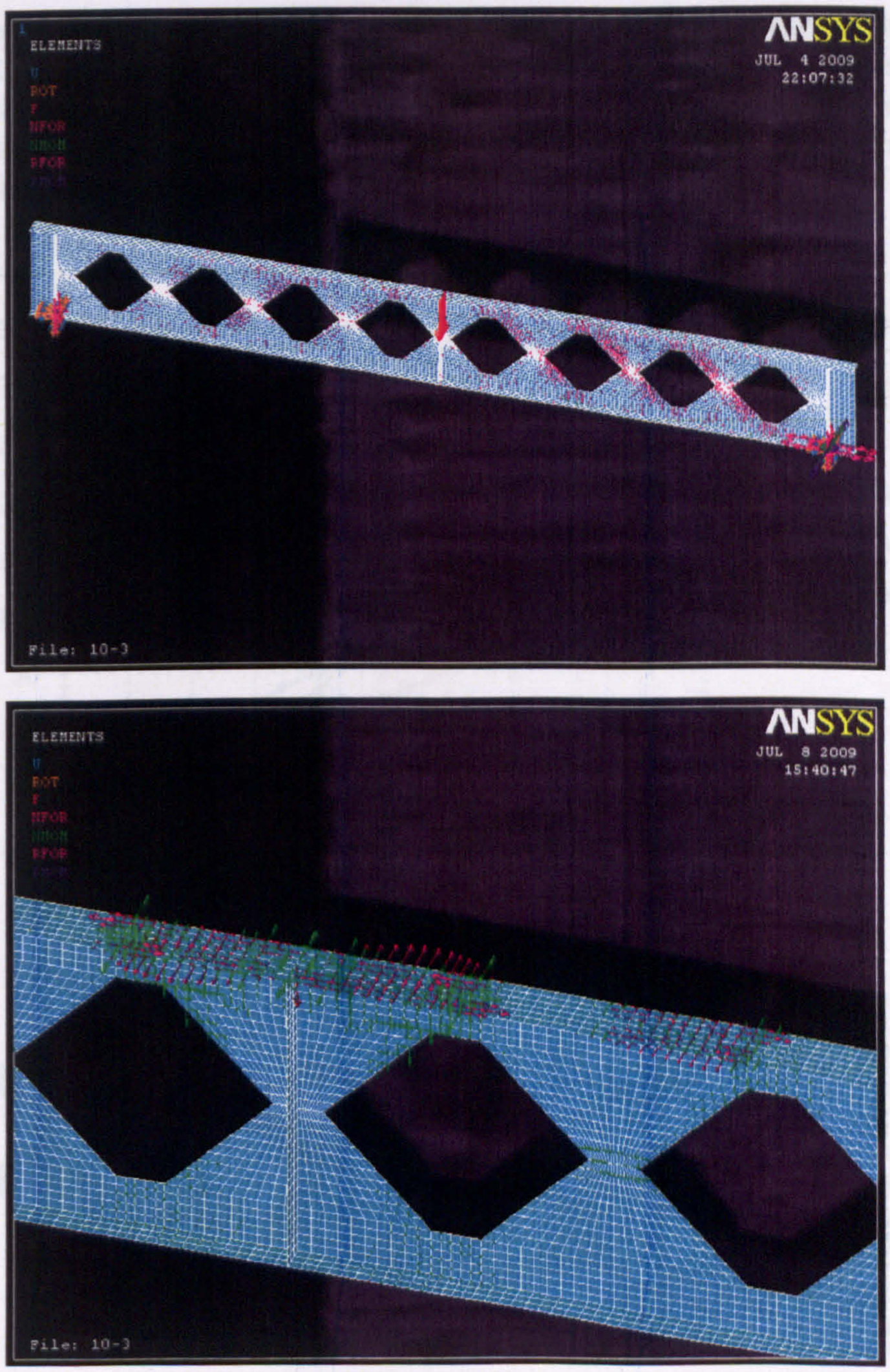

Figure 3: Reaction vectors and vector-loads applied on the nodes

3 FE results

The FE non-linear buckling analysis converges at a load, $P_{cr.FEM}=72.76kN$, which is very close to the experimental one ($P_{test}=73.8kN$), and the failure mode is web-post buckling. In **Figure 4** the out-of-plane displacements of the three web-posts adjacent to each other at the right side of the beam, from the one closer to the load (web-post 1) to the one closer to the support (web-post 3), are illustrated. It is clearly shown that the web-post buckling mode shape and its magnitude change for web-posts under different shear-moment interactions. Von-Mises yield criterion is used for steel beams and such stresses are depicted in **Figure 5** for better understanding of their distribution and concentration in the vicinity of the web

openings. The results are satisfactorily correlated with the experimental ones provided by Zaarour and Redwood (1996). The predicted FE buckling mode shape includes some flange rotation, which is also observed in the test beams. The rotation of the web tee-section associated with the rotation of the flange produces the out-of-plane movement of the web-post and the displacements at the web opening centre-lines.

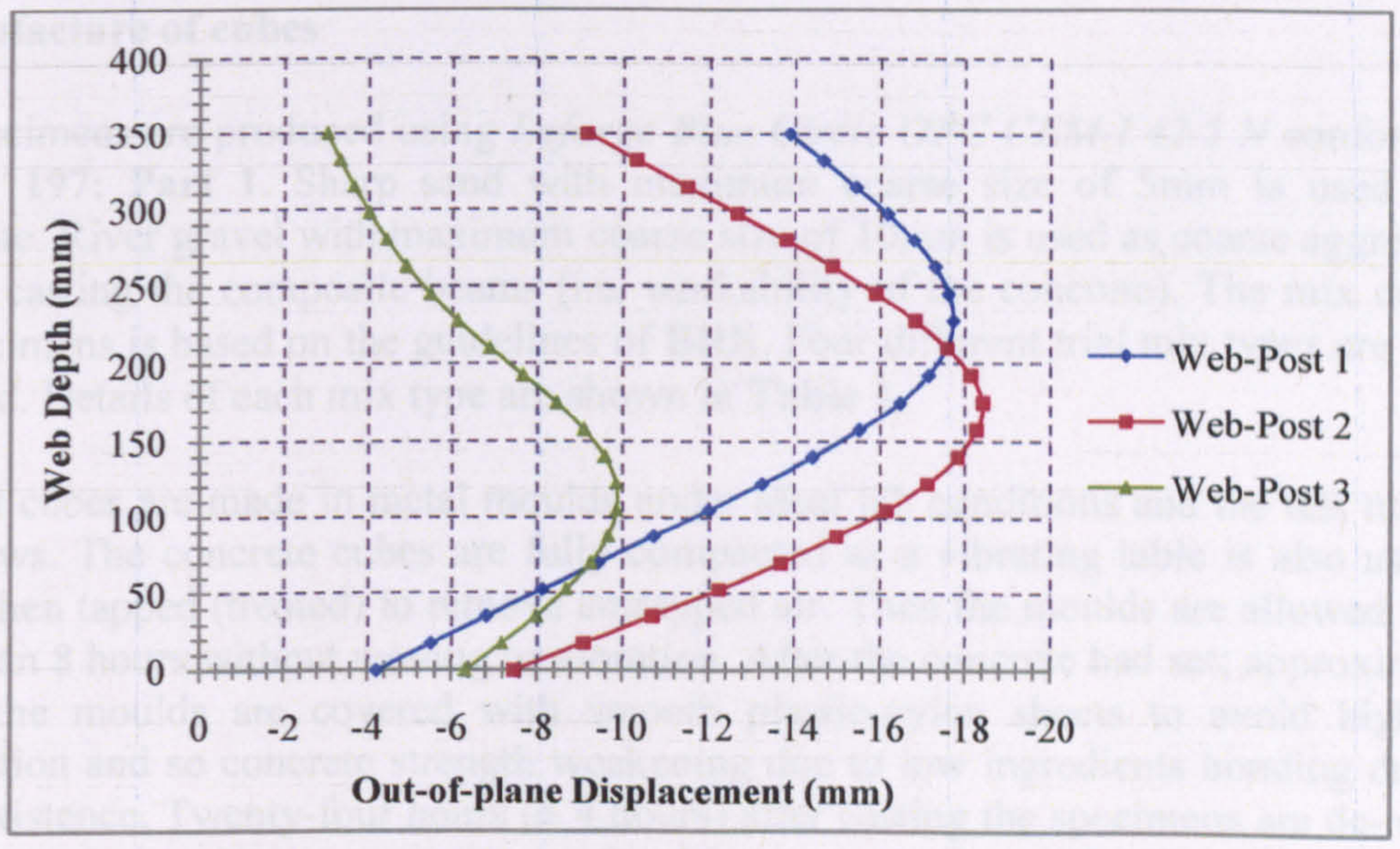

Figure 4: Out-of-plane displacements in three adjacent web-posts

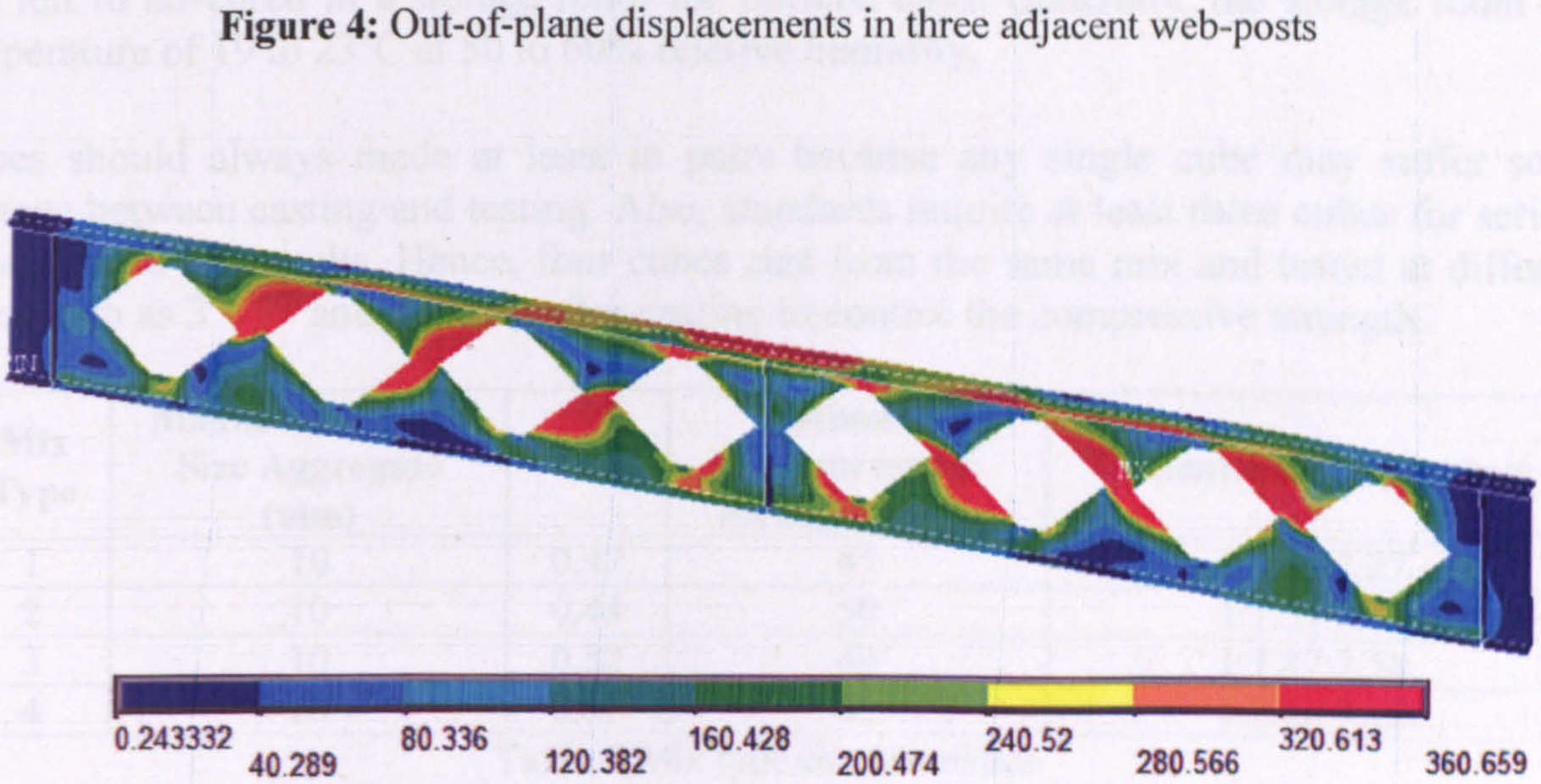

Figure 5: Von-Mises stress distribution

APPENDIX 13

TRIAL MIX DESIGN

1 Manufacture of cubes

The specimens are produced using *Lafarge Blue Circle OPC CEM-I 42.5 N* conforming to **BS EN 197: Part 1**. Sharp sand with maximum coarse size of 5mm is used as fine aggregate. River gravel with maximum coarse size of 10mm is used as coarse aggregate for ease of casting the composite beams (i.e. workability of the concrete). The mix design of the specimens is based on the guidelines of **BRE**. Four different trial mix types are initially designed. Details of each mix type are shown in **Table 1**.

The test cubes are made in metal moulds under ideal lab conditions and the test method is as follows. The concrete cubes are fully compacted as a vibrating table is also used. The side is then tapped (treated) to remove entrapped air. Then the moulds are allowed to stand more than 8 hours without moving or vibration. After the concrete had set; approximately 5 hours, the moulds are covered with smooth plastic-nylon sheets to avoid high water evaporation and so concrete strength weakening due to low ingredients bonding due to no water existence. Twenty-four hours (± 4 hours) after casting the specimens are de-moulded and left to air-cured in a storage room for thirteen days. Generally, the storage room has temperature of 19 to 23°C at 50 to 60% relative humidity.

Cubes should always made at least in pairs because any single cube may suffer some damage between casting and testing. Also, standards require at least three cubes for serious validation of the results. Hence, four cubes cast from the same mix and tested at different times such as 3rd, 7th and 14th day after casting to control the compressive strength.

Mix Type	Maximum Coarse Size Aggregate (mm)	*w/c*	Estimated Compressive Strength (MPa)	Cement:Sand:Aggregate
1	10	0.47	45	1:1.65:2.27
2	10	0.44	50	1:1.51:2.09
3	10	0.52	40	1:1.87:2.58
4	10	0.61	30	1:2.26:3.12

Table 1 Mix type characteristics

Test Results of Cubes

Initially, three mixes (Mix-1, 2 and 3) are designed with nominal compression strength at 28 days according to **BRE** of 45, 50 and 40MPa. Results obtained from this study could not conform to the required concrete strength at the day of the test, so another mix (Mix-4) is designed with nominal compression strength at 28 days of 30MPa.

All specimens are tested following the guidelines of **BS1881: Part 118**. As it is shown in **Figure 1** the results from cube compressive tests are expectable. As the water-cement ratio

is increased the concrete compressive strength is gradually decreased. The descending line of the concrete strength according to **BRE** as the time passes shows that it is not constant. The details of the trial cubes and the measurements of the compressive strength for each cube together with the average evaluations for the 3rd, 7th and 14th day of curing are synopsized in **Table 2**, **3** and **4** below, respectively.

As it is mentioned in **Chapter 5**, the compressive concrete strength at the day of the test (i.e. 14 days after casting) should be within 25 and 30MPa, no more than 35MPa. Hence, from **Figure 1** it is concluded that a water-cement ratio of 0.61 (Mix 4) should be used for casting the USFBs. The details of the tested cubes and the measurements of the compressive strength for each cube together with the average evaluations for USFB No.1 (Mix 5), USFB No.2 (Mix 6), USFB No.3 (Mix 7) and USFB No.4 (Mix 8) are synopsized in **Table 5**, **6**, **7** and **8**, respectively, and also shown in **Figure 6.3**.

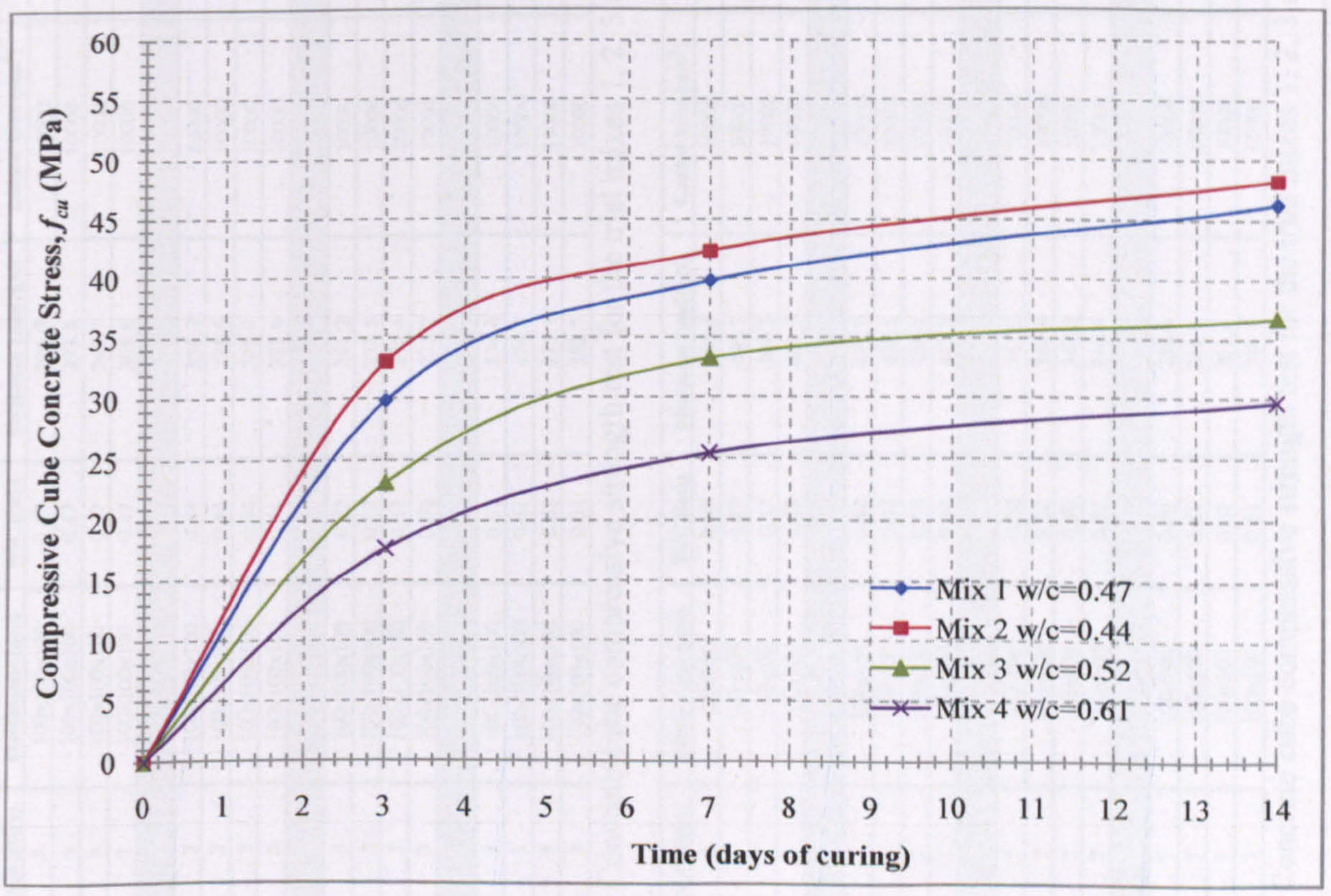

Figure 1: Concrete cube compressive strength for the trial mixes 1, 2, 3 and 4

Cube No.	Reference No.	Date Tested	Age (Days)	Dimensions (mm)	W/C Ratio	Maximum Load (kN)	Loaded Area (mm^2)	Compr. Str. (N/mm^2)	Average Comp. Str. (Mpa)
1	Mix 1	5/4/2008	3	100x100x100	0.47	296.0	10000	29.60	29.85
2	Mix 1	5/4/2008	3	100x100x100	0.47	293.8	10000	29.38	
3	Mix 1	5/4/2008	3	100x100x100	0.47	298.7	10000	29.87	
4	Mix 1	5/4/2008	3	100x100x100	0.47	305.6	10000	30.56	
1	Mix 2	5/4/2008	3	100x100x100	0.44	338.2	10000	33.82	32.97
2	Mix 2	5/4/2008	3	100x100x100	0.44	328.6	10000	32.86	
3	Mix 2	5/4/2008	3	100x100x100	0.44	328.0	10000	32.80	
4	Mix 2	5/4/2008	3	100x100x100	0.44	323.8	10000	32.38	
1	Mix 3	5/4/2008	3	100x100x100	0.52	241.2	10000	24.12	23.18
2	Mix 3	5/4/2008	3	100x100x100	0.52	232.5	10000	23.25	
3	Mix 3	5/4/2008	3	100x100x100	0.52	230.4	10000	23.04	
4	Mix 3	5/4/2008	3	100x100x100	0.52	223.2	10000	22.32	
1	Mix4*	17/4/2008	3	100x100x100	0.61	174.4	10000	17.44	17.68
2	Mix4*	17/4/2008	3	100x100x100	0.61	174.3	10000	17.43	
3	Mix4*	17/4/2008	3	100x100x100	0.61	175.1	10000	17.51	
4	Mix4*	17/4/2008	3	100x100x100	0.61	183.5	10000	18.35	

Table 2: Concrete cube compressive strength test for the trial mixes 1, 2, 3 and 4 at 3 days

Cube No.	Reference No.	Date Tested	Age (Days)	Dimensions (mm)	W/C Ratio	Maximum Load (kN)	Loaded Area (mm^2)	Compr. Str. (N/mm^2)	Average Comp. Str. (Mpa)
1	Mix 1	9/4/2008	7	100x100	0.47	385.4	10000	38.54	39.79
2	Mix 1	9/4/2008	7	100x100	0.47	423.7	10000	42.37	
3	Mix 1	9/4/2008	7	100x100	0.47	380.5	10000	38.05	
4	Mix 1	9/4/2008	7	100x100	0.47	401.9	10000	40.19	
1	Mix 2	9/4/2008	7	100x100	0.44	422.7	10000	42.27	42.29
2	Mix 2	9/4/2008	7	100x100	0.44	438.5	10000	43.85	
3	Mix 2	9/4/2008	7	100x100	0.44	420.3	10000	42.03	
4	Mix 2	9/4/2008	7	100x100	0.44	410.2	10000	41.02	
1	Mix 3	9/4/2008	7	100x100	0.52	312.2	10000	31.22	33.19
2	Mix 3	9/4/2008	7	100x100	0.52	340.9	10000	34.09	
3	Mix 3	9/4/2008	7	100x100	0.52	342.6	10000	34.26	
4	Mix 3	9/4/2008	7	100x100	0.52	246.4	10000	24.64	
1	Mix4*	21/4/2008	7	100x100	0.61	258.4	10000	25.84	25.44
2	Mix4*	21/4/2008	7	100x100	0.61	248.8	10000	24.88	
3	Mix4*	21/4/2008	7	100x100	0.61	261.2	10000	26.12	
4	Mix4*	21/4/2008	7	100x100	0.61	249.1	10000	24.91	

Table 3: Concrete cube compressive strength test for the trial mixes 1, 2, 3 and 4 at 7 days

Cube No.	Reference No.	Date Tested	Age (Days)	Dimensions (mm)	W/C Ratio	Maximum Load (kN)	Loaded Area (mm^2)	Compr. Str. (N/mm^2)	Average Comp. Str. (Mpa)
1	Mix 1	16/4/2008	14	100x100	0.47	467.6	10000	46.76	46.22
2	Mix 1	16/4/2008	14	100x100	0.47	468.9	10000	46.89	
3	Mix 1	16/4/2008	14	100x100	0.47	457.3	10000	45.73	
4	Mix 1	16/4/2008	14	100x100	0.47	455.0	10000	45.50	
1	Mix 2	16/4/2008	14	100x100	0.44	465.0	10000	46.50	48.25
2	Mix 2	16/4/2008	14	100x100	0.44	487.1	10000	48.71	
3	Mix 2	16/4/2008	14	100x100	0.44	494.9	10000	49.49	
4	Mix 2	16/4/2008	14	100x100	0.44	482.9	10000	48.29	
1	Mix 3	16/4/2008	14	100x100	0.52	380.1	10000	38.01	36.75
2	Mix 3	16/4/2008	14	100x100	0.52	377.3	10000	37.73	
3	Mix 3	16/4/2008	14	100x100	0.52	353.7	10000	35.37	
4	Mix 3	16/4/2008	14	100x100	0.52	358.8	10000	35.88	
1	Mix4*	28/4/2008	14	100x100	0.61	303.6	10000	30.36	29.63
2	Mix4*	28/4/2008	14	100x100	0.61	296.0	10000	29.60	
3	Mix4*	28/4/2008	14	100x100	0.61	308.0	10000	30.80	
4	Mix4*	28/4/2008	14	100x100	0.61	277.6	10000	27.76	
	Mix4*	**Casting Date: 14/04/2008**							

Table 4: Concrete cube compressive strength test for the trial mixes 1, 2, 3 and 4 at 14 days

Cube No.	Reference No.	Date Tested	Age (Days)	Dimensions (mm)	W/C Ratio	Maximum Load (kN)	Loaded Area (mm^2)	Compr. Str. (N/mm^2)	Average Comp. Str. (Mpa)
1	Mix 5	5/1/2008	3	100x100	0.61	154.9	9850	15.726	16.005
2	Mix 5	5/1/2008	3	100x100	0.61	157.5	9850	15.990	
3	Mix 5	5/1/2008	3	100x100	0.61	159.8	9850	16.223	
4	Mix 5	5/1/2008	3	100x100	0.61	158.4	9850	16.081	
1	Mix 5	5/5/2008	7	100x100	0.61	225.1	9850	22.853	22.864
2	Mix 5	5/5/2008	7	100x100	0.61	225.3	9850	22.873	
3	Mix 5	5/5/2008	7	100x100	0.61	229	9850	23.249	
4	Mix 5	5/5/2008	7	100x100	0.61	224.8	10000	22.480	
1	Mix 5	5/12/2008	14	100x100	0.61	279.3	10000	27.930	27.907
2	Mix 5	5/12/2008	14	100x100	0.61	281.4	9900	28.424	
3	Mix 5	5/12/2008	14	100x100	0.61	279.5	9900	28.232	
4	Mix 5	5/12/2008	14	100x100	0.61	267.7	9900	27.040	
1	Mix 5	26/5/2008	28	100x100	0.61	336.9	9900	34.030	32.672
2	Mix 5	26/5/2008	28	100x100	0.61	332.2	9800	33.898	
3	Mix 5	26/5/2008	28	100x100	0.61	341.6	9900	34.505	
4	Mix 5	26/5/2008	28	100x100	0.61	278.3	9850	28.254	

Table 5: Concrete cube compressive strength test for USFB No.1 (Mix 5)

Cube No.	Reference No.	Date Tested	Age (Days)	Dimensions (mm)	W/C Ratio	Maximum Load (kN)	Loaded Area (mm^2)	Compr. Str. (N/mm^2)	Average Comp. Str. (Mpa)
1	Mix 6	16/5/2008	3	100x100	0.61	167.4	9800	17.082	17.444
2	Mix 6	16/5/2008	3	100x100	0.61	178.9	10000	17.890	
3	Mix 6	16/5/2008	3	100x100	0.61	176.8	9800	18.041	
4	Mix 6	16/5/2008	3	100x100	0.61	164.3	9800	16.765	
1	Mix 6	20/5/2008	7	100x100	0.61	236	9650	24.456	23.735
2	Mix 6	20/5/2008	7	100x100	0.61	228.5	9750	23.436	
3	Mix 6	20/5/2008	7	100x100	0.61	229.6	9850	23.310	
4	Mix 6	20/5/2008	7	100x100	0.61	235	9900	23.737	
1	Mix 6	27/5/2008	14	100x100	0.61	260.1	9650	26.953	26.765
2	Mix 6	27/5/2008	14	100x100	0.61	257.8	9700	26.577	
3	Mix 6	27/5/2008	14	100x100	0.61	258.5	9600	26.927	
4	Mix 6	27/5/2008	14	100x100	0.61	260.7	9800	26.602	
1	Mix 6	6/10/2008	28	100x100	0.61	300.2	9500	31.600	30.836
2	Mix 6	6/10/2008	28	100x100	0.61	309.9	9800	31.622	
3	Mix 6	6/10/2008	28	100x100	0.61	295.2	9850	29.970	
4	Mix 6	6/10/2008	28	100x100	0.61	298.5	9900	30.152	

Table 6: Concrete cube compressive strength test for USFB No.2 (Mix 6)

Cube No.	Reference No.	Date Tested	Age (Days)	Dimensions (mm)	W/C Ratio	Maximum Load (kN)	Loaded Area (mm^2)	Compr. Str. (N/mm^2)	Average Comp. Str. (Mpa)
1	Mix 8	22/6/2008	3	100x100	0.61	137.2	9900	13.859	16.116
2	Mix 8	22/6/2008	3	100x100	0.61	165.6	9900	16.727	
3	Mix 8	22/6/2008	3	100x100	0.61	170	9900	17.172	
4	Mix 8	22/6/2008	3	100x100	0.61	165.4	9900	16.707	
1	Mix 8	26/6/2008	7	100x100	0.61	229.4	9950	23.055	22.549
2	Mix 8	26/6/2008	7	100x100	0.61	219.7	10000	21.970	
3	Mix 8	26/6/2008	7	100x100	0.61	222.3	9800	22.684	
4	Mix 8	26/6/2008	7	100x100	0.61	221.5	9850	22.487	
1	Mix 8	3/7/2008	14	100x100	0.61	259.8	10000	25.980	25.331
2	Mix 8	3/7/2008	14	100x100	0.61	244.5	9702	25.201	
3	Mix 8	3/7/2008	14	100x100	0.61	254.7	9702	26.252	
4	Mix 8	3/7/2008	14	100x100	0.61	236.5	9900	23.889	
1	Mix 8	17/7/2008	28	100x100	0.61	295.1	9900	29.808	29.600
2	Mix 8	17/7/2008	28	100x100	0.61	300	9900	30.303	
3	Mix 8	17/7/2008	28	100x100	0.61	287.6	9900	29.051	
4	Mix 8	17/7/2008	28	100x100	0.61	291.2	9960	29.237	
						high segregation is observed - highlighted value			

Table 7: Concrete cube compressive strength test for USFB No.3 (Mix 8)

Cube No.	Reference No.	Date Tested	Age (Days)	Dimensions (mm)	W/C Ratio	Maximum Load (kN)	Loaded Area (mm^2)	Compr. Str. (N/mm^2)	Average Comp. Str. (Mpa)
1	Mix 7	16/5/2008	3	100x100	0.61	93.2	10000	9.32	10.04
2	Mix 7	16/5/2008	3	100x100	0.61	104.5	9850	10.61	
3	Mix 7	16/5/2008	3	100x100	0.61	98.9	9700	10.20	
1	Mix 7	20/5/2008	7	100x100	0.61	142.6	10000	14.26	15.05
2	Mix 7	20/5/2008	7	100x100	0.61	142.6	9600	14.85	
3	Mix 7	20/5/2008	7	100x100	0.61	164.0	9850	16.65	
4	Mix 7	20/5/2008	7	100x100	0.61	142.2	9850	14.44	
1	Mix 7	27/5/2008	14	100x100	0.61	178.7	9850	18.14	18.80
2	Mix 7	27/5/2008	14	100x100	0.61	187.7	9650	19.45	
1	Mix 7	10/06/2008	28	100x100	0.61	195.2	9850	19.82	21.14
2	Mix 7	10/06/2008	28	100x100	0.61	219.0	9750	22.46	
1	Mix 7	04/07/2008	52	100x100	0.61	261.3	9800	26.66	25.62
2	Mix 7	04/07/2008	52	100x100	0.61	259.5	9900	26.21	
3	Mix 7	04/07/2008	52	100x100	0.61	247.2	9800	25.22	
4	Mix 7	04/07/2008	52	100x100	0.61	234.0	9600	24.38	

Table 8: Concrete cube compressive strength test for USFB No.4 (Mix 7)